MEDICAL RADIOLOGY

Diagnostic Imaging

A. L. Baert
M. Knauth
K. Sartor

Radiological Imaging of the Digestive Tract in Infants and Children

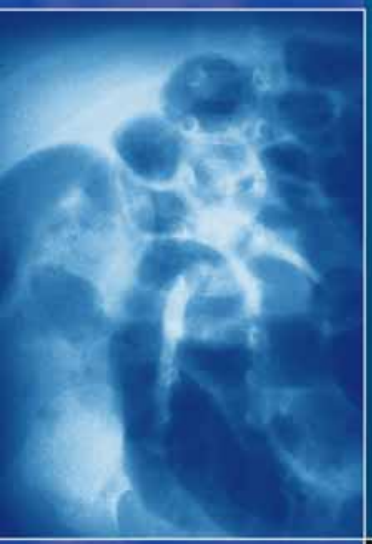

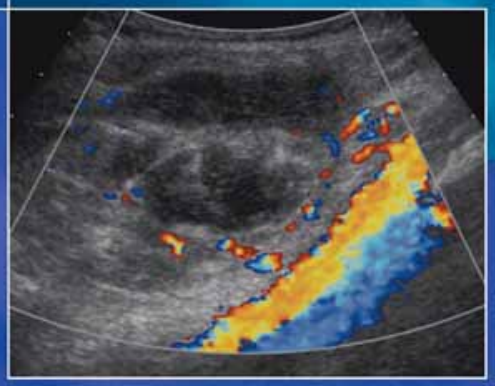

A. S. Devos · J. G. Blickman
Editors

Springer

MEDICAL RADIOLOGY

Diagnostic Imaging

A. S. Devos · J. G. Blickman (Eds.)

Radiological Imaging of the Digestive Tract in Infants and Children

With Contributions by

T. Berrocal · S. A. Connolly · G. del Pozzo · R. B. J. Glass · C. M. Hall · Y. L. Hoogeveen
M. Hiorns · R. M. Jiménez · J. S. Laméris · M. Meradji · E. Nijs · R. R. van Rijn

Foreword by

A. L. Baert

With 227 Figures in 500 Separate Illustrations, 43 in Color

Springer

Annick S. Devos, MD
Erasmus MC
Sophia Children's Hospital
Dr. Molewaterplein 40
P. O. Box 1738
3000 DR. Rotterdam
The Netherlands

Johan G. Blickman, MD, PhD, FACR
Professor and Chairman, Department of Radiology
University Hospital Nijmegen
UMC Nijmegen-667
P. O. Box 9101
Geert Groteplein 10
6500 HB Nijmegen
The Netherlands

Medical Radiology · Diagnostic Imaging and Radiation Oncology
Series Editors:
A. L. Baert · L. W. Brady · H.-P. Heilmann · M. Knauth · M. Molls · C. Nieder · K. Sartor

Continuation of Handbuch der medizinischen Radiologie
Encyclopedia of Medical Radiology

Library of Congress Control Number: 2005935285

ISBN 978-3-540-40733-1 Springer Berlin Heidelberg New York

Medical Editor: Dr. Ute Heilmann, Heidelberg
Desk Editor: Ursula N. Davis, Heidelberg
Production Editor: Kurt Teichmann, Mauer
Cover-Design and Typesetting: Verlagsservice Teichmann, Mauer

Printed on acid-free paper – 21/3180xq – 5 4 3 2 1 0

Foreword

Although conventional radiography and barium studies still play an important role in radiological imaging of the digestive tract in infants and children, the new cross-sectional methods based on ultrasound, CT and, to a lesser extent, MRI have gained considerable importance in this radiological field during recent years.

This volume provides a much needed update on our knowledge and insights on how to provide optimal radiological care to infants and children with digestive malformations and acquired diseases of the digestive tract.

The editors, A. S. Devos and J. G. Blickman, are leading pediatric radiologists with a special interest in pediatric digestive diseases. They have been assisted by a group of internationally renowned experts. Together they have produced a well structured work that, although concise in concept and contents, covers well our actual radiological approach and management of diagnostic pediatric digestive problems.

I am confident that this outstanding volume will find great interest from both general and specialised pediatric radiologists, as well as from radiologists in training, neonatologists and pediatricians.

Leuven

Albert L. Baert

Preface

For the general radiologist, pediatric radiology is not the most frequent part of his or her daily practice. In particular, the pediatric chest and abdomen, relatively common occurrences in a general radiology practice, are often cause for unease of approach and interpretation.

Such unease arises both from a practical point of view, in that it can be physically difficult to image the infant or young child, and from the differential diagnostic point of view, the differential diagnosis often being different at varying ages.

This book is intended to provide the reader with a comprehensive review of all that pertains to the pediatric gastrointestinal (GI) tract and the accessory digestive organs. It is built up in a logical sequence, starting with pathology affecting the oesophagus and culminating with pathology most often encountered at or near the rectum.

While primarily intended for general radiologists, both in training and in daily practice, it also addresses those interested in GI tract imaging, such as pediatricians or general practitioners, as well as trainees therein, of the pediatric and young adult age group.

The book is by no means intended to be exhaustive, but certainly tries to give an up-to-date approach to daily clinical diagnostic issues.

Each author was asked to be exhaustive yet practical and, where possible, to try to incorporate some aspects of "how I do it" in order to illustrate some of his or her personal approaches to each organ system.

In the course of writing this book, a number of things became obvious. The reader should be aware that what the authors describe as state-of-the-art while writing their chapters may already have become outdated, although in pediatric imaging in general this is luckily not often the case.

Also, one must realize that the location of disease processes and approaches to diagnosis also vary, both between institutions but also whether one's focus is the acute patient or an analysis of the entire clinical question. Overlap between some parts of this text are thus unavoidable. Examples include appendicitis and intussusception, but also entities affecting multiple parts of the digestive tract.

To be asked by Prof. Albert Baert to take on this endeavour was a true honour. But in the process he certainly showed me how to stay patient!

Also, and for me this is the real reason for being in academics, this endeavour was an opportunity to encourage a promising 'next-generation pediatric radiologist' to take the lead and 'get one's name in print'. Dr. Annick Devos did an outstanding job, even while having a baby during the process.

Both of us were lucky indeed to have our research associate, Dr. Yvonne Hoogeveen, to keep us on course and spend much time and effort on getting the text in optimal shape. Without her, it would have been difficult, if not impossible, to ensure the completion of this endeavour.

To complicate matters further, we had a number of potential and agreed authors either dropping out due to illness or because of changes in employment situations precluding them from contributing. Nevertheless, the result is a truly international effort that we are proud of.

For this we wish to thank the co-workers of Springer-Verlag, as they were truly exemplary in their cooperation. Ursula Davis, in particular, deserves our thanks.

Dr. Devos and I are extremely thankful to all the authors: you all are the book! They were selected for their prominence in their specialty, and the list of these authors represents a broad combination of experience, teaching ability and stature.

Finally, it was a pleasure to contribute to better imaging in children, something that pediatric radiologists of course have made their aim in life, but also should be aimed for by all radiologists in general.

Nijmegen — Johan G. Blickman

It was a wonderful opportunity for me, and I agree wholeheartedly with the above. Also, I want to thank Prof. Johan G. Blickman for giving me this opportunity and for the trust he had in me during our collaboration. Your enthusiasm is contagious and a source of motivation to persevere and at the same time to remain patient!

Rotterdam — Annick S. Devos

Contents

Imaging in Pediatric Gastrointestinal Emergencies

1

Teresa Berrocal and Gloria del Pozo

CONTENTS

T. Berrocal, MD, PhD
Pediatric Radiologist, Department of Radiology, Division of Pediatric Radiology, University Hospital La Paz. Madrid. Spain
G. del Pozo, MD, PhD
Associate Professor of Radiology, Pediatric Radiologist, Department of Radiology, Pediatric Radiology section, University Hospital 12 de Octubre, Madrid, Spain

1.1 Gastrointestinal Emergencies in the Neonate

1.1.1 Neonatal Intestinal Obstruction

Intestinal obstruction is the most common abdominal emergency in the neonatal period. It is almost always the result of a congenital anomaly of the gastrointestinal tract, which must be rectified surgically if the infant is to survive. Mortality in surgically untreated patients is close to 100%, and the rate of survival is closely related to the time of surgical intervention (Hajivassiliou 2003). The most common clinical findings are abdominal distension, vomiting, and sometimes failure to pass meconium, depending on the level of the obstruction. These findings usually prompt the clinician to consult the radiologist, who must answer three major questions: Is the obstruction present? What is the location of the obstruction? What is the aetiology? The most valuable means of determining whether or not obstruction is present is the plain abdominal radiograph. Plain radiographs are often diagnostic. When not diagnostic, they may provide important clues suggesting the subsequent most valuable diagnostic procedure (Singleton et al. 1977).

Knowledge of the many variations in both the distribution and quantity of intestinal air in infants is useful in the interpretation of pathologic findings. In a healthy neonate, air can usually be identified in the stomach within minutes after birth, and reaches the proximal portion of the small bowel during the first 6 h of life. By 6–12 h the entire small bowel usually contains air, and after 12–24 h normal neonates show rectosigmoid air in a plain abdominal radiograph.

When an intestinal obstruction is present, since air proceeds distally in the gastrointestinal tract until stopped at the obstruction, an abdominal radiograph will show dilated air-filled loops proximal to the obstruction and no air distal to it. The number of dilated loops depends on the site of obstruction: the lower the obstruction, the greater the number of dilated loops. Having established that an intestinal obstruction is present, the radiologist should still determine the location of the obstruction and, if possible, the etiology. In order to arrive at a useable differential diagnostic list of possible etiologies, neonatal obstructions can be classified as high or low obstruction. High or upper intestinal obstructions are those that occur proximal to the mid-ileum and include obstructions involving the stomach, duodenum, jejunum, and proximal ileum. Obstructions that involve the distal ileum or colon are called low intestinal obstructions. The distinction between high and low obstruction is also critical since children with high obstructions usually need little or no radiologic evaluation after plain radiograph, and the specific diagnosis is made in the operating room. Newborns with low obstructions need a contrast enema, which usually provides a specific diagnosis and may be therapeutic (Buonomo 1997). In general, plain radiographs in neonates with high obstruction reveal one, two, or a few dilated air-filled bowel loops, depending on the level of the obstruction, while radiographs in low obstructions show multiple dilated air-filled bowel loops.

Disorders of the intestinal tract in the neonatal period usually present with abdominal distension and dilatation of the bowel. However, not all intestinal dilatations represent obstruction. Infants with medical disorders such as sepsis, electrolyte imbalance or necrotizing enterocolitis may present ileus characterized by uniform dilatation of the bowel to the level of the rectum. Also, infants on continuous positive airways pressure may swallow an excessive amount of air and exhibit important intestinal dilatation. This dilatation must be distinguished from mechanical obstruction, because the treatment is completely different. The differentiation between these two categories can usually be made on the basis of clinical history, laboratory tests, and appropriate radiographs (Hernanz-Schulman 1999).

1.1.1.1 High Obstruction

1.1.1.1.1 Gastric Outlet Obstruction

Complete obstruction involving the gastric outlet is a rare condition usually due to antral or pyloric atresia, although it may be caused by extrinsic pressure from congenital peritoneal bands or by annular pancreatic tissue in the gastric wall. Antral or pyloric atresia accounts for less than 1% of all congenital intestinal obstructions. The condition is thought to be due to localized vascular occlusion in fetal life (Okoye et al. 2000). It is usually produced by a membranous diaphragm in which only the mucosa is involved. An association with epidermolysis bullosa letalis has been described (Toma et al. 2002). It is unknown whether the association is on the basis of a causative effect on the antropyloric mucosa, or whether it is due to a genetic linkage (Dolan et al. 1993). The predominant symptom is vomiting within the first hours after birth, the vomits being free of bile**.** The absence of bile in the vomits indicates that the obstruction is above the ampulla of Vater. A plain radiograph of the abdomen shows distension of the stomach proximal to the obstruction and absence of air in the small bowel and colon, resulting in the characteristic "single bubble" image (Rathaus et al. 1992) (Fig. 1.1). When a single bubble is observed, examination with contrast material is unnecessary and most patients are taken directly to surgery. The membranous atresia may perforate after birth, leaving variable degrees of stenosis. In these cases, plain radiography will show distension of the stomach and some air in the small bowel depending upon the degree of obstruction (Bell et al. 1977).

Pyloric stenosis may lead to obstruction of the lumen and usually presents beyond the neonatal period. However, it has been diagnosed in utero and can be seen in the neonatal period after administration of prostaglandin E to infants with ductus-dependent congenital heart disease. The stenosis is produced by central foveolar hyperplasia. On sonography, mucosal thickening often with polypoid or lobular appearance is observed, different from the muscular thickening observed in hypertrophic pyloric stenosis (Peled et al. 1992; Babyn et al. 1995) (Fig. 1.2).

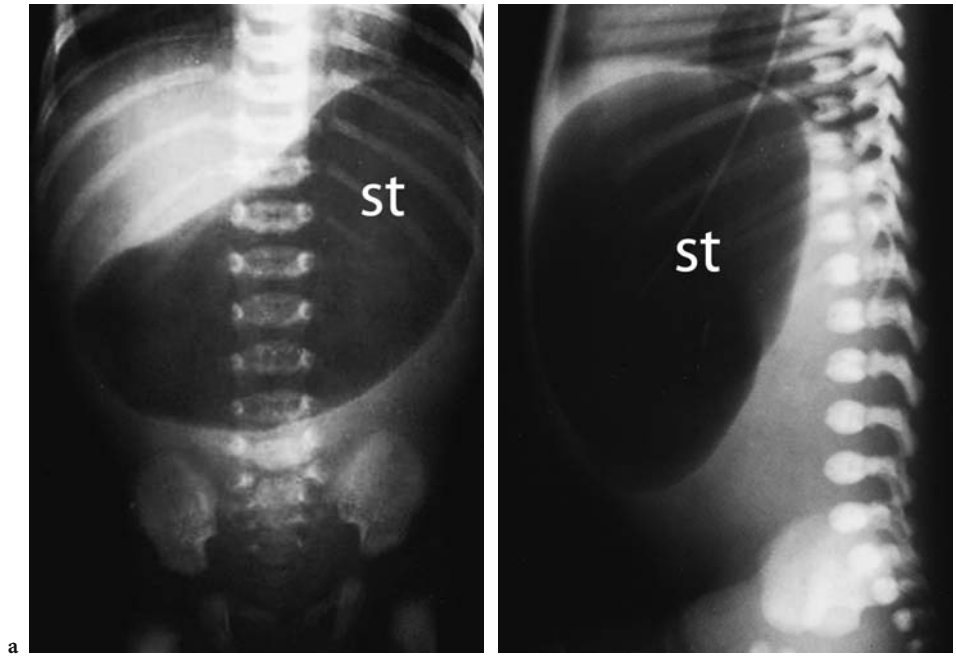

Fig. 1.1a,b. Pyloric atresia. Anteroposterior (**a**) and lateral (**b**) plain abdominal radiograph in a newborn infant that shows distension of the stomach (*st*) and absence of air in the small bowel and colon, resulting in the characteristic "single bubble" image

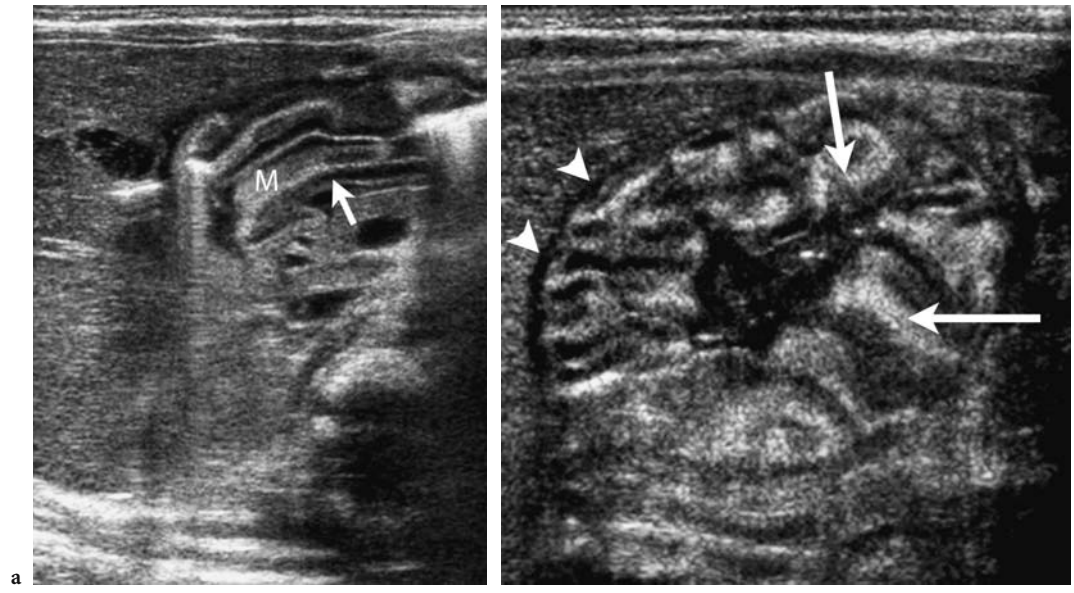

Fig. 1.2a,b. Prostaglandin therapy-induced gastric outlet obstruction. Neonate with ductus-dependent congenital heart disease treated with prostaglandin E to maintain ductus patency. **a** Longitudinal US scan through the pyloric channel shows mucosal thickening (*M*), and a thin muscular layer (*arrows*), different from the muscular thickening seen in hypertrophic pyloric stenosis. **b** Axial scan through the gastric antrum reveals markedly hypertrophic mucosa (*arrows*) and an undulating appearance. The thickness of the muscular layer of the gastric wall is normal (*arrowheads*)

1.1.1.1.2 Duodenal Obstruction

Complete duodenal obstruction is much more frequent than congenital gastric obstruction.

Persistent vomiting is the cardinal sign, but abdominal distension may not be a conspicuous feature. The vomiting is bile-stained when the obstruction is below the ampulla of Vater (70% of cases), and clear but persistent in supra-ampullary lesions.

The classic plain radiographic finding is the so-called double bubble image (Rathaus et al. 1992) (Fig. 1.3). The higher, more leftward and larger bubble is the stomach, and the other bubble is the dilated proximal duodenum, above the area of obstruction. Two distinct air-fluid levels are usually demonstrated on erect or horizontal beam radiographs. There is no air more distally in the gastrointestinal tract. Newborns showing evidence of complete duodenal obstruction on their abdominal radiograph rarely require further radiologic investigation. An upper gastrointestinal series provides no additional information, and there is a potential hazard of vomiting with barium aspiration. Sometimes vomiting can result in a lack of air in the obstructed segment; in these cases a small amount of air can be injected via a nasogastric tube when the abnormal pathology will present (Fig. 1.4). A contrast enema is not necessary when the diagnosis is obvious, although it can be performed to exclude additional more distal areas of atresia (McAlister et al. 1996). In the case of isolated duodenal obstruction, the colon should be normal.

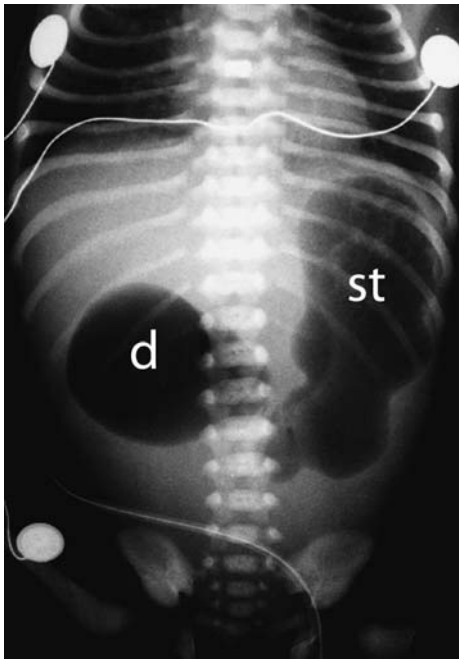

Fig. 1.3. Complete duodenal obstruction caused by a congenital duodenal web. The stomach (*st*) and duodenum (*d*) are dilated and with absence of air more distally in the gastrointestinal tract, producing the classical "double bubble" image

The main causes for a "double bubble" are duodenal atresia, annular pancreas, and midgut volvulus. Less frequently it may be secondary to duodenal web, Ladd´s band, or preduodenal portal vein (Crowe and Sumner 1978).

Duodenal atresia is the most important cause of complete duodenal obstruction (Fig. 1.4). It occurs in approximately 1 in 10,000 births, and 60% of the infants are premature. The etiology of this condition is thought to be failure of recanalization of the duodenum, approximately between the 9th and 11th week of gestation. Unlike jejunal and ileal atresia, this condition does not appear to be related to intrauterine vascular accidents (Boyden et al. 1967). Major associated anomalies are present in about 50% of the patients. Approximately 30% have Down´s syndrome. Other anomalies include malrotation of the small bowel, esophageal atresia, congenital heart disease, imperforate anus, small bowel atresia, biliary atresia, annular pancreas, and renal anomalies (Auringer and Sumner 1994; Bailey et al. 1993).

Annular pancreas is an anomalous band of pancreatic tissue, which arises from the head of the pancreas and encircles the second portion of the duodenum to a variable extent, giving rise to a variable degree of duodenal obstruction. This anatomy results if two ventral pancreatic buds arise from the ventral mesentery and rotate in opposite directions to fuse with the dorsal pancreatic bud (Larsen 1993). If a complete ring is formed, there may be complete obstruction of the duodenum at the time of birth; if the ring is incomplete, obstruction may occur later in life or may never produce symptoms. When a complete ring is formed, radiological findings are indistinguishable from duodenal atresia with the typical double bubble sign, and the diagnosis is made at surgery (Norton et al. 1992) (Fig. 1.5).

Midgut volvulus is the most dramatic consequence of intestinal malrotation. When present at birth, the classic finding on a plain film is partial obstruction of the duodenum, but evidence of complete obstruction may also be present. In such cases, it is impossible to distinguish midgut volvulus from

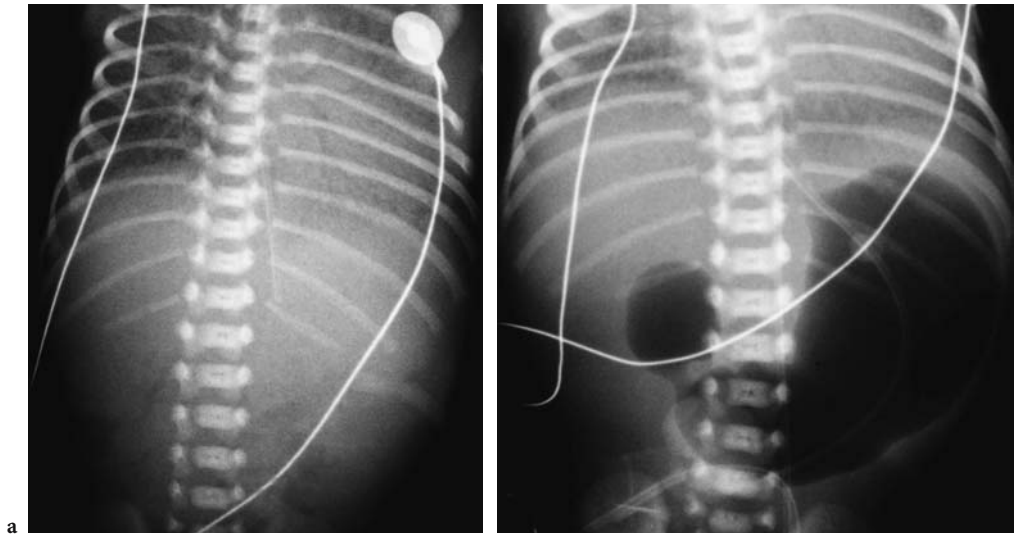

Fig. 1.4a,b. Duodenal atresia. **a** Plain radiograph obtained 6 h after birth shows absence of air in the gastrointestinal tract of this neonate with severe lung disease. **b** Radiograph made after inflation of the stomach through a nasogastric tube demonstrates complete duodenal obstruction ("double bubble" sign)

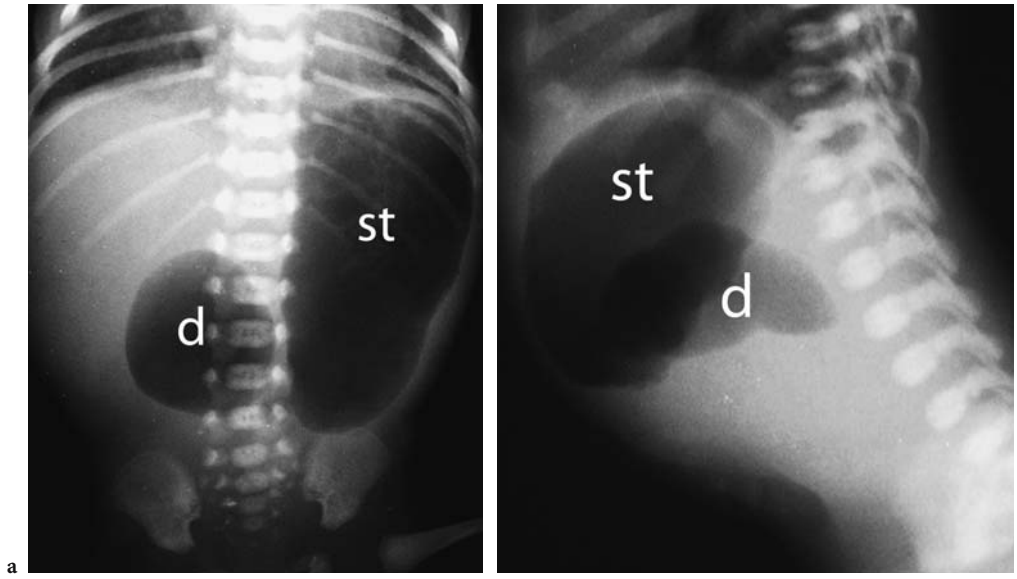

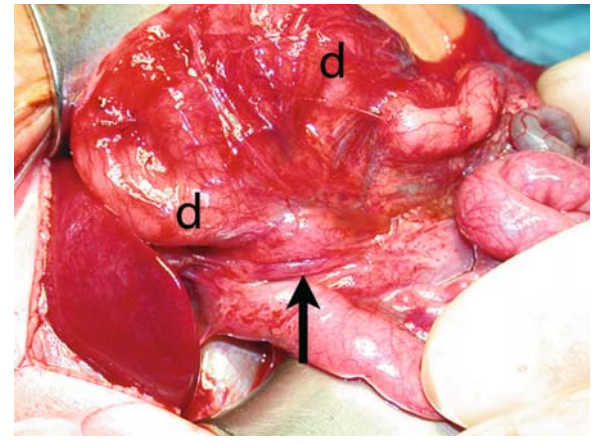

Fig. 1.5a–c. Annular pancreas. Supine (**a**) and lateral (**b**) views of the abdomen show complete obstruction at duodenal level identical to that seen in duodenal atresia. The stomach (*st*) and duodenal bulb (*d*) are distended and there is no distal air. **c** Surgical image shows the pancreatic tissue (*arrow*) encircling the duodenum (*d*)

duodenal atresia or annular pancreas (Fig. 1.6). Past the immediate postnatal period, any duodenal obstruction should be assumed to be midgut volvulus until proven otherwise (Buonomo 1997). It is the only condition mentioned above that may kill the patient.

Antenatal diagnosis of duodenal obstruction is based on sonographic demonstration of polyhydramnios in conjunction with a fluid-filled "double bubble" in the fetal abdomen corresponding to the double bubble sign seen on postpartum radiographs (Nelson et al. 1982). Since there is a high incidence of associated anomalies, identification of a double bubble sign should prompt consideration of fettle karyotyping and a careful search for other fetal anomalies (Hertzberg and Bowie 1990).

Partial duodenal obstruction may be produced by duodenal stenosis, duodenal web, Ladd´s bands, midgut volvulus, annular pancreas, preduodenal portal vein, and duplication cyst. Plain radiographs show gaseous distension of the stomach and duodenum with a normal or diminished quantity of air in the small bowel. Content studies may be necessary to differentiate between midgut volvulus and partial duodenal obstruction caused by a web or stenosis (Auringer and Sumner 1994). Sonography is helpful to rule out extraluminal causes such as a duplication cyst.

1.1.1.1.3 Malrotation and Midgut Volvulus

Malrotation is a general term that includes a wide spectrum of anomalies that occur when intestinal rotation and fixation happens in an abnormal way. Failure of completion of the normal intestinal rotation leads to a continuum of anatomic abnormalities with a common clinical denominator consisting of obstruction with the potential for midgut volvulus. Only its presentation as an abdominal emergency in the neonatal period is discussed here.

Malrotation results not only in the malposition of the bowel but also in the malfixation of the mesentery. When the duodenojejunal junction and the cecum, the normal points of fixation of the mesentery, are not in their usual location, the mesenteric attachment is shortened to a narrow pedicle. Because the entire length of the midgut is attached to this narrow pedicle, there is a tendency for the intestines to twist around the pedicle. This twisting of malfixed intestines around the short mesentery is named midgut volvulus (Fig. 1.7) (Millar et al. 2003; Torres and Ziegler 1993). With volvulus, the small bowel wraps around the axis of the superior mesenteric artery (SMA), resulting in a spiral that impairs blood supply. Twists of 720° and greater are often reported. Increasing degrees of volvulus will

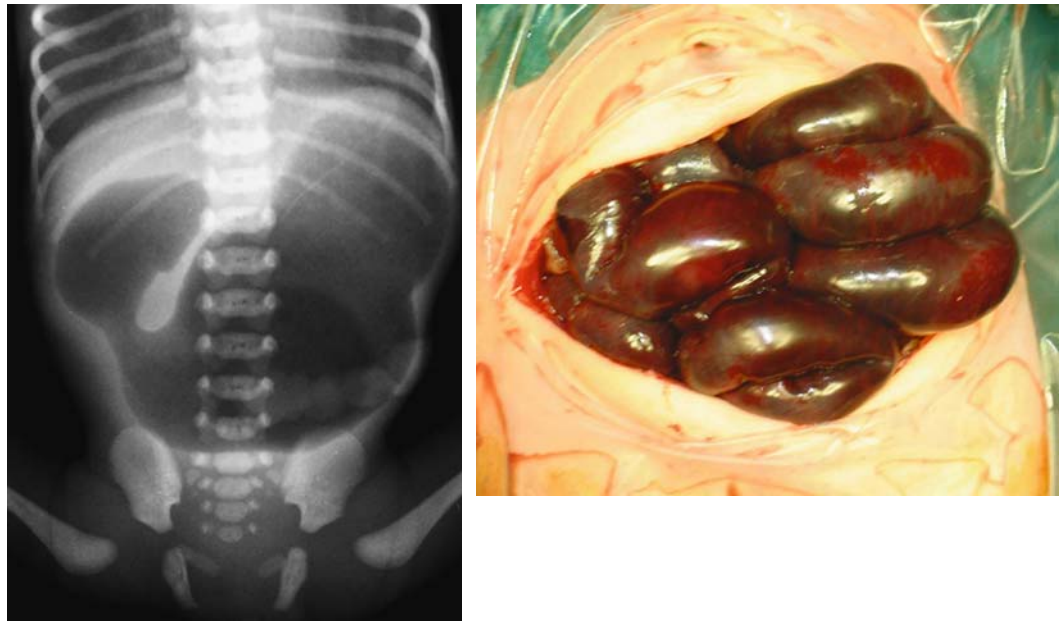

a b

Fig. 1.6a,b. Midgut volvulus. A 5-day-old neonate with severe vomiting. **a** Abdominal plain radiograph shows marked distension of the stomach and duodenal bulb and absence of air more distally. **b** Surgery demonstrated midgut volvulus with necrosis of the entire midgut

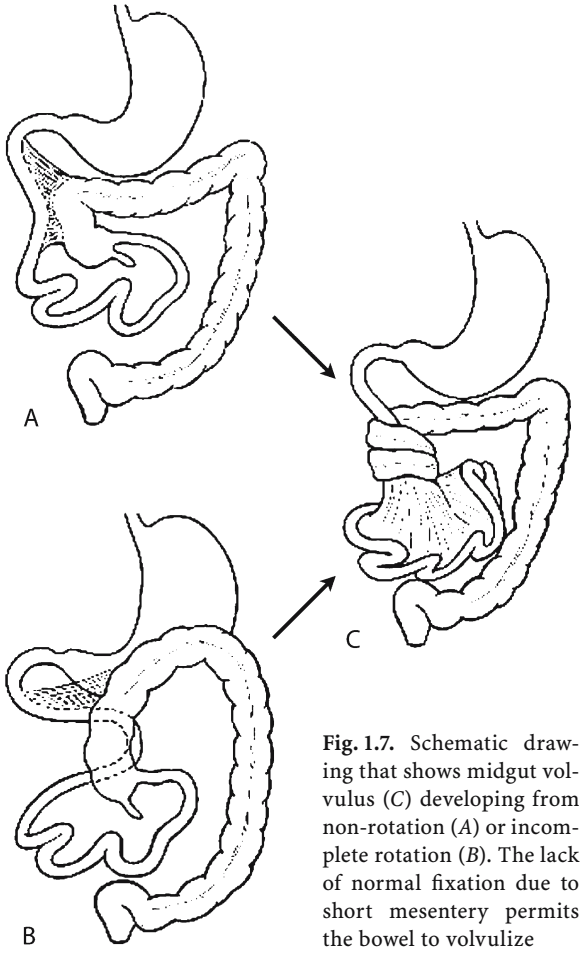

Fig. 1.7. Schematic drawing that shows midgut volvulus (*C*) developing from non-rotation (*A*) or incomplete rotation (*B*). The lack of normal fixation due to short mesentery permits the bowel to volvulize

obstruct the bowel lumen, but also the lymphatic drainage, the venous drainage, and eventually, the arterial supply. Obstruction of the vascular supply can be a life-threatening condition requiring immediate surgical intervention (Spigland et al. 1990; Pickhardt and Bhalla 2002).

A patient with malrotation may also develop dense peritoneal bands, termed Ladd´s bands, that originate in an attempt to fix the bowel. These bands extend from the cecum to the hilum of the liver, posterior peritoneum, or abdominal wall across the duodenum and can cause extrinsic duodenal obstruction.

Volvulus of the midgut may occur at any age but it is more common in the first month of life, most of them presenting in the first week of life (Torres and Ziegler 1993). In general, the symptoms are those of obstruction. The child with obstruction secondary to midgut volvulus typically presents with a sudden onset of bilious vomiting often preceded by initial toleration of feeding. The sudden onset of bilious emesis in a neonate who has been normal for the first few days of life should be considered to be due to a midgut volvulus until proven otherwise (Buonomo 1997). In the early stages, prior to the onset of ischemia, the abdomen is not distended. Patients presenting with shock have a worse prognosis. This manifests as abdominal distension with peritonitis, bloody stools, and hemodynamic comprise (Bonadio et al. 1991).

The imaging work-up begins with a plain radiograph. An anteroposterior supine view and either an upright view or cross-table lateral view should be obtained. In general, the abdominal plain radiograph shows evidence of obstruction, usually in the third portion of the duodenum but occasionally, higher or even lower. The stomach and proximal portion of the duodenum are dilated and some air is usually seen in the jejunum and ileum (Fig. 1.8). These cases are frequently identical in appearance to duodenal stenosis and other incomplete congenital duodenal obstructions. As already noted, complete duodenal obstruction with the double bubble sign may also be a presentation form, this pattern being indistinguishable from other causes of complete congenital duodenal obstruction. The abdominal radiograph may be normal if the obstruction is recent, intermittent, or incomplete, or may demonstrate a relative paucity of bowel air (Kassner and Kottmeier 1975; Frye et al. 1972). The significance of these findings must be recognized in the context of an infant with bilious vomiting, because they are much more alarming than multiple dilated loops of bowel, which denote a more distal obstruction from a cause other than midgut volvulus (Hernanz-Schulman 1999). A gasless abdomen associated with abdominal distension or tenderness may be a sign of strangulated midgut volvulus (Kassner and Kottmeier 1975). Diffuse gaseous distension of the bowel with a "low obstruction" pattern is uncommon and correlates with gangrenous bowel, perhaps because vascular occlusion interferes with resorption of air (Frye et al. 1972) (Fig. 1.9).

An upper gastrointestinal series is the preferred imaging modality for the radiologic diagnosis of a midgut volvulus and should be performed in all patients with bilious emesis, except in those with evidence of complete duodenal obstruction in the plain radiograph or in critically ill infants. A nonionic, water-soluble contrast medium is preferable, although barium can also be used. Ionic hypertonic solutions, such as gastrographin, are to be avoided

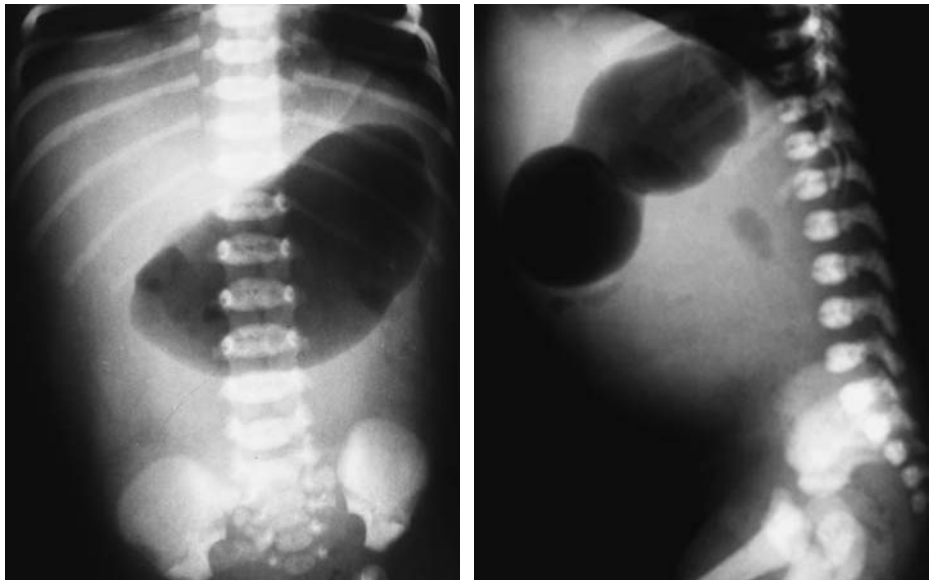

Fig. 1.8a,b. Midgut volvulus. Supine (**a**) and lateral (**b**) radiographs show distension of the stomach and duodenum with some distal intestinal air in a 12-day-old infant with severe vomiting

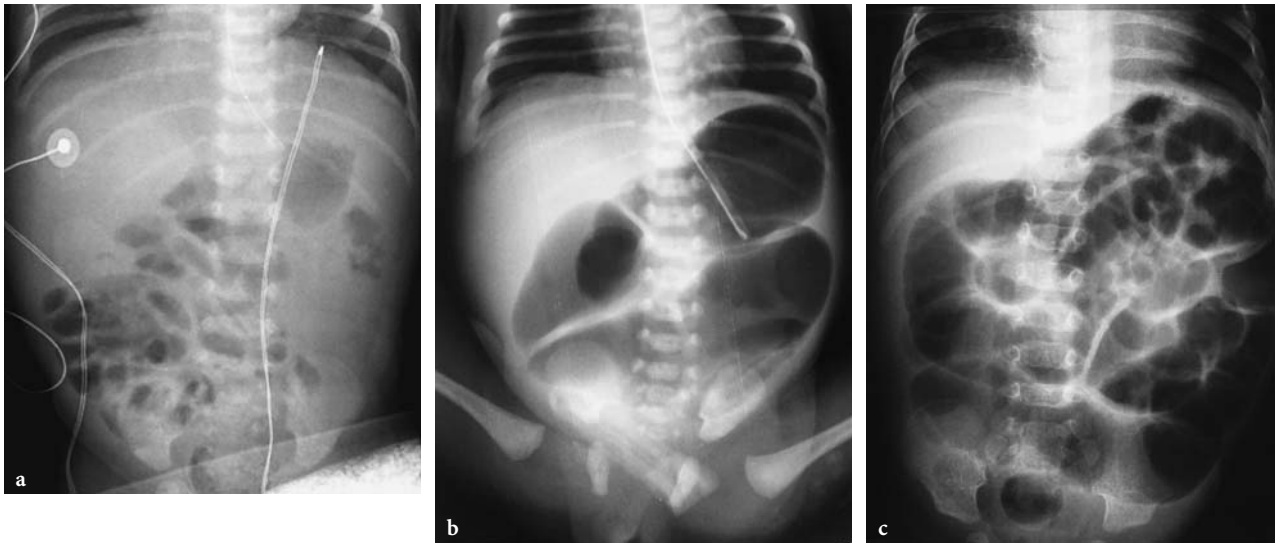

Fig. 1.9a–c. Different patterns of midgut volvulus in plain abdominal radiographs. **a** Normal air pattern in a neonate with bilious vomiting. **b** Another neonate patient with bilious vomiting. There are a few dilated bowel loops suggesting high intestinal obstruction. **c** Obstructed, distended gas pattern suggesting devitalized bowel probably due to venous obstruction and infarction

as aspiration causes pulmonary edema that may be fatal. The contrast medium may be administered orally or, even better, through a nasogastric tube to control the amount of contrast, because a contrast-filled, distended stomach may obscure the course and configuration of the duodenum. The pathognomonic finding of midgut volvulus in the upper gastrointestinal examination is a spiral or "corkscrew appearance" of the twisted distal duodenum and jejunum that are located in the middle of the abdomen (Strouse 2004; Long et al. 1996) (Fig. 1.10). The bowel lumen is narrowed and the duodenum

proximal to the obstruction may be mildly dilated. The contrast pass from the stomach to the duodenum and jejunum showing the characteristic corkscrew course both in the anteroposterior and lateral views. In the lateral view the distal duodenum will exhibit a characteristic anterior course (Fig. 1.10) (Koplewitz and Daneman 1999). When there is complete obstruction, the contrast medium cannot enter the volvulized loops to show the "corkscrew" and only the entrance to the volvulus is identified, with a tapered or "beaked" appearance (Fig. 1.11). In cases of recent complete obstruction, distal air may be seen; however, the contrast cannot enter the volvulized segment, so the corkscrew image cannot be seen. Once the findings of volvulus are confirmed, no further imaging studies are necessary. Surgical intervention is mandatory immediately following the diagnosis.

Obstruction due to Ladd´s bands produces a Z-shaped configuration, outlining the lack of normal rotation and fixation of the duodenum. The Z-configuration may appear similar to the "corkscrew" of volvulus, but it does not indicate volvulus itself (Fig. 1.12). It must be stressed, however, that in most children with malrotation obstruction is caused by the volvulus with the band playing a lesser role or no roll at all (Ford et al. 1992; Torres and Ziegler 1993).

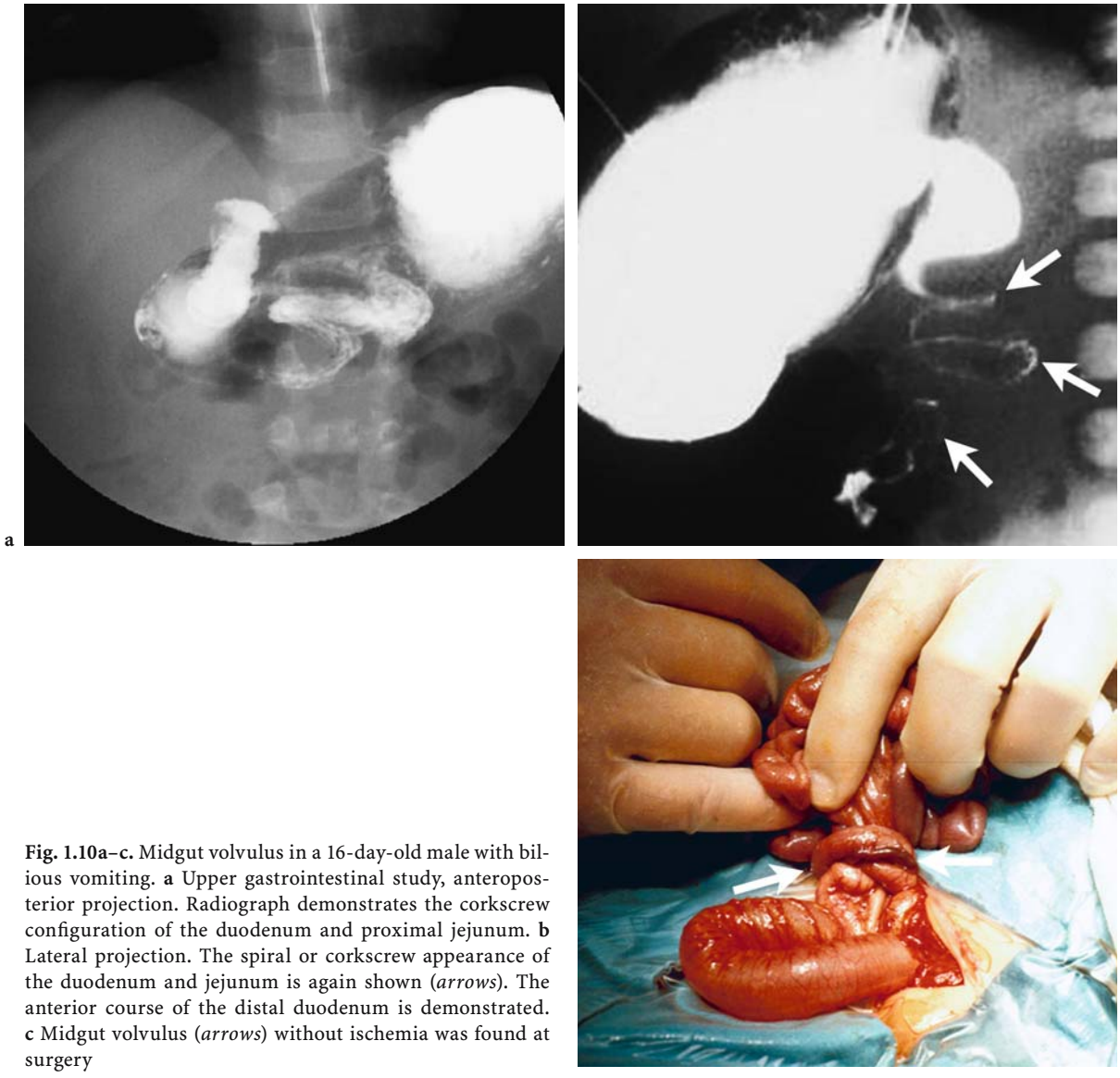

Fig. 1.10a–c. Midgut volvulus in a 16-day-old male with bilious vomiting. **a** Upper gastrointestinal study, anteroposterior projection. Radiograph demonstrates the corkscrew configuration of the duodenum and proximal jejunum. **b** Lateral projection. The spiral or corkscrew appearance of the duodenum and jejunum is again shown (*arrows*). The anterior course of the distal duodenum is demonstrated. **c** Midgut volvulus (*arrows*) without ischemia was found at surgery

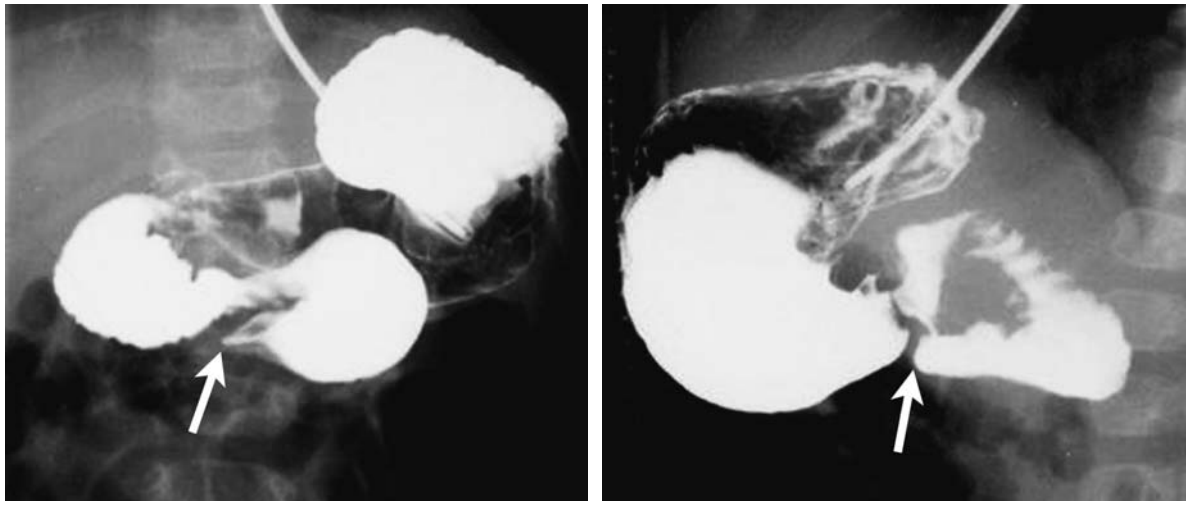

a b

Fig. 1.11a,b. Midgut volvulus in a 7-day-old girl with bilious vomiting. Upper gastrointestinal series. Anteroposterior (**a**) and lateral projections (**b**). The distal duodenum courses anteriorly and tapers to a "beaked" obstruction (*arrow*). No contrast is observed beyond the obstruction, but there is distal air indicating a recent complete obstruction

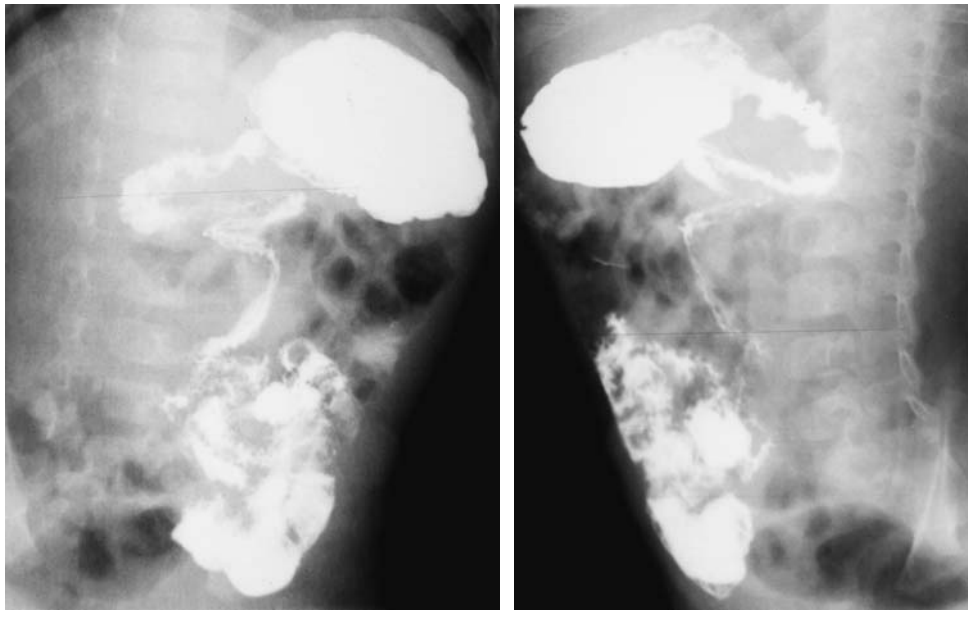

a b

Fig. 1.12a,b. Malrotation with z-shape of the duodenum and jejunum. Upper gastrointestinal series. Anteroposterior (**a**) and lateral (**b**) projections show a central, downward, Z course of the duodenum. No volvulus was found at surgery. Surgery demonstrated the partial obstruction to be produced by Ladd´s bands

Currently, a contrast enema has fallen out of favor for the diagnosis of malrotation and its main complication is that the cecum can be normal in up to 20%–30% of infants with malrotation and, therefore, a normal cecum does not exclude malrotation (Slovis et al. 1980). On the other hand, approximately 15% of patients with normal rotation have a mobile cecum that could be misinterpreted as malfixation (Beasley and De Campo 1987). Nevertheless, demonstration of an unequivocally abnormal cecal position in the setting of an equivocal upper gastrointestinal series may be helpful (Strouse 2004).

Ultrasound may also be a useful tool in the early detection of midgut volvulus because of its availabil-

ity, relative lack of need for preparation, and lack of ionizing radiation. In fact, several authors currently recommend routine US examination before performing a gastrointestinal series in any patient with bilious vomiting if surgery is going to be delayed, for several reasons: (1) It can be performed at the bedside. (2) It provides information about the outside part of the bowel loops and the abdominal cavity not provided by the contrast examination. (3) In complete obstruction, it provides information about the intestinal loops beyond the obstruction (Babcock 2002; Weinberger et al. 1992).

The characteristic finding of midgut volvulus in the US examination is the "whirlpool" sign produced by the twisting of the bowel, mesentery, and superior mesenteric vein around the axis of the superior mesenteric artery (Fig. 1.13). The whirlpool sign, proposed by Pracros et al. (1992), directly indicates the anatomic alteration caused by midgut volvulus. The SMV and tributaries wrap around the SMA as a result of the volvulus, resulting in a partial or complete blockage of the blood supply to the midgut. The whirlpool sign represents this characteristic pattern of the SMV and SMA on sonograms (Chao et al. 2000; Pracros et al. 1992; Shimanuki et al. 1996). Color Doppler reveals a circle of vascularity representing the superior mesenteric vein twisting around the superior mesenteric artery (Patino et al. 2004). Other described findings such as dilated thick-walled bowel loops, mainly to the right of the spine, increased peritoneal fluid, a dilated duodenum, a truncated SMA, and a solitary hyperdynamic pulsating SMA, are also useful findings in a proper clinical setting but are non-specific (Sze et al. 2002; Smet et al. 1991; Chao et al 2000).

1.1.1.1.4 High Small Bowel Obstruction

High small bowel obstruction includes atresia or stenosis of the jejunum or proximal ileum. It is now generally accepted that intestinal atresia and ste-

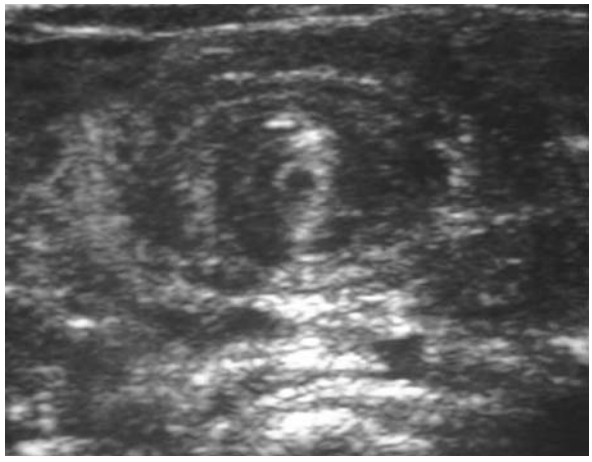

a

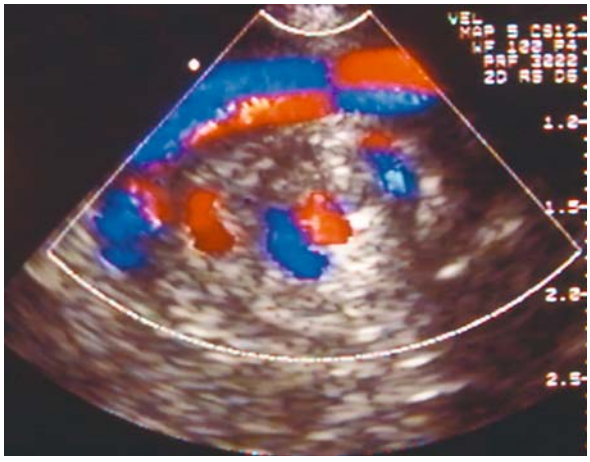

b

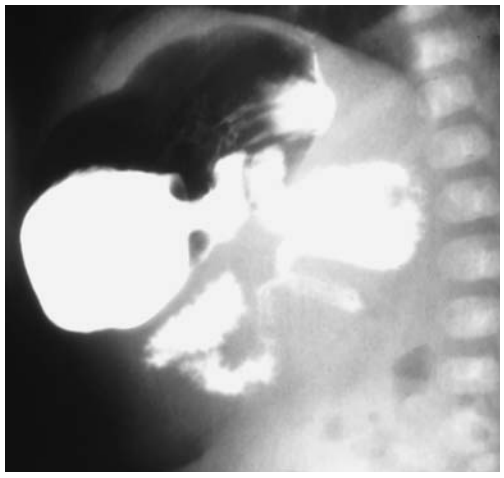

c

Fig. 1.13a–c. "Whirpool" sign of midgut volvulus. A 12-day-old female with bilious vomiting. **a** Transverse B-mode sonography of the upper abdomen shows the twisting of bowel, mesentery, and superior mesenteric vein around the axis of the superior mesenteric artery. **b** Color Doppler image demonstrates a circle of vascularity that represents the superior mesenteric vein twisting around the superior mesenteric artery, producing the characteristic "Whirlpool sign". **c** Upper gastrointestinal series confirms midgut volvulus

nosis below the duodenum are caused by an intra-abdominal vascular accident during intrauterine life. The vascular accident may be primary or secondary to a mechanical obstruction, as in the case of in utero volvulus. This results not merely in a hindrance of growth, but also in an actual disappearance of the affected portion of the fetal bowel (Powell and Raffensperger 1982). Jejunoileal atresias are classified into four types based on their anatomic appearance (Touloukian 1993). Type I is a simple intraluminal diaphragm, and accounts for 32% of jejunal atresias. In type II, the proximal bowel terminates in a blind end and the distal bowel commences similarly, the two ends being joined by a fibrous band. In type III, the proximal and distal blind ends are completely separated with no connecting band. The adjoining mesentery always has a V-shaped defect corresponding to the missing segment. The familial form of multiple atresias is considered type IV. A rare form of inherited jejunal atresia is the "apple-peel mesentery", also called the "Christmas-tree mesentery." This abnormality is the result of a catastrophic in utero vascular accident, producing an interruption of the distal superior mesenteric artery that leads to atresia of a large segment of small bowel and mesentery. The proximal segment is dilated, whereas the collapsed distal segment is spiraled around its vascular supply and resembles an apple peel. The blood supply is retrograde through the anastomotic arcade of the inferior mesenteric artery (Leonidas et al. 1978; Manning et al. 1989). This defect has historically been associated with high mortality, although recent reports suggest an improved prognosis (Waldhausen and Sawin 1997).

Jejunal atresias comprise approximately 50% of small bowel atresias, and in 10% of the cases, there are multiple areas of atresia (De Lorimier et al. 1969). Jejunal atresia is clinically characterized by bilious vomiting, frequently delayed until after the first feeding, and abdominal distension. The lower the obstructive lesion in the small bowel, the more severe the abdominal distension, and the more difficult the accurate localization of the site of obstruction is (Godbole and Stringer 2002).

The diagnosis is usually apparent on the plain films. The abdominal radiograph shows a few dilated bowel loops (three or four air bubbles), more than in the case of duodenal atresia and fewer than in ileal atresia or in other causes of low bowel obstruction (Fig. 1.14). The loop just proximal to the site of the atresia is frequently disproportionately dilated with a bulbous end. There is no air in the lower portion of the abdomen; this is observed most clearly in the upright film (Rathaus and Grunebaum 1992) (Fig. 1.15). The colon cannot be identified and air

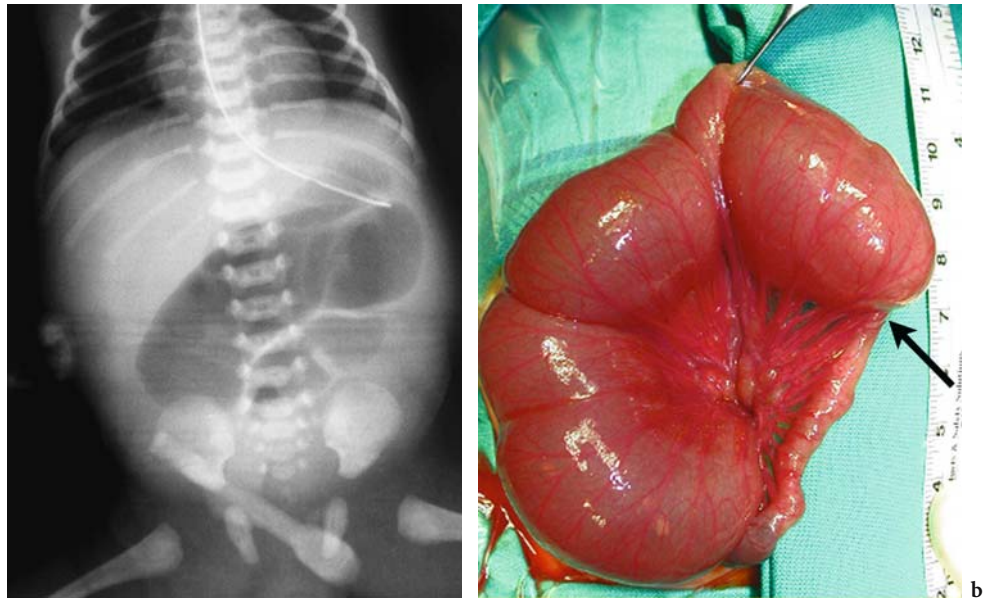

a b

Fig. 1.14a,b. Jejunal atresia. **a** Supine radiograph shows a few dilated, air-filled intestinal loops, about four "bubbles", which indicates a high obstruction. **b** Surgical image demonstrates the location of the atresia (*arrow*), the dilated proximal jejunum, and the small caliber of the bowel distal to the atresia

is not found in the rectum. These signs indicate an obstructive lesion in the small intestine, and surgery is mandatory. Here, also when the obstruction can be definitely identified in the small intestine, there is no need to delay surgery to give contrast material orally. An upper gastrointestinal series is clearly not indicated. In fact, flocculation and dispersion of the contrast given orally may occur, due to the high mucus content of the distended segment, and little information is obtained. Occasionally, the dilated bowel loops may be fluid-filled giving an airless abdomen. In cases of doubt, aspiration and insufflation of air through a nasogastric tube should be carried out (Fig. 1.16).

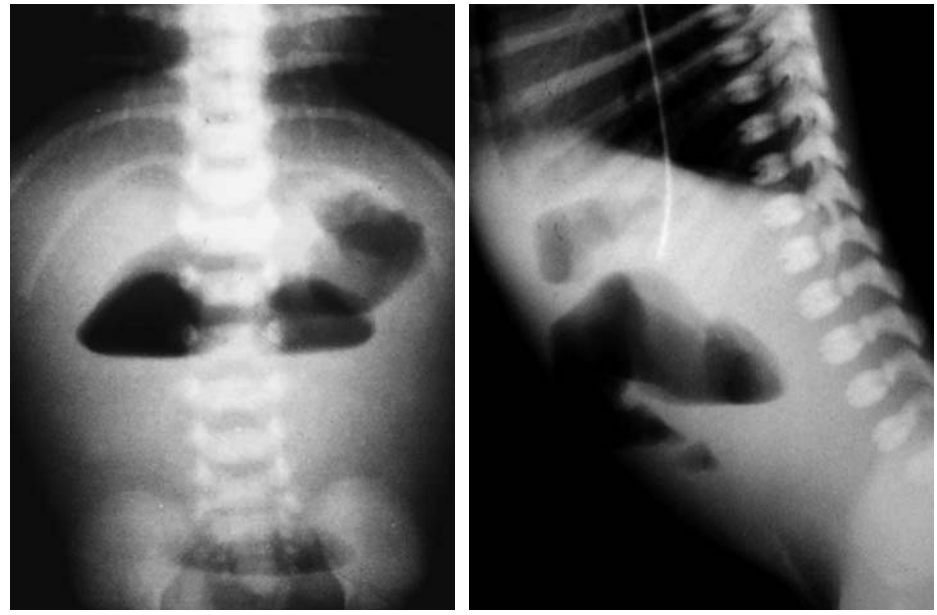

Fig. 1.15a,b. Jejunal atresia. Anteroposterior (**a**) and lateral (**b**) upright radiographs show a few central air-fluid levels indicating high obstruction

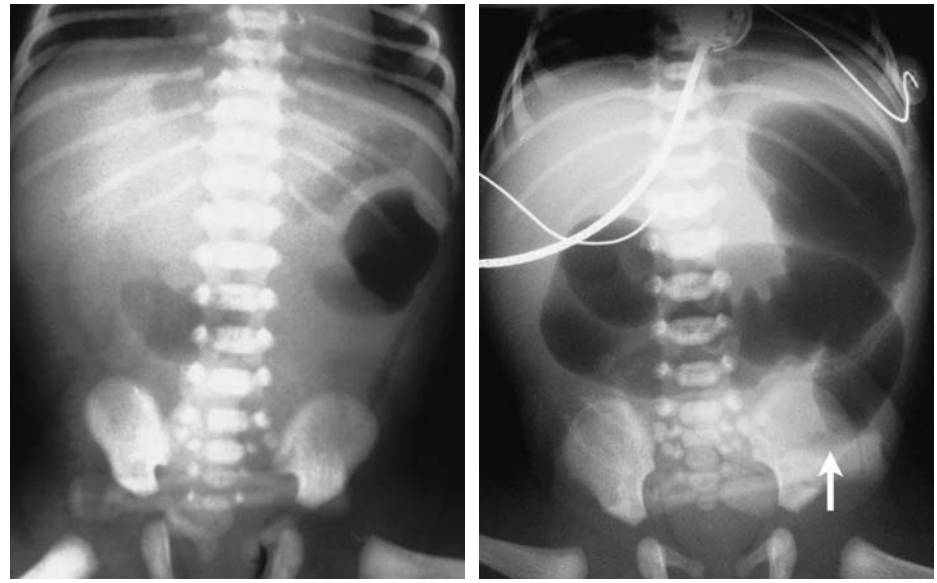

Fig. 1.16a,b. Jejunal atresia. **a** Supine radiograph shows an airless abdomen. **b** Aspiration and insufflation of air through a nasogastric tube was performed and adequately demonstrates the point of obstruction (*arrow*). Massively dilated loops of jejunum but only about three "bubbles" give indication of a high obstruction

Although a patient with jejunal or proximal ileal atresia usually needs no further radiologic investigation, contrast material enema examinations are commonly performed to attempt to exclude second and third areas of atresia lower in the bowel. The colon in isolated jejunal and proximal ileal atresia, as in duodenal atresia, is normal or near normal in size. If a microcolon is encountered, additional distal atresia should be suspected (Hernanz-Schulman 1999). A contrast enema is especially indicated when the scout radiograph shows distension of the flanks and elevation of the diaphragms indicating the presence of multiple dilated loops of the bowel filled with fluid distal to the obstruction. If the ischemic event that produced the atresia caused a perforation, there may be evidence of meconium peritonitis with peritoneal calcification. The apple peel type of atresia does not have distinctive findings on plain film (Fig. 1.17).

Sonography has a role in high intestinal obstruction, especially in patients with lack of air in the gastrointestinal tract whenever marked distension of the flanks and elevation of the diaphragms is observed on the plain radiograph. In such cases, sonography is useful to differentiate the presence of multiple dilated loops filled with fluid from ascites (Fig. 1.18). It is also useful in demonstrating associated anomalies in the abdominal organs (Hayden 1991; Jouppila and Kirkinen 1984).

Severe congenital stenosis of the small bowel is usually accompanied by vomiting and abdominal distension, identical in severity to that seen in atresia. In less severe cases, these symptoms may be mild or even delayed for several days or weeks. Plain abdominal radiographs reveal dilatation of bowel loops proximal to the stenosis and normal or decreased quantity of air in the small bowel distal to the stenosis (McAlister et al. 1996).

1.1.1.2 Low Obstruction

Low intestinal obstruction is defined as one occurring in the distal ileum or colon. The symptoms are vomiting, abdominal distension, and failure to pass meconium.

For practical purposes, the differential diagnosis of low intestinal obstruction in the neonate consists of five conditions. Two conditions involve the distal ileum and include ileal atresia and meconium ileus, and three involve the colon, which are colonic atresia, Hirschsprung´s disease, and functional immaturity of the colon that includes meconium plug

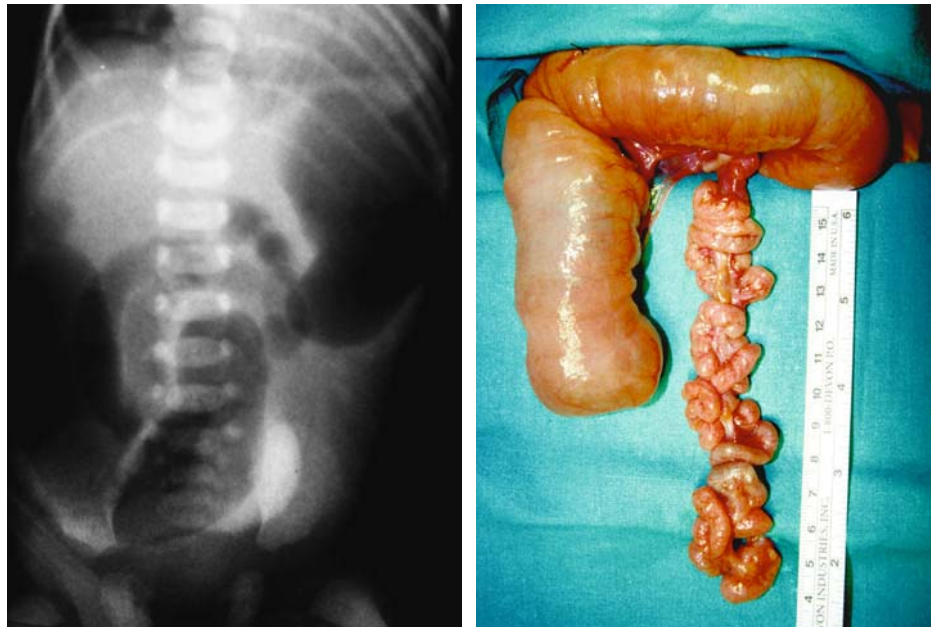

a b

Fig. 1.17a,b. "Apple peel" mesentery. **a** Plain radiograph showing dilated proximal loops suggesting high obstruction. **b** Surgical specimen shows the dilated proximal segment and the collapsed distal segment, which is spiraled around its vascular supply and resembles an "apple peel". The mesentery is short

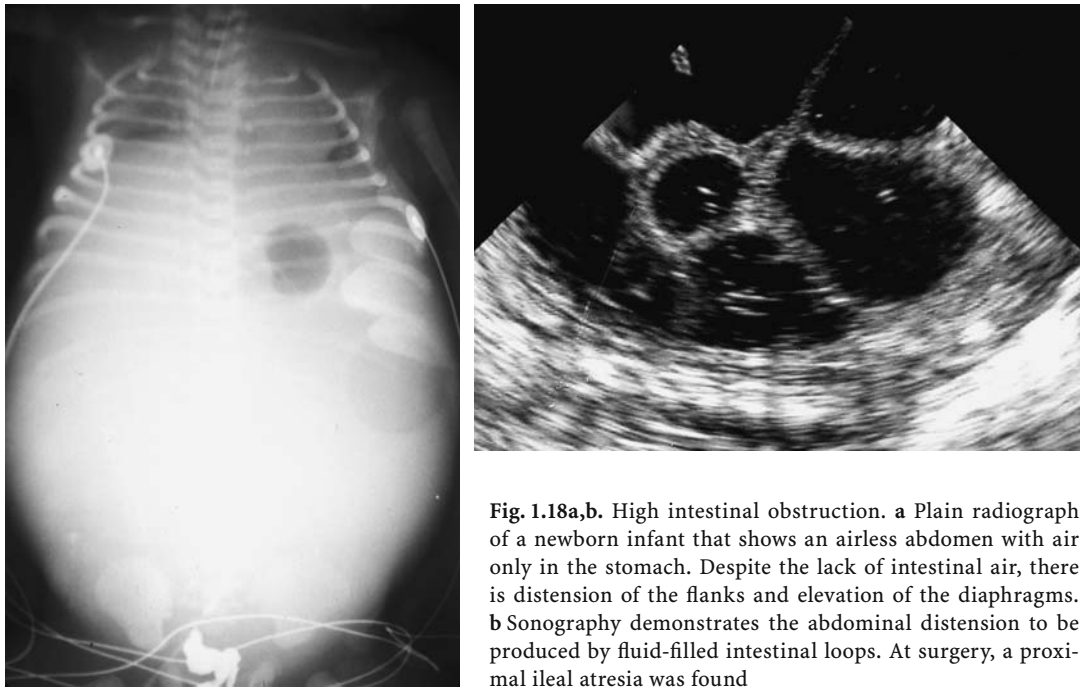

a b

Fig. 1.18a,b. High intestinal obstruction. **a** Plain radiograph of a newborn infant that shows an airless abdomen with air only in the stomach. Despite the lack of intestinal air, there is distension of the flanks and elevation of the diaphragms. **b** Sonography demonstrates the abdominal distension to be produced by fluid-filled intestinal loops. At surgery, a proximal ileal atresia was found

syndrome and small left colon syndrome. Anorectal malformations are also an important cause of low intestinal obstruction, but are almost always evident on physical examination.

A low obstruction is usually obvious on the plain film. Plain radiographs in low obstructions are characteristic, always showing multiple dilated air-filled bowel loops, with air-fluid levels in the upright or horizontal beam radiographs. Whether or not a low obstruction is at the level of the distal ileum or at the level of the colon and, in this case, in what part of the colon, is usually impossible to determine from the plain film. The dilated loops occupy the entire abdominal cavity, and the small and large bowel cannot be distinguished from each other. This distinction can be readily made with a contrast enema. Virtually all neonates with evidence of low obstruction require a contrast enema. The critical differential diagnostic finding on the contrast enema of a newborn with low obstruction is the presence or absence of a microcolon. The term microcolon is synonymous with unused colon. The colon in low intestinal obstruction is small, owing to a lack of use rather than anatomic or functional abnormality (Berdon et al. 1968). The caliber of the colon depends on the passage of intestinal fluid and desquamate mucosal cells from the jejunum and proximal ileum. These small intestinal contents are termed succus entericus. If little or no succus entericus reaches the colon, it is tiny. In low intestinal obstructions, the fetal colon does not receive sufficient contents from the small intestinal to assume its normal caliber, and, therefore, at birth the colon is usually of very small caliber, generally less than 1 cm, and nondistensible. Proximal obstructions such as duodenal or jejunal atresias maintain normal colonic caliber by virtue of passage of succus entericus produced by the remaining small bowel distal to the atresia (Hernanz-Schulman 1999). Normally, meconium reaches the cecum in the fourth month of intrauterine life and is in the rectum by the fifth month. The development of obstruction at an early period will consequently prevent the passage of meconium into the colon, leaving this structure collapsed and narrowed, although potentially distensible. In cases of distal small bowel obstruction of relatively recent onset, the colon has had time to attain a normal caliber, and therefore a microcolon is not present. Thus, the presence of a microcolon is diagnostic of a long-standing distal small bowel obstruction, but a normal colon does not exclude this condition in all cases (Dalla Vecchia et al. 1998). The degree of microcolon in complete obstruction is variable, presumably due to the variable amount of meconium formed by internal secretions below the obstruction. The choice of contrast medium varies among different medical centers. We currently use a low osmolar water-soluble contrast medium.

1.1.1.2.1 Distal Small Bowel Obstruction

Ileal atresia is an important cause for low intestinal obstruction. It represents approximately 50% of small bowel atresias and the etiology is similar to that of jejunal atresia. As jejunal atresias, they are believed to result from an intrauterine vascular injury. Approximately 25% have a history of polyhydramnios (Sweeney et al. 2001).

Plain film shows numerous dilated loops of bowel occupying the entire abdominal cavity, including the pelvic portion, and multiple air-fluid levels in upright film (Fig. 1.19). With this degree of distension the mucosal pattern of the small bowel is effaced and it is impossible to differentiate the small bowel from the colon (Winters et al. 1992). Examination of the colon is then warranted to disclose the presence or absence of a colonic lesion. In ileal atresia, the colon is normally placed but has an abnormally small caliber, the so-called functional microcolon typical of distal small bowel obstruction (Dalla Vecchia et al. 1998) (Fig. 1.19d,e). The presence of pneumoperitoneum indicates that perforation has occurred and a colon examination is contraindicated. Intraperitoneal calcifications, indicative of meconium peritonitis, are not uncommon in ileal atresia.

Meconium ileus is a low intestinal obstruction produced by impaction of abnormal meconium in the distal ileum. It almost always occurs in patients with cystic fibrosis, in which a deficiency of pancreatic enzymes causes the meconium to become abnormally viscous and thick. The effects on the gastrointestinal tract range from temporary meconium retention with delayed but spontaneous evacuation of the meconium, to complete obstruction. When obstruction occurs, the distal ileum is narrowed and contains concretions of grey inspissated meconium pellets (Garza-Cox et al. 2004). Proximal to this the ileum is grossly distended by thick, tenacious, chewing-gum-like meconium due to the viscid, abnormal mucus. Meconium ileus is the earliest manifestation of cystic fibrosis and occurs in 10%–15% of patients. A family history is often elicited. Symptoms usually commence on the first day of life and consist of bile-stained vomiting and abdominal distension. The abdomen may have a doughy feel and it is sometimes possible to indent the bowel contents on pressure. The diagnosis may be confirmed by finding an increased concentration of sodium chloride in the sweat (Burge and Drewett 2004).

Meconium ileus can be complicated or uncomplicated. The plain radiograph in uncomplicated meconium ileus usually demonstrates low obstruction. The abdomen is filled with air-distended loops, and occasionally there is a relative absence of air-fluid levels (Fig. 1.20). In general, patients with meconium ileus have fewer air-fluid levels than patients with small bowel atresias. The sticky, viscid meconium prevents rapid movement of air shadows during changes of posture so that fluid levels do not easily develop. Sometimes, a mixture of air and meconium may be visualized as coarse, granular, ground-glass shadows, giving rise to a "soap bubble" appearance similar to the fecal pattern of the colon in older patients. However, a similar faucial pattern may also be seen in ileal atresia and aganglionosis of the terminal ileum, so these findings are not of much use in the differential diagnosis of low obstruction (Leonidas 1976). On ultrasound, abnormal intestinal contents are hyperechogenic and thick, which is clearly different from that of the ileal atresia, where the bowel is filled with hypoechoic fluid and air (Barki and Bar-Ziv 1985; Sigalas et al. 2003) (Fig. 1.21).

Contrast enema classically demonstrates a microcolon, and multiple small filling defects consisting of meconium pellets may be seen within the microcolon and in the collapsed distal ileum, with dilated small bowel proximal to the obstruction (Fig. 1.22). These findings are diagnostic of meconium ileus. The type of contrast to be used in this examination should be considered carefully, especially given the fact that the etiology of the distal obstruction is not known prior to this examination. Barium is not ideal in patients with meconium ileus and impacted meconium pellets. It is preferable to begin the enema examination with a water-soluble contrast medium. Low osmolar, non-ionic water-soluble agents are the best choice to avoid large fluid shifts into the bowel. These agents are expensive, so a relatively dilute isosmolar ionic water-soluble contrast medium may also be acceptable. Once the diagnosis is made, these patients should undergo a therapeutic enema to help the passage of the sticky meconium and so relieve the obstruction avoiding surgery. The choice of contrast media is controversial, but a hyperosmolar agent such as Gastrografin continues to be used by many radiologists (Burke et al. 2002). Gastrografin is meglumine diatrizoate; a water-soluble, radiopaque solution containing 0.1% polysorbate 80 (Tween 80) and 37% organically bound iodine. The solution's osmolarity is 1900 Osm/L. This very hyperosmolar agent decreases the tenacity of the

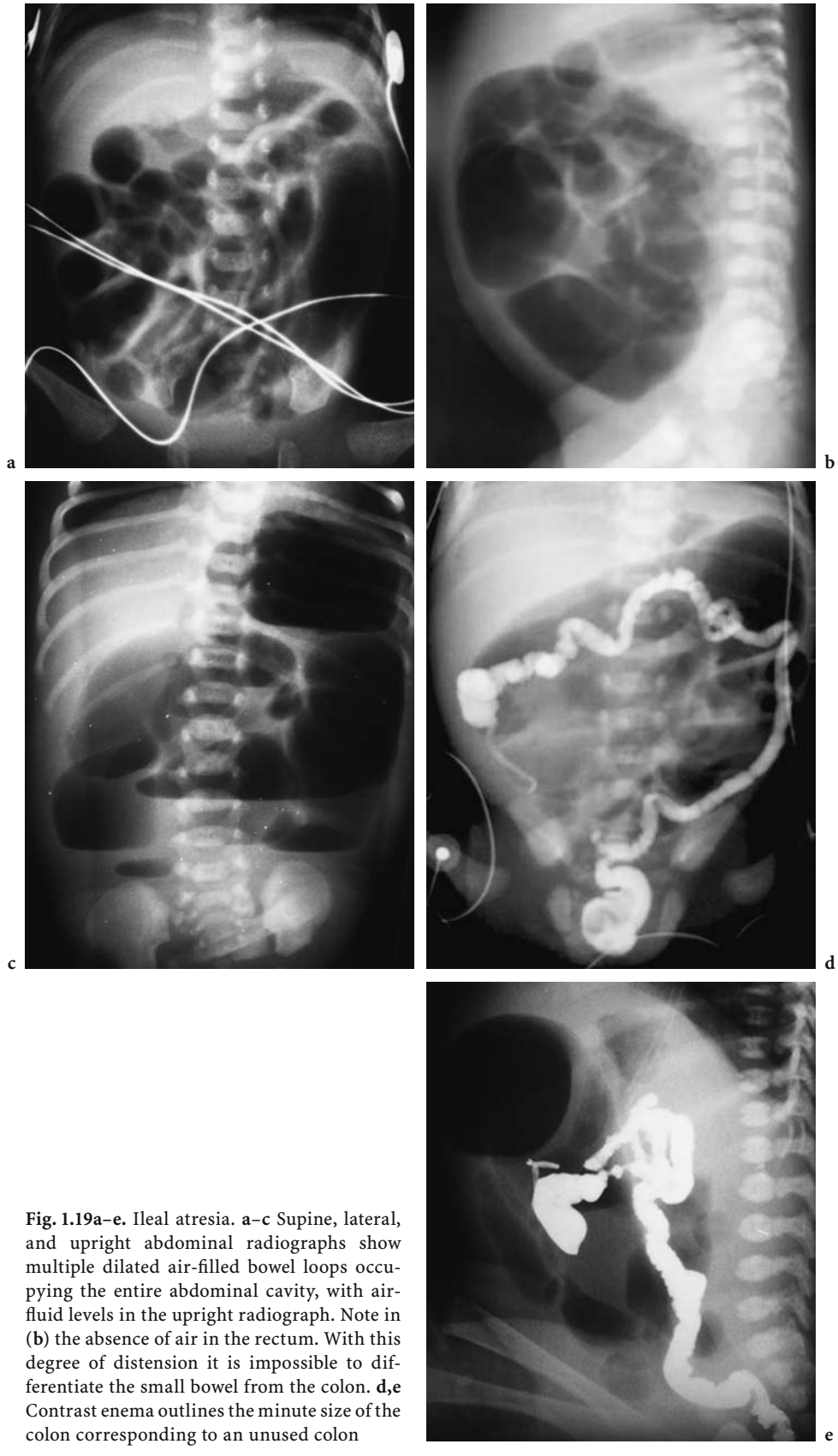

Fig. 1.19a–e. Ileal atresia. **a–c** Supine, lateral, and upright abdominal radiographs show multiple dilated air-filled bowel loops occupying the entire abdominal cavity, with air-fluid levels in the upright radiograph. Note in (**b**) the absence of air in the rectum. With this degree of distension it is impossible to differentiate the small bowel from the colon. **d,e** Contrast enema outlines the minute size of the colon corresponding to an unused colon

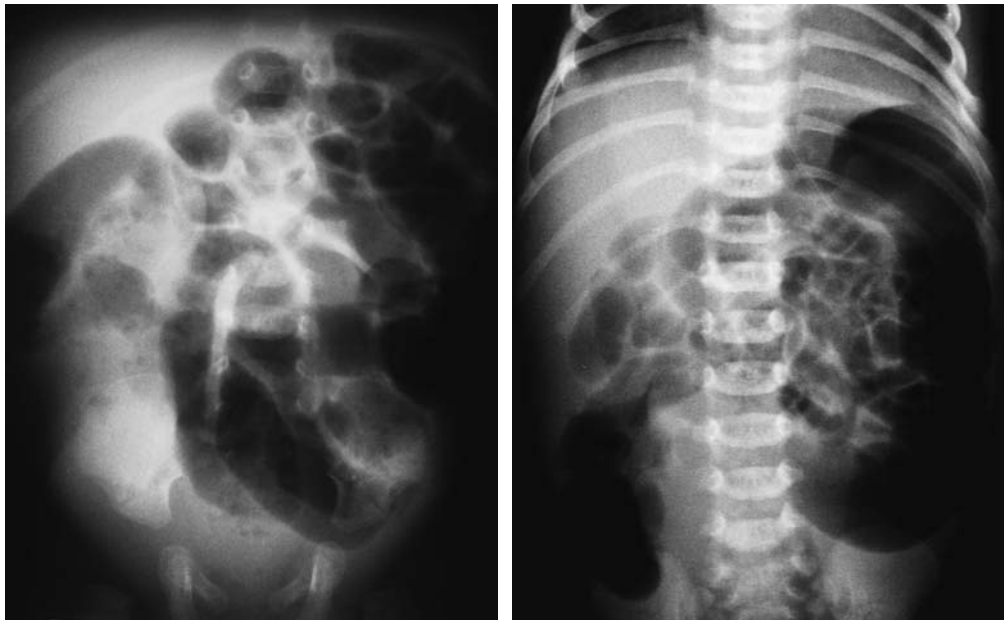

a b

Fig. 1.20a,b. Meconium ileus. **a** Supine plain radiograph shows marked bowel distension with suggestive evidence of mottled air and feces in ascending colon and terminal ileum. **b** Upright film shows absence of well-defined air-fluid levels

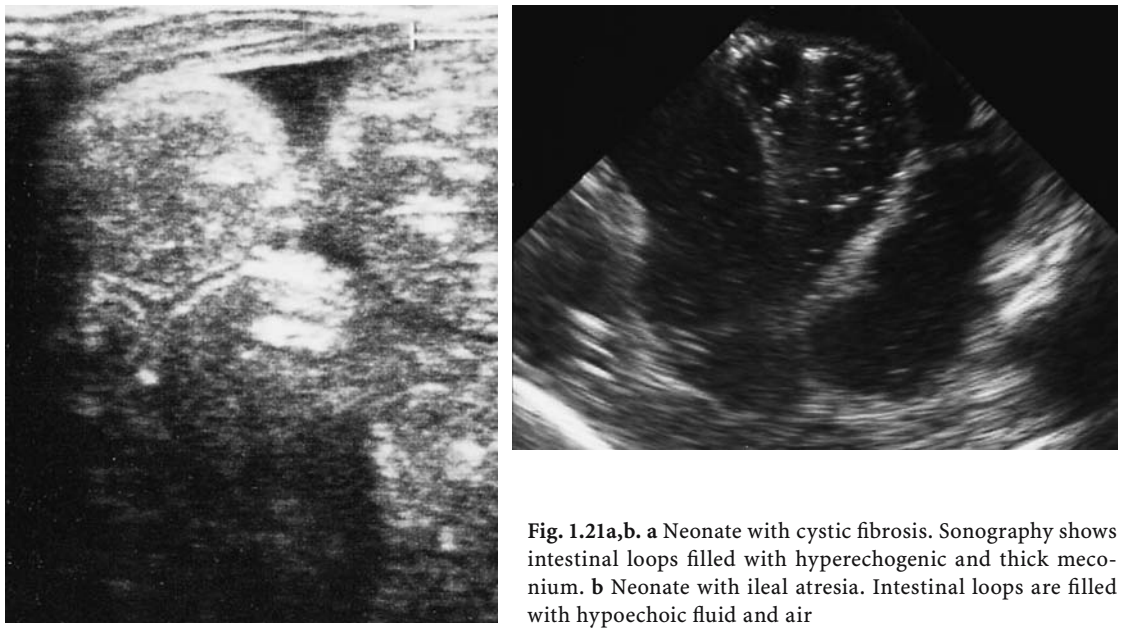

a b

Fig. 1.21a,b. a Neonate with cystic fibrosis. Sonography shows intestinal loops filled with hyperechogenic and thick meconium. **b** Neonate with ileal atresia. Intestinal loops are filled with hypoechoic fluid and air

meconium by drawing water into the bowel lumen. Before proceeding with this therapy, the infant must show signs of uncomplicated meconium ileus and no clinical or radiologic evidence of complicating factors (e.g., volvulus, gangrene, perforation, peritonitis). Under fluoroscopic control, a 25%–50% solution of Gastrografin should be infused slowly at low hydrostatic pressure through a catheter inserted into the rectum. Balloon inflation must be avoided to minimize the risk of rectal perforation.

An expert group convened by the Cystic Fibrosis Foundation Consensus Conference found no scientific evidence that Gastrografin was superior to other low osmolar water-soluble contrast media in the

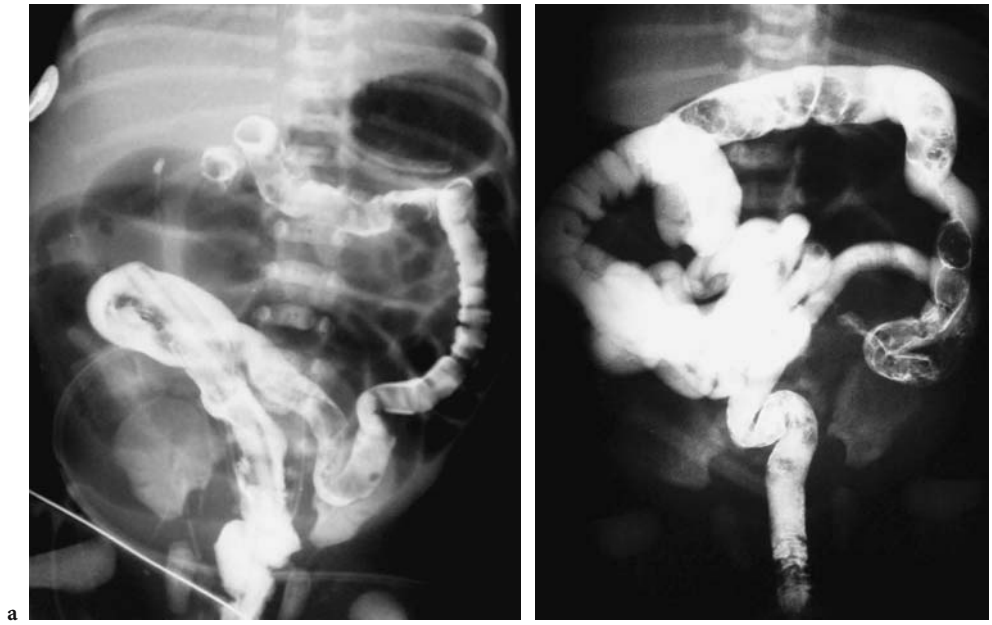

Fig. 1.22a,b. Meconium ileus. **a** Water-soluble contrast enema showing a microcolon with scattered filling defects that correspond to inspissated meconium. **b** The enema was continued with reflux of the contrast medium into the terminal ileum, showing filling defects that represent meconium pellets. The patient was discharged within 48 h of successful treatment

treatment of meconium ileus. As Gastrografin may cause hypotension or circulatory collapse in newborn infants, many radiologists currently favor the use of low osmolar agents in these infants. In any case, the flow of the contrast through the thick meconium is slow, and usually several enemas are required. Efforts must be taken to reflux contrast into the ileum and if possible back into the dilated proximal bowel (Fig. 1.23). Care should be taken that the patient is well hydrated because of fluid shifts. The patient's electrolyte balance must be attended to before, during, and after each enema (Kao and Franken 1995).

Meconium ileus may be complicated by volvulus of a distal intestinal loop, perforation, or atresia. All patients with complicated meconium ileus require surgical intervention (Fig. 1.23), therefore radiographs need to be read carefully for the presence of calcification or pneumoperitoneum which indicates in utero perforation and the need for surgical intervention without further imaging (Rescorla and Grosfeld 1993).

Meconium peritonitis is a condition that is the result of in utero perforation of the fetal gastrointestinal tract during the last 6 months of pregnancy. Sterile meconium escapes through the perforation into the peritoneal cavity producing a marked reaction with dense adhesions, which usually calcify rapidly, in some cases as early as 24 h after it leaves the intestinal lumen. Yellow-green nodules form on the bowel wall and the perforation may be sealed off so well that at birth there may not be any macroscopic evidence of the leak. However, if the perforation is still present after birth and meconium still escapes into the peritoneal cavity, secondary septic peritonitis will develop. Very often a pseudocyst is formed by adjacent loops of the intestine, which tend to wall off the perforation. The wall of this pseudocyst is lined by a thick plaque of greenish-yellow material with areas of calcification (Reynolds et al. 2000) (Fig. 1.24). The intrauterine perforation may be due to any obstructing lesion such as atresia, meconium ileus, volvulus, Meckel´s diverticulum, internal hernia, or bands. In such cases the causative lesion will be found at laparotomy. Frequently, however, no obvious cause for the perforation can be found. Such idiopathic perforations may be produced by localized areas of intestinal infarction due to minute emboli from the placenta (Eckoldt et al. 2003).

The diagnosis is usually obvious on the plain radiographs of the abdomen and is characterized by linear or punctate calcifications over the serosal surfaces of the abdominal viscera. The calcification may consist of a few irregular scattered areas or may be more extensive, consisting of continuous

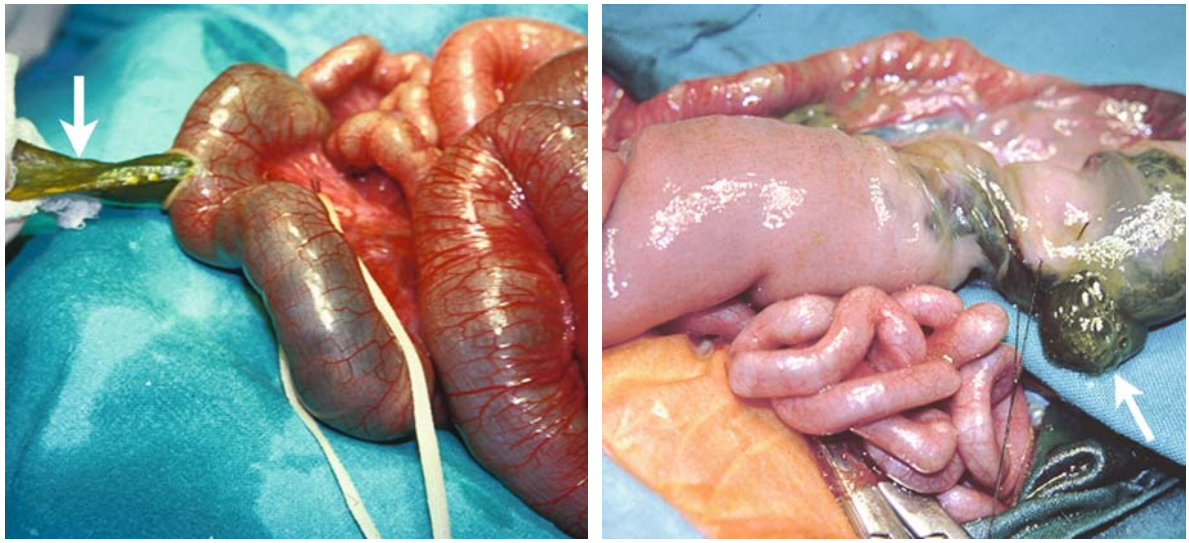

a b

Fig. 1.23a,b. Meconium ileus. **a,b** Intraoperative views illustrating the tenacious nature of the meconium impacted within the distal small bowel loops (*arrows*) in a patient in which contrast enema failed to solve the obstruction

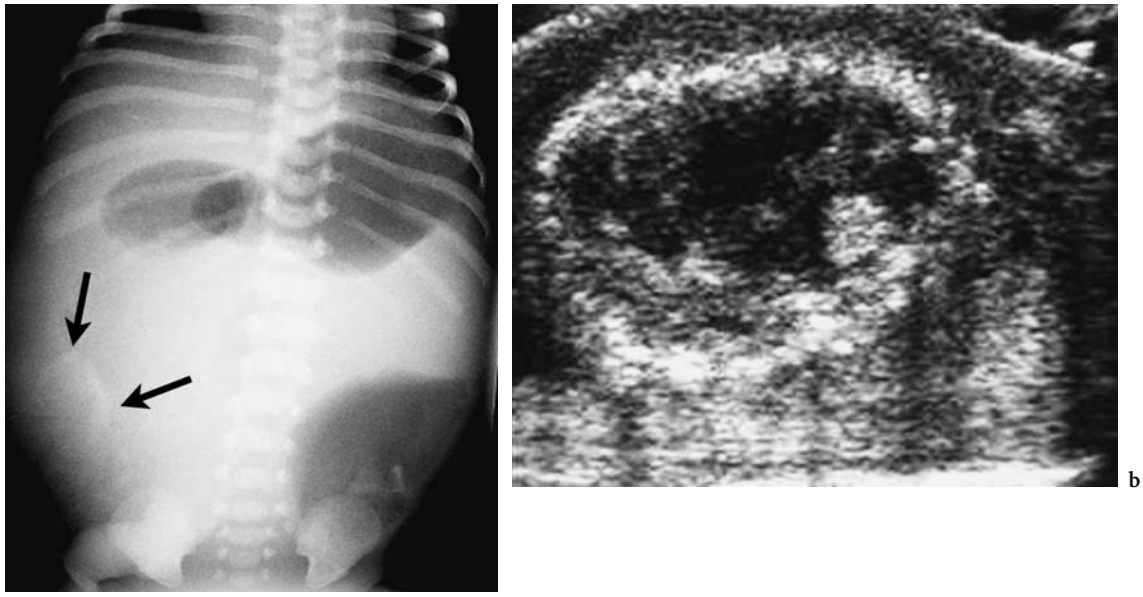

a b

Fig. 1.24a,b. Meconium peritonitis. **a** Abdominal radiograph demonstrates a small amount of gas in a markedly distended abdomen. A calcified mass within the peritoneal cavity is observed (*arrows*). There is no pneumoperitoneum. **b** Sonography of the same patient shows a pseudocyst containing debris with peripheral calcification

linear depositions of calcium localized underlying the anterior or posterior abdominal walls, in the flanks, or beneath the diaphragm. Calcifications may also be observed in the scrotal sac of males owing to communication through a patent processus vaginalis (Salman et al. 1999) (Fig. 1.25). Pseudocysts also may be seen as a solid mass on plain radiographs. In addition, distended loops of the bowel with air-fluid levels may be present due to the underlying intestinal obstruction. Where the perforation is still patent, free air will be seen in the peritoneal cavity (Fig. 1.26) or trapped in a walled-off loculus or pseudocyst. Decubitus radiographs to determine the presence or absence of free air with a persistent perforation are essential. The typical appearances of pneumoperitoneum, how-

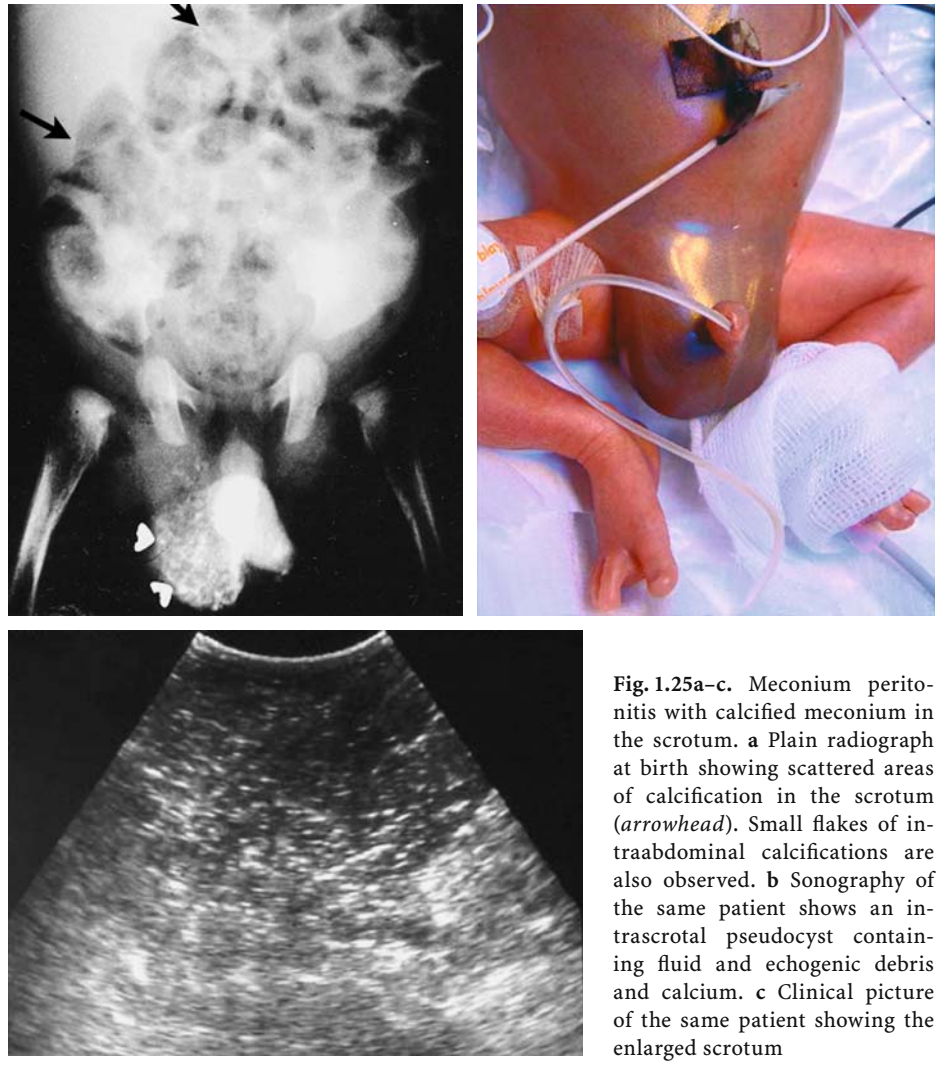

Fig. 1.25a–c. Meconium peritonitis with calcified meconium in the scrotum. **a** Plain radiograph at birth showing scattered areas of calcification in the scrotum (*arrowhead*). Small flakes of intraabdominal calcifications are also observed. **b** Sonography of the same patient shows an intrascrotal pseudocyst containing fluid and echogenic debris and calcium. **c** Clinical picture of the same patient showing the enlarged scrotum

ever, are not usually seen because of the presence of adhesions, which obliterate most of the peritoneal cavity.

Ultrasound may be useful in these patients, especially in the presence of a relatively airless abdomen. Meconium peritonitis predominantly presents two ultrasound appearances: general or cystic abnormality. With the generalized condition, highly echogenic material spreads throughout the abdomen and around the bowel loops (Fig. 1.27), producing a

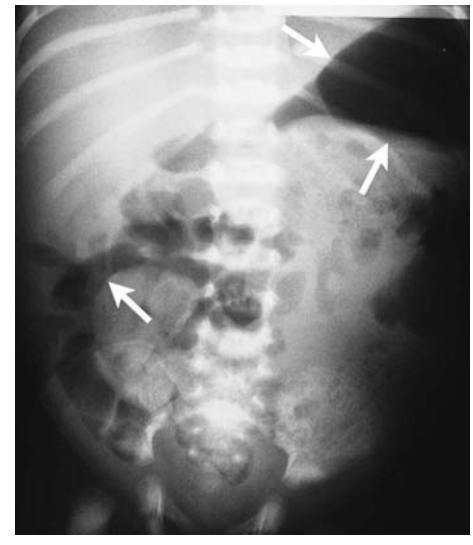

Fig. 1.26. Meconium peritonitis with intrauterine bowel perforation. Free air within the peritoneal cavity is observed (*arrows*) in this neonate with ileal atresia. No bowel distension is observed. A patent bowel perforation was found at surgery

characteristic "snowstorm appearance" (Lawrence and Chrispin 1984). The cystic form is characterized by localized, cystic collections of meconium (meconium pseudocysts) ranging from a few centimeters in size to huge cysts occupying most of the abdominal cavity. The cyst is usually well defined and predominantly echogenic, but may also be less well defined and markedly heterogeneous. The walls are echogenic and may be thick or thin (Bowen et al. 1984; Foster et al. 1987) (Figs. 1.24 and 1.28). Calcified foci may be demonstrated with posterior shadowing in many cases.

Meconium peritonitis may also be diagnosed by prenatal ultrasound. It can present as fetal meconium ascites, giant pseudocysts, small pseudocysts, and calcifications. Associated polyhydramnios is a common finding (Eckoldt et al. 2003; Kamata et al. 2000).

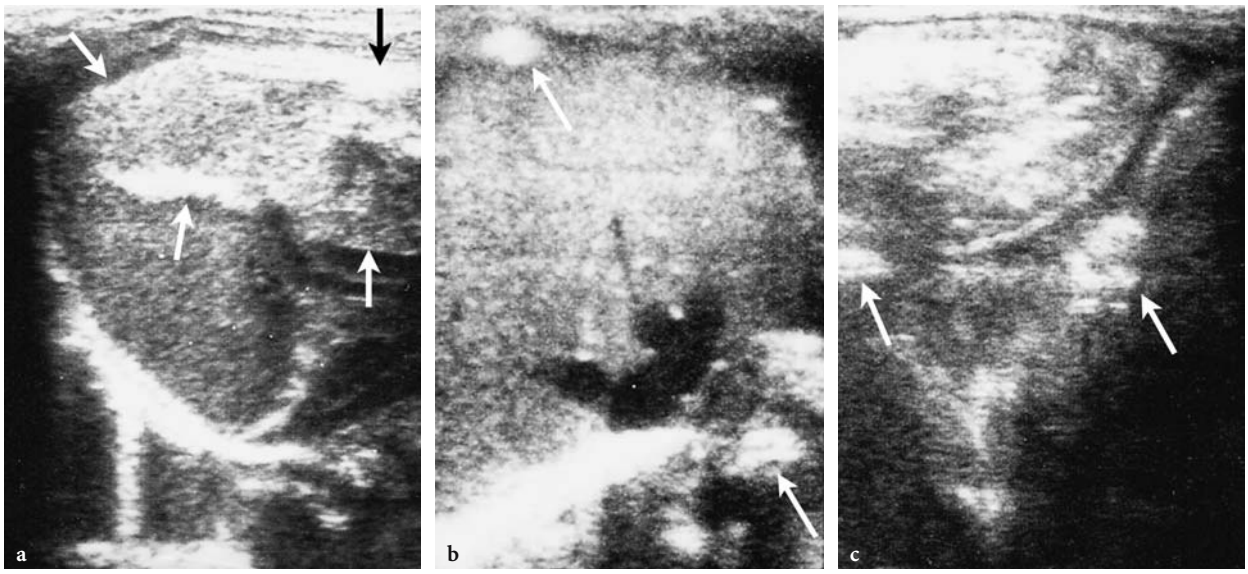

Fig. 1.27a–c. Meconium peritonitis in a neonate with cystic fibrosis. Sonography demonstrates intraabdominal calcifications over the liver surface (**a**), around the spleen (**b**), and around the bowel loops (**c**) (*arrows*). Note the hyperechogenic inspissated meconium into the bowel loops

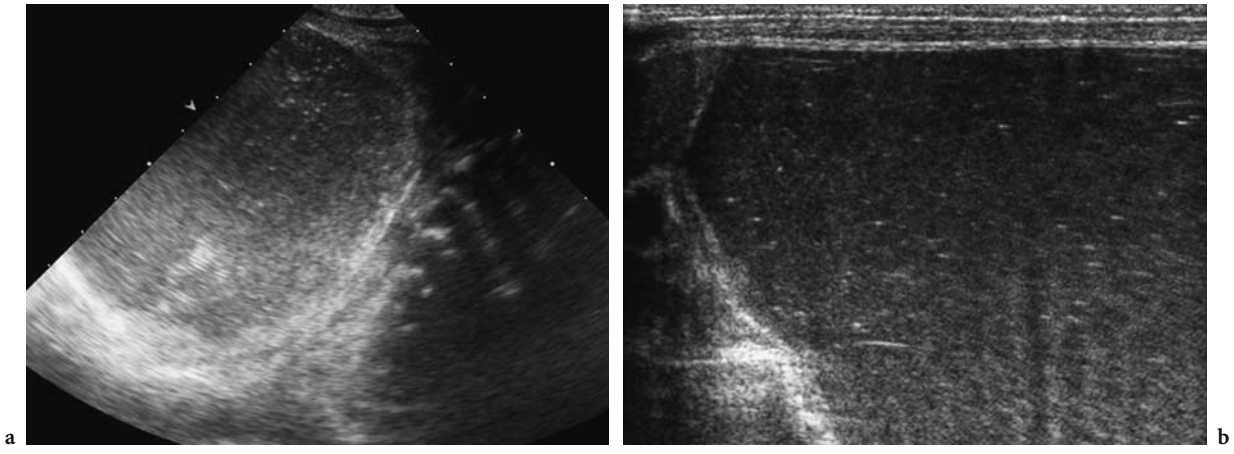

Fig. 1.28a,b. Meconium pseudocyst. **a** Sonography of the right hemiabdomen shows a large fluid-filled mass with echogenic contents. **b** High resolution US scan demonstrates a well-defined walled cyst with striking echogenic content consistent with inspissated meconium

1.1.1.2.2 Colonic Obstruction

Colon atresia, similar to small bowel atresia, is believed to result from an intrauterine vascular insult. The colon is the least frequent location, representing 5%–15% of all intestinal atresias (Powell and Raffensperger 1982). Multiple atresia syndromes may involve the colon in addition to the small bowel. Proximal location is more common than distal, with atresia beyond the splenic flexure being unusual. Clinical presentation may be delayed up to 48 h after birth. The abdominal scout film, in particular when the atresia is in the ascending colon, is often indistinguishable from obstruction of the distal ileum. The colon proximal to the point of atresia is often massively dilated and a mottled pattern of air and meconium may be identified. Plain film is usually unclear prior to 12–24 h of age so that an adequate amount of air can reach the site of obstruction (Hajivassiliou 2003). Sonography can determine the cause of distension before air is present in the distal bowel. The sonographic features of colon atresia are dilated distal small bowel and proximal colon, which often is markedly echogenic secondary to retained meconium.

Contrast-enema usually reveals a microcolon distal to the atresia, with obstruction to the retrograde flow of barium at the site of the atresia (Fig. 1.29). A "wind-sock" appearance may be observed with membranous atresias (Winters et al. 1992). Calcification of meconium peritonitis due to in utero bowel perforation is present in about 12% of atresia cases, and can be diagnosed antenatally by sonography.

Hirschsprung disease is a form of low intestinal obstruction caused by the absence of normal myenteric ganglion cells in the submucosal and intermuscular myenteric plexuses of a segment of the colon. Clusters of enlarged, unmedullated nerve fibers have taken their place. In normal intrauterine development, neuroenteric cells migrate from the neural crest to the upper end of the gastrointestinal tract by 5 weeks and proceed in a caudal direction. These cells reach the rectum by 12 weeks and commence the intramural migration from the myenteric plexus (Auerbach´s plexus) to the submucosal plexus (Meissner´s plexus). Hirschsprung´s disease is caused by abnormal neural crest cell migration resulting in arrested distal migration of these cells (Gershon and Ratcliffe 2004). The length of the aganglionosis is variable but always commences at the lower end of the rectum and extends proximally for a variable distance. In about 80% of cases, the anomaly does not extend beyond the sigmoid (short segment), while in the remainder it extends proximally to involve variable lengths of the colon and may even involve the terminal ileum (long segment). Ultrashort segment disease with aganglionosis essentially limited to the region of the internal sphincter is very rare, as is aganglionosis involving the entire alimentary tract (Meier-Ruge et al. 2004; Dasgupta and Langer 2004). In children with Hirschsprung´s disease, the absence of ganglion cells results in the failure of the distal intestine to relax normally, peristaltic waves do not pass through the aganglionic segment and there is no normal defecation leading to functional obstruction. The aganglionic segment remains unexpanded and the proximal colon becomes distended and hypertrophied. Hirschsprung´s disease is responsible for approximately 15%–20% of cases of neonatal bowel obstruction. Short segment disease is more common in males at a ratio of 4:1. In long segment aganglionosis, male preponderance diminishes to 2.8:1. Gender distribution is almost equal in the cases with extensive involvement (Kleinhaus et al. 1979)

A positive family history is encountered in about 10% of patients with short segment disease and in 25% of patients with total colonic aganglionosis. Hirschsprung´s disease is associated with esophageal dysmotility syndromes, malrotation and ileal or colonic atresia. Approximately 3% of patients with Down's syndrome have Hirschsprung´s disease. The disease has also been associated with other neurocristopathies (neuroblastoma, pheochromocytoma, MEN IIA syndrome) and is thought to be related to their common neuroblastic origin (Rescorla et al. 1992). The severity of the symptoms does not depend entirely on the length of the aganglionic segment. Abdominal distension, failure to pass meconium in the first 24 h of life, constipation, and bilious vomiting are the predominant symptoms, with the signs of obstruction appearing within a few days after birth.

Plain abdominal film of infants with this condition is similar to that of other forms of low small bowel obstruction. The abdomen is filled with several distended loops of the colon and the small bowel often with air-fluid levels. The colon is usually difficult to identify accurately, and air is usually absent in the rectum (Fig. 1.30). About 5% of patients may present with pneumoperitoneum

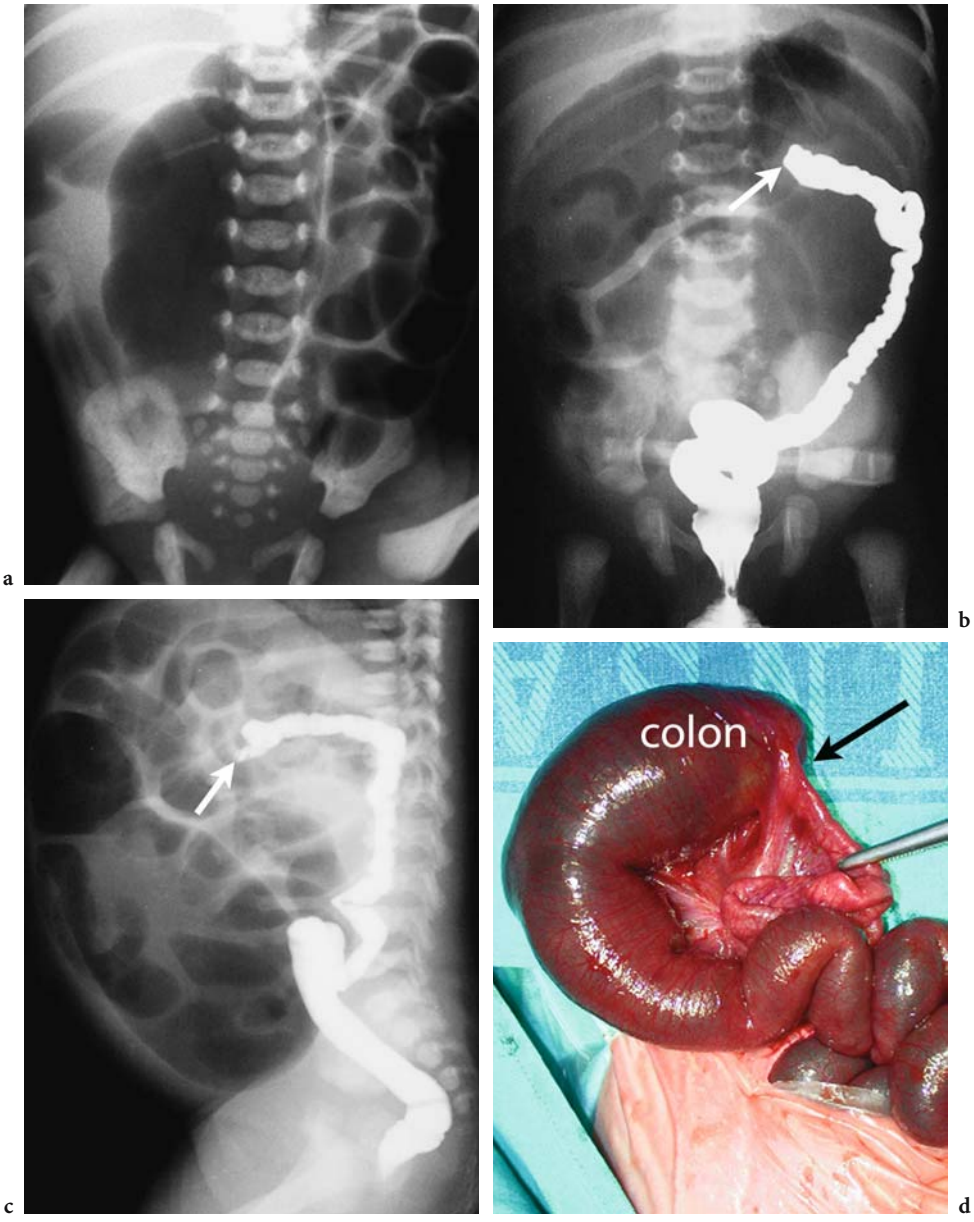

Fig. 1.29a–d. Colon atresia. **a** Supine radiograph shows gaseous distension of bowel. **b,c** Contrast enema, anteroposterior and lateral views show abnormally small colon (microcolon) with complete obstruction to retrograde flow of contrast material proximal to the middle transverse portion of colon. **d** Photograph at operation shows a distended colon up to the site of the atresia (*arrow*) and a microcolon distal to it

secondary to perforation (Dasgupta and Langer 2004). Most of these patients have long segment or total colonic aganglionosis. As in all cases of low intestinal obstruction, a contrast enema is needed. Rectal examination should not be performed prior to the enema as this may mask a low-lying transition zone. The enema examination is started with the patient in a lateral position. The catheter should be placed barely within the rectum, so as not to obscure a transition zone. Balloon catheters should never been used as they may obscure a transition zone or even perforate the aganglionic rectum. Although the contrast enema has classically been performed with barium sulphate, currently low-osmolar water-soluble is the preferred contrast medium because of the risk of barium peritonitis

in the event of colonic perforation. There are many signs of Hirschsprung´s disease on contrast enema studies. The most important is the transition zone between the normal or relatively narrow aganglionic segment and the dilated bowel proximal to it, usually in the shape of an inverted cone (Figs. 1.30 and 1.31). This finding is present in about 65% of neonates (Fotter 1998). When this is observed, the examination should be discontinued, especially if barium is being used, as filling of the more proximal dilated bowel beyond the transition zone may lead to impaction. The transition zone may, however, be difficult to see in newborns. In such cases, the rectosigmoid index may be useful (Siegel et al. 1981). Normally, the rectum is 20%–40% larger than the sigmoid in diameter. In Hirschsprung´s disease, this ratio may equilibrate or reverse. The pathologic transition zone is usually somewhat more proximal than the radiographic one (Jamieson et al. 2004). Abnormal contractions and irregular peristaltic activity of the aganglionic portion of the colon may be a useful indicator of the disease, occurring in about 20% of infants, and should not suggest mucosal ulceration. Retention of contrast medium at 24 h with colonic distension may be a helpful sign, but is nonspecific, as it can be observed in 60% of patients without Hirschsprung´s disease. On the other hand, good evacuation does not rule out the disease (Rosenfield et al. 1984).

The radiologic diagnosis of total colonic aganglionosis is much more difficult. Findings may include normal barium enema, short colon of normal caliber, microcolon, rounding of the colonic flexures, or transition zone in the ileum (Fig. 1.32). Clinical suspicion should be heightened in patients presenting with clear signs and symptoms of distal obstruction, in whom the contrast enema does not demonstrate a specific cause (Hayakawa et al. 2003). Histological confirmation is obtained by means of rectal biopsy (Solari et al. 2003).

Enterocolitis is the major cause of death in patients with Hirschsprung´s disease, with a mortality rate as high as 30%. The patients may present with diarrhoea, hypovolemia and prostration. Enterocolitis of Hirschsprung´s disease can be diagnosed on plain radiograph by the irregular contour of the dilated colonic wall caused by the edema, spasm, and ulceration of the intestinal wall. Patients who present with perforation typically do not have enterocolitis. Enema is contraindicated in patients with suspected enterocolitis because of the possibility of perforation (Vieten and Spicer 2004).

Functional immaturity of the colon is a common cause of neonatal obstruction, particularly in premature infants and in those whose mothers were treated during labor with magnesium preparation or high doses of opiates or other sedatives. The condition has also been encountered in children of diabetic mothers, or children with septicemia, hypothyroidism, or hypoglycemia (Cohen 2003). The term includes meconium plug syndrome and small left colon syndrome. Both entities are associated with dysmotility of the colon. The etiology remains unclear, although they are thought to be associated with immature myenteric plexus ganglia (Burge and Drewett 2004). These infants have difficulty in initiating evacuation, abdominal distension, and sometimes vomiting, but, in general, bowel distension usually is less severe than in organic obstruction. The condition is both diagnosed and treated with contrast material enemas (De Backer et al. 1999).

In cases of meconium plug syndrome the meconium forms a long, thick, snake-like plug, which obstructs the colon. The contrast enema reveals a large meconium plug as a translucent filling defect surrounded by opaque material filling the rectosigmoid, often extending into the descending colon (Fig. 1.33). The contrast medium will sometimes stream around the plug to give a double contrast appearance, with the contrast-lined colonic walls showing up against the negative filling defect of the plug. The large plug is usually evacuated during or soon after the enema examination (Loening-Baucke and Kimura 1999). Typically, following the enema there is clinical improvement, and over the course of hours to days, radiographic and clinical signs of obstruction subside. The only problem is that a few cases of meconium ileus and a few cases of Hirschsprung´s disease may be incorrectly lumped into this group. Then, if the difficulty is not promptly and completely cured a sweat test for cystic fibrosis and further observation for Hirschsprung´s disease should be carried out (LeQuesne and Reilly 1975).

The clinical presentation of patients with small left colon syndrome is very similar to that of patients with meconium plug syndrome. Air-fluid levels are often absent in the upright film, particularly prior to 48 h of life. “Soap bubble” meconium is typically seen in the collapsed left colon on the plain film, and the distended bowel tends to be less than that seen in atresias. The contrast enema reveals a normal or slightly dilated colon and rectum but

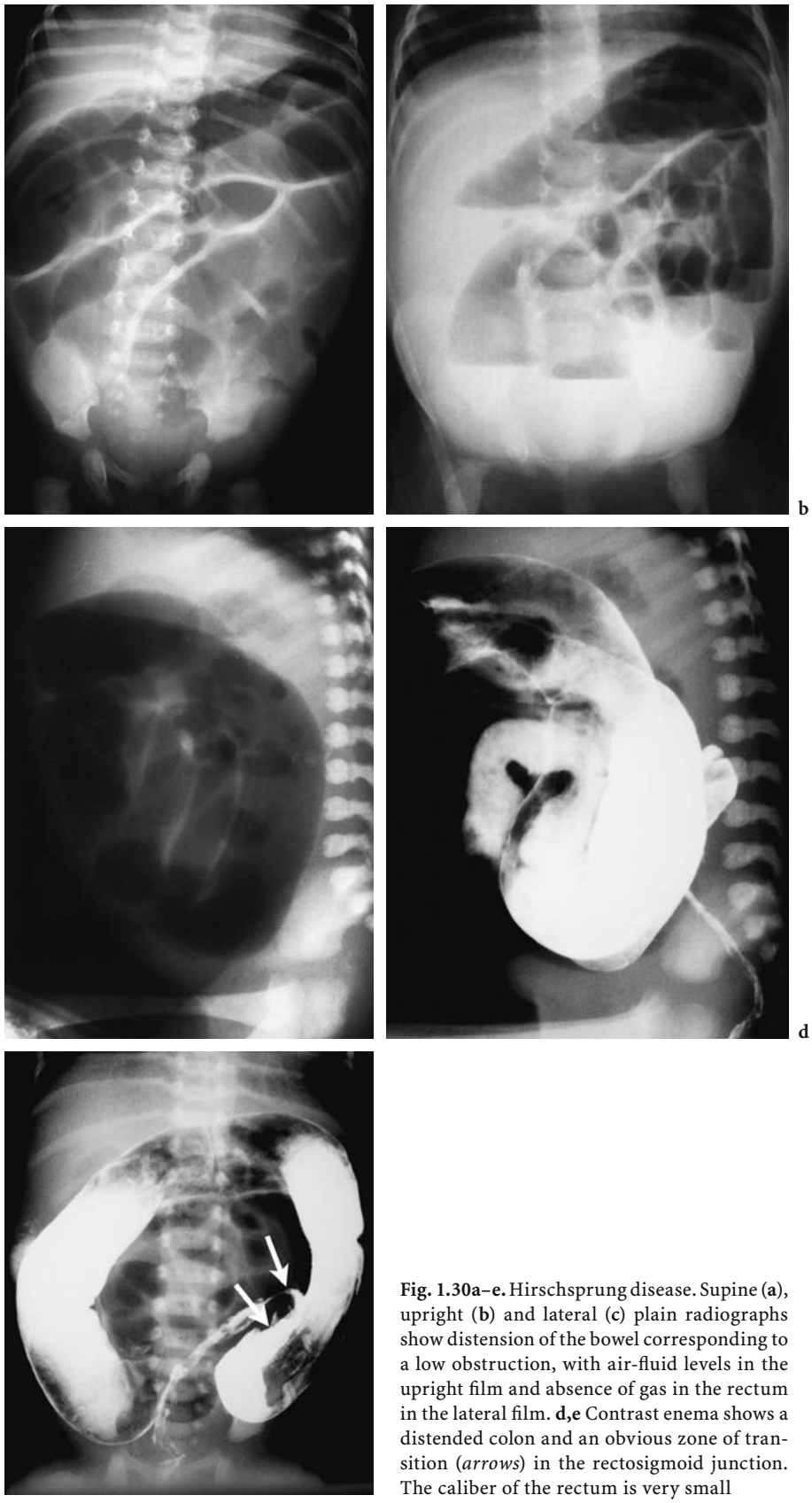

Fig. 1.30a–e. Hirschsprung disease. Supine (**a**), upright (**b**) and lateral (**c**) plain radiographs show distension of the bowel corresponding to a low obstruction, with air-fluid levels in the upright film and absence of gas in the rectum in the lateral film. **d,e** Contrast enema shows a distended colon and an obvious zone of transition (*arrows*) in the rectosigmoid junction. The caliber of the rectum is very small

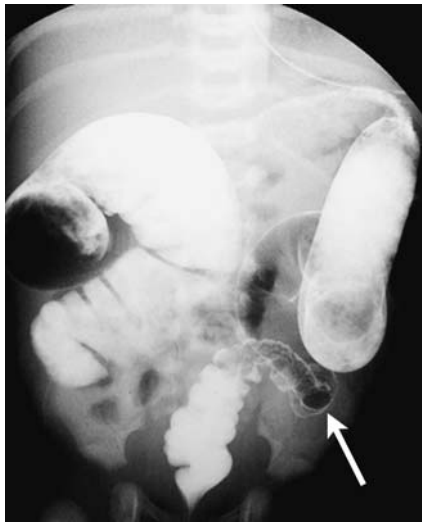

a

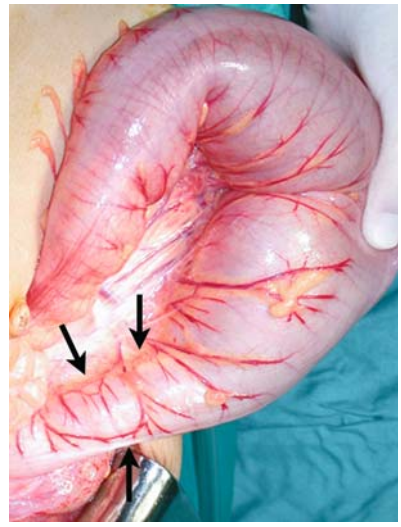

b

Fig. 1.31a,b. Hirschsprung disease. **a** Contrast enema shows a distended colon and a small rectum and portion of the colon. The rectosigmoid index is abnormal. **b** Intraoperative photograph demonstrates the transition zone (*arrows*) with the shape of an inverted cone

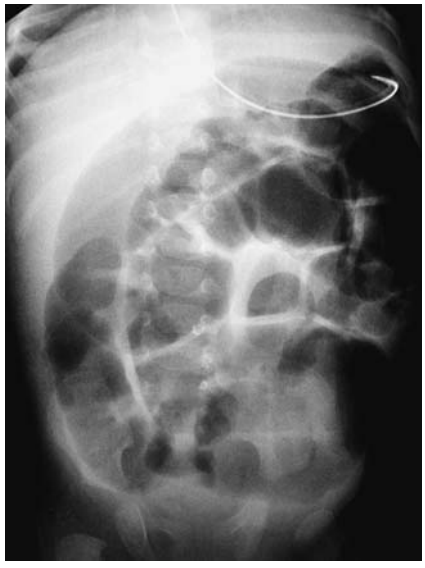

a

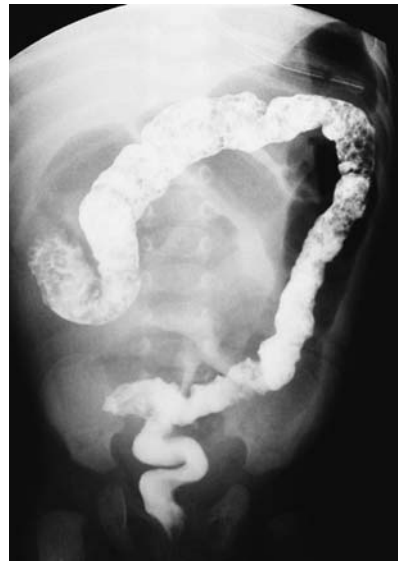

b

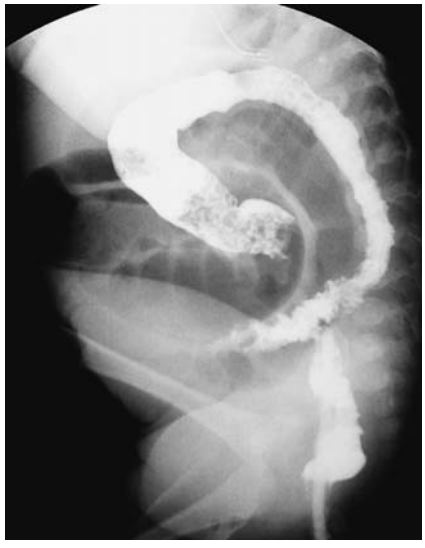

c

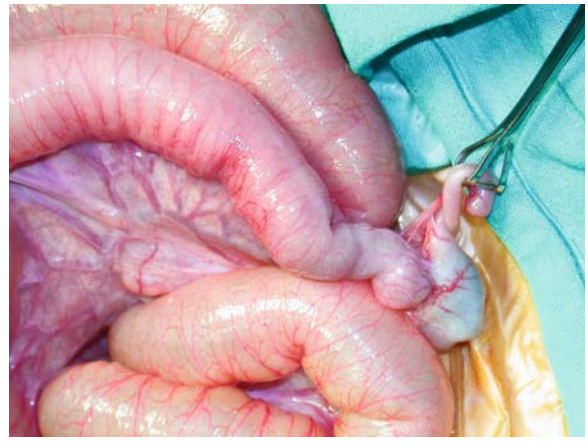

d

Fig. 1.32a–d. Total colonic aganglionosis. **a** Plain radiograph of the abdomen demonstrates low obstruction. **b,c** Anteroposterior and lateral views during contrast enema show the shortened colon compared with the normal redundancy of the neonatal colon, with the flexures pulled down and a normal rectosigmoid index. **d** Intraoperative photograph shows dilated bowel loops with the transition zone at the distal ileum

the left colon up to the splenic flexure is very small, resembling a microcolon (Fig. 1.34). The amount of meconium present in the colon is variable, and discrete plugs of meconium at the point of transition may or may not be seen (Hajivassiliou 2003). Typically, after the enema, there is clinical improvement, and over the course of hours to days radiographic and clinical signs of obstruction resolve. The only important differential diagnosis in babies with these findings is Hirschsprung´s disease with a transition zone at the splenic flexure. There are several findings that can be helpful. The distal rectosigmoid colon is of normal caliber and larger than the left colon, the proximal colon is less dilated than in Hirschsprung´s disease and the transition zone of small left colon syndrome tends to be quite abrupt, whereas in Hirschsprung´s disease it tends to be cone-shaped and gradual. However, the distinction between both entities is not always possible on the basis of radiological findings and a rectal biopsy must then be performed (Amodio et al. 1986; De Backer et al. 1999).

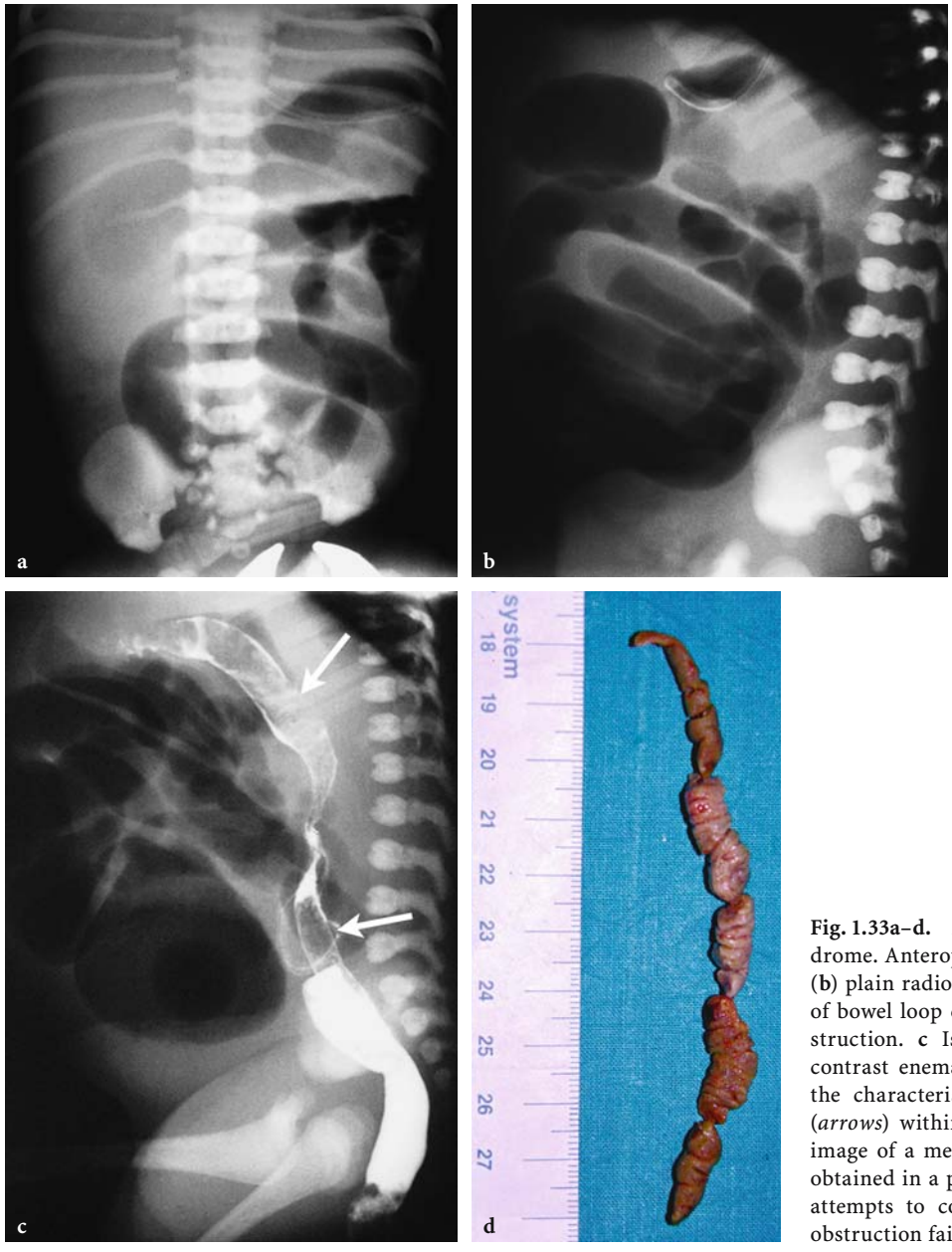

Fig. 1.33a–d. Meconium plug syndrome. Anteroposterior (**a**) and lateral (**b**) plain radiographs show distension of bowel loop consistent with low obstruction. **c** Isosmolar water-soluble contrast enema, lateral view outlines the characteristic long filling defect (*arrows*) within the colon. **d** Clinical image of a meconium plug surgically obtained in a patient in whom several attempts to conservatively solve the obstruction failed

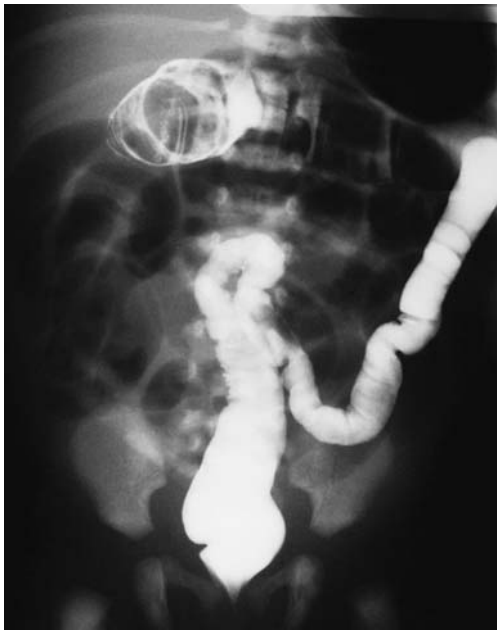

Fig. 1.34. Small left colon syndrome. Isosmolar water-soluble contrast enema in a newborn with low obstruction demonstrates a normal rectum and distal rectosigmoid and a relatively narrow proximal sigmoid and descending colon with a transition to a more dilated colon at the splenic flexure. In 1 week radiographic and clinical signs of obstruction resolved

1.1.2 Necrotizing Enterocolitis

Necrotizing enterocolitis (NEC) is the leading gastrointestinal emergency of the premature infant. In many cases, it happens in apparently healthy premature infants who have no other medical problems. Although it affects mostly premature infants, 10% of affected infants are born at term. Its incidence varies between 0.3 and 2.4 infants/1000 births and between 3.9% and 22.4% amongst infants of less than 1500 g. Males and females are equally affected.

Most infants develop NEC within the first 2 weeks of life (Krasna et al. 1996). Its precise cause remains unclear, but it is thought that factors such as ischemia, decreased mucus production, and diminished immune response of the premature infant may lead to invasion of the intestinal mucosa by intestinal flora resulting in air entering the submucosa and mucosa. Some experimental work suggests that translocation of intestinal flora across an incompetent mucosa may play a role in spreading the disease and systemic involvement. Such a mechanism would account for the apparent protection breast-fed infants have against fulminant NEC (Horton 2005). The terminal ileum and the proximal colon are most commonly affected, though any portion of the intestines may be involved.

The clinical signs are nonspecific and consist of feeding intolerance, increased gastric retention, vomiting, abdominal distension, and the presence of blood in the stools.

The mainstay of diagnostic imaging is abdominal radiography. Because of the possibility of perforation of the necrotic bowel, the supine film should be supplemented with a cross-table lateral or left-lateral decubitus radiograph. The radiograph findings of NEC are nonspecific, especially in early stages. Diffuse nonspecific gaseous distension and thickened bowel walls (suggesting edema/inflammation) is the most common pattern (Fotter and Sorantin 1994; Krasna et al. 1996) (Fig. 1.35). An asymmetric bowel air pattern or distension localized to focal loops only may also be seen. Radiographs can sometimes reveal scarce or absent intestinal air, which is more worrisome than diffuse distension that changes over time. But the pathognomonic finding of NEC is pneumatosis intestinalis, consisting of submucosal or subserosal air (Buonomo 1999). Pneumatosis intestinalis appears as a characteristic train-track lucency configuration within the bowel wall and may be linear or cystic (Figs. 1.36 and 1.37). The cystic collections are usually subserosal, whereas the linear form is usually submucosal. Pneumatosis intestinalis is due to the production of small bubbles of hydrogen by bacteria within the intestinal wall (Albanese and Rowe 1998). Intramural air bubbles may also represent extravasated air from within the intestinal lumen. These changes might not be detectable on digitalized images due to the suboptimal resolution, and a printed X-ray film is often necessary (Morrison and Jacobson 1994). Serial radiographs help assess disease progression.

Abdominal free air is ominous and usually requires emergency surgical intervention (Fig. 1.38). The presence of abdominal free air can be difficult to discern on a flat radiograph, which is why decubitus radiographs are recommended at every evaluation. The football sign is characteristic of intraperitoneal air on a flat plate and manifests as a subtle oblong lucency over the liver shadow. It represents the air bubble that has risen to the most anterior aspect of the abdomen in a baby lying in a supine position and can be demonstrated by left lateral decubitus imaging (Buonomo 1999). Although free air in the

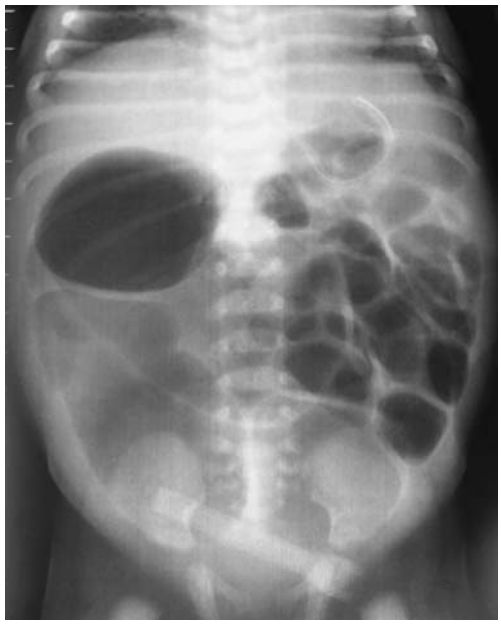

a

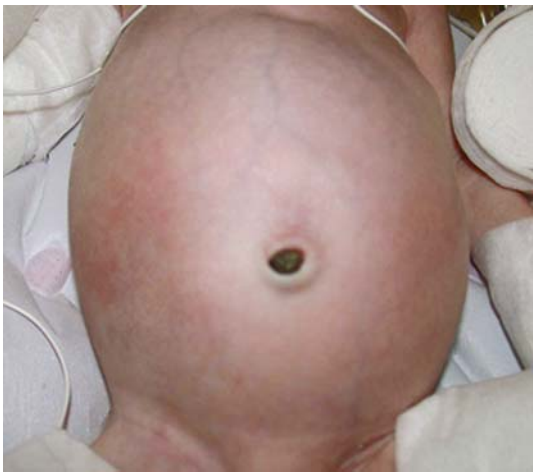

b

Fig. 1.35a,b. Necrotizing enterocolitis. **a** Photograph of a 3-week-old premature neonate showing important abdominal distension. **b** Plain abdominal radiograph shows diffuse nonspecific gaseous distension of the bowel loops

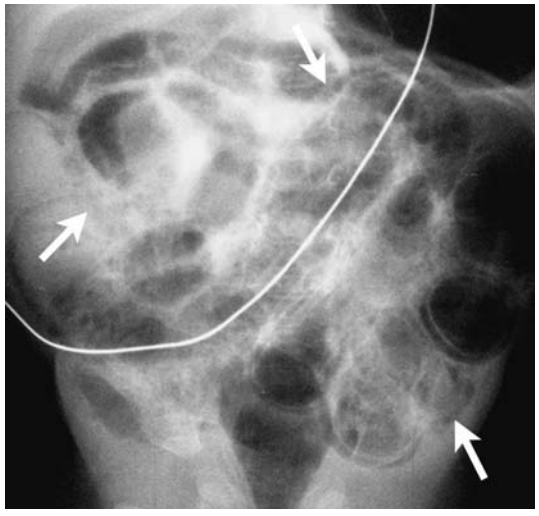

a

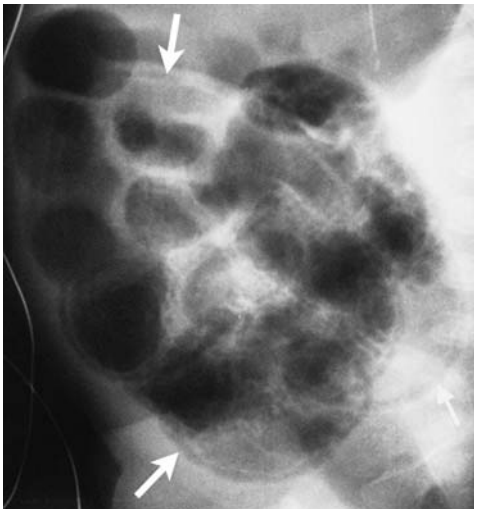

b

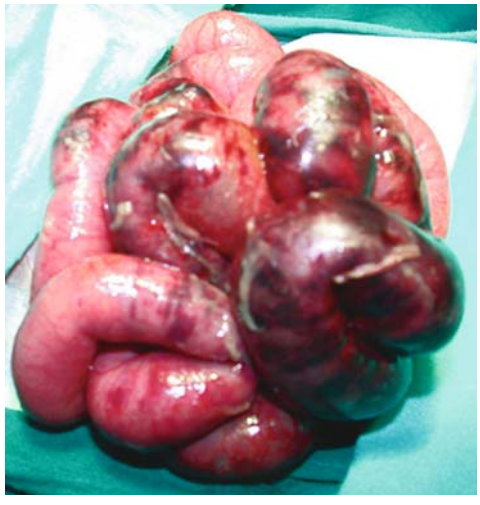

c

Fig. 1.36a–c. Pneumatosis intestinalis in a 1-week-old infant. Anteroposterior (**a**) and lateral (**b**) plain radiographs show small and large bowel loops sharply outlined by collections of gas in bowel wall. Most of these collections of gas are linear, indicating a submucosal location. **c** Surgical image of the same patient demonstrates diffuse bowel necrosis

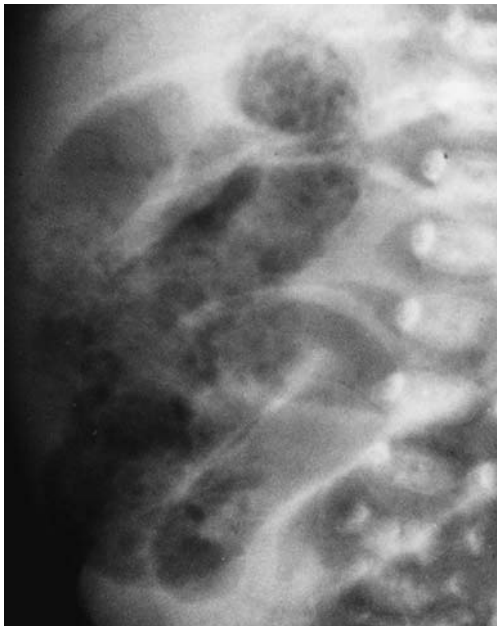

Fig. 1.37. Pneumatosis intestinalis in 12-day-old infant. Abdominal radiograph demonstrates increase in the amount of gas in the small bowel. Pneumatosis intestinalis is identified as cystic lucencies in the right upper and lower quadrant. These cystic lucencies are usually subserosal

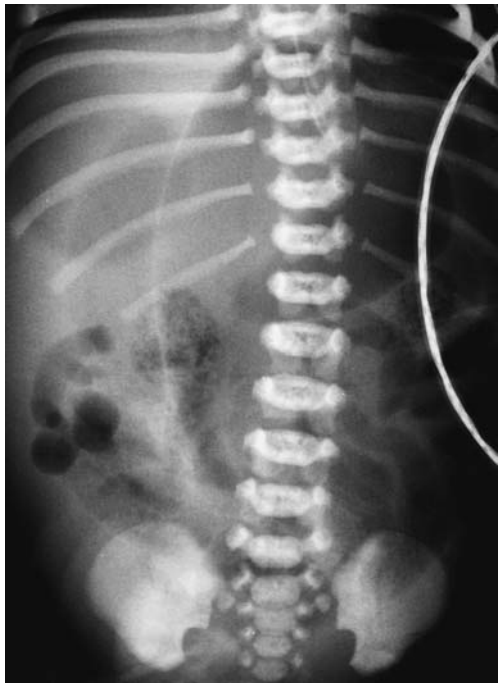

Fig. 1.38. Pneumoperitoneum complicating necrotizing enterocolitis. Supine in a 1-month-old premature infant radiograph shows intramural gas in the small bowel and free intraperitoneal air secondary to bowel perforation. The central lucency and the falciform ligament are observed

abdominal cavity confirms it, bowel wall perforation might be present in the absence of free air in one third of the cases.

Another pathognomonic sign of NEC is portal vein air. Portal vein air is more frequent and less ominous than was previously thought. It is seen as finely branching radiolucencies extending from the porta hepatis to the periphery of the liver (Fotter and Sorantin 1994) (Fig. 1.39). Ascites is a late finding that usually develops some time after perforation when peritonitis is present. Ascites is observed on an AP radiograph as centralized bowel loops that appear to be floating on a background of density. It is better observed on ultrasonography (Albanese and Rowe 1998).

Abdominal ultrasonography is a relatively new technology for evaluating suspected NEC in neonates. Ultrasonography can be used to identify areas of loculation and/or abscess consistent with a walled-off perforation when patients with indolent NEC have scarce air or a fixed area of radiographic density. Ultrasonography is excellent for identifying and quantifying ascites. Serial examinations can be used to monitor the progression of ascites as a marker for the disease course. Portal air may be demonstrated on ultrasound as bright, shifting echogenic foci within the portal vein (Morrison et al. 2004) (Fig. 1.40). This finding has been termed informally the "champagne sign" because of its similar appearance to a champagne flute. Sonography can also show thickened bowel loops, and bowel air pneumatosis (Fig. 1.41). Recent data suggests that Doppler study of the splanchnic arteries early in the course of NEC can help distinguish developing NEC from benign feeding intolerance in a mildly symptomatic baby. A markedly increased peak flow velocity (> 1.00) of arterial blood flow in the celiac and superior mesenteric arteries in early NEC has been demonstrated (Deeg et al. 1993). Such a finding at the presentation of symptoms can further aid in diagnosis and therapy, potentially sparing those individuals at low risk for NEC from unnecessary interventions. Recently, color Doppler US has been used to evaluate bowel wall perfusion. Early stages of the disease show increase in color Doppler signals in the bowel wall and mesentery, reflecting marked

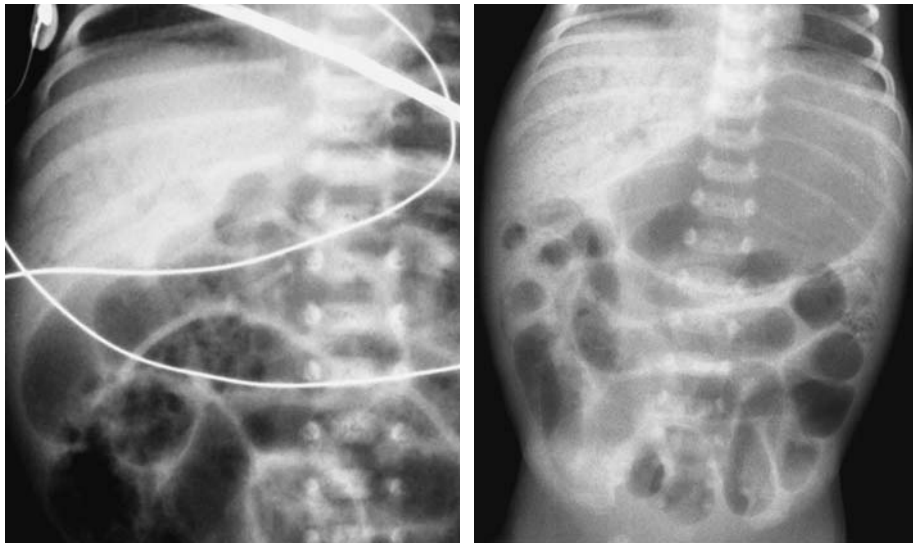

Fig. 1.39a,b. Portal vein air. Plain radiographs. **a** Air is observed within the portal vein branches complicating pneumatosis intestinalis in a 3-week-old premature infant. **b** Another premature infant with pneumatosis intestinalis and air within the portal vein

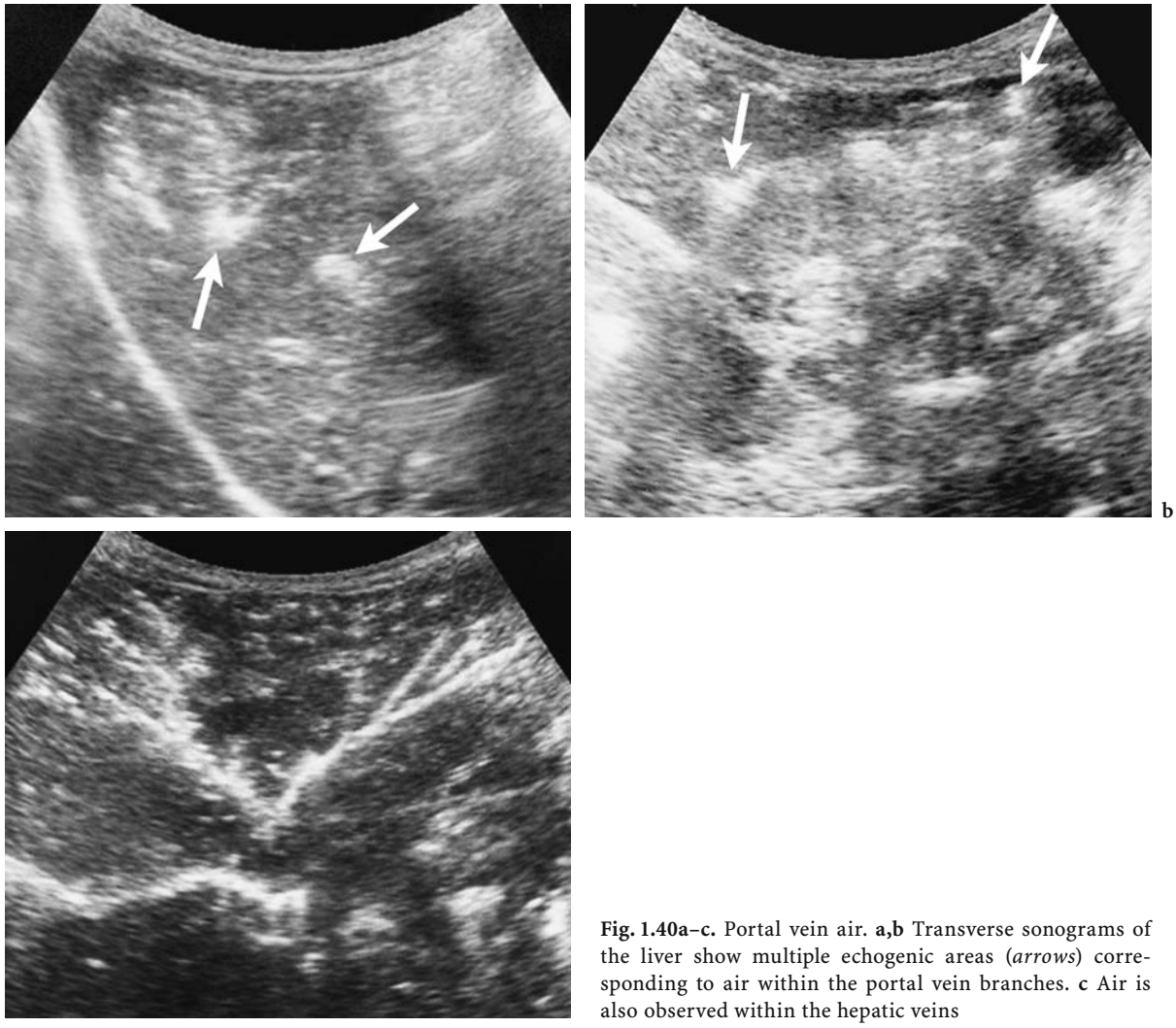

Fig. 1.40a–c. Portal vein air. **a,b** Transverse sonograms of the liver show multiple echogenic areas (*arrows*) corresponding to air within the portal vein branches. **c** Air is also observed within the hepatic veins

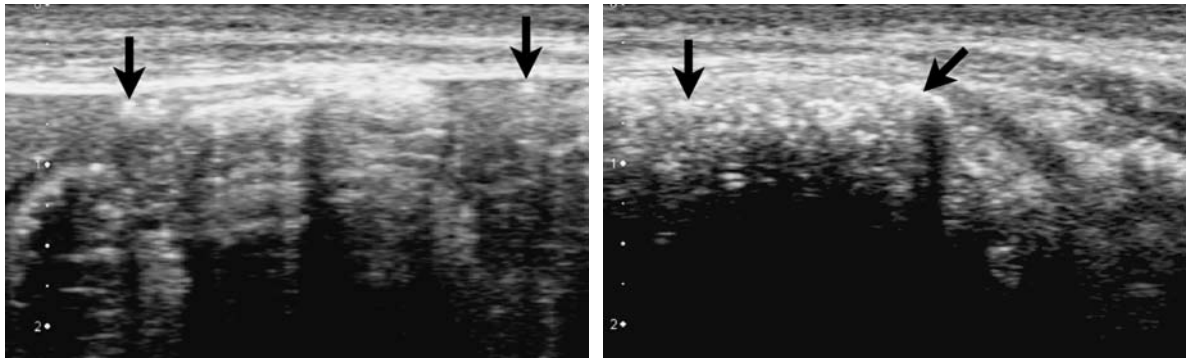

Fig. 1.41a,b. Necrotizing enterocolitis. **a,b**. Longitudinal US scans at the transverse colon show air bubbles (*arrows*) within the colonic wall corresponding to pneumatosis intestinalis

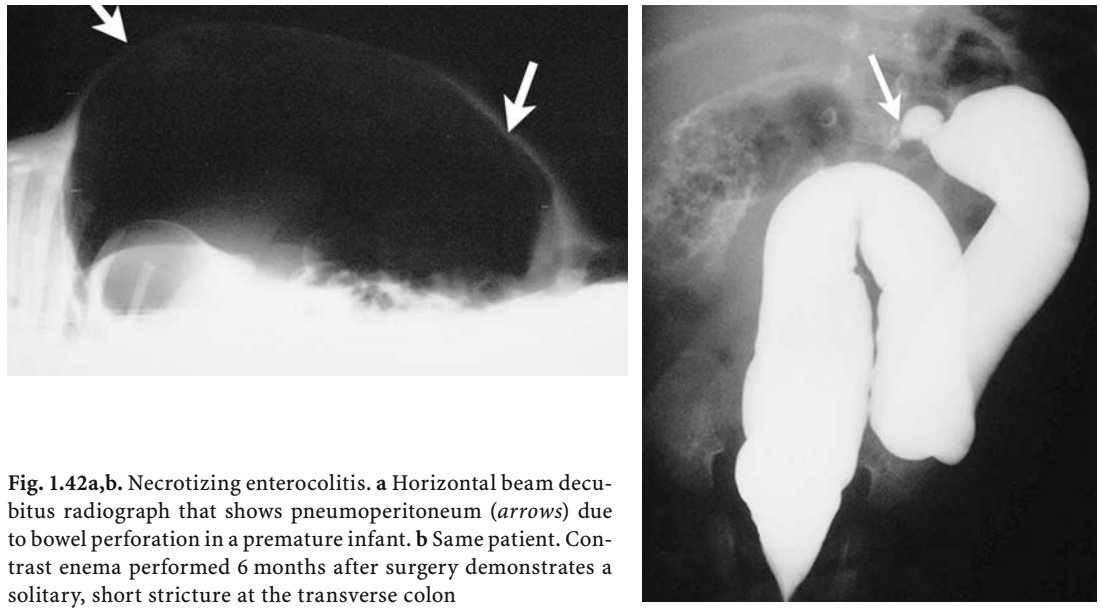

Fig. 1.42a,b. Necrotizing enterocolitis. **a** Horizontal beam decubitus radiograph that shows pneumoperitoneum (*arrows*) due to bowel perforation in a premature infant. **b** Same patient. Contrast enema performed 6 months after surgery demonstrates a solitary, short stricture at the transverse colon

hyperemia due to vasodilatation. Absence of blood flow in the bowel wall reflecting absence of perfusion to the involved loop, has been correlated with necrotic bowel (Faingold et al. 2005).

NEC mortality ranges from 9% to 28% and is due to refractory shock, disseminated intra-vascular coagulation, multiple organ failure, intestinal perforation, sepsis, extensive bowel necrosis, and complication of short bowel syndrome. Proper selection of patients for medical versus surgical managements has resulted in significant improvement in survival of infants with NEC. The only universally accepted indication for surgery is the presence of perforation, which may manifest as pneumoperitoneum or free fluid in the peritoneal cavity. Unfortunately, only 50%–75% with perforation have free air detectable on decubitus or horizontal beam radiographs. The presence of intraperitoneal fluid at US, particularly if it is complex or echogenic, is suggestive of perforation (Miller et al. 1993). About 20% of patients treated medically or surgically develop one or multiple strictures, at previously affected sites, especially in the large bowel. The strictures may be asymptomatic but also may cause bowel obstruction several weeks or months after the episode of NEC (Hofman et al. 2004; Pierro and Hall 2003) (Fig. 1.42). Strictures may develop even in patients whose NEC was not severe. Therefore, any patient with symptoms of obstruction after completion of treatment for necrotizing enterocolitis should undergo a contrast enema.

1.1.3 Pneumoperitoneum

Pneumoperitoneum or free intraperitoneal air in the neonatal period is usually the result of a hollow viscous perforation. In healthy neonates, the perforation is usually iatrogenic, secondary to the insertion of a tube or a rectal thermometer (Fig. 1.43). Necrotizing enterocolitis is the most common cause of pneumoperitoneum in the neonatal intensive care unit. Intestinal atresia is also an important cause, the perforation usually occurring in the dilated loops above the atresia. Ruptured or perforated Meckel, sigmoid, and jejunal diverticula, toxic megacolon, and idiopathic gastric perforation in premature infants are also common causes of pneumoperitoneum in the

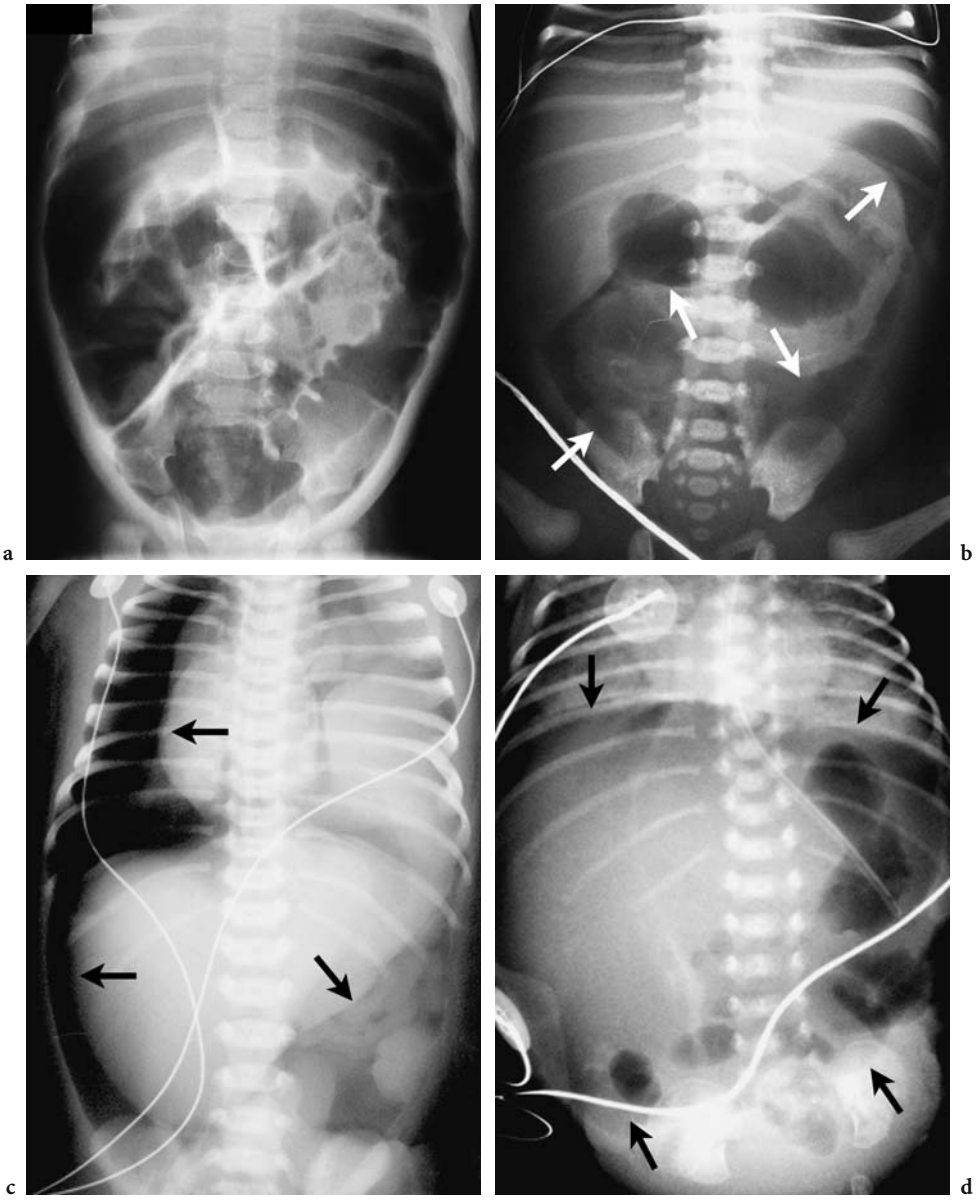

Fig. 1.43a–d. Pneumoperitoneum. **a** Massive pneumoperitoneum complicating the insertion of a rectal tube. **b** Pneumoperitoneum (*arrows*) in a newborn with ileal atresia. **c** Massive pneumothorax, pneumomediastinum and pneumoperitoneum (*arrows*) in a patient that had been supported by mechanical ventilation. **d** Neonate with abdominal distension following the insertion of a rectal thermometer. A supine radiograph shows a lucency occupying the entire abdominal cavity (*arrows*) and the falciform ligament outlined by air

neonatal period. At times, free intraperitoneal air may be seen in neonates supported by mechanical ventilation. It occurs following a pathway through the normal diaphragmatic foramina. There is no perforation of the gastrointestinal tract in these cases.

1.2 Gastrointestinal Emergencies in the Infant and Young Child

Acute abdominal pain is a common complaint in the pediatric age group. A total of 10% of school-age children have recurrent abdominal pain and in only 10% of these children can etiology be detected. The majority of these children have self-limited disease. The most common associated conditions include upper respiratory tract infection, pharyngitis, viral syndrome, gastroenteritis, and constipation (Henderson et al. 1992). Therefore, it is uncommon for the underlying condition in these children to require surgical intervention.

Acute abdomen is defined as a severe abdominal pain that starts suddenly, so that the possibility of immediate surgery must be considered. The causes of the acute abdomen in children vary depending on the ages of the children and can be divided into diseases that can be treated with medical care and those in which emergency surgical intervention may be necessary.

The most frequent surgically treated causes of acute abdomen are appendicitis, intussusception, adhesions causing bowel obstruction, incarcerated hernia, midgut volvulus and complicated Meckel's diverticulum. Non-surgically treated conditions frequently have a digestive origin including gastroenteritis, severe constipation, mesenteric lymphadenitis, ileocecitis, Schönlein-Henoch purpura, inflammatory bowel disease, or paralytic ileus.

Furthermore, a large-scale of intraabdominal or extraabdominal disorders can cause acute abdominal pain. Intraabdominal causes may have a genitourinary (urinary tract infection, ovarian torsion) or biliopancreatic origin (colecistitis, pancreatitis, etc.). Extraabdominal causes include abdominal pain referred from non-abdominal organs (pneumonia, discitis) and abdominal pain related to a systemic disease, such as diabetic acidosis, hypothyroidism, lead metals poisoning, sickle cell anemia, and porphyria. Fortunately, these different causes differ with the age group, thus simplifying the differential diagnosis (Table 1.1).

The role of diagnostic imaging is to determine whether the acute abdominal pain is due to a surgically or medically treated disease and, if possible, to diagnose the exact nature of the ailment. Since

Table 1.1. Causes of acute abdomen in children

Abdominal
● Gastrointestinal
Surgical
Appendicitis
Intussusception
Small Bowel Obstruction
– Adhesions
– Incarcerated hernia
– Volvulus Strangulation
Meckel's Diverticulum
Nonsurgical
Gastroenteritis
Ileocecitis
Crohn's disease
Schönlein-Henoch purpura
Mesenteric adenitis
Primary fat epiploic lesions
Peritonitis
Constipation
Paralytic ileus
● Genitourinary
Urinary tract infection
Lithiasis
Pelviureteric junction obstruction
Ovarian cyst
Ovarian torsion
Hydrometrocolpos
● Biliopancreatic
Cholecystitis
Lithiasis
Choledochal cyst
Pancreatitis
Extraabdominal
● Referred
Thorax: pneumonia, effusion
Musculoskeletal: discitis
● Systemic
Endocrinologic disorders (diabetes, hypothyroidism)
Porphyry

Note: Entities that at their natural evolution usually require surgery are listed under "Surgical" causes. This list is not complete

intussusception or appendicitis are the main surgically treated causes to keep in mind, imaging tests should be directed to rule out intussusception in infants and young children and appendicitis in older children. Plain abdominal radiographs have historically been used as the initial imaging examination in children with acute abdominal pain of equivocal etiology but they are usually unhelpful in establishing the cause of the acute abdominal pain as an isolated symptom. The traditional indications for plain abdominal radiography – bowel obstruction, pneumoperitoneum, and the search of ureteral calculi – have been questioned by cross-sectional imaging (Marincek 2002). However, in many centers plain radiographs serve as the initial radiological approach. The presence of an appendicolith in the right iliac fossa supports the diagnosis of acute appendicitis. If the abdominal pain is accompanied by vomiting, or if there is any clinical suspicion of bowel obstruction or perforation, a supine plain film of the abdomen can be useful, with an additional decubitus or upright view to exclude perforation where indicated. If an abdominal pain is accompanied by fever, a chest radiograph should also be obtained, as pneumonia is a well-recognized cause of abdominal pain (Hayes 2004).

The principal imaging technique used for evaluating acute abdominal pain in children is sonography. In the majority of cases, an ultrasound can provide a specific diagnosis, whereas in others valuable supplemental information can be obtained. It is widely available and relatively inexpensive. It does not involve the use of ionizing radiation, which is a major advantage in pediatric practice; however, US of the gastrointestinal tract requires experience and patience. CT will be reserved for selected patients when further information is needed. Magnetic resonance (MR) imaging is seldom required as a primary imaging technique but supplements CT and ultrasound in select cases (jaundice, malignancy) (Carty 2002). The use of MR imaging is increasing on an emergency or semi-emergency basis in some instances including anomaly of the internal genitalia, ovarian torsion, and congenital biliary dilatation (Nosaka 2000; Carty 2002).

1.2.1 Intussusception

Intussusception is one of the most common causes of acute abdomen in infancy. Intussusception occurs when a portion of the digestive tract becomes telescoped into the adjacent bowel segment. This condition usually occurs in children between 3 months and 2 years of age. In almost all cases intussusceptions are idiopathic, that is, they do not have a demonstrated anatomic abnormality that functions as a lead point except for hypertrophied lymphoid tissue. The vast majority of childhood cases of intussusception are ileocolic. In the past, intussusception was a severe condition with high morbidity and mortality rates. Today, prompt diagnosis and effective nonsurgical reduction lead to a favorable outcome in most cases.

1.2.1.1 Diagnosis

The classic clinical presentation is characterized by acute (colic) abdominal pain with drawing up of the legs, currant-jelly stools or hematochezia, and a palpable abdominal mass. These findings, however, are present in less than 50% of children with intussusception (Daneman and Alton 1996). The onset of nonspecific abdominal symptoms in which vomitus predominates, the absence of passage of blood via the rectum (usually in cases of less than 48 h duration), and the inability to obtain a reliable clinical history may lead to dismissal of the diagnosis of intussusception in some cases. In some instances lethargy or convulsion is the predominant sign or symptom, this situation resulting in consideration of a neurologic disorder. Some cases in which the diagnosis is considerably delayed manifest as shock of unknown origin due to the progression of the disease to mechanical obstruction causing vascular comprise and bowel infarction. On the other hand, less than 50% of children with clinical findings suggestive of intussusception are shown to have this condition (del Pozo et al. 1999). Therefore, it is desirable to use diagnostic tools that are as innocuous as possible to avoid potential harm to these children, diminish any adverse effects on the actual diseases, and to lessen the discomfort of the children who are not shown to have intussusception. To this end, the traditional diagnostic approach to childhood intussusception of plain radiography and enema examination has been changed to plain radiography and US at most institutions, keeping the enema for therapeutic purposes.

Many plain radiographic signs of intussusception have been described. The most common is a soft-tissue mass, which is most often seen in the

right upper quadrant effacing the adjacent hepatic contour. Other signs include reduced air in the small intestine or a gasless abdomen, air in a displaced appendix, and obstruction of the small bowel (Gilsanz 1984; Sargent et al. 1994). The most specific plain radiographic findings are the "target sign" and "meniscus sign". The "target sign" consists of a soft-tissue mass that contains concentric circular or nearly circular areas of lucency, which are due to the mesenteric fat of the intussusceptum. The mass is most often seen in the upper right quadrant projecting over the right kidney (Ratcliffe et al. 1992) (Fig. 1.44). The "meniscus sign" consists of a crescent of gas within the colonic lumen that outlines the apex of the intussusception (the intussusceptum) (Fig. 1.45). Conversely, identification of a cecum filled with air or feces in the normal location is the finding that allows exclusion of intussusception with the most confidence (Sargent et al. 1994). However, plain abdominal radiography is normal in 40%–50% (Sargent et al. 1994; Meradji et al. 1994). Therefore, several authors do not recommend plain radiography if there is high clinical suspicion of intussusception (Verschelden et al. 1992), especially when the symptoms are of short duration. In such cases, US should be the initial imaging procedure (Woo et al. 1992; Daneman and Alton 1996; Riebel et al. 1993).

US has a high sensitivity for the diagnosis of intussusception (98%–100%) (Pracros et al. 1987; Riebel et al. 1993; Wang and Liu 1988). Because deep penetration of the ultrasound beam is not necessary in small children, a high-resolution transducer (5–10 MHz) can be used to improve the definition of the image. The majority of intussusceptions (i.e. the ileocolic type) occur in the

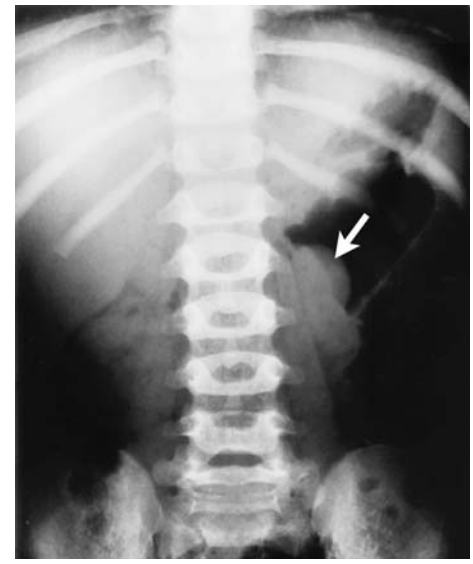

Fig. 1.45. Meniscus sign. Plain radiograph shows the meniscus sign: a rounded soft-tissue mass (the intussusceptum) protruding into the gas-filled transverse colon (*arrow*) [From del Pozo (1999)]

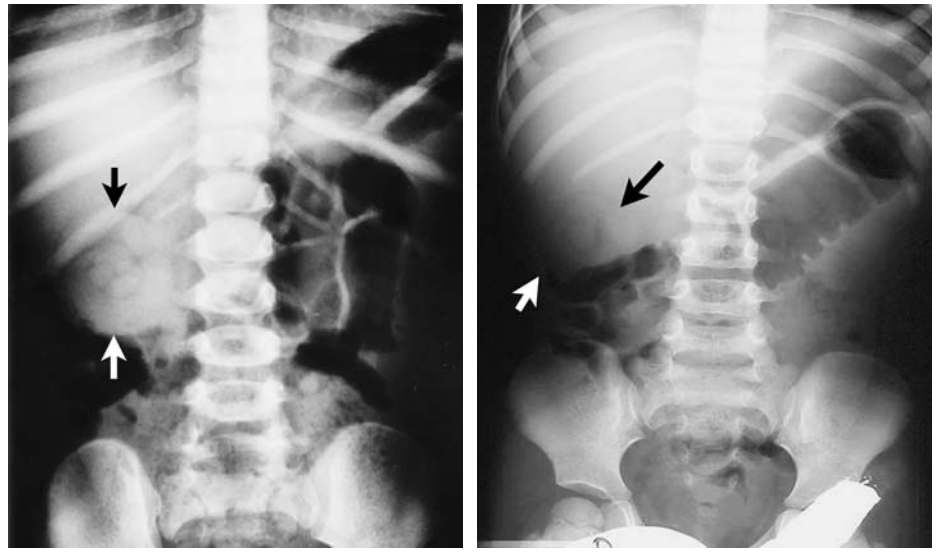

Fig. 1.44a,b. Target sign. **a,b** Two different patients. Plain radiographs show a round soft-tissue mass in the right upper quadrant (*arrows*). The masses contain a ring-like area of lucency [From del Pozo (1999)]

subhepatic region. The intussusception mass is a large structure, usually greater than 5 × 2.5 cm, that often displaces adjacent bowel loops. Early studies of the US appearance of intussusception reported a doughnut or pseudokidney appearance composed of a hypoechoic outer ring and a hyperechoic center (Swischuck et al. 1985). This appearance is similar to the US findings in other pathologic conditions of the gastrointestinal tract that cause thickening of the bowel wall. Appearances that are characteristic of intussusception include the "multiple concentric ring" sign (Holt and Samuel 1978) and "crescent-in-doughnut" sign (del Pozo et al. 1996a) on axial scans, and the "sandwich" sign (Pracros et al. 1987; Montali et al. 1983) and "hayfork" sign (Alessi and Salerno 1985) on longitudinal scans. In US of intussusception, the terms axial and longitudinal refer to the axis of the intussusception.

An intussusception is a complex structure (Fig. 1.46). The intussuscipiens (the receiving loop) contains the folded intussusceptum (the donor loop), which has two components: the entering limb and returning limb. The attached mesentery is dragged between the entering and returning limbs. The thickest component of the intussusceptum is the everted returning limb, which, together with the thin intussuscipiens, forms the hypoechoic outer ring seen on axial scans. The center of the intussusception contains the central or entering limb, which is of normal thickness and is eccentrically surrounded by the hyperechoic mesentery.

On axial US scans, intussusception has a variable appearance, which is primarily due to the amount of enclosed mesentery. Enclosed mesentery is absent at the apex of the intussusception and progressively increases toward the base (Figs. 1.46 and 1.47). Conversely, the everted limb of the intussusceptum is thicker at the apex than at the base. Therefore, an axial US scan obtained at the apex shows

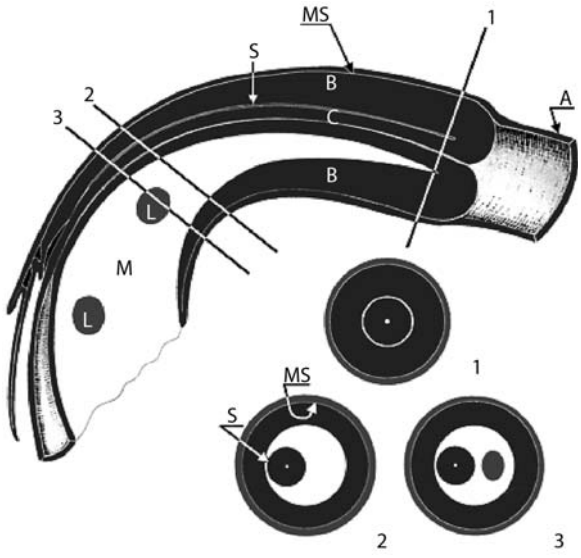

Fig. 1.46. Structure of an intussusception. Diagram shows a longitudinal view and three axial views of an intussusception; three bowel loops and the mesentery can be seen. The intussuscipiens (*A*) contains the two limbs of the intussusceptum: the everted returning limb (*B*), which is edematous, and the central entering limb (*C*), which is located at the center of the intussusception with the accompanying mesentery (*M*). The mesentery contains some lymph nodes (*L*). *MS*, contacting mucosal surfaces of the intussuscipiens and everted limb; *S*, contacting serosal surfaces of the everted limb and central limb. [From del Pozo (1999)]

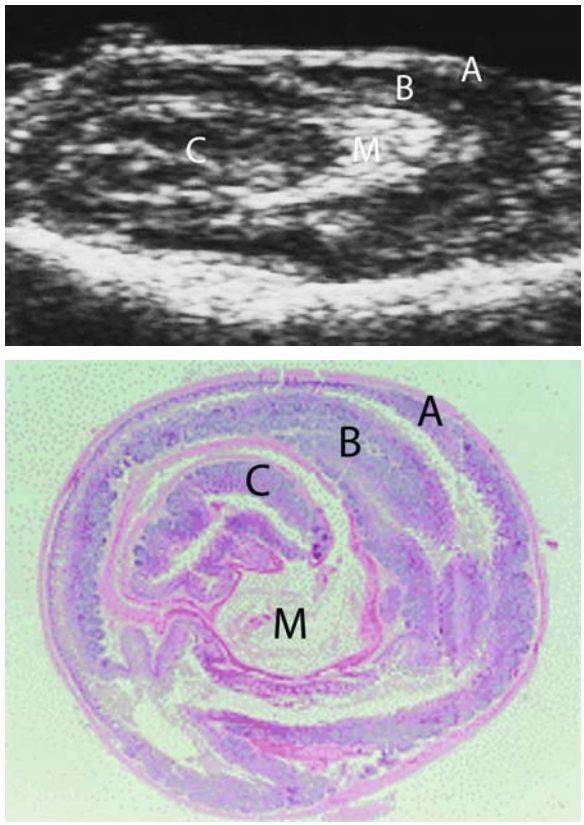

a

b

Fig. 1.47a,b. Correlation of sonographic and pathologic findings in intussusceptions in pigs. **a** Axial US scan; **b** corresponding pathologic specimen. Axial sections at the base show a doughnut sign with a peripheral hypoechoic ring (formed by the everted limb of the intussusceptum and the intussuscipiens) and a hyperechoic crescent shaped center due to the mesentery enclosing the hypoechoic central limb of intussusceptum (crescent-in-doughnut sign). *A*, intussuscipiens; *B*, everted limb of intussusceptum; *C*, central limb of intussusceptum; *M*, mesentery [From del Pozo (1996a)

a hypoechoic outer ring with a hypoechoic center. In some instances, multiple concentric rings can be seen near the apex. As the axial US study proceeds toward the base, the appearance changes gradually as increasing amounts of mesentery are included in the image. At the base, the amount of enclosed mesentery is maximal; the result is a hypoechoic outer ring with a hyperechoic, crescentic center (the crescent-in-doughnut sign) (Fig. 1.48).

On longitudinal US scans, it is the arrangement of the mesentery that causes variation in the appearance. If the middle of the intussusception is imaged along the longitudinal axis, three parallel hypoechoic bands separated by two nearly parallel hyperechoic bands are seen. The outer hypoechoic bands represent the edematous everted limb of the intussusceptum and the thin intussuscipiens; the central hypoechoic band is the central limb of the intussusceptum. The hyperechoic bands are caused by the mesentery that is dragged along with the bowel loop. This appearance is known as the sandwich sign (Fig. 1.49a). The hayfork sign is a variant of the sandwich sign that is seen at the apex of the intussusception. The pseudokidney sign occurs if the intussusception is curved or is imaged obliquely and the mesentery (at the point of maximal thickness) is demonstrated on only one side of the central limb of the intussusceptum (Fig. 1.49b). The hyperechoic mesentery often contains hypoechoic areas that correspond to lymph nodes, the cecoappendiceal complex, or vessels (del Pozo et al. 1999) (Fig. 1.50).

The presence of trapped peritoneal fluid within an intussusception correlates significantly with ischemia and irreducibility (del Pozo et al. 1996b). Such fluid, which reflects vascular compromise of the everted limb, accumulates between the serosal layers of both limbs of the intussusceptum. The mesentery acts as a wedge and impedes the exit of fluid into the peritoneal cavity (Fig. 1.51). On axial US scans, this complication appears as the double-crescent-in-doughnut sign. In addition to the usual crescent-in-doughnut appearance, there is an anechoic crescent that represents the trapped ascites (Fig. 1.51). Conversely, small amounts of free peritoneal fluid are seen in up to 50% of cases. The presence of this finding alone has not been definitely related to ischemia or an increased risk of perforation (Swischuk and Stansberry 1991). The absence of blood flow within the intussusception on Doppler US correlates with irreducibility but not definitely with bowel necrosis (Kong et al. 1997). The presence of blood flow at Doppler US suggests that the intussusception would be reduced (Fig. 1.52).

Most childhood cases of intussusception are idiopathic. Intussusception lead points such as a Meckel diverticulum, duplication cyst, polyp, or tumor (e.g. lymphoma) are uncommon in infants (< 5% of cases). Intussusception lead points are more common in neonates, older children (> 5 years old), and cases restricted to the small intestine. For example, intussusception of the small intestine is common in Peutz-Jeghers syndrome, Schönlein-Henoch purpura, and after surgery. US allows

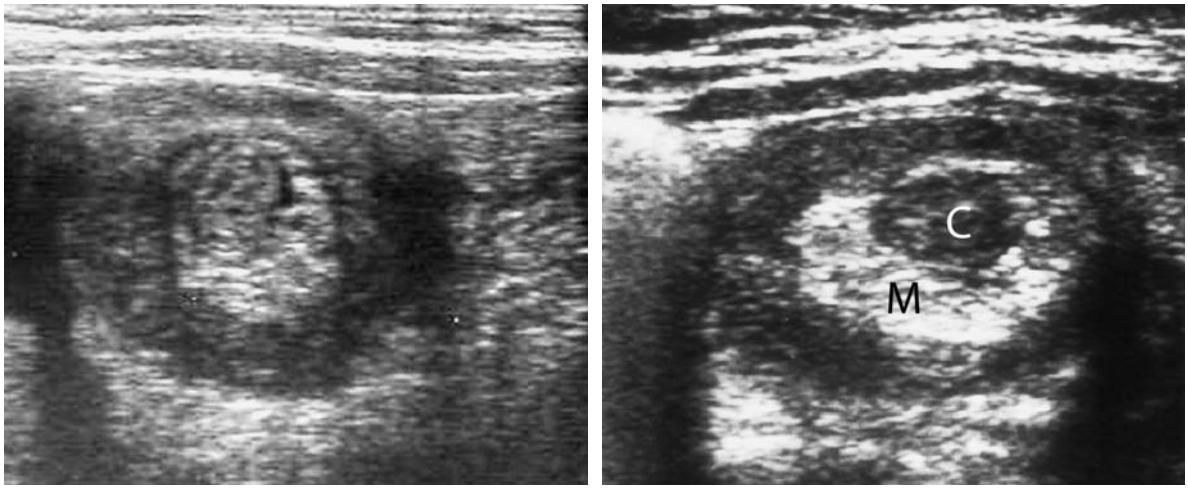

a b

Fig. 1.48a,b. The crescent-in-doughnut sign. Axial US scans obtained at the middle (apex proximal regions) (**a**) and at the base (**b**) of an intussusception, show the central limb of the intussusceptum (*C*) eccentrically surrounded by the hyperechoic mesentery (*M*), a situation that produces the crescent-in-doughnut sign [From del Pozo (1999)]

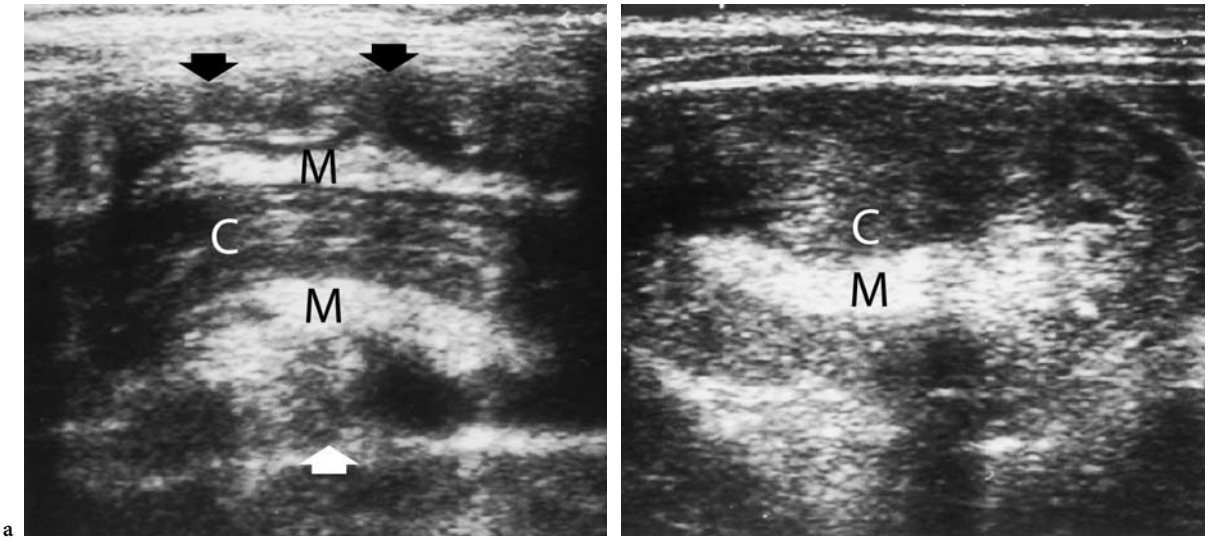

a b

Fig. 1.49a,b. Intussusception on longitudinal US scans. Variable appearance of intussusception on longitudinal US scans depending on which side of the central limb of the intussusceptum the mesentery is imaged. It may be depicted at one side (pseudo-kidney) or at both sides (sandwich). **a** US scan obtained in the strict longitudinal plane of an intussusception slightly away from the apex shows the sandwich sign. The outer hypoechoic bands (*arrows*) represent the everted limb of the intussusceptum beside the intussuscipiens. The two hyperechoic bands represent the mesentery. The central hypoechoic band represents the central limb of the intussusceptum. **b** US scan shows the pseudokidney sign. The mesentery is demonstrated on one side of the central limb of the intussusceptum. *C*, central limb of the intussusceptum; *M*, mesentery [From del Pozo (1999)]

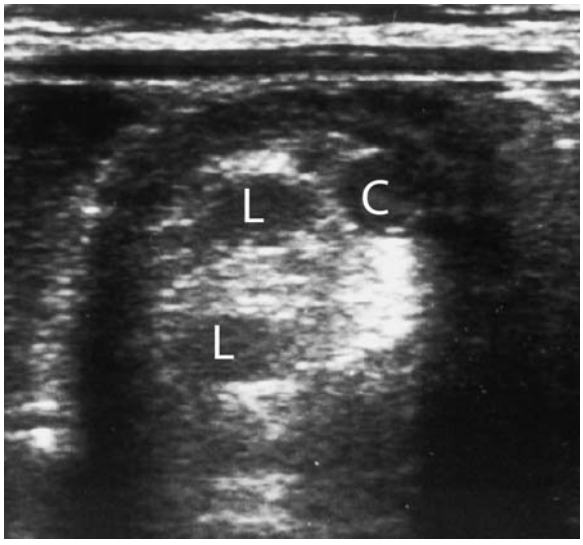

Fig. 1.50. Intussusception with lymph nodes (variant of the mesenteric crescent). Axial image at the base of the intussusception. The crescent-in-doughnut contains round mesenteric lymph nodes (*L*). *C*, the entering limb of the intussusceptum [From del Pozo (1999)]

better detection and characterization of lead points than a contrast enema study (Miller et al. 1995; Navarro and Daneman 2004b). Transient small-bowel intussusceptions that may reduce spontaneously are not infrequently identified on US or on CT studies (Navarro and Daneman 2004a; Strouse et al. 2003).

Barium enema examination has been the standard of reference for the diagnosis of intussusception for many years. The classic signs of intussusception at enema examination are the "meniscus" sign and "coiled spring" sign. The "meniscus" sign at enema examination is analogous to the "meniscus" sign at plain radiography and is produced by the rounded apex of the intussusceptum protruding into the column of contrast material. The "coiled spring" sign is produced when the edematous mucosal folds of the returning limb of the intussusceptum are outlined by contrast material in the lumen of the colon (Fig. 1.53).

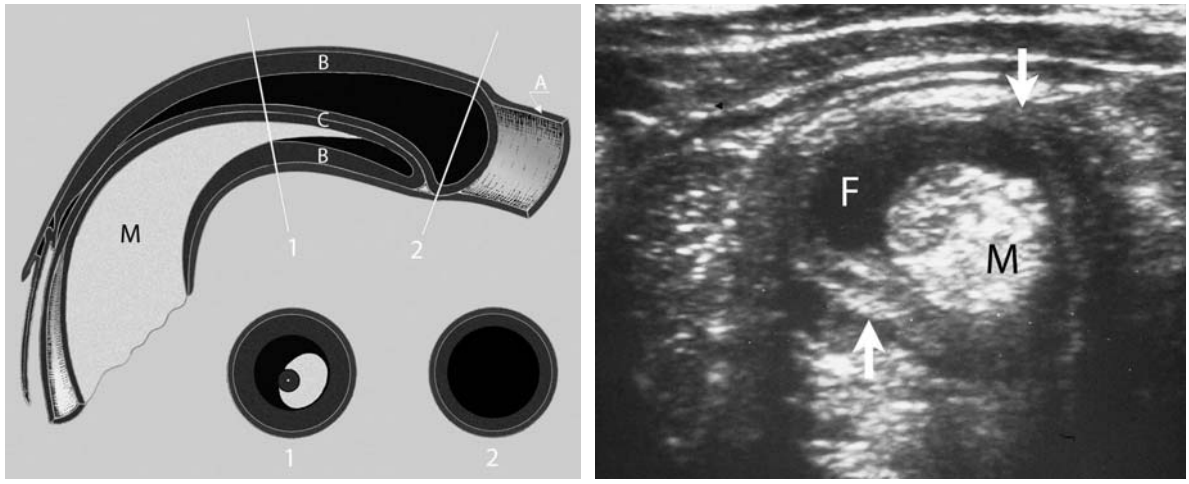

a b

Fig. 1.51a,b. Intussusception with trapped peritoneal fluid. **a** Schematic representation of an intussusception with the presence of fluid. Sagittal and axial images were obtained at different levels. Fluid collects between the serosal layers of both limbs of the intussusceptum; the returning limb is everted and compromised. The mesentery acts as a wedge which makes the exit of fluid into the peritoneum difficult. Dilatation at the apex of the intussusceptum, probably secondary to ischemia and to the increase in trapped fluid, occurs mainly at the antimesenteric border. This fact results in the asymmetric disposition of the area of fluid, which explains the appearance on axial US images. *1*, crescent-in-doughnut sign with additional anechoic crescent; *2*, everted intussusceptum filled with peritoneal fluid; *A*, intususcipiens; *B*, returning limb of the intussusceptum; *C*, entering limb of the intussusceptum; *M*, mesentery. The black areas represent fluid in the intussusception. **b** US scan of an intussusception with trapped peritoneal fluid. Axial US scan shows the double crescent-in-doughnut sign (*arrows*). There is the crescent-in-doughnut sign with an additional echo-free crescent that represents the trapped fluid (*F*). *M*, mesentery [From del Pozo (1996b)]

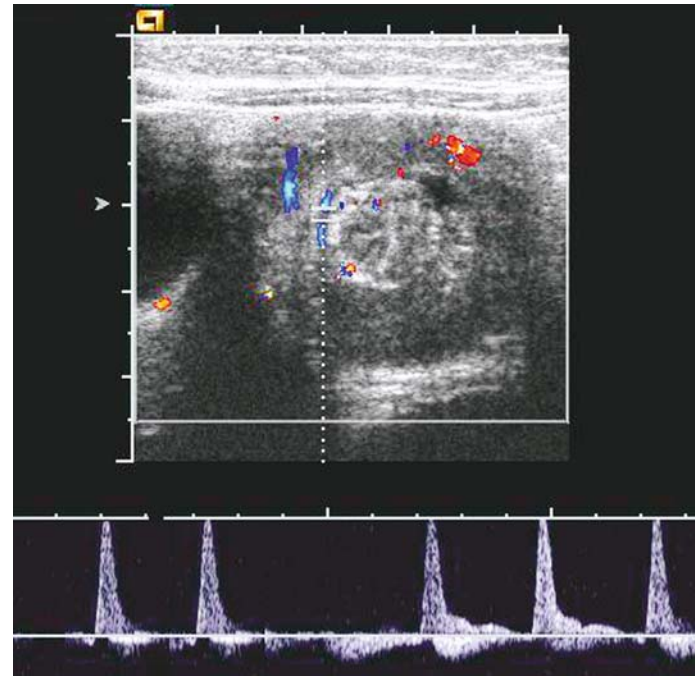

Fig. 1.52. Intussusception. Duplex Doppler sonography. Color Doppler indicates wall vascularity. High resistive index is observed in the vessels within the intussusception. This intussusception could be reduced

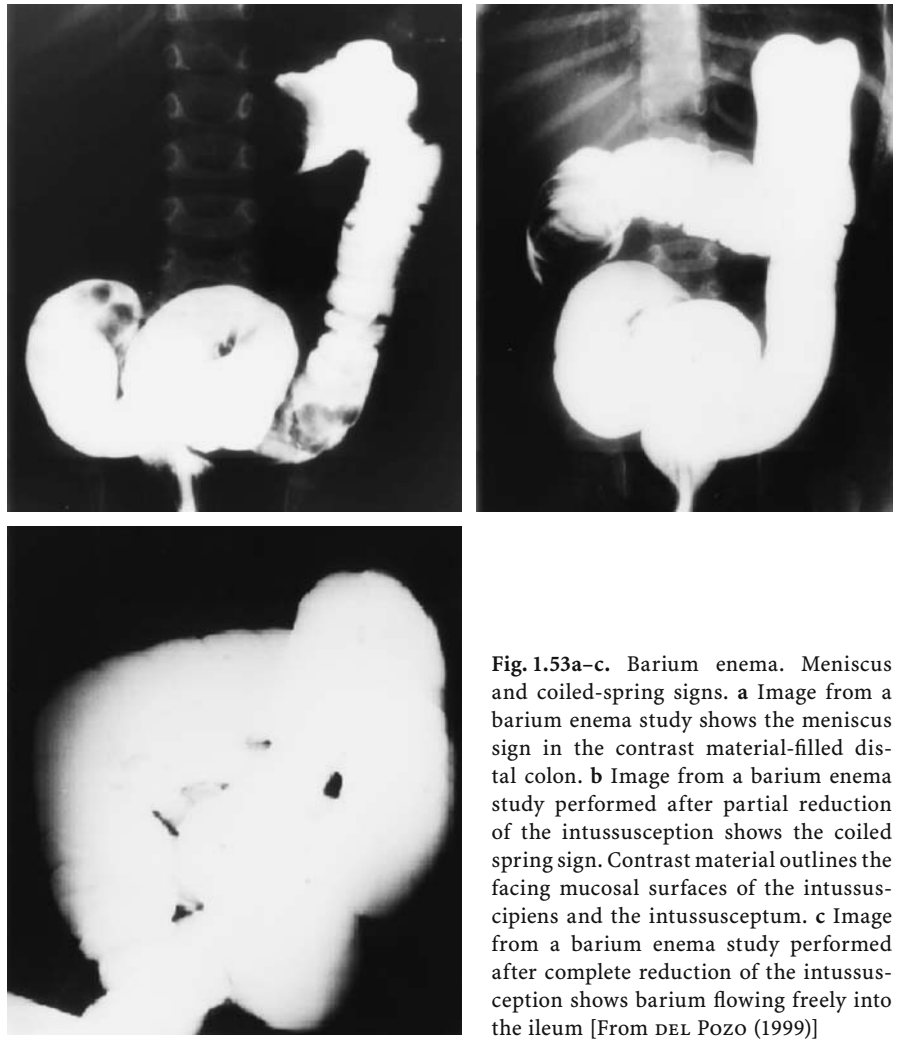

Fig. 1.53a–c. Barium enema. Meniscus and coiled-spring signs. **a** Image from a barium enema study shows the meniscus sign in the contrast material-filled distal colon. **b** Image from a barium enema study performed after partial reduction of the intussusception shows the coiled spring sign. Contrast material outlines the facing mucosal surfaces of the intussuscipiens and the intussusceptum. **c** Image from a barium enema study performed after complete reduction of the intussusception shows barium flowing freely into the ileum [From DEL POZO (1999)]

1.2.1.2 Treatment

Although there are reports of spontaneous reduction of intussusception (SWISCHUCK et al. 1994; NAVARRO and DANEMAN 2004a), chronic and recurrent intussusceptions, and rare cases of spontaneous sloughing of the gangrenous intussusceptum through the rectum (RAVITCH 1986), the usual course of an untreated intussusception is bowel obstruction followed by bowel perforation with peritonitis and septic shock. Currently, the overall perforation rate in developed countries is low (0%–3%).

Enema reduction is the standard non-operative method of treatment of intussusception. This may be guided with fluoroscopy when a barium, water-soluble, or air enema is used. US guidance is used when therapy is performed with a saline, water, or air enema. There is continuing discussion without vast agreement about which type of enema is the best for the reduction of intussusception. The few randomized studies that have been performed did not show statistically significant differences in reduction and perforation rates between air and liquid enemas (MEYER et al. 1993). The goal of any type of enema therapy is to reduce the intussusception by exerting pressure on the apex of the intussusceptum to push it from the pathologic position back to the original position. The reduction and perforation rates for a specific type of enema therapy are directly proportional to the pressure applied. RAVITCH (1986) found that the intracolonic pressure achieved by placing the barium enema bag 3.5 ft (105 cm) above the table did not reduce any intussus-

ception in which the intestine was necrotic or incarcerated. Further studies found that a pressure that did not exceed 120 mm Hg for hydrostatic enemas and 108 mm Hg for air enemas did not perforate the colon in animals (Shiels et al. 1993). The pressure can be controlled by measuring the height of the bag containing the fluid for a hydrostatic enema or using a manometer for an air enema. A pressure of 120 mm Hg is equivalent to a 100-cm column of barium or a 150-cm column of water or water-soluble contrast material (Kuta and Benator 1990). This theoretical pressure is reached during liquid enema therapy only if the diameter of the tubing of the system is sufficiently large to easily transmit the pressure. In hydrostatic enema therapy, the use of a rectal tube of large caliber may be more effective in increasing the actual intracolonic pressure than use of an increased column height (Schmitz-Rode et al. 1991). According to some experimental studies, the likelihood of perforation is smaller with the use of liquid compared to air enemas (Zambuto et al. 1995). There is no agreement on the number and duration of reduction attempts, the efficacy of premedication or sedation, the use of rectal tubes with inflatable retention balloons, or the use of transabdominal manipulation (Meyer 1992; Katz and Kolm 1992). This lack of agreement reflects the fact that no large studies have demonstrated a definite improvement in the reduction rate with any of these factors. According to the classic "rule of threes" the barium bag is suspended 3 ft above the examination table and three attempts over a maximum of 3 min are performed for reduction. This rule has been discarded at some institutions, and some authors use a nearly unlimited number of attempts. These authors even use delayed attempts, that is, they repeat the reduction attempt after the patient rests for up to several hours. The aim is to improve the reduction rate (Gonzalez-Spinola et al. 1999). Use of US guidance permits an even more liberal approach to enema therapy due to the lack of radiation exposure. Use of sedation had been thought to improve the reduction rate. However, sedation prevents the patient from performing the Valsalva maneuver during straining. This maneuver improves the effectiveness of enema therapy and protects against perforation, particularly during air enema therapy (Bramson et al. 1997). In theory, use of a rectal tube with a retention balloon creates a closed system that transmits the effective pressure of the enema material (liquid or air) without a loss of pressure. Use of such a rectal tube could increase the speed and effectiveness of enema therapy. However, this closed system could block the spontaneous expulsion of liquid or air when the pressure suddenly increases (Rohrschneider and Tröger 1995).

1.2.1.3 Types of Enema Therapies

Barium enema has been validated as an effective therapy by extensive experience over a long period. At some institutions, it remains the therapy of choice. However, there is a tendency to replace barium with other contrast agents, primarily because of the sequelae if perforation occurs during barium enema therapy (Bramson and Blickman 1992; Meyer 1992). The advantages and disadvantages of barium enema therapy are summarized in Table 1.2.

The use of water-soluble contrast agents in enema therapy has been supported in North America (Swischuk et al. 1994). The principal reason for use of these agents is to avoid the chemical peritonitis caused by barium if perforation occurs. There are few reports on the use of water-soluble contrast media. The reduction rate (80%) and perforation rate (3%) do not surpass those of other contrast agents (Swischuk et al. 1994).

Air enema therapy was not used for a long time in the Western Hemisphere but it has become popular in some countries, chiefly in North America (Gu et al. 1988; Shiels et al. 1991; Daneman and Navarro 2004), after successful experiences in Argentina and China (Guo et al. 1986) were reported. This method is quick and clean with a high reduction rate (73%–95%) and less radiation exposure than barium enema therapy (Fig. 1.54). The decreased radiation exposure is related to the shortened time required to achieve reduction and the milder (in terms of kilovolts and milliamperes) radiographic technique used. The average dose to reduce an intussusception by fluoroscopy is roughly estimated as 2567 mR (Henrikson et al. 2003). Air enema therapy requires precise control of the pressure and a thorough knowledge of the technique and potential complications. Immediate paracentesis using a large-caliber needle may be necessary if tension pneumoperitoneum is produced secondary to perforation during pneumatic reduction (Kirks 1994). The advantages and disadvantages of air enema therapy are summarized in Table 1.3. The most important studies of US guidance of intussusception reduction have been performed in the Eastern Hemisphere, where there is extensive experience with the technique, and in

Europe. The procedure is usually performed with saline solution (Fig. 1.55). Studies have shown a high reduction rate (76%–95%) with few complications, results similar to those of other hydrostatic methods (Wang and Liu 1988; Woo et al. 1992; Riebel et al. 1993; Rohrschneider and Tröger 1995). The principal advantage of this technique is the lack of radiation exposure. As a result, there is no limit to the procedure time, a fact that may improve the success rate. US has a high accuracy and reliability for monitoring the reduction process and for the visualization of all components of the intussusception, with easy recognition of pathologic lead points and residual intussusception when they exist. The easiest way to initiate an US-guided enema service could be to replace the contents of the barium bag with saline or warm water. To easily visualize the reduction process, the procedure should start at low pressures with the enema bag 60 cm above the table, and slowly raising the height of the bag. If the apex of the intussusception stops its retrograde course, the bag is progressively elevated. The reduction process can be easily monitored. If the apex of the intussusception has not been visualized passing through the

Table 1.2. Advantages and disadvantages of barium enema therapy

Advantages
– Maximum experience with this method
– Good results with optimized method (55%–90% of cases)
– Good evaluation of ileoileal residual intussusceptions
– Low perforation rate (0.39%–0.7%)
Disadvantages
– X-ray exposure required, thus limiting procedure time
– Perforation causes chemical peritonitis
– Visualization of only intraluminal content

Table 1.3. Advantages and disadvantages of air enema therapy

Advantages
– Excellent results (70%–95.6% of cases)
– Less X-ray exposure than with barium enema
– Easy, quick, clean technique
Disadvantages
– X-ray exposure required, thus limiting procedure time
– Higher perforation rate (0.14%–2.8%) with risk of tension pneumoperitoneum
– Visualization of only intraluminal content
– Less control of residual ileoileal intussusceptions

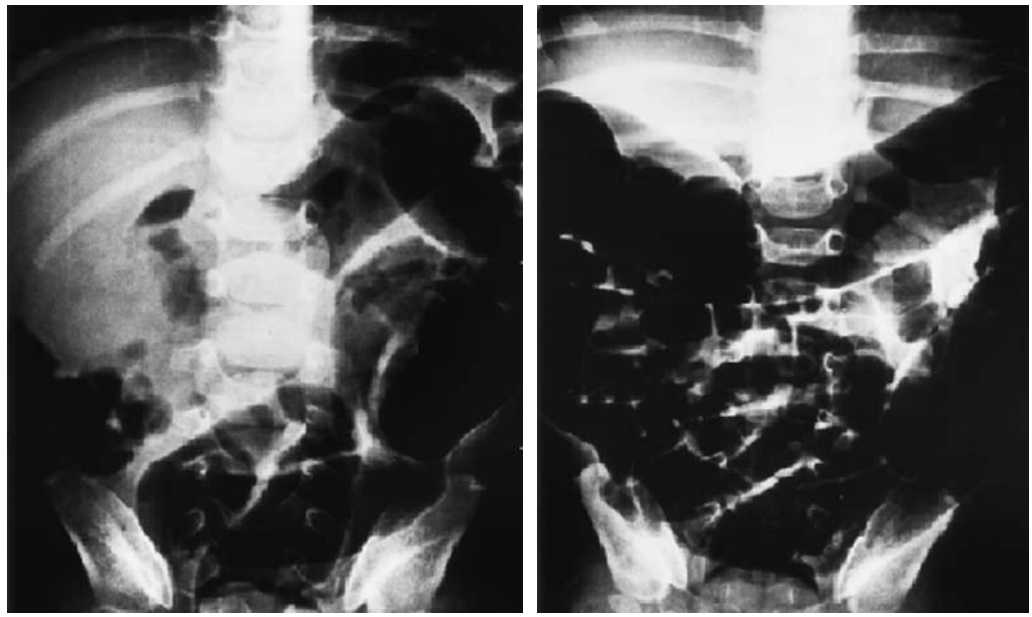

a b

Fig. 1.54a,b. Air enema therapy. **a** Image obtained at the beginning of an air enema study shows the meniscus sign and a mass in the middle of the upper abdomen. **b** Image obtained after complete reduction shows gas passing freely into the small intestine [From del Pozo (1999)]

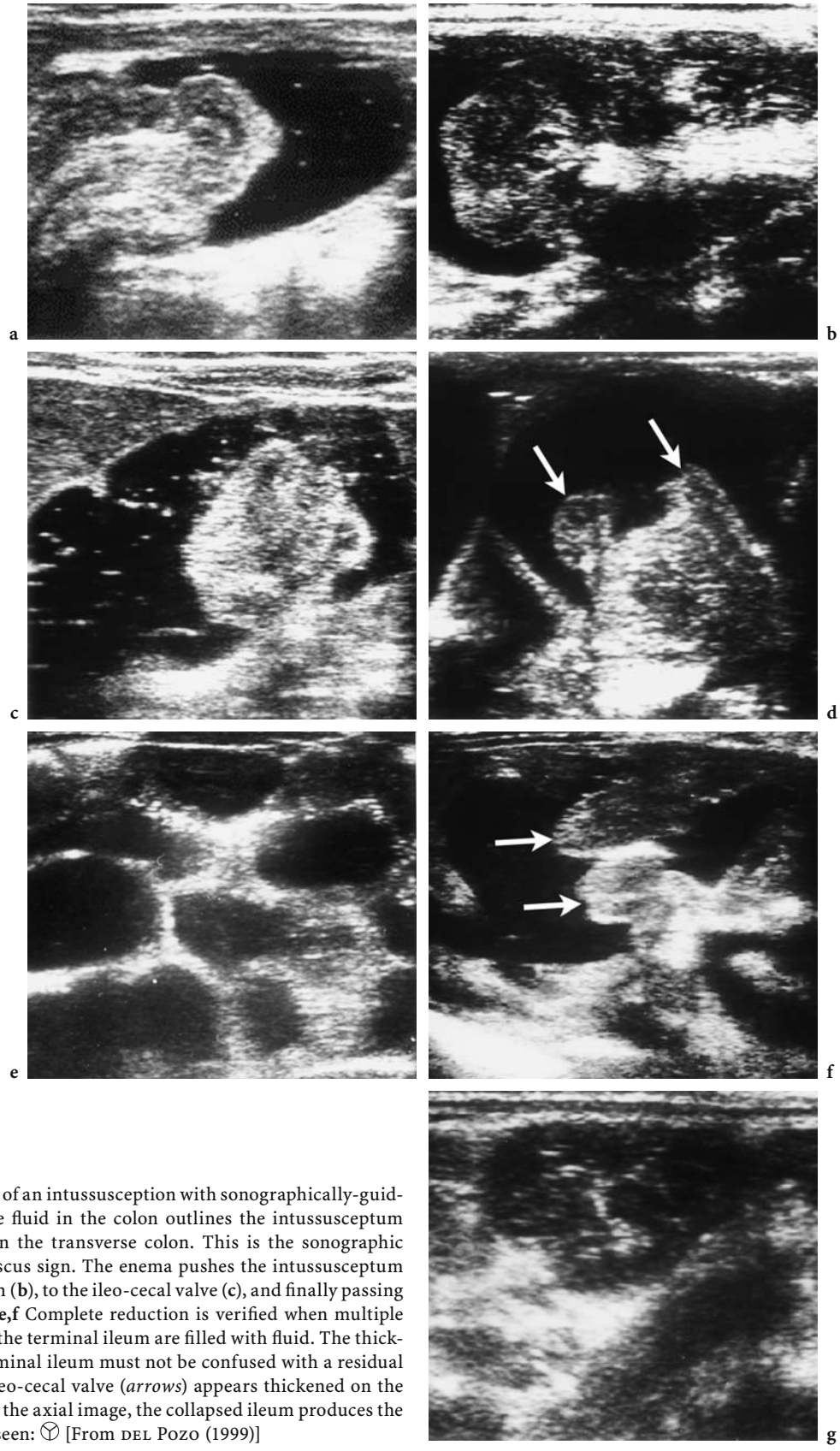

Fig. 1.55a–g. Reduction of an intussusception with sonographically-guided saline enema. **a** The fluid in the colon outlines the intussusceptum in its initial location in the transverse colon. This is the sonographic equivalent of the meniscus sign. The enema pushes the intussusceptum into the ascending colon (**b**), to the ileo-cecal valve (**c**), and finally passing through the valve (**d**). **e,f** Complete reduction is verified when multiple bowel loops, including the terminal ileum are filled with fluid. The thickened and collapsed terminal ileum must not be confused with a residual intussusception. The ileo-cecal valve (*arrows*) appears thickened on the longitudinal scan. **g** On the axial image, the collapsed ileum produces the "mercedes-benz" sign seen: ⊛ [From DEL POZO (1999)]

ileocecal valve and you are not sure that the reduction has been achieved, an ultrasound examination may be repeated some hours later (del Pozo 2005). The advantages and disadvantages of US-guided saline enema therapy are summarized in Table 1.4.

There has been little experience with US-guided air enema therapy. This modality attempts to unite the advantages of air enema therapy (quick and clean method, high reduction rate) with those of US guidance (no radiation exposure). Despite air preventing or hindering passage of the ultrasound beam, adequate visualization of the ileocecal valve and thus detection of perforation with pneumoperitoneum are possible and good results have been reported (Gu et al. 2000; Yoon et al. 2001). However, small residual ileoileal intussusceptions can be obscured by the presence of a large amount of intraluminal air. Intraluminal air could also interfere with a subsequent US study if one is required.

Definite contra-indications to enema therapy are shock that is not readily corrected with intravenous hydration, and an established perforation with clinical signs of peritonitis. Criteria that are linked to a lower reduction rate and a higher perforation rate, especially if more than one is present, are as follows: (a) patient age less than 3 months or greater than 5 years; (b) long duration of symptoms, especially if greater than 48 h; (c) passage of blood via the rectum (hematochezia); (d) significant dehydration; (e) obstruction of the small intestine; and (f) visualization of the dissection sign during enema therapy (Katz et al. 1993). The dissection sign refers to contrast material within the lumen of the intussuscipiens that "dissects" for a long distance over the surface of the intussusceptum. Two indicators of ischemia and irreducibility at US are fluid trapped within the intussusception (del Pozo et al. 1996b) and absence of blood flow at Doppler imaging (Kong et al. 1997). In cases with clinical or imaging high-risk factors, a more cautious and gentle approach is advisable during enema therapy.

In conclusion, plain radiography is of limited value in the diagnosis of intussusception. US, an accurate and safe modality, may also allow one to detect lead points and identify alternative diagnoses. Nonsurgical treatment of intussusception is possible in most cases. There is a trend toward performing enema therapy with agents other than barium (e.g. air, saline solution, water-soluble agents) as other agents will not stay in the peritoneal cavity if perforation occurs. In the absence of large, randomized studies, the reported differences in reduction and perforation rates are probably due more to complications that occurred before enema therapy, the pressures exerted, and the patient selection criteria than to the type of enema used. However, liquid agents appear to cause fewer perforations. Use of US guidance eliminates the disadvantage of radiation exposure, thus allowing a greater number of attempts at hydrostatic reduction.

Table 1.4. Advantages and disadvantages of US-guided saline enema therapy

Advantages
– No X-ray exposure, thus procedure time not limited
– Excellent results (76%–95.5% of cases)
– Visualization of all components of the intussusception
– Easier recognition of lead points and residual intussusceptions
– Low perforation rate (0.26%)
Disadvantages
– Less clean technique

1.2.2 Appendicitis

Acute appendicitis is the most common reason for emergency abdominal surgery in children. Up to 98% of operations required for abdominal pain are for suspected appendicitis.

Epidemiologic studies reveal that the lifetime risk of appendicitis is 8.6% for males and 6.7% for females. The lifetime risk of appendectomy is 12.0% for males and 23.1% for females (Addiss et al. 1990). These data stress the social and economic impact of appendicitis and the need to improve the diagnosis. The pathogenesis of appendicitis is conditioned by the specific "cul-de-sac" anatomy of the appendix being prone to develop ectasia, fecalith formation, obstruction and/or infection followed by ischemia, necrosis and perforation (Gray and Ashley 1986).

Diagnosis is based on clinical symptoms that include periumbilical or right lower quadrant (RLQ) pain, vomiting, nausea, fever and leucocytosis. Nevertheless, more than 30% of cases of appendicitis have atypical clinical presentations (Lewis et al. 1975), particularly in small children and in cases of unusual appendiceal location (Rothrock et al. 1991; Poole 1990). In addition, the presentation signs and symptoms of many nonsurgical condi-

tions may mimic those of acute appendicitis, and most children with suspected appendicitis do not have it. Cross-sectionals imaging have contributed to a marked reduction of unnecessary laparotomies and have decreased the complications caused by a delayed or wrong diagnosis (Ooms et al. 1991; Kosloske et al. 2004). Surgery is the treatment of choice. Early surgical intervention in patients with acute appendicitis prevents appendiceal perforation, which is associated with increased morbidity and mortality compared with nonperforating appendicitis. The most notable characteristic of perforated appendicitis is the presence of an appendiceal disruption and/or pus or feces in the abdominal cavity (Ooms et al. 1991). Histological diagnosis is divided into early, phlegmonous suppurative, and gangrenous appendicitis depending on the grade of the parietal polymorphonuclear infiltration and necrosis (Cotran et al. 1989).

1.2.2.1 Appendicitis Imaging

Plain abdominal radiographs have been used as the first imaging technique in suspected appendicitis. However, its diagnostic accuracy is limited. More than 50% of them are normal and when positive, radiological signs usually indicate perforation (Johnson and Coughlin 1989). This fact makes abdominal plain radiography useless in the early diagnosis of appendicitis and adds unnecessary cost and radiation exposure. Appendicolith is the only specific sign (10% of cases) of appendicitis. When this finding is associated with abdominal pain, the chance of having appendicitis is 90%, and at least 50% of them have perforated or gangrenous appendicitis (Holgersen and Stanley-Brown 1971) (Fig. 1.56a).

US is a widely available and inexpensive modality with the potential for highly accurate imaging in the patient suspected of having acute appendicitis. The utility of US lies primarily in children with equivocal clinical findings, both to establish the diagnosis of appendicitis and to aid in diagnosis of other abdominal and pelvic conditions that may mimic appendicitis, particularly gynecological diseases. In experienced hands, the inflamed appendix can be demonstrated in 90% of patients with appendicitis (Puylaert 2001). High-resolution transducers (5 and 15 MHz), familiarity with the RLQ anatomy, experience, and patience are necessary. The graded compression US technique described by Puylaert (Puylaert 1986) is helpful in positioning the appendix into the most focused area of the ultrasonographic beam and to displace and compress bowel loops, but is not always required in children. The peritoneal cavity is screened for bowel pathology with five or six vertically orientated, overlapping lanes using a broad-based probe. Puylaert (2003) refers to this as "moving the lawn." The examination begins with identification of the ascending colon, which appears as a nonperistaltic structure containing gas and fluid. The transducer is then moved inferiorly to identify the terminal ileum, which is easily compressible and displays active peristalsis. The cecal tip where the appendix arises is approximately 1–2 cm below the terminal ileum (Sivit 2001).

The normal appendix can be detected on US in more than 80% of asymptomatic patients (Rioux 1992; Wiersma et al. 2005). It may be identified as a tubular, mobile and blind-ended structure, measuring 6 mm or less in the anteroposterior diameter (Jeffrey et al. 1988; Vignault et al. 1990). As with any intestinal bowel loop, five concentric layers that are alternately hyperechoic and hypoechoic can be identified corresponding from inner to outer: hyperechoic mucosal surface, hypoechoic mucosa, hyperechoic submucosa (due to vessels, connective tissue and fat content), hypoechoic muscular, and hyperechoic serosa sometimes in smooth continuity with the hyperechoic periappendicular fat (Kimmey et al. 1989) (Fig. 1.57). The most prominent layer of the normal appendix in children is the hypoechoic mucosa due to the follicular lymphoid tissue of the mucosal lamina propria (Spear et al. 1992).

Several authors have reported a marked overlap of diameters of normal and acutely inflamed appendices measured on US in children. In 1997, Hahn et al. found diameters of 6 mm or more in 79 (82%) of 96 cases of histologically proven normal appendices with lymphatic hyperplasia. They therefore concluded that high diagnostic accuracy in children can be achieved only by considering several US criteria simultaneously, including appendiceal compressibility, location of the point of tenderness, presence of hyperechoic periappendiceal inflamed fatty tissue, appendiceal shape, appendicoliths, air in the appendiceal lumen, and blood flow in the appendiceal wall detected on color Doppler US (Rettenbacher et al. 2001). Furthermore, the analysis of morphologic appendiceal changes may add enough information to avoid the limitation of the nonspecific numerical (6-mm diameter) criteria in

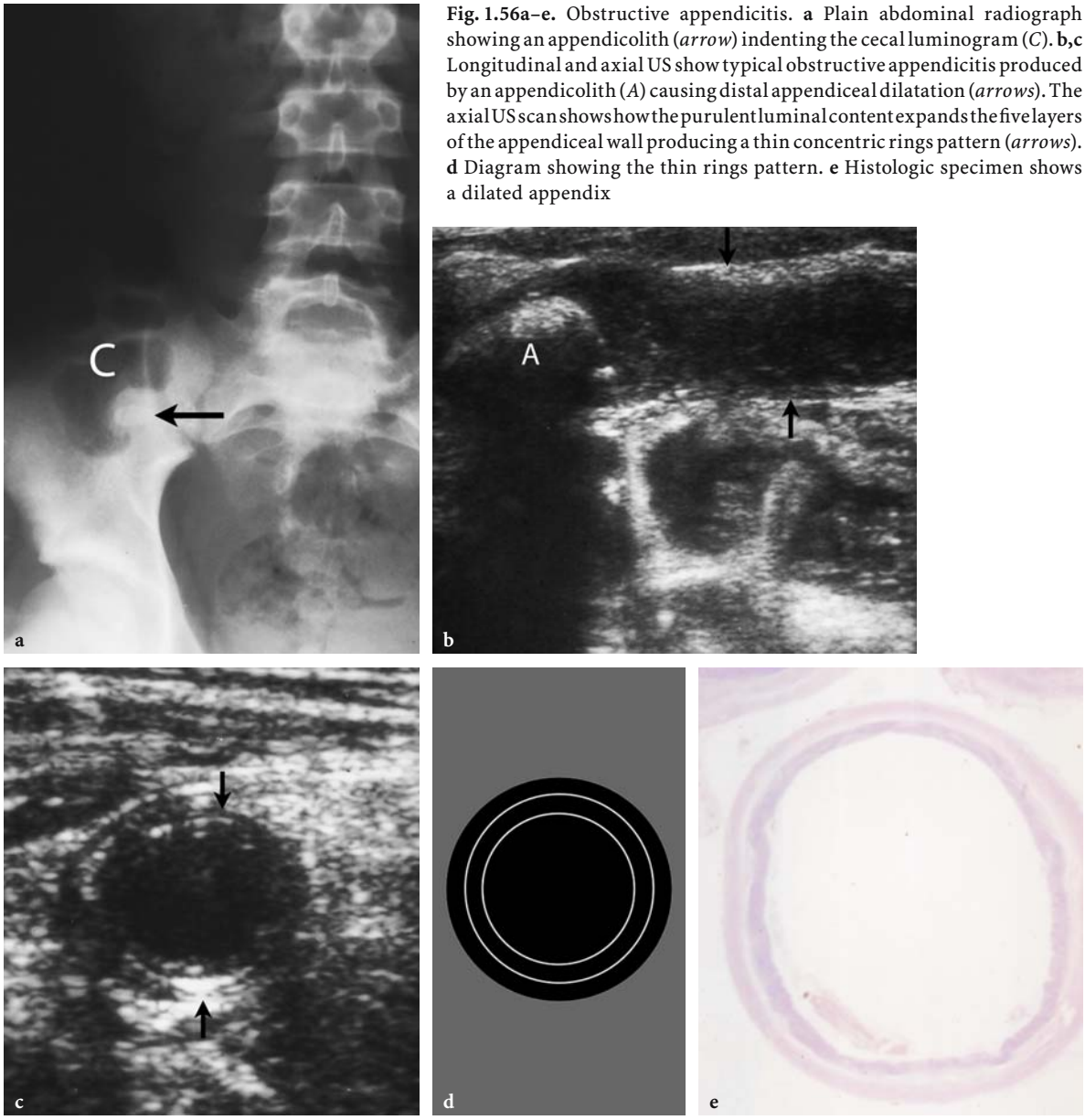

Fig. 1.56a–e. Obstructive appendicitis. **a** Plain abdominal radiograph showing an appendicolith (*arrow*) indenting the cecal luminogram (*C*). **b,c** Longitudinal and axial US show typical obstructive appendicitis produced by an appendicolith (*A*) causing distal appendiceal dilatation (*arrows*). The axial US scan shows how the purulent luminal content expands the five layers of the appendiceal wall producing a thin concentric rings pattern (*arrows*). **d** Diagram showing the thin rings pattern. **e** Histologic specimen shows a dilated appendix

the accurate diagnosis of appendicitis. Based on our own experience (del Pozo et al. 1992) and appendiceal anatomic considerations (Spear et al. 1992; Puylaert 1990; Borushok et al. 1990), distinctive axial US patterns have been organized (three/two/one ring) to help in appendiceal identification and in evaluating the involvement stage. Each of the three rings closely correlates to one of the hyperechoic anatomical layers, from inner to outer: mucosal surface, submucosa, and serosa. Like a countdown, the progressive loss of those rings leads to perforation (3 rings, 2 rings, 1 ring, perforation) (Fig. 1.58). The centrifugal loss of the hyperechoic appendiceal layers (rings) and, outside the organ, the periappendicular fat prominence, the irregularity of the appendiceal contour, and the presence of collections or echogenic ascites, are linked to increasing inflammation and necrosis.

In US examination, the inflamed appendix enlarges (greater than 6 mm in AP diameter), becoming a noncompressible structure (Puylaert 1986; Jeffrey et al. 1988). Initially, the transmural involvement stresses the concentric layered appearance of the normal appendix, turning from a rela-

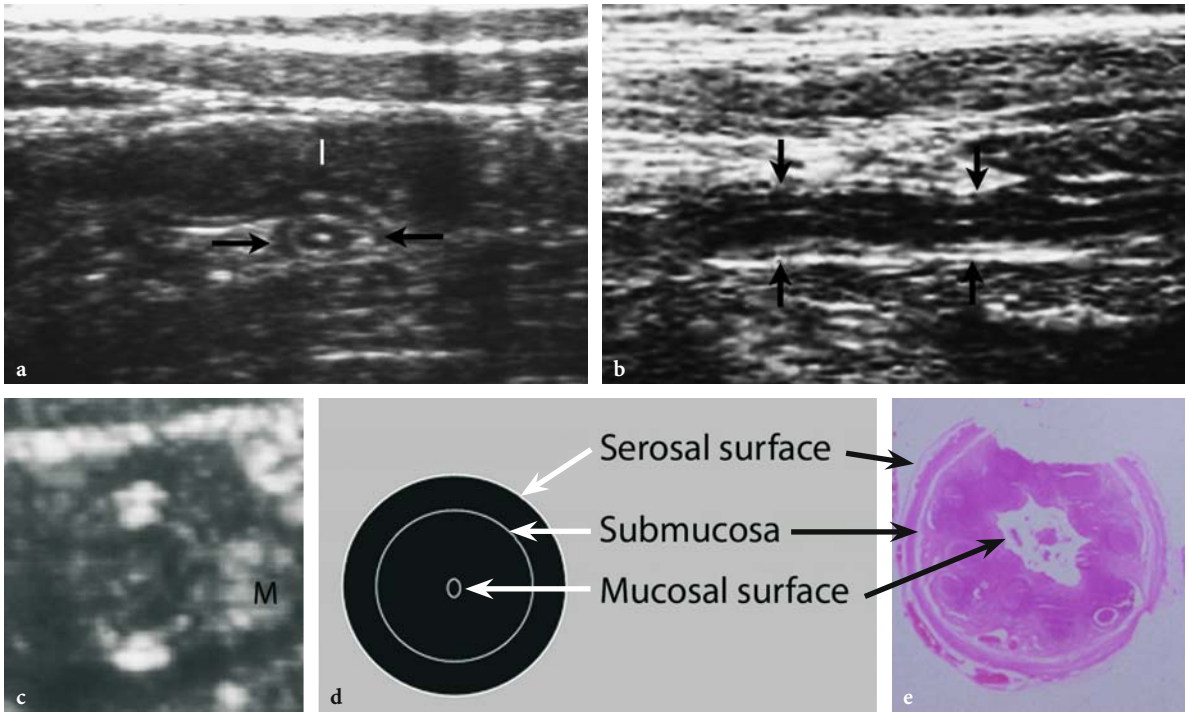

Fig. 1.57a–e. US images of the normal appendix. **a** Round transverse section of the proximal part of a normal appendix (*arrow*) behind the terminal ileum (*I*). "Target" appearance with patent concentric layers. **b** Longitudinal section of a normal appendix (*arrows*) showing five layers that are alternately hyperechoic and hypoechoic from inner to outer: hyperechoic mucosal surface, hypoechoic mucosa, hyperechoic submucosa, hypoechoic muscular, and hyperechoic serosa. The hypoechogenicity of the mucosa corresponds to the follicular lymphoid tissue of the mucosal lamina propria, the most prominent layer of the normal appendix in children. **c** Normal appendix with the lumen collapsed surrounded by ascites. The fatty mesoappendix (*M*) appears as a tiny hyperechoic structure close to the appendix. Compared **c** with **d**, **e** Diagram and histologic specimen show the hyperechoic appendiceal layers as three concentric rings, **e** Histologic specimen showing lymphoid hyperplasia

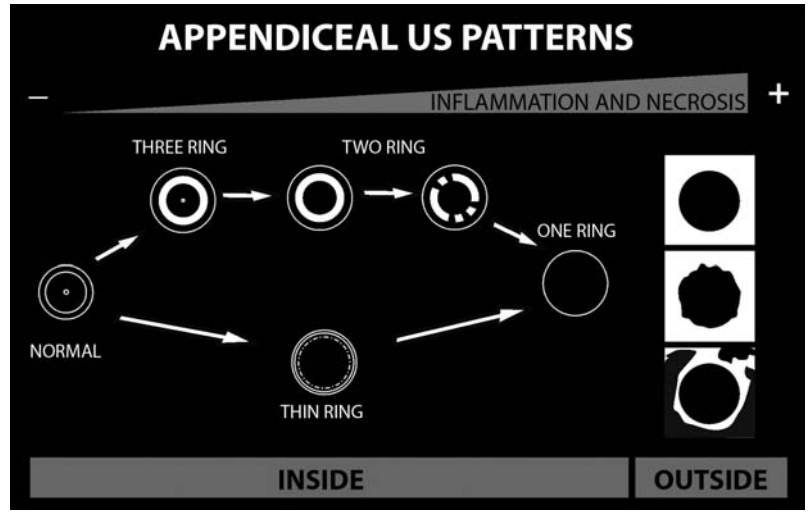

Fig. 1.58. The illustration represents US axial slides of the appendix. The hyperechoic layers (*RINGS*) correspond to the mucosal surface (*MS*), submucosa (*SB*) and serosa layers (*SE*). When inflammation progresses, these rings gradually disappear from inner to outer. Normal appendix: AP diameter ≤ than 6 mm, mucosal predominance. Three rings pattern: AP diameter > than 6 mm, collapsed lumen and submucosal prominence. Thin rings pattern: AP diameter > than 6 mm, dilated lumen and thinned wall: Patent SB and SE with subtle mucosal surface. Two rings pattern: non-visible central spot or inner ring (*MS*). The appendiceal center may represent either the inflamed mucosa or hypoechoic content. Both the submucosa and serosa are preserved. One ring pattern: Appendix homogeneously hypoechoic. Only serosal layer is preserved. Non-visible mucosa and submucosa. When inflammation progresses, outside the appendix prominence of periappendicular fat, appendicular contour irregularity and, finally, the presence of loculated collections or echogenic ascites are observed. As in a count-down, the progressive loss of those rings leads to perforation (3 - 2 - 1 - perforation) [From DEL POZO (1994)]

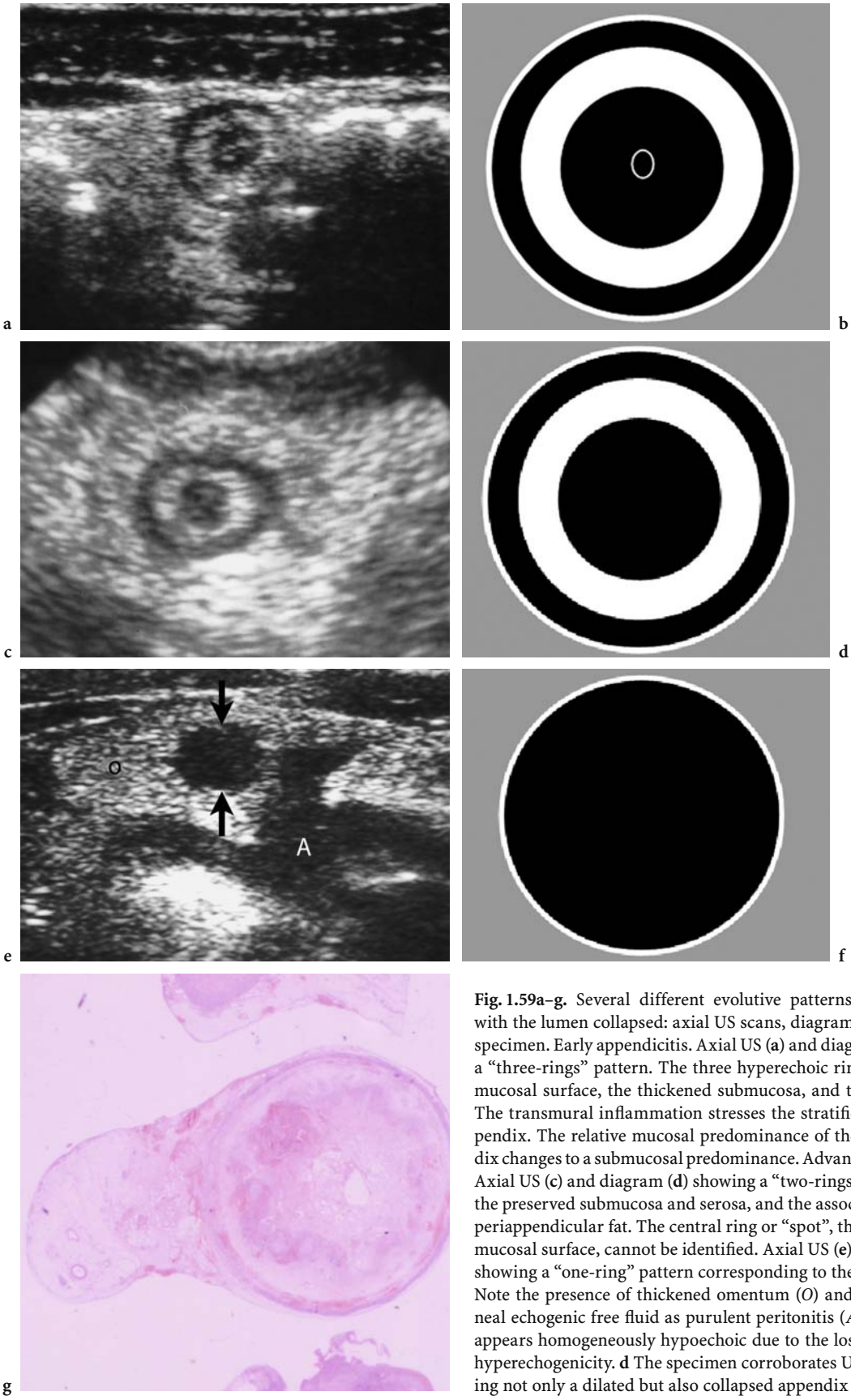

Fig. 1.59a–g. Several different evolutive patterns of appendicitis with the lumen collapsed: axial US scans, diagrams, and histologic specimen. Early appendicitis. Axial US (**a**) and diagram (**b**) showing a "three-rings" pattern. The three hyperechoic rings represent the mucosal surface, the thickened submucosa, and the serosa layers. The transmural inflammation stresses the stratification of the appendix. The relative mucosal predominance of the normal appendix changes to a submucosal predominance. Advanced appendicitis. Axial US (**c**) and diagram (**d**) showing a "two-rings" pattern. Notice the preserved submucosa and serosa, and the associated prominent periappendicular fat. The central ring or "spot", that represents the mucosal surface, cannot be identified. Axial US (**e**) and diagram (**f**) showing a "one-ring" pattern corresponding to the serosa (*arrows*). Note the presence of thickened omentum (*O*) and the intraperitoneal echogenic free fluid as purulent peritonitis (*A*). The appendix appears homogeneously hypoechoic due to the loss of submucosal hyperechogenicity. **d** The specimen corroborates US findings showing not only a dilated but also collapsed appendix in appendicitis

tive mucosal to a submucosal predominance. In this early stage the appendix may be found with the lumen collapsed appearing as a target or a three-ring pattern (Fig. 1.59a,b), or with the lumen dilated and some grade of wall thinning, which would lead to a thin-rings pattern on axial US scan (Fig. 1.56). In this last appearance, the layers are expanded by a usually hypoechoic purulent content. In a more advanced stage the appendiceal diameter increases and the central ring or "spot" corresponding to the mucosal surface cannot be identified, making it difficult to evaluate whether the hypoechoic center corresponds to the inflamed mucosa or to the intraluminal content. The serosa and submucosa are preserved giving rise a two-rings pattern (del Pozo et al. 1994) (Fig. 1.59c,d). Finally, necrosis and suppuration lead to the loss of the submucosa hyperechogenicity, and the appendix tends to appear homogeneously hypoechoic surrounded by the serosa: one-ring pattern (Figs. 1.59e–g and 1.60) (Borushok et al. 1990; Vignault et al. 1990). The accurate identification of the different appendiceal layers demands a careful technique examination and the use of an appropriate transducer. Otherwise, we can easily mistake thin rings for a one-ring pattern, misinterpreting as a higher grade of involvement than really exists. Because of fluid content, the structure should have posterior enhancement, but its identification is often impaired due to the small appendiceal size and the particular echogenic quality of the surrounding structures.

All patterns may coexist in the same appendix. Furthermore, one of the appendiceal ends may remain normal while the opposite is inflamed, so it is very important to image the full appendix (Nghiem and Jeffrey 1992). An appendicolith may also be identified coexisting with each pattern, even in normal appendices. Appendicoliths appear as bright, echogenic foci with clean distal acoustic shadowing. Their identification within the appendix or in the adjacent perienteric soft tissue after perforation is highly associated with a positive diagnosis. Failure to see an appendicolith, in contrast, is noncontributory (Birnbaum and Wilson 2000) (Fig. 1.56).

A significant number of appendicitis may have an atypical location, producing a long-standing process and, less frequently, involving other organs. If the appendix cannot be identified in the RLQ, the entire abdomen should be systematically examined, because it may locate retrocecally (20%–25% of cases) or pelvic (7.9% of cases) (Collins 1932). Lateral approach through the flank may facilitate the US identification of retrocecal appendix, which lies posterolaterally to the cecum and would be hidden by the cecal air (Ceres et al. 1990).

Loss of visualization of submucosa layer, prominent periappendicular fat and periappendicular fluid (loculated fluid collection) have been related to a higher rate of perforation (Borushok et al. 1990) (Fig. 1.61). Perforation is more frequent in infants and small children and, at these ages, it is often free. The pneumoperitoneum secondary to an appendiceal perforation is extremely rare. Echogenic ascites implies purulent peritonitis in a free perforation, being the most important finding. A perforated

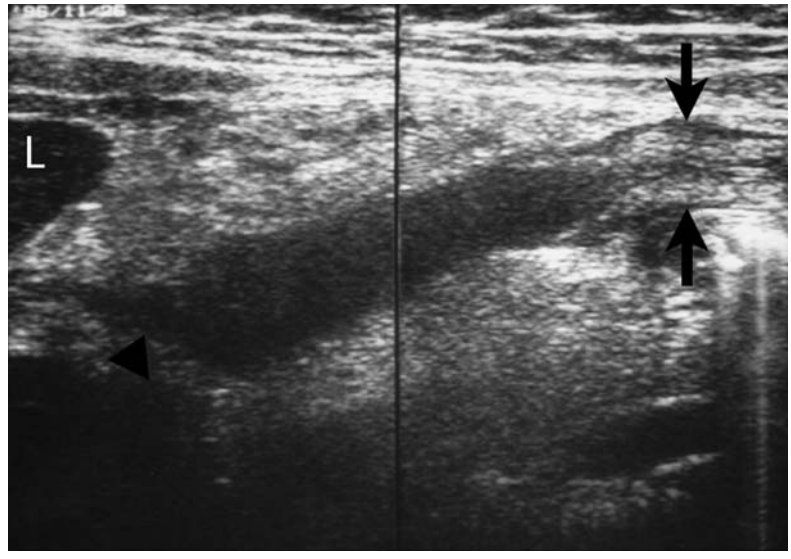

Fig. 1.60. Several patterns of appendicitis in the same appendix. Longitudinal US scan, from the right lower quadrant to the subhepatic region summarizes all the different appearances of appendicitis, showing at the base (*arrows*) the five conspicuous appendiceal layers with the patent mucosal surface and the prominent submucosa layer. These layers begin disappearing from the appendiceal base to the tip. Notice the associated thickened omentum encircling the appendix and trying to prevent the dissemination of the process. Also note the irregularity at the tip contour due to discrete inflammatory collection in the appendicular periphery (*arrowhead*). *L,* liver

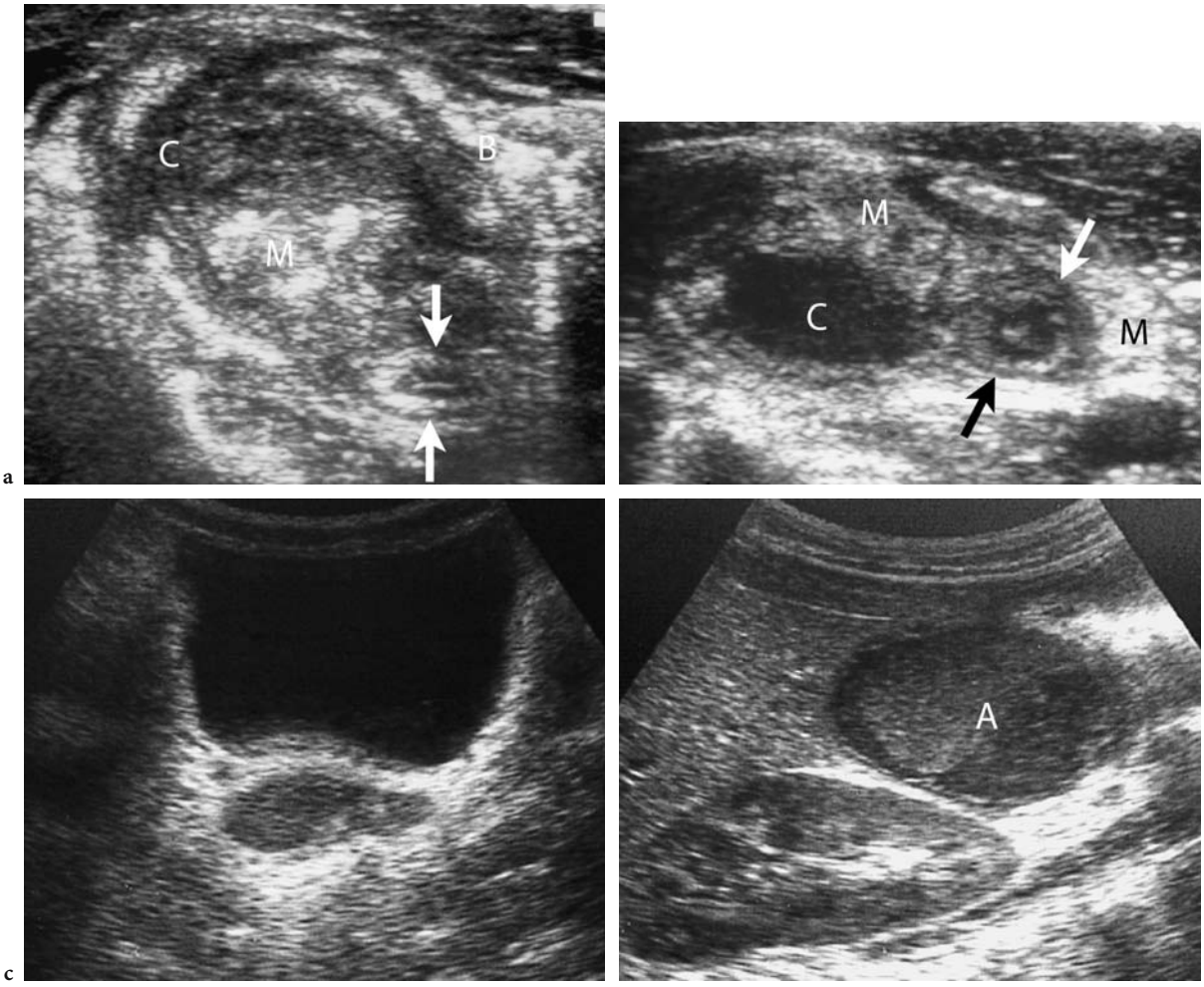

Fig. 1.61a–d. Perforated appendicitis: phlegmon and abscess. **a,b** Phlegmon. Inflammatory mass composed of a complex fluid collection (*C*), prominent mesenteric fat (*M*), and adjacent thickened poorly defined intestinal bowel loops (*B*) just close to the appendiceal remnants (*arrows*). **c,d** Abscesses. Distant multiple abscesses in the pouch of Douglas and in the subhepatic region. *A*, abscess

appendix is difficult to identify, as it tends to be collapsed, partially destroyed, and generally hidden behind the dilated loops. Generalized peritonitis can produce distant abscesses (Fig. 1.61c,d).

Appendicitis may resolve spontaneously either in noncomplicated or perforated forms. Follow-up US examinations have shown these infrequent spontaneous resolutions. They are considered as a false positive diagnosis in most of the published studies, due to unavailability of surgical and pathological confirmation (Jeffrey et al. 1987). Spontaneously resolving appendicitis occurs in at least 1 in 13 cases of appendicitis and has an overall recurrence rate of 38%, with the majority of cases recurring within 1 year. It is difficult to make therapeutic recommendations with this intermediate recurrence rate (Cobben et al. 2000). The lack of US criteria in predicting the evolution of these cases leaves conservative management an alternative. On the other hand, when resolution is achieved, recurrence is not the rule, and interval or prophylactic appendectomies may be unnecessary (Puylaert 1990).

Color Doppler US may be useful in easily identifying the inflamed appendix. Color Doppler US is useful as an additional positive finding of appendicitis in uncertain cases of borderline appendiceal size (around 6 mm). Circumferential color in the wall of the inflamed appendix on color Doppler US images reflecting inflammatory hyperperfusion is strongly supportive evidence of active inflamma-

tion (Birnbaum and Wilson 2000) (Fig. 1.62). With gangrene, color Doppler US may show decreased or no perfusion. With perforation of the appendix, the hyperemia seen in the inflamed appendix extends to the inflamed periappendiceal fat, as seen at color Doppler US (Fig. 1.63).

CT is a highly accurate and effective cross-sectional imaging technique for diagnosing and staging acute appendicitis. The advantages over US are reduced operator dependence, superior contrast sensitivity, and the capability for viewing the entire range of air, soft-tissue, fat, and bone attenuation values inherent to the abdomen (Sivit et al. 2000). CT is also more useful than US for evaluating complications such as phlegmon and abscess formation, as well as for delineating the location and extent of associated fluid collections. The smaller amount of intraabdominal fat in children compared with that of adults may contribute to the relative low rate of normal appendix detection at CT (12%) published in some studies (Kaiser et al. 2002) (Fig. 1.64). Controversy remains in the literature regarding the use of oral, rectal, or intravenous contrast agents and the question of whether the area scanned should be limited to the lower abdomen and pelvis or extended to the full abdominopelvic cavity (Taylor 2004). The highest diagnostic efficacy has been obtained with the use of rectal contrast material and thin collima-

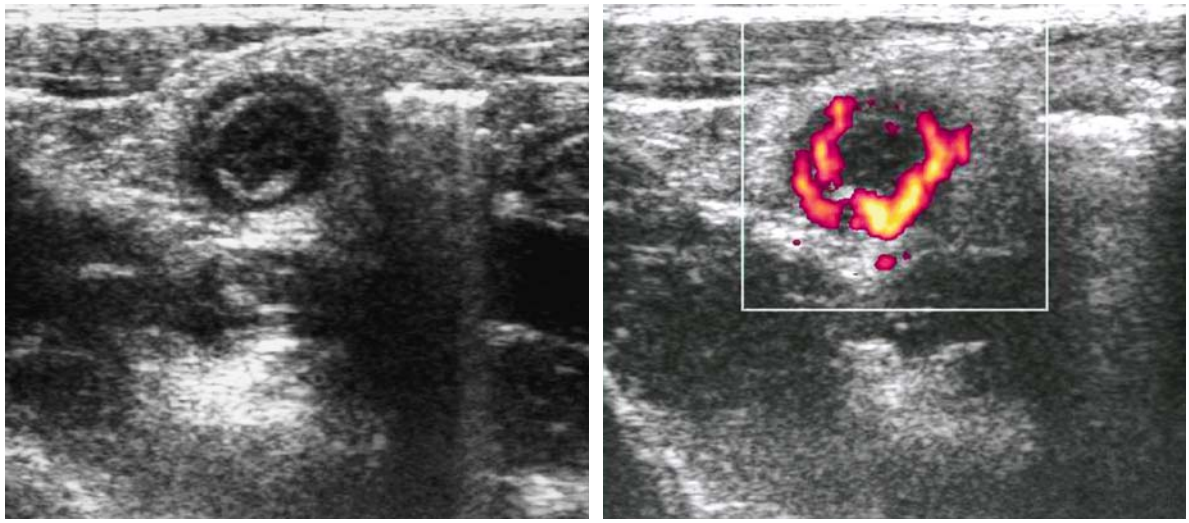

a b

Fig. 1.62a,b. Acute appendicitis on color Doppler US. **a** B-mode US axial scan showing a two-ring-pattern appendicitis. **b** Color Doppler demonstrates hyperemia of the appendiceal wall manifested as an increased circumferential color flow, mostly in the submucosal layer

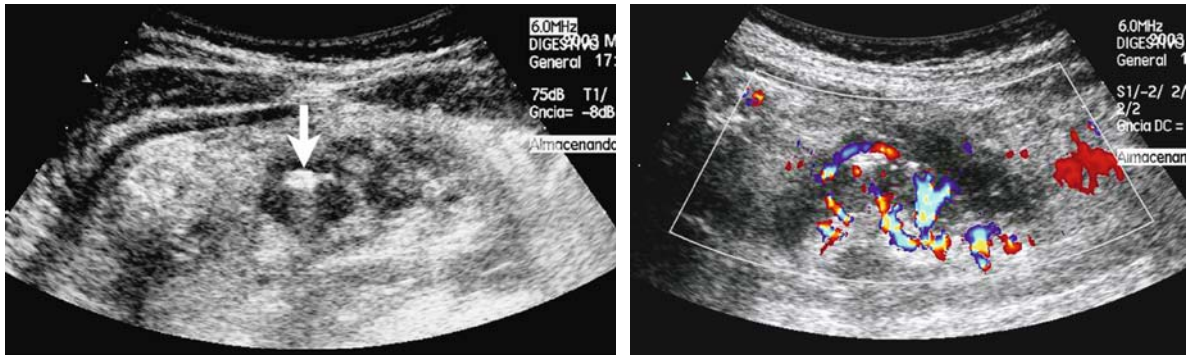

a b

Fig. 1.63a,b. Perforated appendicitis. **a** Axial US scan shows air within the appendiceal dilated lumen (*arrow*) and enlargement of the periappendicular fat. **b** Color Doppler demonstrates the enlarged periappendicular tissue to correspond to an inflammatory mass

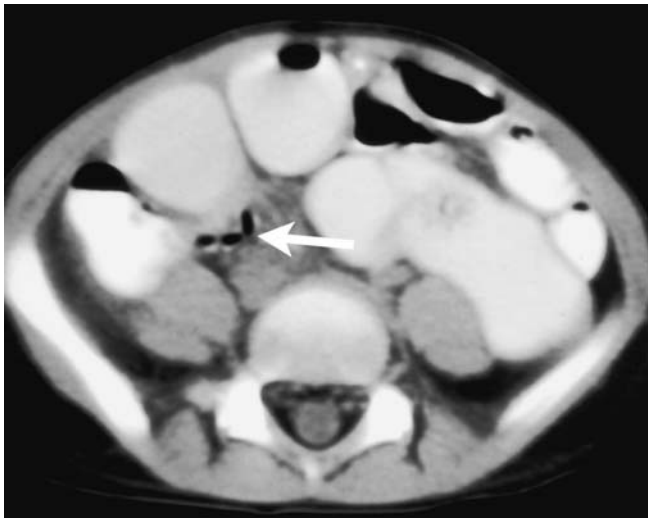

Fig. 1.64. Normal gas-filled appendix (*arrow*) on CT. Some dilated bowel loops filled with oral contrast are depicted. Note the small amount of intraabdominal fat that contributes to the low rate of normal appendix detection in children at CT

tion through the lower abdomen and pelvis (Rao et al. 1998; Garcia-Pena et al. 1999). The amount of intracolonic contrast material administered depends on the size of the patient, ranging from 500 ml in small children to 1000 ml in adolescents. Thin-collimation scanning is performed with 4-mm collimation, 4-mm/s table speed (1.0 pitch), and 4-mm reconstruction beginning 2–3 cm above the iliac wing (Sivit et al. 2001). Visualization of the appendix is strongly dependent on the type and quality of the CT examination, although appendiceal size, the amount of periappendicular fat, and the degree of bowel opacification are important influencing factors (Birnbaum and Jeffrey 1998). Optimal cecal opacification and distension are essential to maximize the diagnostic yield of the examination. When seen, the normal appendix appears as a tubular or ring-like pericecal structure that is either totally collapsed or partially filled with fluid, contrast material, or air. The periappendiceal fat should appear homogeneous, although a thin mesoappendix may be present. The appearance of the abnormal appendix varies with the stage and severity of the disease process. In patients with mild, nonperforating appendicitis the appendix may appear as minimally distended, fluid-filled, tubular structure 5 mm in diameter surrounded by the homogeneous fat attenuation of the normal mesentery. This appearance, however, occurs in less than 5% of patients. Most patients demonstrate greater degrees of luminal distention and evidence of transmural inflammation (Fig. 1.65). The inflamed appendix usually measures 7–15 mm in diameter. Circumferential and symmetric wall thickening is nearly always present and is best demonstrated on images obtained with intravenous contrast material enhancement (Birnbaum and Wilson 2000). The thickened wall is usually homogeneously enhanced, although mural stratification in the form of a target sign may be noted. Other common findings include an appendicolith, circumferential or focal apical cecal thickening, pericecal fat thickening, and the arrowhead sign. The latter finding occurs when cecal contrast material funnels symmetrically at the cecal apex to the point of the appendiceal occlusion (Rao et al. 1997). Perforated appendicitis is usually accompanied by pericecal phlegmon or abscess formation (Fig. 1.65). Associated findings include extraluminal air, marked ileocecal thickening, peritonitis, and small bowel obstruction.

The only CT features specific for appendicitis are an enlarged appendix and cecal apical changes, which represent contiguous spread of the inflammatory process to the cecum. The identification of cecal apical changes is particularly useful in allowing a confident diagnosis of acute appendicitis if there is difficulty in identifying an enlarged appendix. Identification of an appendicolith in an individual with acute right lower quadrant pain is also considered highly suggestive of acute appendicitis. The remaining CT findings are nonspecific and may be seen with a variety of right lower quadrant and pelvic infectious or inflammatory conditions. The main disadvantage of CT remains the radiation dose to the patient. The emergence of helical and multidetector CT technology has been followed by higher diagnostic efficacy, with no increase in the ionizing radiation exposure. Low-dose CT protocols

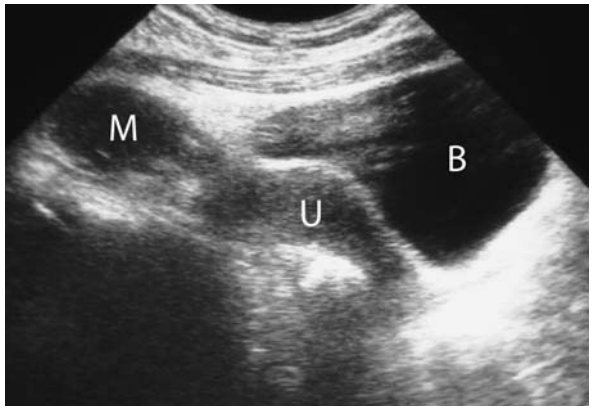

a

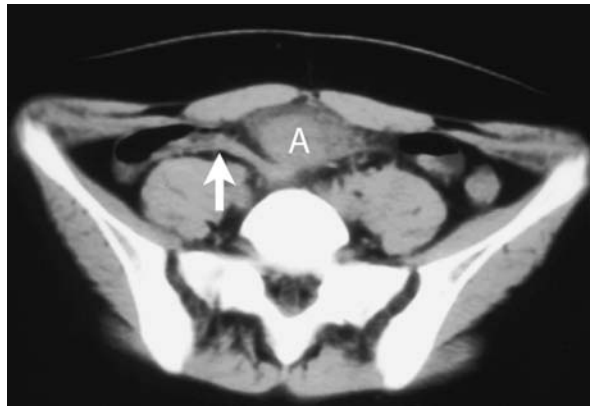

b

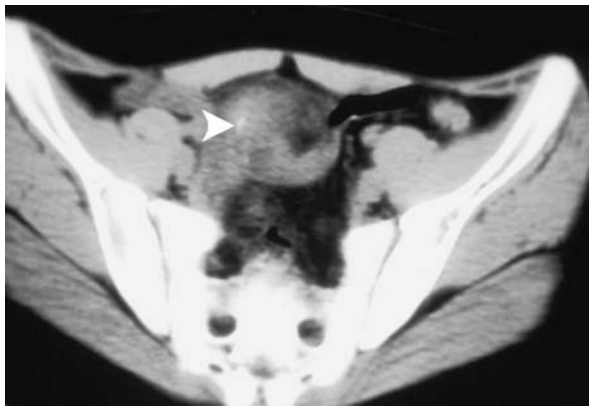

c

Fig. 1.65a–c. CT in appendicitis. A 13-year-old girl treated with antibiotics for pelvic pain and fever. **a** US shows a non-specific cystic mass (*M*) cranial to the uterus (*U*). No flow was observed on color Doppler study. **b,c** CT clearly demonstrates the close relationship between the mass (*A*) and the enlarged appendix (*arrow*) with an appendicolith (*arrowhead*). An appendiceal abscess was demonstrated at surgery. *B*, Bladder; *A*, abscess

using an effective current-time product of 30 mAs have proven to be highly accurate (Keyzer et al. 2004). In spite of these considerations, as stated by Kaiser et al. (2004), "the greatest possible decrease in risk from ionizing radiation at CT is a result of an unnecessary study not being performed". In the interests of radiation protection CT scanning should be reserved for complex problems or for patients whose body habitus precludes adequate US examination.

In conclusion, in cases of high clinical suspicion of appendicitis, surgery is indicated without cross-sectional imaging examination. When clinical presentation is unclear, US should be performed. A positive diagnosis followed by a prompt appendectomy decreases the complication rate. Additionally, a conservative treatment alternative to the surgical option can be used: antibiotics, occasionally followed by delayed appendectomy in cases of phlegmon, and percutaneous drainage in abscess formation. If US examination is accurately shown to be negative for appendicitis, no further studies are required, except for those indicated for the proper management of other possible diagnoses (intussusception, ovarian cyst, etc.). If a nonconclusive diagnosis is made (bowel air interposition, obesity, etc.), different options should be considered, depending on the clinical findings and on the resources available in each institution: observation followed by a second US examination (Kosloske et al. 2004), or CT in order to obtain the most accurate diagnosis. Protocol-based in-patient clinical evaluations by pediatric surgeons, with selective use of diagnostic imaging methods, have shown high accuracy in the diagnosis of appendicitis. Low negative appendicectomy rates (5%) and perforation rates (17%) have been achieved without the radiation exposure and potential costs derived from excessive use of radiological examinations (Kosloske et al. 2004; Ziegler 2004). On the other hand, lower negative appendicectomy rates have been demonstrated in high volume hospitals (Smink et al. 2004).

Several non-surgical abdominal processes such as enteritis (ileocecitis, inflammatory bowel disease), mesenteric adenitis, primary fat epiploic lesions (right segmentary omental infarction and epiploic appendagitis), typhlitis, peritonitis, and functional gynecologic pathology may clinically mimic appen-

dicitis. A precise diagnosis to avoid unnecessary surgery is essential in these cases.

1.2.3 Small Bowel Obstruction

Besides perforated appendicitis and intussusception, the most common causes of small bowel obstruction are incarcerated hernias and adhesions. Other causes of small bowel obstruction comprise a miscellaneous group of rare conditions, such as midgut volvulus, Meckel's diverticulum, advanced stages of Crohn's disease, and bezoars. Adhesions usually result from prior surgery and are often multiple. There is an increasing tendency for initial conservative management rather than immediate operative intervention, as a proportion of cases will resolve spontaneously.

The diagnosis of bowel obstruction is established on clinical grounds and usually confirmed with plain abdominal radiographs. Plain radiographs usually show distended bowel loops with air-fluid levels (Fig. 1.66). In inguinal incarcerated hernia, plain film will also show thickening of the right inguinoscrotal fold (Fig. 1.67a). Because of the diagnostic limitations of plain films, cross-sectional methods are increasingly used. At US, dilated, fluid-filled small bowel loops are seen, which are recognized by the presence of the valvulae conniventes. The bowel wall may become edematous due to vascular and lymphatic obstruction, and ascites may be an accompanying feature of intestinal obstruction. In patients with mechanical bowel obstruction, hyperperistalsis with a to-and-fro motion of the bowel contents is often observed during real-time imaging. Once the obstruction becomes high-grade or complete, peristalsis may be absent (O'Malley and Wilson 2003). Peristalsing fluid and air-filled loops of bowel or mesenteric fat passing down the canal into the scrotum can be readily identified in inguinal hernias (Fig. 1.67b). At US or CT a diagnosis of adhesion is assumed when there is no identifiable lesion at the transition zone between the dilated and the collapsed bowel loops, because the adhesive band itself is not visualized (Marincek 2002).

Closed loop obstruction is a form of mechanical bowel obstruction in which two points along the course of the bowel are obstructed at a single

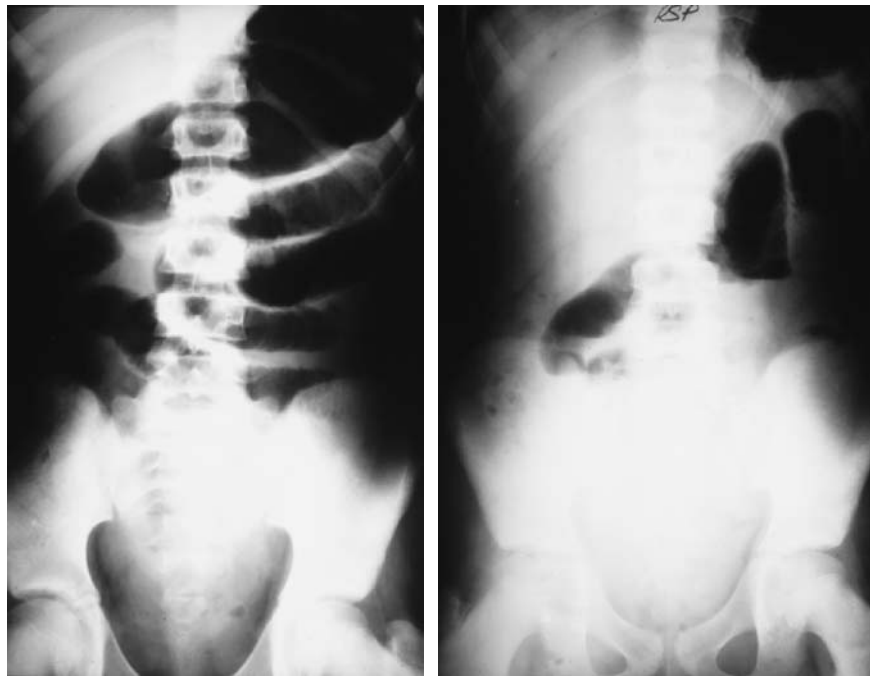

a b

Fig. 1.66a,b. Small bowel obstruction due to adhesive band. **a** Supine plain radiograph shows multiple dilated loops of proximal small bowel. **b** Erect film demonstrates multiple air-fluid levels

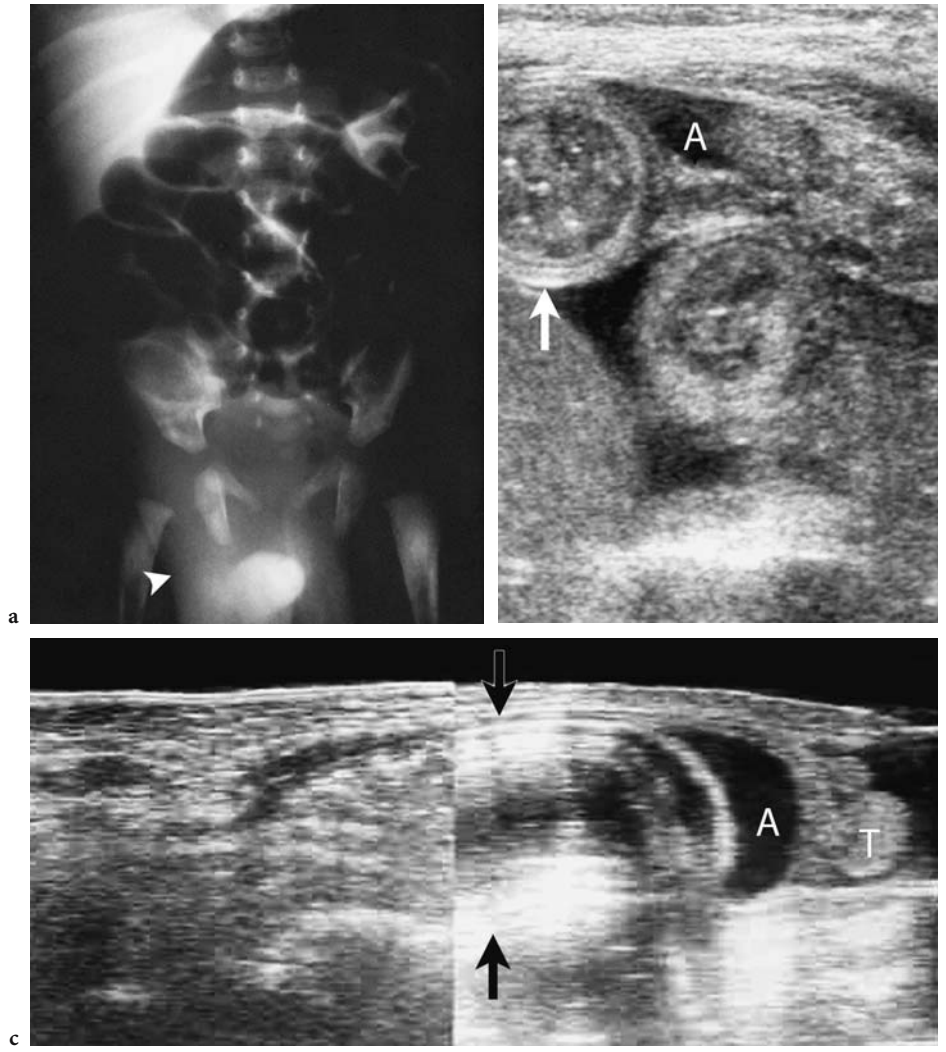

Fig. 1.67a–c. Incarcerated right inguinal hernia. **a** Plain film shows dilated loops of small bowel and thickening of the right inguinoscrotal fold (*arrowhead*). **b** US scan shows dilated small bowel loops and ascites. Note the typical appearance of the bowel wall with five layers (*arrow*). **c** Longitudinal US of the right inguinoscrotal fold performed with an interposed gel-pad, shows an air-filled loop (*arrows*) passing down the canal into the scrotum. The scrotum shows a normal appearance. Normal testis (*T*) and fluid. *A*, ascites

site. It is usually secondary to an adhesive band or a hernia. Because a closed loop tends to involve the mesentery and is prone to produce a volvulus, it represents the most common cause of strangulation. Characteristic findings of closed-loop obstructions are a C-shaped, U-shaped, or "coffee bean" configuration of the bowel loop (Marincek 2002) (Fig. 1.68). Mechanical obstruction of the gut must be differentiated from paralytic ileus. Numerous causes exist for both diffuse and localized paralytic ileus and gaseous distention of the small and the large intestine are seen. Paralytic ileus is a common problem after abdominal surgery. It may be secondary to inflammatory or infectious disease, abnormal electrolyte, metabolite, drug or hormonal level, or innervation defects. Plain radiographs show diffuse dilated bowel loops with distal air, as well as air-fluid levels in the upright or decubitus radiograph (Marincek 2002) (Fig. 1.69). Differentiation of paralytic vs mechanical ileus can also be documented by M-mode US (Riccabona 2001).

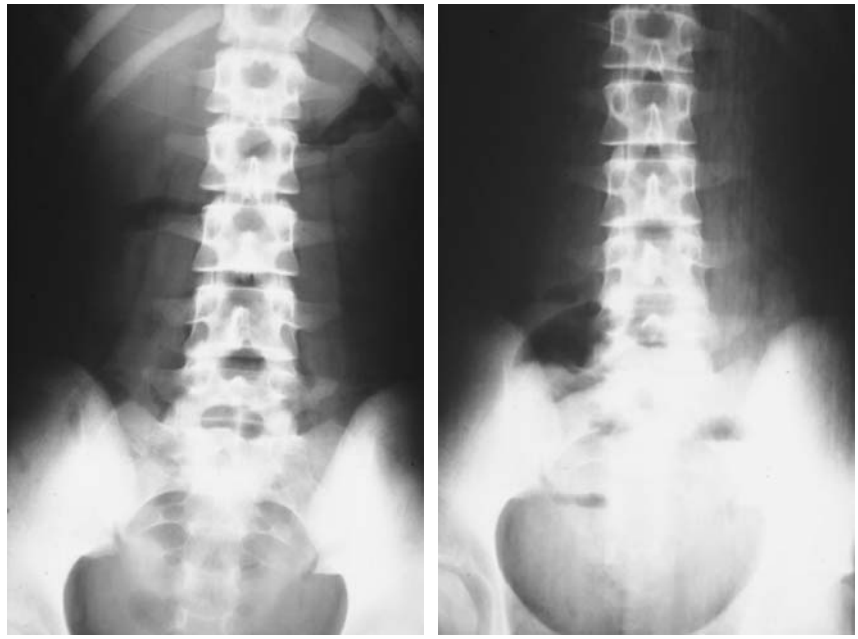

a b

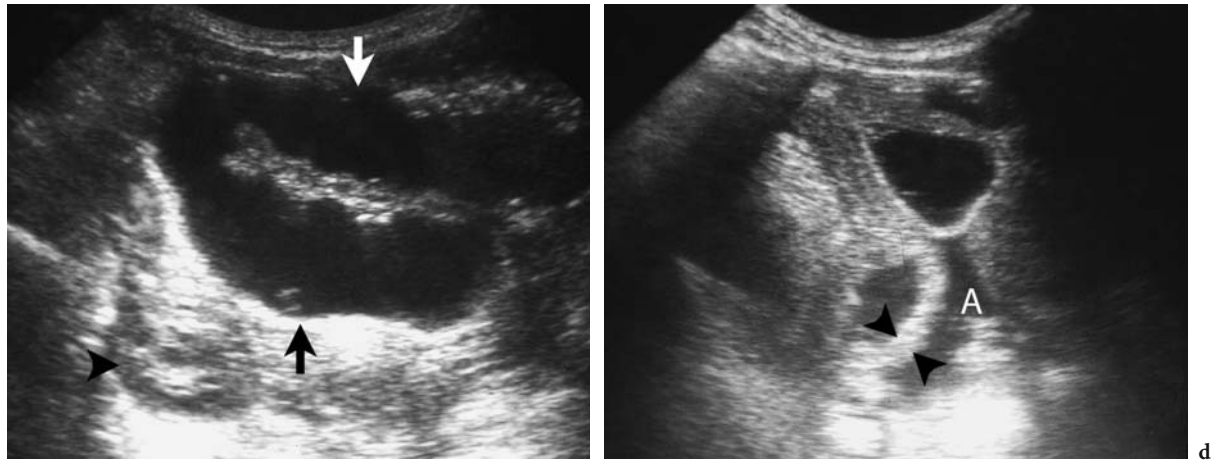

c d

Fig. 1.68a–d. Ileal adhesions from previous appendicectomy causing small bowel obstruction. Supine (**a**) and upright (**b**) plain abdominal radiographs show a paucity of abdominal air and a few air-fluid levels indicating small bowel obstruction indistinguishable from any other cause of obstruction. **c,d** Sonography at the right and left lower quadrants demonstrate a U-shaped, or "coffee bean", configuration of the dilated bowel loops (*arrows*). Some bowel loops present a thickened wall (*arrowhead*) and ascites (*A*), suggesting strangulation

1.2.4 Midgut Volvulus

Midgut volvulus is a complication of malrotation in which clockwise twisting of the bowel around the SMA axis occurs because of the narrowed mesenteric attachment. This life-threatening condition is a clear indication for emergent surgery. The clinical diagnosis of midgut volvulus in older children and adolescents is difficult because the presentation is usually nonspecific and malrotation is rarely considered. Recurrent episodes of colicky abdominal pain with vomiting over a period of months or years are typical and may eventually lead to imaging. Diarrhea and malabsorption from chronic venous and lymphatic obstruction may also occur (Berdon 1995). Findings on abdominal radiographs in midgut volvulus are usually abnormal but nonspecific. Upper gastrointestinal examination (the study of choice in neonates) shows the typical corkscrew appearance of the proximal small bowel. However, in older patients with acute symptoms, US or CT are generally performed instead of a barium examination. Sonographically, an abnormal location of the mesenteric vein to the left or anterior to the corresponding artery can raise the suspicion of malrotation. When a volvulus occurs, twisting of the bowel loops around the mesenteric artery axis leads to the whirlpool sign (Pracros 1992), best shown in Doppler color studies (Patino

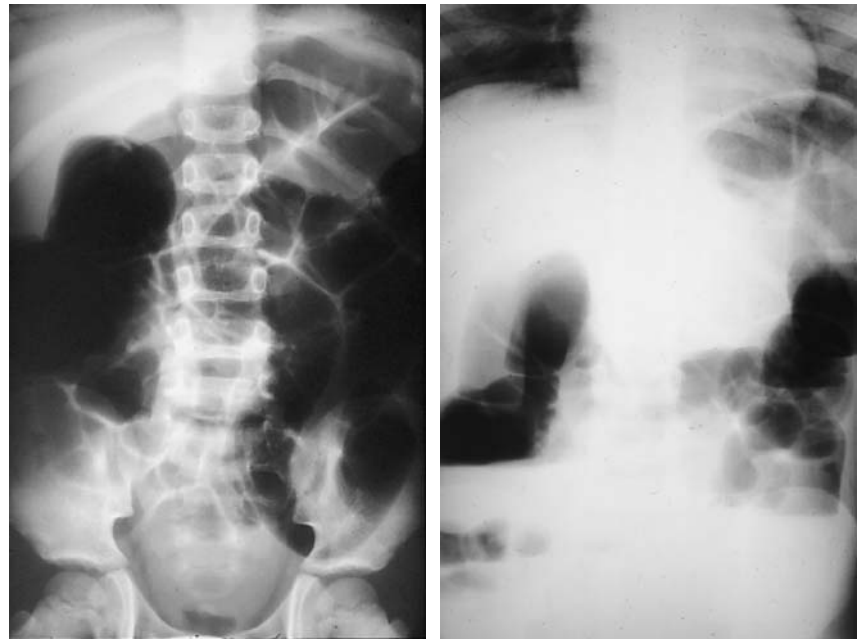

Fig. 1.69a,b. Paralytic ileus due to gastroenteritis. **a** Supine film shows generalized dilated bowel loops and distal gas. **b** Upright film demonstrates multiple air-fluid levels

and Munden 2004) (Fig. 1.13). In the last step of the process, the presence of free fluid and wall thickening may indicate vascular compromise. A similar appearance can be seen on CT (Bernstein and Russ 1998; Pickhardt and Bhalla 2002). Additional CT findings include duodenal obstruction, congestion of the mesenteric vasculature, and evidence of underlying malrotation. The presence of intestinal ischemia or necrosis is an ominous sign. Internal hernia caused by abnormal peritoneal bands is an under-recognized complication of malrotation after childhood (Maxson et al. 1995). This condition may also be life-threatening because of the risk of bowel obstruction and strangulation. CT findings of malrotation and small-bowel obstruction (without volvulus) may be seen in patients with this complication (Pickhardt and Bhalla 2002). Evidence of ischemic bowel again portends a poor prognosis. Some patients may present with a combination of midgut volvulus and internal hernia. These life-threatening events in adolescents who may be otherwise healthy underscore the importance of earlier detection and treatment.

1.2.5 Meckel´s Diverticulum

Meckel´s diverticulum is a remnant of the omphalomesenteric duct. It is located in the antimesenteric side of the ileum, usually within 60 cm of the ileocecal valve. This anomaly occurs in 0.5%–4% of the population, and is generally asymptomatic. Meckel´s diverticulum can present clinically with rectal bleeding, inflammation, or obstruction. Obstruction can be produced by small bowel volvulus around an associated omphalomesenteric band (Fig. 1.70), incarceration in a hernia, herniation of other bowel loops through the mesentery of the diverticulum or also the diverticulum may act as a lead point in intussusception. The most frequent form of presentation is painless hemorrhage in children under 5 years old. Bleeding is related to ulceration of heterotopic gastric mucosa, present in less than 25% of cases. The 99m-Tc pertechnetate scan has demonstrated high accuracy in detecting a diverticulum when isotope is taken up by ectopic gastric mucosa (Hayes 2004). It is difficult to prospectively diagnose a Meckel´s diverticulum causing abdominal pain despite the wide variety of imaging techniques available, particularly if symptoms regress and diverticula bowel walls return to the normal appearance of any adjacent bowel loop. Radiographic findings are nonspecific in most cases of obstruction. Sonography is useful showing a piriform cystic or echogenic everted Meckel´s diverticulum acting as a lead point in the apex of intussusception cases. US may also show an inflamed or torsioned diverticulum mimicking appendicitis. In these cases, localization of the lesion far from

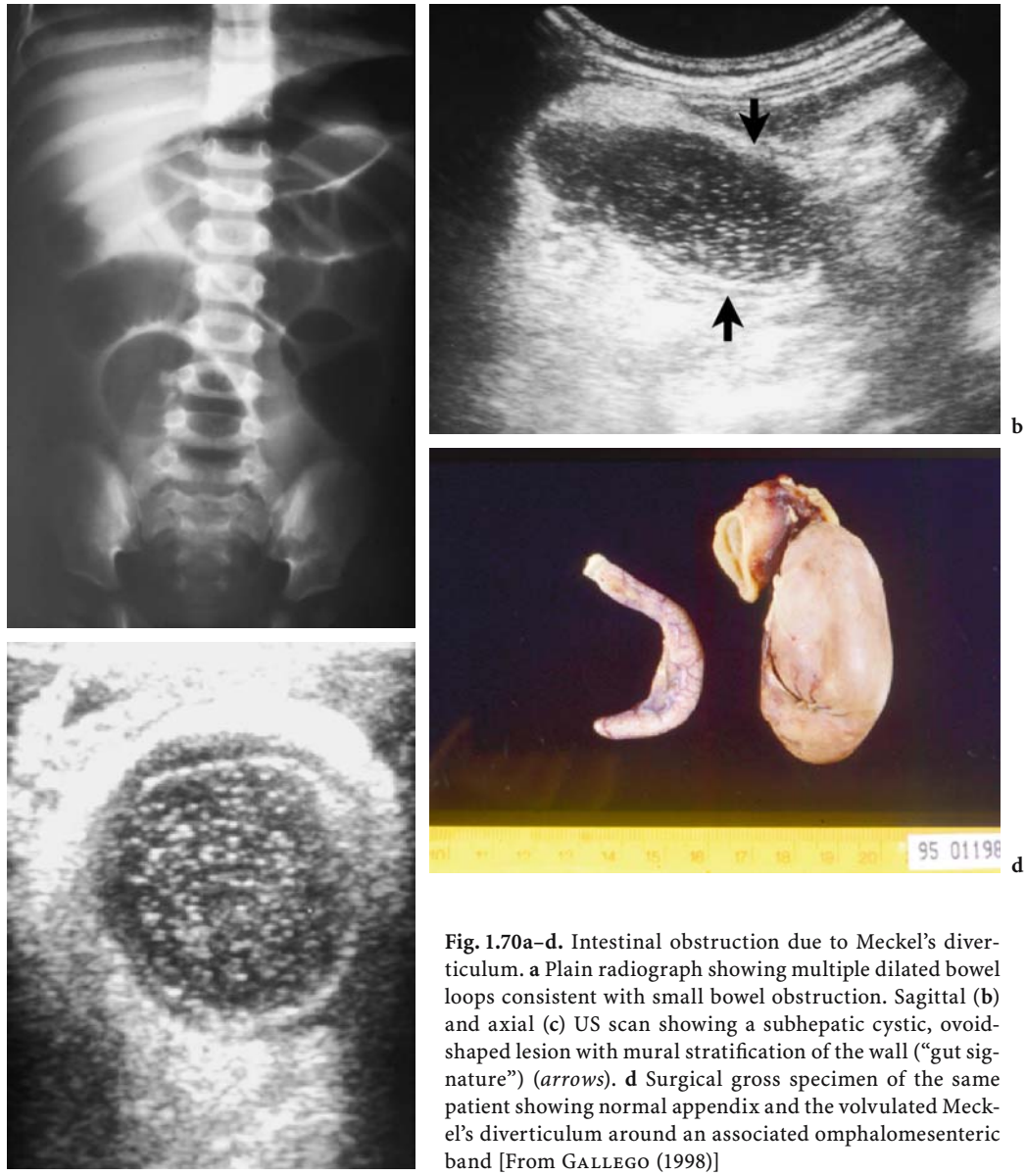

Fig. 1.70a–d. Intestinal obstruction due to Meckel's diverticulum. **a** Plain radiograph showing multiple dilated bowel loops consistent with small bowel obstruction. Sagittal (**b**) and axial (**c**) US scan showing a subhepatic cystic, ovoid-shaped lesion with mural stratification of the wall ("gut signature") (*arrows*). **d** Surgical gross specimen of the same patient showing normal appendix and the volvulated Meckel's diverticulum around an associated omphalomesenteric band [From Gallego (1998)]

the cecum, as well as an anteroposterior diameter superior to 2.5 cm, can help to make an accurate diagnosis (Gallego et al. 1998) (Fig. 1.70). As with the appendix, enteroliths may produce obstruction of the diverticulum and inflammation.

1.2.6 Enteritis

Gastroenteritis is the most frequent cause of abdominal pain in children. Several organism may cause this usually self-limited disease in developed countries. Diarrhea, vomiting, and abdominal pain are common symptoms. There is overlap of symptoms with some cases of appendicitis; for this reason imaging is required in cases of atypical course. Plain film may show diffuse small and large bowel distension, with air-fluid levels on positional views (the pattern of an ileus) (Fig. 1.71a). US may detect generalized dilated bowel loops without wall thickening or significant ascites in non-invasive gastroenteritis cases (Fig. 1.71b). In cases of viral gastroenteritis, there are multiple loops of fluid-filled as well as air-filled intestine, with some patients demonstrating hyperperistalsis, whereas others demonstrate variable

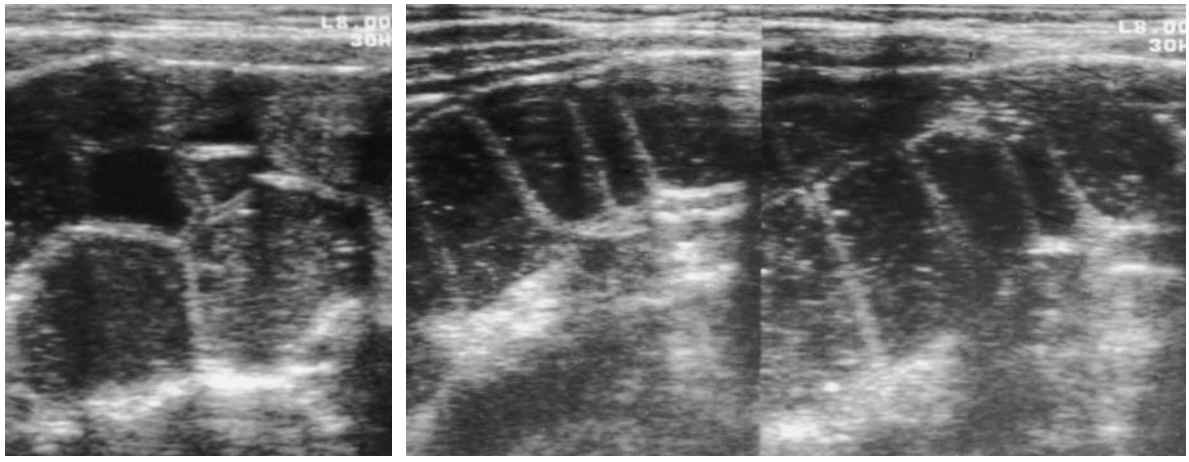

Fig. 1.71a,b. Gastroenteritis. **a,b** US images show dilated loops of small bowel and colon without bowel wall thickening or ascites

degrees of hypoperistalsis. Transient small bowel intussusceptions can be observed in those patients with hyperperistalsis (Hayden 1996). The normal appendix is not usually seen. Differential diagnosis with appendicitis may be difficult because appendicitis may produce similar US findings linked to adynamic or mechanical ileus, mostly in evolutionated cases. However, the absence of echogenic peritoneal fluid or enlarged omental fat makes the probability of perforated appendicitis remote.

Acute terminal ileitis or ileocecitis (bacterial enteritis limited to the ileocecal region).

The term ileocecitis, proposed by Puylaert et al. (1989), defines those bacterial enteritises that affect primarily the ileocecal region, mimicking clinically appendicitis. *Yersinia, Campylobacter*, and *Salmonella* are the most frequent infective organisms. In these cases, diarrhea is often absent or moderate. Sonographic diagnosis of these entities may avoid a significant number of unnecessary laparotomies. Sonographic findings consist of mural thickening of the terminal ileon, ileocecal valve, and the cecum, and the presence of multiple enlarged mesenteric lymph nodes. The thickened ileon appears mostly hypoechoic related to mucosal follicular hyperplasia. This finding may help differentiate it from Crohn's disease, which exhibits a transmural affectation. Abnormalities often extended along the proximal colon, giving rise to a prominent haustral pattern on the longitudinal view. The exaggeration of the haustrations leads to the "accordion" sign (Fig. 1.72). In many cases the appendix cannot be visualized. Nevertheless, the exclusion of appendicitis is justified when sonography reveals other pathology rather than lymph nodes that could explain the patient´s symptoms (Puylaert et al. 1989). Crohn's disease may also be confused with bacterial infection of the ileocecal region. In this case no surgical dilemma will ensue since appendicectomy is not indicated (Puylaert et al. 1989).

1.2.7 Inflammatory Bowel Disease

Crohn's disease may affect any part of the gastrointestinal tract, being the commonest site in the ileocecal region. In children, 20% of cases of Crohn's disease present with acute abdominal pain mimicking acute appendicitis (Hayes 2004). In fact, Crohn's disease may cause, though rarely, appendicitis. Parietal involvement is often discontinuous in Crohn's disease with intervals of apparently normal bowel, producing "skip lesions." Another specificity of the disease is the transmural inflammation extending through all layers of the intestinal wall and involving the mesentery (Valette et al. 2001). Imaging shows stratified transmural thickening of the bowel wall usually involving distal ileum, proximal colon, as well and mesentery. The transmural pattern of the disease is often associated with an irregular thickening of the submucosa and muscular layers. The involved segment appears rigid and shows no peristalsis on US (Fig. 1.73) (Hayes 2004). Differential diagnosis with an infectious ileocolitis may be more difficult than with acute appendici-

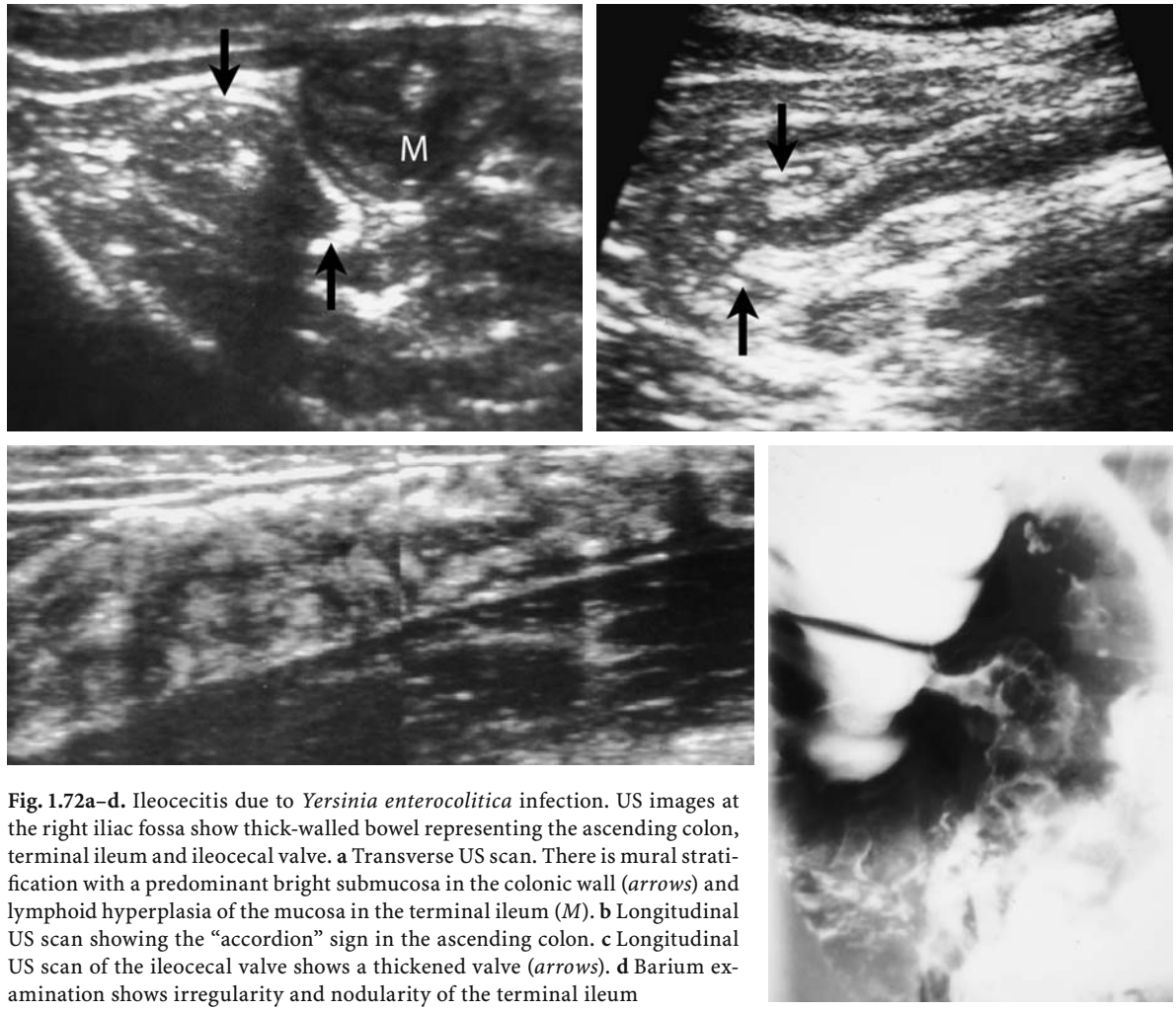

Fig. 1.72a–d. Ileocecitis due to *Yersinia enterocolitica* infection. US images at the right iliac fossa show thick-walled bowel representing the ascending colon, terminal ileum and ileocecal valve. **a** Transverse US scan. There is mural stratification with a predominant bright submucosa in the colonic wall (*arrows*) and lymphoid hyperplasia of the mucosa in the terminal ileum (*M*). **b** Longitudinal US scan showing the "accordion" sign in the ascending colon. **c** Longitudinal US scan of the ileocecal valve shows a thickened valve (*arrows*). **d** Barium examination shows irregularity and nodularity of the terminal ileum

tis. Wall thickening is usually – though not always – transmural, with inflammation of the surrounding fatty tissue, which makes distinction from infectious ileocecitis easy (Puylaert 2001). Characteristic CT findings include terminal ileal thickening with or without a target sign enhancement pattern on contrast-enhanced CT, fibrofatty proliferation of the ileal mesentery, reactive adenopathy and perienteric sinus tracts and mesentery abscesses in cases of severe extramural inflammation (Birnbaum and Jeffrey 1998). Crohn's disease may involve the appendix as distinct from acute obstructive or suppurative appendicitis. The appendix appears collapsed with transmural thickening of the wall, usually maintaining the stratification (three-ring pattern). Recommended treatment is conservative if the appropriate diagnosis can be established with noninvasive techniques.

1.2.8 Schönlein-Henoch Purpura

Schönlein-Henoch syndrome or anaphylactoid purpura, is a vasculitic disease of unknown origin, although is has been suggested to be a viral-induced, allergic, or hypersensitive reaction. Schönlein-Henoch syndrome most commonly occurs in children under 10 years old. It may involve the small blood vessels of the skin, joints, gut and/or kidney. More than 50% of cases have abdominal symptoms, which may precede the cutaneous rash and cause a diagnostic dilemma (Hayden 1996). Sonographically, several degrees of localized or diffuse involvement can be demonstrated in the small bowel loops. Most commonly, there is symmetrical transmural thickening of the bowel wall, secondary to submucosal edema and hemorrhage (Hayden 1996)

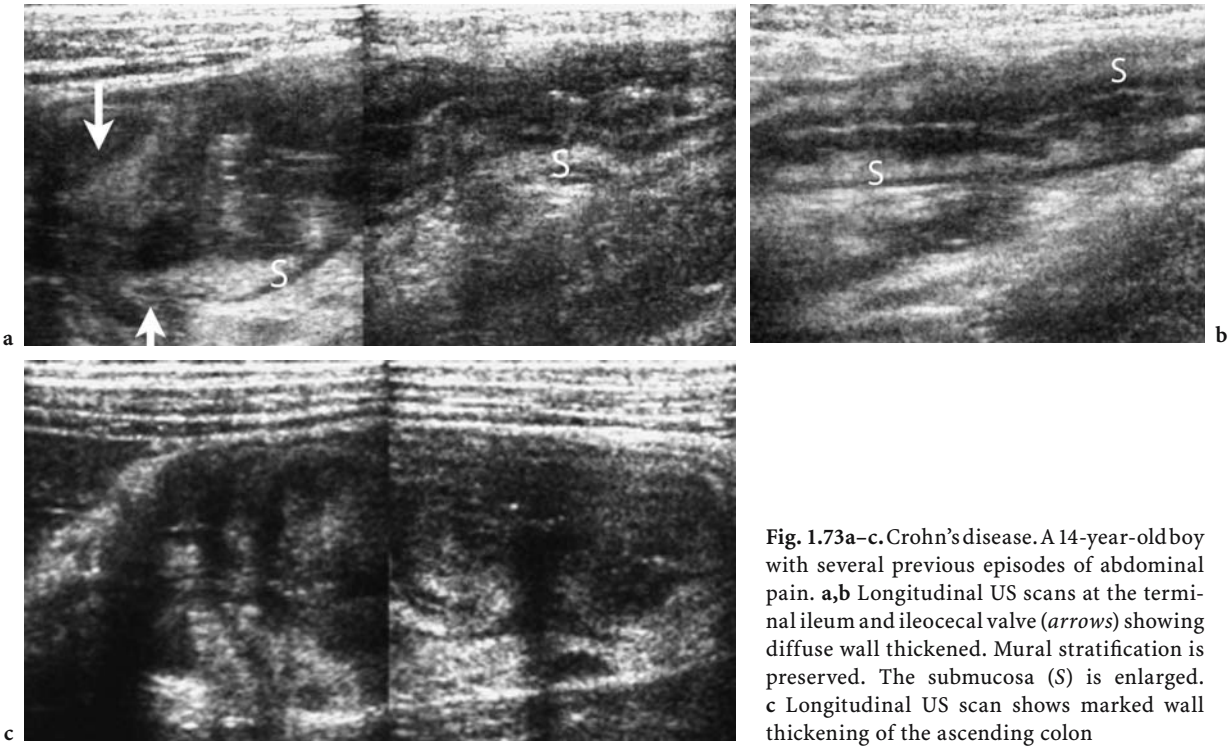

Fig. 1.73a–c. Crohn's disease. A 14-year-old boy with several previous episodes of abdominal pain. **a,b** Longitudinal US scans at the terminal ileum and ileocecal valve (*arrows*) showing diffuse wall thickened. Mural stratification is preserved. The submucosa (*S*) is enlarged. **c** Longitudinal US scan shows marked wall thickening of the ascending colon

(Fig. 1.74). Luminal narrowing and ascites may be significant. Some transient small bowel intussusceptions can be observed. Schönlein-Henoch syndrome, in general, is a self-limited process with a very good clinical outcome.

1.2.9 Mesenteric Lymphadenitis

Mesenteric adenitis is a consequence of an enteric infection, usually viral, that predominantly affects mesenteric lymph nodes. It is the most frequent diagnosis in children who are found to have a normal appendix at surgery (Hayes 2004). Mesenteric lymphadenitis is a self-limiting condition requiring only symptomatic treatment. Mesenteric lymph nodes located at the middle abdomen to the right of the umbilicus, or less frequently at the RLQ, are visualized on US as oval, hypoechoic masses increased in number or size (Fig. 1.75a). In nearly 25% of asymptomatic patients more than five lymph nodes can be observed (Wiersma et al. 2005). Otherwise, a short-axis diameter of 8 mm on CT and 10 mm on US have been proposed as the upper limit of normal lymph node size (Karmazin et al. 2005; Wiersma et al. 2005). Lymphadenopathy due to normal immunization process can be seen in almost 50% of asymptomatic children or in association with a number of abdominal and pelvic disorders. Increased color Doppler flow in tender enlarged lymph nodes reflects its pathologic nature (Fig. 1.75b). Although exuberant blood flow can be demonstrated in inflamed lymph nodes, this still does not differentiate the cause of the inflammation (Hayden 1996). In about half of appendicitis cases, moderately enlarged mesenteric lymph nodes can be seen (Puylaert 1990). Rarely, they are prominent, but in such cases a diagnosis of mesenteric lymphadenitis cannot be establish, except when a full identification of a normal appendix is achieved. Therefore, mesenteric adenitis is an exclusion diagnosis that can only be made if normal appendix is identified and other digestive pathologies excluded.

1.2.10 Primary Fat Epiploic Lesions: Right Segmentary Omental Infarction Including Omental Torsion and Epiploic Appendagitis

Epiploic appendagitis and omental infarction are benign self-limiting conditions that are more frequent than generally assumed. Both disorders fre-

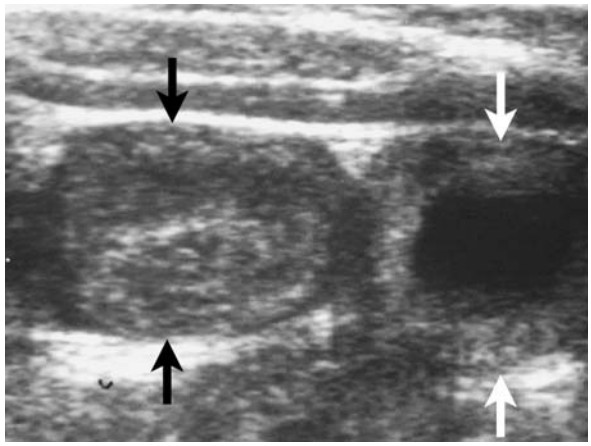

a

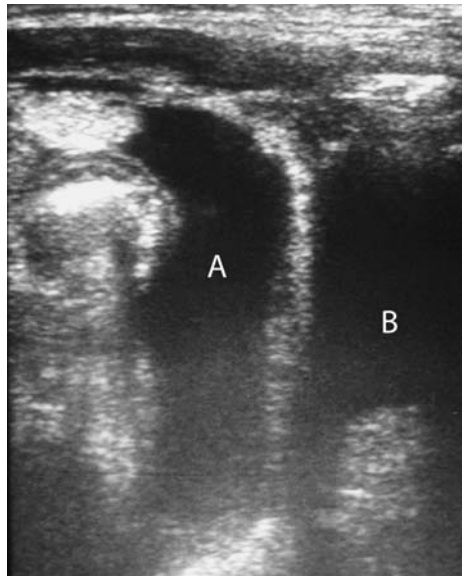

b

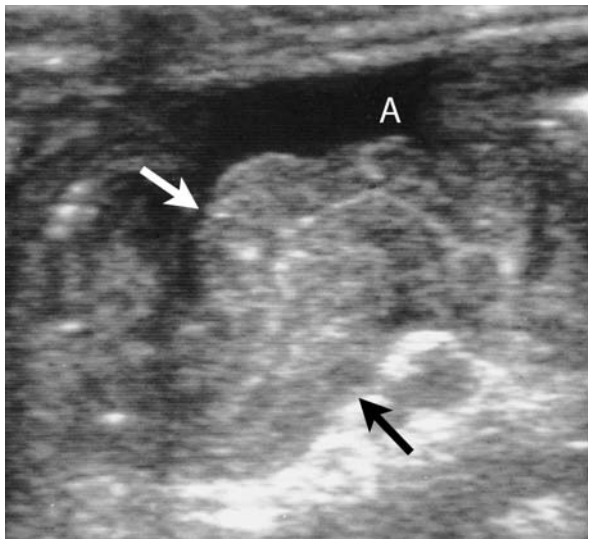

c

Fig. 1.74a–c. Schönlein-Henoch purpura.Sonography shows symmetrical transmural ileal bowel wall thickening and ill-defined wall layers (*arrows*). Anechoic ascites (*A*). *B*, bladder

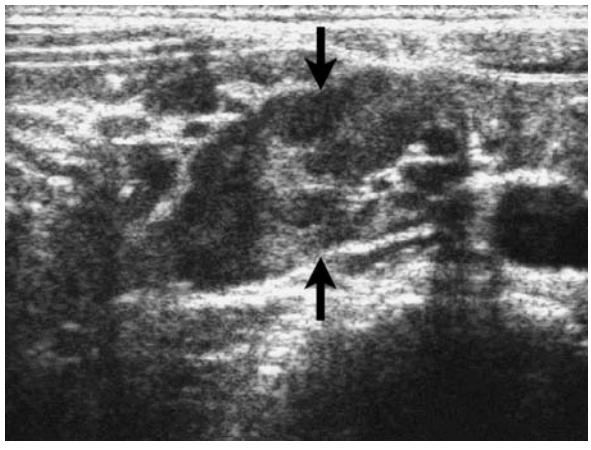

a

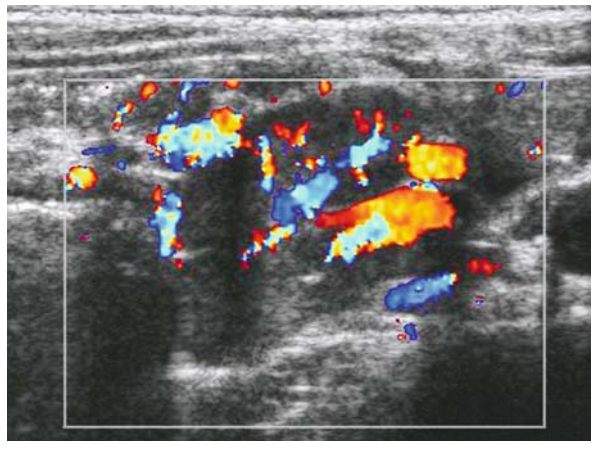

b

Fig. 1.75a,b. Mesenteric lymphadenitis. **a** US image shows enlarged mesenteric lymph nodes in the region to right of the umbilicus (*arrows*). **b** Color Doppler image shows increased flow reflecting hyperemia. Appendix was normal

quently mimic symptoms of an abdominal surgical emergency, often leading to clinical misdiagnosis of appendicitis. Discriminating between both conditions is of no practical relevance since treatment and prognosis are identical (van Breda Vriesman and Puylaert 2002). Spontaneous and complete resolution of symptoms, typically within 2 weeks, is the rule. Obesity seems to be an important risk factor for primary omental torsion in children. Varjavandi et al. (2003) postulated that the increased fat deposition in obese children outstrips the blood supply to the developing omentum. This could lead to either relative ischemia as the inciting event, increased omental weight leading to torsion, or traction to the most distal parts of the omentum. At gray-scale and color Doppler sonography, the more frequent appearance is a hyperechoic mass containing poorly defined nodular or linear hypoechoic areas with few vessels within the mass and hyperemia in the peripheral area. The hyperechoic area corresponds to preserved omental tissue with edema and vascular congestion, the avascular hypoechoic areas corresponding to infarcted tissue (Baldisserotto et al. 2005). Sometimes a progressive sound attenuation is detected (Fig. 1.76). Small amounts of free intraabdominal fluid between bowel loops and in the cul-de-sac are routinely observed (Theriot et al. 2003). The lesion is more conspicuous on CT studies, appearing as a well-circumscribed region of inflamed omental mass interspersed with hyperattenuating stripes and inflammatory stranding (Fig. 1.76). The underlying colon, terminal ileum, and appendix remain unaffected (Birnbaum and Jeffrey 1998).

Epiploic appendices are pedunculated adipose structures protruding from the serosal surface of the colon. An epiploic appendix might incidentally undergo infarction because of torsion or spontaneous venous thrombosis. The condition has been called epiploic appendagitis (van Breda Vriesman and Puylaert 2002). It is considered, as with omental infarction, a self-limited process, and the appropriate management is conservative. The inflamed mass is often delineated by a hypoechoic ring on US.

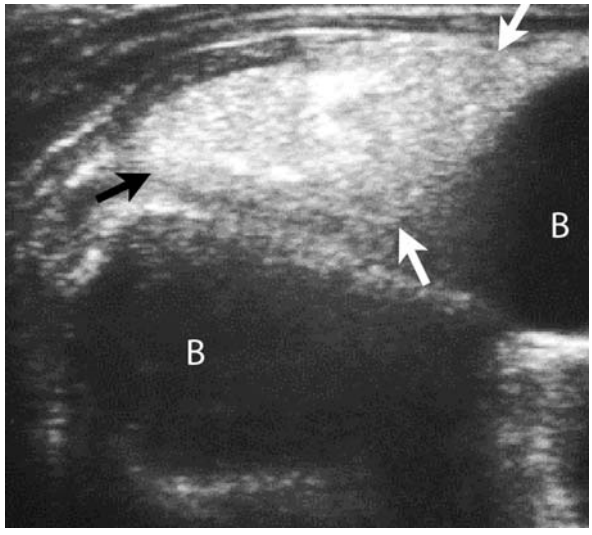

a

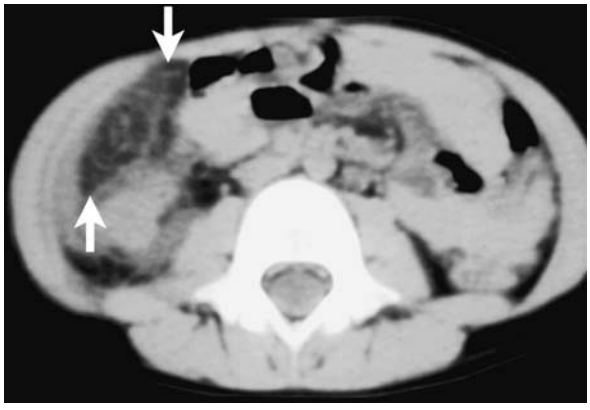

b

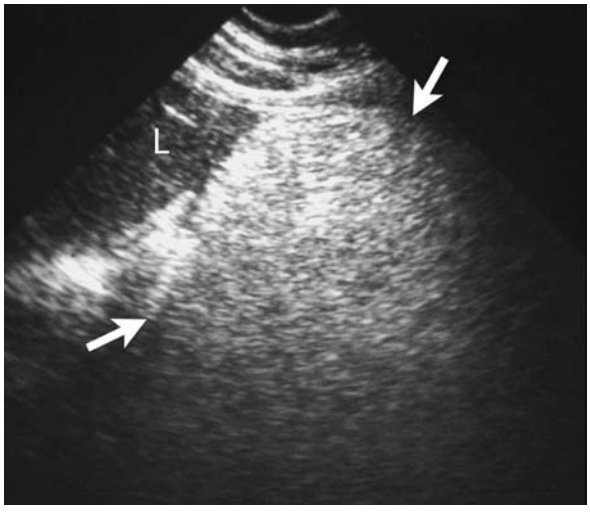

c

Fig. 1.76a–c. Omental infarction. **a** Hyperechoic mass just behind the abdominal wall (*arrows*). **b** Axial CT image shows an area of fat stranding indicating inflamed mesenteric fat (*arrows*). **c** Another patient. Longitudinal US at the subhepatic region shows a hyperechoic mass just underneath the anterior abdominal wall that progressively attenuates the sound suggesting a fat origin (*arrows*). *B*,dilated bowel loops; *L*, liver

The corresponding CT findings consist of a small pedunculated fat-attenuation mass with a hyperattenuating rim (Birnbaum and Jeffrey 1998).

1.2.11 Peritonitis

Peritonitis is often secondary to perforated appendicitis. Primary bacterial peritonitis is an inflammatory process of the peritoneum without an identifiable intraabdominal source. Although this rare entity has been typically associated with underlying systemic processes such as nephrotic syndrome, liver failure, and the presence of ventriculoperitoneal shunt catheter, primary bacterial peritonitis may also occur in otherwise healthy children. The sonographic and CT finding of complex ascites is relatively nonspecific, most commonly thought to be associated with perforated appendicitis. However, when the imaging findings of peritonitis are disproportionately greater than the degree of abnormal appendiceal changes or are associated with non-visualization of the appendix, the diagnosis of primary bacterial peritonitis should be considered in addition to that of perforated appendicitis. The diagnosis can be confirmed by paracentesis and demonstration of a single species of gram-positive cocci on stained smears, findings that would be highly unlikely to be caused by appendicitis. The demonstration of multiple bacterial species, especially if gram-negative bacilli are present, still warrants exclusion of hollow viscus perforation (Dann 2005).

Inflammation of the peritoneum caused by *Mycobacterium tuberculosis* can be produced by direct spread from gastrointestinal tuberculosis or after hematogenous dissemination from a pulmonary focus. Involvement of the omentum in peritoneal tuberculosis is diffuse and different to the focal involvement of the omentum in appendicitis or in omental infarction on US or CT. The correct diagnosis is suggested by additional findings such as lymphadenopathy, involvement of the mesentery, bowel wall thickening, or loculated ascites (van Breda Vriesman and Puylaert 2002).

1.2.12 Hepatobiliary Causes of Acute Abdominal Pain

Hepatitis, space occupying hepatic lesions, and biliary pathology such as cholecystitis or those characteristics of the childhood (hydrops, choledochal cyst) may also cause abdominal pain.

Acute cholecystitis in children is relatively rare, but certain pediatric patients are prone to these diseases. Acute cholecystitis may be calculous or acalculous. The triad of right upper quadrant pain, vomiting, and fever is the usual clinical presentation (Tsakayannis et al. 1996). Jaundice occurs in 25%–45% of patients probably secondary to inflammation around the bile duct. US should be the primary screening in patients with these symptoms. US findings include gallbladder wall thickening and distension and, sometimes, gallstones. A gallbladder wall thickness over 3 mm is abnormal, although it can be observed in many conditions unrelated to cholecystitis such as hypoalbuminemia, ascites, and portal hypertension. The ultrasonographic Murphy´s sign (maximal tenderness over the sonographically-localized gallbladder) is a useful secondary sign. The presence of intraluminal membranes and echoes with or without gallbladder wall irregularity may indicate hemorrhagic or gangrenous cholecystitis (Chinn et al. 1987).

Until recently, biliary lithiasis was considered infrequent in childhood, but the frequency of the diagnosis has been increasing. In children, up to 75% of gallstones are pigmented stones. Their etiology is often unknown (Rescorda 1997). Symptom-free stones usually have a benign course and spontaneous resolution can occur. The most frequent clinical presentation is abdominal pain, with or without vomiting. Ultrasound is very accurate in the detection of calculi in the gallbladder, but less so in the intrahepatic and extrahepatic ducts (Fig. 1.77). MRCP can be used when choledocholithiasis needs to be excluded and ultrasound is negative.

Choledochal cysts are localized dilatations of the biliary ductal system. Five types have been described: type I (80%–90%), dilatation of the common bile duct (IA cystic, IB focal, IC fusiform); type II, diverticulum; type III, choledochocele; type IV, multiple cysts (IVA intra- and extrahepatic, IVB extrahepatic); type V, Caroli disease. The pathogenesis is related to an anomalous relation of the common bile duct and the pancreatic duct, which allows reflux of pancreatic secretion into the biliary tree. It is more frequently seen in female and Asian infants. It may be found in all ages from neonate to adult, but is now frequently discovered during prenatal sonogram (Benya 2002). Clinical symptoms include episodic abdominal pain, jaundice, and a right upper quadrant mass. At US and MRCP this appears as a cyst

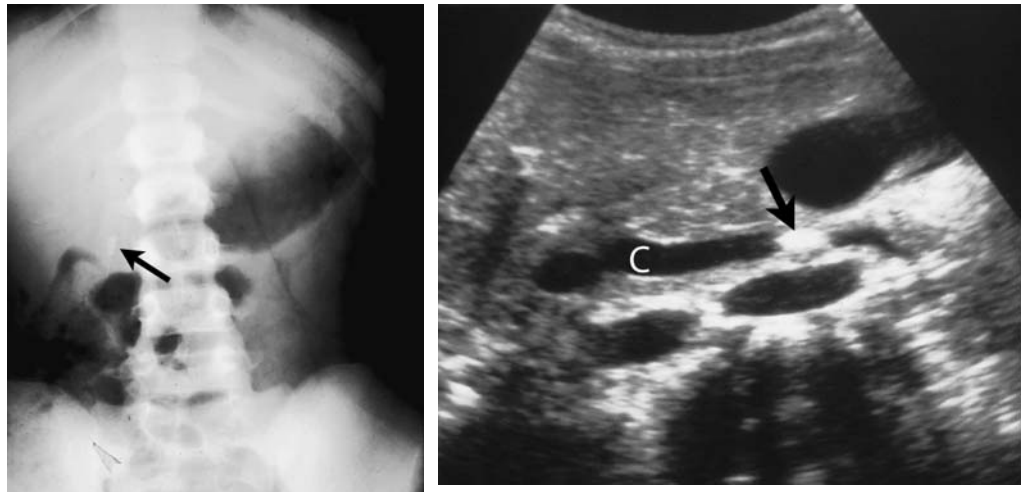

a b

Fig. 1.77a,b. Choledocholithiasis presenting as an acute abdomen in an 8-year-old boy. **a** Plain film shows a paraspinal calcification (*arrow*). **b** US demonstrates a calculus (*arrow*) in the distal choledochus (*C*) producing dilatation of the proximal bile duct

in the porta hepatis, separated from the gallbladder and communicated with the biliary ductal system (to differentiate extrahepatic biliary atresia) (Fig. 1.78). Complications include cholelithiasis, choledocholithiasis, pancreatitis, malignant degeneration, and cirrhosis.

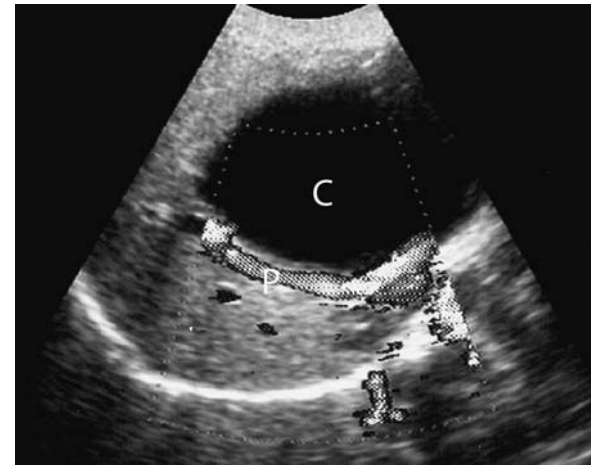

Fig. 1.78. Choledochal cyst. Transverse US scan through the liver shows a cystic mass (*C*) in the porta hepatis. Hepatobiliary scintigraphy confirmed communication of the cystic structure with the biliary system. *P*, portal vein

1.2.13 Acute Pancreatitis

Acute pancreatitis is an uncommon clinical entity in children that is caused by a wide variety of etiological agents, the most common of which is blunt abdominal trauma. Other causes include viral infections, drugs, and hereditary abnormalities. Clinical presentation depends on the severity of the disease, but abdominal pain is invariable. Other symptoms are vomiting, fever, jaundice, and an abdominal mass if a pseudocyst is present. When pancreatitis is suspected in a child, US should be the primary imaging investigation (Berrocal et al. 1995). The most common US finding is diffuse or focal glandular enlargement and decreased echogenicity, with poorly defined borders (Fig. 1.79). Dilatation of the pancreatic duct may be present. In cases of mild pancreatitis the pancreas may appear normal on US. CT or MRI are usually reserved for patients with complications, especially those requiring intervention. CT shows diffuse pancreatic enlargement, heterogeneous attenuation, a poorly defined pancreatic contour, and peripancreatic fluid collections, which are most commonly found in the anterior pararenal space and lesser sac (Baltazhar 2002). More than one third of patients with acute pancreatitis have an initially normal CT. MRI should be preferred to CT when available because of the lack of ionizing radiation. Pseudocyst formation is the most common complication of the acute pancreatitis and

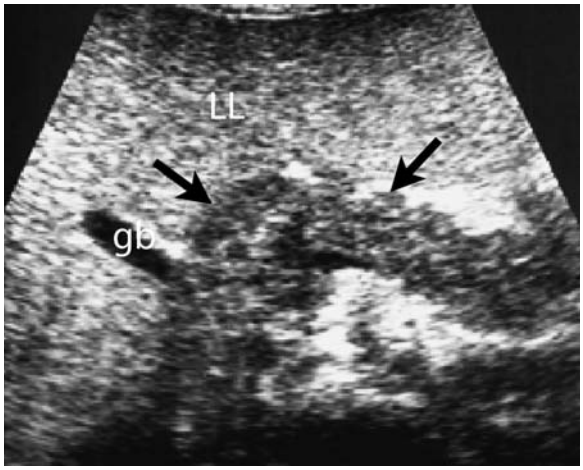

Fig. 1.79. Acute pancreatitis. Diffuse acute pancreatitis in a 5-year-old girl with acquired immunodeficiency syndrome. Transverse US scan through the pancreas shows a globally enlarged pancreas with diffuse decreased echogenicity and irregulars borders (*arrows*). Note the poor definition of the splenic vein. Gallbladder (*gb*), left lobe of the liver (*LL*)

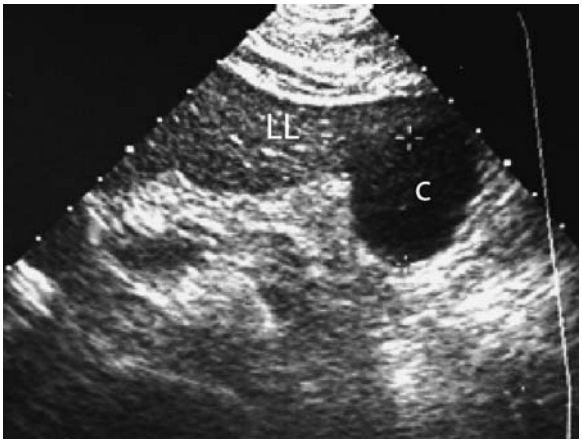

Fig. 1.80. Pseudocyst. Transverse US scan through the pancreas shows a cystic mass (*c*) with posterior reinforcement anterior to the pancreatic tail (*arrows*). Left lobe of the liver (*LL*)

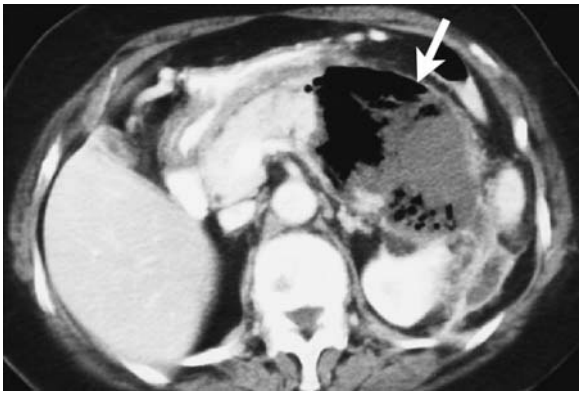

Fig. 1.81. Pancreatic abscess. CT shows a complex, gas-containing fluid collection in the pancreatic tail (*arrow*)

they are the most usual type of cysts occurring in the pancreas. Pseudocysts may be extrapancreatic (usually in the lesser sac) or intrapancreatic, and require at least 4 weeks following an episode of acute pancreatitis. On US they appear as anechoic structures with well-defined borders and posterior reinforcement (Fig. 1.80). These lesions are usually homogeneous, and of water signal intensity on T1-weighted and T2-weighted HASTE images (Ly and Miller 2002) (Fig. 1.12b,c). Pancreatic abscesses can have imaging features similar to pseudocysts, but may be distinguished by means of the clinical history or when there is gas within the collection (Baltazhar 2002) (Fig. 1.81).

1.2.14 Renal Causes of Acute Abdominal Pain

The most common renal causes of an apparent acute abdomen are upper urinary tract infection, especially pyelonephritis, renal colic due to a stone in the urinary tract, and acute presentation of a pelviureteric junction obstruction. Children may localize the pain to the abdomen, not the loin. Urinary tract infections, usually related to vesicoureteral reflux, may cause similar symptoms to those of intussusception, mostly in young children. In most of these cases US is normal and only in high-grade reflux (grades III–IV) pyelocaliceal dilatation may point to the right urologic diagnosis. When evident, foci of infection are often hypoechoic with focal loss of the corticomedullary differentiation (Riccabona 2002a,b). A renal abscess appears as a heterogeneous mass lesion with central necrosis. Structural abnormalities of the urinary tract that may be found in children presenting with infection include duplex systems, renal ectopia, horseshoe kidney, and renal malrotation. A VCUG is indicated in children presenting with an acute urinary tract infection, but should not be performed during acute infection. The child should remain on antibiotic prophylaxis and the VCUG should be done as a planned investigation (Pennington and Zerin 1999).

Renal lithiasis is more common in infants than in older children, and 20% of cases manifest as renal colic. Underlying causes are multiple, proteus being the most common pathogen. The role of imaging is to diagnose lithiasis, to detect any underlying anatomical abnormality, and to demonstrate the effect on the urinary tract so that treatment can be appropriate. Renal lithiasis can be detected radiographically or sonographically. The latter method may also substantiate the presence of obstructive uropathy and in many cases it may demonstrate its level and etiology. A calculus manifests as a hyperechoic area with acoustic shadowing located within the pelvicaliceal system or ureter (Fig. 1.82). In suspected obstruction by a calculus, US examination should include the kidneys, ureters, and bladder to determine the level of obstruction. On plain abdominal radiographs, calculi are seen as radiopacities in the renal areas, the line of the ureters or the bladder region. Differential diagnosis includes appendicolith, intracolic foreign body, calcified ovarian mass, or adenopathy. CT should not be used as a routine investigation tool due to its associated radiation dose (Eshed and Witzling 2002); however, it is useful in patients with renal colic and a negative US study, and in patients with US findings suggestive of ureteric obstruction in which US failed to demonstrate the calculus. In such cases, a non-contrast, low-dose CT scan usually allows demonstration of the stone, even a non- or poorly radiopaque stone (Meaghar et al. 2001).

Pelviureteric junction obstruction may be detected on prenatal US or on US examination of infants who have a urinary tract infection; however, a significant proportion of cases present later in childhood with abdominal pain. US demonstrates a dilated renal collecting system with no associated dilated ureter. There are multiple hypoechoic cystic spaces, the largest being medial and representing the dilated pelvis. The cysts intercommunicate and infundibula and calyces, as well as surrounding renal parenchyma, can usually be identified (Ward et al. 1998). In severe cases the distended renal pelvis has a classically convex contour (Fig. 1.83). The patient should be well hydrated at the time of examination. Follow-

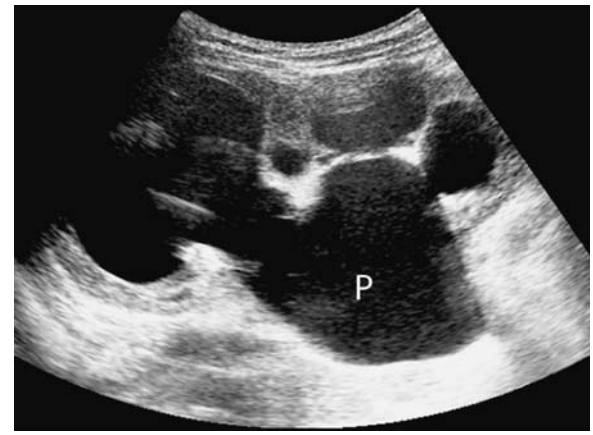

Fig. 1.83. Ureteropelvic junction obstruction. Longitudinal US scan of the right kidney demonstrates dilated calyces communicating with a markedly dilated renal pelvis (*P*). No dilated ureter is identified

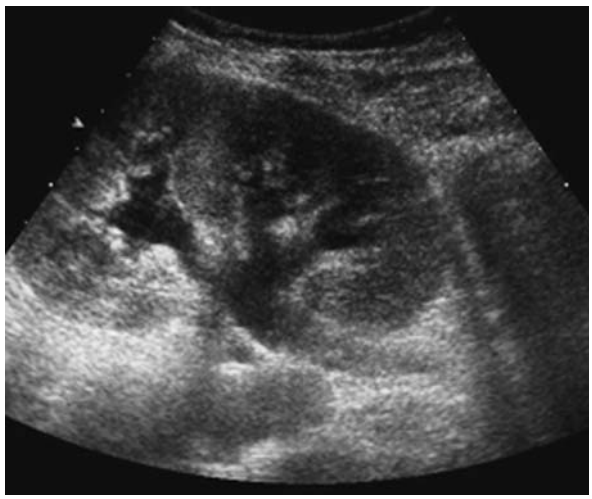

a

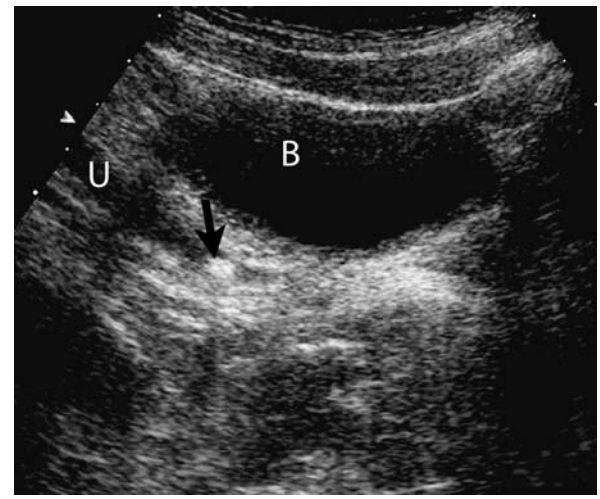

b

Fig. 1.82a,b. Calculus in the distal ureter. Longitudinal US scan through the right kidney shows a dilated collecting system produced by a calculus (*arrow*) in the right distal ureter (*U*). *B*, bladder

ing a US diagnosis of pelviureteric junction obstruction, the patient should have a Mag 3 renogram after IV furosemide, to assess the degree of obstruction and the relative filtration of the obstructed kidney. The excretion curves that are generated during this examination provide useful information regarding the degree of obstruction. They also provide a useful baseline for future follow-up in patients in whom immediate surgical treatment of their obstruction is not warranted. Intravenous urograms may be useful when further anatomical details are required prior to surgery; however, this imaging modality is being substituted by MR urography if facilities are available (Riccabona 2002). Most patients with severe pelviureteric junction obstruction are surgically treated with a dismembered pyeloplasty, while those with mild or moderate pelviureteric junction obstruction are followed-up with periodic US.

1.2.15 Gynecological Causes of Acute Abdominal Pain

The main gynecological conditions causing acute abdominal pain are functional ovarian cysts, ovarian torsion, and hydrometrocolpos. Transabdominal US will commonly show the lesion. Transvaginal US should not be routinely done as a primary investigation in adolescent girls, but may supplement the abdominal examination in sexually active patients.

Ovarian cysts usually result from failure of involution during the normal menstrual cycle. They may cause acute lower abdominal or pelvic pain in pre-pubertal and pubertal girls if they are complicated by rupture, torsion, or hemorrhage, or if they become significantly enlarged. Transabdominal US in uncomplicated cysts usually show a thin-walled, well-defined, echo-free ovarian mass, and excellent through-transmission (Carty 2002). Simple cysts may be quite large, but most of them resolve spontaneously, only requiring clinical and sonographic follow-up. Rarely, there is a complication, the most common being ovarian torsion. Functional cysts may also rupture and result in free fluid in the pelvis. Despite the high frequency of presentation of these cysts, they should not be assumed to be the cause of the acute symptoms until other pathologies, especially appendicitis, have been excluded.

Functional cysts may develop internal hemorrhage. Hemorrhagic ovarian cysts typically present with sudden and severe lower abdominal pain. On US, they may appear echogenic or hypoechoic, but never anechoic (Fig. 1.84). Most of them are heterogeneous in echogenicity and show through-transmission due to their underlying cystic nature. They may contain internal clots, septations, as well as fluid-debris levels. The cyst wall may be thin or thick and irregular. A changing US appearance over time can help make the diagnosis. The initial bright echogenicity of acute hemorrhage, produced by fibrin deposition, becomes less echogenic and eventually fluid-like as the fibrin dissolves and the clot lyses (Surratt and Siegel 1991). A complex cystic ovarian mass may often be treated conservatively, particularly if there are no features suggesting the presence of torsion. In these cases, US follow-up is necessary until complete resolution.

In adnexal torsion, the ovary twists with the vascular pedicle. Torsion leads initially to compromise of lymphatic and venous drainage, followed later by arterial occlusion and thrombosis and eventual hemorrhagic infarction of the involved organs. It is most common in prepubertal girls, due to increased adnexal mobility prior to menarche. Right-sided torsion is more common as the sigmoid colon prevents excessive movements of the left ovary and fallopian tube. Adnexal torsion is a true surgical emergency which clinically may mimic acute appendicitis, gastroenteritis, or intussusception. The pain may be intermittent and localized to one or other lower quadrant, or it may be severe, acute, and generalized. Associated nausea, vomiting, or constipation may occur. A palpable abdominal mass and a paralytic ileus may also be present. US is the most important imaging modality for the diagnosis of adnexal torsion. The US findings are variable. Typically, the ovary involved appears noticeably enlarged, with multiple enlarged peripheral follicles (Graif and Itzchak 1988) (Fig. 1.85), being hard to delineate from the little uterus that is often displaced anteriorly. This appearance is seen in 60%–75% % of cases of torsed normal adnexa. However, the ovary appearance may vary depending on the degree of internal hemorrhage, stromal edema, and infarction which has occurred by the time it is diagnosed. Other gray-scale imaging appearances include a purely cystic, a mixed cystic-solid, or a solid adnexal mass lesion. Fluid may be present in the pouch of Douglas.

Doppler studies may demonstrate absent or reduced central venous and arterial flow. However, complete absence of Doppler signal alone is not a specific finding as flow may be difficult to obtain even in normal ovaries. In addition, low velocity peripheral arterial flow (less than 5 cm/s) may per-

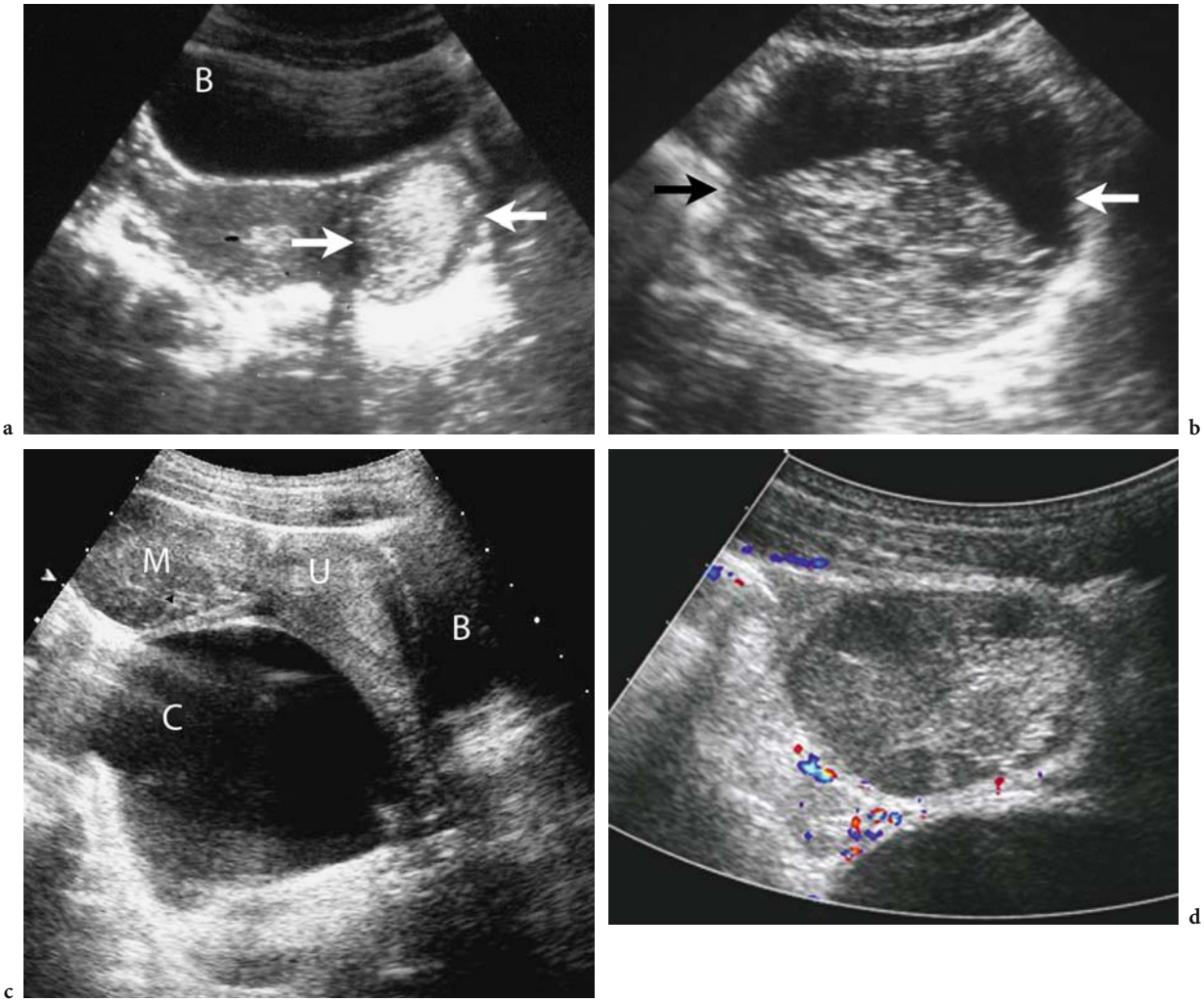

Fig. 1.84a–d. Several appearances of symptomatic ovarian cysts. **a** Luteinic cyst. Well-defined hyperechogenic mass in the left ovary (*arrows*). Regardless of its echo pattern, it typically shows through-transmission due to its underlying cystic nature. Control performed 6 weeks later demonstrated a normal left ovary. **b** Hemorrhagic ovarian cyst. Complex cystic mass (*arrows*). **c** Longitudinal US scan in an adolescent patient with acute abdominal symptoms. A cystic mass (*C*) is observed behind the uterus (*U*) in the cul-de-sac. Another complex mass (*M*) is present above the cyst and uterus. **d** Axial US scan of the same patient demonstrates no flow within the mass on color Doppler sonography. Surgery demonstrated the cystic mass to be a teratoma and the complex mass to be a hemorrhagic cyst. *B*, bladder

sist due to ovarian dual blood supply. The presence of damped arterial and venous flow or absent arterial and damped venous flow has also been described as being associated with adnexal torsion. If torsion is intermittent or incomplete, then Doppler study may be normal (Hurth et al. 2002).

Pelvic inflammatory disease is increasing in incidence in sexually active adolescents, and is due to either *Chlamydia trachomatis* or *Neisseria gonorrhea* infection. Infection ascends from the cervix to involve the endometrium and fallopian tubes. The fallopian tubes become edematous and hyperemic and are filled with pus, which may spill over into the peritoneum causing peritonitis. If the fimbriated ends of the fallopian tubes become adherent to the ovaries, the tubes may obstruct and distend with fluid, resulting in a hydrosalpinx, or with pus, resulting in a pyosalpinx. The infection may extend to the ovaries, resulting in a tubo-ovarian abscess. Clinically, patients with pelvic inflammatory disease present with pelvic pain that may worsen during or just after menstruation. Dysfunctional uterine bleeding and dysuria may also appear. Ultrasound is the primary imaging modality, the sonographic

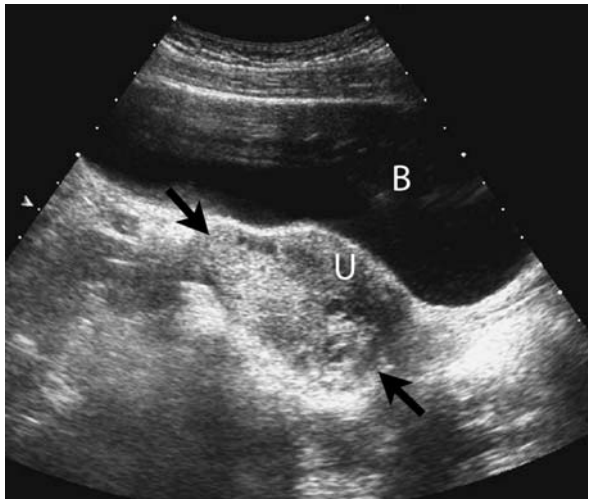

a

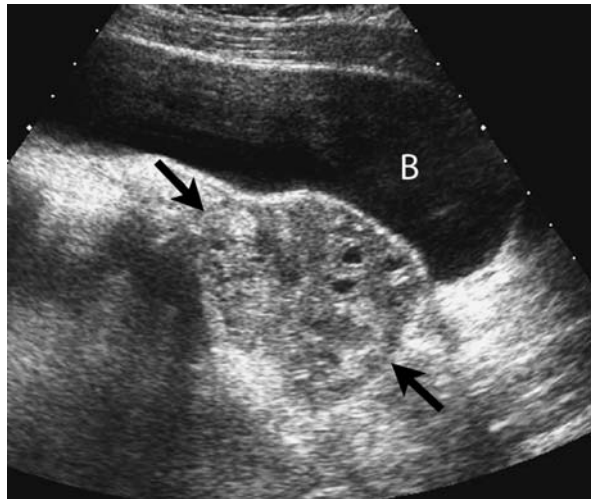

b

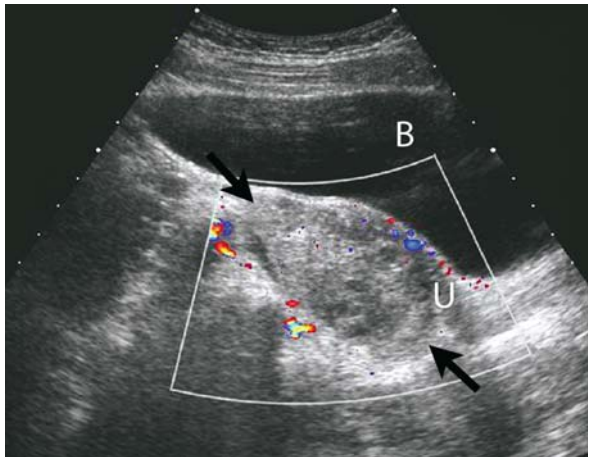

c

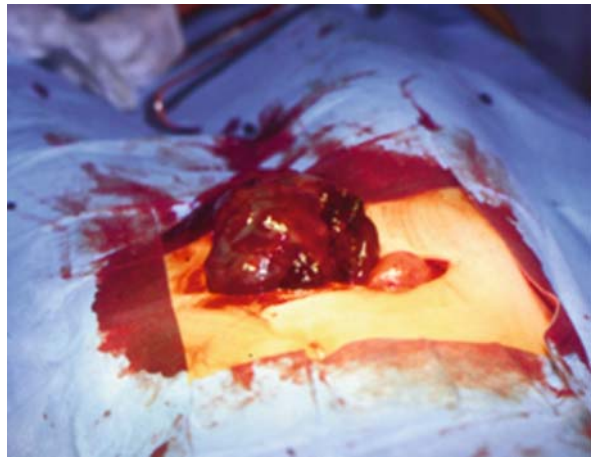

d

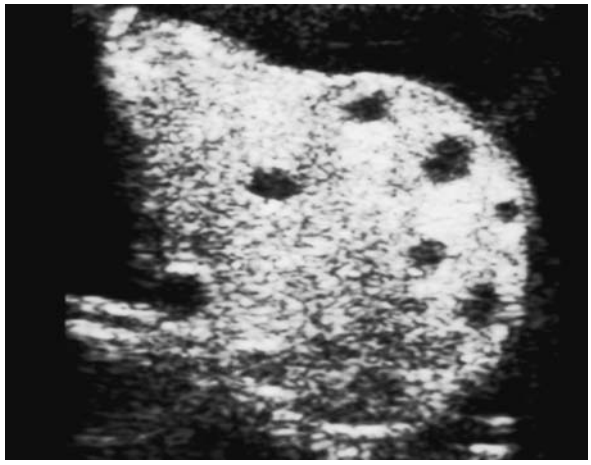

e

Fig. 1.85a–e. Ovarian torsion. **a,b** Longitudinal US scan shows an echogenic mass with tiny cyst behind the uterus (*U*) in the cul-de-sac. The little prepuberal uterus is displaced anteriorly, and it is hard to delineate it from the mass (*arrows*). **c** Color Doppler showing the absence the flow in the center of the ovary. **d** Surgical specimen. **e** In vitro study of the ovary. Multiple edematous immature follicles may be visualized in the ovary not only in the periphery but in the whole ovary. *B,* bladder

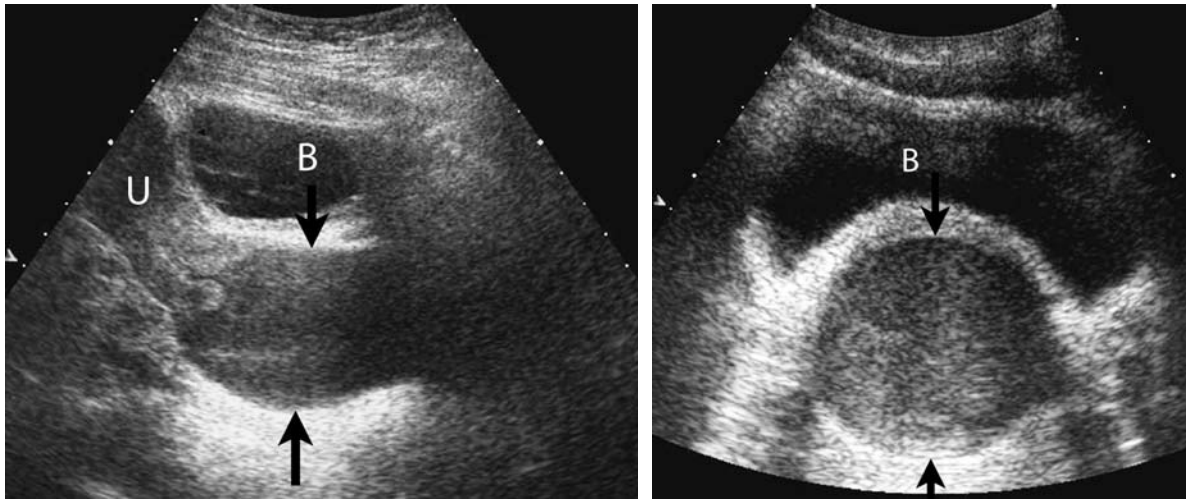

a b

Fig. 1.86a,b. Hydrocolpos due to an imperforate hymen. **a,b** Transversal and longitudinal US images show a dilated vagina (*arrows*) behind the bladder. *U,* uterus. *B*, bladder

findings varying according to the extent of the disease. Endometritis may lead to enlargement of the endometrium and fluid may be seen in the endometrial cavity. Pyosalpinx manifests as thickened and dilated fallopian tubes containing debris-laden fluid and septations. A tubo-ovarian abscess usually appears as a complex and heterogeneous adnexal mass, commonly accompanied by free fluid in the pouch of Douglas. Transvaginal US gives better anatomical detail of the inflamed adnexal structures and may obviate the need for laparoscopy in adolescents with pelvic inflammatory disease (Bulas et al. 1992). In severe cases, CT and MRI can be useful in demonstrating the extent of the disease throughout the abdomen and pelvis.

Genital tract obstruction may also be a cause of acute abdominal pain. It may present with pain and amenorrhea in adolescence and is usually due to an imperforate hymen, but it may also be due to vaginal or cervical atresia. With an imperforate hymen, the menstrual products during menarche collect in the vagina and uterus, producing an hydrometrocolpos. In vaginal or cervical atresia, the products may collect in the fallopian tubes and broad ligament. The diagnosis is easily made by US when the fluid-filled vagina and dilated uterus are seen behind the bladder (Fig. 1.86). It is not unusual that, after a urine culture is performed for suspected urinary tract infection, the patient undergoes US with an empty bladder. In these situations, special attention must be paid not to mistake a fluid-filled vagina with a full bladder. Identification of the dilated uterus in the cranial aspect of the cystic structure that occupies the pelvis can help make the right diagnosis.

References

Addiss DG, Shaffer N, Fowler BS et al (1990) The epidemiology of appendicitis and appendectomy in the United States. Am J Epidemiol 132:910–25

Albanese CT, Rowe MI (1998) necrotising enterocolitis. In: O´Neil JA, Rowe MI, Grosfeld JL, et al (eds.): Paediatric Surgery, 5th ed, vol 2. St. Louis, Mosby-Year Book, pp 1297–1320

Alessi V, Salerno G (1985) The "hay-fork" sign in the ultrasonographic diagnosis of intussusception. Gastrointest Radiol 10:177–179

Amodio J, Berdon WE, Abramson SJ (1986) Microcolon of prematurity: a form of functional obstruction. AJR Am J Roentgenol 146:239–244

Auringer ST, Sumner TE (1994) Pediatric upper gastrointestinal tract. Radiol Clin North Am 32:1051–1066

Babcock DS (2002) Sonography of the acute abdomen in the pediatric patient. J Ultrasound Med 21:887–899

Babyn P, Peled N, Manson D et al (1995) Radiologic features of gastric outlet obstruction in infants after long-term prostaglandin administration. Pediatr Radiol 25:41–43

Bailey PV, Tracy TF Jr, Connors RH et al (1993) Congenital duodenal obstruction: a 32-year review. J Pediatr Surg 28:92–95

Baldisserotto M, Maffazzoni DR, Dora MD (2005) Omental infarction in children: color Doppler sonography correlated with surgery and pathology findings. AJR Am J Roentgenol 184:156–162

Balthazar EJ (2002) Complications of acute pancreatitis: clinical and CT evaluation. Radiol Clin North Am 40:1211–1229

Barki Y, Bar-Ziv J (1985) Meconium ileus: ultrasonic diagnosis of intraluminal inspissated meconium. J Clin Ultrasound 13:509–512

Beasley SW, De Campo JF (1987) Pitfalls in the radiological diagnosis of malrotation. Australas Radiol 33:376–383

Bell MJ, Ternberg JL, McAlister W et al (1977) Antral diaphragm – a cause of gastric outlet obstruction in infants and children. J Pediatr 90:196–202

Benya EC (2002) Pancreas and biliary system. Imaging of developmental anomalies and diseases unique to children. Radiol Clin North Am 40:1355–1362

Berdon WE (1995) The diagnosis of malrotation and volvulus in the older child and adult: a trap for radiologists. Pediatr Radiol 25:101–103

Berdon WE, Baker DH, Santulli TV et al (1968) Microcolon in newborn infants with intestinal obstruction. Radiology 90:878–885

Bernstein SM, Russ PD (1998). Midgut volvulus: a rare cause of acute abdomen in an adult patient. AJR Am J Roentgenol 171:639–641

Berrocal T, Lamas M, Gutiérrez J et al (1999) Congenital anomalies of the small intestine, colon and rectum. Radiographics 19:1219–1236

Berrocal T, Prieto C, Ignacio P et al (1995) Sonography of pancreatic disease in infants and children. Radiographics 15:301–313

Birnbaum BA, Wilson SR (2000) Appendicitis at the millennium. Radiology 215:337–348

Birnbaum BA, Jeffrey RB Jr (1998) CT and sonographic evaluation of acute right lower quadrant pain. AJR Am J Roentgenol 170:361–371

Bley W, Franken EA Jr (1973) Roentgenology of colon atresia. Pediatr Radiol 1:105–108

Bonadio WA, Clarkson T, Naus J (1991) The clinical features of children with malrotation of the intestine. Pediatr Emerg Care 7:348–349

Borushok FK, Jeffrey RB Jr, Laing FC et al (1990) Sonographic diagnosis of perforation in patients with acute appendicitis. AJR Am J Roentgenol 154:275–278

Bowen A, Mazer J, Zarabi M, et al (1984) Cystic meconium peritonitis: ultrasonographic features. Pediatr Radiol 14:18–22

Boyden EA, Cope JG, Bill AH (1967) Anatomy and embryology of congenital intrinsic obstruction of the duodenum. Am J Surg 114:190–193

Bramson RT, Blickman JG (1992) Perforation during hydrostatic reduction of intussusception: proposed mechanism and review of the literature. J Pediatr Surg 27:589–591

Bramson RT, Shiels II WE, Eskey CJ et al (1997) Intraluminal colon pressure dynamics with Valsalva maneuver during air enema study. Radiology 202:825–828

Bulas DI, Ahlstrom PA, Sivit CJ et al (1992) Pelvic inflammatory disease in the adolescent: comparison of transabdominal and transvaginal sonographic evaluation. Radiology 183:435–439

Buonomo C (1997) Neonatal gastrointestinal emergencies. Radiol Clin North Am 35:845–864

Buonomo C (1999) The radiology of necrotizing enterocolitis. Radiol Clin North Am 37:1187–1198

Burge D, Drewett M (2004) Meconium plug obstruction. Pediatr Surg Int. 20:108–110

Burke MS, Ragi JM, Karamanoukian HL et al (2002) New strategies in nonoperative management of meconium ileus. J Pediatr Surg 37:760–764

Carty HM (2002) Paediatric emergencies: non-traumatic abdominal emergencies. Eur Radiol 12:2835–2848

Ceres L, Alonso I, Lopez P et al (1990) Ultrasound study of acute appendicitis in children with emphasis upon the diagnosis of retrocecal appendicitis. Pediatr Radiol 20:258–261

Chao HC, Kong MS, Chen JY et al (2000) Sonographic features related to volvulus in neonatal intestinal malrotation. J Ultrasound Med 19:371–376

Chinn DH, Millar EI, Piper N (1987) Hemorrhagic cholecystitis. Sonographic and clinical presentation. J Ultrasound Med 6:313–317

Cobben LP, de Van Otterloo AM, Puylaert JB (2000) Spontaneously resolving appendicitis: frequency and natural history in 60 patients. Radiology 215:349–352

Cohen MM Jr (2003) Infants of diabetic mothers and neonatal small left colon. Am J Med Genet A 122:301–302

Collins DC (1932) The length and position of the vermiform appendix. A study of 4680 specimens. Ann Surg 96:1044–1048

Connolly B, Alton DJ, Ein SH et al (1995) Partially reduced intussusception: when are repeated delayed reduction attempts appropriate? Pediatr Radiol 25:104–107

Cotran RS, Kumar V, Robbins SL (1989) Appendix. In: Saunders WB (ed) Robbins pathologic basis of disease, 4th edn. Saunders, Philadelphia, pp 902–904

Crowe JE, Sumner TE (1978) Combined esophageal and duodenal atresia without tracheoesophageal fistula: characteristic radiographic changes. AJR Am J Roentgenol 130:167–168

Dalla Vecchia LK, Grosfeld JL, West KW et al (1998) Intestinal atresia and stenosis. Arch Surg 133:490–497

Daneman A, Alton DJ (1996) Intussusception. Issues and controversies related to diagnosis and reduction. Radiol Clin North Am 34:743–756

Daneman A, Navarro O (2004) Intussusception. Part 2: an update on the evolution of management. Pediatr Radiol 34:97–108

Dann PH, Amodio JB, Rivera R et al (2005) Primary bacterial peritonitis in otherwise healthy children: imaging findings. Pediatr Radiol 35:198–201

Dasgupta R, Langer JC (2004) Hirschsprung disease. Curr Probl Surg 41:942–988

De Backer AI, De Schepper AM, Deprettere A et al (1999) Radiographic manifestations of intestinal obstruction in the newborn. JBR-BTR 82:159–166

De Lorimier A, Fonkalsrud E, Hays D (1969) Congenital atresia and stenosis of the jejunum and ileum. Surgery 65:819–827

Deeg KH, Rupprecht T, Schmid E (1993) Doppler sonographic detection of increased flow velocities in the celiac trunk and superior mesenteric artery in infants with necrotizing enterocolitis. Pediatr Radiol 23:578–582

del Pozo G (2005) Intussusception: still work in progress. Pediatr Radiol 35:92–94

del Pozo G, Sánchez L, Miralles M et al (1992) Appendicitis in children: usual and unusual appearances. Radiology 185[Suppl]:349–360

del Pozo G, Miralles M, Sánchez L et al (1994) Apendicitis aguda en la infancia. Hallazgos ecográficos frecuentes e infrecuentes. Radiología 36:411–424

del Pozo G, Albillos JC, Tejedor D (1996a) Intussusception: US findings with pathologic correlation. The crescent-in-doughnut sign. Radiology 199:688–692

del Pozo G, González-Spinola J, Gómez-Ansón B et al (1996b) Intussusception: trapped peritoneal fluid detected with US-relationship to reducibility and ischemia. Radiology 201:379–386

del Pozo G, Albillos JC, Tejedor D et al (1999) Intussusception in children: current concepts in diagnosis and enema reduction. RadioGraphics 19:299–319

Dolan CR, Smith LT, Sybert VP (1993) Prenatal detection of epidermolysis bullosa letalis with pyloric atresia in a fetus by abnormal ultrasound and elevated alpha-fetoprotein. Am J Med Genet 47:395–400

Eckoldt F, Heling KS, Woderich R et al (2003) Meconium peritonitis and pseudo-cyst formation: prenatal diagnosis and post-natal course. Prenat Diagn 23:904–908

Eshed I, Witzling M (2002) The role of enhanced helical CT in the evaluation of suspected renal colic and atypical abdominal pain in children. Pediatr Radiol 32:205–208

Faingold R, Daneman A, Tomlinson G et al (2005) Necrotizing enterocolitis: assessment of bowel viability with color Doppler US. Radiology 235:587–594

Ford EG, Senac MO Jr, Srikanth MS et al (1992) Malrotation of the intestine in children. Ann Surg 215:172–178

Foster MA, Nyberg DA, Mahony BS et al (1987) Meconium peritonitis: prenatal sonographic findings and their clinical significance. Radiology 165:661–663

Fotter R (1998) Imaging of constipation in infants and children. Eur Radiol 8:248–258

Fotter R, Sorantin E (1994) Diagnostic imaging in necrotizing enterocolitis. Acta Paediatr 396[Suppl]:41–44

Frye TR, Mah CL, Schiller M (1972) Roentgenographic evidence of gangrenous bowel in midgut volvulus with observations in experimental volvulus. Am J Roentgenol Radium Ther Nucl Med 114:394–401

Gallego C, del Pozo G, Marin C et al (1998) Torsion of a Meckel's diverticulum: sonographic findings. Pediatr Radiol 28:599–601

Garcia-Pena BM, Taylor GA, Lund DP et al (1999) Effect of computed tomography on patient management and costs in children with suspected appendicitis. Pediatrics 104:440–446

Garza-Cox S, Keeney SE, Angel CA et al (2004) Meconium obstruction in the very low birth weight premature infant. Pediatrics 114:285–290

Gershon MD, Ratcliffe EM (2004) Developmental biology of the enteric nervous system: pathogenesis of Hirschsprung's disease and other congenital dysmotilities. Semin Pediatr Surg 13:224–235

Gilsanz V (1984) Displacement of the appendix in intussusception. AJR Am J Roentgenol 142:407–408

Godbole P, Stringer MD (2002) Bilious vomiting in the newborn: how often is it pathologic? J Pediatr Surg 37:909–911

Gonzalez-Spinola J, del Pozo G, Tejedor D et al (1999) Intussusception: the accuracy of ultrasound-guided saline enema and the usefulness of a delayed attempt at reduction. J Pediatr Surg 34:1016–1020

Graif M, Itzchak Y (1988) Sonographic evaluation of ovarian torsion in childhood and adolescence. AJR Am J Roentgenol 150:647–651

Gray GF, Ashley P (1986) Surgical pathology of the vermiform appendix. In: Soumers SC, Rosen PP, Fechner RE (eds) Pathology annual. Part 2. Appleton-Century-Crofts, Norwalk, Connecticut, 21:111–144

Gu L, Alton DJ, Daneman A et al (1988) Intussusception reduction in children by rectal insufflation of air. AJR Am J Roentgenol 150:1345–1348

Gu L, Zhu H, Wang S et al (2000) Sonographic guidance of air enema for intussusception reduction in children. Pediatr Radiol 30:339–342

Guo JZ, Ma XY, Zhou QH (1986) Results of air pressure enema reduction of intussusception: 6,396 cases in 13 years. J Pediatr Surg 21:1201–1203

Hahn H, Hoepner F, Kalle T, et al. (1997) Appendicitis in childhood (German). Radiologe 37:454-458

Hajivassiliou CA (2003) Intestinal obstruction in neonatal/pediatric surgery. Semin Pediatr Surg 12:241–253

Hayakawa K, Hamanaka Y, Suzuki M et al (2003) Radiological findings in total colon aganglionosis and allied disorders. Radiat Med 21:128–134

Hayden CK Jr (1991) Advances in the ultrasonographic evaluation of the pediatric gastrointestinal tract. Ultrasound Quatr 9:139–169

Hayden, CK Jr (1996) Ultrasonography of the acute pediatric abdomen. Radiol Clin North Am 34:791–806

Hayes R (2004) Abdominal pain: general imaging strategies. Eur Radiol 14:L123–L137

Henderson J, Goldacre MJ, Fairweather JM (1992) Conditions accounting for substantial time spent in hospital in children age 1–14 years of age. Arch Dis Child 67:83–86

Henrikson S, Blane CE, Koujok K et al (2003) The effect of screening sonography on the positive rate of enemas for intussusception. Pediatr Radiol 33:190–193

Hernanz-Schulman M (1999) Imaging of neonatal gastrointestinal obstruction. Radiol Clin North Am 37:1163–1186

Hertzberg BS, Bowie JD (1990) Fetal gastrointestinal abnormalities. Radiol Clin North Am 28:101–114

Hoffman FN, Bax NM, van der Zee DC et al (2004) Surgery for necrotizing enterocolitis: primary anastomosis or enterostomy? Pediatr Surg Int 20:481–483

Holgersen LO, Stanley-Brown EG (1971) Acute appendicitis with perforation. Am J Dis Child 122:288–293

Holt S, Samuel E (1978) Multiple concentric ring sign in the ultrasonographic diagnosis of intussusception. Gastrointest Radiol 3:307–309

Horton KK (2005) Pathophysiology and current management of necrotizing enterocolitis. Neonatal Netw 24:37–46

Hurth PJ, Meyer JS, Shaaban A (2002) Ultrasound of a torsed ovary: characteristic gray-scale appearance despite normal arterial and venous flow on Doppler. Pediatr Radiol 32:586–588

Hussain SM, Meradji M, Robben SG et al (1991) Plain film diagnosis in meconium plug syndrome, meconium ileus and neonatal Hirschsprung's disease. A scoring system. Pediatr Radiol 21:556–559

Jamieson DH, Dundas SE, Belushi SA et al (2004) Does the transition zone reliably delineate aganglionic bowel in Hirschsprung's disease? Pediatr Radiol 34:811–815

Jeffrey RB Jr, Laing FC, Lewis FR (1987) Acute appendicitis: high-resolution real-time ultrasound findings. Radiology 163:11–14

Jeffrey RB Jr, Laing FC, Townsend RR (1988) Acute appendicitis: sonographic criteria based on 250 cases. Radiology 167:327–329

Johnson JF, Coughlin WF (1989) Plain film diagnosis of appendiceal perforation in children. SeminUltrasound CT MR 10:306–313

Jouppila P, Kirkinen P (1984) Ultrasonic and clinical aspects in the diagnosis and prognosis of congenital gastrointestinal anomalies. Ultrasound Med Biol 10:465–468
Kaiser S, Frenckner B, Jorulf HK (2002) Suspected appendicitis in children: US and CT – a prospective randomized study. Radiology 223:633–638
Kaiser S, Finnbogason T, Jorulf HK et al (2004) Suspected appendicitis in children: diagnosis with contrast-enhanced versus nonenhanced helical CT. Radiology 231:427–433
Kamata S, Nose K, Ishikawa S, Usui N, Sawai T, Kitayama Y, Okuyama H, Imura K et al (2000) Meconium peritonitis in utero. , Pediatr Surg Int 16:377–379
Kao SC, Franken EA Jr (1995) Nonoperative treatment of simple meconium ileus: a survey of the Society for Pediatric Radiology. Pediatr Radiol 25:97–100
Karmazyn B, Werner EA, Rejaie B et al (2005) Mesenteric lymph nodes in children: what is normal? Pediatr Radiol 35:774–777
Kassner EG, Kottmeier PK (1975) Absence and retention of small bowel gas in infants with midgut volvulus: mechanisms and significance. Pediatr Radiol 4:28–30
Katz M, Phelan E, Carlin JB et al (1993) Gas enema for the reduction of intussusception: relationship between clinical signs and symptoms and outcome. AJR Am J Roentgenol 160:363–366
Katz ME, Kolm P (1992) Intussusception reduction 1991: an international survey of pediatric radiologists. Pediatr Radiol 22:318–322
Keyzer C, Tack D, Bohy P et al (2004) Acute appendicitis: comparison of low-dose and standard-dose unenhanced multi-detector row CT. Radiology 232:164–172
Kimmey MB, Martin RW, Haggitt RC et al (1989) Histologic correlates of gastrointestinal ultrasound images. Gastroenterology 96:433–441
Kirks DR (1994) Diagnosis and treatment of pediatric intussusception: how far should we push our radiologic techniques? Radiology 191:622–623
Kleinhaus S, Boley SJ, Sheran M et al (1979) Hirschsprung's disease – a survey of the members of the Surgical Section of the American Academy of Pediatrics. J Pediatr Surg 14:588–597
Kong MS, Wong HF, Lin SL et al (1997) Factors related to detection of blood flow by color Doppler ultrasonography in intussusception. J Ultrasound Med 16:141–144
Koplewitz BZ, Daneman A (1999) The lateral view: a useful adjunct in the diagnosis of malrotation. Pediatr Radiol 29:144–145
Kosloske AM, Love CL, Rohrer JE et al (2004) The diagnosis of appendicitis in children: outcomes of a strategy based on pediatric surgical evaluation. Pediatrics 113:29–34
Krasna IH, Rosenfeld D, Salerno P (1996) Is it necrotizing enterocolitis, microcolon of prematurity, or delayed meconium plug? A dilemma in the tiny premature infant. J Pediatr Surg 31:855–858
Kuta AJ, Benator RM (1990) Intussusception: hydrostatic pressure equivalents for barium and meglumine sodium diatrizoate. Radiology 175:125–126
Larsen W (1993) Human embryology. Churchill Livingston, New York
Lawrence PW, Chrispin A (1984) Sonographic appearances in two neonates with generalized meconium peritonitis: the "snowstorm" sign. Br J Radiol 57:340–342
Leonidas JC, Amoury R, Ashcraft K et al (1976) Duodenojejunal atresia with "apple peel" small bowel: a distinct form of intestinal atresia. Radiology 118:661–665
LeQuesne G, Reilly B (1975) Functional immaturity of the large bowel in the newborn infant. Radiol Clin North Am 13:331–342
Lewis FR, Holcroft JW, Boey J et al (1975) Appendicitis: a critical review of diagnosis and treatment in 1,000 cases. Arch Surg 110:677–684
Loening-Baucke V, Kimura K (1999) Failure to pass meconium: diagnosing neonatal intestinal obstruction. Am Fam Physician 60:2043–2050
Long FR, Kramer SS, Markowitz RI et al (1996) Radiographic patterns of intestinal malrotation in children. Radiographics 16:547–556
Ly JN, Miller FH (2002) MR imaging of the pancreas: a practical approach. Radiol Clin North Am 40:1289–1307
Manning C, Straus A, Gyepes MT (1989) Jejunal atresia with apple peel deformity. A report of eight survivors. J Perinatol 9:281–286
Marincek B (2002) Nontraumatic abdominal emergencies: acute abdominal pain: diagnostic strategies. Eur Radiol 12:2136–50
Maxson RT, Franklin PA, Wagner CW (1995). Malrotation in the older child: surgical management, treatment, and outcome. Am Surg 61:135–138
McAlister WH, Kronemer KA (1996) Emergency gastrointestinal radiology of the newborn. Radiol Clin North Am 34:819–844
Meaghar T, Sukumar VP, Collingwood J et al (2001). Low-dose computed tomography in suspected acute renal colic. Clin radiol 56:873–876
Meier-Ruge WA, Bruder E, Holschneider AM et al (2004) Diagnosis and therapy of ultrashort Hirschsprung's disease. Eur J Pediatr Surg 14:392–397
Meradji M, Hussain SM, Robben SGF et al (1994) Plain film diagnosis in intussusception. Br J Radiol 67:147–149
Meyer SE (1992) The current radiologic management of intussusception: a survey and review. Pediatr Radiol 22:323–325
Meyer JS, Dangman BC, Buonomo C et al (1993) Air and liquid contrast agents in the management of intussusception: a controlled, randomized trial. Radiology 188:507–511
Millar AJ, Rode H, Cywes S (2003) Malrotation and volvulus in infancy and childhood. Semin Pediatr Surg 12:229–236
Miller SF, Landes AB, Dautenhahn LW et al (1995) Intussusception: ability of fluoroscopic images obtained during air enemas to depict lead points and other abnormalities. Radiology 197:493–496
Miller SF, Seibert JJ, Kinder DL et al (1993) Use of ultrasound in detection of occult bowel perforation in neonates. J Ultrasound Med 12:531–535
Montali G, Croce F, de Pra L et al (1983) Intussusception of the bowel: a new sonographic pattern. Br J Radiol 56:621–623
Morrison SC, Jacobson JM (1994) The radiology of necrotizing enterocolitis. Clin Perinatol 21:347–363
Morrison SC, Reid JR, Harrison M et al (2004) Systemic arterial pneumatosis in a neonate with necrotizing enterocolitis. Pediatr Radiol 34:337–339
Navarro O, Daneman A (2004a) Intussusception. Part 3: diagnosis and management of those with an identifiable

or predisposing cause and those that reduce spontaneously. Pediatr Radiol 34:305–312
Navarro OM, Daneman A, Chae A (2004b) Intussusception: the use of delayed, repeated reduction attempts and the management of intussusceptions due to pathologic lead points in pediatric patients. AJR Am J Roentgenol 182:1169–1176
Nelson LH, Clark CE, Fishburne JI (1982) Value of serial sonography in the in utero detection of duodenal atresia. Obstet Gynecol 59:657–660
Nghiem HV, Jeffrey RB (1992) Acute appendicitis confined to the appendiceal tip: evaluation with graded compression sonography. J Ultrasound Med 11:205–207
Norton KI, Tenreiro R, Rabinowitz JG (1992) Sonographic demonstration of annular pancreas and a distal duodenal diaphragm in a newborn. Pediatr Radiol 22:66–67
Nosaka S (2000) Diagnostic radiology in acute pediatric abdomen. Nippon Igaku Hoshasen Gakkai Zasshi 60:5–13
Okoye BO, Parikh DH, Buick RG et al (2000) Pyloric atresia: five new cases, a new association, and a review of the literature with guidelines. J Pediatr Surg 35:1242–1245
O'Malley ME, Wilson SR (2003) US of gastrointestinal tract abnormalities with CT correlation. Radiographics 23:59–72
Ooms HWA, Koumans RKJ, Ho Kang You PJ et al (1991) Ultrasonography in the diagnosis of acute appendicitis. Br J Surg 78:315–318
Patino MO, Munden MM (2004) Utility of the sonographic whirlpool sign in diagnosing midgut volvulus in patients with atypical clinical presentations. J Ultrasound Med 23:397–401
Peled N, Dagan O, Babyn P et al (1992) Gastric-outlet obstruction induced by prostaglandin therapy in neonates. N Engl J Med 327:505–511
Pennington DJ, Zerin MJ (1999) Imaging of the UTI. Pediatr Ann 28:678–686
Pickhardt PJ, Bhalla S (2002) Intestinal malrotation in adolescents and adults: spectrum of clinical and imaging features. AJR Am J Roentgenol 179:1429–143
Pierro A, Hall N (2003) Surgical treatments of infants with necrotizing enterocolitis. Semin Neonatol 8:223–232
Ping AJ, Blane CE, Garver KA (1998) Current prognosis in necrotizing enterocolitis with portal vein gas. Can Assoc Radiol J 49:237–240
Poole GV (1990) Anatomic basis for delayed diagnosis of appendicitis. South Med J 83:771–773
Powell RW, Raffensperger JG (1982) Congenital colonic atresia. J Pediatr Surg 17:166–170
Pracros JP, Sann L, Genin G et al (1992) Ultrasound diagnosis of midgut volvulus: the "whirlpool" sign. Pediatr Radiol 22:18–20
Pracros JP, Tran-Minh VA, Morin de Finfe CH et al (1987) Acute intestinal intussusception in children. Contribution of ultrasonography (145 cases). Ann Radiol 30:525–530
Puylaert JB (1986) Acute appendicitis: US evaluation using graded compression. Radiology 158:355–360
Puylaert JB (1990) Diagnosis of appendicitis by ultrasound. In: Puylaert JBCM (ed) Ultrasound of appendicitis and its differential diagnosis, Springer-Verlag, Berlin Heidelberg New York, pp 29–62
Puylaert JB (2001) Ultrasound of acute GI tract conditions. Eur Radiol 11:1867–1877
Puylaert JB (2003) Ultrasonography of the acute abdomen: gastrointestinal conditions. Radiol Clin N Am 41:1227–1248
Puylaert JB, Vermeijden RJ, Van der Werf SD et al (1989) Incidence and sonographic diagnosis of bacterial ileocaecitis masquerading as appendicitis. Lancet 2(8654):84–86
Rao PM, Rhea JT, Novelline RA et al (1997) Helical CT technique for the diagnosis of appendicitis: prospective evaluation of a focused appendix CT examination. Radiology 202:139–144
Rao PM, Rhea JT, Novelline RA et al (1998) Effect of computed tomography of the appendix on treatment of patients and use of hospital resources. N Engl J Med 338:141–146
Ratcliffe JF, Fong S, Cheong I et al (1992) Plain film diagnosis of intussusception: prevalence of the target sign. AJR Am J Roentgenol 158:619–621
Rathaus V, Grunebaum M, Ziv N et al (1992) The bubble sign in the gasless abdomen of the newborn. Pediatr Radiol 22:18–20
Ravitch MM (1986) Intussusception. In: Ravitch MM (ed) Pediatric surgery, 4th edn. Year Book Medical, Chicago, 868–882
Rescorda FJ (1997) Cholelithiasis, cholecystitis, and common bile duct stones. Curr Opin Pediatr 9:276–282
Rescorla FJ, Grosfeld JL (1993) Contemporary management of meconium ileus. World J Surg 17:318–325
Rescorla FJ, Morrison AM, Engles D et al (1992) Hirschsprung's disease. Evaluation of mortality and long-term function in 260 cases. Arch Surg 127:934–941
Rettenbacher T, Hollerweger A, Macheiner P et al (2001) Outer diameter of the vermiform appendix as a sign of acute appendicitis: evaluation at US. Radiology 218:757–762
Reynolds E, Douglass B, Bleacher J (2000) Meconium peritonitis. J Perinatol 20:193–195
Riccabona M (2001) Paediatric ultrasound. I. Abdominal. Eur Radiol 11:2354–2368
Riccabona M (2002a) Potential of modern techniques in paediatric uroradiology. Eur J Radiol 43:110–121
Riccabona M, Simbrunner J, Ring E et al (2002b) Feasibility of MR-urography in neonates and infants with anomalies of the upper urinary tract. Eur J Radiol 12:1442–1450
Riebel TW, Nasir R, Weber K (1993) US-guided hydrostatic reduction of intussusception in children. Radiology 188:513–516
Rioux M (1992) Sonographic detection of the normal and abnormal appendix. AJR Am J Roentgenol 158:773–778
Rohrschneider WK, Tröger J (1995) Hydrostatic reduction of intussusception under US guidance. Pediatr Radiol 25:530–534
Rosenfield NS, Ablow RC, Markowitz RI et al (1984) Hirschsprung disease: accuracy of the barium enema examination. Radiology 150:393–400
Rothrock SG, Skeoch G, Rush JJ et al (1991) Clinical features of misdiagnosed appendicitis in children. Ann Emerg Med 20:45–50
Salman AB, Karaoglanoglu N, Suma S (1999) Abdominal, scrotal, and thoracic calcifications owing to healed meconium peritonitis. J Pediatr Surg 34:1415–1416
Sargent MA, Babyn P, Alton DJ (1994) Plain abdominal radiography in suspected intussusception: a reassessment. Pediatr Radiol 24:17–20

Schmitz-Rode T, Müller-Leisse C, Alzen G (1991) Comparative examination of various rectal tubes and contrast media for the reduction of intussusceptions. Pediatr Radiol 21:341–345
Shiels WE II, Kirks DR, Keller GL et al (1993) Colonic perforation by air and liquid enemas: comparison study in young pigs. AJR Am J Roentgenol 160:931–935
Shiels WE II, Maves CK, Hedlung GL et al (1991) Air enema for diagnosis and reduction of intussusception: clinical experience and pressure correlates. Radiology 181:169–172
Shimanuki Y, Aihara T, Takano H et al (1996) Clockwise whirlpool sign at color Doppler US: an objective and definite sign of midgut volvulus. Radiology 199:261–264
Siegel MJ, Shackelford GD, McAlister WH (1981) The rectosigmoid index. Radiology 139:497–499
Sigalas I, Dafopoulos K, Galazios G et al (2003) Fetal small bowel obstruction: report of two cases. Clin Exp Obstet Gynecol 30:161–163
Singleton EB, Wagner ML, Dutton RV (1977) Radiology of the alimentary tract in infants and children, 2nd edn. Saunders, Philadelphia
Sivit CJ, Applegate KE, Stallion A et al (2000) Imaging evaluation of suspected appendicitis in a pediatric population: effectiveness of sonography versus CT. AJR Am J Roentgenol 175:977–980
Sivit CJ Siegel MJ, Applegate KE et al (2001) When appendicitis is suspected in children. Radiographics 21:247–262
Slovis TL,Klein MD,Watts FB (1980) Incomplete rotation of the intestine with a normal cecal position. Surgery 87:325–330
Smet MH, Marchal G, Ceulemans R et al (1991) The solitary hyperdynamic pulsating superior mesenteric artery: an additional dynamic sonographic feature of midgut volvulus. Pediatr Radiol 21:156–157
Smink DS, Finkelstein JA, Kleinman K et al (2004) The effect of hospital volume of pediatric appendectomies on the misdiagnosis of appendicitis in children. Pediatrics 113 (1 Pt 1):18–23
Solari V, Piotrowska AP, Puri P (2003) Histopathological differences between recto-sigmoid Hirschsprung's disease and total colonic aganglionosis. Pediatr Surg Int 19:349–354
Spear R, Kimmey MB, Wang KY et al (1992) Appendiceal US scans: histologic correlation. Radiology 183:831–834
Spigland N, Brandt ML, Yazbeck S (1990) Malrotation presenting beyond the neonatal period. J Pediatr Surg 25:1139–1142
Stringer MD, Pablot SM, Brereton RJ (1992) Paediatric intussusception. Br J Surg 79:867–876
Strouse PJ (2004) Disorders of intestinal rotation and fixation („malrotation"). Pediatr Radiol 34:837–851
Strouse PJ, DiPietro MA, Saez F (2003) Transient small-bowel intussusception in children on CT. Pediatr Radiol 33:316–320
Surratt J, Siegel M (1991) Imaging of pediatric ovarian masses. Radiographics 11:533–547
Sweeney B, Surana R, Puri P (2001) Jejunoileal atresia and associated malformations: correlation with the timing of in utero insult. J Pediatr Surg 36:774–776
Swischuck LE, Hayden CK, Boulden T (1985) Intussusception: indications for ultrasonography and explanation of the doughnut and pseudokidney signs. Pediatr Radiol 15:388–391
Swischuck LE, John SD, Swischuck PN (1994) Spontaneous reduction of intussusception: verification with US. Radiology 192:269–271
Swischuk LE, Stansberry SD (1991) Ultrasonographic detection of free peritoneal fluid in uncomplicated intussusception. Pediatr Radiol 21:350–351
Sze RW, Guillerman RP, Krauter D et al (2002) A possible new ancillary sign for diagnosing midgut volvulus: the truncated superior mesenteric artery. J Ultrasound Med 21:477–480
Taylor GA (2004) Suspected appendicitis in children: in search of the single best diagnostic test. Radiology 231:293–295
Theriot JA, Sayat J, Franco S et al (2003) Childhood obesity: a risk factor for omental torsion. Pediatrics 112 (6 Pt 1): e460
Toma P, Mengozzi E, Dell'Acqua A et al (2002) Pyloric atresia: report of two cases (one associated with epidermolysis bullosa and one associated with multiple intestinal atresias). Pediatr Radiol. 32:552–555
Torres AM, Ziegler MM (1993) Malrotation of the intestine. World J Surg 17:326–331
Touloukian RJ (1993) Diagnosis and treatment of jejunoileal atresia. World J Surg 17:310
Tsakayannis DE, Kozakewich HP, Lillehei CW (1996) Acalculous cholecystitis in children. JPediatr Surg 31:127–131
Valette PJ, Rioux M, Pilleul F et al (2001) Ultrasonography of chronic inflammatory bowel diseases. Eur Radiol 11:1859–1866
van Breda Vriesman AC, Puylaert JBCM (2002) Epiploic appendagitis and omental infarction: pitfalls and look-alikes. Abdom Imaging 27:20–28
Varjavandi V, Lessin M, Kooros K et al (2003) Omental infarction: risk factors in children. J Pediatr Surg. 38:233–235
Verschelden P, Filiatrault D, Garel L et al (1992) Intussusception in children: reliability of US in diagnosis – a prospective study. Radiology 184:741–744
Vieten D, Spicer R (2004) Enterocolitis complicating Hirschsprung's disease. Semin Pediatr Surg 13:263–272
Vignault F. Filiatrault D, Brandt ML et al (1990) Acute appendicitis in children: evaluation with US. Radiology 176:501–504
Waldhausen JHT, Sawin RS (1997) Improved long-term outcome for patients with jejunoileal apple peel atresia. J Pediatr Surg 32:1307–1309
Wang GD, Liu SJ (1988) Enema reduction of intussusception by hydrostatic pressure under ultrasound guidance: a report of 377 cases. J Pediatr Surg 23:814–818
Ward AM, Kay R, Ross JH (1998) Ureteropelvic junction obstruction in children. Unique considerations for open operative intervention. Urol Clin North Am 25:211–217
Weinberger E, Winters WD, Liddell RM (1992) Sonographic diagnosis of intestinal malrotation in infants: importance of the relative positions of the superior mesenteric vein and artery. AJR Am J Roentgenol 159:825–828
Wiersma F, Sramek A, Holscher HC (2005) US features of the normal appendix and surrounding area in children. Radiology 235:1018–1022
Winters WD, Weinberger E, Hatch EI (1992) Atresia of the colon in neonates: radiographic findings. AJR Am J Roentgenol 159:1273–1276

Woo SK, Kim JS, Suh SJ et al (1992) Childhood intussusception: US-guided hydrostatic reduction. Radiology 182:77–80

Yoon CH, Kim HJ, Goo HW (2001) Intussusception in children: US-guided pneumatic reduction-initial experience. Radiology 218:85–88

Zambuto D, Bramson RT, Blickman JG (1995) Intracolonic pressure measurements during hydrostatic and air contrast barium enema studies in children. Radiology 196:55–58

Ziegler MM (2004) The diagnosis of appendicitis: an evolving paradigm. Pediatrics 113 (1 Pt 1):130–132

The Esophagus

2

Ronald B. J. Glass

CONTENTS

R. B. J. Glass, MD
Department of Radiology, Children's Memorial Hospital, 2300 Children's Plaza, Chicago, IL 60614, USA
and
Associate Professor of Radiology, Feinberg School of Medicine, Northwestern University, Chicago, IL, USA

2.1 Anatomy and Development of the Esophagus

2.1.1 Development

The esophagus and trachea form from a single common tubular structure that separates into an anterior laryngotracheal groove and a posterior esophagus (Collins 1995). Development of the esophagus begins in the fourth week of fetal life when the respiratory diverticula, or lung buds, appear on the ventral wall of the foregut at the border with the pharyngeal gut. Lateral invagination of the mesodermal esophagotracheal septum gradually partitions this diverticulum from the foregut, thus dividing into the ventral respiratory primordium and the dorsal esophagus. Epithelial growth obliterates the lumen, which recanalizes at the tenth week (Sadler 2000). The esophagus is initially short, but lengthens rapidly with descent of the heart and lungs, and attains normal length by 7 weeks. Occasionally, the esophagus fails to lengthen sufficiently, and the stomach is pulled up into the esophageal hiatus through the diaphragm, resulting in a congenital hiatal hernia (Sadler 2000). The commonest congenital anomalies, i.e. the tracheoesophageal fistula/esophageal atresia complex, esophageal stenosis, duplication cysts and bronchopulmonary foregut malformations, are the result of disruption of the normal sequence of separation of the airway from the foregut. The upper esophageal sphincter and normal peristaltic activity are well developed by 33 weeks, and continue to mature in the post-natal period (Jadcherla et al. 2005).

2.1.2 Anatomy

The esophagus is a muscular tube that connects the pharynx at the level of the inferior border of the cricoid cartilage at C6 to the cardia of the stomach at the level of T11 (Meschan 1975). The course of the esophagus is approximately vertical, with a gentle curve to the level of the lower neck. The esophagus gradually returns medially at the level of T5, inclining again to the left at the level of T7, and finally inclining anteriorly to traverse the diaphragm at T10 (Bannister 1995). The esophagus lies anterior to the spine, and its course parallels the curves of the cervical and thoracic spine. Apart from the appendix, the esophagus has the narrowest lumen of the alimentary tract. Four anatomic sites of constriction occur at which the esophageal lumen becomes even narrower. These include: at the cricopharyngeus muscle, the level where the aortic arch crosses the esophagus, the level at which the left main stem bronchus crosses the esophagus just below the carina, and the level of the esophageal hiatus in the diaphragm. A foreign body or a large food bolus may lodge at one of these natural constrictions and thereby obstruct the esophagus. The lower esophageal sphincter, or vestibule, is at the level of, or below, the diaphragm and is held in place by the phrenico-esophageal membrane. The lower esophageal sphincter is formed by smooth muscle fibers that surround the intra-abdominal esophagus. These fibers remain contracted except during swallowing and vomiting. Sphincteric action is also provided by the diaphragmatic crura that surround the esophagus. The crural muscle fibers constrict the esophagus during inspiration and when intra-abdominal pressure is raised and prevent gastroesophageal reflux (Bannister 1995). The acuteness of the angle of the gastroesophageal junction also prevents reflux.

The esophagus is lined by a thick mucosa of non-keratinized squamous epithelium that provides an impermeable barrier and, together with surface mucus, protects against mechanical injury. The muscularis mucosae is made up of longitudinal smooth muscle that becomes thicker distal to the pharynx. The mucosa is loosely attached to the muscularis mucosae. The muscularis consists of an outer, thicker longitudinal layer and an inner circular layer. Accessory slips of muscle fibers attach and anchor the esophagus to adjacent thoracic organs and to the pleura. Striated skeletal muscle occurs in the upper two-thirds of the esophagus, while only smooth muscle is found distally. In the empty state, the mucosa is thrown into a series of parallel longitudinal folds. It is these folds that give the esophageal lumen a stellate appearance so characteristic in cross section. Mucosal folds are not a feature of the neonatal esophagus, which is smooth in outline.

2.2 Radiological Techniques of Examination

An empty esophagus is not visible on plain radiographs or CT. However, the esophagus is not uncommonly outlined by air in a child that is crying and swallowing large amounts of air (Fig. 2.1). An air-filled esophagus is also frequently seen in neonates ventilated with continuous positive airway pressure (CPAP), as well as in those with tracheo-esophageal fistula, esophageal stricture and achalasia (Fig. 2.2). In children with developmental delay, air in the esophagus is a common finding, and is usually secondary to reflux.

Despite the current emphasis on the superb diagnostic possibilities of CT and MR, the conventional barium examination still remains the most important modality for evaluating patients with dysphagia, gastroesophageal reflux and other symptoms referable to the esophagus (Levine and Rubesin 2005). The barium swallow, or esophagram, provides anatomic and functional information about the esophagus along its entire course. Radiation safety and dose reduction are important factors to consider for pediatric imaging, and fluoroscopy time must be carefully monitored. Dose reduction is achieved with low-dose pulsed fluoroscopy. "Last image hold" on the monitor helps to reduce fluoroscopy exposure. Because fine mucosal detail is not the main object in routine esophagrams, image capture from the disc provides sufficient information without additional radiation.

Barium suspension is the most frequently used contrast medium. Children above 6 months of age who are reluctant to drink barium may be encouraged by adding additional flavoring to the barium. Any commercially available chocolate syrup or instant drinking chocolate powder renders the barium more palatable without altering its radiographic characteristics. It is advisable to check for allergies and to be aware that some commercial flavoring preparations contain allergenic products.

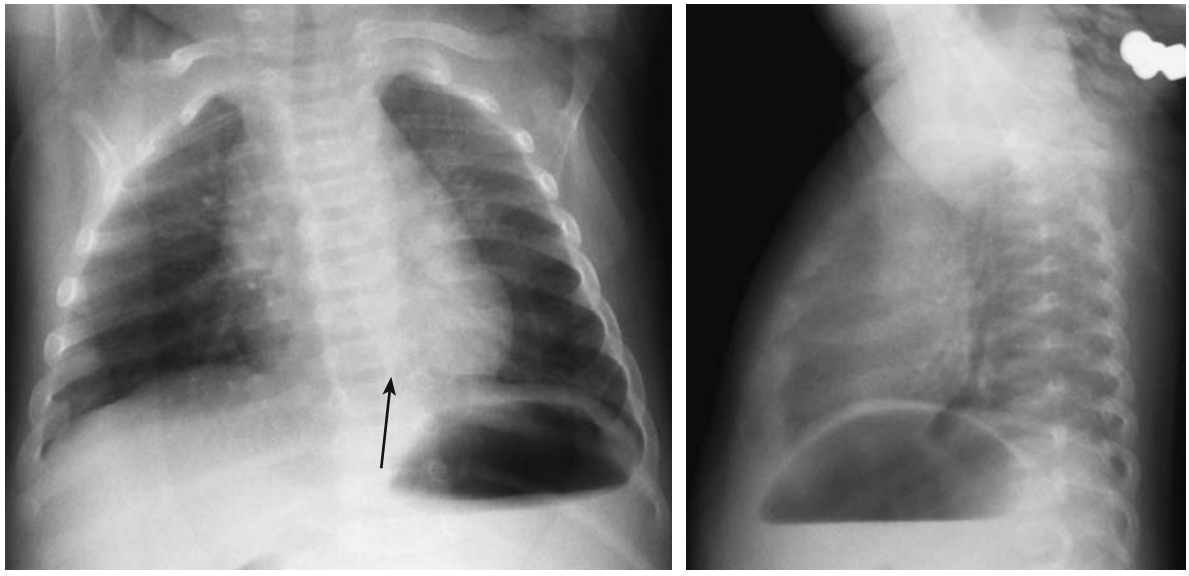

Fig. 2.1a,b. Air outlining a normal esophagus. AP (**a**) and lateral chest (**b**) radiographs of a crying infant with an air-filled esophagus (*arrow*)

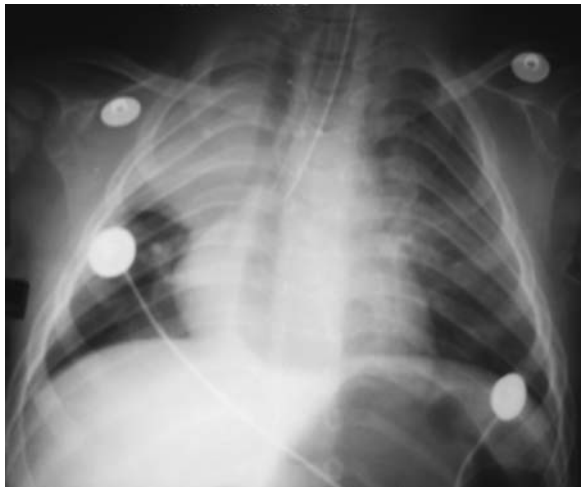

Fig. 2.2. Air-filled esophagus. Esophageal malposition of the endotracheal tube with resultant gaseous gastric and esophageal distention and right upper lobe atelectasis

Some children find chilled barium more palatable. Barium must not be used if either esophageal perforation or massive aspiration is suspected. Such patients are best studied with water-soluble low osmolar non-ionic contrast media. Gastrografin, due to its high osmolality, should never be used in infants or in any patients lacking adequate airway protection. Its use must be restricted to older, stable and neurologically unimpaired patients.

Children who are to undergo barium swallow examinations must be fasting. A child who is not hungry will simply refuse to drink barium. The duration of fasting depends on the child's age, and should be no longer than the child's routine time between feeds. Premature infants should fast 2–3 h, and infants up to 3 months fast 3–4 h. Children above 2 years can fast up to 6 h. To minimize parental and patient discomfort, fasting children are best scheduled for examinations early in the morning. Older children and adolescents will be most comfortable swallowing barium in the erect position. Infants and younger children are examined recumbent, and require immobilization. Effective immobilization decreases fluoroscopy time, and ensures clear and diagnostic images. Safe and convenient immobilization is accomplished with a device such as the Octagon board (Octostop, Laval, Qc, Canada) which enables immobilization, as well as rotation of the child into any position, including true lateral and oblique. This device facilitates positioning with the infant's arms above the neck so that the esophagus is not obscured during fluoroscopy. Barium can be very conveniently administered with the modified Poznanski technique using an 8-F feeding tube inserted through the end hole of a nipple and injected via syringe (Kuhns and Poznanski 1972; Poznanski 1969). The side holes of the feeding tube are further from the tip, so the tube must be advanced all the way through the nipple and

the protruding 1-cm cut so that the tube is almost flush with the nipple in order to prevent gagging. When the nipple is loosely attached to the face with paper tape, this "hands free" technique ensures that no hand or bottle obscures the mouth or pharynx during the examination and also decreases exposure to the radiologist. Barium is injected at a rate that is easily judged by observing a few trial sips of contrast medium prior to commencing fluoroscopy. This rate of administration of barium should be maintained to prevent aspiration. Older children may be fed from a cup or they may drink through a straw if they are examined in the upright position. When evaluating for gastroesophageal reflux, the volume of barium administered should be the same as that of a normal feed. If the child refuses to drink sufficient barium, the volume can be augmented with milk or juice after the anatomy to the level of the duodenojejunal flexure has been evaluated.

Swallowing begins in the mouth when chewed food or liquid reach the back of the tongue which then elevates and propels the oral contents posteriorly to the pharynx while the soft palate elevates to occlude the nasopharynx. The larynx and hyoid bone are seen to elevate as the oropharynx contracts, propelling the bolus distally while the epiglottis closes to protect the airway. The oral and pharyngeal phases of swallowing are evaluated in the lateral position to avoid overlap with the skull and spine. Peristalsis begins in the cervical esophagus, and the bolus passes inferiorly with a smooth primary stripping wave (Schlesinger and Parker 2004). Distal to the cervical esophagus, the esophagus is evaluated in the oblique position and true lateral, thus projecting the esophagus off the spine and avoiding overlap. Gravity helps the esophagus to clear, and infants with poor esophageal motility may benefit by tilting the fluoroscopy table into a more upright position. The distended esophagus has a smooth and regular outline. In its collapsed state, the mucosal folds appear as parallel, longitudinal lines 1–2 mm thick (Fig. 2.3). The esophagram in children should always include the stomach and the duodenum to the level of the duodenojejunal flexure to observe gastric emptying and to document normal bowel rotation. Cross-sectional imaging has limited application in evaluation of the esophagus, but is invaluable in cases with extrinsic compressive masses and vascular rings.

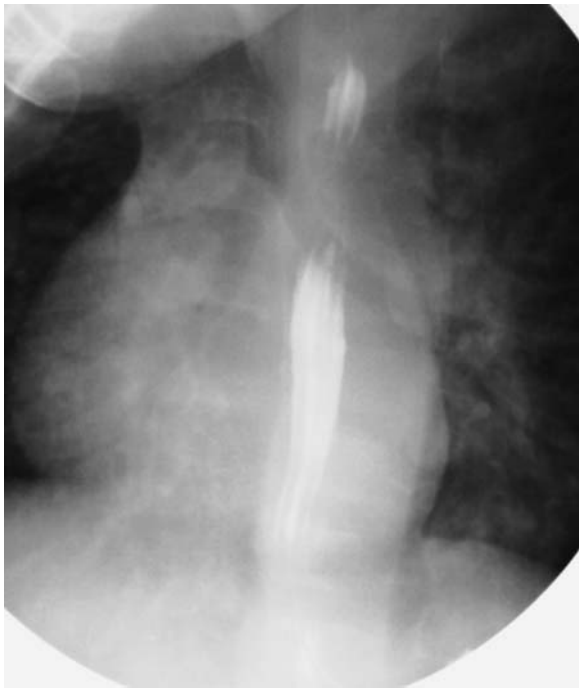

Fig. 2.3. Normal mucosal folds. Parallel linear mucosal in an infant's empty esophagus

2.3 Disorders of Swallowing

Feeding difficulty is not an uncommon symptom in children, reportedly occurring in 25% of children (Miller and Willging 2003). The causes of pediatric dysphagia are varied and complex, and may be physiologic or behavioral. The majority of children with dysphagia have a neurological cause, and may be due to cranial nerve palsies, cerebral palsy and meningomyelocele. Structural craniofacial anomalies predispose to dysphagia (Lifschitz 2001; Miller and Willging 2003). Swallowing dysfunction with aspiration is common in full-term infants less than 1 month of age and improves with age (Vazquez and Buonomo 1999).

The video esophagram, or modified barium swallow, is the standard technique to evaluate dysphagia. This examination is more sensitive than clinical evaluation of aspiration (DeMatteo et al. 2005), and is also more sensitive than the conventional upper GI series for the detection of aspiration (Vazquez and Buonomo 1999). A scout radiograph of the chest should be obtained to assess for evidence of aspiration. For the examination, the child must be securely

maintained sitting in the true lateral position, best accomplished in an infant feeding seat. Participation of the parents and caregivers helps to reassure the child, and recreates some aspect of daily feeding. The child's own speech therapist or feeding therapist should optimally be present during the examination to witness the events. The therapist can observe the optimal food volume and consistency and compensatory maneuvers that assist swallowing (Fernbach 1994). Boluses of different consistencies are fed. Young children are given liquids, though the density of various liquids may vary. The examination in older children begins with thin liquid barium, proceeding to feeds with a mixture of barium thickened with pudding or pureed food, and finally with more solid food such as barium-coated crackers. Barium density influences the swallowing mechanism. High-density barium has a slower transit time, causing the upper esophageal sphincter to open later, to remain open for longer and to delay its closure (Dantas et al. 1989). The actions of swallowing occur too rapidly to be observed fluoroscopically, therefore the entire examination is recorded on videotape, or if unavailable, with standard fluoroscopy set at a frame rate of 2–3/s. The recorded examination can be repeatedly reviewed without additional radiation. Review of the tapes is important when there is a need to assess the patient multiple times as treatment or the disease progresses. Multiple swallows in each series must be reviewed because changes can occur in the same cycle after episodes of normal swallowing. Infants may tire as feeding progresses, and may have difficulty maintaining their airway so the study should be continued after the first few uneventful swallows (Newman et al. 2001). Pulsed fluoroscopy cannot be used during video esophagrams as it may prevent detection of fleeting episodes of penetration and microaspiration (Mercado-Deane et al. 2001). The unfortunate necessity of using standard fluoroscopy results in the child's receiving a higher radiation exposure to the thyroid gland than during a conventional esophagram.

Abnormalities occur at all levels during swallowing: in the oral, pharyngeal and esophageal phases. The modified barium swallow is used to identify the level of pathology so that therapy or treatment can be given. In the oral phase of swallowing, the abnormality may have an anatomic etiology such as micrognathia or macroglossia. Children on long term tube feeding may be unused to feeding, and they may simply refuse to eat. Severely neurologically impaired children may be unable to suck or they may lack sufficient tongue control to latch onto and maintain control of the nipple. Suckling deficits also manifest with weak and deficient tongue motion, inability to compress the nipple and early tiring (Kramer 1989). Oral motor dysfunction occurs with moderate or severe cerebral palsy and developmental delay. Incomplete buccal closure leads to drooling, and abnormal tongue and jaw motion (Kramer 1989). Those neurologically impaired children unable to elevate the soft palate experience nasopharyngeal incoordination and nasopharyngeal reflux (Fig. 2.4). Occasional nasopharyngeal incoordination is most commonly due to transient swallowing incoordination. Retropharyngeal masses such as teratoma, lymphoma and abscess can rarely cause dysphagia. Cricopharyngeal achalasia, or failure of relaxation of the cricopharyngeus muscle, is most commonly secondary to gastroesophageal reflux. Signs of cricopharyngeal achalasia include absent, delayed or incomplete opening or early closure of the sphincter. Laryngeal penetration occurs when barium enters an incompletely protected airway below the level of the vocal cords and trachea during swallowing. It is important to document whether aspiration induces

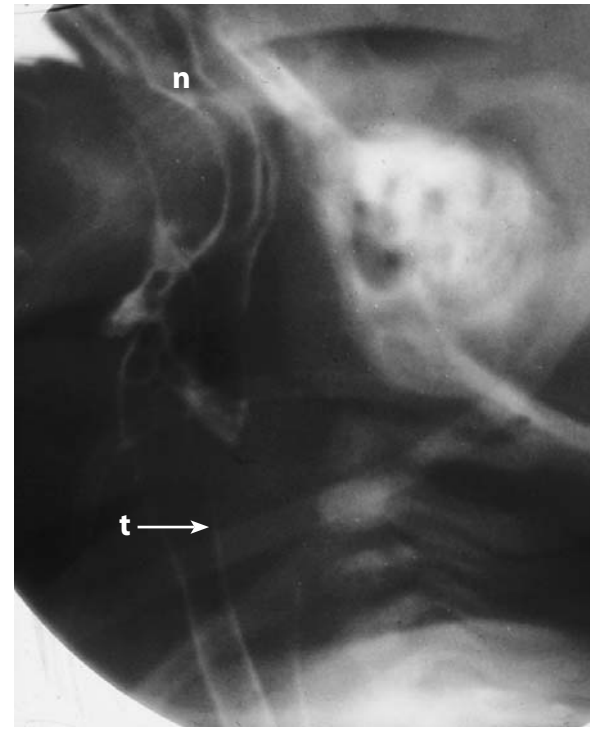

Fig. 2.4. Nasopharyngeal and tracheal aspiration. Barium outlines the nasopharynx (*n*) and the trachea (*t*). Only a trace of barium remains in the esophagus

a cough reflex. Penetration is different from aspiration, which occurs during respiration (Kramer 1989). Aspiration should be documented with a post-examination chest radiograph. The examination must be terminated if aspiration occurs and causes changes in vital signs. If the child remains stable after aspiration, the examination can proceed. The aim of the study is to determine if there is a safe way that food can be given, and after aspiration, it may be necessary to change to barium of another density, to use another type of nipple or to change the pace of feeding. Co-ordination of swallowing improves with age, and follow up examinations are an effective means to monitor improvement.

2.4 Congenital Abnormalities

2.4.1 Esophageal Atresia and Tracheo-esophageal Fistula

Esophageal atresia (EA) and tracheo-esophageal fistula (TEF) are common congenital anomalies, encountered in approximately 1 in 3,500 births (Shaw-Smith 2005). They are part of a spectrum of congenital anomalies that arise from defective formation of the esophagus or abnormal communication between the esophagus and trachea. It has been suggested that tracheo-esophageal fistula is the result of incomplete infolding of the lateral mesodermal walls that separate the developing esophagus from the trachea. Atresia is thought to result when the lateral folds of mesoderm occlude the esophageal lumen (Berrocal et al. 1999). Intrauterine anoxia and vascular compromise can cause focal esophageal necrosis that may result in atresia or a fistulous connection between the esophagus and adjacent trachea (Barnard 1956). Five types of anomalies occur: EA with a distal fistula to the trachea, accounts for more than 80% of cases, esophageal atresia without a fistula occurs in 10%, and an isolated H-fistula accounts for 6%. Atresia with a distal and a proximal fistula occurs in about 1%, and the rarest, atresia with a proximal fistula, accounts for fewer than 1% (Cumming 1975). Children with esophageal atresia have the most urgent clinical presentation due to their inability to swallow salivary secretions which then overflow and are aspirated into the airway. Respiratory distress may be exacerbated by gastroesophageal reflux from the distal esophageal segment into the airway when a distal fistula is present. Inability to pass an orogastric tube confirms the clinical diagnosis. Fistulae between the esophagus and trachea are in the midline. Although classically described as an H-fistula, the connection to the esophagus has an upward, oblique course that assumes an N-shape. A small isolated fistula without atresia may be less symptomatic and asymptomatic until late childhood (Kappelman et al. 1969) whereas a large fistula will be more likely to present earlier. Intrauterine distention of the blind-ending esophageal pouch compresses the adjacent trachea, inhibits development of the normal C-shaped tracheal rings and causes tracheomalacia which most commonly affects the proximal two-thirds of the airway. The trachea retains a U-shape with a wide posterior membranous portion, leading to tracheomalacia (Kovesi and Rubin 2004).

EA and TEF are frequently not isolated and occur in association with other congenital anomalies in 25% of children; in children with isolated EA, the incidence of associated anomalies is even higher, affecting 50%–70% of patients (Kovesi and Rubin 2004). The VACTERL association is an acronym for a complex of anomalies that may affect various systems (vertebral, anorectal, cardiovascular, tracheoesophageal, renal and the limbs) (Quan and Smith 1973; Fernbach and Glass 1988). The most frequently encountered anomalies associated with EA and TEF are cardiac (35%), genitourinary (24%), gastrointestinal (24%), skeletal (13%) and central nervous system (10%) (Kovesi and Rubin 2004). Approximately 8% of infants with esophageal atresia have aortic arch anomalies, and approximately 5% of infants with EA have a right aortic arch (Babu et al. 2000). Once the diagnosis of EA is established, prompt evaluation of clinically significant abnormalities (cardiac and renal) should be undertaken. Limb anomalies can be evaluated later as they are not of critical importance.

Until the twentieth century, esophageal atresia was a condition incompatible with life. Survival is now routine, dependent on the severity of other associated anomalies. Treatment of a TEF is surgical closure of the communication. Primary surgical anastomosis is the treatment of choice for EA, but this may be complicated with a long atretic segment. Staged repair is reserved for very ill and unstable children, or those with a long atretic gap (Cumming 1975).

2.4.1.1 Radiological Findings

The radiological appearance varies with the type of lesion, whether there is esophageal atresia, fistula or both. The initial radiograph must include the entire abdomen to assess for the presence of bowel gas (Figs. 2.5 and 2.6). The abdomen is characteristically gasless in the absence of a fistula, whereas in the presence of a distal fistula, the abdomen has a normal bowel gas pattern. Features of esophageal atresia are characteristic. The proximal blind-ending pouch is lucent and distended with air, often with a coiled esophageal tube. The lateral chest radiograph confirms the distended esophagus which displaces the airway anteriorly, markedly narrowing the tracheal lumen (Fig. 2.7). The cervical esophagus can become quite distended in children on nasal continuous positive airway pressure (CPAP) and have a similar appearance to EA (Walor et al. 2005). A right-sided aortic arch occurs in 5% of children with EA/TEF and may be difficult to see on the plain chest radiograph of infants (Berdon et al. 1979). Pre-operative echocardiography should be routinely done in these babies to evaluate the heart and the aortic arch in order to plan surgical access on the side contralateral to the aortic arch. The radiograph should be evaluated for vertebral and limb anomalies (Fig. 2.8).

A "pouchogram" of the atretic proximal esophagus is not usually necessary because of the low incidence a fistula from the proximal pouch (Fig. 2.9). In addition, this is a dangerous procedure if improperly performed. Air or non-ionic isotonic contrast medium can be injected to distend the pouch (Fig. 2.10). Over distention of the pouch with contrast medium will invariably result in aspiration so only a small volume of contrast medium, not exceeding 1–2 ml, is injected into the blind-ending pouch with the child in the true lateral position. Contrast medium must be removed at the end of the procedure.

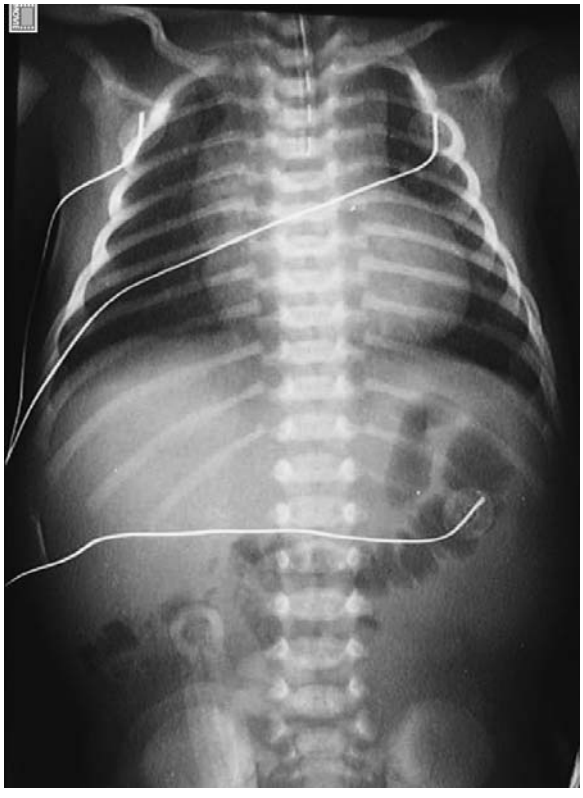

Fig. 2.5. Esophageal atresia with distal tracheoesophageal fistula. The orogastric tube tip is in the blind-ending esophagus and gas is present in loops of bowel in the abdomen. Note the right cervical rib and left 13th rib

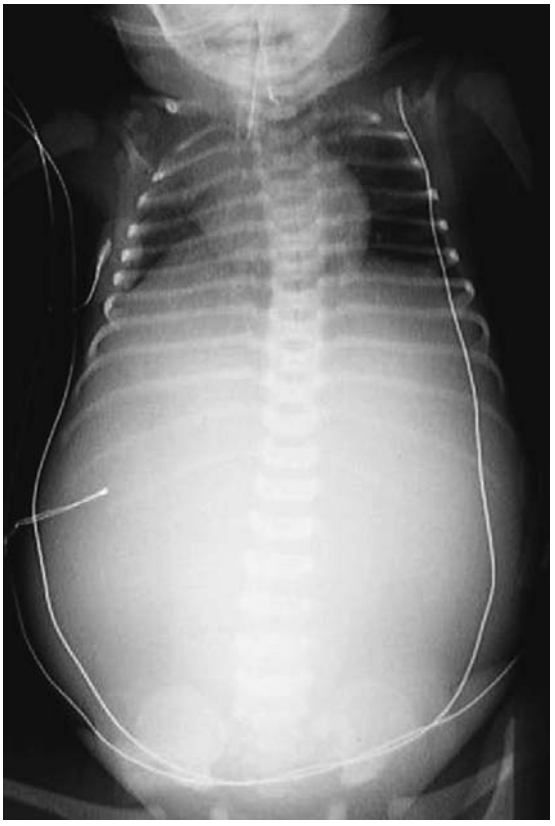

Fig. 2.6. Esophageal atresia without distal tracheoesophageal fistula. The abdomen is gasless. Duodenal atresia was diagnosed at the time of surgical repair

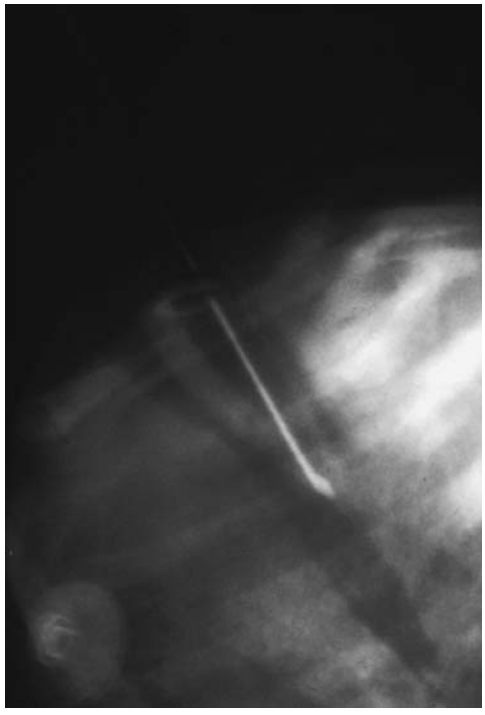

Fig. 2.7. Tracheomalacia. Lateral radiograph with the orogastric tube in the distended atretic proximal esophagus and markedly decreased caliber of the airway at the same level

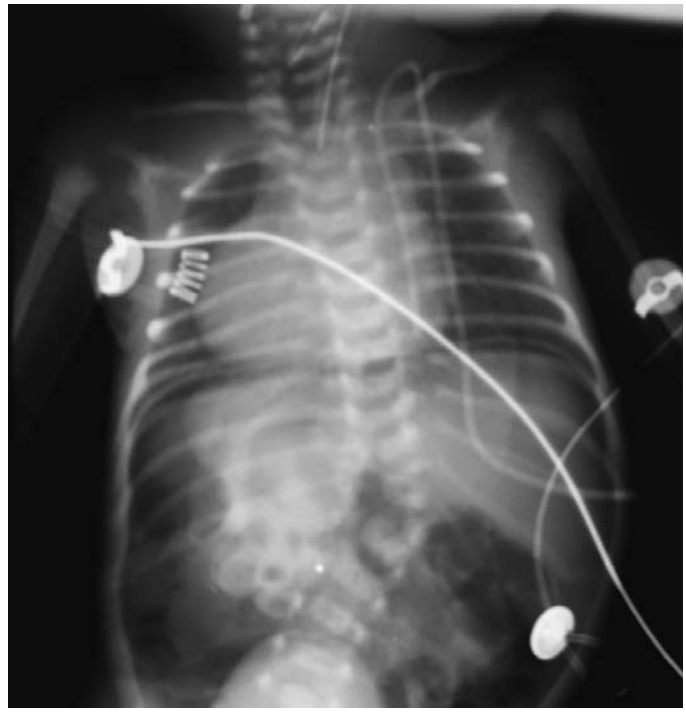

Fig. 2.8. Esophageal atresia with vertebral anomalies. Newborn with EA and a long gap not amenable to primary repair. Pneumoperitoneum followed the recent laparotomy. The esophageal tube is in the blind-ending esophagus. Note the vertebral segmentation anomalies and corresponding missing right sided ribs

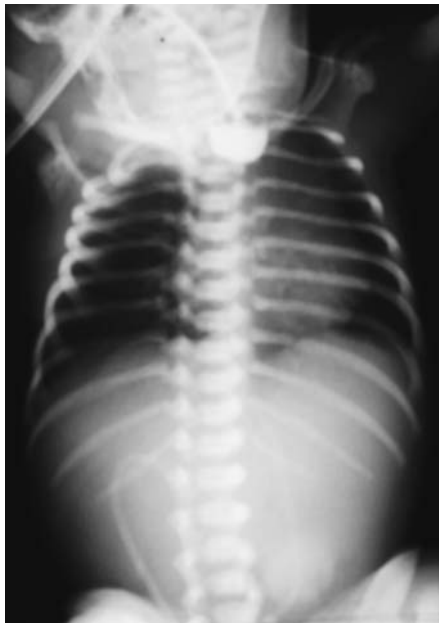

Fig. 2.9. AP "pouchogram". Contrast medium demonstrates esophageal atresia. The abdomen is gasless in the absence of a distal fistula. The left scapula is winged and elevated (Sprengel deformity)

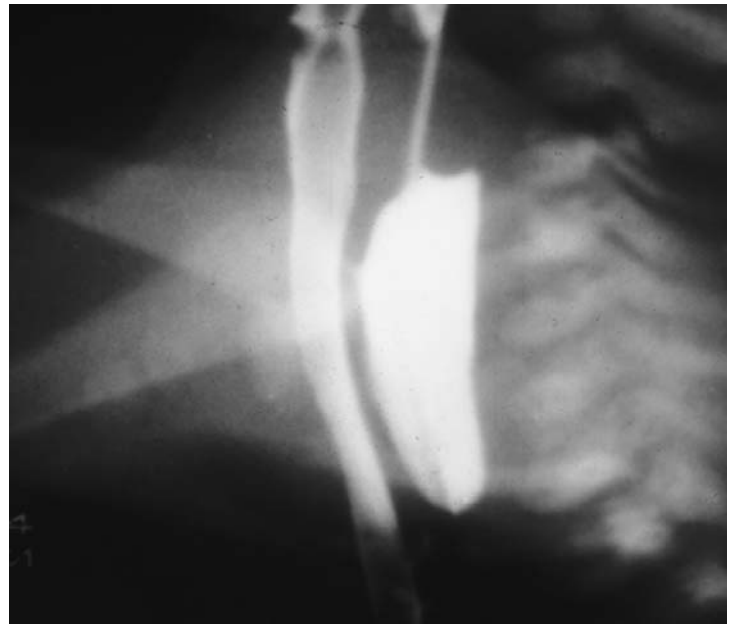

Fig. 2.10. Lateral "pouchogram" with esophageal atresia and proximal tracheoesophageal fistula. Contrast medium fills the blind-ending esophageal pouch and a narrow fistula connects to the trachea

An H-type fistula is often difficult to demonstrate. The barium esophagram, performed to evaluate swallowing and possible aspiration, may reveal the TEF (Fig. 2.11). If the barium esophagram is normal, and suspicion of TEF is high in an infant with recurrent aspiration pneumonias or cyanotic episodes, a more invasive investigation is required. For this procedure, the infant is placed on the octagon board in the true lateral position. Prone positioning is not necessary. The lateral position will give the best unobstructed view of the esophagus and airway, and gives the best access for suctioning. The correct examination technique is with a nasogastric tube inserted into the esophagus to the level of the carina. The tube is slowly withdrawn while low-osmolar non-ionic contrast medium is being injected at a rate sufficient to distend the esophagus. The fluoroscopist must always visualize the larynx during the esophagram to be able to differentiate whether tracheal contrast entered through a fistulous connection or by aspiration. The upper cervical esophagus is the commonest location for an H-type fistula, and it is here that greatest care must be taken in order not to overfill the esophagus and cause spill into the airway and aspiration, and also not to miss a subtle fistulous track. The fistulae are muscular tubes that are not constantly open. They are thought to open during respiration and with swallowing. The fistula will be missed if it is temporarily plugged with food or mucus. It is not uncommon for the fistula not to be demonstrated the first time, thus requiring more than one contrast examination.

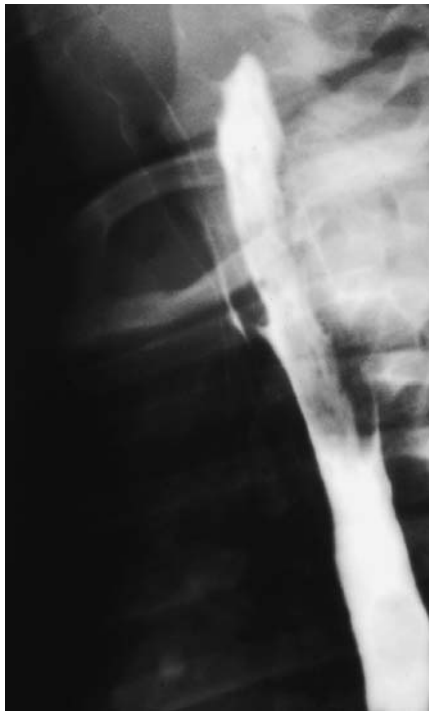

Fig. 2.11. Tracheoesophageal fistula. The fistulous connection to the trachea was opacified during the barium swallow examination. The fistula has an oblique cephalad course

2.4.2 Post-operative Appearance and Complications

The immediate post-operative changes, as well as the later complications, have specific appearances. The underlying abnormalities of the esophagus and airway may produce problems throughout the child's life.

The earliest acute complication of surgery may be an anastomotic leak, occurring in up to 17% of cases (Kovesi and Rubin 2004). Most leaks resolve spontaneously with conservative management: drainage of the leak and esophageal rest. However, up to 50% of those with a prior anastomotic leak will develop an esophageal stricture (Kovesi and Rubin 2004). The commonest late complication in all children with EA and TEF is esophageal stricture, affecting between 6%–40% (Engum et al. 1995). Strictures are more common in the presence of gastroesophageal reflux (GER). Strictures are not uncommonly complicated by foreign body impaction. Strictures, when present, must be differentiated from congenital esophageal stenosis. Re-fistulization occurs in approximately 9% of patients, and may occur as early as 11 days up to 18 months after primary repair (Cumming 1975; Benjamin 1981). Poor esophageal motility and reflux occur in 75%–100% of children with EA and TEF surgery, caused by abnormal in utero development of the esophageal myenteric plexus. GER and dysphagia are common throughout the lives of affected children. GER may be due to the abnormal esophageal myenteric plexus (Kovesi and Rubin 2004) or due to post-operative changes at the gastroesophageal junction. Reflux is exacerbated by poor antegrade esophageal peristalsis. Esophageal obstruction is commonly encountered due to poor esophageal motility or strictures.

2.4.2.1 Radiological Findings

An esophagram with non-ionic water-soluble contrast medium is routinely performed 4–7 days after

surgery to assess the integrity of the anastomosis prior to commencing feeding. The surgical anastomosis is always narrower than the previously obstructed proximal pouch, and should not be confused with a stricture (Fig. 2.12). A normal anastomosis will not impede or obstruct the flow of contrast medium.

A barium esophagram should be performed with a change in eating pattern or new onset of dysphagia that may indicate a stricture. Strictures are usually treated by repeated dilatation, but treatment is less successful when associated with reflux (Kovesi and Rubin 2004). Drooling and refusal to eat are usually signs of foreign body or food impaction. Removal of foreign bodies may be difficult with balloon extraction because of the capaciousness of the esophagus that allows the foreign body to fall back into this segment (Cumming 1975). CT performed years after surgical repair of EA and TEF shows the esophagus to be dilated and filled with air and fluid that is likely a mixture of pooled saliva and refluxed gastric contents, and predisposes to aspiration in the recumbent position (Griscom and Martin 1990). The trachea of these children exhibits more variable cross-sectional variation than in normal subjects (Griscom and Martin 1990). Acquired chest wall deformities and scoliosis are not uncommon after thoracotomy for EA repair (Chetcuti et al. 1989).

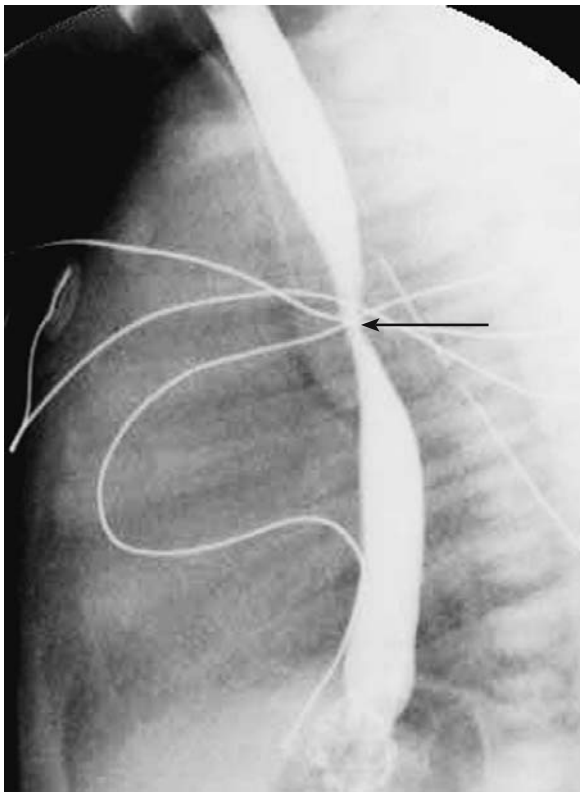

Fig. 2.12. Post-anastomotic narrowing of the esophagus. Routine post-operative swallow with non-ionic isotonic contrast medium shows esophageal narrowing at the primary anastomosis without evidence of hold up. No leak was demonstrated. Tracheomalacia is evident. Contrast medium in the airway is the result of an episode of aspiration (*arrow*)

2.4.3 Congenital Esophageal Stenosis

This is an uncommon anomaly, occurring in 1 in 25,000 to 1 in 50,000 live births (Murphy et al. 1995). Some consider esophageal stenosis to be a very mild variant of EA (Berrocal et al. 1999). The association with TEF in one-third of cases and other congenital anomalies in 17%–33% (Vasudevan et al. 2002) may support this theory. Most strictures are localized, 2- to 3-mm areas of narrowing approximately at the junction of the middle third and the distal one-third of the esophagus. Congenital esophageal stenosis may occur as an isolated narrowing due to ectopic cartilaginous tracheobronchial remnants, as an incomplete membranous diaphragm or web, or a localized segmental hypertrophy of the muscularis and submucosal layers with diffuse fibrosis (Murphy et al. 1995). There is a higher incidence of post-operative anastomotic leaks in children with TEF who have an associated congenital esophageal stenosis (Newman and Bender 1997). Esophageal stenosis usually presents when solid food is introduced or after impaction of a foreign body. In older children the differential diagnosis includes strictures due to reflux, caustic ingestion and sequelae from surgery. The diagnosis should be considered in an infant with dysphagia or with an impacted foreign body after EA repair. Esophageal stenosis must be considered in any child with acute dysphagia or foreign body impaction even without the antecedent history of atresia.

Treatment is resection with end-to-end esophageal anastomosis. Dilatation has a high incidence of esophageal perforation, especially in young children, and may be related to the length of the stricture and its transmural involvement (Newman and Bender 1997). The diameter of the lumen increases with age and growth of the patient, and with repeated dilatations, but will never be normal (Newman and Bender 1997). Some patients will benefit from initial dilatation, but most ultimately require surgery (Amae et al. 2003).

2.4.3.1 Radiological Findings

A congenital web appears as an oblique or transverse filling defect in the column of barium, and may be at the same level as a TEF. The esophageal narrowing is smooth and well defined, without evidence of ulceration. Barium swallow reveals an abrupt narrowing in the lower esophagus or a gradually tapering stenosis (Fig. 2.13) (Amae et al. 2003). Dilatation of the proximal esophagus reflects a high grade stenosis. Filling defects in the barium column can represent a foreign body or food bolus. The entire esophagus must be evaluated after surgical correction of EA. The contrast swallow may reveal an unsuspected congenital esophageal stricture (Vasudevan et al. 2002). The stenosis will be missed if the bolus of contrast medium is insufficient to cause adequate distention of the esophagus. Occasionally, a nasogastric tube is required to administer an adequate bolus to distend the entire esophagus. The esophagus must be evaluated dynamically during fluoroscopy to ensure that a stenosis is not missed or confused with spasm or peristalsis (Newman and Bender 1997).

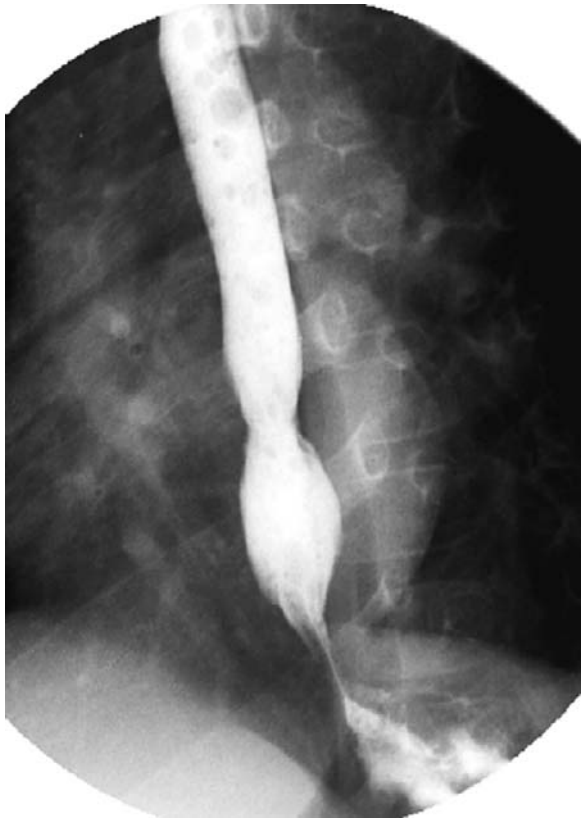

Fig. 2.13. Congenital esophageal stenosis. Barium swallow reveals a discrete annular narrowing in the distal esophagus. Tracheobronchial rests were found at pathology

2.4.4 Esophageal Duplication

The esophagus is the second most common location of duplication after the ileum, and accounts for 15%–20% of all duplications. It has been suggested that duplications result from aberrant luminal recanalization (Bremer 1944). In the 5^{th}–6^{th} week of intrauterine life, the foregut is covered by cells similar to those of the respiratory tract. The epithelium grows and obliterates the lumen, later producing secretions that form intercellular vacuoles that coalesce to form the new lumen. Failure of localized vacuole formation results in a cyst, which then migrates laterally into the esophageal wall and becomes surrounded by the muscular layer. Due to elongation of intrathoracic viscera, the cysts are commonly found in the lower esophagus. Complete esophageal duplication is extremely rare, and is often associated with gastric duplication (Singleton and King 1971; Herman et al. 1991). Esophageal duplication cysts are treated by excision.

2.4.4.1 Radiological Findings

Most esophageal cysts are detected incidentally on chest radiographs as mediastinal masses (Fig. 2.14). The esophagram demonstrates a well defined extrinsic soft tissue mass displacing the esophagus. The role of cross-sectional imaging is to differentiate the cyst from a solid mass such as neuroblastoma or sequestration and to show its relationship to adjacent vital structures. CT reveals a well defined fluid containing, non enhancing mass. Cyst contents have water-like characteristics on MR.

2.4.5 Esophageal Bronchus

Bronchopulmonary foregut malformations are rare congenital anomalies that are characterized by a fistula between an isolated portion of respiratory tissue and the foregut (Srikanth et al. 1992). Of these malformations, the esophageal bronchus communicating with the lower esophagus is the most common. Com-

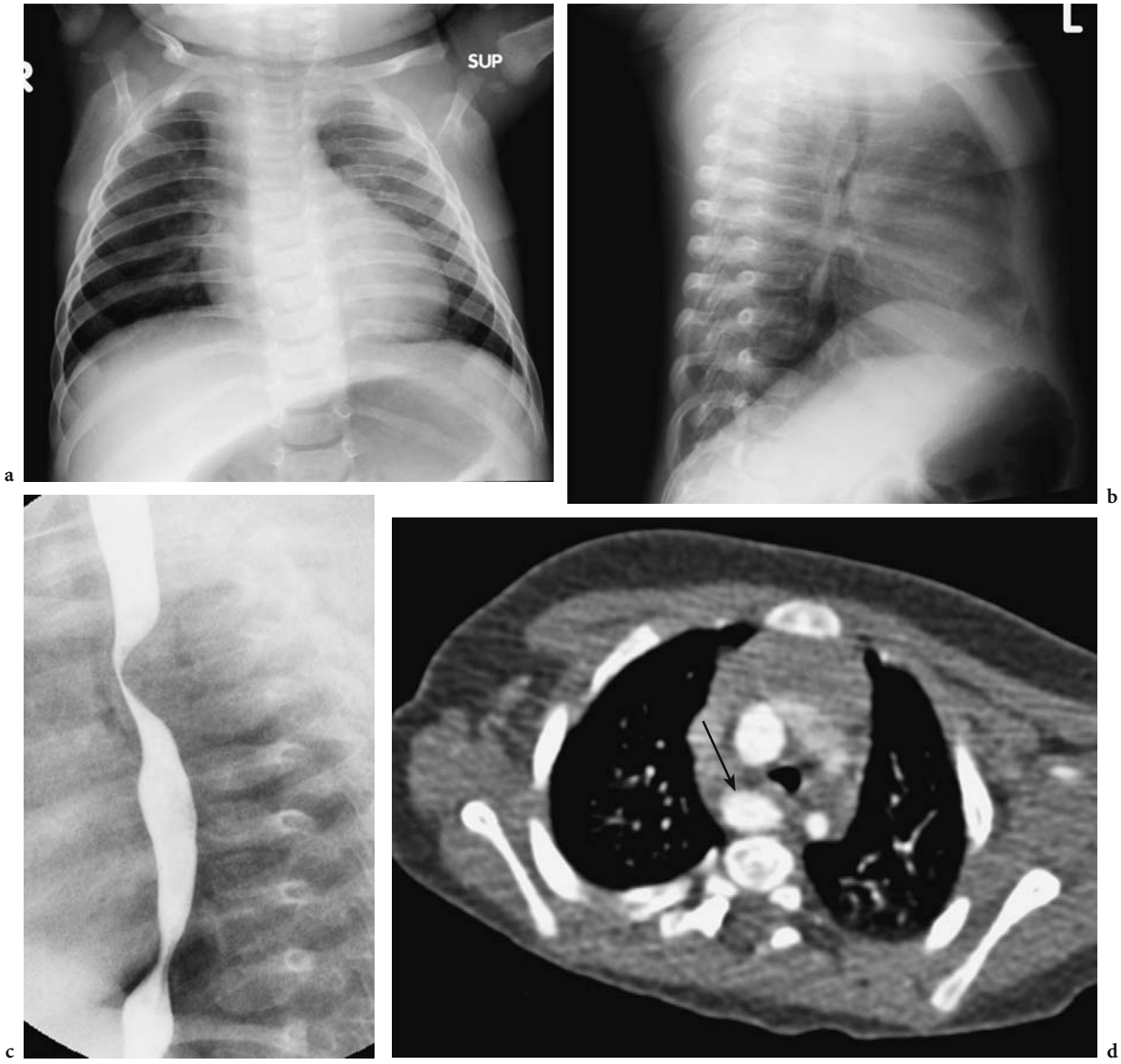

Fig. 2.14a–d. Esophageal duplication cyst. **a** AP chest radiograph without appreciable abnormality. **b** Lateral chest radiograph with anterior bowing and narrowing of the airway above the carina. **c** Barium esophagram confirms the presence of a soft tissue mass. **d** Contrast-enhanced CT shows the cyst posterior to the airway, and deforming the airway (*arrow*)

munication with the stomach is rarer. The abnormal communication develops when the lung sacs come into close contact with the esophagus and a part of the lung bud connects with the esophagus through a focal mesodermal defect. The attached portion of lung tissue, covered by mesenchyme, is carried away by the rapidly elongating esophagus (Srikanth et al. 1992). The arterial supply is variable and may arise from the pulmonary artery or the aorta and its branches. Venous drainage is commonly to the left atrium, but may also be systemic (Leithiser et al. 1985). This malformation is frequently associated with other anomalies. The abnormal connection to the respiratory tract causes respiratory distress, coughing with feeds and recurrent pneumonias.

Treatment is resection of the anomalous pulmonary tissue which is often hypoplastic and destroyed by infection. If detected early enough before pulmonary damage has occurred, tracheal reimplantation is preferred to resection (Michel et al. 1997).

2.4.5.1 Radiological Findings

The chest radiograph reveals opacification of the involved lung, and the communication is confirmed with a contrast examination of the esophagus and stomach (Fig. 2.15). Non-ionic isotonic contrast medium is the safest choice to minimize pulmonary complications such as acute pulmonary edema. Angiography is necessary to demonstrate adequate blood supply and venous drainage. CT will reveal signs of destroyed pulmonary parenchyma, which include atelectasis, bullae and abscesses. CT angiography (CTA) can demonstrate the source of arterial blood supply, its adequacy and venous drainage. Lung volume estimation can also be done with CT as part of the pre-surgery evaluation.

2.4.6 Vascular Ring Abnormalities

Vascular rings are uncommon. They are formed by vascular and ligamentous structures that encircle the airway and esophagus, causing extrinsic compression and obstruction of these hollow structures. Rings form as a result of developmental failure of parts of the paired 4^{th}–6^{th} aortic arches (Bonnard et al. 2003). Almost 20% of vascular ring malformations occur in association with congenital cardiac anomalies. Some rings are incomplete and asymptomatic, and are only incidentally discovered on chest radiographs or esophagrams. Symptoms vary with the degree of constriction of the vascular ring around the airway and esophagus. It is not surprising that the double aortic arch, which encircles the airway and the esophagus, causes the most severe symptoms. A double aortic arch is formed by a larger superior right aortic arch and a more inferior smaller left aortic arch. Symptoms from vascular rings are principally respiratory. Gastrointestinal symptoms and dysphagia are less common, and are more often encountered with a left retroesophageal subclavian artery arising from a right aortic arch (Bonnard et al. 2003). A right aortic arch with mirror-image branching acts like a vascular ring if the left ductus arteriosus passes between the right descending aorta and the left pulmonary artery.

The treatment is surgical relief of the constriction. The basic principle of vascular ring surgery is to divide non-functional or non-critical components of the ring. Surgical relief of the double aortic arch entails dividing the lesser of the two arches. An atretic portion is an optimal location for division of the arch. In cases with a right aortic arch and ligamentum arteriosum, the ductus remnant is divided, and the trachea and esophagus are released from adhesive bands (Backer et al. 2005).

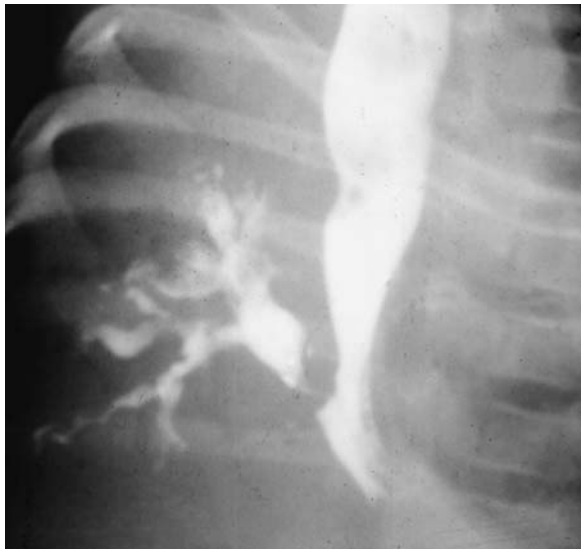

Fig. 2.15. Esophageal bronchus. Barium esophagram demonstrates that the right main bronchus arises from the esophagus. The right lung is completely opacified

2.4.6.1 Radiological Findings

The chest radiograph and esophagram demonstrate extrinsic esophageal impressions and tracheomalacia, as well as the side of the aortic arch. A right sided aortic arch in a child with respiratory symptoms is suggestive of a double aortic arch. The next examination is often a barium esophagram. A normal esophagram will clearly rule out the presence of a vascular ring. Symptomatic vascular rings caused by double aortic arches with bilateral arch patency cause significant narrowing and anterior bowing of the trachea, which are apparent on the lateral chest radiograph and barium esophagram. On the frontal projection, right and left indentations assume an "S" configuration. The barium esophagram is helpful to determine which component of a double aortic arch is larger. Barium swallow can show the right arch and a posterior esophageal impression (Fig. 2.16). This type of arch is usually associated with congenital heart disease. Advantages of the barium swallow include its ready availability, that

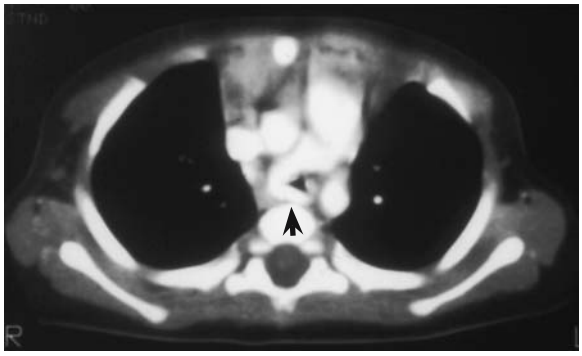

Fig. 2.16. Anomalous left pulmonary artery. CT with intravenous contrast medium shows the anomalous left pulmonary artery originating from the right main pulmonary artery, passing posterior to the trachea between the airway and the esophagus (*arrowhead*)

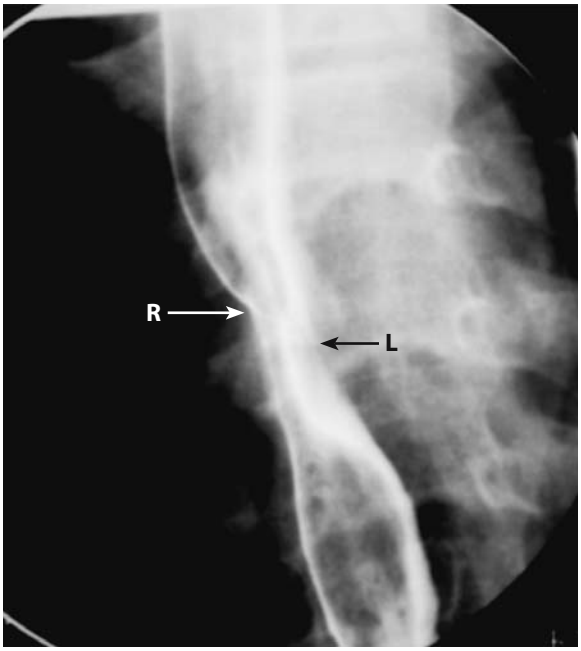

Fig. 2.17. Double aortic arch. Barium esophagram with double extrinsic impressions on the barium column. The dominant right arch (*R*) is higher than the smaller left arch (*L*)

it does not require sedation, an important feature for children who have airway compromise, and that it can show extrinsic compression by an atretic vascular segment not delineated by CT or MRI (Woods et al. 2001).

Over the last decade, however, the diagnosis of esophageal rings has changed from barium swallow and angiography to cross-sectional imaging (Figs. 2.17 and 2.18). CT angiography and MRI are optimal for more precise pre-operative delineation of the anatomy of the vascular ring (Hernanz-Schulman 2005). CT is more quickly performed, and can often be done without sedation. CT angiography can be completed in 20–30 s, whereas MR often requires sedation or immobilization for studies that can take as long as 45 min. The advantage of CT is visualization of the lungs and bronchi, and the diagnostic yield is even enhanced with multiplanar reformations. High-resolution 3D FISP (fast imaging with steady precession) MRA will accurately define vascular rings. This bright blood technique differentiates between vascular and non-vascular structures with higher spatial resolution than spin-echo (Greil et al. 2005). The choice of imaging modality varies with institutional preferences.

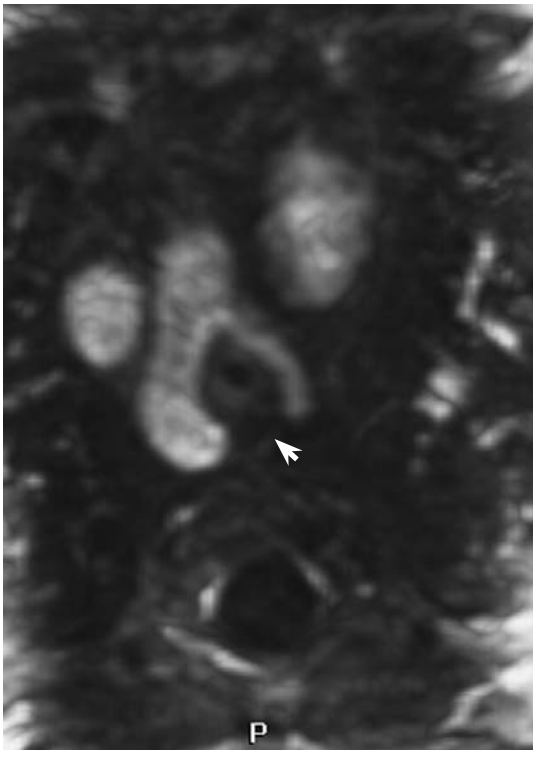

Fig. 2.18. Double aortic arch. MRI with contrast medium. The dominant right aortic arch and smaller left arch encircle the airway and the esophagus. The posterior limb of the vascular ring is atretic (*arrowhead*)

2.4.7 Hiatal Hernia

Hiatal hernia and intrathoracic stomach are uncommon in children. This condition may be congenital and inherited (Chana et al. 1996). Hiatal hernia may be secondary to congenital esophageal short-

ening (Chacko et al. 1998). Abnormally lax gastric ligamentous attachments and non-fixation of the stomach result in intrathoracic herniation in Marfan syndrome (Al-Assiri et al. 2005). Though usually an isolated anomaly, hiatal hernia can occur with other congenital abnormalities (Wang et al. 1993).

Esophageal clearance time and duration of gastroesophageal reflux are prolonged in children with hiatal hernia, thereby increasing esophageal exposure to acid and causing a higher failure rate of conservative therapy (Gorenstein et al. 2001).

2.4.7.1 Radiological Findings

Chest radiographs may reveal gas lucency in an intrathoracic stomach, occasionally with compressive atelectasis of adjacent lung. The next examination is the esophagram to confirm intrathoracic gastric malposition (Fig. 2.19). Gastric rugal folds of the hiatal hernia extend above the diaphragm or a portion of the gastric fundus protrudes through the esophageal hiatus. Sonography can demonstrate gastroesophageal reflux, as well as delineate the abnormally short length of abdominal esophagus and loss of the acute gastroesophageal angle that occur with a hiatus hernia (Westra et al. 1990).

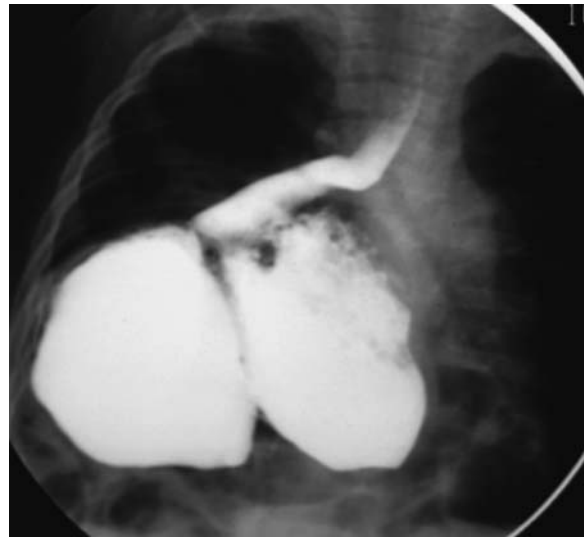

Fig. 2.19. Hiatal hernia. This infant with Marfan syndrome has intrathoracic gastric malposition

2.5 Acquired Abnormalities

2.5.1 Gastroesophageal Reflux

Gastroesophageal reflux (GER) is very common in infants and children, and may be physiological in young infants. The incidence ranges from 18% in all infants up to 70% in children with underlying conditions such as tracheoesophageal fistula, neurological deficits and anatomic abnormalities of the esophagus (McGuirt 2003). GER decreases spontaneously from an incidence of 67% at 4–5 months, declining to 21% by 6–7 months and to less than 5% by 12 months (Nelson et al. 1997). In young infants, the short length of the intraabdominal esophagus and physiologic immaturity of the developing lower esophageal sphincter contribute to GER, which invariably improves with the introduction of solid food. GER resolves spontaneously when most infants learn to sit up in the latter part of the first year of life, suggesting that gravity likely plays a role in aiding downward passage of esophageal contents. The presentation of GER is variable. In infants, GER manifests as regurgitation and "spitting up". Abdominal pain is a common symptom of GER in school-age children (Hassal 2005a).

There is a distinction between the common physiologic GER of childhood and pathological gastroesophageal reflux disease (GERD). This more severe form of reflux can interfere with growth, and cause gastroesophageal and respiratory symptoms. GER has been linked to asthma, and pulmonary symptoms are significantly higher in children with GER than those without (Gold 2005). Children and adolescents with GER are more likely to present with cough and other respiratory symptoms than complaints of "heartburn". Asthma itself causes GER by a variety of mechanisms. Hyperinflation changes the pressure gradient across the lower esophageal sphincter, increases negative intrathoracic pressure and alters the relationship between the diaphragm and lower esophageal sphincter. This may be exacerbated by some asthma medications that decrease lower esophageal sphincter pressure.

While most children with "physiologic" GER will naturally outgrow the reflux, those children with underlying abnormalities will not (Boix-Ochoa and Canals 1976). The initial treatment for GER is most commonly thickening of the infant's formula, feeding smaller amounts per meal and maintaining the

infant in an upright position after each feed. Esophageal pH monitoring is the standard and reliable method to document abnormal gastric acid reflux, as well as to assess the efficacy of therapy in patients who do not respond to acid suppression treatment (Rudolph et al. 2001). Early diagnosis and treatment will prevent and mitigate complications such as failure to thrive, refusal to feed and respiratory disorders. Children above 3 years with GER have a higher rate of related complications and frequently require medical or surgical intervention (McGuirt 2003). Fundoplication augments the lower esophageal sphincter with a wrap of the gastric fundus; it is the most common surgical treatment for GER, but has a high rate of failure, which ranges from 30%–70% within 1–3 years (Hassal 2005b). Ironically, those with the greatest need for good reflux control with neurologic impairment, repaired esophageal atresia, chronic lung disease have underlying pathophysiological mechanisms that lead to wrap failure (Hassal 2005a).

2.5.1.1 Radiological Findings

GER is the commonest indication for performing barium esophagram and upper gastrointestinal series in children. To optimize the examination, the stomach should be filled with the same volume as with a normal feed. If the child refuses to drink sufficient barium, the ingested volume can be increased with formula or fruit juice. The volume can be supplemented with fluid injected through an indwelling gastrostomy tube, or the stomach can be filled through a nasogastric tube which is removed after filling. Nasogastric tubes maintain patency of the lower esophageal sphincter and compromise its function. Tubes must be removed when evaluating for reflux. The barium swallow has only 50% sensitivity and specificity for reflux diagnosis in children (Rudolph et al. 2001). Reflux of barium is not diagnostic of GERD, and nor does absence of reflux rule it out (Rudolph et al. 2001). The most important aspect of the barium examination is to exclude anatomic abnormalities of the esophagus, to define the level of the duodenojejunal junction and to define the cephalad anatomic level of reflux, as well as to document aspiration (Fig. 2.20). Aspiration with reflux may be seen, but is very uncommon (Fernbach 1994). A carefully performed upper GI series may miss significant GER because of the limited use of fluoroscopic monitoring time and the relatively short duration of the entire examination.

The radionuclide "milk scan" is a sensitive test for diagnosing GER (Blumhagen et al. 1980; Seibert et al. 1983). Milk, formula or juice mixed with Tc 99m sulphur colloid is administered to the child who is then scanned. Radionuclide scanning is continuous, an advantage over fluoroscopy. Radionuclide scanning allows documentation of episodes of GER, and

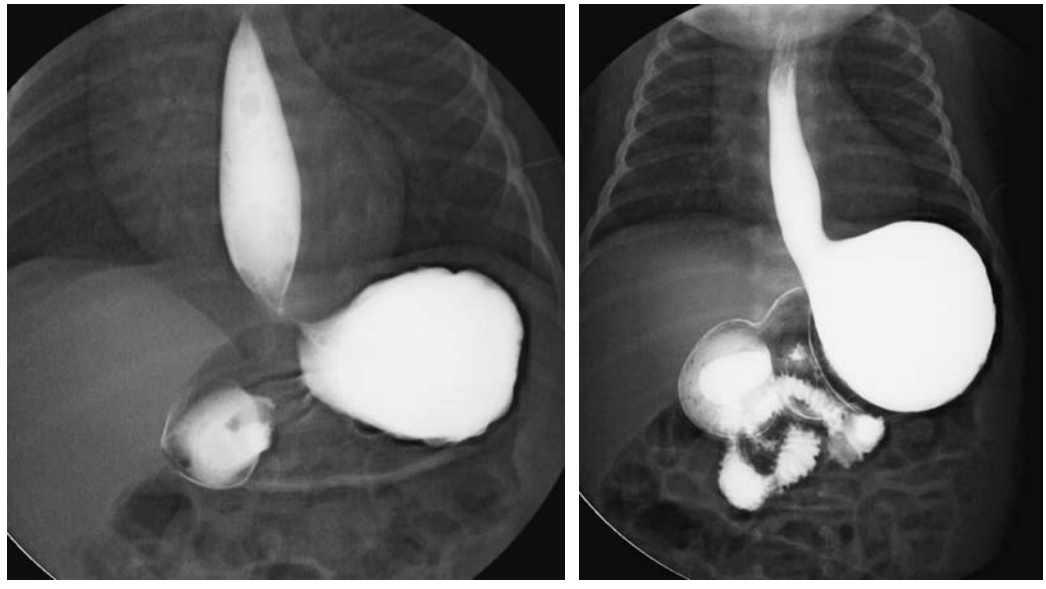

a b

Fig. 2.20a,b. Gastroesophageal reflux. **a** During swallowing, the gastroesophageal junction is closed. **b** The gastroesophageal junction is widely patent, and barium refluxes to the upper esophagus

cephalad extent of GER, as well as the rate of gastric emptying.

GER can be demonstrated sonographically into the distal esophagus (Koumanidou et al. 2004). Gastric contents can be observed as they reflux into the esophagus. This technique is limited because the degree of reflux and proximal extent cannot be evaluated in the chest where the esophagus is obscured by the lungs.

2.5.2 Achalasia

Achalasia is rare in children with an incidence estimated at approximately 0.05–1 per 100,000. Fewer than 5% of those with achalasia present in childhood (Emblem et al. 1993; Mayberry and Mayell 1998). This condition is characterized by defective relaxation of the cardia and absence of esophageal peristalsis with normal upper esophageal sphincter and pharyngeal function. Pathological findings are characterized by marked fibrotic hypertrophy of the myenteric plane between the muscle layers and a significant reduction in the number of myenteric ganglia and myenteric neurons (Khelif et al. 2003). It is not uncommon for children with achalasia to present before the age of 5 (Hussain et al. 2002). Clinical symptoms are age-related. Infants present with symptoms similar to gastroesophageal reflux, including frequent regurgitation, choking, apnea and pneumonia. Symptoms in older children are similar to those of adults and include dysphagia, chest pain, cough, vomiting of undigested food and poor weight gain (Vane et al. 1988). As a result of its rarity in children and non-specific symptomatology, the diagnosis and treatment are frequently delayed.

Injection of botulinum toxin temporarily relieves the symptoms of achalasia, and half of the patients treated with botulinum toxin will require an additional procedure. Botulinum toxin is only recommended for patients who are poor candidates for pneumatic dilatation or surgery (Hurwitz et al. 2000). Pneumatic dilatation has a higher success rate and lower failure rate than botulinum toxin. Modified Heller myotomy has 94% efficacy and pneumatic dilatation has 90% efficacy (Vaezi and Richter 1999). Myotomy alone has a high incidence of gastroesophageal reflux (Emblem et al. 1993), and some children ultimately require an antireflux procedure (Vane et al. 1988). Laparoscopic modified Heller myotomy is increasingly more commonly performed in children and can be performed in patients as young as 10 years. The myotomy relieves symptoms of obstruction, yet the underlying esophageal dysmotility persists through the patient's life. These patients must be monitored and followed up for life.

2.5.2.1 Radiological Findings

The chest radiograph may reveal a dilated esophagus with an air fluid level, changes of chronic aspiration and tracheal displacement (Fig. 2.21). The stomach

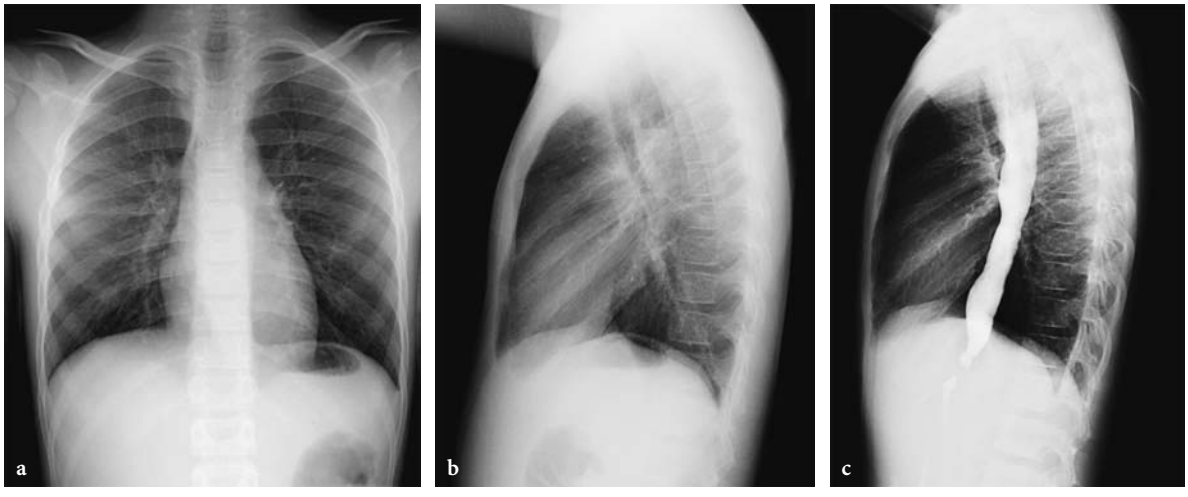

Fig. 2.21a–c. Achalasia. AP (**a**) and lateral (**b**) chest radiographs reveal an air-fluid level in the distended esophagus. **c** Delayed lateral chest radiograph. Barium fills the entire length of the esophagus, which tapers distally. There has been minimal flow of barium into the stomach

bubble is not visualized in cases with high grade obstruction. The esophagram is the initial diagnostic study, followed by esophageal manometry and endoscopy. Barium esophagram reveals a dilated esophagus that tapers smoothly distally to a "bird's beak". Occasionally, a leiomyoma may mimic the symptoms and radiographic appearance of achalasia (Hussain et al. 2002).

2.5.3 Foreign Body Ingestion

Infants and young children experiment with unfamiliar objects by placing them in their mouths. Most swallowed foreign objects pass uneventfully. The age range of children who swallow foreign bodies is from 6 months–3 years. A higher incidence of obstructed ingested foreign bodies occurs with esophageal pathology, especially after repaired esophageal atresia and among children with psychiatric disease and retardation. Foreign bodies are most likely to be caught at the normal anatomic sites of esophageal narrowing. Foreign bodies at other levels are indicative of a stricture or vascular ring (Fig. 2.22). Foreign bodies lodge at the level of the thoracic inlet (53%) in the thoracic esophagus (32%), and the least common site is the cervical esophagus (15%) (Harned et al. 1997). Presentation is usually with dysphagia and chest pain. Salivation and drooling occur with esophageal obstruction. Swallowed objects may be unchewed or partially chewed food, or other foreign objects, 66% of which are coins in children (Fig. 2.23) (Webb 1995).

More than one coin may occasionally be ingested (Fig. 2.24). The older the children, the larger the coins ingested (Cheng and Tam 1999). Acute coin ingestion is rarely symptomatic unless the coin is above the thoracic inlet (Sharieff et al. 2003). The majority of coins will not pass spontaneously. However, some coins will pass spontaneously and can be followed for 24 h, thereby decreasing the need for operative removal (Sharieff et al. 2003). The coin should be removed if repeat radiography reveals non-passage. Flexible endoscopy is safer than blind removal, and provides immediate information about the esophagus at the site of impaction.

Button battery ingestion is rare, but the incidence is increasing (Yardeni et al. 2004). Most are less than 15 mm in diameter, and pass uneventfully. Button batteries contain alkali and cause injury by direct corrosion, voltage burns and pressure necrosis. Those that lodge can cause severe complications within a short time after ingestion and must be removed endoscopically as soon as possible.

Complications of foreign body ingestion include perforation and abscess formation. Flexible endoscopy is the most common method for removal.

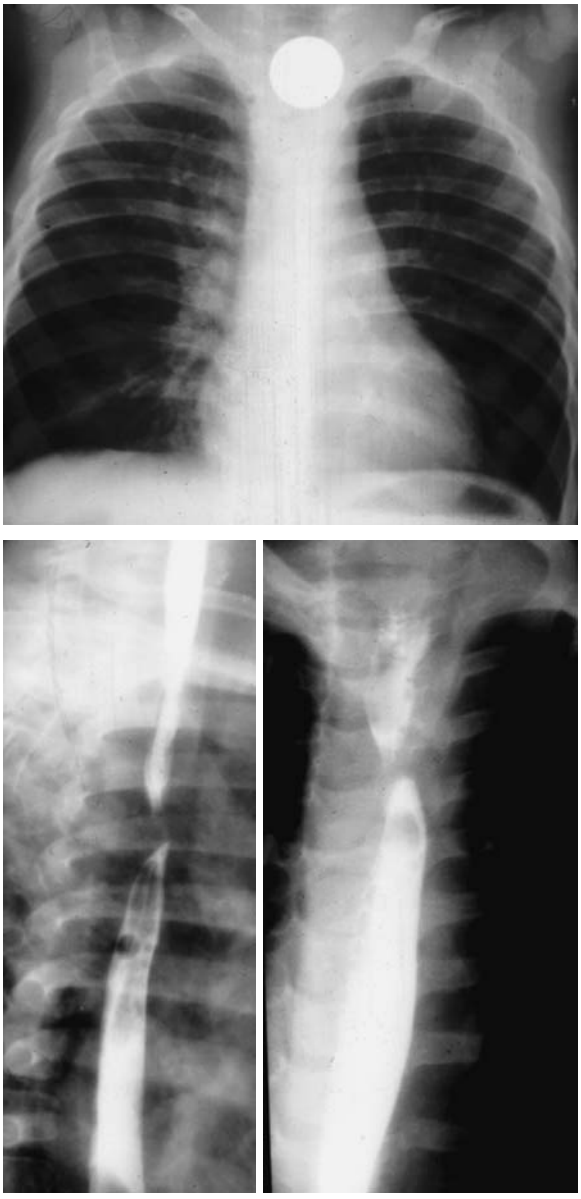

Fig. 2.22a,b. Impacted coin above an unsuspected vascular ring. **a** Frontal chest radiograph shows the coin lodged in the proximal esophagus above the aortic arch. **b** Barium esophagram reveals an aberrant retroesophageal right subclavian artery

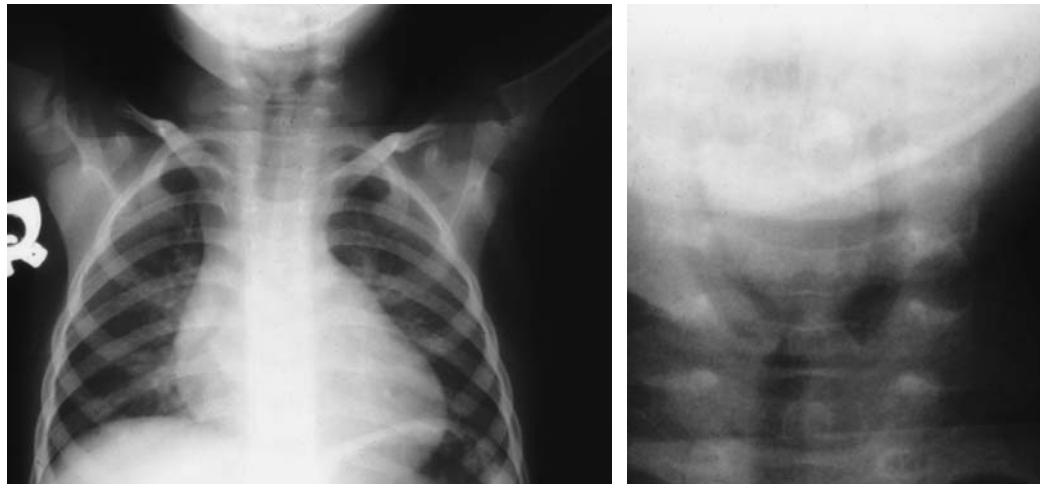

Fig. 2.23a,b. Radiolucent foreign body. AP (**a**) chest radiograph and magnified view (**b**) reveal an impacted piece of unchewed chicken in the cervical esophagus outlined by esophageal air

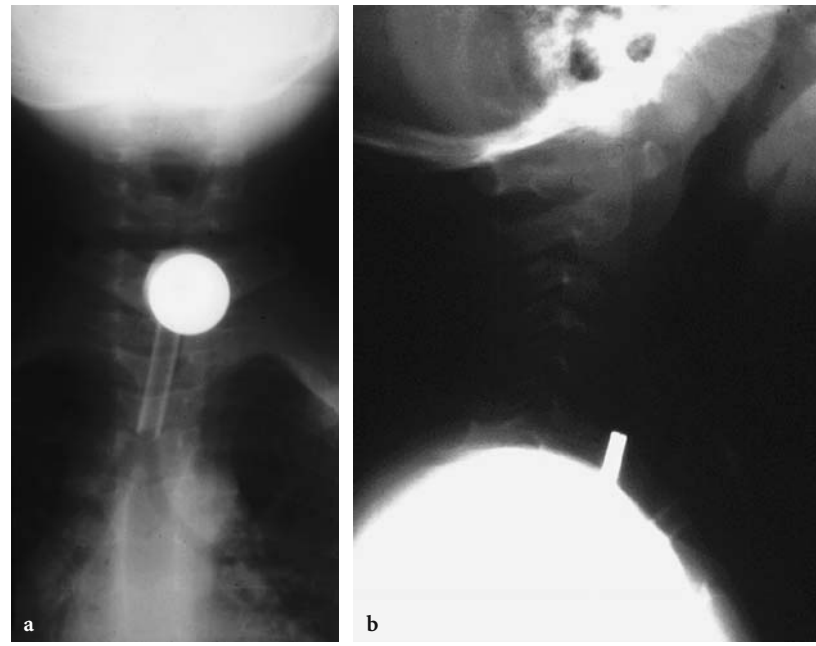

Fig. 2.24a,b. Two impacted coins. **a** The AP view of the airway is confusing. The metallic density resembles part of the tracheostomy tube. **b** The lateral radiograph reveals two coins in the esophagus

2.5.3.1 Radiological Findings

When suspicion for an ingested foreign body is high, frontal and lateral radiographs should be obtained from the nasopharynx to the abdomen. Radiology reveals 100% of metal objects, 86% of glass and 26% of fish bones (Cheng and Tam 1999). Commonly ingested foreign bodies such as medications, small plastic toys and organic material are not seen on plain radiography. These radiolucent foreign bodies may show on the barium esophagram as filling defects in the barium. A contrast examination must not be performed with a high grade obstruction because of the aspiration risk. Chronically lodged foreign bodies cause inflammation, edema of the esophageal wall and narrowing of the lumen (Fig. 2.25).

Fluoroscopic Foley catheter removal has a high (91%) success rate with coins that have been in place for less than 3 days. The rate of successful removal is lower with coins that have been lodged for a longer time period (Schunk et al. 1994). The success rate is

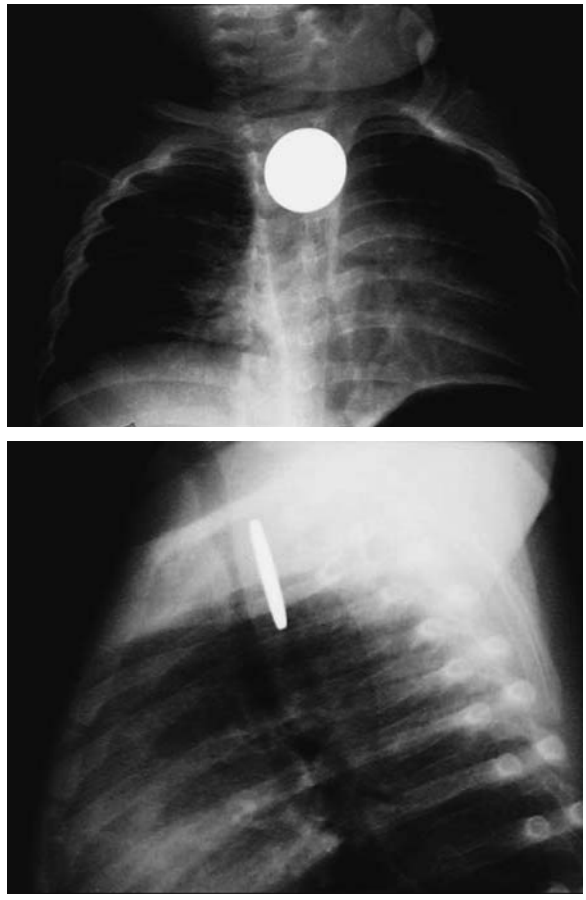

Fig. 2.25a,b. Chronically impacted coin. Frontal (**a**) and lateral (**b**) chest radiographs with an impacted coin and inflammatory narrowing of the adjacent airway. The space between the trachea and the esophagus is thickened, evidence of chronic inflammatory change

also lower (83%) in cases with underlying esophageal pathology (Schunk et al. 1994). An underlying stricture will not permit passage of the Foley catheter, and may be a cause for failure. Foley catheter removal is limited to objects without sharp edges. This technique must not be attempted in children with clinical or radiological airway compromise and should not be attempted in the presence of esophageal edema (Schunk et al. 1994).

Patients for fluoroscopic removal should not be sedated in order to maintain their airway. However, patients must be restrained and placed in the prone oblique position. A Foley catheter size 8–12 is placed through the nose or mouth under fluoroscopy to below the foreign body. The balloon is then inflated with 3–5 ml of contrast medium, taking care not to over distend the esophagus. The catheter is gently withdrawn, and the foreign body is delivered into the hypopharynx from where it can either be spontaneously expectorated, or manually removed by the radiologist whose fingers are in the child's mouth. A useful tip is to don two pairs of rubber gloves as these offer protection from being bitten by the patient. Occasionally, the Foley catheter will push the foreign body distally into the stomach. Complications are minor, and may include epistaxis and vomiting, but esophageal laceration may occur (Schunk et al. 1994). Although effective, this procedure is not widely performed and many pediatric radiologists defer to endoscopic extraction.

2.5.4 Caustic Ingestion

Caustic ingestion is rare in children. Most are accidental, and 58% occur in children younger than 6 years (Duncan and Wong 2003). Ingestion may be acid or alkaline products. Injury depends on ingestant characteristics, i.e. corrosive properties, the amount and concentration as well as the physical form of the substance, as well as the duration of mucosal contact. Alkalis initially cause liquefactive necrosis, and the most severe type of caustic injury, followed by scar formation and strictures. Most damage occurs in the middle and lower esophagus. Alkali granules cause strictures at any level where they may lodge. The esophagus tends to be spared injury in acid ingestion because acids, which tend to be liquids, pass through the esophagus more quickly than alkalis. Acids require longer contact to cause deep tissue injury and it is the stomach that sustains most injury.

Treatment is initially with volume resuscitation and airway management. Sips of water are encouraged to dislodge lye particles. Emetics and neutralizing agents are contra-indicated because heat damage can occur during neutralization, and emesis of acid gastric contents can damage the esophageal mucosa. Surgery is rarely required. Colonic interposition or gastric pull up are performed if the stricture is long and does not respond to dilatation (Fig. 2.26).

2.5.4.1 Radiological Findings

Chest and abdomen radiographs are obtained to screen for signs of perforation. The initial radio-

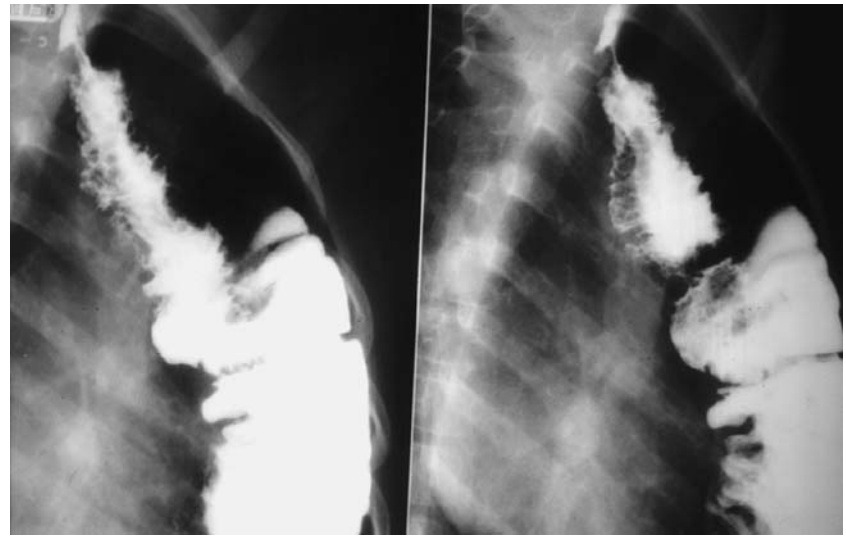

Fig. 2.26. Alkali ingestion. Barium swallow shows a long segment of narrowing of the mid esophagus approximately 3 weeks after swallowing drain cleaner

logic examination is the esophagram which is best performed with water soluble non-ionic isotonic contrast medium in case of perforation. The earliest signs are epiglottic swelling, esophageal dysmotility, mucosal edema and ulceration (Fig. 2.27). Intramural contrast and persistent gaseous dilatation of the esophagus are signs of severe injury and may precede perforation (Fernbach 1994). CT is recommended if suspicion for perforation is high. Deep esophageal burns are investigated by serial esophagrams to detect early stricture formation. Follow up barium esophagrams are important to evaluate the development of scarring and the length of the resulting strictures which are typically long.

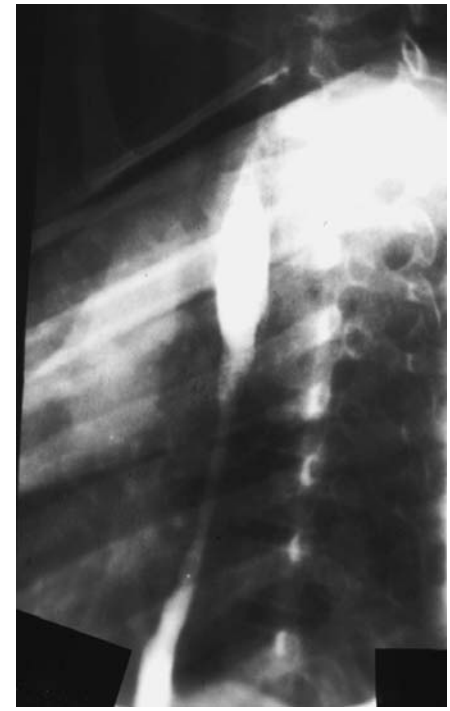

Fig. 2.27. Colonic interposition. Treatment for a high-grade long segment caustic stricture

2.5.5 Esophageal Strictures

Acquired strictures in children are most commonly encountered after surgical repair of EA and TEF. Strictures in the pediatric population may be caused by caustic ingestion, esophagitis and epidermolysis bullosa. Symptoms vary with the degree of tightness of the stricture, and include dysphagia, chest pain, cough and vomiting of undigested food. Drooling and refusal to eat may be signs of a foreign body causing complete obstruction of the stricture.

Balloon dilatation is the preferred treatment above traditional bougienage, and surgery is rarely indicated.

2.5.5.1 Radiological Findings

The chest radiograph is usually normal. Occasionally, an esophageal air-fluid level can be seen above an esophageal obstruction. Barium esophagram, the modality of choice, demonstrates strictures as nar-

rowing of the esophageal lumen and lack of distensibility which may be localized or diffuse (Fig. 2.28) (Karasick and Lev-Toaff 1995). The radiological appearance varies with the type of stricture and its caliber.

Fluoroscopic dilatation has many advantages over bougienage because balloon dilatation is not limited by the diameter of the nose or pharynx, and the incidence of perforation with balloon dilatation is much lower than with bougie dilatation (Fasulakis and Andronikou 2003). Serial balloon dilatation is recommended because progressive stretching of scar tissue prevents tears and perforations. Scar tissue can limit success since fibrosis and altered blood supply reduce tissue elasticity (Fasulakis and Andronikou 2003). The balloon is inflated under fluoroscopy at the level of the stricture, applying uniform radial force that is less traumatic than the shearing force of bougienage. Fluoroscopy has the added advantage of allowing the radiologist to check that the stricture is dilated to a suitable diameter. After dilatation, the success of the procedure can be monitored immediately with the introduction of water soluble contrast medium to show an increase in esophageal caliber and to evaluate for a leak or perforation (Fasulakis and Andronikou 2003).

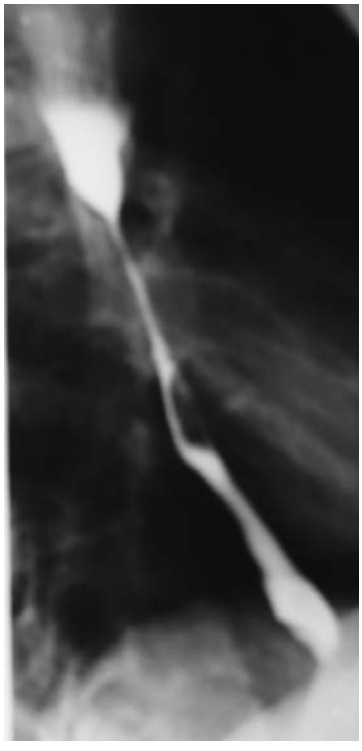

Fig. 2.28. Esophageal stricture. Barium swallow shows a long stricture involving almost the entire length of the esophagus years after ingesting an unknown corrosive agent

Although strictures may not be completely resolved after balloon dilatation, the procedure will provide functional relief, often further aided by forceful swallowing by the patient (Allmendinger et al. 1996). Balloon dilatation has to be repeated as the child grows (Allmendinger et al. 1996). Ongoing and progressive diseases such as repaired esophageal atresia and epidermolysis bullosa require repeated dilatation as the disease progresses (Fig. 2.29).

2.5.6 Esophageal Perforation

Esophageal perforations are rare in children, but the incidence is increasing as more diagnostic and therapeutic endoscopies are performed. Iatrogenic esophageal perforation is the cause in 33%–75% of cases (Martinez et al. 2003). The incidence is low in upper endoscopy, and higher with rigid dilators. Esophageal perforations are more likely to occur if a foreign body has been present more than 24 h and caused pressure necrosis. Other etiologies are pill-induced, caustic damage, infectious, including candida, herpes and tuberculosis. Cervical esophageal perforation may result from penetrating trauma by objects in the mouth, including lollipops and pencils. Esophageal perforation is potentially life-threatening because it allows entry of bacteria and digestive enzymes into the pleural and subphrenic spaces and the mediastinum, causing sepsis. Perforation of the intraabdominal esophagus may lead to sepsis and shock.

Conservative non-operative therapy for esophageal perforation is preferred. In children this consists of antibiotic coverage, drainage of pleural effusions, esophageal rest and total parenteral nutrition if there is no evidence of contrast leak at esophagram. Successful outcome depends on early diagnosis and treatment, young age and absence of underlying disease (Martinez et al. 2003). Operative treatment may be required with esophageal perforation or gross leakage.

2.5.6.1 Radiological Findings

Esophageal perforation can be diagnosed on frontal and lateral chest radiographs. Findings include pneumomediastinum, pneumothorax, hydro-pneumothorax, subcutaneous emphysema and pleural effusions (Fig. 2.30). Chest radiography is not useful

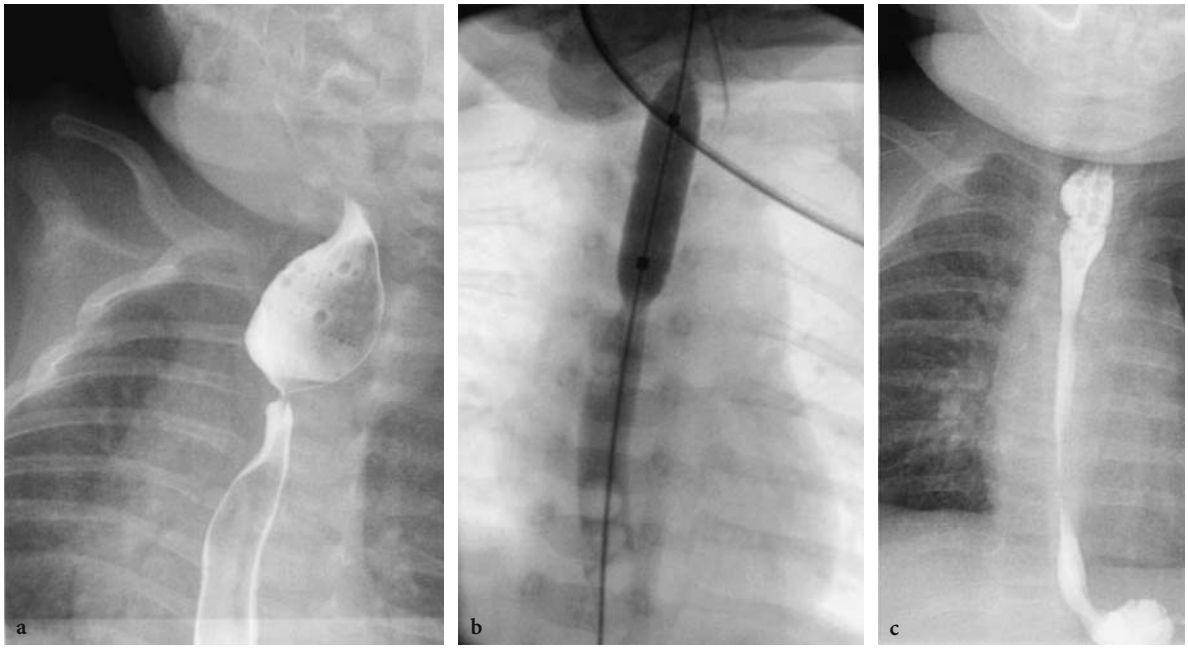

Fig. 2.29a–c. Balloon dilation of an esophageal stricture. **a** Severe stenosis of the proximal esophagus 3 months after repair. **b** Dilatation balloon expanded across the narrowing, no extravasation. **c** Post-dilatation appearance

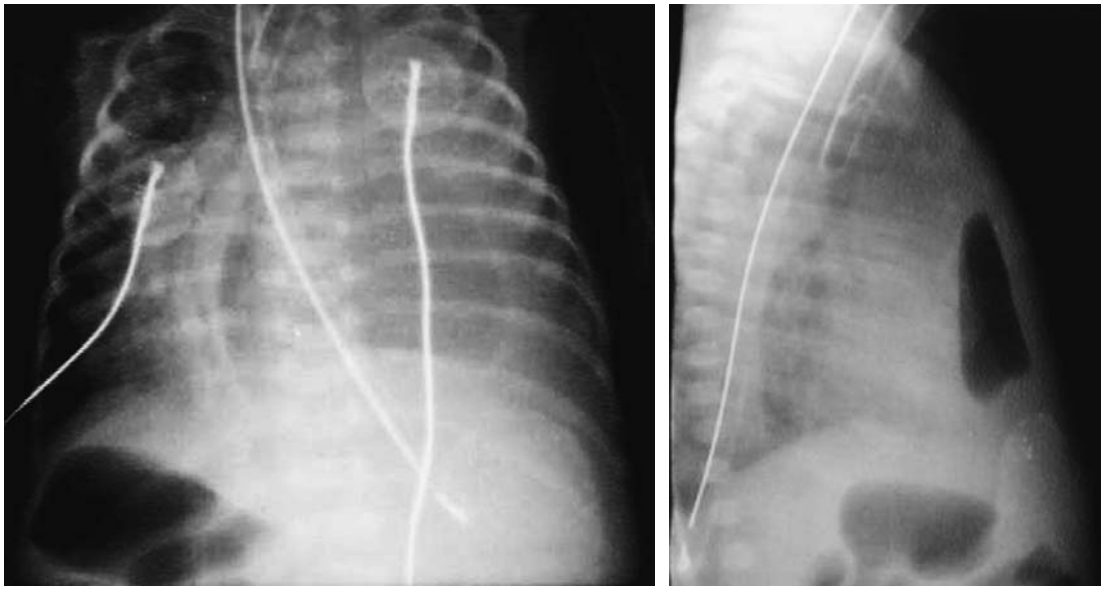

Fig. 2.30a,b. Esophageal perforation after orogastric tube malposition. **a** Frontal chest radiograph with left pleural effusion, left pulmonary atelectasis and mediastinal shift. Free air overlies the cardiac silhouette. **b** Lateral chest radiograph confirms the traumatic pneumothorax

with cervical esophageal perforation. Airway films are required if there is concern for cervical esophageal perforation. Contrast swallow is falsely negative in 10% (Gimenez et al. 2002). CT is recommended when the esophagram is negative and there is high suspicion of perforation.

2.5.7 Epidermolysis Bullosa

Epidermolysis bullosa is a rare inherited genodermatosis resulting from a mutation in COL7A1, the gene encoding type VII collagen (Horn and Tidman 2002). Clinical manifestations are caused by the extreme vulnerability of squamous epithelium of the skin and mucous membranes to minor trauma. The most affected subtype is the recessive epidermolysis bullosa dystrophica, in which the most severely affected individuals will develop blisters within the first 24 h of life (Horn and Tidman 2002). Most cases with esophageal involvement become symptomatic during the first two decades of life. Gastrointestinal manifestations can occur in the absence of active blistering (Horn and Tidman 2002). Swallowing is sufficiently traumatic to cause bullae and erosions that rupture, ulcerate and scar. Oral changes compromise the child's ability to chew food properly and further exacerbate the esophageal trauma (Anderson et al. 2004). Scarring and fibrosis cause shortening of the esophagus that may result in gastroesophageal reflux and further stricturing (Anderson et al. 2004).

Epidermolysis bullosa is an ongoing and progressive disease and repeated dilatations are necessary (Demirogullari et al. 2001). Dilatation is best performed in the inactive stage of the disease rather than during the active stages of blistering.

2.5.7.1 Radiological Findings

Affected individuals have a 15% incidence of developing squamous carcinoma at an early age (Hoeffel et al. 1992). Therefore, fluoroscopy must be prudently limited in these children and repeated fluoroscopy and fluoroscopically guided esophageal dilatation are discouraged

Children with epidermolysis bullosa must be treated very carefully to prevent trauma to their extremely fragile skin and mucosa. They should lie on soft padding on the fluoroscopic table and should not be restrained for radiographic procedures. Affected children should drink the barium spontaneously, and nasogastric tubes must be avoided (Fordham 2005). Barium esophagram will demonstrate strictures, approximately half which are in the proximal third of the esophagus near the cricopharyngeus muscle, 25% in the distal one-third, and the remainder in multiple sites (Fig. 2.31) (Kern et al. 1989). The strictures may be several centimeters in length, and are likely exacerbated by gastroesophageal reflux. Annular strictures are usually less than 3 cm in length.

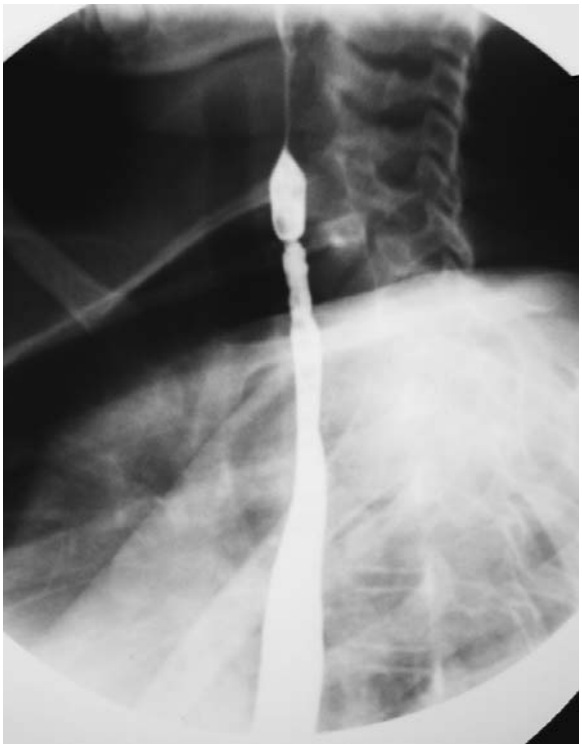

Fig. 2.31. Epidermolysis bullosa. Barium swallow reveals a proximal annular stricture and a long segment of diffuse irregularity of the esophagus

2.5.8 Infectious and Inflammatory Conditions

2.5.8.1 Infectious Esophagitis

Infectious esophagitis is rare in children. Candida is the most common cause, and usually occurs

in immunocompromised patients (Levine and Rubesin 2005). Candida esophagitis is common in the absence of oral thrush. Barium esophagram demonstrates linear or irregular filling defects separated by normal mucosa (Levine and Rubesin 2005). Herpes and cytomegalovirus are other frequent causes of esophagitis in immunosuppressed patients. They manifest on barium swallow as discrete well defined areas of ulceration (Levine and Rubesin 2005). HIV infection itself can cause large esophageal ulcers (Sor et al. 1995).

2.5.8.2 Inflammatory Esophagitis

Eosinophilic esophagitis is an atopic condition in which esophageal inflammation occurs with a predominantly eosinophilic infiltrate that extends into the muscularis. The annual incidence is 1 in 10,000, and is increasing (Noel and Rothenberg 2005). Symptoms mimic reflux esophagitis, are unresponsive to acid suppression therapy and respond to steroids. The esophagram shows a narrow esophageal lumen, caused by thickening of the esophageal wall, a feature also demonstrated on CT (Sant'Anna et al. 2004).

2.5.9 Esophageal Varices

Esophageal varices in children are a manifestation of portal hypertension that causes hepatofugal flow through esophageal collateral veins to drain into the superior vena cava. The most common children's diseases that cause portal hypertension include umbilical venous catheterization, biliary atresia, alpha-1 antitrypsin deficiency, autosomal recessive polycystic renal disease and cystic fibrosis.

2.5.9.1 Radiological Findings

On barium swallow, varices are demonstrated as serpiginous filling defects, best seen in the collapsed esophagus. The normal parallel course of the mucosal folds is interrupted by the varices that appear as filling defects. At the present time, barium swallow is uncommonly performed to make this diagnosis. Instead, the diagnostic work up includes Doppler sonography, MR cholangiography and MR angiography.

References

Al-Assiri A, Wiseman N, Bunge M (2005) Prenatal diagnosis of intrathoracic stomach (gastric herniation). J Pediatr Surg 40:E15–E17

Allmendinger N, Hallsey MJ, Markowitz SK et al (1996) Balloon dilatation of esophageal strictures in children. J Pediatr Surg 31:334–336

Amae S, Nio M, Kamiyama T (2003) Clinical characteristics and management of congenital esophageal stenosis: a report on 14 cases. J Pediatr Surg 38:565–570

Anderson SHC, Meenan J, Williams KN et al (2004) Efficacy and safety of endoscopic dilatation of esophageal strictures in epidermolysis bullosa. Gastrointest Endoscop 59:28–32

Babu R, Pierro A, Spitz L et al (2000) The management of oesophageal atresia in neonates with right-sided aortic arch. J Pediatr Surg 35:56–58

Backer CL, Mavroudis C, Rigsby CK, Holinger LD (2005) Trends in vascular ring surgery. J Thorac Cardiovasc Surg 129:1339–1347

Bannister LH (1995) Chapter 12. The alimenatary system. In: Banister LH, Berry MM, Colllins P et al. (eds) Gray's anatomy, 38th edn. Churchill Livingstone, Edinburgh, pp 1683–1812

Barnard CN (1956) The genesis of intestinal atresia. Surg Forum 7:393–402

Benjamin B (1981) Endoscopy in esophageal atresia and tracheo-esophageal fistula. Ann Otol Rhinol 90:376–382

Berdon WE, Baker DH, Schulinger JN, Santulli TV (1979) Plain film detection of right aortic arch in infants with esophageal atresia and tracheoesophageal fistula. J Pediatr Surg 14:436–437

Berrocal T, Torres I, Guttierrez J et al (1999) Congenital anomalies of the upper gastrointestinal tract. Radiographics 19:855–872

Blumhagen JD, Rudd TG, Christie DL (1980) Gastroesophageal reflux in children: radionuclide gastroesophagography. AJR Am J Roentgenol 135:1001–1004

Boix-Ochoa J, Canals J (1976) Maturation of the lower esophagus. J Pediatr Surg 11:749–756

Bonnard A, Auber F, Fourcade L et al (2003) Vascular ring abnormalities: a retrospective study of 62 cases. J Pediatr Surg 38:539–543

Bremer JL (1944) Diverticula and duplications of the intestinal tract. Arch Pathol 38:132–140

Chacko J, Ford WDA, Furness ME (1998) Antenatal detection of hiatus hernia. Pediatr Surg Int 13:163–164

Chana J, Crabbe DC, Spitz L (1996) Familial hiatus hernia and gastro-oesophageal reflux. Eur J Pediatr Surg 6:175–176

Cheng W, Tam PKH (1999) Foreign-body ingestion in children: experience with 1,265 cases. J Pediatr Surg 34:1472–1476

Chetcuti P, Myers NA, Phelan PD et al (1989) Chest wall deformity in patients with repaired esophageal atresia. J Pediatr Surg 24:244–247

Collins P (1995) Chapter 3. Embryology and development. In: Banister LH, Berry MM, Collins P et al (eds) Gray's anatomy, 38th edn. Churchill Livingstone, Edinburgh, pp 91–342

Cumming WA (1975) Esophageal atresia and tracheoesophageal fistula. Radiol Clin North Am 13:277–295

Dantas RO, Dodds WJ, Massey BT, Kern MK (1989) The effect of high- vs low-density barium preparations on the quantitative features of swallowing. AJR Am J Roentgenol 153:1191–1195

DeMatteo C, Matovich D, Hjartarson A (2005) Comparison of clinical and video fluoroscopic evaluation of children with feeding and swallowing difficulties. Dev Med Child Neurol 47:149–157

Demirogullari B, Sonmez K, Turkyilmaz Z et al (2001) Colon interposition for esophageal stenosis in a patient with epidermolysis bullosa. J Pediatr Surg 36:1861–1863

Duncan M, Wong RKH (2003) Esophageal emergencies: things that will wake you from a sound sleep. Gastroenterol Clin N Am 32:1035–1052

Emblem R, Stringer MD, Hall CM, Spitz L (1993) Current results of surgery for achalasia of the cardia. Arch Dis Child 68:749–751

Engum SA, Grosfeld JL, West KW et al (1995) Analysis of morbidity and mortality in 227 cases of esophageal atresia and/or tracheoesophageal fistula over two decades. Arch Surg 130:502–508

Fasulakis S, Andronikou S (2003) Balloon dilatation in children for esophageal strictures other than those due to primary repair of oesophageal atresia, interposition or restrictive fundoplication. Pediatr Radiol 33:682–687

Fernbach SK, Glass RBJ (1988) The expanded spectrum of limb anomalies in the VATER association. Pediatr Radiol 18:215–220

Fernbach SK in: Gore RM, Levine MS, Laufer I (eds) (1994) Textbook of gastrointestinal radiology, 1st edn. WB Saunders Company. Philadelphia, pp 1380–1497

Fordham LA (2005) Imaging of the esophagus in children. Radiol Clin North Am 43:283–302

Gimenez A, Franquet T, Erasmus JJ et al (2002) Thoracic complications of esophageal disorders. Radiographics Spec No:S247–258

Gold B (2005) Asthma and gastroesophageal disease in children: exploring the relationship. J Peds 146:S13–S20

Gorenstein A, Cohen AJ, Cordova C et al (2001) Hiatal hernia in pediatric gastroesophageal reflux. J Pediatr Gastroenterol Nutr 33:554–557

Greil GF, Kramer U, Dammann F, Schick F et al (2005) Diagnosis of vascular rings and slings using an interleaved 3D double-slab FISP MR angiography technique. Pediatr Radiol 35:396–401

Griscom NT, Martin TR (1990) The trachea and esophagus after repair of esophageal atresia and distal fistula: computed tomographic observations. Pediatr Radiol 20:447–450

Harned RK, Strain JD, Hay TC, Douglas MR (1997) Esophageal foreign bodies: safety and efficacy of Foley catheter extraction of coins. AJR Am J Roentgenol 168:443–446

Hassal E (2005a) Decisions in diagnosing and managing chronic gastroesophageal reflux disease in children. J Pediatr 146:S3–S12

Hassal E (2005b) Outcomes of fundoplication: causes for concern, newer options. Arch Dis Child 90:1047–1052

Herman TE, Oser AB, McAlister WH (1991) Tubular communicating duplications of esophagus and stomach. Pediatr Radiol 21:494–496

Hernanz-Schulman M (2005) Vascular rings: a practical approach to imaging diagnosis. Pediatr Radiol 35:961–979

Hoeffel JC, Bigard MA, Merle M, Hoeffel C (1992) Epidermolysis bullosa: radiological patterns in childhood. Rofo 157: 427–428

Horn HM, Tidman MJ (2002) The clinical spectrum of dystrophic epidermolysis bullosa. Br J Dermatol 146:267–274

Hurwitz M, Bahar R, Ament ME et al (2000) Evaluation of the use of botulinum toxin in children with achalasia. J Pediatr Gastroenterol Nutr 30:509–514

Hussain SZ, Thomas R, Tolia V (2002) A review of achalasia in 33 children. Dig Dis Sci 47:2538–2543

Jadcherla SR, Duong HK, Hofmann C et al (2005) Characteristics of upper esophageal sphincter and oesophageal body during maturation in healthy human neonates compared with adults. Neurogastroenterol Motil 17:663–670

Kappelman MM, Dorst J, Haller JA et al (1969) H-type tracheo-esophageal fistula. Diagnostic and operative management. Am J Dis Child 118:568–575

Karasick S, Lev-Toaff AS (1995) Esophageal strictures: findings on barium radiographs. AJR Am J Roentgenol 165:561–565

Kern IB, Eisenberg M, Willis S (1989) Management of oesophageal stenosis in epidermolysis bullosa dystrophica. Arch Dis Child 64:551–556

Khelif K, De Laet MH, Chaouachi B et al (2003) Achalasia of the cardia in Allgrove's (Triple A) syndrome: histopathological study of 10 cases. Am J Surg Pathol 27:667–672

Koumanidou C, Vakaki M, Pitsoulakis G et al (2004) Sonographic measurement of the abdominal esophagus length in infancy: a diagnostic tool for gastroesophageal reflux. AJR Am J Roentgenol 183:801–807

Kovesi T, Rubin S (2004) Long term complications of esophageal atresia and/or tracheoesophageal fistula. Chest 126:915–925

Kramer SS (1989) Radiologic examination of the swallowing impaired child. Dysphagia 3:117–125

Kuhns LR, Poznanski AK (1972) A device for control of esophageal tubes in infants. Radiology 102:438–439

Leithiser RE, Capitanio MA, Macpherson RI, Wood BP (1985) "Communicating" bronchopulmonary foregut malformations. AJR Am J Roentgenol 146:227–231

Levine MS, Rubesin SE (2005) Diseases of the esophagus: diagnosis with esophagography. Radiology 237:414–427

Lifschitz CH (2001) Feeding problems in infants and children. Curr Treat Options Gastroenterol 4:451–457

Martinez L, Rivas S, Hernandez F et al (2003) Aggressive conservative treatment of esophageal perforations in children. J Pediatr Surg 38:685–689

Mayberry JB, Mayell MJ (1998) Epidemiological study of achalasia in children. Gut 29:90–93

McGuirt WF (2003) Gastroesophageal reflux and the upper airway. Pediatr Clin N Am 50:487–502

Mercado-Deane MG, Burton EM, Harlow SA et al (2001) Swallowing dysfunction in infants less than 1 year of age. Pediatr Radiol 31:423–428

Meschan I (1975) An atlas of anatomy basic to radiology. WB Saunders Company, Philadelphia

Michel JL, Revillon Y, Salakos C et al (1997) Successful bronchotracheal reconstruction in esophageal bronchus: two case reports. J Pediatr Surg 32:739–742

Miller CK, Willging JP (2003) Advances in the evaluation and management of pediatric dysphagia. Curr Opin Otolaryngol Head Neck Surg 11:442–446

Murphy SG, Yazbeck S, Russo P (1995) Isolated congenital esophageal stenosis. J Pediatr Surg 30:1238–1241

Nelson SP, Chen EH, Syniar GM, Christoffel KK (1997) Prevalence of symptoms of gastroesophageal reflux during infancy: a pediatric practice-based survey. Arch Pediatr Adolesc Med 151:569–572

Newman B, Bender TM (1997) Esophageal atresia/tracheoesophageal fistula and associated congenital esophageal stenosis. Pediatr Radiol 27:530–534

Newman LA, Keckley C, Petersen MC, Hammer A (2001) Swallowing function and medical diagnoses in infants suspected of dysphagia. Pediatrics 108:E106

Noel RJ, Rothenberg ME (2005) Eosinophilic esophagitis. Curr Opin Pediatr 17:690–694

Poznanski A (1969) A simple device for administering barium to infants. Radiology 93:1106

Quan L, Smith WL (1973) The VATER association: vertebral defects, anal atresia, T-E fistula with esophageal atresia, radial and renal dysplasia: a spectrum of associated defects. J Pediatr 82:104–107

Rudolph CD, Mazur LJ, Liptak GS et al (2001) Guidelines for evaluation and treatment of gastroesophageal reflux in infants and children: recommendations of the North American Society for Pediatric Gastroenterology and Nutrition. J Pediatr Gastroenterol Nutr 32:S1–S32

Sadler TW (2000) Langman's medical embryology, 8th edn. Lippincott Williams and Wilkins, Baltimore, MD

Sant'Anna AM, Rolland S, Fournet JC et al (2004) Eosinophilic esophagitis in children: symptoms, histology, and pH probe results. J Pediatr Gastroenterol Nutr 39:373–377

Schlesinger AE, Parker BP in: Kuhn JP, Slovis TL, Haller JO (eds) (2004) Caffey's pediatric diagnostic imaging, 10th edn. Mosby, Philadelphia, pp 1539–1583

Schunk JE, Harrison MA, Corneli HM, Nixon GW (1994) Fluoroscopic Foley catheter removal of esophageal foreign bodies in children: experience with 415 episodes. Pediatrics 94:709–714

Seibert JJ, Byrne WJ, Euler A, et a. (1983) Gastroesophageal reflux – the acid test: scintigraphy or the pH probe? AJR Am J Roentgenol 140:1087–1090

Sharieff GQ, Brousseau TJ, Bradshaw JA, Shad JA (2003) Acute esophageal coin ingestion: is immediate removal necessary? Pediatr Radiol 33:859–863

Shaw-Smith CJ (2005) Oesophageal atresia, tracheo-esophageal fistula and the VACTERL association: review of genetics and epidemiology. J Med Genet 43:545-554 [Epub ahead of print]

Singleton EB, King BA (1971) Localized lesions of the stomach in children. Semin Roentgenol 6:220–234

Sor S, Levine MS, Kowalski TZ et al (1995) Giant ulcers of the esophagus in patients with human immunodeficiency virus: clinical, radiographic, and pathologic findings. Radiology 194:447–451

Srikanth MS, Ford EG, Stanley P, Mahour GH (1992) Communicating bronchopulmonary foregut malformations: classification and embryogenesis. J Pediatr Surg 27:732–736

Vaezi MF, Richter JE (1999) Current therapies for achalasia: comparison and efficacy. J Clin Gastroenterol 27:21–35

Vane DW, Cosby C, West K, Grosfeld JL (1988) Late results following esophagomyotomy in children with achalasia. J Pediatr Surg 23:515–519

Vasudevan SA, Kerendi F, Lee H, Ricketts RR (2002) Management of congenital esophageal stenosis. J Pediatr Surg 37:1024–1026

Vazquez JL, Buonomo C (1999) Feeding difficulties in the first days of life: findings on upper gastrointestinal series and the role of videofluoroscopic swallowing study. Pediatr Radiol 29:894–896

Walor D, Berdon W, Anderson N et al (2005) Gaseous distention of the cervical esophagus with nasal CPAP: mimicker of pharyngeal perforation and esophageal atresia. Pediatr Radiol 35:1196–1198

Wang JK, Chang MH, Li YW et al (1993) Association of hiatus hernia with asplenia syndrome. Eur J Pediatr 142:418–420

Webb WA (1995) Management of foreign bodies of the upper gastrointestinal tract: update. Gastrointest Endosc 41:39–51

Westra SJ, Wolf BH, Staalman CR (1990) Ultrasound diagnosis of gastroesophageal reflux and hiatal hernia in infants and young children. J Clin Ultrasound 18:477–485

Woods RK, Sharp RJ, Holcomb GW 3rd et al (2001) Vascular anomalies and tracheoesophageal compression: a single institution's 25-year experience. Ann Thorac Surg 72:438–439

Yardeni D, Yardeni H, Coran AG, Golladay ES (2004) Severe esophageal damage due to button battery ingestion: can it be prevented? Pediatr Surg Int 20:496–501

Stomach

3

Els Nijs

CONTENTS

E. Nijs, MD
Department of Radiology, University Hospitals Gasthuisberg, Katholieke Universiteit Leuven, Herestraat 49, 3000 Leuven, Belgium

3.1 Normal Embryology and Anatomy

In the normal embryo, the abdominal portion of the foregut is visibly divided into the esophagus, stomach and proximal duodenum by the fifth week (Larsen 2001). During the fifth week, the stomach starts out as a straight tube but since there is differential growth of its dorsal and ventral wall, the greater curvature will become more elongated than the lesser curvature. Continued differential expansion of the superior part of the greater curvature gives rise to the fundus and cardiac incisure by the end of the seventh week.

During the seventh and eighth weeks, the stomach will rotate 90° around a craniocaudad axis. The former anterior portion will form the right side of the stomach and the former posterior portion becomes the left side of the stomach.

The stomach is relatively fixed in the abdominal cavity at the esophagogastric junction and at the pyloroduodenal junction. Furthermore, there are four different ligaments which will fix the stom-

ach: the gastrohepatic ligament, the gastrosplenic ligament, the gastrocolic ligament and the gastrophrenic ligament.

The stomach is classically divided into the fundus, being the upper most portion, the body, which is the largest part, the antrum, at the distal end, and the pylorus.

Due to the above mentioned rotations of the stomach, the presumptive duodenum will bend into a C shape and will be displaced to the right until it lies against the dorsal body wall and becomes secondarily retroperitoneal. A system of digestive glands develops from endodermal buds of the duodenum, including the liver parenchyma, the gall bladder and their ducts (derived from the hepatic diverticulum), as well as the pancreatic parenchyma and its ducts (derived from the fusion of the dorsal and ventral pancreatic ducts) (Fig. 3.1).

The duodenum is typically divided into four portions. The first portion is relatively mobile in contrast to the rest of the duodenum which is fixed in the retroperitoneal cavity. The second descending portion of the duodenum is in close contact with the pancreas and receives the common bile duct and duct of Wirsung in its midportion. The third portion is horizontally oriented and is ventrally crossed by the superior mesenteric artery (SMA) and superior mesenteric vein (SMV). The fourth ascending portion will turn ventrally to the duodenojejunal junction, which is additionally held in place by the ligament of Treitz.

The stomach and proximal duodenum are derived from the embryonic foregut and will therefore receive their blood supply from the celiac axis. Part of the third portion and the entire fourth portion of the duodenum depend on the superior mesenteric artery because of their midgut origin.

The gastrointestinal (GI) tract also starts out as a short, straight tube (Larsen 2001). This tube will then elongate and will become fixed in the abdominal cavity by a very complicated process. The proximal duodenojejunal loop and the distal cecocolic loop are able to pull adjacent bowel along with them. Before the tenth week of embryonic life, both loops will independently rotate 270° in a counterclockwise direction around the SMA and return to the abdominal cavity. This results in the actual position of the duodenum with the duodenojejunal junction at the left side in the upper abdomen. On the other hand, the cecum will finally lie in the right lower quadrant and the transverse colon anterior to the SMA. When the process of rotation is finalized, the bowel is fixed in this position by the mesentery. The normal mesentery extends from the left upper quadrant at the ligament of Treitz to the cecum in the right lower quadrant and is broad based.

The bolus from the esophagus will arrive in the stomach, where digestion takes place until ingredients are sufficiently broken down to be passed into the intestine for further digestion and absorption. The gastric wall consists of the mucosa with the muscularis mucosae, submucosa, muscularis externa and serosa. The mucus produced by the mucous surface cells and mucous cells of the glands protects the stomach lining from damage due to hydrochloric acid and pepsin secreted by the gastric glands. The rugae or longitudinal folds of the empty stomach are consistent with the mucosa and

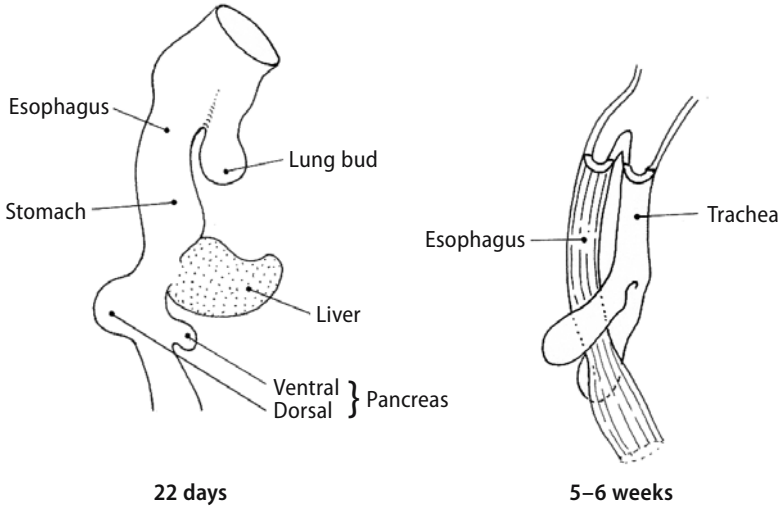

Fig. 3.1. Normal embryology and anatomy of the foregut and organs of digestion

submucosa. The muscularis externa of the stomach consists of three smooth muscle layers: an inner oblique, a middle circular and an outer longitudinal. These muscle layers are responsible for the 'gastric motility' in receiving large volumes of ingested food and fluids during a meal, in mixing the ingested food with gastric juices and in propelling the gastric contents into the small intestine.

The wall of the duodenum is, like the gastric wall, divided into the mucosa, submucosa, muscularis externa and serosa. The main function of the duodenum is the digestion of nutrients (Ross and Romrell 1989).

3.2 Examination of the Upper GI Tract

3.2.1 Abdominal X-Ray: Air as a Contrast Agent

The plain film of the abdomen is still very useful in the evaluation of the neonate. Air can be used as a contrast agent since newborns will start swallowing air immediately after birth, and gas should be present in the stomach within minutes. After 3 h, air should be seen throughout the entire small bowel, while the sigmoid colon is seen after 8–9 h (Berrocal et al. 1999). Some congenital anomalies can be readily diagnosed without the need for other contrast media (Fig. 3.2), for instance a duodenal obstruction with the typical "double-bubble" appearance, which may be caused for instance by duodenal atresia or midgut volvulus.

3.2.2 Fluoroscopy/Upper GI Study

Roughly, the recommended fasting time before the study is equal in length to the regular time between meals for the patient, being longer in adolescents than in newborn babies. Typically in children under 1 year of age, a 3-h fasting period is sufficient to empty the normal stomach. A longer fasting time bares the risk of dehydration in this patient group. Older children will be kept fasting overnight (Schlesinger and Parker 2003).

Traditionally barium will be used as contrast agent. However, in a patient with suspected risk of aspiration (e.g. neurologically impaired children) or a neonate with a congenital proximal obstruction and suspicion of perforation (risk of barium peritonitis), non-ionic low-osmolar contrast agents will be used. The main advantages of the latter contrast agents are lack of large fluid shifts, absence of con-

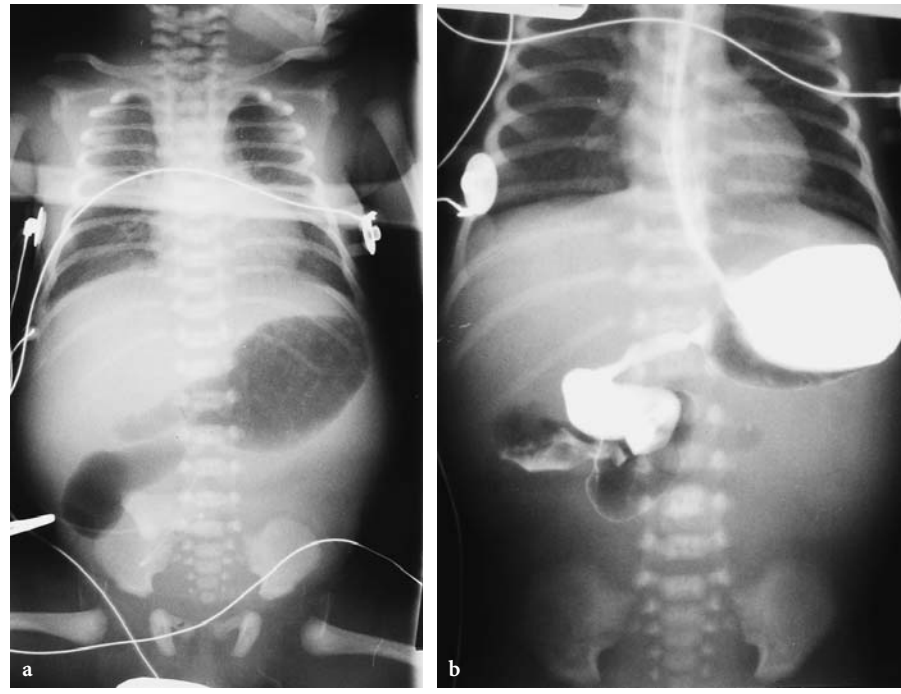

Fig. 3.2. a Radiograph with air as contrast agent: malrotation. **b** Radiograph with high density contrast agent: confirmation of malrotation. (Courtesy of Dr. Carlo Buonomo, Boston, MA, USA)

trast dilution, lack of injury to the bowel mucosa, low absorption from the bowel and relatively low risk of pulmonary edema if aspirated.

An upper GI study will always include the evaluation of the esophagus, stomach and duodenum.

An upper GI study in newborns and small infants will be different from those performed in adolescents. In the former group of children, the study will be performed to evaluate a (known) congenital proximal obstruction (evaluation of antral or duodenal web) or, more importantly, to evaluate the position of the duodenojejunal flexure (the ligament of Treitz). The study will be tailored to answer these specific questions and these will always be single contrast studies. In older children, however, double contrast studies may occasionally be necessary depending on the clinical question (e.g. polyps).

On barium studies, the contour of the stomach typically will appear smooth in newborns and young infants, while in older children the normal gastric rugal folds will be visible as seen in adults.

Pulsed fluoroscopy is always recommended in children together with careful collimation and gonadal shielding. Furthermore, photo spot-film cameras or digital fluoroscopy should be used (Schlesinger and Parker 2003).

3.2.3 Ultrasound

Ultrasound (US) is now increasingly used for the evaluation of the upper GI tract, for instance to evaluate for wall thickness or a duplication cyst. In other instances, it may be necessary to fill the stomach with fluid before the examination, e.g. in the evaluation of gastroesophageal reflux or hypertrophic pyloric stenosis.

Abdominal vector probes can be used for a good overview of the stomach, but linear high frequency transducers are necessary for a more detailed view.

Typically the patient will be scanned in the supine position. A right posterior oblique position is used to evaluate the antrum and pyloric region since fluid will displace the air to the gastric body and fundus.

3.2.4 Cross-Sectional Imaging

Computed tomography (CT) and magnetic resonance (MR) imaging are not routinely used to evaluate the stomach in children, except in cases of a suspected or known malignancy for staging purposes.

3.2.5 Scintigraphic Studies

Several scintigraphic studies may be indicated to evaluate for gastric pathology in children. Radionuclide gastric emptying study may be performed to evaluate for gastric motility and emptying. 99Tcm-pertechnetate scintigraphy can be performed to evaluate for the presence and location of functioning ectopic gastric mucosa. Technetium-99m HMPAO-labeled leukocyte imaging can be used in the evaluation of inflammatory bowel disease.

3.3 Congenital Gastric Disorders

3.3.1 Fetal Study (US and/or MR)

The stomach will appear as a cystic structure in the left hypochondrium of the fetus and should be constantly visible at around 11–12 weeks of gestation during fetal US.

When the stomach is small or not visible in the second or third trimester, first US should be repeated to confirm or exclude these findings. If the above can be confirmed, it raises the suspicion of an abnormality. The most common etiology is esophageal atresia. This diagnosis can be confirmed on US when the dilated pharyngeal pouch is seen. MR can more easily demonstrate the dilated pharyngeal pouch or can exclude the diagnosis by documenting a normal esophagus. Another condition in which the stomach appears small or cannot be visualized, is intra-uterine growth retardation with associated oligohydramnios.

If the stomach is too big in the third trimester on two consecutive studies, the main cause is duodenal atresia with the typical "double-bubble" appearance. A total of 30% of these patients will have trisomy 21 (Buonomo et al. 1998). These patients also have an increased risk of an esophageal atresia, in which case they will not always present with a "double-bubble" appearance due to the obstruction of the GI tract more proximally, unless they have an associated

H-type tracheo-esophageal fistula. The differential diagnosis for the double-bubble should include duodenal stenosis and annular pancreas (Rathaus et al. 1992; Poki et al. 2005).

When the stomach does not lie in the left hypochondrium but is located in the midline, this may indicate an intestinal malrotation with or without obstruction. A postnatal work-up is strictly indicated in these patients.

Further description of the above-mentioned entities/anomalies are given in the sections below.

3.3.2 Gastric Duplication

The gastric duplication cyst represents only 4% of all enterogenous duplications and thus is the least common of all GI duplications (Pruksapong et al. 1979). It can be seen as an isolated finding or in association with other anomalies such as an aberrant pancreas, vertebral anomalies (Schlesinger and Parker 2003) or a pulmonary sequestration (Chen et al. 2006; Granata et al. 2003). Duplication anomalies are usually adjacent to involved bowel and will mainly be located along the greater curvature of the stomach, often in the antrum. They will be spherical or occasionally tubular in configuration and may communicate with the lumen. The duplication is composed of a smooth muscle wall continuous with the muscle layer of the intestinal wall and an inner mucosal lining.

Presenting symptoms may include vomiting (obstruction), hematemesis, melena or palpable mass.

Plain abdominal X-ray may demonstrate a soft tissue mass in between the greater curvature of the stomach and superior to the transverse colon (Barlev and Weinberg 2004). This is seldom seen.

On barium studies, a large gastric duplication may be recognized as an intramural, extraluminal soft tissue mass which causes displacement of the gastric lumen. However the diagnosis will often be made by US where the typical bowel wall can be recognized: an inner thin echogenic line, consistent with the mucosa, and an outer hypoechoic layer, consistent with the muscular layer (Fig. 3.3). Furthermore, the gastric duplication is located intramurally and is filled with anechoic fluid. Less commonly it is filled with echogenic material, representing hemorrhage, infection or proteinaceous fluid.

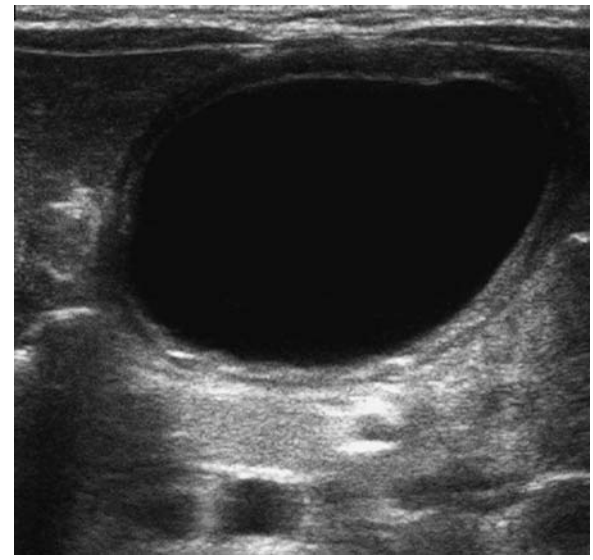

Fig. 3.3. US of duplication cyst of the greater curvature of the stomach: classic double echo pattern of the GI mucosa. (Courtesy of Dr. Carlo Buonomo, Boston, MA, USA)

The imaging diagnosis can also be made by CT or MR, on which the gastric duplication cyst is filled with low attenuation fluid/low signal intensity on T1-weighted images and high signal intensity on T2-weighted images, or less commonly with high attenuation fluid/high signal intensity on T1-weighted images.

3.3.3 Gastric Diverticula

True congenital gastric diverticula are rare in children. All elements of the normal gastric wall are present and they can be regarded as incomplete gastric duplications. They are usually located posteriorly near the esophagogastric junction, are asymptomatic and can be seen on upper gastrointestinal studies when filled with contrast material (Elliot et al. 2006).

3.3.4 Microgastria

Congenital microgastria was first described in 1894 (Dide 1894) and is extremely rare with less than 50 cases reported to date (Sharma and Menon 2005). It is thought to be the result of an early gastric development arrest from the foregut between the 4th and

5th week of gestation; there is no fetal rotation and the greater and lesser curvatures fail to develop. The spleen arises in the dorsal mesogastrium by mesenchymal differentiation at around the same time, which may explain the frequent association of microgastria with asplenia or polysplenia.

Complete lack of gastric development or agastria is the most extreme form of microgastria (Schlesinger and Parker 2003).

Presenting symptoms of microgastria are recurrent postprandial vomiting, respiratory distress/infection, failure to thrive and malnutrition. These are all consequences of the small stomach and the associated gastroesophageal reflux (Hoehner et al. 1994; Waasdorp et al. 2003).

The diagnosis is made by an upper GI study which will demonstrate an abnormally small tubular or saccular stomach in the midline (Kroes and Festen 1998) (Fig. 3.4).

Megaesophagus is almost always associated with microgastria, which may be secondary to the gastroesophageal reflux or caused by the esophagus taking over the reservoir capacity of the stomach (Moulton et al. 1994).

There is a very high incidence of other associated anomalies with esophageal stenosis, such as a left-sided diaphragmatic hernia (Sharma and Menon 2005), right-sided diaphragmatic hernia (Velasco et al. 1990), growth hormone deficiency and diabetes insipidus (Herniaz Driever et al. 1997), intestinal malrotation, cardiopulmonary anomalies, central nervous system anomalies (hydrocephalus, arrhinencephaly, microphthalmia) (Schlesinger and Parker 2003), renal anomalies (Kroes and Festen 1998), laryngo-tracheo-bronchial clefts (Ryan et al. 1991; Samuel et al. 1997), limb reduction defects (Cunniff et al. 1993), Pierre Robin sequence and partial trismus (Giurgea et al. 2000). Isolated congenital microgastria is extremely rare.

The treatment of choice in patients with microgastria, if no other life-threatening anomalies are present, is gastric augmentation (Menon et al. 2003), classically a Hunt-Lawrence pouch (a double-lumen jejunal pouch anastomosed to the greater curvature of the stomach with a distal Roux-en-Y jejunostomy). Prolonged medical management of gastroesophageal reflux in these patients is not beneficial, since the stomach size will not increase significantly over time (Blank and Chisholm 1973). Operating at an early stage is indicated to allow normal growth and development. Life expectancy is determined mostly by the associated anomalies, being the most frequent cause of death (Moulton et al. 1994).

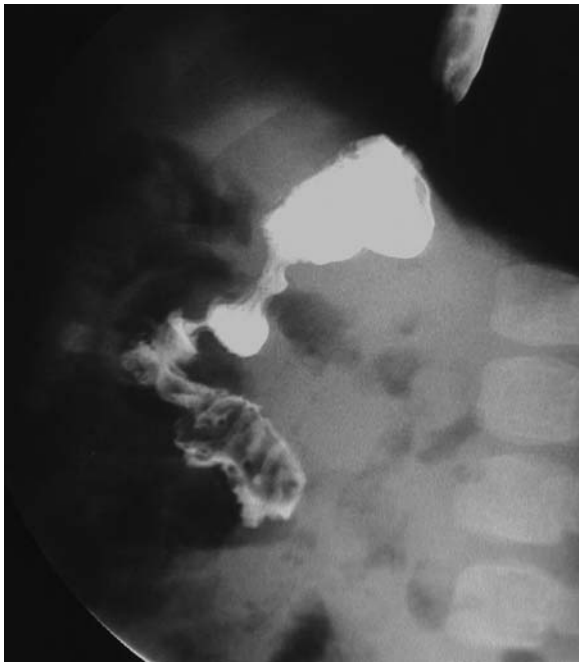

Fig. 3.4. UGI reveals a markedly small stomach: microgastria. (Courtesy of Dr. Carlo Buonomo, Boston, MA, USA)

3.3.5 Pyloric and Prepyloric/Antral Atresias, Stenoses and Webs

Congenital (pre-)pyloric atresias, stenoses and webs are rare. These lesions are thought to be the consequence of an intrauterine vascular insult (Schlesinger and Parker 2003). There are three different types of pyloric atresia: (1) complete atresia and absence of a connection between stomach and duodenum; (2) complete atresia with a fibrous band between stomach and duodenum; and (3) gastric membrane or diaphragm (Gupta and Guglani 2005). The association of pyloric atresia and epidermolysis bullosa has been described and the responsible genetic mutation for this association has been identified (Schlesinger and Parker 2003).

Symptoms will vary among patients, depending on the degree of obstruction: true atresias will result in a complete obstruction while patients with stenoses or webs will only have obstruction depending on relative size of orifice and bolus. This will also affect the time of presentation: patients with atresias will present very early in life, while patients with steno-

ses or webs of the pylorus may present later in life, including adulthood.

The findings described above will correlate with the imaging findings. In patients with atresia, there may be no air distal to the body of the stomach while the stomach is usually dilated. With stenoses and webs, varying degrees of distal air may be seen. In case of an incomplete obstruction, webs are more common than stenoses. On barium studies these can be seen as linear filling defects. Sometimes the diagnosis can also be made with US where a membrane can be seen in the antrum if the stomach is filled with clear liquid (Gupta and Guglani 2005).

3.3.6 Gastric Volvulus

Gastric volvulus can be defined as an abnormal rotation of more than 180° of the stomach around its long (organoaxial) and/or short (mesentericoaxial) axis, creating a closed loop obstruction that may result in incarceration, strangulation and gastric perforation (due to ischemia and necrosis) leading to sepsis and cardiovascular collapse. It is rare in children, but acute gastric volvulus in neonates and infants is a life-threatening emergency. It was first described in children in 1899 (Kiel 1899). To date, more than 150 patients with gastric volvulus in the pediatric population have been described (Darani et al. 2005).

The normal stomach is fixed in the peritoneal cavity by four different ligaments. Absence or loosening of these anatomic attachments results in abnormal mobility of the stomach. Gastric volvulus is the result of the absence or laxity (e.g. post surgical) of the gastrocolic and gastrosplenic ligaments (Dalgaard 1952) as seen in congenital diaphragmatic hernia, paraesophageal hernia or wandering spleen (Lin et al. 2005). Gastric volvulus may be iatrogenic, e.g. after the placement of a percutaneous endoscopic gastrostomy (Sookpotarom et al. 2005).

Acute as well as recurrent subacute or chronic forms have been described. The symptoms are related to the degree of rotation and gastric obstruction. In the acute form, patients will present with sudden vomiting, intractable retching and acute abdominal pain as well as acute vegetative symptoms with hypotonia, pallor and ocular revulsion. It is thought that during acute gastric volvulus, a vagal reflex is triggered by direct irritation of the parasympathetic nervous system. Prompt resuscitation in patients with acute vegetative symptoms may be needed. In the subacute or chronic forms only nonspecific symptoms will be apparent, including recurrent abdominal pain, vomiting and gastric distention.

On abdominal X-ray studies, a gastric volvulus may be suspected. In organoaxial volvulus, a subtle inferiorly displaced gastroesophageal junction may be seen. More typically in mesentericoaxial volvulus, the stomach appears spherical on supine films and a double air-fluid level can be seen in the upright position: a superior one in the antrum, and an inferior one in the fundus. On chest radiograph, a retrocardiac gas-filled structure, consistent with a diaphragmatic hernia and/or an intrathoracic stomach may be seen (Fig. 3.5).

The gold standard for the diagnosis of acute as well as subacute or chronic forms is the upper GI study (Darani et al. 2005). The organoaxial type will be characterized by a stomach in horizontal position with the pylorus facing downward but with a greater curvature, projecting higher than the lesser curvature and in front of the distal portion of the esophagus. In this case the stomach rotates around the long axis, which connects the gastroesophageal junction and pylorus. In contrast, the mesentericoaxial type can be recognized by a stomach in vertical position with a pylorus projecting above the gastroesophageal junction (Fig. 3.6a). The inverted antrum, pylorus and proximal duodenum can form a 'beak' at the usual location of the gastroesophageal junction. In this type, the short axis bisects the lesser and greater curvatures and runs parallel to the hepatoduodenal ligament. The antrum then rotates anteriorly and superiorly so that the posterior surface of the stomach lies anteriorly (Fig. 3.6b,c).

The diagnosis of gastric volvulus can sometimes be suggested on US, when it is performed in search of other diagnoses (Anagnostara et al. 2003).

Definitive treatment will be performed by gastropexy, which can be done laparoscopically. In some patients an anti-reflux procedure may be needed, but this is not always necessary at first (Darani et al. 2005).

3.3.7 Ectopic Gastric Mucosa

Kumar et al. (2005) described a series of 11 (male) children in which the diagnosis of ectopic gastric mucosa could be made by the use of 99Tcm-

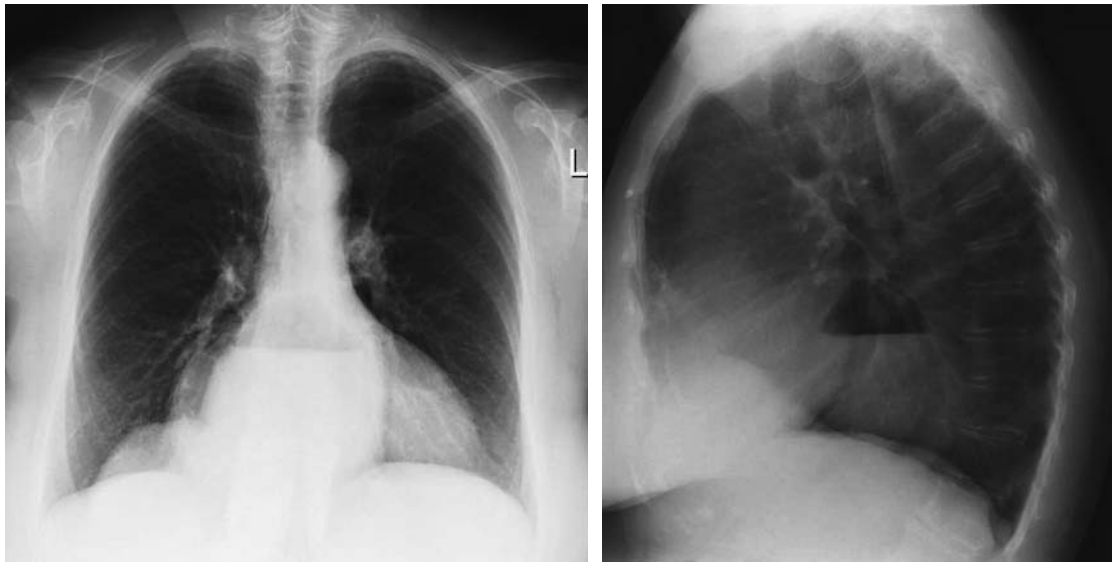

Fig. 3.5a,b. The chest radiograph shows in this 14-year-old girl retrocardial an air fluid level, consistent with a diaphragmatic hernia. (Courtesy of Dr. Carlo Buonomo, Boston, MA, USA)

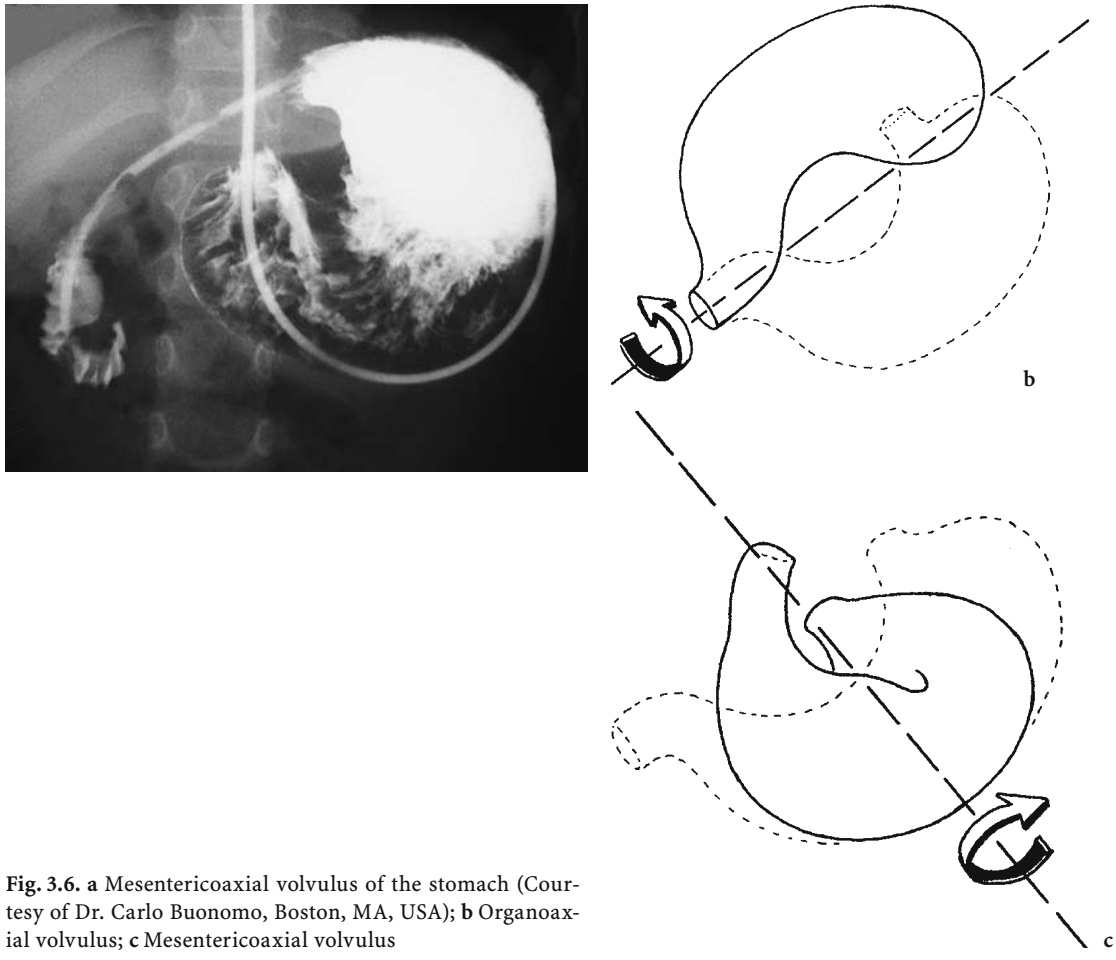

Fig. 3.6. a Mesentericoaxial volvulus of the stomach (Courtesy of Dr. Carlo Buonomo, Boston, MA, USA); **b** Organoaxial volvulus; **c** Mesentericoaxial volvulus

pertechnetate scintigraphy. Functioning ectopic gastric mucosa was found in Meckel diverticulum in three patients, in small bowel duplications in four, in a gastric duplication in one and in intrathoracic foregut duplication cysts in three patients. They stress the importance of performing a dynamic and static sequence as well as delayed images (up to 24 h) since only the latter can document the presence of ectopic gastric mucosa in patients with intrathoracic duplication cysts; this is much later than the visualization of the stomach activity. In contrast, the tracer activity in ectopic gastric mucosa in intestinal duplication cysts may be seen before gastric tracer activity. The uptake of 99Tcm-pertechnetate in the ectopic gastric mucosa of Meckel diverticulum and gastric duplication is visualized simultaneously with the stomach (Fig. 3.7).

Meckel diverticulum is the most common congenital anomaly of the GI tract and is the most common site for ectopic gastric mucosa. GI duplications (non-communicating or more rarely communicating) are less common and 20%–30% of these will contain ectopic gastric mucosa. It is also more commonly seen in tubular duplications (in contrast to cystic).

Patients with functioning ectopic gastric mucosa will present with pain, bleeding and perforation. However, patients with intrathoracic foregut duplication cysts, mainly younger patients, will present with respiratory distress caused by compression of the airway.

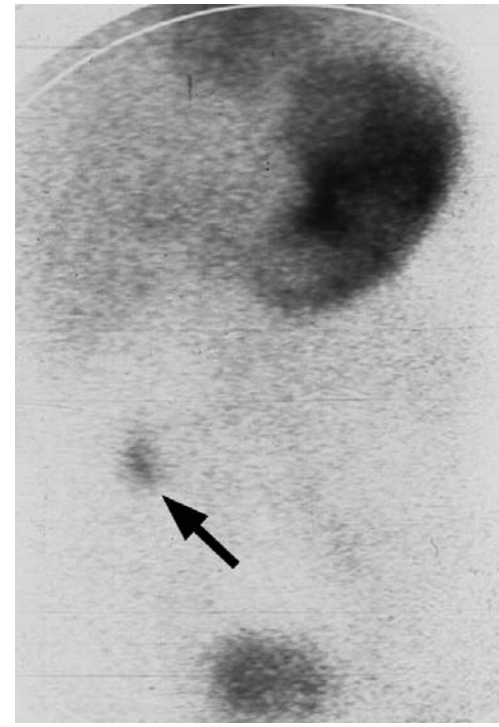

Fig. 3.7. A 2-year old boy with bright red blood per rectum and a normal UGI study: ectopic gastric muscosa (Meckel diverticulum) (*arrow*)

3.3.8 Ectopic Pancreatic Tissue

In this condition pancreatic tissue will be found in the antropyloric region or less frequently in the duodenum. It is usually asymptomatic, but these patients may present with pain, GI bleeding or obstruction due to ulceration, bleeding or inflammation (pancreatitis) or rarely malignant degeneration. On barium studies, a rounded filling defect can be noted in the antropyloric region with a central niche, representing an attempt at duct formation (Fig. 3.8). This entity can also be identified on US (Schlesinger and Parker 2003) or CT (Fig. 3.9a–c).

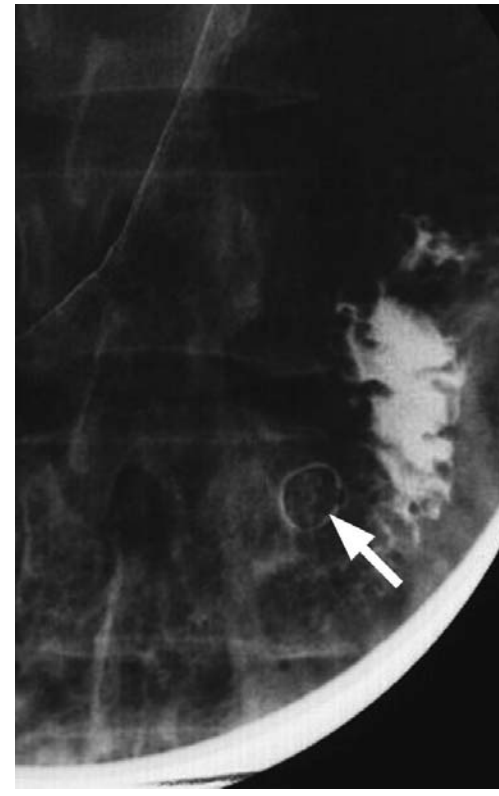

Fig. 3.8. Ectopic pancreatic tissue (*arrow*)

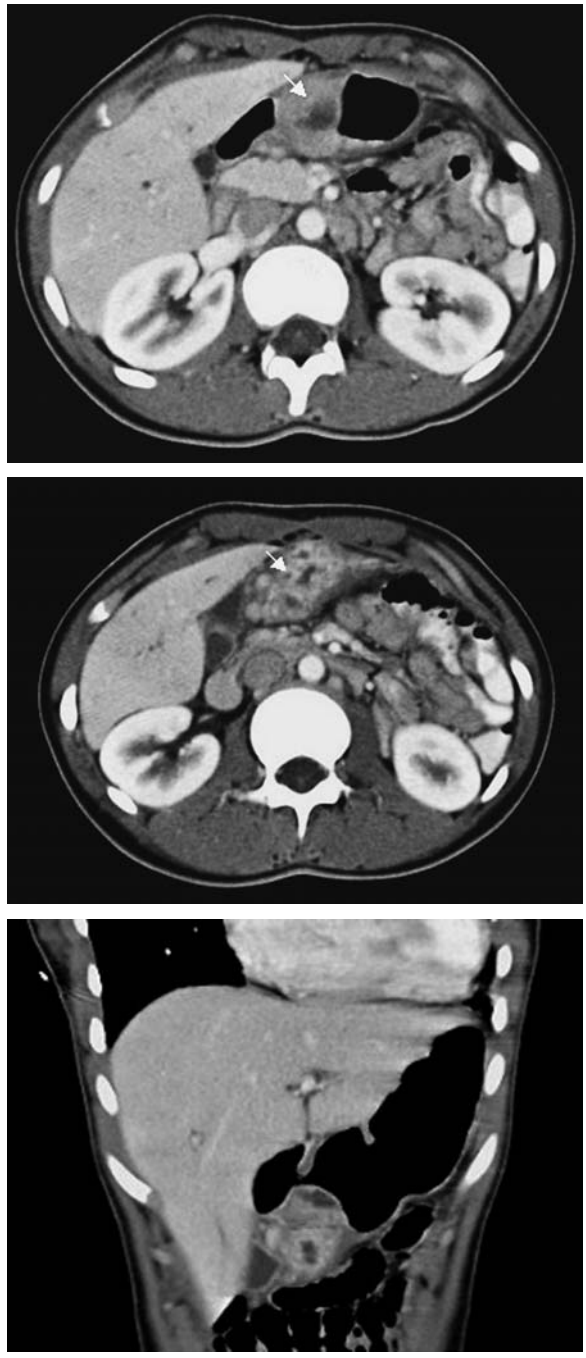

Fig. 3.9a–c. Contrast-enhanced CT showing pancreatitis in ectopic pancreatic tissue in the antropyloric region (*arrow*) causing an extrinsic mass on the greater curvature of the stomach in a 16-year-old girl. **a,b** Axial and **c** Coronal

3.4 Acquired Gastric Disorders

3.4.1 Hypertrophic Pyloric Stenosis (HPS)

Congenital hypertrophic pyloric stenosis is characterized by hypertrophy of the circular muscle layer and represents the most common cause of gastric outlet obstruction (Hernanz-Schulman 2003). Takahashi (2003) suggested that impaired neuronal nitric oxide synthase synthesis in the myenteric plexus is an important contributing factor in the pathogenesis of HPS as well as of achalasia, diabetic gastroparesis, Hirschsprung disease and Chagas disease.

Children usually present at the age of 3–6 weeks, but with a range from 1 week to 3 months. It is unusual in premature infants and older children. There is a definite male predominance and is also more commonly seen in firstborns in comparison with their younger siblings. The patient will typically present with increasing vomiting, leading to projectile vomiting. The vomitus is not bile stained since the obstruction is proximal to the ampulla of Vater.

The diagnosis can be made by physical examination by palpating the typical olive in the epigastrium. Peristaltic waves may also be seen on the abdominal wall.

An abdominal X-ray may be nonspecific or demonstrate a distended stomach with a small amount of air distally (Fig. 3.10). In some instances gastric pneumatosis can be seen, which resolves spontaneously after nasogastric tube placement in order to decompress the stomach. The imaging diagnosis using an upper GI study has been replaced by US in many countries worldwide, since US allows direct visualization of the hypertrophied muscle (Fig. 3.11). Typically, the patient is given water or a dextrose solution orally, and is subsequently placed in the right posterior oblique position. The left liver lobe can be used as an acoustic window to evaluate the pylorus in the supine position. The muscle thickness, as well as the muscle length, the pyloric channel length, the pyloric muscle index (calculated using pyloric length, pyloric muscle thickness and pyloric diameter) and the muscle volume have all been used as indicators of HPS (Westra et al. 1989). Overall the muscle thickness seems to be the most important criterion, with a muscle thickness equal

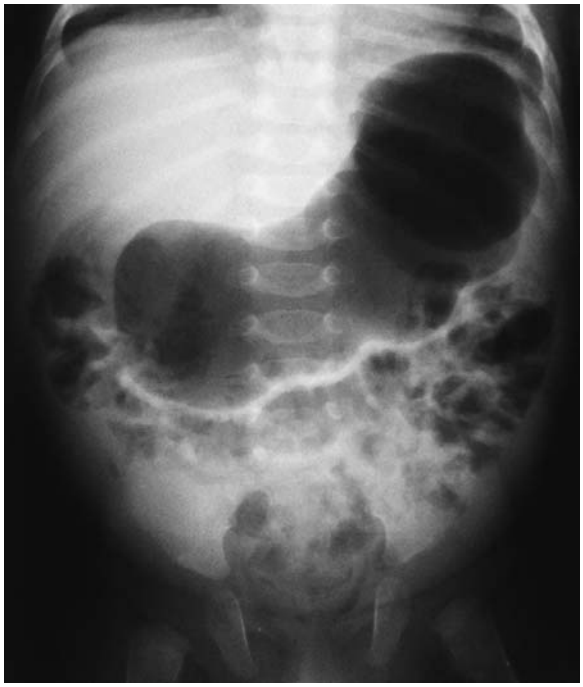

Fig. 3.10. Plain abdominal radiograph reveals a markedly distended stomach and hyperperistalsis. (Courtesy of Dr. Carlo Buonomo, Boston, MA, USA)

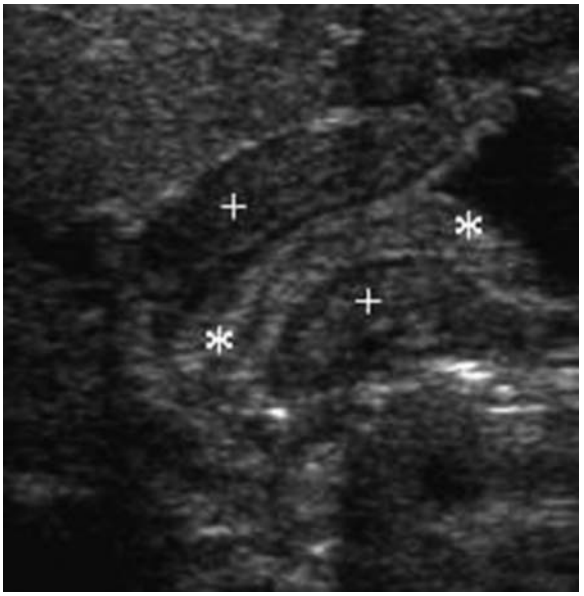

Fig. 3.11. US reveals an elongated pyloric channel (*asterisks*) and a thickened longtitudinal pyloric muscle (*crosses*). (Courtesy of Dr. Carlo Buonomo, Boston, MA, USA)

or greater than 3 mm, indicating HPS, and 2 mm or less, indicating a normal pylorus muscle. The channel length should be greater than 15 mm to support the diagnosis of HPS (Blumhagen et al. 1988).

The differential diagnosis includes pylorospasm (which may cause an increased muscle thickness, but only transiently), (eosinophilic) gastroenteritis, gastric and duodenal ulcers. If the US findings are not clearly diagnostic, an upper GI examination is next.

On a barium study almost all children will show some degree of pylorospasm, which may cause a delay as long as 20–25 min in the passage of barium through the antropyloric region. Classical findings on upper GI include: the "string" sign, consistent with a narrowing of the pyloric channel, is almost always seen in conjunction with an elongated and upward curved pyloric channel. The "double track/string" sign is caused by barium which is caught between folds overlying the hypertrophied muscle. A similar sign can be seen on US, without being pathognomonic for HPS since it can also be seen in patients with pylorospasm (Cohen et al. 2004). The "beak" sign is the result of the thickened muscle narrowing the barium column as it enters the pyloric channel. The thickened and enlarged muscle mass resembles an 'apple core lesion' with undercutting of the distal antrum and proximal duodenum. The "pyloric tit" can be seen along the lesser curvature of the stomach, just proximal to the impression of the pyloric mass and may be consistent with a blocked peristaltic wave. The "shoulder" sign is caused by impression of the hypertrophied muscle on the antrum. All of the above mentioned findings can also be seen transiently in normal children, therefore the study should be done carefully, with documentation of the persistence of these signs. The treatment of choice is pyloromyotomy, surgically or laparoscopically. However, some countries (Sweden, Japan) also have experience with nonsurgical therapy.

3.4.2 Peptic Ulcer Disease

There is important evidence to document the involvement of *Helicobacter pylori* as a causative agent of peptic ulcer disease, antral atrophic gastritis, gastric adenocarcinoma and gastric lymphoma (Konturek et al. 2006a,b). Although these diseases are much more common in adulthood, colonization with this pathogen occurs mostly during

childhood. Prevalence rates vary from almost 10% of children under the age of 10 years in industrialized countries to 56.8%–83.1% of children in the poorest Brazilian regions (Bittencourt et al. 2006). In theory, childhood is a good time to eradicate *H. pylori* because children are usually not infected long enough to develop gastric cancer (Bourke 2005). In this way, gastric cancers may be prevented. However, since prevalence and incidence of gastric cancer are decreasing rapidly in developed nations, screening programs would be extremely expensive. Only in high-risk areas or in families with a strong positive history, a test-and-treat strategy can be justified (Bourke 2005; Graham and Shiotani 2005).

Peptic ulcer disease is much less common in the pediatric population than in adulthood. The classification of peptic ulcers is based on the region of involvement (gastric versus duodenal ulcers) and on the presence or absence of a known etiology (primary or secondary due to an underlying disease). Primary peptic ulcers are associated with *H. pylori* infection. Gastric ulcers are mostly seen in neonates (with or without the development of gastric perforation) while duodenal ulcers are much more common after the neonatal period.

Drumm et al. (2004) demonstrated that single-contrast barium studies have a high false-negative rate for ulcer disease, when compared with endoscopy. Double contrast studies are indicated because of the higher sensitivity, but cannot be performed in young children and imply a higher radiation dose in all children. When perforation is suspected, however, a single contrast study with a low-osmolar nonionic contrast agent should be performed. As a general rule, endoscopy is the preferred method of choice in the diagnosis of peptic ulcers. It has the highest sensitivity and allows the collection of fragments from the gastric mucosa for diagnosis of the infection and for histopathological analysis (Bittencourt et al. 2006).

An ulcer will be visible on an upper GI study as a round or ovoid collection of barium with radiating folds, consistent with edema/inflammation of surrounding mucosa. On US, thickening of the antropyloric mucosa can be seen as well as elongation of the antropyloric canal, persistent spasm and delayed gastric emptying. US is not routinely used for the diagnosis of peptic ulcer disease. The presence or absence of intra-abdominal free air can be seen on an abdominal X-ray (upright, left lateral decubitus or with horizontal beam radiographs) in case of a gastric perforation (Fig. 3.12).

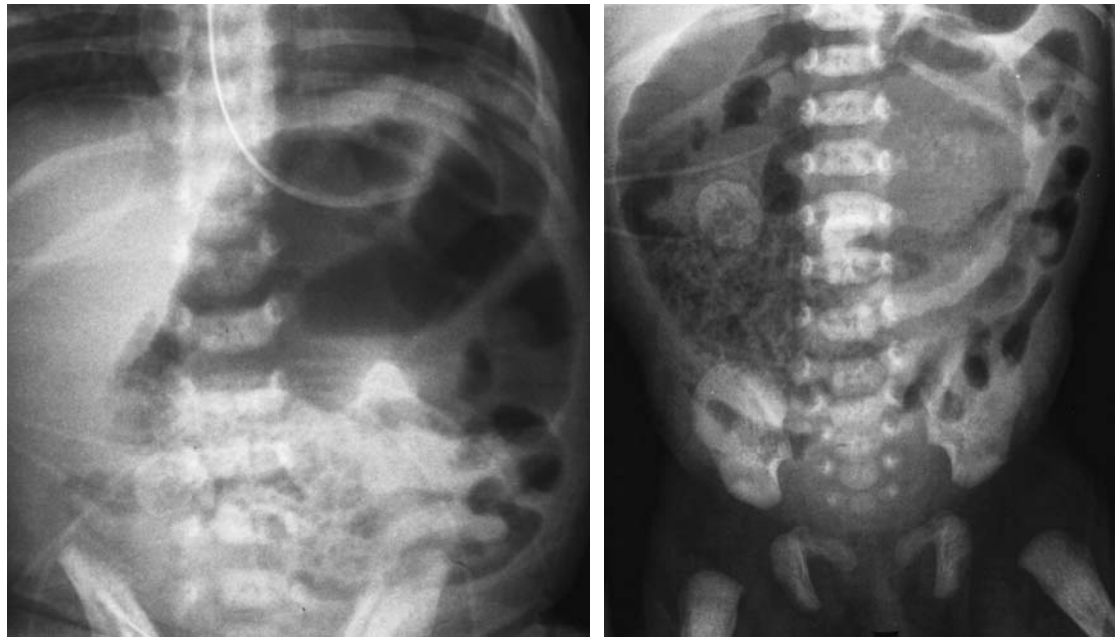

a **b**

Fig. 3.12. a Stress ulcer disease: free air supine. **b** Stress ulcer disease: supine radiograph reveals free air due to duodenal ulcer

3.4.3 Gastritis

3.4.3.1 Infectious Gastritis

H. pylori infection is well known as the causative agent of antral gastritis and peptic ulcer disease (see Sect. 3.4.2). On barium studies, the most frequent finding will be (markedly) thickened gastric folds, or even thickened and lobulated gastric folds can be seen.

AIDS patients can develop infectious gastritis, the most common including cytomegalovirus (CMV), *Toxoplasma gondii* and *Cryptosporidium*.

3.4.3.2 Caustic Ingestion with Chemical Gastritis

Ingestion of caustic agents may lead to severe damage of the gastrointestinal tract: the esophagus is more commonly involved, but also stomach and duodenum may be involved (Schlesinger and Parker 2003). Chemical esophagitis and/or gastritis can be caused by a variety of substances as there are strong alkaline agents (e.g. concentrated sodium hydroxide) which will typically affect the esophagus, while strong acid agents will affect the stomach (e.g. common are calcium chloride, zinc chloride, iron sulfate tablets and acids) although an overlap certainly exists where acids can cause esophagitis as well and vice versa. Chemical gastritis can vary from mild antral gastritis to extensive necrosis of the stomach, in which case it can be lethal. Patients will present with abdominal pain, vomiting, hematemesis, fever and shock.

Contrast studies can be done for the evaluation of chemical gastritis and imaging findings will depend on the time interval between the acute ingestion and the contrast study. During the acute necrotic phase (1–4 days after the event), contrast studies should be performed with caution. Free air should be excluded before the start of the study by abdominal X-ray, including upright, left lateral decubitus or horizontal-beam radiographs. If perforation is suspected, no barium should be used. Instead, low-osmolar nonionic contrast agents or water-soluble contrast are indicated. Thickened mucosal folds can be seen due to severe edema, ulceration, gastric atony or mural defects. Sometimes intramural air can be seen in the stomach of patients with severe gastric necrosis; this can be due to either mechanical disruption of the gastric wall or to surinfection by gas-forming organisms. In the former case, contrast leakage may be seen which is almost always confined; free leakage in the peritoneal cavity is rare.

At 5–28 days after the caustic ingestion, an ulceration-granulation phase will take place. At 3–4 weeks after the initial event, cicatrization and scarring will begin. Chemical gastritis can resolve with minor sequelae or it can heal with gastric wall calcifications with cicatricial constrictions several weeks after the ingestion (Schlesinger and Parker 2003). In this phase, barium can be used as a contrast agent (Fig. 3.13). Typically, the scarring will take place in the antrum or body antrum of the stomach since caustic agents tend to flow down the lesser curvature of the stomach into the antrum, causing severe pylorospasm that delays emptying into the duodenum. Therefore, the duodenum may be unaffected. In other patients, however, severe duodenal injury may have occurred and can be seen as thickened folds, spasm, atony and ulceration leading to scarring, fibrosis and stricture formation. Almost all of these patients will have associated gastric injury. Patients with chemical gastritis and/or duodenitis will typically develop a gastric outlet obstruction after 3–4 weeks due to the scarring and strictures (Levine 2000).

3.4.3.3 Ménétrier's Disease

Ménétrier's disease is a rare disorder in children and is probably different from the adult disease. It is typically self-limiting and may be caused by cytomegalovirus (Sferra et al. 1996; Kovacs et al. 1993; Eisenstatt et al. 1995).

Children will present with abdominal pain, nausea and vomiting. Also peripheral edema, ascites and pleural effusions are commonly associated with Ménétrier's disease due to an associated protein-losing enteropathy.

On barium studies of the upper gastrointestinal tract, markedly enlarged folds (rugae) are typically seen at the gastric fundus along the greater curvature (Fig. 3.14). US can also demonstrate the rugal hypertrophy with thickening of the mucosa. When the stomach is completely filled, however, these thickened folds will collapse. Typically high frequency (8–13 Mhz) linear transducers will be used. Serial US can be used in the follow-up of the disease. CT can also confirm these findings.

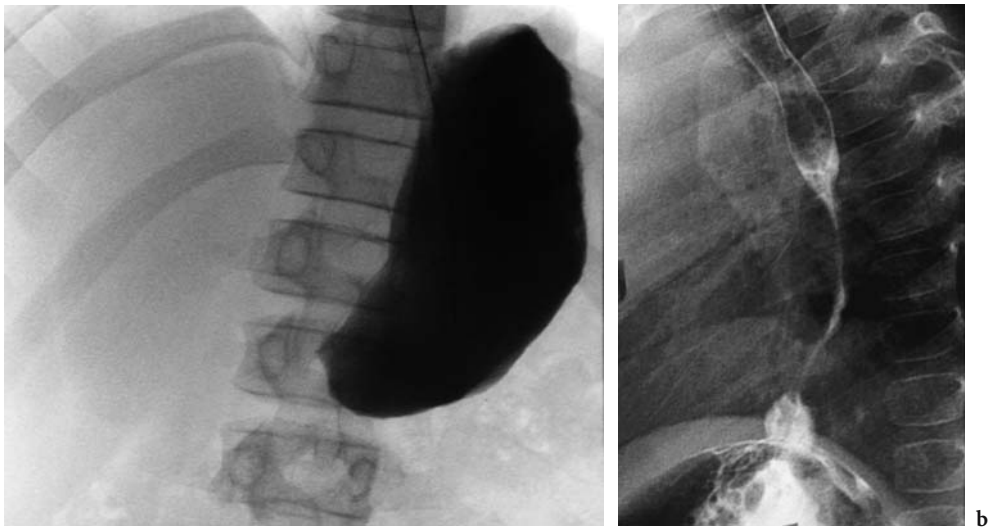

Fig. 3.13. a Caustic ingestion: gastric obstruction in a 9-year-old after drinking gasoline. **b** Esophageal stricture after alkaline ingestion in a 2-year-old

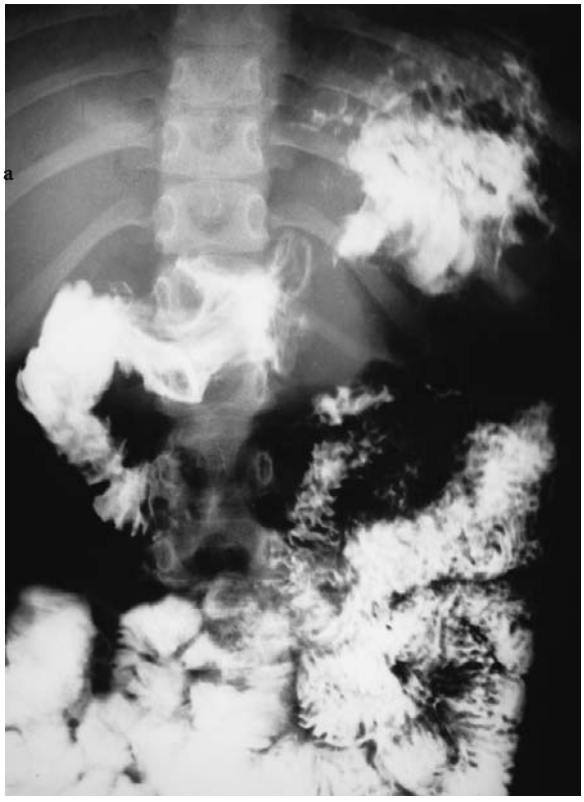

Fig. 3.14. Ménétrier's disease: Thickened gastric rugae with no detectable peristalsis in an 8-year-old boy

3.4.3.4 Eosinophilic Gastritis

Almost all patients with eosinophilic gastroenteritis have a peripheral eosinophilia. A history of allergy can be obtained in half of the patients. The stomach can be solely involved, but more commonly the small bowel also participates in the disease process. If patients only have eosinophilic gastritis, they present with epigastric pain, nausea and vomiting or hematemesis and/or melena, while patients with eosinophilic enteritis will have diarrhea, malabsorption or a protein-losing enteropathy.

On barium studies a strikingly nodular pattern in the gastric antrum can be seen with relative sparing of the body and fundus (Teele et al. 1979) (Fig. 3.15). Hummer-Ehret et al. (1998) reported that eosinophilic gastroenteritis could mimic hypertrophic pyloric stenosis on US.

3.4.3.5 Chronic Granulomatous Disease of Childhood (CGDC)

Chronic granulomatous disease results from an inability of phagocytic cells to produce bactericidal superoxide anions caused by a defect in the nicotinamide adenine dinucleotide phosphate (reduced form) oxidase enzyme of phagocytes. This leads to recurrent life-threatening bacterial and fungal infections. About two thirds of patients inherit

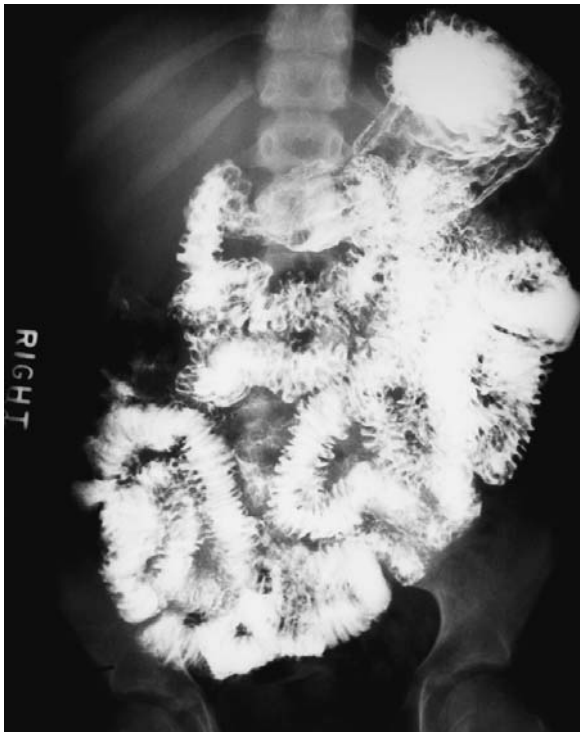

Fig. 3.15. Eosinophic gastritis: thickened mucosal folds and a suggestion of nodularity in a patient with diarrhea and eosinophilia. (Courtesy of Dr. Carlo Buonomo, Boston, MA, USA)

X-linked defects; one-third inherit this disease in autosomal recessive fashion. Over 75% of patients present during the first 5 years of life. The most commonly involved organs are those that serve as barriers against the entry of microorganisms from the environment (e.g. lymph nodes, lungs, skin, GI tract, skeleton, upper respiratory tract and central nervous system) (Movahedi et al. 2004; Garcia-Eulate et al. 2006).

Patients with GI tract involvement will present with abdominal pain (periumbilical or diffuse) with lower abdominal cramping, diarrhea with or without blood in the stool, nausea and vomiting, constipation growth delay or hypoalbuminemia (Marciano et al. 2004).

A barium study (Fig. 3.16) will demonstrate narrowing of the antropyloric region (occurring in up to 16% of patients) (Griscom et al. 1974) secondary to chronic inflammation and fibrosis, which can eventually lead to gastric outlet obstruction. In some cases, the proximal duodenum will also be involved. Ultrasound will also reveal a thickening of the antropyloric wall, simulating HPS. Most patients, however, will be older than the typical HPS patient.

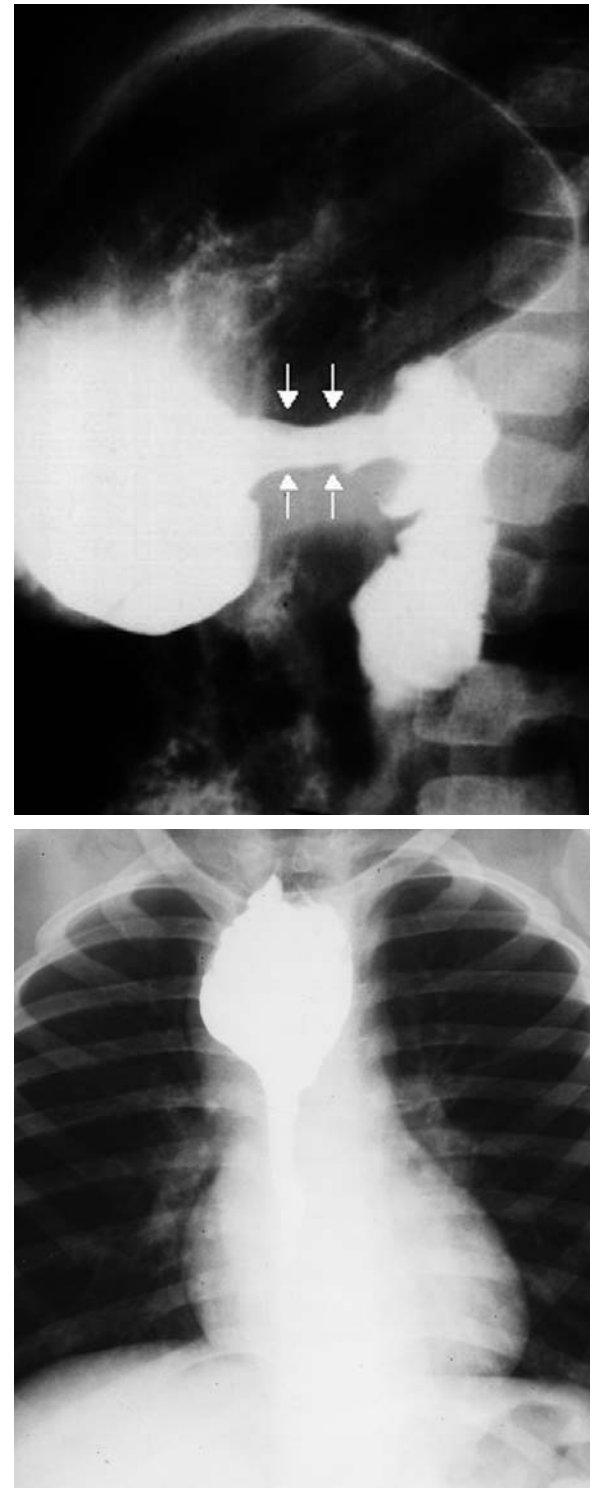

a

b

Fig. 3.16. a CGDC stomach. Antral narrowing in a 7-year-old with CGDC. **b** Mid-esophageal stenosis caused by enlarged lymph nodes in CGDC

3.4.3.6 Crohn Disease

Crohn disease of the upper GI tract is more common than previously thought. Several studies performed by different authors confirm these findings (Lenaerts et al. 1989; Cameron 1991; Mashako et al. 1989; Ruuska et al. 1994; Oberhuber et al. 1998).

Patients can be asymptomatic of the upper gastrointestinal tract involvement and can present with features of distal ileocolic Crohn disease (crampy abdominal pain, diarrhea) or they can present with weight loss, epigastric pain, recurrent vomiting or hematemesis and melena (Griffiths et al. 1989).

In the detection of Crohn disease of the upper GI tract, double contrast studies are classically used to detect the aphthae (a punctate collection of barium surrounded by a radiolucent halo of edema), which are typical for onset of the disease. Other findings include: larger ulcers, thickened folds, distorted, effaced or rarely cobblestoned mucosa, fistula and sinus tracts and formation of pseudodiverticula (Fig. 3.18b). Progressive antral narrowing will develop over the course of time due to scarring and fibrosis of the antrum, pylorus or duodenum. Contrast studies can also be replaced by upper endoscopy with biopsy, or MR (Godefroy et al. 2005; Castellaneta et al. 2004; Lemberg et al. 2005). US can also be used to follow Crohn disease in the terminal ileum and colon (Bremner et al. 2006), although no studies have yet been published to evaluate its use in the stomach and duodenum.

3.4.4 Gastric Perforation

Gastric rupture is mainly seen in neonates due to acute distention of the stomach, ischemic necrosis associated with perinatal asphyxia and distal obstruction such as annular pancreas (Ibach and Inouye 1965) or duodenal atresia/stenosis. On the other hand, duodenal rupture in neonates is rare.

Gastric perforation beyond infancy in the pediatric population is also rare. It can be seen in cases of iatrogenic trauma (tubes and catheters), after Nissen or other fundoplications in patients with distal small bowel instruction, after caustic ingestion or in patients with blunt trauma to a distended stomach. Gastric rupture can also be seen in patients with perforated peptic ulcer and dermatomyositis, although duodenal rupture is seen more frequently.

Abdominal X-ray will reveal free intraperitoneal air on upright or decubitus films (Fig. 3.12), no gastric air-fluid level can be demonstrated.

3.4.5 Bezoars

Bezoars consist of ingested materials that accumulate within the GI tract, most commonly the stomach. They are classified according to the composition of the ingested material: lactobezoar consisting of milk products; trichobezoar consisting of hair; and phytobezoar consisting of fruit and vegetable fibers. A trichobezoar is commonly seen in young females and sometimes an underlying psychiatric illness can be associated. Presenting symptoms may include nausea, emesis, epigastric pain and an epigastric mass.

Ulceration, bleeding, obstruction and perforation are the most common complications of bezoars (Sinzig et al. 1998); an intussusception may also be seen (Ben Cheikh et al. 2004).

Upper GI studies were the gold standard for the diagnosis of gastric bezoar in the past. This has now been replaced by US, CT or MR (Sinzig et al. 1998; Ben Cheikh et al. 2004; Ripollés et al. 2001).

On abdominal radiographs, a bezoar can be recognized as an area with a mottled gas appearance, which can be mistaken for an abdominal abscess or for feces in the colon (Ripollés et al. 2001). On US an intraluminal mass with a hyperechoic arc-like surface and a marked acoustic shadow can be detected, which must be differentiated from retained food products in the stomach. Small gastric bezoars are rounded or ovoid, tend to float and have lower density than food particles on CT. Large gastric bezoars fill the gastric lumen and will demonstrate multiple small air bubbles throughout the mass on CT. On MR a gastric bezoar is characterized by a very low signal intensity, similar to air, on T1- as well as T2-weighted sequences, which makes it difficult to diagnose on MR if it is not suspected. In most cases, giving water prior to the examination in order to enhance contrast in the stomach contents is not necessary (Ripollés et al. 2001).

In the evaluation of a gastric bezoar it is important to evaluate the extent of the disease as some patients will have multiple (other) intestinal locations.

3.4.6 Foreign Body Ingestion

Foreign body ingestion is not infrequently observed in children between the ages of 6 months and 3 years. Most objects will pass without problem, thus in many patients a conservative approach will be taken. In some, however, (immediate) removal is mandatory. Open safety pins, objects larger than 6 cm in the stomach (Welch et al. 1986) and button batteries (not because of their size but because of their content) need to be removed, as well as foreign bodies retained in the stomach or duodenum for more than 1 week.

A "mouth-to-anus" image is essential to find the foreign body, an en-face appearance in the neck of a small round coin proves that it is in the esophagus (Fig. 3.17a,b).

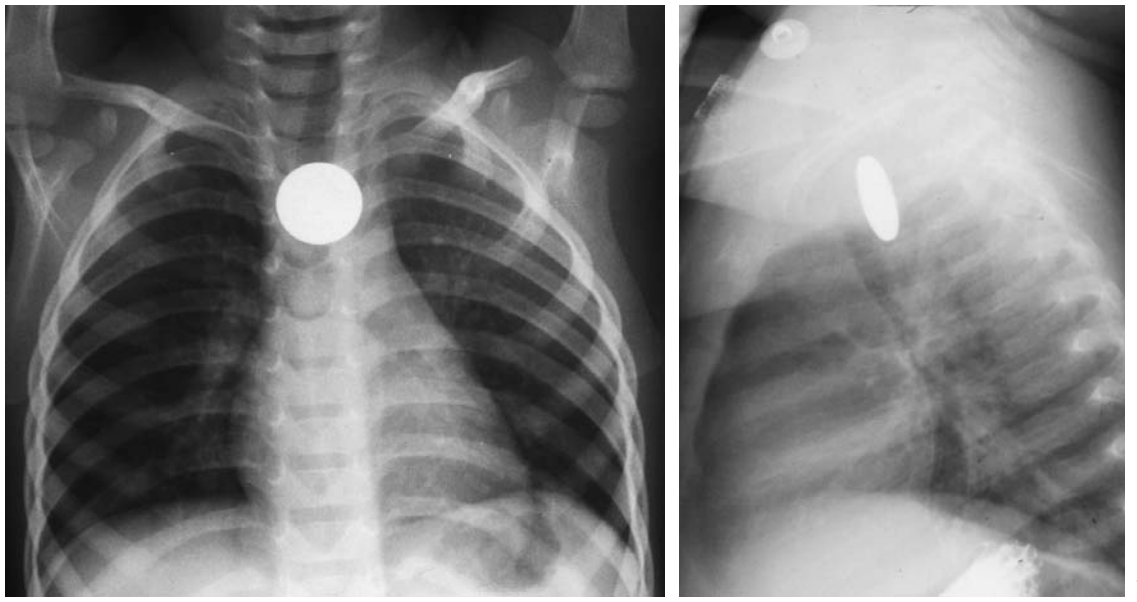

Fig. 3.17a,b. Coin en-face on AP radiograph, thus located in the esophagus as confirmed on the lateral view

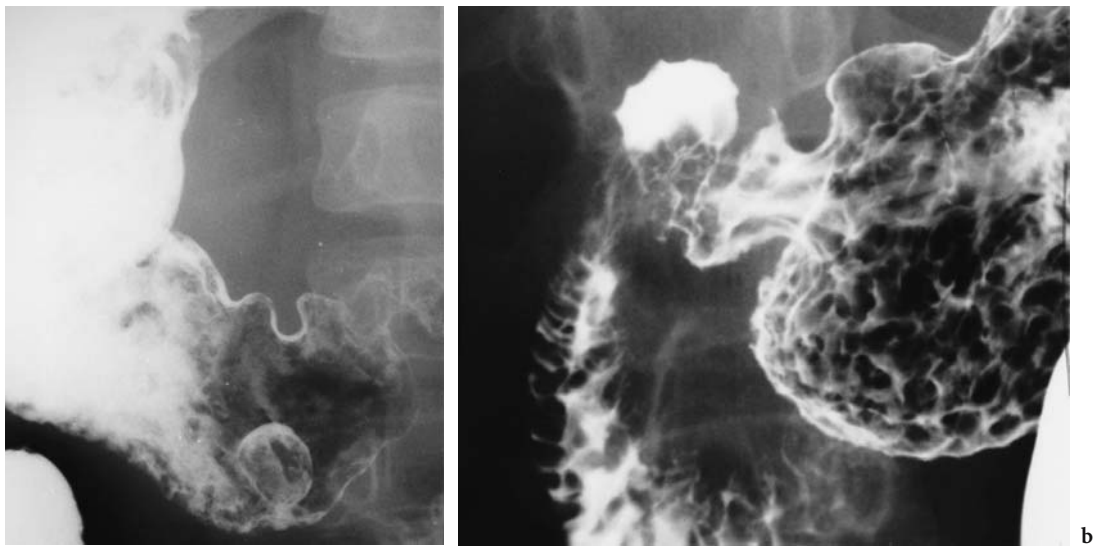

Fig. 3.18. a Juvenile polyposis: gastric polyps in a patient with peroral mucositis (Courtesy of Dr. Carlo Buonomo, Boston, MA, USA). **b** Gastritis/duodenitis in an 8-year-old eventually diagnosed with Crohn disease

3.4.7 Tumors and Tumor-Like Conditions

3.4.7.1 Gastric Polyps

3.4.7.1.1 Familial Adenomatous Polyposis Syndrome (FAPS)

This syndrome is caused by the presence of an abnormal tumor suppressor gene (APC gene) on chromosome 5 and it includes Gardner syndrome (previously known as familial polyposis coli). More than 50% of these patients will have gastric involvement. Two different types of polyps have been recognized: the fundic gland (hamartomatous) polyp and adenoma. The former are mostly multiple and appear as small, sessile lesions ranging from 1–5 mm in size in the fundus and body of the stomach (Fig. 3.22). There is generally no association with chronic nonspecific gastritis and these lesions are not precancerous. On the other hand, adenomas are pre-malignant lesions. The radiographic appearance is similar, but gastric adenomas are located in the antrum and are multiple in over half of the cases (Buck and Harned 2000).

3.4.7.1.2 Hamartomatous Polyposis Syndrome

These syndromes are not as common as FAPS and include Peutz-Jeghers syndrome, multiple hamartoma syndrome (Cowden disease), juvenile polyposis (Fig. 3.18a), Cronkhite-Canada syndrome and Bannayna-Riley-Ruvalcaba syndrome.

Patients with Peutz-Jeghers syndrome have a unique type of gastrointestinal hamartoma, which can be found on barium studies throughout the alimentary tract from the stomach to the rectum, but mostly in the jejunum and ileum (followed by duodenum, colon and stomach). The polyps vary in size, may be sessile or pedunculated and have a lobulated surface (larger lesions), tending to occur in clusters. Clinically, these patients will present with abdominal pain due to intussusception of one of the polyps; less frequently they will present with GI bleeding. These patients are at increased risk of developing adenocarcinoma of the gastrointestinal tract (majority located in the stomach, duodenum and colon) (Peutz 1921).

3.4.7.1.3 Other Gastric Polyps

Gastric polyps and nodules can be seen in children receiving long-term omeprazole therapy. Pashankar and Israel (2002) suggested in their study of 31 pediatric patients that there is an association rather than a coincidental relationship between these two entities.

Other gastric polyps in children include inflammatory fibroid polyp, solitary hyperplastic polyp and polypoid focal foveolar hyperplasia (Teele and Share 2000).

3.4.7.2 Gastric Lymphoma

GI tumors represent no more than 5% of all malignancies in children (Sasaki et al. 1999). Most frequently, GI malignancy in children is a lympma or sarcoma (Kurugoglu et al. 2002). The majority of primary gastric lymphomas (Fig. 3.19, 3.20a,b) are high-grade non-Hodgkin lymphomas of B-cell origin. A notable number, however, are low-grade B-cell lymphomas that are derived from mucosa-associated lymphoid tissue (MALT) that is not found in the stomach. *H. pylori* infection triggers the development of MALT in the stomach and is the prerequisite in the development of MALT lymphoma. Primary Burkitt lymphoma of the stomach is very rare (Moschovi et al. 2003).

Patients will present with non-specific signs and symptoms. On US a hypoechoic thickening of the gastric wall or a mural mass can be seen. The presence or absence of adenopathy can also be evaluated. CT is used in the initial staging and is able to evaluate the extension of the primary tumor with or without invasion of adjacent structures as well as the coexistence of enlarged lymph nodes. On barium studies, mucosal nodularity, rugal thickening, shallow and/or deep ulceration(s), mass formation or diffusely enlarged area gastricae can be seen as solitary findings or as a combination of the above mentioned observations.

3.4.7.3 Gastric Gastrointestinal Stromal Tumor (GIST)

GISTs are rare in children with a broad spectrum varying from benign to malignant tumors. Miettinen et al. (2005) suggested in their study including 44 patients that the pathogenesis of gas-

tric GISTs may differ from that of adults because no KIT or PDGFRA mutations could be found. They also report that these tumors are often found in the antrum and have a somewhat unpredictable but slow course of disease. The patients usually presented with anemia due to chronic insidious GI blood loss, abdominal pain or a palpable mass (Egloff et al. 2005). On imaging studies, a GIST will present as a well-defined solid or partially cystic mass; sometimes hemorrhage, necrosis or calcification (extensive or in a mottled pattern) can be seen. Mucosal alteration, intracavitary air-fluid levels and fistulas to the alimentary tract have been described (Fig. 3.21a,b).

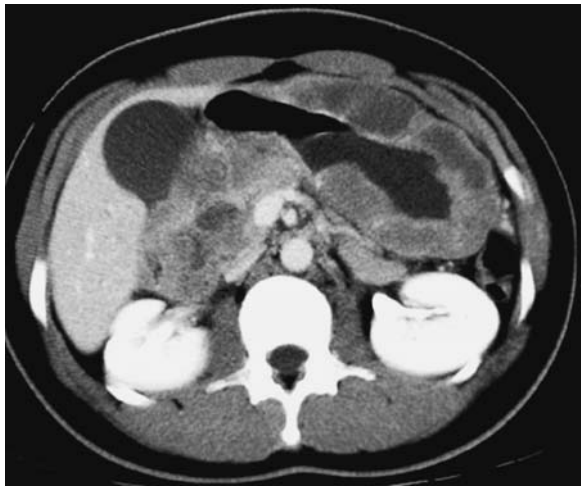

Fig. 3.19. NHL of the stomach and descending duodenum. (Courtesy of Dr. Carlo Buonomo, Boston, MA, USA)

3.4.7.4 Gastric Adenocarcinoma

Primary gastric adenocarcinoma is extremely rare in children; it represents only 0.05% of all malignant pediatric gastrointestinal tumors (Sasaki et al. 1999). Nearly 10% of all gastric cancers will present in patients younger than 41 years (Kokkola and Sipponen 2001). There are three different forms of presentation in the pediatric population: de novo, as part of a polyposis syndrome (e.g. Peutz-Jeghers syndrome as mentioned above) and following treatment of a gastric lymphoma (Dokucu et al. 2005). The prognosis of these patients is very compromised, as described by Dokucu et al. (2005) and Reut et al. (2001).

On upper GI series, loss of distensibility, distortion of the normal surface pattern of the stomach with thickened irregular folds and mucosal nodularity or irregular narrowing with or without ulceration (the ulcer is located intraluminally in contrast to a benign ulcer which is located beyond the expected border of the stomach) can be seen anywhere in the stomach (Fig. 3.22).

CT will be used for staging purposes to assess lymphadenopathy and to assess invasion of adjacent organs.

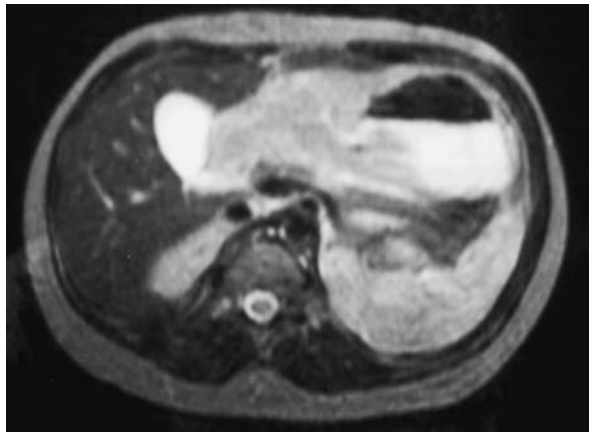

a

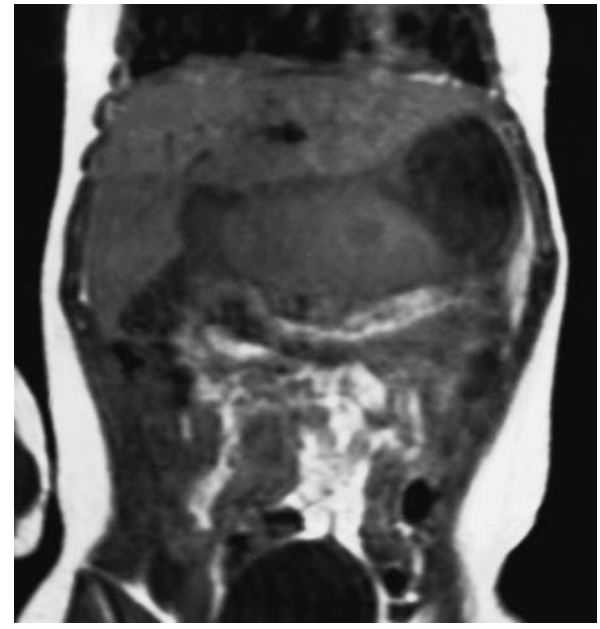

b

Fig. 3.20. a A predominantly antral lesion in a 6-year-old with NHL on this T2-weighted axial image. **b** A predominantly antral lesion in a a 6-year-old with NHL on this T1-weighted coronal image. (Courtesy of Dr. Carlo Buonomo, Boston, MA, USA)

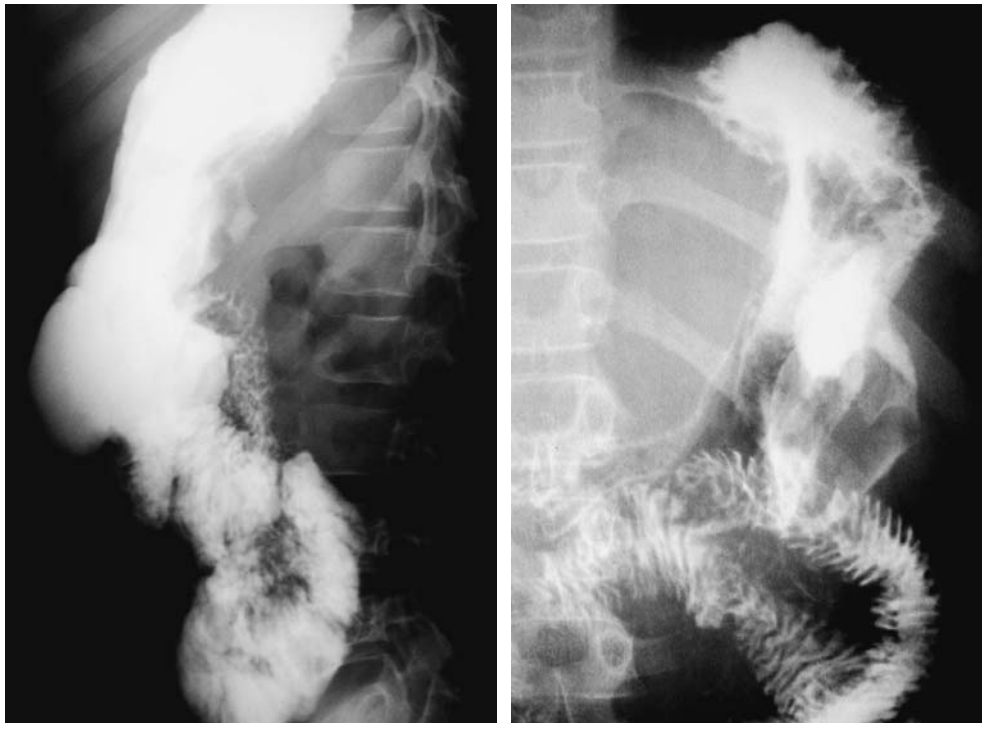

Fig. 3.21. a B-cell lymphoma of the stomach on upper GI. **b** B-cell lymphoma of the stomach in a 12-year-old. (Courtesy of Dr. Carlo Buonomo, Boston, MA, USA)

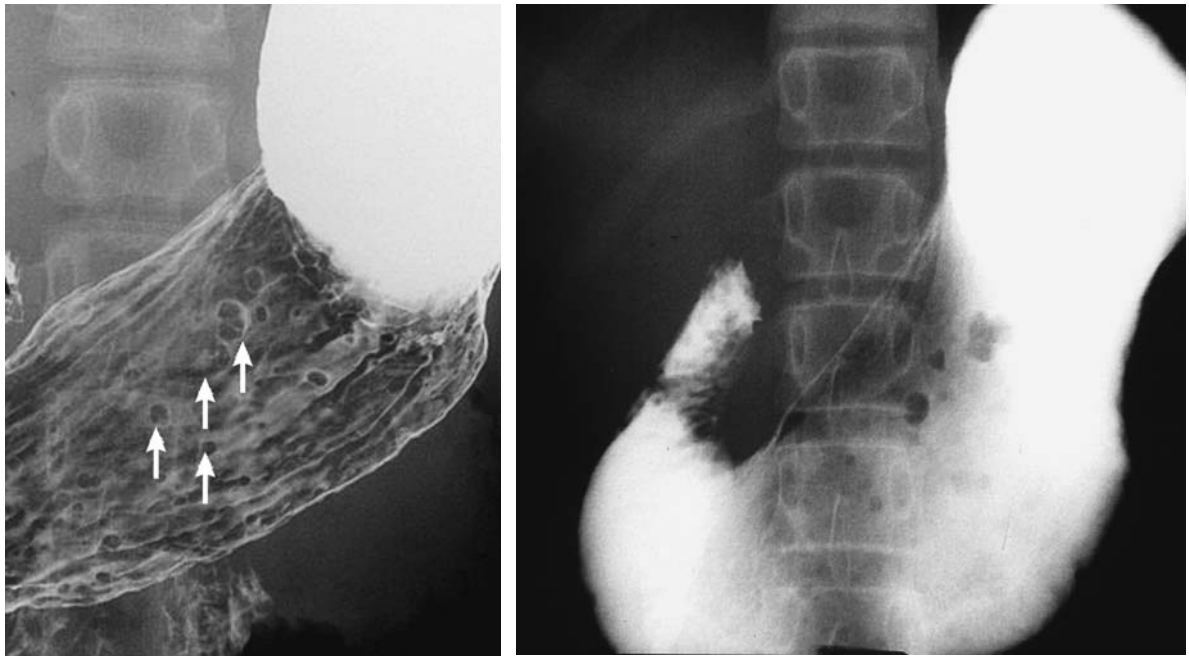

Fig. 3.22. a Multiple polyps (*arrows*) in Peutz-Jeghers with malignant degeneration (adenocarcinoma). **b** This 12-year-old had a giant osteoma in the left frontal sinus: Gardner syndrome

3.4.7.5 Gastric Teratoma

Gastric teratoma is an extremely rare gastric tumor, comprising less than 1% of all teratomas in children (Chandrasekharam et al. 2000). They typically occur in infancy (during the first year of life), most commonly in boys. The patients will present with an upper abdominal mass with evidence of proximal GI obstruction or GI hemorrhage. The therapy of choice should be resection. It has an excellent prognosis as described in a series of seven patients by Wakhlu and Wakhlu (2002).

Abdominal X-ray may reveal calcifications within a mass that displaces the stomach. CT is superior as it can better demonstrate the anatomical relationships with the surrounding organs and suggest the diagnosis.

3.4.7.6 Gastric Inflammatory Pseudotumor

This entity can simulate a malignant tumor on radiographic studies and should be considered in children with other unusual problems such as retroperitoneal fibrosis, sclerosing cholangitis or in patients with Castleman's syndrome. It should be added to the differential diagnosis when a gastric mass contains an ulcer or confined perforation.

3.4.8 Varices

Patients with portal hypertension will develop collateral pathways over time. Esophageal varices are very common, but gastric varices may also be observed (Schlesinger and Parker 2003; Itha and Yachha 2006).

Barium studies will reveal serpentine filling defects, which are compressible, typically in the fundus and along the lesser curvature or less commonly in the antrum of the stomach or proximal duodenum. US and CT can directly demonstrate the different collaterals.

3.4.9 Gastrostomy

Percutaneous gastrostomy is a well-accepted, widely performed procedure in three main groups

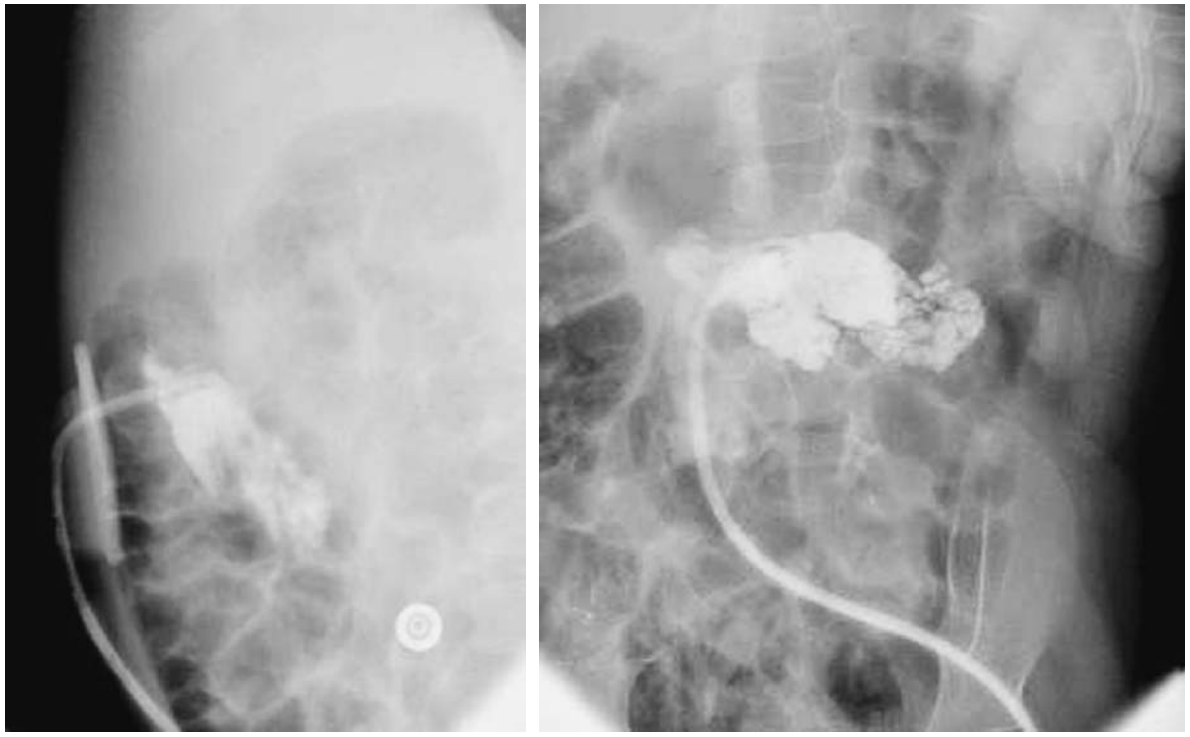

a b

Fig. 3.23a,b. A misplaced gastrostomy catheter, with contrast agent spillage into the peritoneal cavity

of patients. The first group includes children with anatomic disorders of the proximal upper GI tract, including mouth, pharynx and esophagus, in which normal feeding is not possible. The second group consists of neurologically impaired children where normal swallowing is not possible or safe. The third group consists of patients who need more nutrition than normal feeding allows.

Imaging may be performed if a complication is suspected, such as duodenal obstruction by balloon, leakage around the gastrostomy tube, malposition of the gastrostomy tube (Fig. 3.23), gastrocolic and gastrojejunal fistula and duodenal hematoma. In most cases, water-soluble contrast agents or non-ionic low-osmolar contrast agents will be used, while barium should be used, if at all, with caution (van Rijn et al. 2006).

3.4.10 Post-Operative Appearances of Stomach

One of the most commonly performed procedures on the stomach in children is pyloromyotomy for hypertrophic pyloric stenosis. Barium study findings will depend on the time interval between the surgical procedure and barium study. In the immediate postoperative setting, the radiographic findings will be the same as discussed above in the preoperative setting. Gradually this will change over time with the persistence of asymmetry of the pyloric channel. However, after 6 weeks, the pyloric channel will appear normal again in most patients, although some patients will continue to have a degree of antropyloric dysfunction (which even may occasionally lead to the retention of foreign bodies) (Bramson et al. 1994).

Another frequently performed surgical procedure in the pediatric population is antireflux surgery or the Nissen fundoplication. Post-operative imaging is focussed on demonstrating normal antegrade flow and the cuff or "pseudotumor" (Fig. 3.24), its slippage leading to recurrence of gastroesophageal reflux.

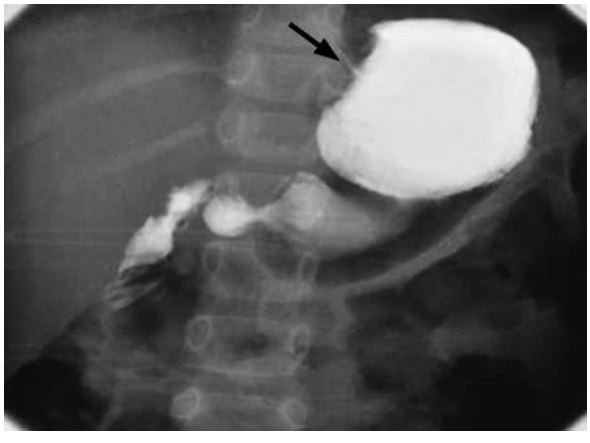

Fig. 3.24. Typical appearance of a Nissen fundoplication (*arrow*)

References

Anagnostara A, Koumanidou C, Vakaki M, Manoli E, Kakavakis K (2003) Chronic gastric volvulus and hypertrophic pyloric stenosis in an infant. J Clin Ultrasound 31:383–386

Barlev DM, Weinberg G (2004) Acute gastro-intestinal hemorrhage in infancy from gastric duplication: imaging findings. Emerg Radiol 10:204–206

Ben Cheikh A, Gorincour G, Dugougeat-Pilleul F, Duipuis S, Basset T, Pracros JP (2004) Trichobézoard gastrique révélé par une anémie chez une adolescente: association échograpie-imagerie par résonance magnétique (IRM). J Radiol 85:411–413

Berrocal T, Lamas M, Gutieerrez J, Torres I, Prieto C, del Hoyo ML (1999) Congenital anomalies of the small intestine, colon and rectum. Radiographics 19:1219–1236

Bittencourt PF, Rocha GA, Penna FJ, Queiroz DM (2006) Gastroduodenal peptic ulcer and Helicobacter pylori infection in children and adolescents. J Pediatr (Rio J) 82:325–334

Blank E, Chisholm AJ (1973) Congenital microgastria; a case report with a 26-year follow-up. Pediatrics 51:1037–1041

Blumhagen JD, Maclin L, Krauter D, Rosenbaum DM, Weinberger E (1988) Sonographic diagnosis of hypertrophic pyloric stenosis. AJR Am J Roentgenol 150:1367–1370

Bourke B (2005) Will treatment of Helicobacter pylori infection in childhood alter the risk of developing gastric cancer? Can J Gastroenterol 19:409–411

Bramson RT, Buonomo C, Blickman JG (1994) Barium extravasation discovered some years after pyloromyotomy. Pediatr Radiol 24:216–217

Bremner AR, Griffiths M, Argent JD, Fairhurst JJ, Beattie RM (2006) Sonographic evaluation of inflammatory bowel disease: a prospective, blinded, comparative study. Pediatr Radiol 36:947–953

Buck JL, Harned KH (2000) Polyposis syndromes. In: Textbook of gastrointestinal radiology, 2nd edn. WB Saunders Company, Philadelphia, pp 1075–1088

Buonomo C, Taylor GA, Share JC, Kirks DR (1998) Specific abnormalities of the abdomen. In: Kirks DR, Griscom NT (eds) Practical pediatric imaging: diagnostic radiology of infants and children, 3rd edn. Lippincott-Raven, Philadelphia, pp 838–953

Cameron DJ (1991) Upper and lower gastrointestinal endoscopy in children and adolescents with Crohn's disease: a prospective study. J Gastroenterol Hepatol 6:355–358

Castellaneta SP, Afzal NA, Greenberg M, Deere H, Davies S, Murch SH, Walker-Smith JA, Thomson M, Srivistrava A (2004) Diagnostic role of upper gastrointestinal endoscopy in pediatric inflammatory bowel disease. J Pediatr Gastroenterol Nutr 39:257–261

Chandrasekharam VV, Gupta AK, Bhatnagar V (2000) Infantile gastric teratoma. Trop Gastroenterol 21:192–193

Chen CP, Liu YP, Hsu CY, Lin SP, Wang W (2006) Prenatal sonography and magnetic resonance imaging of pulmonary sequestration associated with a gastric duplication cyst. Prenat Diagn 26:483–491

Cohen HL, Blumer SL, Zucconi WB (2004) The sonographic double-track sign: not pathognomonic for hypertrophic pyloric stenosis; can be seen in pylorospasm. J Ultrasound Med 23:641–646

Cunniff C, Williamson-Kruse L, Olney AH (1993) Congenital microgastria and limb reduction defects. Pediatrics 91:1192–1194

Dalgaard JB (1952) Volvulus of the stomach. Acta Clin Scand 103:131–136

Darani A, Mendoza-Sagaon M, Reinberg O (2005) Gastric volvulus in children. J Ped Surg 40:855–858

Dide M (1894) Sur en estomac d'adulte a type foetal. Bull Soc Anat (Paris) 69:669

Dokucu AU, Özturk H, Kilinç N, Önen A, Bukte Y, Soker M (2002) Primary gastric adenocarcinoma in a 2.5-year-old girl. Gastric Cancer 5:237–239

Drumm B, Day AS, Gold B, Gottrand F, Kato S, Kawakami E, Madrazo A, Snyder J, Thomas J (European Society for Paediatric Gastroenterology, Hepatology and Nutrition) (2004) Helicobacter pylori and peptic ulcer: Working Group Report of the second World Congress of Pediatric Gastroenterology, Hepatology, and Nutrition. J Pediatr Gastroenterol Nutr 39[Suppl 2]:S626–631

Egloff A, Lee EY, Dillon JE (2005) Gastrointestinal stromal tumor of stomach in pediatric patient. Pediatr Radiol 35:728–729

Eisenstat DD, Griffiths AM, Cutz E, Petric M, Drumm B (1995) Acute cytomegalovirus infection in a child with Menetrier's disease. Gastroenterology 109:592–595

Elliot S, Sander AD, Meekan JJ, Lawrence JP (2006) Surgical treatment of a gastric diverticulum in an adolescent. J Ped Surg 41:1467–1469

Garcia-Eulate R, Hussain N, Heller T, Kleiner D, Malech H, Holland D, Choyke PJ (2006) CT and MRI of hepatic abscess in patients with chronic granulomatous disease. AJR Am J Roentgenol 187:482–490

Giurgea I, Raqbi F, Nihoul-Fekete C, Couly G, Abadie V (2000) Congenital microgastria with Pierre Robin sequence and partial trismus. Clin Dysmorphol 9:307–308

Godefroy C, Pilleul F, Dugougeat F, Yzebe D, Lachaux A, Pracros JP, Valette PJ (2005) Value of contrast enhanced MR enterography in pediatric Crohn disease. J Radiol 86:1685–1692

Graham DY, Shiotani A (2005) The time to eradicate gastric cancer is now. Gut 54:735–738

Granata C, Dell'Acqua A, Lituania M, Oddone M, Rossi U, Toma P (2003) Gastric duplication cyst: appearance on prenatal US and MRI. Pediatr Radiol 33:148–149

Griffiths AM, Alemayehu E, Sherman P (1989) Clinical features of gastroduodenal Crohn's disease in adolescents. J Pediatr Gastroenterol Nutr 8:166–171

Griscom NT, Kirkpatrick JA Jr, Girdany BR, Berdon WE, Grand RJ, Mackie GG (1974) Gastric antral narrowing in chronic granulomatous disease of childhood. Pediatrics 54:456–460

Gupta AK, Guglani B (2005) Imaging of congenital anomalies of the gastrointestinal tract. Indian J Ped 72:403–414

Hernanz-Schulman M (2003) Infantile hypertrophic pyloric stenosis. Radiology 227:319–331

Herniaz Driever P, Gohlich Ratmann G, Konig R (1997) Congenital microgastria, growth hormone deficiency and diabetes insipidus. Eur J Pediatr 156:37–40

Hoehner JC, Kimura K, Soper RT (1994) Congenital microgastria. J Pediatr Surg 29:1591–1593

Hummer-Ehret Bh, Rohrschneider WK, Oleszczuk-Raschke K, Darge K, Nutzenadel W, Troger J (1998) Eosinophilic gastroenteritis mimicking hypertrophic pyloric stenosis. Pediatr Radiol 28:711–713

Ibach JR, Inouye WY (1965) Neonatal gastric perforation secondary to annular pancreas. Am J Surg 110:985–987

Itha S, Yachha SK (2006) Endoscopic outcome beyond esophageal variceal eradication in children with extrahepatic portal venous obstruction. J Ped Gastroenterol Nutr 42:196–200

Kokkola A, Sipponen P (2001) Gastric carcinoma in young adults. Hepatogastroenterology 48:1552–1555

Konturek PC, Konturek SJ, Brzozowski T (2006a) Gastric cancer and Helicobacter pylori infection. J Physiol Pharmacol. 57[Suppl 3]:51–65

Konturek SJ, Konturek PC, Konturek JW, Plonka M, Czesnikiewicz-Guzik M, Brzozowski T, Bielanski W (2006b) Helicobacter pylori and its involvement in gastritis and peptic ulcer formation. J Physiol Pharmacol 57[Suppl 3]:29–50

Kovacs AA, Churchill MA, Wood D, Mascola L, Zaia JA (1993) Molecular and epidemiologic evaluations of a cluster of cases of Menetrier's disease associated with cytomegalovirus. Pediatr Infect Dis J 12:1011–1014

Kroes EJ, Festen C (1998) Congenital microgastria: a case report and review of the literature. Pediatr Surg Int 13:416–418

Kumar R, Tripathi M, Chandrashekar N, Agarwala S, Kumar A, Dasan JB, Malhotra A (2005) Diagnosis of ectopic gastric mucosa using 99Tc m-pertechnetate: spectrum of scintigraphic findings. Br J Radiol 78:714–720

Kurugoglu S, Mihmanli I, Celkan T, Aki H, Aksoy H, Korman U (2002) Radiological features in paediatric primary gastric MALT lymphoma and association with Helicobacter pylori. Pediatr Radiol 32:82–87

Larsen WJ (2001) Development of the gastrointestinal tract. In: Larsen WJ (ed) Human embryology, 3rd edn. Churchill Livingstone, Philadelphia, pp 235–264

Lemberg DA, Clarkson CM, Bohae TD, Day AS (2005) Role of esophagogastroduodenoscopy in the initial assessment of children with inflammatory bowel disease. J Gastroenterol Hepatol 20:1696–1700

Lenaerts C, Roy CC, Vaillancourt M, Weber AM, Morin CL, Seidman E (1989) High incidence of upper gastrointestinal tract involvement in children with Crohn disease. Pediatrics 83:777–781

Levine MS (2000) Inflammatory conditions of the stomach and duodenum. In: Textbook of gastrointestinal radiology, 2nd edn, vol. 1. Gore and Levine. WB Saunders Company, pp 546–574

Lin CH, Wu SF, Lin WC, Chen AC (2005) Wandering spleen with torsion and gastric volvulus. J Formos Med Assoc 104:755–758

Marciano BE, Rosenzweig SD, Kleiner DE (2004) Gastrointestinal involvement in chronic granulomatous disease. Pediatrics 114:462–468

Mashako MN, Cezard JP, Navarro J, Mougenot JF, Sonsino E, Gargouri A, Maherzi A (1989) Crohn's disease lesions in the upper gastrointestinal tract: correlation between clinical, radiological, endoscopic and histological features in adolescents and children. J Pediatr Gastroenterol 8:442–446

Menon P, Rao KLN, Cutinha HP, Thapa BR, Nagi B (2003) Gastric augmentation in isolated congenital microgastria. J Ped Surg 38:4–6

Miettinen M, Lasota J, Sobin L (2005) Gastrointestinal stromal tumors of the stomach in children and young adults: a clinicopathologic, immunohistochemical, and molecular genetic study of 44 cases with long-term follow-up and review of the literature. Am J Surg Path 29:1373–1381

Moschovi M, Menegas D, Stefanaki K, Van-Vliet Constantinidou C, Tzortzatou-Stathopoulou F (2003) Primary gastric Burkitt lymphoma in childhood: associated with Helicobacter pylori? Med Pediatr Oncol 41:444–447

Moulton SL, Bouvet M, Lynch FP (1994) Congenital microgastria in a premature infant. J Pediatr Surg 29:1594–1595

Movahedi M, Aghamohammadi A, Rezaei N, Shahnavav N, Jandaghi AB, Farhoudi A, Pourpak Z, Moin M, Gharagozlou M, Mansouri D (2004) Chronic granulomatous disease: a clinical survey of 41 patients form the Iranian primary immunodeficiency registry. Int Arch Allergy Immunol 134:253–259

Oberhuber G, Hirsch M, Stolte M (1998) High incidence of upper gastrointestinal tract involvement in Crohn's disease. Virchows Arch 432:49–52

Oltman H (1899) Inaugural discussion. Kiel

Pashankar DS, Israel DM (2002) Gastric polyps and nodules in children receiving long-term omeprazole therapy. J Ped Gastroenterol Nutr 35:658–662

Peutz JLA (1921) Very remarkable case of polyposis of mucous membrane of intestinal tract and nasal pharynx. Ned. Maandschrift Geneesk 10(134)

Poki HD, Holland AJ, Pitkin J (2005) Double bubble, dubble trouble. Ped Surg Int 21:428–431

Pruksapong C, Donovan RJ, Pinit A, Heldrich FJ (1979) Gastric duplication. J Pediatr Surg 14:83–85

Rathaus V, Grunebaum M, Ziv N, Kornreich L, Horev G (1992) The bubble sign in the gasless abdomen of the newborn. Pediatr Radiol 22:106–109

Reut J, Russell JC, Weiss R, Leonard E, Gillan E, Krugman D (2001) Adenocarcinoma of the stomach in an adolescent presenting as pneumoperitoneum: a brief report. Conn Med 65:131–133

Ripollés T, Garcia-Aguayo J, Martinez, MJ, Gil P (2001) Gastrointestinal bezoars: sonographic and CT characteristics. AJR Am J Roentgenol 177:65–69

Ross MH, Romrell LJ (1989) Digestive system II: esophagus and gastrointestinal tract. In: Ross MH, Romrell LJ (eds) Histology. A text and atlas, 2nd edn. Williams and Wilkins, Baltimore, pp 421–470

Ruuska T, Vaajalahti P, Arajarvi P, Maki M (1994) Prospective evaluation of upper gastrointestinal mucosal lesions in children with ulcerative colitis and Crohn's disease. J Pediatr Gastroenterol Nutr 19:181–186

Ryan DP, Muehrcke DD, Doody DP, Kim SH, Donahoe PK (1991) Laryngotracheo-esophageal cleft (type IV): managment of lesions beyond the carina. J Pediatr Surg 26:962–970

Samuel M, Burge DM, Griffiths DM (1997) Prenatal diagnosis of laryngotracheoesophageal clefts. Fetal Diagn Ther 12:260–265

Sasaki H, Sasano H, Ohi R, Imaizumi M, Shineha R, Nakamura M, Shibuya D, Hayashi Y (1999) Adenocarcinoma at the esophageal gastric junction arising in an 11-year-old girl. Path Int 49:1109–1113

Schlesinger AE, Parker BR (2003), Scafidi DE, Young LW (2000) Diseases of the pediatric pancreas. In: Gore R, Levine M (eds) Textbook of gastrointestinal radiology. Saunders, Philadelphia, pp 2162–2172 Congenital gastric and duodenal abnormalities and acquired gastric and duodenal disorders. In: Kuhn JP, Slovis TL, Haller JO (eds) Caffey's pediatric diagnostic imaging, 10th edn. Mosby, Philadelphia, pp 1587–1615

Sferra TJ, Pawel BR, Qualman SJ, Li BU (1996) Menetrier disease of childhood: role of cytomegalovirus and transforming growth factor alpha. J Pediatr 128:213–219

Sharma SC, Menon P (2005) Congenital microgastria with esophageal stenosis and diaphragmatic hernia. Pediatr Surg Int 21:292–294

Sinzig M, Umschaden HW, Haselbach H et al. (1998) Gastric trichobezoar with gastric ulcer: MR findings. Pediatr Radiol 28:296

Sookpotarom P, Vejchapipat P, Chongsrisawat V, Mahayosnond A (2005) Gastric volvulus caused by percutaneous endoscopic gastrostomy: a case report. J Ped Surg 40: E21–E23

Takahashi T (2003) Pathophysiological significance of neuronal nitric oxide synthase in the gastrointestinal tract. J Gastroenterol 38:421–430

Teele RL, Katz AJ, Goldman H, Kettell RM (1979) Radiographic features of eosinophilic gastroenteritis (allergic gastroenteropathy) of childhood. AJR Am J Roentgenol 132:575–580

Teele RL, Share JC (2000) Diseases of the pediatric stomach and duodenum. In: Textbook of gastrointestinal radiology, 2nd edn. WB Saunders Company, Philadelphia, pp 2029–2107

van Rijn RR, van Lienden KP, Fortuna TL, D'Alessandro LC, Connolly B, Chait PG (2006) Membranous duodenal stenosis: initial experience with balloon dilatation in four children. Eur J Radiol 59:29–32

Velasco Al, Holcomb GW III, Templeton JM Jr, Ziegler MM. Management of congenital microgastria. J Pediatr Surg 1990;25:192–197

Waasdorp CE, Rooks V, Sullivan C (2003) Congenital microgastria presenting as stridor. Pediatr Radiol 33:662–663

Wakhlu A, Wakhlu AK (2002) Paediatric gastric teratoma. Eur J Pediatr Surg 12:375–378

Welch KJ, Randolph JG, Ravitch MM et al (eds) (1986) In: Pediatric surgery, 4th edn. Year Book Medical, Chicago, pp 907–908

Westra SJ, de Groot CJ, Smits NJ, Staalman CR (1989) Hypertrophic pyloric stenosis: use of the pyloric volume measurement in early US diagnosis. Radiology 172:615–619

Accessory Organs of Digestion

4

Rafael M. Jiménez, Susan Connolly, Johan G. Blickman, and Yvonne L. Hoogeveen

CONTENTS

R. M. Jiménez, MD; S. Connolly, MD
Department/Division Radiology, Area of Clinical Expertise, Musculoskeletal Radiology, Children's Hospital Boston, Department of Radiology, 300 Longwood Avenue, Main 2, Boston, MA 02115, USA
J. G. Blickman, MD, PhD, FACR; Y. L. Hoogeveen, PhD
Department of Radiology, UMCN St Radboud, Box 9101, route 667, 6500 HB Nijmegen, The Netherlands

4.1 The Liver

At birth a normal liver can extend below the costal margin, and occupy two fifths of the abdominal cavity. However, when the child starts growing, these proportions will change to adult proportions. Of the modalities useful in imaging of the liver in children, ultrasound (US) in particular has proved to be an excellent screening and diagnostic tool in children (Siegel 2001a). Conventional radiology can only indirectly "image" the liver, CT "costs" ionizing radiation, while MR is cumbersome and only useful in targeted instances [magnetic resonance cholangiopancreaticography (MRCP), etc.].

Different liver measurements have been reported for normal neonates, infants, and older children (Table 4.1), and although those measurements can be a guideline, the diagnosis of hepatomegaly is usually a clinical one. On US evaluation a normal liver in a young infant should not be more than 1 cm beneath the costal margin, and should be above the costal margin in older infants and children. At birth in 50% of neonates the renal cortical echogenicity is higher than that of the liver of the liver (Sporcq et al. 2007), otherwise the echo texture of the liver must be similar to the adult echo texture, with a similar echogenicity between the hepatic parenchyma and the renal cortex. However, by 6 months of age, the echogenicity of the liver will be greater than that of the kidney (Gubernick et al. 2000; Teele and Share 1991). Evaluation of the intrahepatic and extrahepatic biliary ducts in order to rule out ductal dilation is an integral part of US evaluation of the liver. In neonates, the normal common bile duct measures less than 1 mm, thus making it too small to be visualized. A normal measurement expected in an infant of less than 1 year of age is 2 mm, and up to 4 mm in older children (Soyupak et al. 2002; Gubernick et al. 2000).

Table 4.1. Longitudinal dimensions of right lobe of liver in neonates, infants, and older children (Soyupak et al. 2002)

Subjects		Longitudinal dimensions of right liver lobe (mm)	
Body height (cm)	Age range (months)	Mean	SD
47–64	1–3	64	10.4
54–73	4–6	73	10.8
65–78	7–9	79	8.0

On the underside of the liver, a round structure with a teardrop shape (not spherical) will be seen by US that corresponds to the gallbladder. A normal gallbladder should be smaller than the contiguous kidney and a thin hyperechogenic wall should be present. In the fasting state, the wall thickness can be up to 3 mm (Siegel 2001a). The normal gallbladder length ranges from 1.5 to 3 cm (mean 2.5 cm) in infants (< 1 year old) and 3–7 cm in older children (Gubernick et al. 2000) (Fig. 4.1).

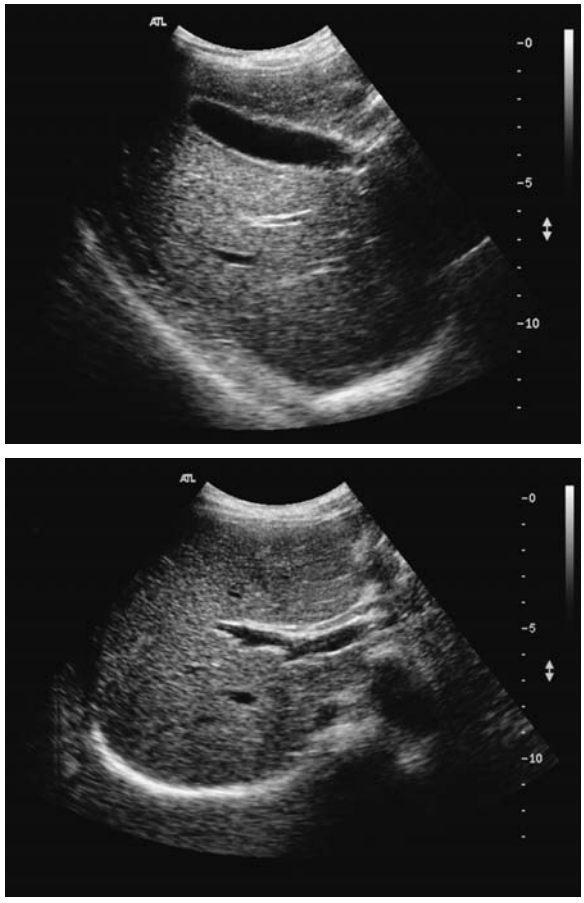

Fig. 4.1. a Longitudinal US image shows the normal texture and a normal gallbladder. **b** Transverse US image reveals normal echo texture and a normal portal vein/common bile duct

4.1.1 Neonatal Jaundice

Shortly after birth, the sclerae and skin may acquire a yellow appearance secondary to the accumulation of bilirubin in these tissues. This is called neonatal jaundice.

There are two types of jaundice, physiologic and pathologic. Physiologic jaundice is a common condition that can be observed in 80% of pre-term newborns and in 60% of normal newborns. It is a benign condition with increased levels of bilirubin at the end of the first week of life. Patients are active and no signs of sepsis or anemia should be present (Gubernick et al. 2000).

On the other hand, pathologic bilirubinemia will be characterized by jaundice presenting within the first day of life or persistent after 1 week in term newborns and 2 weeks in pre-term infants. It is characterized by an increase of bilirubin levels greater than 5 mg/dl in one day, with levels of direct bilirubin greater than 2 mg/dl and total bilirubin greater than 15 mg/dl. The child is often lethargic and quiet. The differential diagnosis includes infectious etiologies such as hepatitis (caused by the TORCH entities toxoplasmosis, rubella, cytomegalovirus, Herpes simplex), syphilis, and metabolic diseases such as alpha 1 antitrypsin deficiency and cystic fibrosis (Gubernick et al. 2000).

Once these causes of jaundice have been excluded, neonatal hepatitis, biliary atresia (BA) or duct paucity syndromes will account for more than two thirds of the remaining cases of conjugated hyperbilirubinemia in the neonate. In conjunction with nuclear medicine, US is the primary imaging modality for differentiating among these diseases and differentiation is important, as surgery is the treatment for BA but not for the other entities (Kelly 1999; Mortele et al. 2006; Gazelle et al. 1998).

4.1.2 Biliary Atresia

Biliary atresia (BA) accounts for the majority of chronic liver diseases without a genetic cause, and

is the most common cause of liver transplantation in children. Although BA is an idiopathic disease, most cases are thought to be secondary to viral, metabolic, or vascular insults in susceptible individuals. Girls are more affected than boys, and a worldwide incidence of 1:14,000 has been reported for this condition (Sokol et al. 2003; Hinds et al. 2004).

BA can be viewed as two different entities, the embryonic and the postnatal form. Approximately 10%–35% of patients will be afflicted by cholestasis from the first hours of life, and the association of this cholestasis with different congenital malformations in these patients will constitute the embryonic or fetal form. On the other hand, a gradual increase in bilirubin levels with a clinically evident jaundice after the sixth week of life will characterize the postnatal form. Acholic stools and hepatomegaly are other common manifestations (Suchy 2003; Rosenthal 1999).

Antenatally, US is a useful tool for detection of biliary malformations. The presence of a cystic structure localized at the hepatic hilum can occur in BA or may present as a choledochal cyst. However, if this cyst is small and anechoic it will be more suggestive of an atresia of the biliary canals, while the presence of an echoic cyst that gradually increases in size supports a choledochal cyst. The specificity of these US findings with BA, however, is not well known (Kim et al. 2000).

Postnatally, the parenchymal pattern of the liver in a patient with BA may be normal or slightly heterogeneous on US examination. The vast majority of patients will have a small gallbladder with a length less than 1.5 cm or an absent gallbladder. Absence of the gallbladder is therefore highly suspicious of BA, while a normal size gallbladder or a change in its size after feeding will support neonatal hepatitis (Teele and Share 1991; Kanegawa et al. 2003; Kirks and Griscom 1998). Some studies have reported the presence of fibrous tissue close to the porta hepatis, and US may depict this tissue as a triangular or tubular echogenic structure. Although a positive predictive value of 95%, and a sensitivity between 84%–93% has been noted between this "triangular cord" and BA, inflammatory diseases and cirrhosis can mask this finding (Gubernick et al. 2000; Jaw et al. 1999; Norton 2002; Mowat et al. 1976) (Fig. 4.2a,b).

Other congenital anomalies such as polysplenia, midline liver, interrupted inferior vena cava, situs inversus, preduodenal portal vein, and intestinal malrotation will support the diagnosis of heterotaxy syndrome (Sokol et al. 2003; Kim et al. 2000).

A 99Tc-IDA derivate isotope scan (scintigraphy) can also differentiate between BA and neonatal hepatitis. Phenobarbital must be administered for 3–5 days to jump-start hepatocellular function. If the tracer reaches the duodenum, biliary atresia can be excluded. However, some authors recommend imaging at 24 h to exclude delayed excretion. Scintigraphy has 50%–75% specificity and 90%–100% sensitivity for BA (Petersen and Ure 2003) (Fig. 4.2c,d).

MRCP using T2-weighted turbo spin echo sequences has been helpful in the diagnosis and visualization of choledochal cysts and dilated common bile ducts. However, in neonates and young infants the intrahepatic ducts are very thin and their visualization can be challenging. The triangular cord sign may be seen on MRCP as a high signal intensity area on T2-weighted images along the portal tract, and this corresponds to inflammatory tissue and fluid (Kim et al. 2000; Jaw et al. 1999).

Finally, an intraoperative cholangiogram will finally depict the anatomy of the biliary ducts and will assess whether the main right and left hepatic ducts have the caliber necessary to perform the Kasai hepatic portoenterostomy (Gazelle et al. 1998) (Fig. 4.2e).

A percutaneous liver biopsy will clinch the diagnosis. Histological analysis will show bile plugs, lymphocytic infiltration in the portal tracts and proliferation of the small intrahepatic bile ducts. There may also be an absence of the extrahepatic biliary ducts and the presence of periportal fibrosis, which will progress to cirrhosis. The accuracy of this procedure is reported to be greater than 90% (Gubernick et al. 2000).

Surgical success depends on several factors, such as the time of operation, extent of fibrosis, and jaundice disappearance. Surgical timing of the Kasai procedure is one of the most important factors, showing a 17% success rate when the surgery is done after 90 days of age, and 91% success rate if it is done before 60 days of age. Disappearance of jaundice after surgery has been correlated with survival rates of between 73%–92% after 10 years; however, if the jaundice continues, the 3-year survival can be as low as 20% (Sokol et al. 2003).

In general, after surgery, one third of patients will require liver transplantation in the first year of life; another third by their teenage years and the remaining third will have a good outcome.

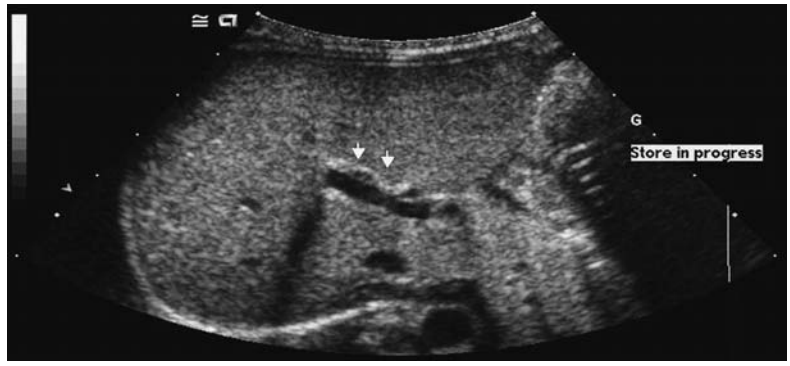

a

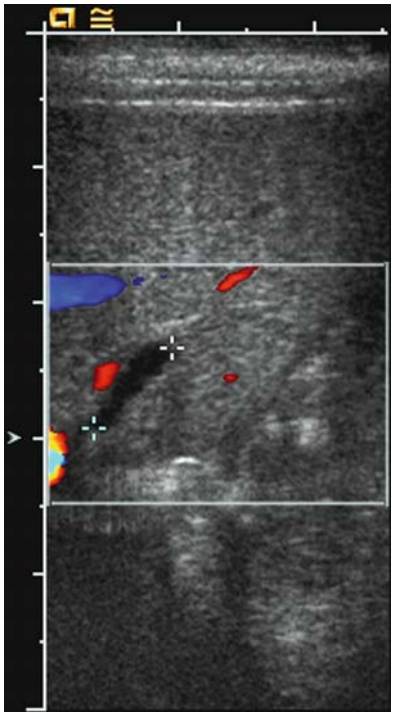

b

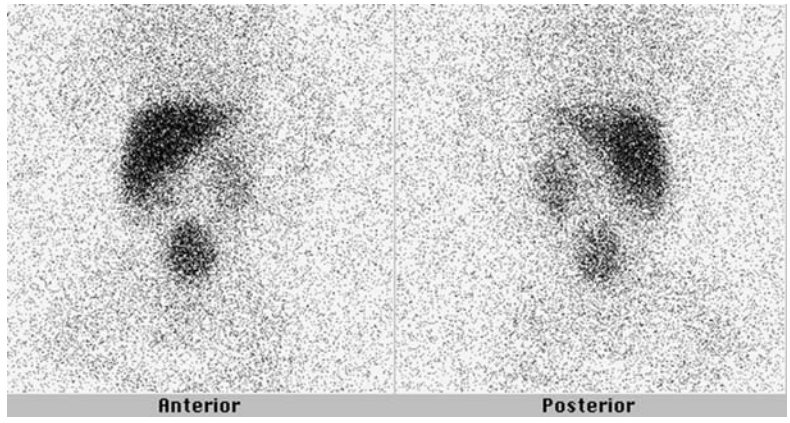

c

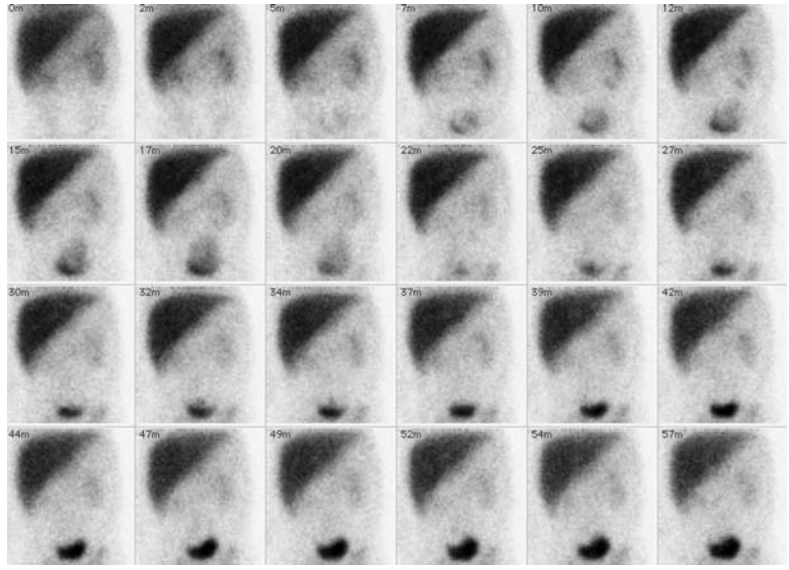

d

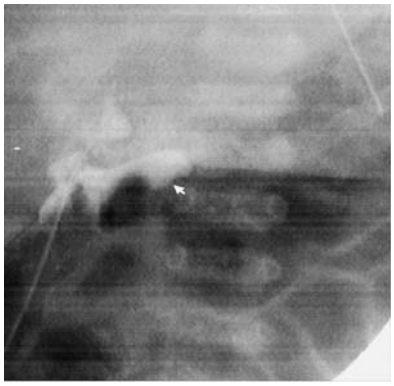

e

Fig. 4.2a–e. Biliary atresia (BA). **a** Slightly inhomogeneous echo texture of the liver, prominent wall of common bile duct (CBD) (*arrows*). **b** Tiny gallbladder. **c,d** Tracer uptake in liver, both kidneys, and bladder, but not in a gallbladder or duodenum. **e** Transhepatic cholangiography reveals atretic CBD (*arrow*)

4.1.3 Idiopathic Neonatal Hepatitis

Idiopathic neonatal hepatitis is an inflammation of the liver parenchyma responsible for most cases of intrahepatic cholestasis, and accounts for at least 25%–40% of patients with neonatal cholestasis. A multitude of etiologies can be the cause (Gubernick et al. 2000).

Treatment of these patients is medical, with a generally good prognosis in 80% of cases. However, up to 20% of cases are progressive and have a mortality of between 13%–25%. Poor outcome predictors include: familial occurrence, persistence of jaundice for more than 6 months, and evidence of severe inflammatory infiltration on histology (Gubernick et al. 2000).

The clinical presentation of a patient with idiopathic neonatal hepatitis can be similar to BA; however, these patients are more likely premature or between 1–4 weeks of age than those with BA.

Histologically there is a transformation of hepatocytes into giant cells, with lobular disarrangement. Although the bile ducts appear normal, the differentiation among idiopathic neonatal hepatitis and BA may be difficult.

US examination will show a normal or enlarged liver with hyperechogenicity of the parenchyma, and poor delineation of the peripheral portal venous vasculature. Typically the gallbladder has a normal size but in some cases it can become small after severe hepatocyte damage. A decrease in the length of the gallbladder after feeding will indicate a normal contraction and supports a diagnosis of idiopathic neonatal hepatitis.

Scintigraphy will show a decreased uptake of 99m Tc-IDA with excretion into the duodenum. Nevertheless, patients with BA for more than 3 months may depict a scintigraphic pattern similar to those with idiopathic neonatal hepatitis.

4.1.4 Cystic Changes in the Liver and Biliary Tree

A choledochal cyst is a dilatation of the common bile duct that presents with neonatal jaundice (Fig. 4.3). They are more frequent in females and in the Asian population with a worldwide frequency of 1:15,000. Many theories regarding the etiology of choledochal cysts have been proposed (Gazelle et al. 1998). In the neonate a congenital etiology has been proposed, while in older children it is thought to be secondary to a pancreatobiliary obstruction that will produce an increased intraductal pressure and a reflux of the activated pancreatic enzymes into the common bile duct. Other possible etiologies include a deficient autonomic innervation with few ganglion cells in the distal common bile duct, a retrovirus infection, and an immune or familial cause.

There are five types of choledochal cysts (Fig. 4.4a):

- Type I: Dilatation of the common bile duct, which may be cystic, focal, or fusiform (subtypes A, B and C, respectively).
- Type II: Saccular diverticulum of the common bile duct.
- Type III: Cystic dilatation of the intramural portion of the common bile duct and is contended by some to represent a duodenal diverticulum rather than a choledochal cyst.
- Type IV-A: Intrahepatic and extrahepatic dilatation of the biliary tree.
- Type IV-B: Multiple extrahepatic cysts
- Type V: Multiple intrahepatic biliary dilatations, synonymous with Caroli disease

Type V cyst is a rare congenital disease characterized by segmental-saccular ductal dilatation. Recurrent bacterial cholangitis and stone formation have been associated with "Caroli disease" (Fig. 4.4b,c) (Todani et al. 2003).

On US a choledochal cyst will be seen as a cystic lesion with a thin wall, well defined borders, and echogenic material inside the cyst that corresponds to biliary sludge. However, it is important in the US evaluation to determine if the cyst is really a dilated choledochus, if the intrahepatic ducts are compromised, and if there is portal hypertension. As US has shown a specificity of 97% for choledochal cysts, it is widely used as the first diagnostic tool (Gubernick et al. 2000; Teele and Share 1991).

Endoscopic retrograde cholangiopancreatography (ERCP) is an excellent tool that affords good visualization of the biliary ducts, and the extent of the choledochal cyst. However, in pediatric patients, and especially in the very young, it can be a challenging procedure, with an unsuccessful outcome in 5%–30% of all patients.

CT might also play an important role. It allows for good characterization of intrahepatic cysts, the distal part of the common bile duct, and the head of the pancreas, and in post-surgical patients it gives a very accurate evaluation of the biliary-enteric anastomosis. However, cholangiography can dem-

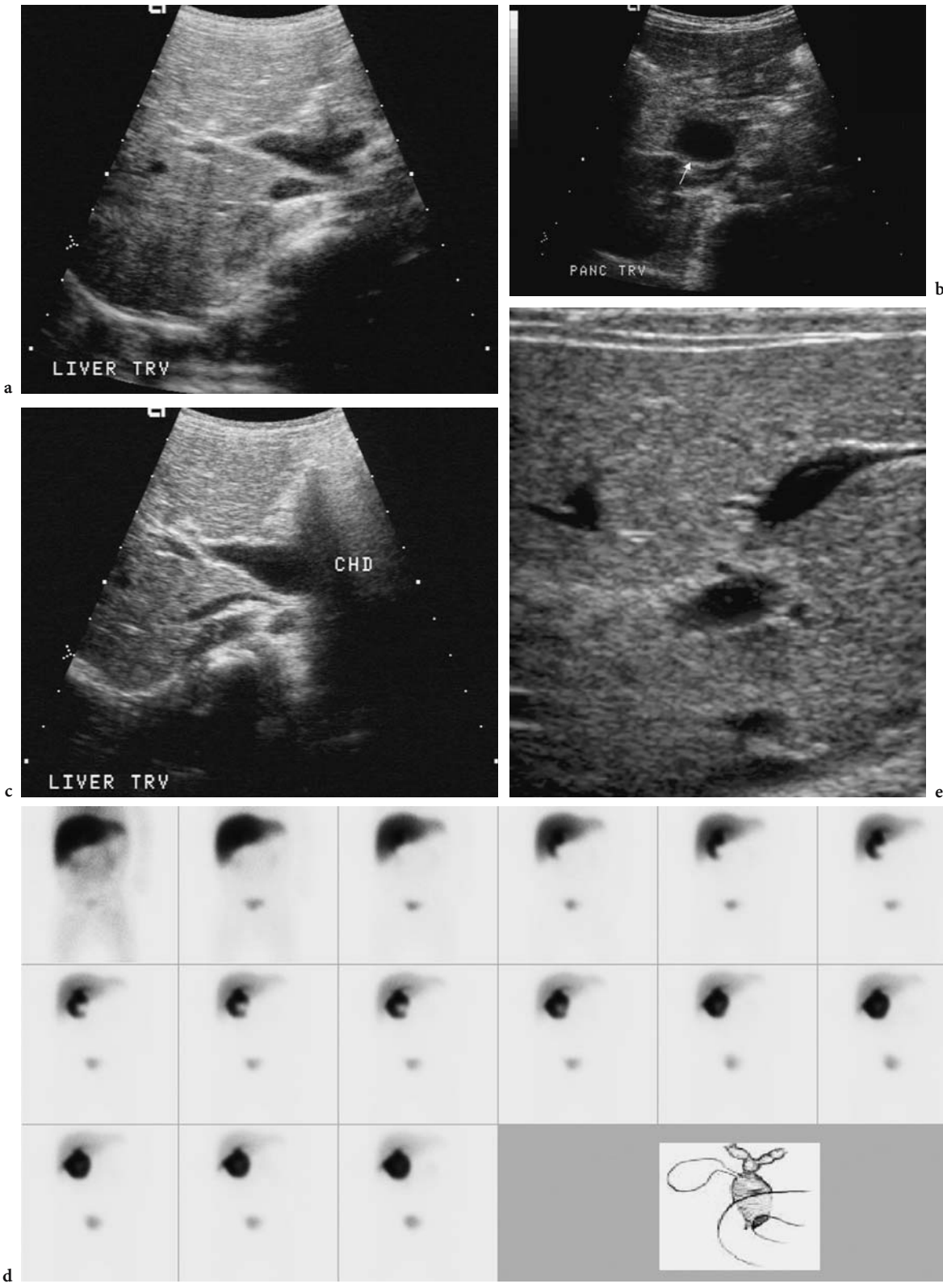

Fig. 4.3a–e. Choledochal cyst dilatation. **a–c** Cystic dilatation of the CBG at successive caudad levels (type I). **d** Cystic dilatation noted on 99Tc-IDA scan. **e** Cystic dilatation of an intrahepatic duct (type III)

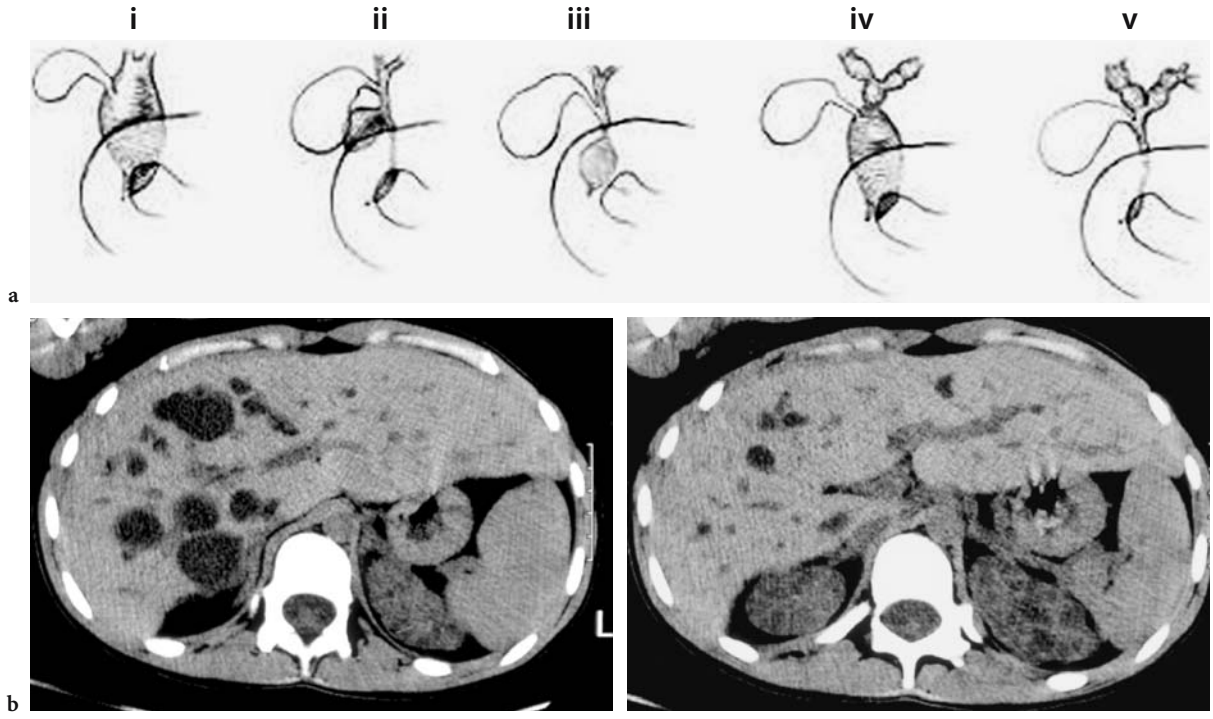

Fig. 4.4. a Classification of choledochal cysts. **b,c** CT demonstrates multiple cystic dilatation (saccular), signifying Caroli's "disease"

onstrate the biliary ducts as well, or better, than CT, with less radiation exposure but with a morbidity and sedation risk (Kuhn et al. 2004).

In some instances neither US nor CT can determine whether the cyst has communication with the biliary tract. Scintigraphy with 99tc at 30 min, 6 h, and 24 h could then be used. The sensitivity of the examination may be as high as 100% for type I cysts or as low as 66% for type IV cysts. However, scintigraphy will not delineate the intrahepatic compromise by choledochal cysts (Lam et al. 1999).

Magnetic resonance cholangiography (MRCP) T2-weighted sequences provide an evaluation of the intra- and extrahepatic bile ducts. Other sequences such as a T1 post-contrast injection provide fine detail on the periportal spaces, parenchyma, and blood vessels. Visualization of the entire biliary tree and the choledochal cysts using MRCP has been reported (Krause et al. 2002). MRCP provides information for the operative planning with less potential risks than ERCP or percutaneous transcutaneous cannulation (PTC).

Although CT-cholangiography can depict intrahepatic stones and the pancreatic duct better than MRCP, CT radiation exposure and potential contrast reactions have limited CT use (Mowat et al. 1976).

Cyst excision and hepaticoenterostomy is the definitive treatment of the disease, and will reduce the 20-fold risk of biliary carcinoma with choledochal cyst. Infants with choledochal cyst may present with the classic triad of jaundice, pain, and right upper quadrant mass; however, this is true only in 15%–20% of cases. Usually, only one of the triad will be present. Ascites, liver dysfunction, and coagulopathy may be found in some patients with progressive disease and without treatment (Behrman et al. 2004).

4.1.5 Polycystic Liver Disease

Two types of polycystic liver disease (PLD) have been identified: one is related to the autosomal dominant polycystic kidney disease (ADPKD) linked to PKD 1 or PKD 2, while the second form is an isolated form totally unlinked to PKD 1 or PKD 2. Patients with PLD will present liver involvement in approximately 45% of cases (Suchy 2003; Pirson et al. 1996). While ADPKD is usually a disease of adults, about 1%–2% of patients display an early manifesting clinical course and may die perinatally.

Early manifesting cases of ADPKD may mimic the autosomal recessive form (ARPKD) that is usually an infantile disease and an important cause of renal- and liver-related morbidity and mortality in children. Most cases manifest peri-/neonatally with a high mortality rate in the first month of life while the clinical spectrum of surviving patients is much more variable (Fig. 4.5a).

Patients with PLD can present with abdominal pain, hepatomegaly, and symptoms associated with renal involvement. Complications of hepatic cysts include compression of the biliary tree and fever secondary to cyst infection or abscess formation (Fig. 4.5b–d).

These hepatic cysts are thought to arise from dilatation of biliary microhamartomas (BMH). They demonstrate a cuboidal epithelial lining with the same histological appearance as that of the biliary epithelium, and may contain fluid. These lesions are generally smaller than 10 cm, surrounded by fibrotic tissue and localized close to the portal tracts (Suchy 2003).

On US hepatic cysts will be seen as multiple anechoic lesions that do not communicate with the liver. Occasionally echogenic debris may be present inside the cyst, which will correspond to hemorrhage. Renal evaluation by US demonstrating enlarged hyperechogenic kidneys will be obvious prenatally as well as later (Kuhn et al. 2004) (Fig. 4.5e,f).

On CT the cyst has lower attenuation than the surrounding parenchyma. There is usually no indication for CT in this condition.

On MRI these cysts may show low signal intensity on T1-weighted images and high signal intensity on T2-weighted images. A heterogeneous signal inside the cyst suggests hemorrhage. Some patients with PLD may have portal hypertension and hepatic venous obstruction. In these cases MRI allows evaluation of flow direction and compression in the hepatic vein, portal vein, and inferior vena cava (Kuhn et al. 2004).

Treatment of PLD is very controversial. Ethanol injection has been used resulting in relief of symptoms for 10 years after serial needle aspiration. However, following this procedure multiple small cysts might replace the treated cyst. Other alternative treatments used include stent placement, resection, or fenestration of the cyst wall. Liver transplantation, however, is the definitive treatment in a patient with end-stage PLD and portal hypertension (Chauveau et al. 2000; Arrivé and Tubiana 2003).

4.1.6 Neoplasms

A total of 6% of all abdominal tumors in the pediatric age group occur in the liver, i.e., 30% of all benign abdominal lesions, and 0.5%–2.0% of all malignant abdominal lesions (Suchy 2003). An incidence of 1.6 cases/million has been reported (Darbari et al. 2003).

The malignant neoplasms of the liver most commonly seen in children are hepatoblastoma and hepatocellular carcinoma. Although the incidence of hepatoblastoma is higher, and has been increasing over the last two decades compared with that of hepatocellular carcinoma, the survival rates for hepatocellular carcinoma are lower than those of hepatoblastoma (Darbari et al. 2003).

US, CT, and MR imaging are very useful tools in the evaluation of hepatic tumors. They can help in the differentiation between benign versus malignant neoplasms, the extent of the tumor, resectability, and the response to treatment (Kirks and Griscom 1998; Pobiel and Bisset 1995; Helmberger 1999).

4.1.6.1 Benign Neoplasms

4.1.6.1.1 Infantile Hemangioendothelioma

The infantile hemangioma accounts for the majority of benign hepatic neoplasms of the liver in infants. Girls are affected five times more frequently than boys. The typical age of presentation is in the first year of life, with approximately 85% of cases having presented by 6 months of age (Suchy 2003) (Fig. 4.6a).

Clinical symptoms may vary but abdominal pain and nausea are common. Other symptoms such as hemorrhage, consumptive coagulopathy, thrombocytopenia (Kasabach-Merrit syndrome), and cardiac failure may be seen (Suchy 2003).

On histological examination, hemangiomas of the liver will present with multiple vascular channels lined by a single layer of endothelial cells. Based on the endothelial layer and proliferation, hemangiomas have been subclassified into type I and II. In type I, multiple vascular spaces with immature endothelial cells will be seen, while in type II the vascular spaces will be larger and the endothelial component will be predominant. Sometimes hemorrhage, fibrous tissue, and calcifications may be found inside the lesion.

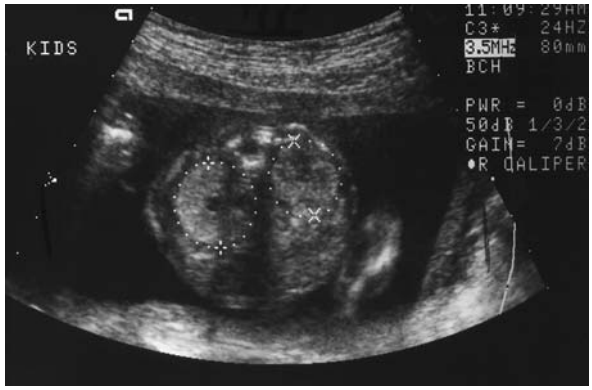

a

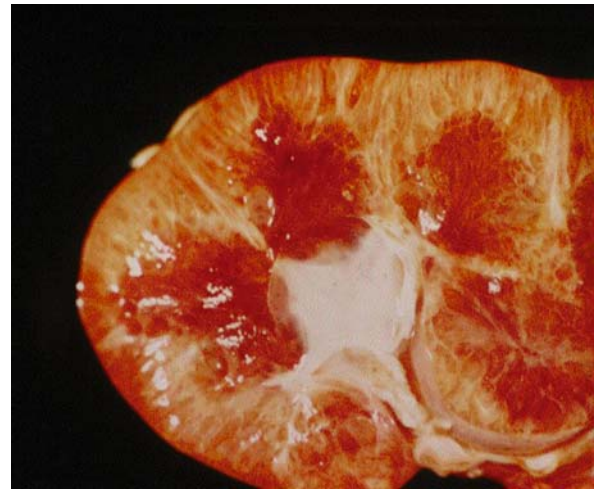

b

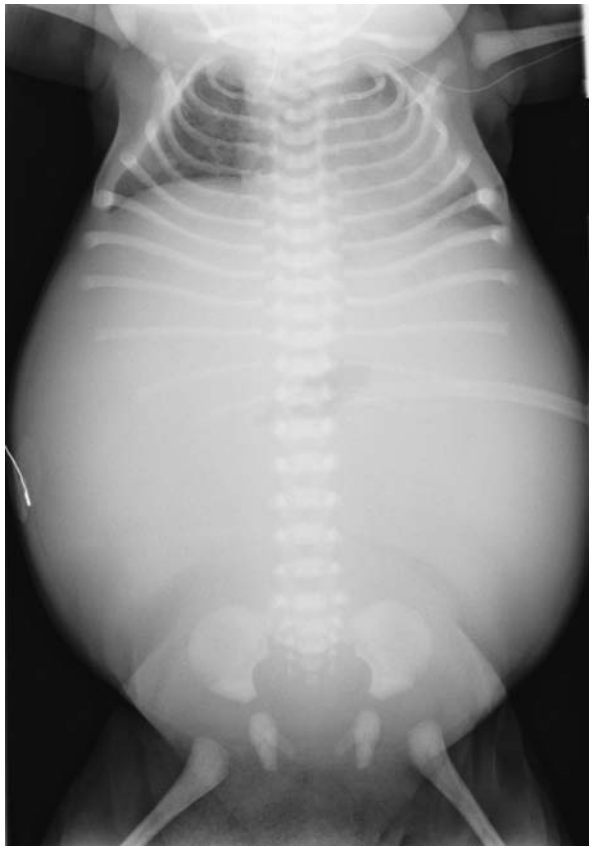

c

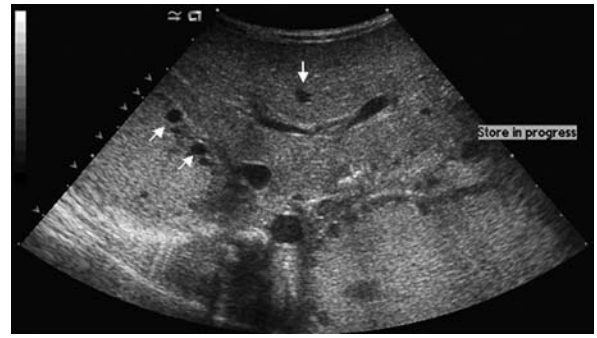

d

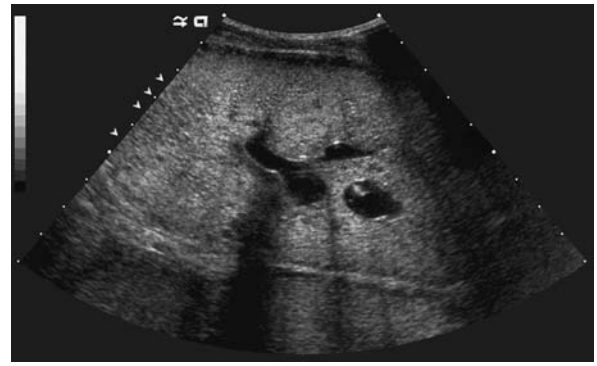

e

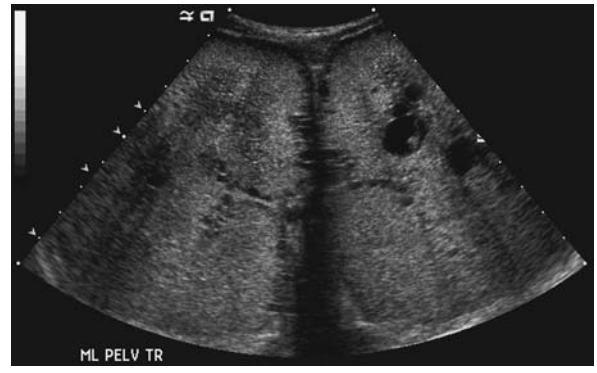

f

Fig. 4.5a–f. Autosomal recessive polycystic kidney disease (ARPKD). **a** Pre-natal depiction of ARPKD. **b** Gross pathology of microcysts in ARPKD. **c** Hepatomegaly with ascites suggested on neonatal abdominal radiograph with overall deformity suggesting ARPKD. **d** Echogenic liver with a few cysts (*arrows*). **e** Longtitudinal left, **f** transverse bilaterally midpole. Echogenic, massively enlarged kidneys with "pepper and salt" pattern

Hemangiomas usually show as echogenic lesions on US; however, sometimes a lesion with heterogenous echogenicity or a hypoechoic lesion may correspond with a hemangioma (Fig. 4.6b,c). This variable echogenicity depends on the extent of vessels and thrombi inside the structure (Siegel 2001a). Besides the hepatic mass, a decrease in the aortic diameter distal to the hepatic artery with an increase in the diameter of the hepatic and celiac arteries will support the diagnosis. On color Doppler the lesion will show mixed arterial and venous flow with a high-frequency peak of systolic shift and high diastolic flow (Swischuk 2005).

On CT, a typical hemangioma will be seen as a mass with lower attenuation than the adjacent liver. After contrast injection it will show a peripheral enhancement followed by centripetal filling on late images. Some necrotic areas or calcifications might not enhance. More than 50% of hemangiomas will contain calcifications on CT.

On MRI hemangiomas will have low signal intensity on T1-weighted sequences, and high signal intensity on T2-weighted sequences (Fig. 4.6d). Hemorrhage and hemosiderin deposition may be responsible for a heterogeneous signal pattern. Acute hemorrhage will have high signal intensity on T1-weighted images while hemosiderin will depict low signal intensity. After contrast injection an enhancement pattern similar to that seen on enhanced CT occurs with central enhancement and uniform distribution to the periphery on delay images (Fig. 4.6e,f). Other findings include a small infrahepatic aorta with increase caliber of the celiac and hepatic arteries (Siegel 2001b; Fulcher and Sterling 2002; Mortele et al. 1998).

Angiographic evaluation can be performed if embolization is a consideration. On angiography the hepatic arteries will show an increased diameter with early fill of hepatic veins (Mortele 2002).

4.1.6.1.2 Mesenchymal Hamartoma

Mesenchymal hamartoma of the liver (MHL) is another benign neoplasm in children. Boys are slightly more affected than girls. It is very unusual to find an MHL after 5 years of age. The lesion usually has a good prognosis (Ramirez-Garredo et al. 2003; Yen et al. 2003).

Typically, patients with MHL will present with a painless abdominal mass before the first year of life in 55% of cases. Other symptoms such as decreased appetite, or cardiac heart failure due to arteriovenous shunting are very uncommon (Fig. 4.7a).

Mesenchymal hamartomas are considered to be a developmental anomaly more than true neoplasm. A total of 75% of cases are located in the right lobe of the liver. Histologically MHR arise from the mesenchyma of the portal tract and will have connective tissue, blood vessels, lymphatic spaces, bile ducts and normal hepatocytes (Konez et al. 2001; Cetin et al. 2002).

The characteristic appearance of MHL on US is a large multicystic mass surrounded by solid areas ("Swiss cheese" appearance) with internal septations within the cyst. Another distinctive US finding is the presence of a large cystic space with thin, mobile septations. The cyst represents accumulation of fluid in bile ducts and degeneration of mesenchyma. Some echogenic material may be seen within the cyst and most likely represents blood. Some of these tumors may present with a high amount of solid tissue. Usually these are the tumors with a high vascular component and can be depicted with Doppler. The hepatic origin of mesenchymal hamartomas of the liver can usually be determined by US; however, in some exophytic tumors the origin and continuity are difficult to evaluate (Konez et al. 2001).

Typically, MHL will show on CT as a mass with multilocular elements and with enhancement of the noncystic components after contrast injection. The imagenologic characteristics of MHL on CT will depend on the predominance of the cystic or mesenchymatous tissue (Cetin et al. 2002).

On MRI the cystic component of the tumor will show low signal intensity on T1 and high signal intensity on T2-weighted images, while the stromal component of the mass will depict low signal intensity on T1-weighted images due to fibrosis. However, heterogeneous signal intensity may be seen as well, secondary to protein or blood within the cyst (Cetin et al. 2002) (Fig. 4.7b–d).

4.1.6.1.3 Focal Nodular Hyperplasia

Focal nodular hyperplasia (FNH) arises in utero as an overgrowth of the hepatic parenchyma secondary to an arteriovenous malformation of the liver (Swischuk 2005; Somech et al. 2001). Although it commonly presents in the adult population, some children with FNH have also been reported with a presentation peak in the pediatric age group between 6–10 years of age (39% of cases) (Somech et al. 2001).

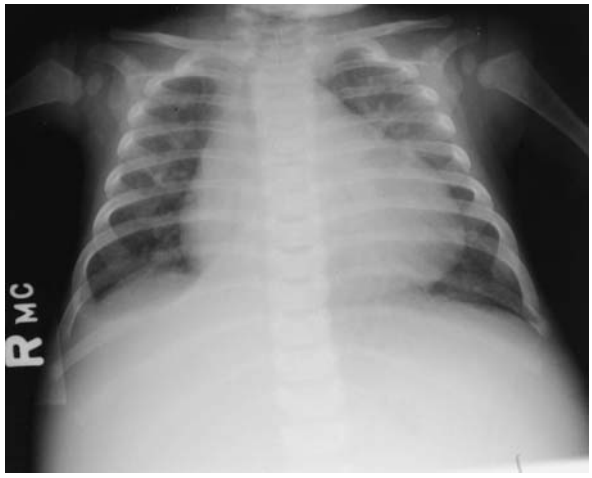

a

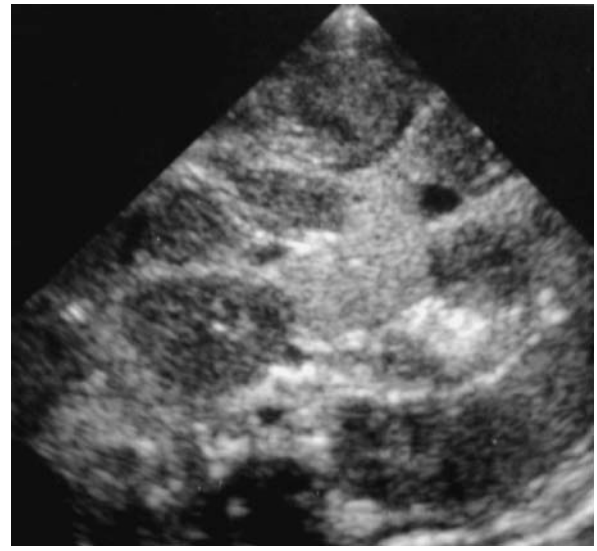

b

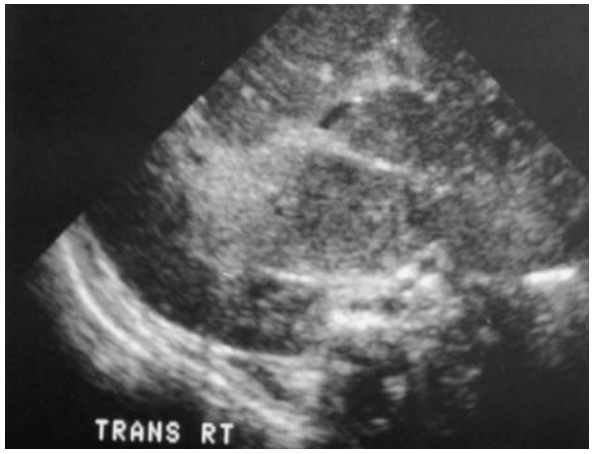

c

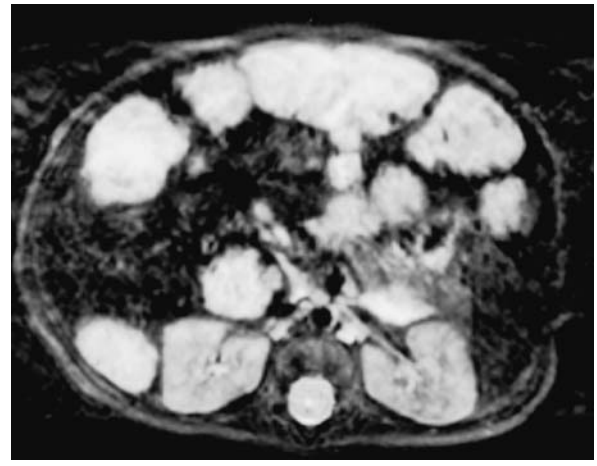

d

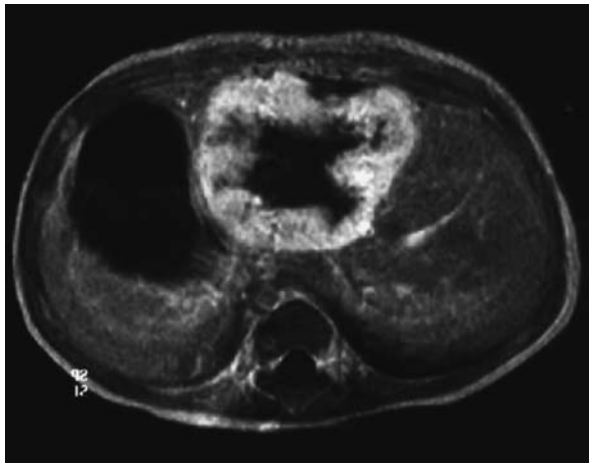

e

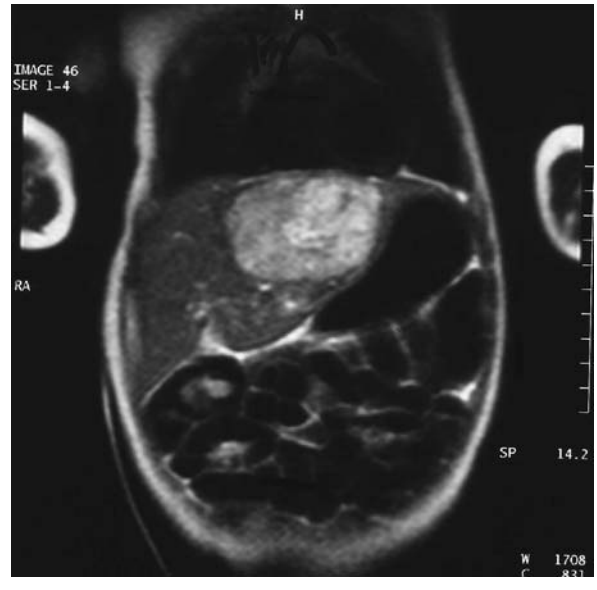

f

Fig. 4.6a–f. Infantile hemangioendothelioma. **a** Shunt vascularity and an enlarged heart in a 4-month-old with a murmur and hepatomegaly. **b,c** US depicts multiple rounded lesions of heterogeneous echo texture. **d** Multiple hemangiomas on T2 imaging. **e,f** Classic early (**e**), and late (**f**) contrast enhancement pattern on contrast MR

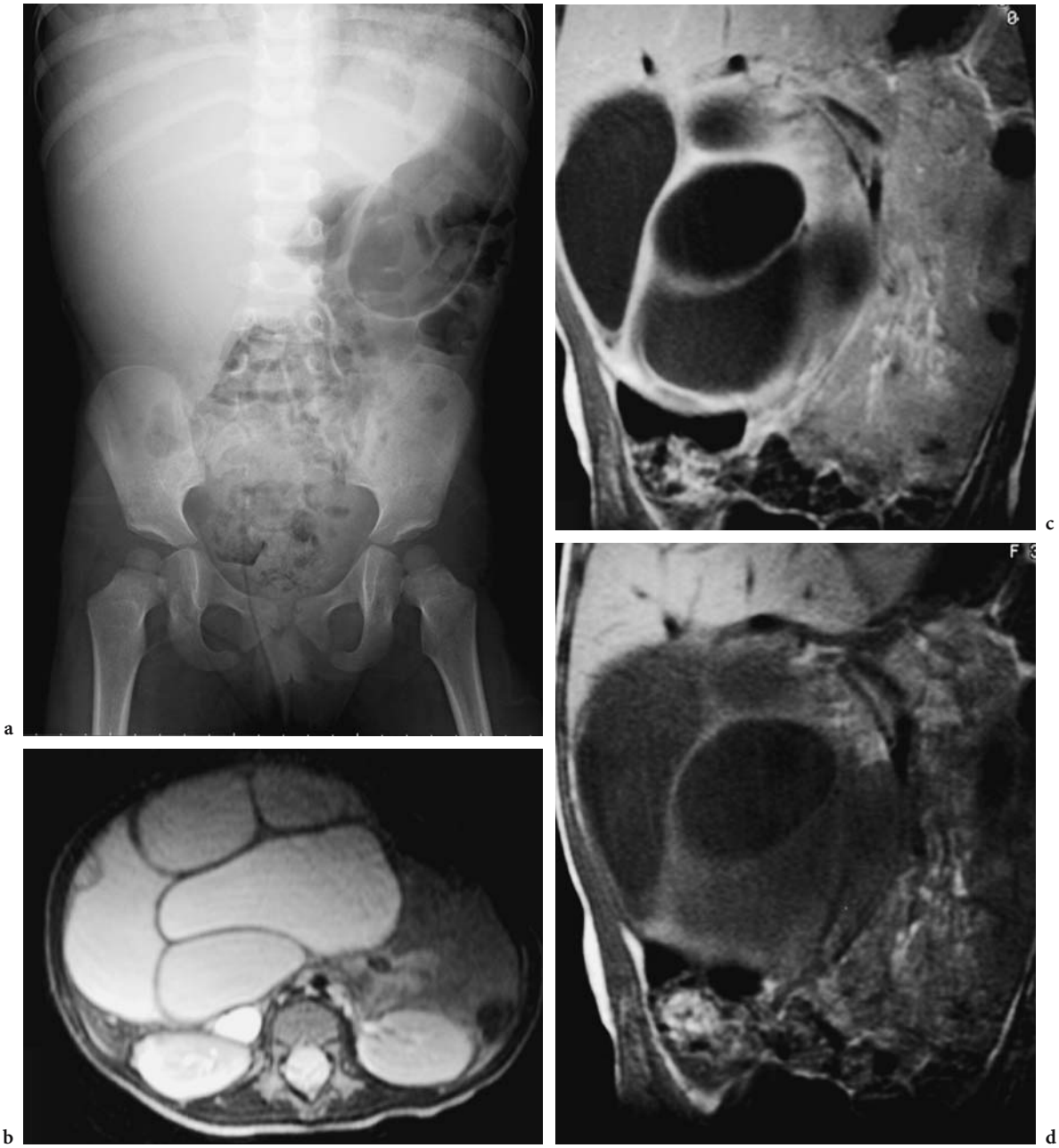

Fig. 4.7a–d. Mesenchymal hamartoma. **a** Plain film suggest hepatomegaly; no ascites. **b** T2 MR image depicts a large cystic lesion with septations. **c,d** T1 MR confirms the predominantly cystic mesenchymal hamartoma

Typically, these children will present with a painless abdominal right upper-quadrant mass on routine examination. Other symptoms include vomiting, diarrhea, and weight loss.

Histologically, a single mass involving the left lobe will be seen in 90% of cases. Only 23% of cases will present with a multifocal disease. On histology a lesion with abnormally organized hepatocytes, Kupffer cells, bile ductules, and well-defined margins are characteristic. All the bile ductules and arterial vessels will be dilatated and multiple fibrotic bands secondary to a central scar will separate the nodules of hepatocytes.

FNH will show a single slightly hypoechoic lesion on US; a central scar may be seen, as well as normal surrounding parenchyma (Carlson et al.

2000). The biliary tree may or may not be dilated (Fig. 4.8a–d).

On unenhanced CT, FNH may appear as isodense or hypodense compared to the liver parenchyma with the presence of a low attenuation central scar. On contrast CT this benign tumor may reveal an enhancement greater than that of the adjacent liver during the early phase (arterial and early portal venous) and may be indistinguishable from adjacent liver in delayed images, indicating rapid washout of contrast material from the lesion. Homogeneous enhancement, smooth surface, a subcapsular location, and ill-defined margins may also be shown (Fig. 4.8e).

As FNH is a tumor with normal hepatic elements, the signal on MRI will be similar to the surrounding liver, showing slightly low signal intensity or an isointense signal on T1 weighted images, and a slightly high signal intensity or isointense signal on T2 weighted images. Usually FNH will present with a central scar, which will be better depicted on T2-weighted images as a high signal lesion. Post-gadolinium images will show an enhancement pattern that resembles that seen on CT (Carlson et al. 2000; Mortele et al. 2000) (Fig. 4.8f–g).

4.1.6.2 Malignant Neoplasms

4.1.6.2.1 Hepatoblastoma

Hepatoblastoma is the third most common intra-abdominal malignancy (after neuroblastoma and Wilms tumour) in children. Almost all patients with hepatoblastoma are younger than 3 years, with a peak presentation at between 18 and 24 months. With an overall incidence of 1 per million, premature children with extremely low birth weight and long hospitalization have a higher risk for hepatoblastoma with a poor prognosis; these patients should be screened with abdominal US and serum alpha-fetoprotein early in life. Beckwith-Wiedemann syndrome, trisomy 18, familial adenomatous polyposis, Gardner's syndrome, and glycogen storage disease have been associated with increased risk of hepatoblastoma. Unlike hepatocellular carcinoma, hepatoblastoma has no association with cirrhosis (Oue et al. 2003; Dachman et al. 1987).

Typically, a hepatoblastoma will present with hepatomegaly. Increased levels of alpha-fetoprotein will be present in 90% of cases and will be helpful in following the patient. Weight loss, fever, and loss of appetite are other symptoms. When metastases occur, the lungs and regional lymph nodes are commonly involved, but also the skeleton, ovaries, brain, and eyes.

Abdominal radiography may show hepatomegaly as evidenced by elevation of the right hemidiaphragm and displacement of intraluminal air by an enlarged liver (Fig. 4.9a). Although not diagnostically specific, coarse, stippled and solid hepatic calcifications may be present in the right upper quadrant. Chest radiography may demonstrate pulmonary metastases and can aid in the differential diagnosis. Plain films cannot localize the tumor to the liver definitively, distinguish between the solid or cystic nature of a neoplasm, or provide information regarding tumor vascularity (Kuhn et al. 2004).

An hepatoblastoma can present as a solitary mass, with or without satellite lesion or as multiple nodules throughout the liver (Roebuck 2006). On US, hepatoblastoma presents as a mass with ill-defined borders, and heterogeneous echogenicity, showing slightly more echogenic areas compared to the surrounding parenchyma and anechoic areas that correspond to necrosis or hemorrhage. Calcifications can also be present (Fig. 4.9b).

Visualization and evaluation of intrahepatic vascular structures is important because hepatoblastomas can invade or compress the portal and the hepatic veins. Absence of the portal branch or presence of a thrombus supports portal vein invasion. Although the inferior vena cava can be invaded, US examination overestimates the incidence of obliteration of this vessel (Siegel 2001a; Kuhn et al. 2004).

Sulfur-colloid liver scintigraphy may show large filling defects in the hepatic parenchyma, with prominent tracer avidity at the site of the tumor within a few seconds of the appearance of the bolus in the abdominal aorta. This increased activity persists into the venous phase. Hepatoblastomas may demonstrate increased uptake on delayed imaging, but this is rare (Suchy 2003).

On CT, the appearance of hepatoblastoma varies greatly. Prior to contrast administration, the tumor may appear as a, or multiple, homogeneous hypodense mass(es) (epithelial-type tumor); however, it may demonstrate a more heterogeneous appearance (mixed mesenchymal-epithelial tumor), corresponding to areas of necrosis or hemorrhage (Fig. 4.9c–g). Vascular compression and tumor extension is also well assessed. Calcifications may be present and follow-up CT after chemotherapy may

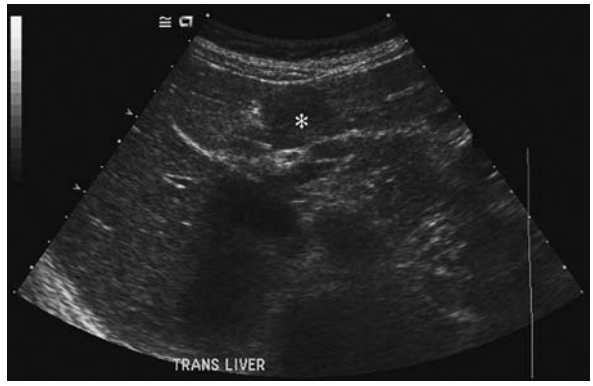

a

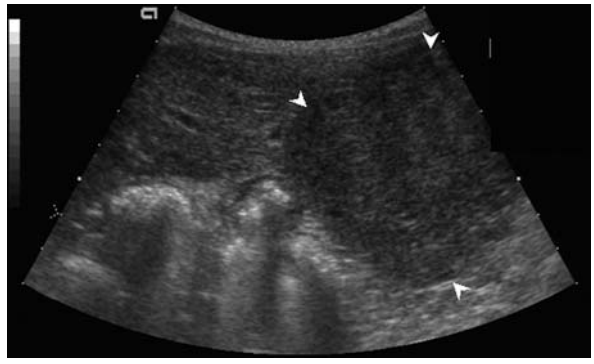

b

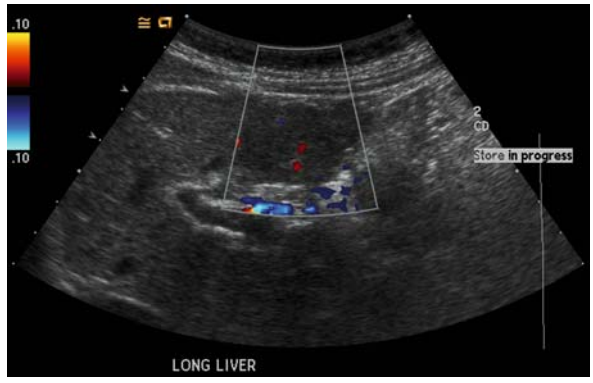

c

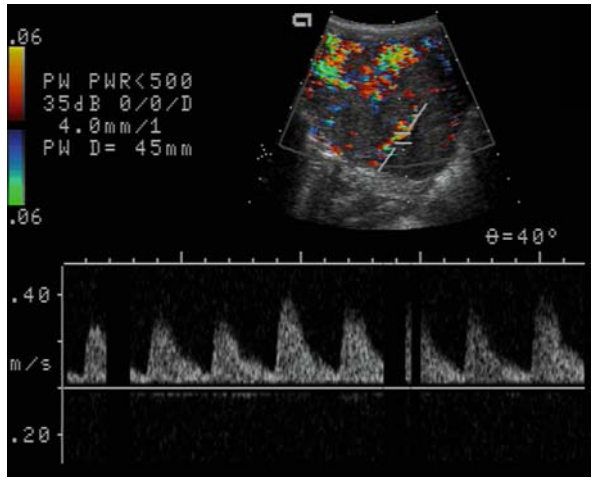

d

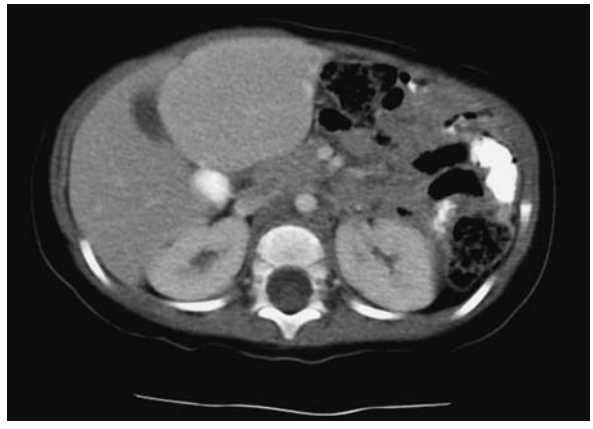

e

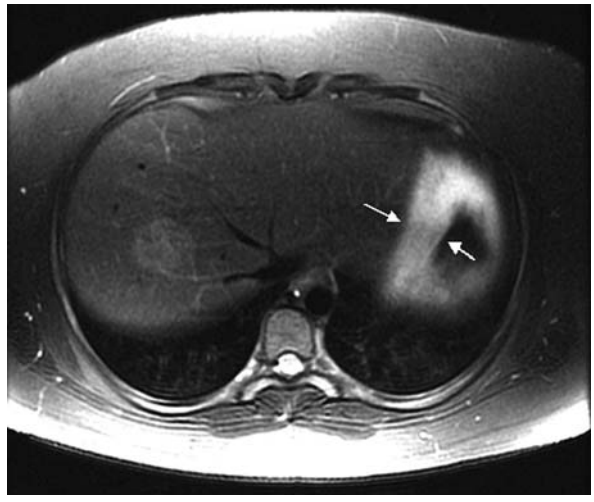

f

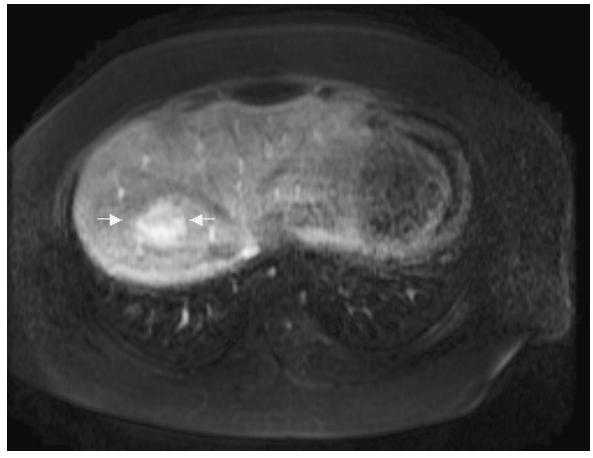

g

Fig. 4.8a–g. Focal nodular hyperplasia. **a** Area of decreased echogenicity in the left lobe of the liver (asterisk). **b** Enlarged view of (**a**) (*arrowheads*). **c** Low Doppler signal. **d** Arterial Doppler signal of same. **e** CT liver demonstrates enhancing of the lesion. **f** MR of FNH (*arrows*). **g** Pooling of contrast agent in FNH (*arrows*)

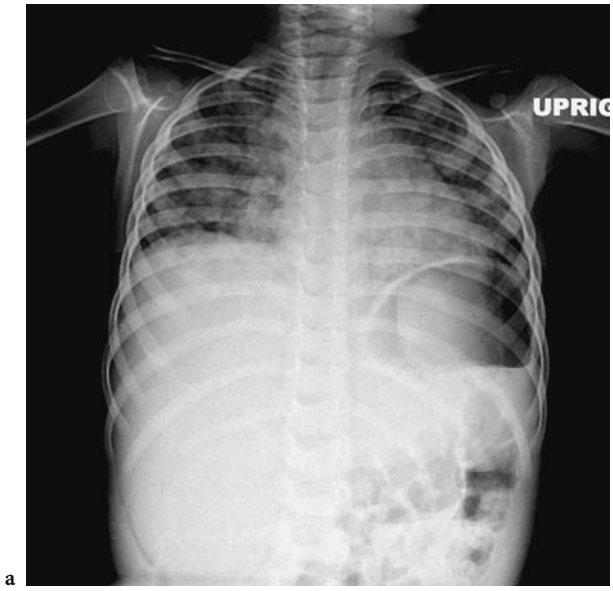

a

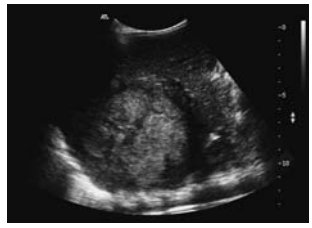

b1

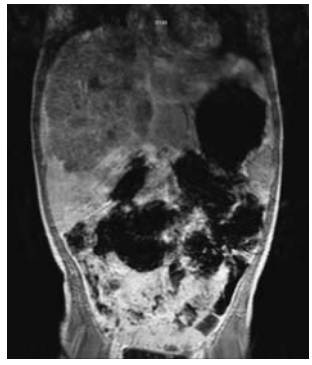

b2

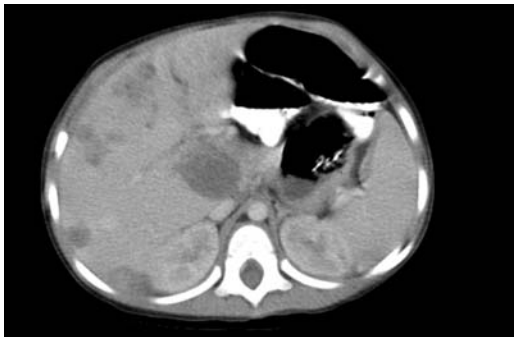

c

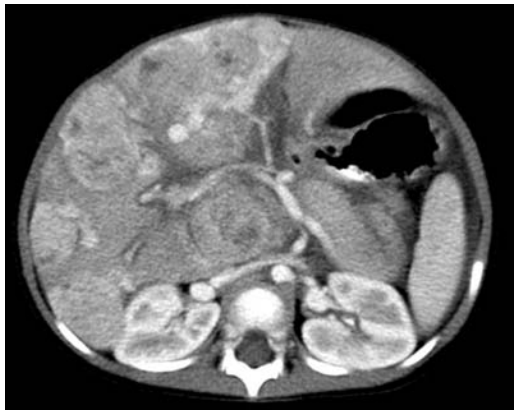

d

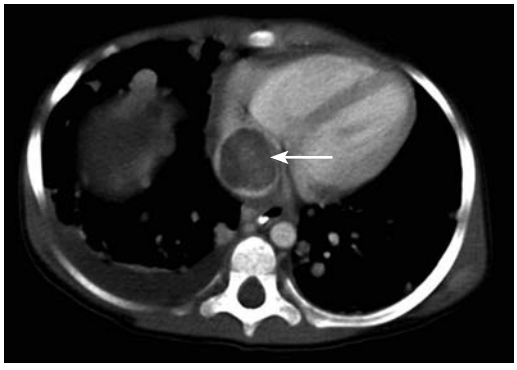

e

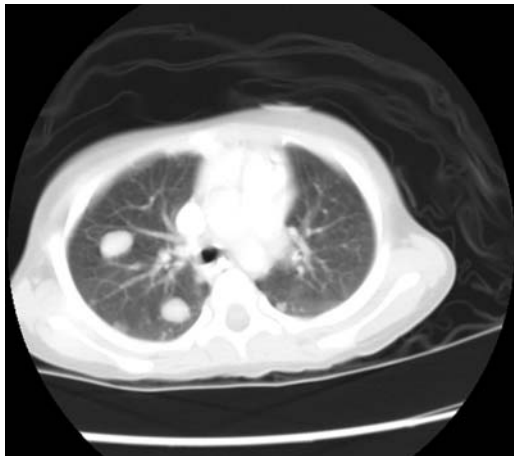

f

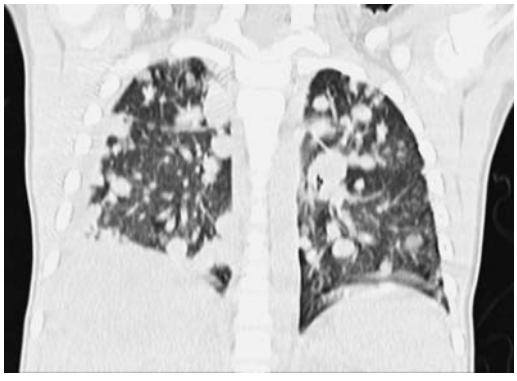

g

Fig. 4.9a–g. Hepatoblastoma. **a** Plain film demonstrates hepatomegaly and multiple round lesions in the chest. Patient with hepatoblastoma in which (**b1**): US shows highly echogenic lesion posteriorly in the liver; scar may be visible; and (**b2**): MR image of same, in the coronal plane. **c–e** CT of the abdomen depicts heterogeneous enhancement of multiple lesions, with tumor extension into the IVC (*arrow*). **f,g** CT of chest reveals multiple metastatic lesions

show an increase in these calcifications as a normal finding (Kirks and Griscom 1998).

Following the injection of IV contrast, hepatoblastomas may demonstrate an inhomogeneous enhancement pattern, usually with a higher density compared to the surrounding liver parenchyma. A peripheral rim of enhancement, which corresponds to compressed parenchyma may be observed if imaging is performed during the early arterial phase. If peripheral enhancement is seen, delayed serial scans at a single level of the tumor can be performed to distinguish hepatoblastoma from hemangioendothelioma.

On MRI, hepatoblastoma will have low signal intensity on T1-weighted images, and heterogeneous high signal intensity on T2. Sometimes high signal lesions can be seen on T1-weighted images and represent hemorrhage. Hypointense bands on T1- and T2-weighted images might also be seen and will correspond to fibrotic tissue. However, MRI has been used more in the evaluation of tumor extension, vascular compression, and complications than for diagnosis. In the evaluation of parenchymal extension of the tumor and lymph node infiltration, MRI, and STIR sequences in particular, have proved to be a useful tool. Although STIR is very effective in determining abnormal abdominal nodes, it cannot differentiate between reactive lymph node versus malignant infiltration (Kirks and Griscom 1998).

Evaluation of the hepatic vasculature is essential before tumor resection. MRI or CT can show vascular involvement even without contrast enhancement. Other modalities such as 3D MRA have been used for this purpose, with the advantage that the images can be studied in both the arterial and venous phases (Haliloglu et al. 2000).

In patients in whom noninvasive cross-sectional images fail to demonstrate crucial anatomy prior to resection or transplantation, angiography may be required. Sometimes a "spoke-wheel" arrangement of the arteries is present (Gazelle et al. 1998; Kirks and Griscom 1998).

4.1.6.2.2 Hepatocellular Carcinoma

After hepatoblastoma, hepatocellular carcinoma (HCC) account for the majority of malignant tumors of the liver in patients between 5 and 15 years. Males are affected more than females, and 25% of these patients will usually have an underlying liver condition such as cirrhosis, biliary atresia, hereditary tyrosinemia, glycogen storage disease, or chronic hepatitis. At diagnosis, half of the patients will have metastatic disease and elevated levels of alpha-fetoprotein will be found. In the United States, HCC has a prevalence of 0.2%–0.7% of children, while in Asia and sub-Saharan Africa a prevalence of 5.5% has been reported (Katzenstein et al. 2003).

A total of 65% of patients with HCC will be older than 10 years of age. The typical presentation will be a child with an abdominal mass or abdominal distension on physical examination. Although not common, abdominal pain, anorexia, weight loss, or hemoperitoneum may also be present (Katzenstein et al. 2003).

Macroscopically, a mass that involves both the right and left lobes will be found in 70% of cases. On histological analysis HCC will show giant tumor cells with large trabeculae arranged in an acinar pattern. Necrosis and vascular involvement are commonly seen. Often there is vascular invasion of the portal system and less frequently that of the hepatic vein and IVC. A variant of HCC is fibrolamellar HCC, which will present with a central scar in 76% of patients on macroscopic examination.

HCC can be represented on US as a hypo- or hyperechogenic mass depending on the amount of fat, or even as a heterogeneous mass with ill-defined borders located in the hepatic parenchyma. It may look identical to a hepatoblastoma. The presence of shadowing foci within the tumor will suggest intratumor calcifications. Evaluation of vascular invasion and dilatation of the portal vein will be seen with color Doppler with conventional gray-scale US (Siegel 2000) (Fig. 4.10a).

On unenhanced CT, HCC is shown as a low attenuation heterogeneous mass. Heterogenicity in attenuation indicates either necrosis or hemorrhage. Lesions may be missed if early vascular imaging is not performed. On enhanced CT, a heterogeneous hypervascularity may be seen. Tumors smaller than 3 cm tend to enhance on arterial phase, while in larger tumors this enhancement pattern is non-specific. Fibrolamellar HCC has specific features on CT. It will be seen as a mass with well-defined borders, calcifications, central scar and abdominal lymphadenopathy. The tumor will enhance in a heterogeneous pattern and show areas of hypervascularity (Siegel 2000; Ichikawa et al. 1999). The central scar does not enhance in the arterial phase but may do so in the portal or equilibrium phase (Fig. 4.10b,c).

On MRI, HCC will show low signal intensity on T1-weighted images and high signal intensity or isoin-

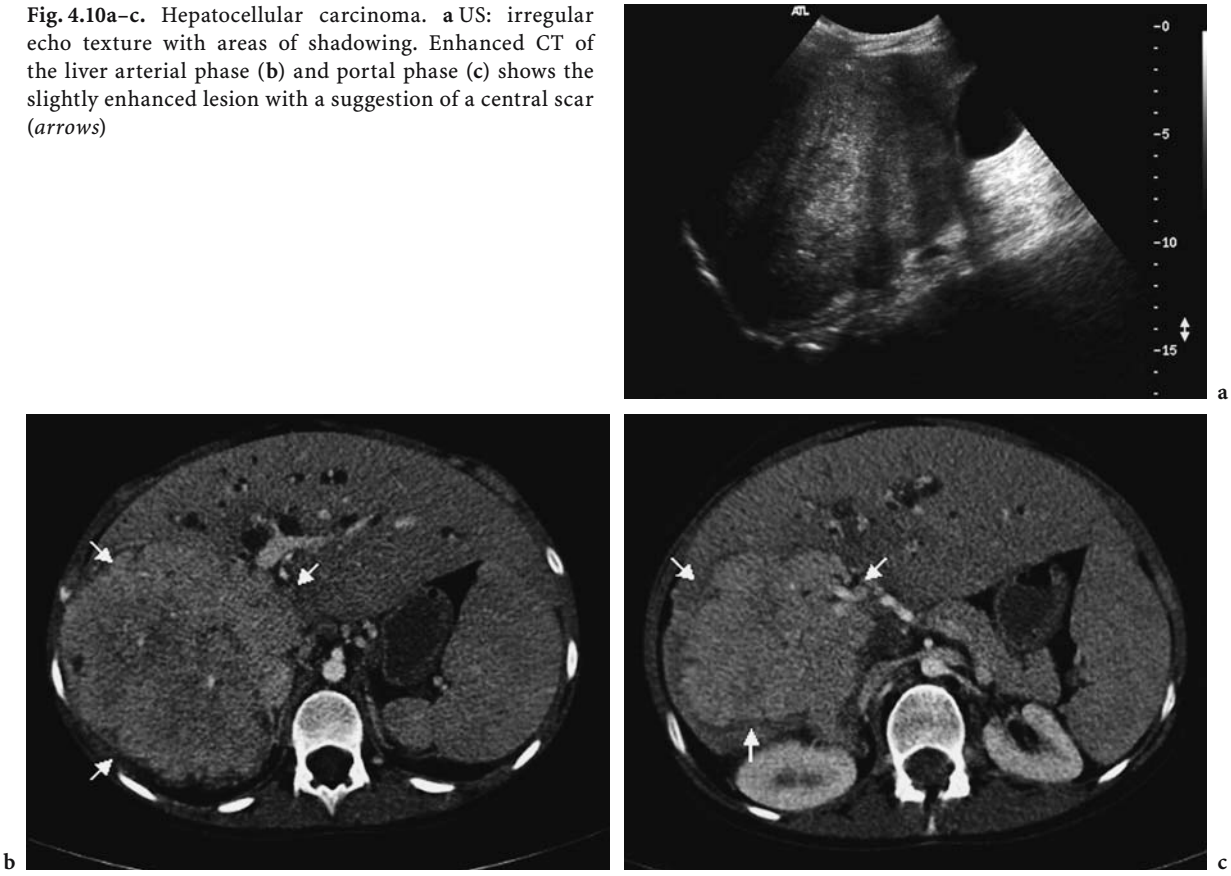

Fig. 4.10a–c. Hepatocellular carcinoma. **a** US: irregular echo texture with areas of shadowing. Enhanced CT of the liver arterial phase (**b**) and portal phase (**c**) shows the slightly enhanced lesion with a suggestion of a central scar (*arrows*)

tense to surrounding liver on T2-weighted images. Sometimes hyperintense areas might be seen on T1-weighted images and will represent hemorrhage or steatosis. A central scar may be present and is characteristic of fibrolamellar HCC. Other neoplasias such as focal nodular hyperplasia may also present with a central scar, but in fibrolamellar HCC the central scar will depict lower signal intensity compared with the surrounding tumor, while in focal nodular hyperplasia the central scar has high signal intensity on T2-weighted images. Vascular evaluation for thrombus detection involving the portal vein can be carried out with MRI. If the thrombus enhances, this indicates that it is composed of tumor, and will contraindicate embolization or transplantation (Siegel 2000).

4.1.6.2.3 Embryonal Rhabdomyosarcoma of the Biliary Tree

Embryonal rhabdomyosarcoma is responsible for only 1% of rhabdomyosarcoma (RMS) in children. There is no difference between genders and it occurs typically in children less than 5 years of age.

Since the tumor arises in the intrahepatic ducts, intrahepatic cyst, gallbladder, extrahepatic ducts, or in a choledochal cyst, jaundice will develop in 60%–80% of patients. Other manifestations include vomiting, fever, and abdominal distension (Roebuck et al. 1998).

US is used to evaluate the size of the tumor, the vascular involvement, and biliary tract compromise. Usually, biliary dilation, an intraductal mass with or without portal vein displacement, may be seen. Necrosis might be present in these tumors, especially when they are extensive (Gazelle et al. 1998).

On CT, embryonal rhabdomyosarcoma will be seen as a hypodense lesion with heterogeneous attenuation localized in the hilum, but sometimes may be seen in one lobe. After contrast injection the tumor will have a very variable enhancement. Contrast CT is very helpful in the evaluation of vascular involvement, and after surgery it helps to identify post-surgical abscess or hematomas (Gazelle et al. 1998) (Fig. 4.11a).

On MRI, embryonal RMS may show low signal intensity on T1-weighted sequences and high signal

intensity on T2-weighted sequences. After contrast injection a heterogeneous enhancement pattern will occur. Bile duct dilatation and bile duct irregularities are also easily noted. However, if the tumor arises in an intrahepatic duct the diagnosis may be challenging (Gazelle et al. 1998) (Fig. 4.11b–e).

On percutaneous transhepatic cholangiography (PTC), extensive filling defects in the biliary tree may be seen with or without obstruction of the extrahepatic bile ducts. PTC can be performed in cases of RMS without biliary dilation and is very useful if there is an obstructive jaundice (Gazelle et al. 1998).

4.1.6.2.4
Undifferentiated Embryonal Sarcoma

Undifferentiated embryonal sarcoma (UES) is a rare and highly malignant hepatic neoplasm, affecting almost exclusively the pediatric population. A total of 63% of patients are between 6–10 years of age, and it commonly occurs in the first two decades of life. It has a survival rate of 40% at 3 years (O'Sullivan et al. 2001; Lack et al. 1991).

Abdominal pain located in the right upper quadrant or epigastrium and an abdominal mass are the principal findings in the initial examination. Other manifestations such as jaundice, chest pain, fever, and cardiac murmur (due to extension of the tumor into the right atrium and ventricle) are very rarely seen.

Usually the tumor is a cystic or necrotic mass that involves the right lobe of the liver.

On histologic analysis a mass with spindle shaped cells surrounded by a mucopolysaccharide rich stroma with necrosis or hemorrhagic tissue, and surrounded by a fibrous pseudocapsule will be seen in a great number of cases.

On US, UES may show a heterogeneous mass with multiple anechoic or hypoechoic areas that correspond to cysts and may involve as much as one-fifth of the liver. Other areas will show a heterogeneous signal with isoechoic and hyperechoic areas compared with the adjacent liver (Gazelle et al. 1998; Moon et al. 1994; Buetow et al. 1997).

On non-enhanced CT, the mass will appear as a large lesion with low attenuation, septations, and a peripheral rim. On enhanced CT, besides solid components, (peripheral) septa may also enhance. Central areas of increased attenuation may be present and likely represent acute hemorrhage, while fibrous tissue surrounding the lesion constitute the peripheral rim.

MRI reveals a lesion that is predominantly hypointense on T1-weighted images and hyperintense on T2-weighted images. However, in T1-weighted images, areas of high signal intensity may be seen within the tumor, which correspond to hemorrhagic tissue on pathologic analysis. If a pseudocapsule is present, it will be of low signal intensity on both T1- and T2-weighted images (Chowdhary et al. 2004).

4.1.6.2.5
Metastatic Lesions

Neuroblastoma, Wilms tumor, and lymphoma are the major tumors of childhood that spread to the liver. Metastatic tumors can also be classified as hypervascular or non-hypervascular metastatic tumors. Hypervascular metastatic tumors include carcinoid tumors, pancreatic islet tumors, melanomas, choriocarcinomas, pheochromocytomas, thyroid carcinoma and renal cell carcinomas. These tumors will show an intense enhancement on CT and MR images, with usually low signal intensity on T1-weighted images and high signal intensity on T2-weighted images. Metastatic neuroblastoma will be seen on US as small hypoechoic lesions within the liver parenchyma (Kirks and Griscom 1998; Lack et al. 1991; Brody et al. 1989; Weinreb et al. 1984) (Fig. 4.12).

4.1.7
Hepatitis

Hepatitis is a general term that refers to acute or chronic inflammation of the liver. This condition may result from various infectious and noninfectious etiologies. Infectious etiologies include viral, bacterial, fungal, and parasitic organisms (Gazelle et al. 1998; Suchy 2003; Kirks and Griscom 1998).

4.1.7.1
Viral Infection

Usually hepatitis is caused by a viral infection, mostly hepatitis virus type A and B; however, hepatitis C, D, E and other viruses such as CMV, Epstein Barr, herpes, and AIDS-HIV may also be involved. The clinical manifestations depend on the insult with jaundice, nausea, vomiting, and pyrexia commonly seen.

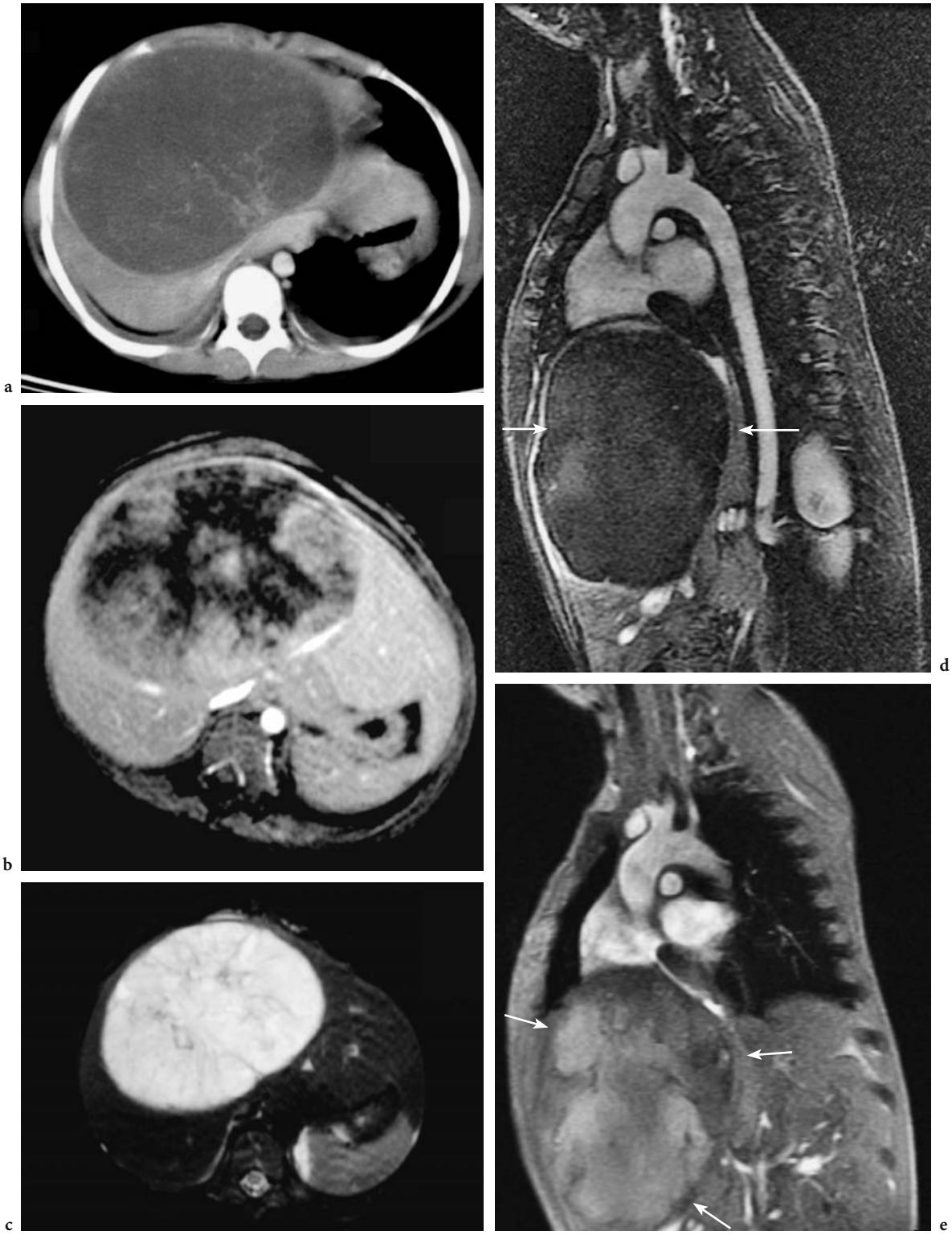

Fig. 4.11a–e. Embryonal rhabdomyosarcoma of the biliary tree. **a** CT reveals a large mainly cystic mass. **b,c** Pre- and post-contrast MR images show irregular yet florid enhancement. **d,e** Thrombus is shown in the hepatic veins secondary to the obstructing lesion

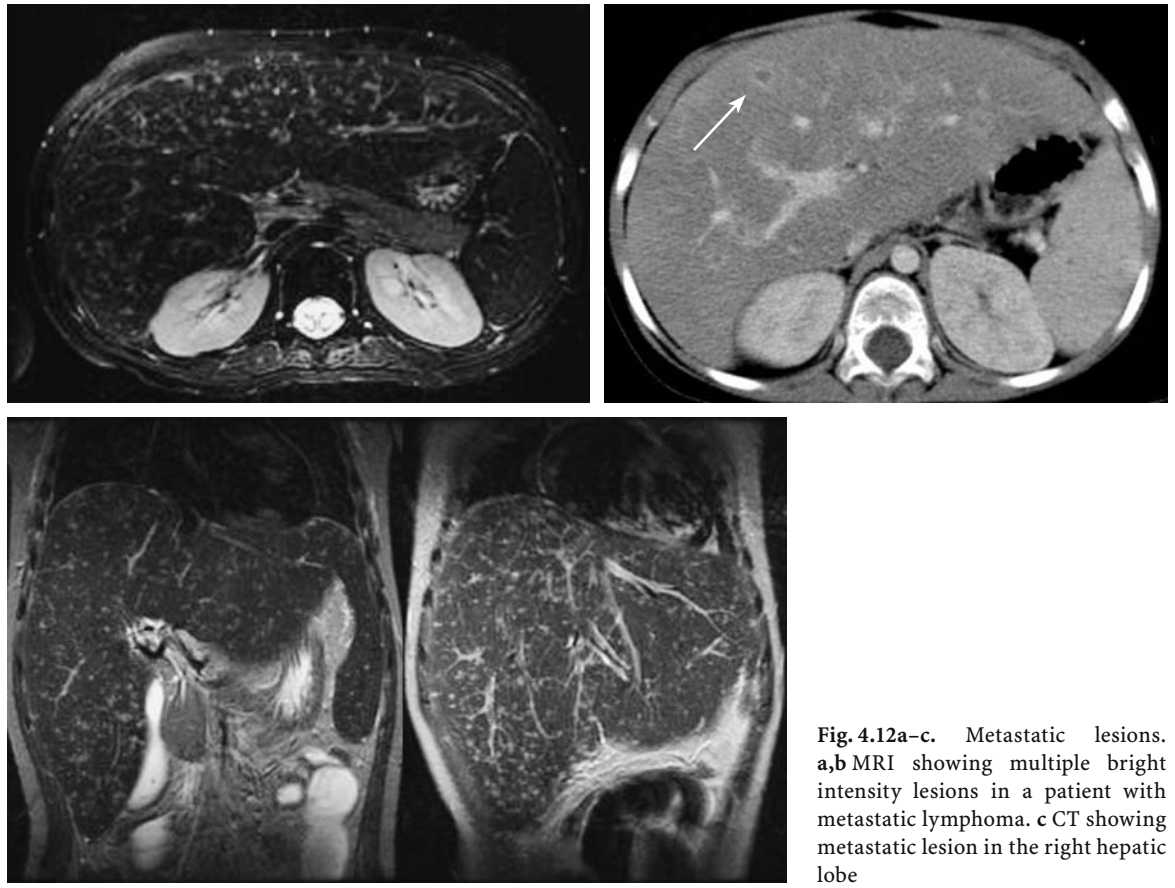

Fig. 4.12a–c. Metastatic lesions. **a,b** MRI showing multiple bright intensity lesions in a patient with metastatic lymphoma. **c** CT showing metastatic lesion in the right hepatic lobe

On US the liver will usually have a normal echo signal. However, in severe cases, the hepatocytes will swell and fatty infiltration will occur, and this may appear as a hyperechoic liver with increased echoes in the portal vein radicles. The gallbladder wall may be thickened and an increase in the size of the lymph nodes around the portal vein and around the cystic duct may be visualized.

Children with chronic hepatitis will initially have a hypoechoic liver that will advance to a heterogeneous liver and finally to a small liver with a hyperechoic signal.

On CT, livers with acute hepatitis are usually heterogeneous in attenuation, with areas of low attenuation due to the presence of edema and lymphocytic portal infiltration. Areas of nodular regeneration will have high attenuation on unenhanced CT and low attenuation after contrast injection. Necrotic areas will be seen as low attenuation areas on unenhanced CT, and will show higher attenuation than surrounding parenchyma on contrast CT. Enlarged lymph nodes close to the hilum or hepatogastric ligament may also be present.

In 80% of patients with acute hepatitis, MRI may demonstrate areas of high signal intensity close to the periportal region on T2-weighted images. Necrotic tissue may be seen in fulminant hepatitis and will have high signal intensity on T2-weighted images and low signal intensity on T1-weighted images. After an episode of fulminant hepatitis, peripheral regeneration in the liver will be seen as nodular areas of high signal intensity on T1-weighted images and low signal on T2-weighted images.

4.1.7.2 Bacterial Infection

Pyogenic liver abscess is a rare disease in the pediatric patients with an incidence of 25 per 100,000 hospital admissions; however, it has a high mortality rate, especially in immunocompromised patients, patients with multiple (or ruptured) abscesses, and patients with chronic granulomatous disease.

Patients usually present with fever, abdominal pain, right upper quadrant tenderness, and hepatomegaly. Although the principal etiologic agent involved is

Staphylococcus aureus in immunocompromised and immunocompetent patients, other organisms such as Streptococcus, Escherichia coli, Klebsiella, pseudomonas, and proteus anaerobic bacteria are also common. Diagnosis is by aspiration or biopsy.

Elevation of the right hemidiaphragm, infiltration, atelectasis, and pleural effusion is often seen on conventional radiography.

US examination is the primary imaging tool for evaluation of immunocompromised patients with intrahepatic or extrahepatic abscess. Usually, pyogenic liver abscesses are localized in the posterior right lobe, and will be seen as hypoechoic lesions with ill-defined borders and good sound transmission in 75% of cases. Image characteristics can vary from a sonolucent to echogenic mass; the wall can be thick or thin and/or ill defined (containing fluid or gas/air).

CT will define the abscess cavity well, and also allows for evaluation of the ductal system.

On MRI, a hepatic cyst will be evident if the lesion is greater than 5 mm. Usually, MRI will demonstrate a low signal intensity lesion on T1-weighted images and high signal intensity lesion compared to the surrounding liver on T2-weighted images. Absence of signal inside the lesion will represent air, and low signal intensity signal on T2 inside the abscess may correspond to protein debris. In post-contrast images, the abscess will be seen as a low signal intensity mass with a peripheral ring with high intensity signal. Some necrotic or cystic tumors may resemble hepatic cyst. Diffusion weighted MRI has been used to differentiate these lesions: liver abscesses will typically show hyperintensity on DW images and hypointensity on ADC maps, while cystic or necrotic tumors will show hypointensity on DW images and hyperintensity on ADC maps (Chan et al. 2001).

4.1.7.3 Fungal Infections

Fungal infections of the liver are very rare in normal patients. They are more typically seen in immunocompromised patients secondary to chemotherapy or AIDS-HIV.

The clinical presentation will vary depending on the area of infection and the systems involved. Symptoms such as fever, abdominal pain, hepatomegaly or splenomegaly may be present but are very unspecific. Candida is the most common etiological agent isolated in these patients. Other etiologic agents include aspergillus, cryptococcus, and mucormycosis.

US may demonstrate different patterns of hepatic lesions depending on the stage of the disease. In acute candidiasis, an echogenic lesion with a peripheral hypoechoic rim may be seen, while in the healing stage the lesion will be pure echogenic with varying intensity of the posterior acoustic shadow, the so-called "wheel-within-wheel" appearance.

On CT, hepatic candidiasis may be seen as a non-enhancing low attenuation lesion within both lobes of the liver and spleen. Sometimes a central high attenuation foci may be seen and represent the candidal hyphae. Some of these lesions may also show rim enhancement (Fig. 4.13).

MRI has replaced the liver biopsy in the evaluation and diagnosis of immunocompromised patients with a suspected fungal infection in the liver. Liver candidiasis will be encountered as discrete areas of high signal intensity on T2-weighted images with a progressive decrease in the signal intensity as the lesion is treated (Siegel 2001b; Sallah et al. 1998).

4.1.7.4 Parasitic Disease

4.1.7.4.1 Hydatid Cysts

The two most prevalent subtypes of hydatid disease are: a unilocular cyst caused by Echinococcus granulosus (worldwide prevalence) and will have a right lobe localization; and a multilocular cyst caused by E. alveolaris (northern hemisphere only) (Czermak et al. 2001). Children usually become infected through exposure to canine feces or by eating food contaminated with tapeworm eggs, which hatch in human small intestine under the influence of gastric and intestinal secretions.

An abdominal mass with pain is a common manifestation. Loss of appetite is a frequent symptom, and weight loss and weakness may occur. Approximately 80% of hydatid cysts will be localized in the liver, and may compress the porta and biliary ducts producing jaundice or cholangitis.

Hepatic echinococcal cysts have been classified into four groups based on US findings: type I is a simple anechoic fluid-filled cyst; type IR is a cyst with undulating membrane secondary to rupture; type II is a cyst with a daughter cyst, and type III is a densely calcified, echogenic cyst with shadowing. It has been proposed that the natural progression is from type I to III.

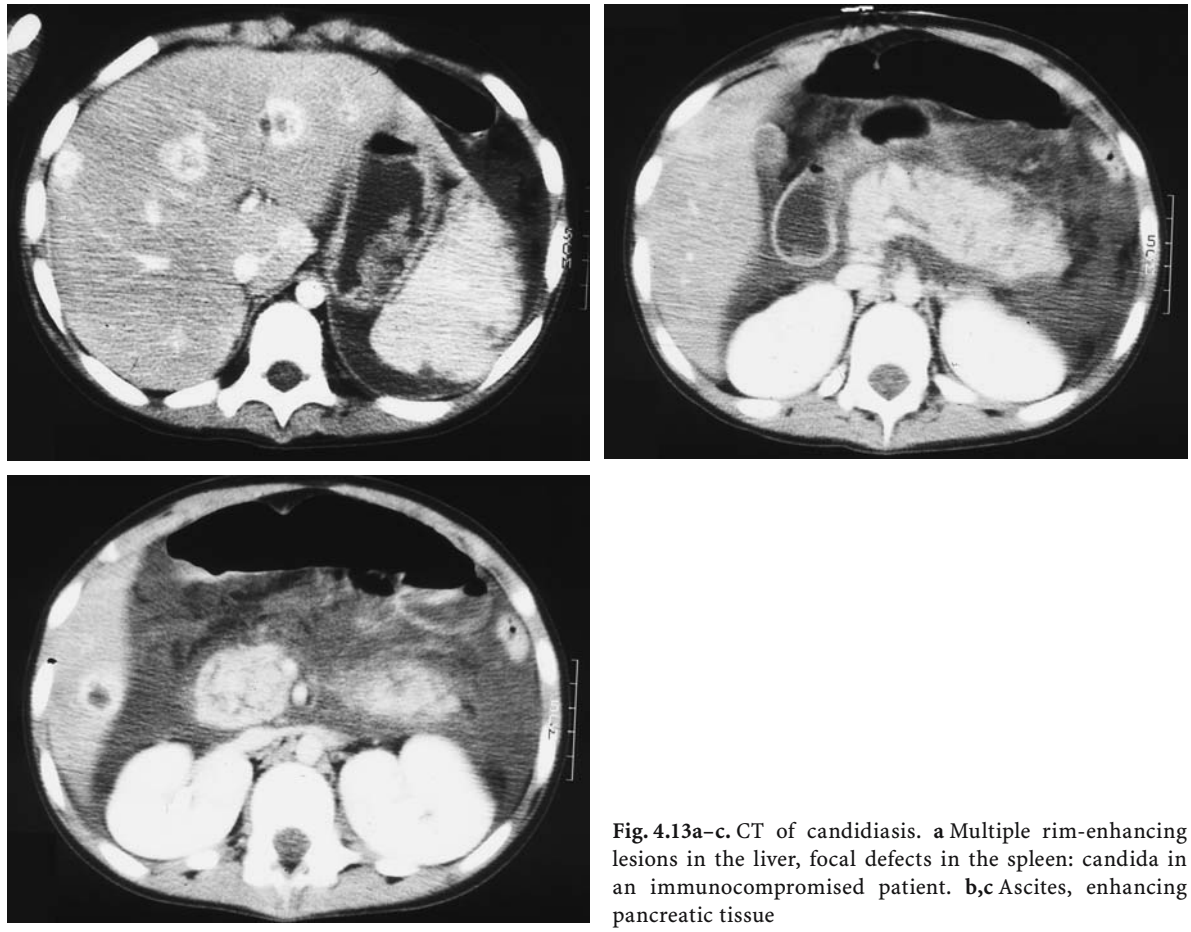

Fig. 4.13a–c. CT of candidiasis. **a** Multiple rim-enhancing lesions in the liver, focal defects in the spleen: candida in an immunocompromised patient. **b,c** Ascites, enhancing pancreatic tissue

On CT, E. granulosus cysts appear as well-demarcated thin or thick walled hypo-attenuating structures. CT can identify the small dissections of the parasitic fluid into the pericystic space with collapse of the parasitic membrane. This is pathognomonic of E. granulosus and has been called the "snake" sign because of the undulated membrane appearance. Peripheral calcifications may be seen in advanced stages.

Hydatid cyst can be identified on MRI as unilocular structures with low signal intensity inside the cyst on T1-weighted images. At the bottom of the cyst a structure with intermediate signal intensity can be visualized and it represents the hydatid sand. On T2 sequences, the cyst will have high signal intensity with a low intensity rim surrounding the lesion. Typically, a mother cyst will have greater signal intensity than a daughter cyst. In some patients, the unilocular cyst will have an increased intensity inside the cyst on T1-weighted images, which corresponds to proteins and lipids (Kuhn et al. 2004).

4.1.7.4.2 Amebiasis

Amebiasis is a parasitic infection caused by the protozoon *Entamoeba histolytica*. It is the third leading parasitic cause of death worldwide, surpassed only by malaria and schistosomiasis. *Amebiasis* can localize in many different locations besides the bowel. One of the most common extraintestinal manifestations is the amebic liver abscess, which usually occurs in children less than 3 years of age, with a peak incidence in the first year of life (Elizondo et al. 1987; Giovagnoni et al. 1993).

The child will present with abdominal pain, fever, and hepatomegaly at the initial examination. An acute abdomen may be the initial manifestation of a ruptured amebic abscess in some patients; however, this is very uncommon.

US is preferred for the evaluation of amebic liver abscess because of its low cost, rapidity, and lack of adverse effects (Kuhn et al. 2004). Amebic abscess

can be identified on US as hypoechoic lesions with good sound transmission through the cyst. Sometimes it may be difficult to differentiate between amebic versus pyogenic abscesses by US. However, amebic abscesses are usually multiple and in very close proximity to one another. They have a central area of liquefaction that will be seen on US as a central hypoechoic area. Some are more likely to have a peripheral halo and better defined borders compared to pyogenic abscesses.

CT may demonstrate multiple cysts adjacent to the liver capsule, with ill-defined margins.

On MRI, a well-defined lesion with heterogeneous signal intensity on T1-weighted images and with high signal intensity on T2-weighted images can be identified. Some abscesses may show a peri-lesional rim with increased signal intensity that corresponds to edema. After treatment the abscesses are typically seen as homogeneous lesions with low signal intensity on T1-weighted images, and with concentric rims and decreased of edema on T2-weighted images.

4.2 The Pancreas

4.2.1 Anatomy and Embryology

There are differences between the pancreas in adults and children. In children, the pancreas will be considered enlarged if the pancreatic neck is bigger than 1.5 cm in its anteroposterior diameter. The anteroposterior measurement of the head and body should be similar and not exceed 1 cm in the newborn and 2 cm in the adolescent and it is usually more transverse in orientation allowing oblique US scans a nice view of the whole gland (Kuhn et al. 2004).

The normal pancreas will form at week 6 from the rotation and fusion of the ventral and dorsal buds. The ventral bud will constitute the posterior and inferior part of the pancreatic head and the uncinate process, while the dorsal bud will constitute the body, tail, and the anterior head. During the 7th week, the main pancreatic duct of Wirsung and the accessory duct (Santorini) will fuse and migrate to the papilla of Vater, close to the common bile duct.

Deviation of this process will result in different congenital anomalies of the pancreas. For instance, in some patients, the pancreatic ducts will not connect. In these patients the duct of Santorini will drain the main portion of the pancreas into the papilla minor, while the main pancreatic duct of Wirsung will drain only the posterior and inferior portion of the head and uncinate process in the duodenum through the papilla major after joining the common bile duct. This congenital anomaly is called a pancreas divisum (Fig. 4.14).

4.2.2 Congenital Anomalies

Congenital anomalies of the pancreas are typically incidental findings. In few patients are these anomalies associated with important clinical symptoms.

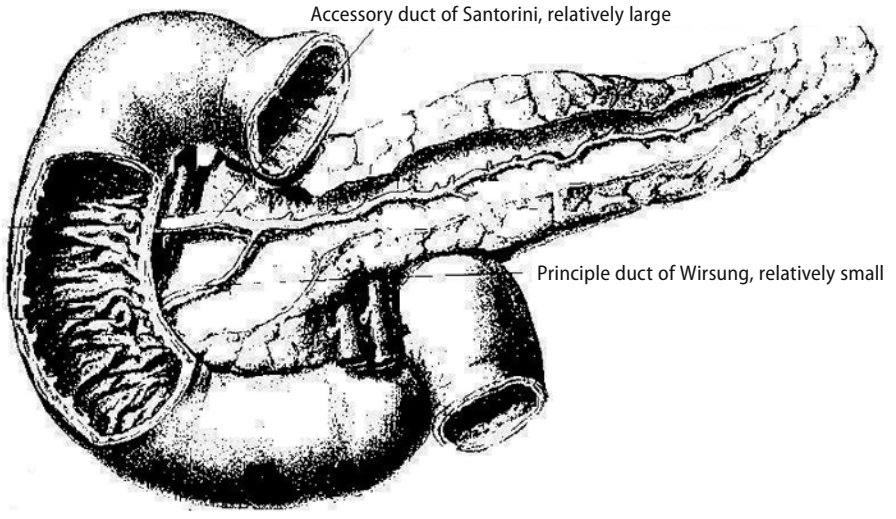

Fig. 4.14. Scheme of the anatomy and relationship of the pancreatic in pancreas divisum. Note the reversal of the relative size of the ducts. (Drawing adapted from F.N. Netter [1964] The Netter Collection of Medical Illustrations-Digestive System-part III)

4.2.2.1 Annular Pancreas

An annular pancreas is the result of an abnormal fusion of ventral and dorsal buds during the 6th week of embryogenesis. These patients will have a "ringed" pancreas surrounding the duodenum that, with growth, may lead to narrowing of the descending duodenum. These patients may present in the newborn period with complete duodenal obstruction, often after the first feeding. Some symptoms include polyhydramnios in utero, feeding intolerance in newborns, vomiting or recurrent pancreatitis. Other anomalies such as esophageal atresia, tracheoesophageal fistula, duodenal stenosis, duodenal atresia, trisomy 21, and malrotation have been associated with annular pancreas (Gazelle et al. 1998).

In annular pancreas, the duodenum is often compressed at a point distal to the ampulla of Vater, making bilious vomiting a hallmark symptom. Abdominal distention is typically not a feature because of the proximal location of the obstruction. Patients may not pass meconium, or bowel movements may cease abruptly. A more insidious form of chronic partial duodenal obstruction may also occur.

In neonates, plain radiographs may reveal a spectrum from a "double-bubble" sign with little or no air in the distal bowel to a normal plain film abdomen. This radiographic finding correlates with a high gastrointestinal obstruction such as malrotation/midgut volvulus, duodenal atresia, and duodenal web (Gazelle et al. 1998) (Fig. 4.15a).

US may show an enlarged pancreatic head or a solid band of pancreatic tissue around the (possibly dilated) duodenum with gastric dilatation (Gazelle et al. 1998).

On CT, an annular pancreas (with or without pancreatitis) may be seen as enlargement of the pancreatic head, surrounding the second portion of the duodenum. Follow up CT may demonstrate calcifications limited to the annulus of the pancreas (Gazelle et al. 1998).

On ERCP, various ductal configurations may be seen. A classification of six types of annular pancreas according to the site into which the duct of the annulus drains has been reported (Gazelle et al. 1998).

On MRI, the normal pancreatic tissue has higher signal intensity compared with other tissues on T1-weighted images with fat saturation. This signal is due to the high concentration of proteins inside the acini. An annular pancreas will be seen on MRI as

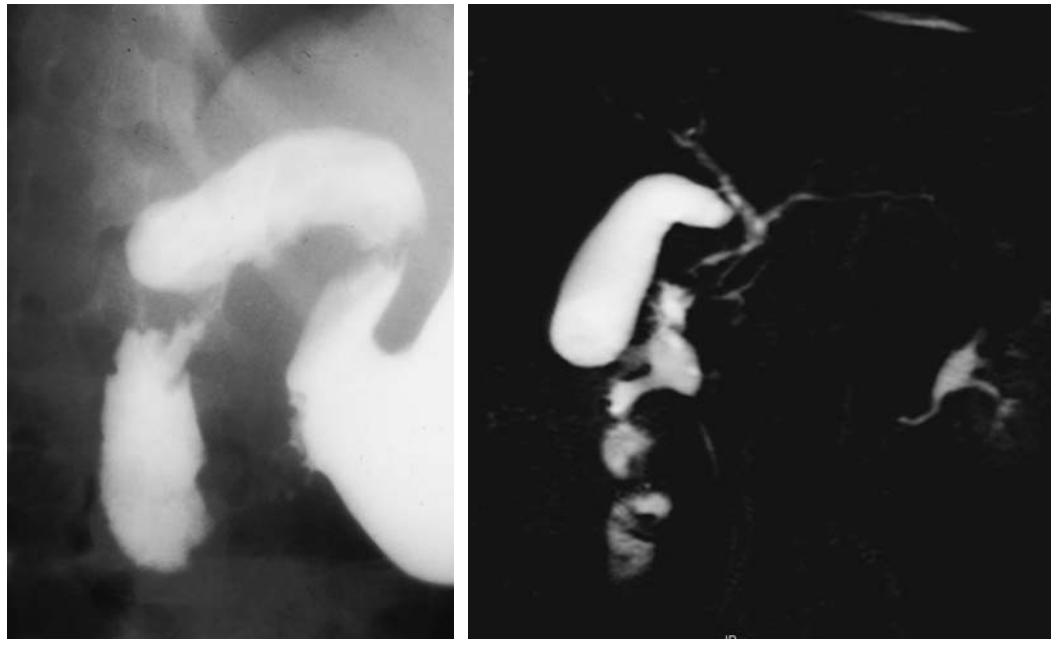

a b

Fig. 4.15. a Classic UGI image of annular pancreas. **b** MRCP image of an annular pancreas causing relative obstruction of the descending duodenum

a high signal intensity tissue encircling the second part of the duodenum (Fig. 4.15b). MRCP has been used to classify the annular pancreas according to the different duct subtypes and to evaluate the concomitant presence of pancreas divisum (Nijs 2005; Chevallier et al. 1999).

4.2.2.2 Ectopic Pancreas

Ectopic pancreas is described as the presence of pancreatic tissue without an anatomic or vascular connection with the pancreatic body. This ectopic tissue may be localized anywhere in or outside of the gastrointestinal tract. Common sites in the gastrointestinal tract are the stomach, duodenum, and the proximal jejunum, and less commonly in the appendix, the diverticulum of Meckel in 5% of cases, or the ileum in just 1% of cases. Extraintestinal localization, such as in the wall of the gallbladder, the bile ducts in the liver, the hilum of the spleen, the omentum, the perigastric or periduodenal area, may be seen in only 4% of cases (Gazelle et al. 1998).

If the ectopic pancreatic tissue is localized in the stomach or duodenum it may be detected on a barium study as a small broad-based submucosal mass with central umbilication. This central umbilication corresponds to remnants of pancreatic ducts. The "bull's eye" appearance represents barium accumulation inside these remnants (Gazelle et al. 1998).

Better delineation of ectopic pancreas may be seen on CT as a round mass with a variation of borders in the antral wall of the stomach; a localization in the fundus is very unusual. After contrast injection the ectopic pancreatic tissue will enhance with a similar pattern to the normal pancreas. Cystic dilation of an ectopic pancreatic duct, ectopic pancreatic tissue in the perigastric fat, or malignant transformation of ectopic pancreas have been described but are rarely seen (Cho et al. 2000).

4.2.2.3 Pancreas Divisum

Pancreas divisum is the most common congenital anomaly of the pancreatic duct system. It arises from an incomplete fusion of the dorsal and ventral pancreatic ducts. The incidence of pancreas divisum at autopsy ranges between 4.7% and 11%, but in patients with unexplained pancreatitis the incidence can be as high as 25.6%. Multiple attacks of pancreatitis with severe and intermittent epigastric pain but with normal amylase levels are common manifestations of pancreas divisum. Affected children are usually between 5–18 years of age (Gazelle et al. 1998).

ERCP is a very useful tool for the evaluation of pancreas divisum. It will show a short duct of Wirsung, limited to the head of the pancreas, without filling of the main pancreatic duct. The accessory papilla can be cannulated and the accessory duct of santorini draining the residual part of the gland will be found.

Absence of union between the dorsal and ventral ducts, with a ventral duct directly entering the common bile duct, will be encountered on thin-section CT (Fig. 4.16a).

The ductal abnormality in pancreas divisum may be diagnosed by MRCP often only after secretin stimulation (S-MRCP) (Fig. 4.16b,c). The duct of Santorini may be enlarged and the pancreas may demonstrate the characteristic features of pancreatitis. However, the detection of pancreas divisum at S-MRCP might be more difficult when stones or strictures are present in the ventral or dorsal pancreatic ducts (Manfredi et al. 2000).

4.2.2.4 Pancreatic Agenesis, Hypoplasia, and Dysplasia

Complete agenesis of the pancreas is usually incompatible with life. Therefore, pancreatic aplasia or hypoplasia is uncommon in humans. Patients with pancreatic hypoplasia will have a normal development of the pancreas in size and shape but later in life will have a replacement of the glandular elements with fatty tissue. Some of these patients will present with an abnormal exocrine pancreatic insufficiency and normal endocrine function. Children with syndromes such as Schwachman-Diamond, Beckwith-Wiedemann, polysplenia bilobed lungs, and congenital heart disease have a higher relative risk of hypoplasia of the pancreas (Gazelle et al. 1998).

4.2.2.5 Cystic Fibrosis

Cystic fibrosis (CF) is a common autosomal recessive disorder of the sodium and chloride channels, and it is characterized by dysfunction of exocrine glands and secondary failure to thrive, frequent foul stools and pancreatic insufficiency. The damage to

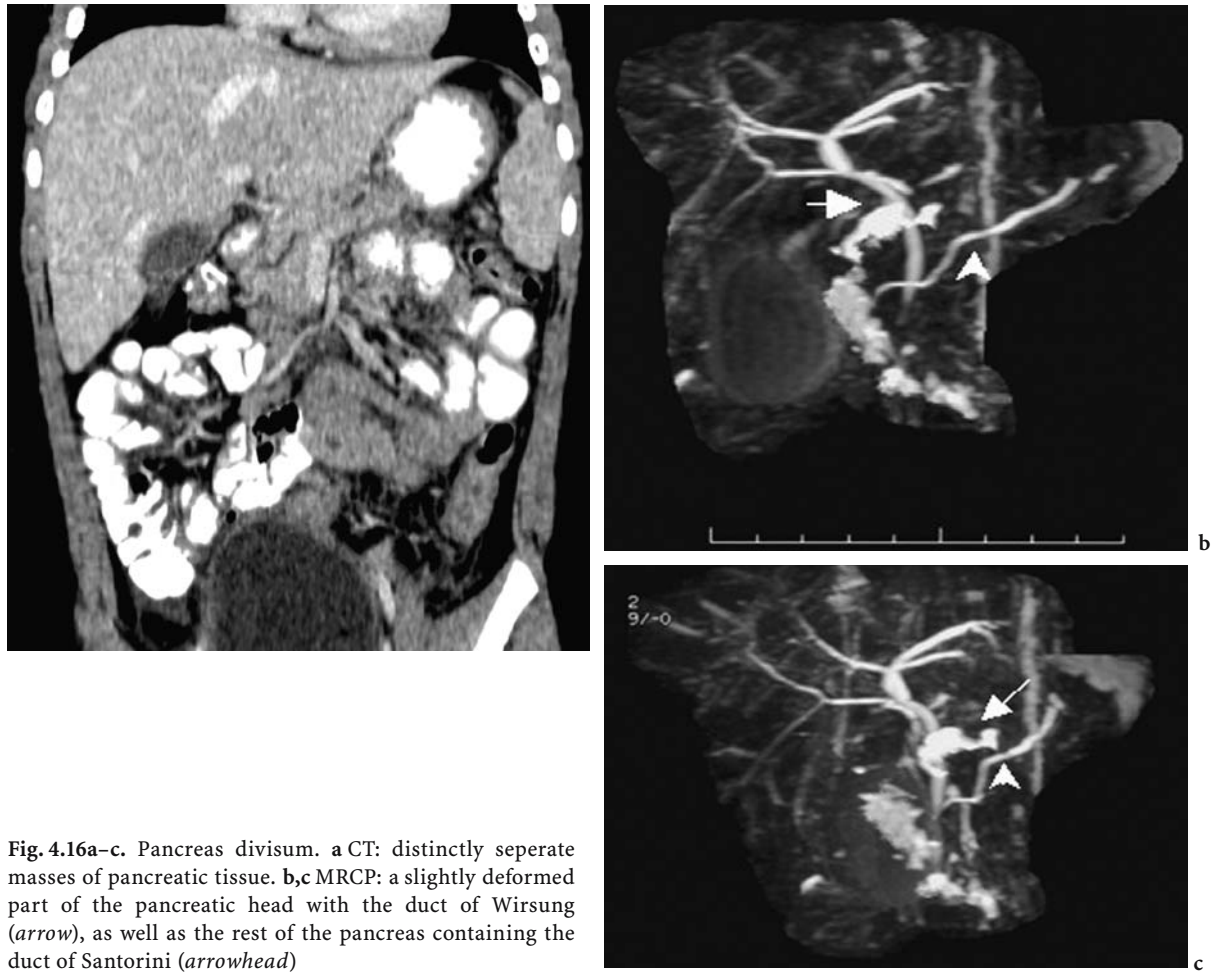

Fig. 4.16a–c. Pancreas divisum. **a** CT: distinctly seperate masses of pancreatic tissue. **b,c** MRCP: a slightly deformed part of the pancreatic head with the duct of Wirsung (*arrow*), as well as the rest of the pancreas containing the duct of Santorini (*arrowhead*)

the pancreas starts in utero, with a progressive dilatation of the acini and pancreatic ducts with secondary fibrosis and fatty replacement. Microscopic findings will include atrophy and cyst formation of the pancreatic stroma before the first year of life.

On US, the pancreas with CF is characteristically of an echogenic texture secondary to fatty infiltration (Fig. 4.17). An enlarged pancreas may be seen initially with a subsequent atrophy later in life. Pancreatic duct dilatation and calcifications may be seen. Small cysts (anechoic areas) without vascular communication can be identified. Although a hyperechogenic pancreas is very typical of CF, some other diseases such as Schwachman-Diamond syndrome (exocrine pancreas insufficiency associated with bone marrow dysfunction, cyclic neutropenia, metaphyseal diastasis and growth retardation), hemosiderosis, chronic pancreatitis, and administration of steroids may also reveal this feature (Feigelson et al. 2000).

CT may demonstrate an atrophic, fatty pancreas with heterogeneous attenuation. Areas of low attenuation will correspond to cysts, while areas of high attenuation will represent calcifications. Partial or total fatty and fibrous replacement are also commonly seen in these patients. There may be a correlation between the degree of fatty infiltration and the pancreatic exocrine dysfunction (Feigelson et al. 2000).

MRI of CF can depict four different patterns. In the first pattern, a diffuse, high signal intensity with lobular features will be seen; the second will show a diffuse homogeneous hyperintensity without lobular features; in the third, the pancreas will have high signal intensity with focal areas of no change in signal intensity; and in the fourth, a normal pancreas might be observed. In some cases the multiple cysts can be seen throughout the entire gland, replacing the normal tissue. This feature has been called pancreatic cystosis (Feigelson et al. 2000).

4.2.2.6 Von Hippel-Lindau Disease

Von Hippel-Lindau disease (VHL) is an autosomal dominant condition secondary to an alteration in a tumor suppressor gene on chromosome 3. It has incomplete penetrance and is characterized by hemangioblastomas in the retina, CNS, renal cell carcinoma, endolymphatic sac tumors, pheochromocytomas, papillary cystadenoma of the epididymis, angiomas of the liver and kidney, cysts of the liver, kidney and epididymis, and pulmonary arteriovenous shunts (Fig. 4.18a–c). In the pancreas, VHL may have multiple presentations, the most common being the presence of multiple small pancreatic cysts with calcifications in 40% of cases. Serous cystadenomas, solid nonfunctional islet cell tumors, and adenocarcinoma are less common (Richard et al. 2004).

US will reveal pancreatic cysts. On CT these cysts will have lower attenuation than the normal pancreatic parenchyma, and calcifications might be seen with unenhanced and enhanced CT (Choyke et al. 1990; Hough et al. 1994).

On MRI, clusters of cyst may be resemble microcystic adenoma of the pancreas; however, this lesion is most commonly found in adult patients. Microcystic adenomas show high signal intensity on T2-weighted images and are lobulated, with internal septations. Blood inside the cyst may be seen on T1-weighted images as high signal intensity lesions. Post-gadolinium images will show enhancement of the septations (Tattersall and Moore 2002).

4.2.2.7 Pancreatic Cysts

The pancreatic cyst can be congenital or acquired and can be subclassified depending on the epithelium lining the cyst. Congenital pancreatic cysts may present as solitary, multiple, or alimentary tract duplications. Von Hippel-Lindau syndrome, trisomy 9, tuberous sclerosis, Meckel-Gruber syndrome, and polycystic kidney disease have been associated with multiple congenital cysts. These cysts may be numerous and can transform the pancreas into a cystic mass (Gazelle et al. 1998; Baker et al. 1990) (Fig. 4.18d,e).

Solitary congenital cysts may be the least common cystic pancreatic lesion, with only 25 documented cases having been reported. Two additional patients were identified on prenatal US scan. Patients with pancreatic cysts may present with an asymptomatic mass upon physical examination or a symptomatic mass with abdominal distension.

CT and US may demonstrate a low attenuating lesion or an anechoic defect typically located in the tail of the pancreas. This lesion can be unilocular or multilocular with multiple septae. The differential diagnosis includes cyst of renal origin, as well as choledochal, mesenteric, ovarian, and urachal cysts. ERCP and HIDA scans can be used to identify communication with the pancreatic duct or biliary tree.

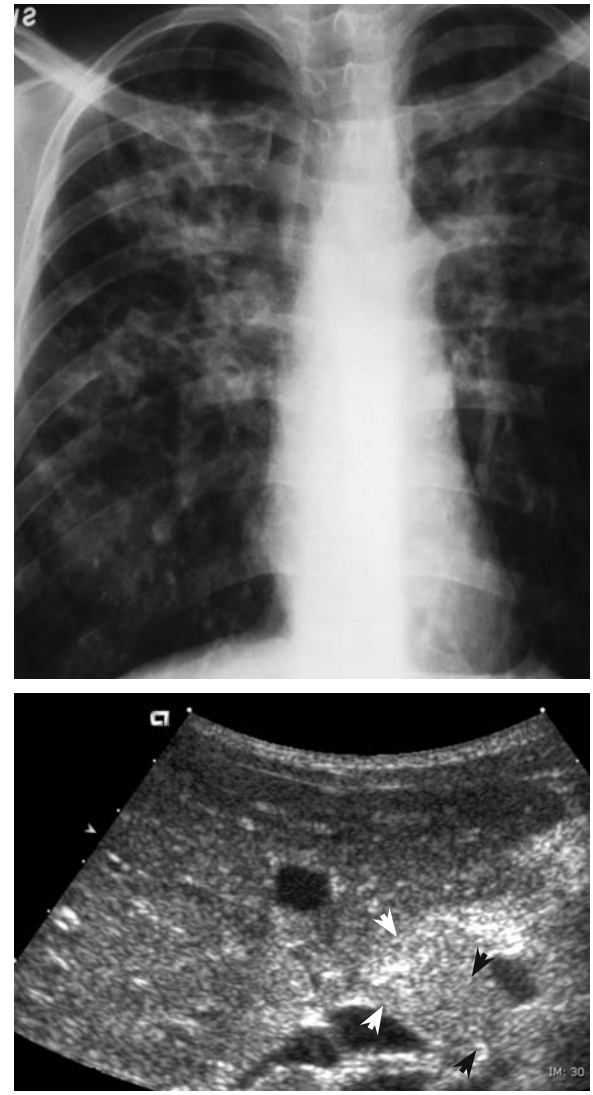

a

b

Fig. 4.17a,b. Cystic fibrosis. **a** Classic chest radiograph. **b** Echogenic pancreas on US (*arrowheads*)

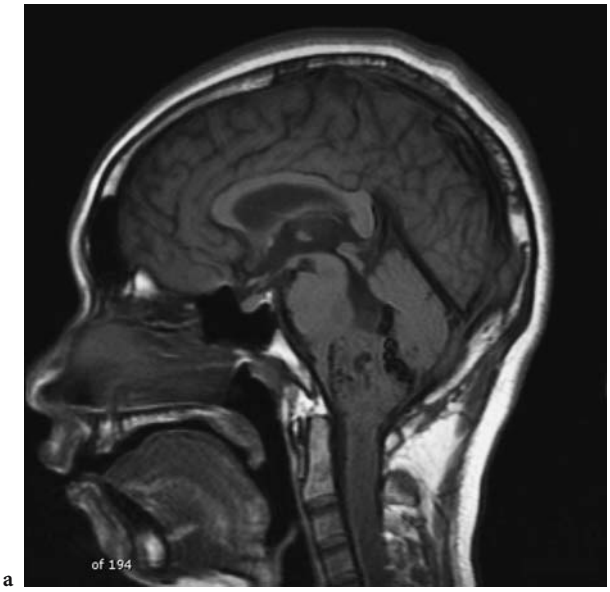

a

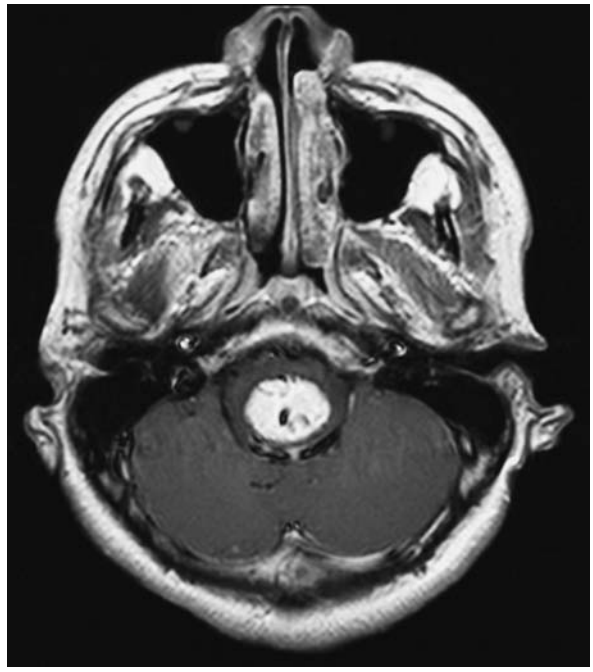

b

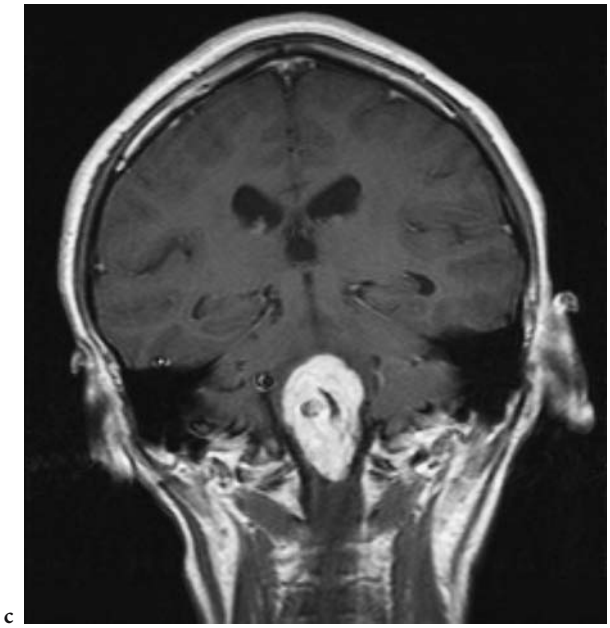

c

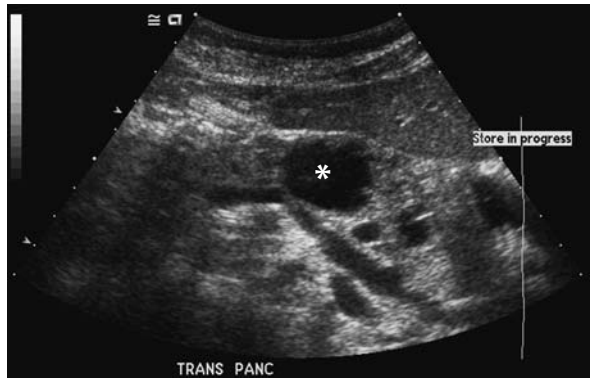

d

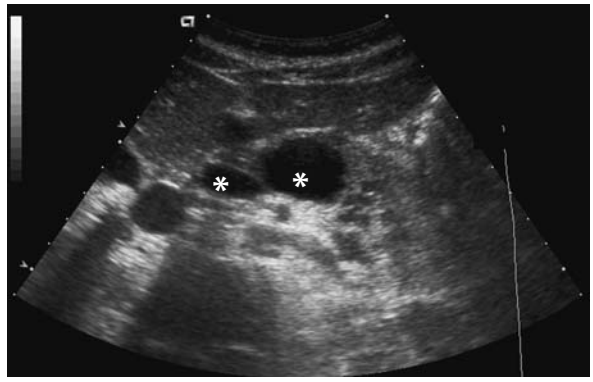

e

Fig. 4.18a–e. Von Hippel-Lindau. **a–c** MRI: Inhomogeneous hemangioblastomas in the pons. **d,e** US: multiple cysts of varying sizes in the pancreas (*asterisks*)

On the other hand, pancreatic pseudocysts represent the most common cystic masses in the pancreas. Pseudocysts are usually fluid collections with a thick wall that arise secondary to infections or trauma. Differentiation between a true cyst and a pseudocyst by imaging is very difficult and can only be done by microscopic examination.

4.2.3 Pancreatic Neoplasia

In the pediatric population, pancreatic tumors are very unusual entities. They account for less than 5% of all malignancies in children. These tumors may arise from the exocrine or endocrine pancreas. Exocrine neoplasias include ductal adenocarcinoma, acinar adenocarcinoma, pancreaticoblastoma, or infantile adenocarcinoma. Endocrine tumors or islet cell tumors are named after the hormone produced, with insulinoma being the most common in children (Walker 1996).

4.2.3.1 Carcinoma of Exocrine Pancreas

4.2.3.1.1 Adenocarcinoma

Adenocarcinoma of the pancreas in childhood is exceedingly rare, with the majority of patients diagnosed between 3 and 18 years. Abdominal pain and mass are the most common manifestations in the initial exam. This tumor has a bad prognosis in children, and patients with Peutz-Jeghers syndrome have been associated with a higher risk (×100-fold) of pancreatic adenocarcinoma.

On US, pancreatic adenocarcinoma will be seen as a heterogeneous mass with hyperechoic and anechoic areas. Involvement of the vessels can be identified on US.

CT may demonstrate a mass with heterogeneous density, due to cystic elements, hemorrhagic tissue, loss of fat planes, dilatation of bile and pancreatic ducts.

ERCP is useful in the evaluation of a small mass causing obstruction of the ductal system. MRCP is as sensitive as ERCP and may prevent inappropriate explorations of the pancreatic and bile ducts in patients with suspected pancreatic carcinoma in whom interventional endoscopic therapy is unlikely (Gazelle et al. 1998; Chung 2006).

4.2.3.1.2 Pancreaticoblastoma

Pancreaticoblastoma, or infantile adenocarcinoma, is a rare tumor in children (Montemarano et al. 2000; Roebuck et al. 2001). It usually presents in the fourth year of life with males being more affected than females. This tumor commonly arises from the head or tail of the gland, and has been associated with Beckwith-Wiedemann syndrome. Microscopic analysis will show proliferation of poor differentiated squamous cells surrounded by a fibrous capsule. Although it has a better prognosis than the adult adenocarcinoma, metastases can occur and are commonly present at the time of the initial exam or diagnosis. Common sites for metastases include the liver and lymph nodes. Lung and brain metastasis are rarely seen. Usually, vanillylmandelic acids (VMA) are not elevated but the alpha-fetoprotein is.

US evaluation may show a large mass with hemorrhage, necrosis, and degeneration within the tumor.

On CT, a well-defined mass with multiple lobules and septal enhancement after contrast injection may be found. The tumor may encase mesenteric vessels and the inferior vena cava. A complex mass with areas of hyperechogenicity and hypoechogenicity may also be seen.

On MRI, pancreatoblastomas are heterogeneous lesions with predominant low signal intensity on T1-weighted images and high signal intensity on T2-weighted images. After contrast injection, the tumor will reveal intermediate signal intensity and will be isointense compared with the spleen on T1-weighted images, with lower signal intensity relative to the spleen on T2-weighted images. In some patients, MRCP has been used to define and determine the level of obstruction of the biliary system.

4.2.3.1.3 Frantz Tumor

Solid-pseudopapillary tumor of the pancreas (SPT), the so-called Frantz tumor, is an exceptionally rare neoplasm in children almost exclusively seen in adolescent girls. Its origin remains enigmatic. It is of low malignant potential. Although SPT is a rare differential diagnosis of a pancreatic mass in children, it is mandatory to establish this diagnosis since complete surgical removal of the tumor (even in case

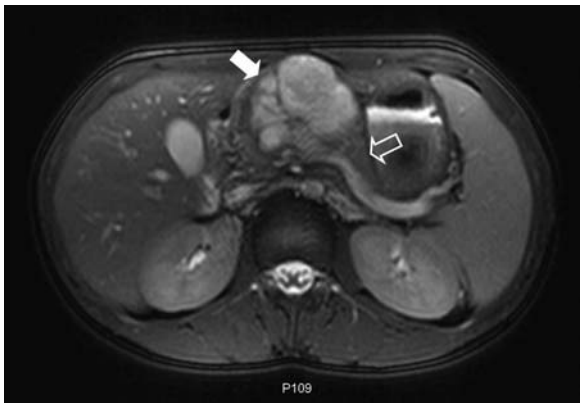

Fig. 4.19. Frantz Tumor

of metastases or local invasion) offers an excellent prognosis (Rebhandl et al. 2001) (Fig. 4.19)

4.2.3.2 Endocrine Pancreatic Neoplasia

Neoplasias that arise from the endocrine portion of the pancreas can be classified as secretory or non-secretory (Gouya et al. 2003). When secretory, the endocrine tumor will be subclassified according to the type of hormone produced (insulin hormone, gastrin hormone, or active peptides). Insulinomas are the most common endocrine tumors, while glucagonomas or somatostatinomas have not been reported in children.

Nesidioblastosis is a hyperplasia of primitive pancreatic islet cells, i.e., B cells secreting insulin, and may be responsible for 5% of cases of hyperinsulinism and hypoglycemia in pediatric patients.

The clinical presentation of patients with endocrine pancreatic tumors will vary according to the type of hormone released. Hyperinsulinism manifested with diarrhea, abdominal pain, and low levels of glucose will be found in the majority of patients. Nesidioblastosis is a primitive pancreatic B cells hyperplasia. Approximately 5% of patients with hyperinsulinism may have this type of tumor. Hunger, jitteriness, lethargy, apnea, and seizures are common manifestations in newborns with nesidioblastosis, while older children may show diaphoresis, confusion, or unusual behavior. Zollinger-Ellison syndrome will present with intractable peptic ulcers. Patients with vipomas will have watery diarrhea, hypokalemia, and achlorhydria, while multiple endocrine neoplasias have been reported with multiple endocrine neoplasia type 1 (MEN I).

Islet cell tumors are very difficult to visualize on US; however, sometimes small and well-defined hypoechoic round lesions with a hyperechoic capsule may be found.

On CT, an area of low attenuation with calcifications and disruption of the normal contour can be identified. On enhanced CT, the tumor will show a momentary enhancement that will be higher in the arterial phase compared with the portal venous phase.

On MRI, a low signal intensity mass compared to a high signal pancreas will be seen on T1-weighted fat suppressed spin-echo images. Because of the high vascular component of these tumors, they will appear on dynamic or contrast enhanced MR more hyperintense and with greater conspicuity than the normal pancreas.

4.2.4 Pancreatitis

Pancreatitis is defined as an inflammation of the pancreas, which can be classified as acute or chronic (Gazelle et al. 1998). Acute pancreatitis can be subclassified in acute interstitial (edematous) or acute hemorrhagic form. Typically, patients with pancreatitis will present with abdominal pain, nausea, vomiting, and elevation of the pancreatic enzymes in the acute form.

4.2.4.1 Acute Pancreatitis

In children, the incidence of acute pancreatitis is 2.7 cases per 100,000 children younger than 15 years. Many etiologic factors have been associated with pancreatitis in childhood, with the most common cause being blunt trauma. Other etiologies such as organ transplantation, malignancies, drug induced (valproic acid), biliary tract disease, viral infections, and idiopathic have been described. These etiologies are different from those seen in adults.

On US, an acute inflammation may show an increase in the duct calibers, with a diffuse swollen hypoechoic gland (Chao et al. 2000). Extrapancreatic fluid collections occur in about 50% of patients, mostly in the anterior pararenal space and this may be the only finding. Some studies have found a correlation between the diameter of the pancreatic duct and serum lipase level. Early US is a helpful tool for identification of stones in the biliary tract in jaundice patients, and Doppler US may diagnose splenic vein thrombosis.

CT may demonstrate duct dilatation, focal areas of low attenuation in the pancreatic parenchyma that correspond to fluid collections (King et al. 1995). Necrosis is recognized as a focal or diffuse area of non-enhancing pancreatic tissue. The pancreas can be enlarged or normal. Other findings include extrapancreatic fluid collections located in the anterior pararenal space, lesser sac, lesser omentum, and transverse mesocolon. Peripancreatic fat stranding and pancreatic pseudocyst are sometimes encountered (Geier et al. 1990).

It is not uncommon to find pancreatic pseudocysts after an episode of traumatic pancreatitis or chronic pancreatitis, and some pseudocysts complicating hemolytic uremic syndrome or mediastinal pseudocysts have been reported. CT will reveal a round hypodense structure with a thin or thick wall, which may enhance after contrast injection. Some of these pseudocysts can cause complications, presenting with obstruction of the common bile duct, infection, abscess formation, rupture of the pseudocyst, and can be responsible for splenic vein thrombosis or splenic hemorrhage. CT is the primary imaging tool to visualize and identify these complications (Geier et al. 1990).

MRCP is a very useful imaging tool used to identify possible etiologies of pancreatitis such as abnormal union of the pancreatobiliary junction, choledochal cyst, or pancreas divisum, in patients with unknown cause (Arcement et al. 2001; Hirohashi et al. 1997).

4.2.4.2 Chronic Pancreatitis

Chronic pancreatitis is a rare entity in children. Amongst the principal causes of chronic pancreatitis are hereditary pancreatitis, autoimmune conditions (sclerosing cholangitis), and CF. CT features of chronic pancreatitis include a focal or diffuse increase in pancreatic size, dilatation of the main pancreatic duct (almost always present), intraductal calcifications, or pseudocyst formation. ERCP can be used in children with unknown pancreatitis to identify and treat cases of biliary obstruction and structural cases of chronic pancreatitis.

4.2.4.3 Hereditary Pancreatitis

Hereditary pancreatitis is an autosomal dominant disorder that presents as a dysfunction of the pancreas (inflammation) during the first decade of life. Usually each episode will last between 2 days and 2 weeks. US will reveal a shrunken fibrotic pancreas with calcifications, and CT will show dilatation of the ductal system, pancreatic stones or pancreatic complications (Fig. 4.20). Approximately 15% of patients with hereditary pancreatitis may have pancreatic carcinoma in adulthood.

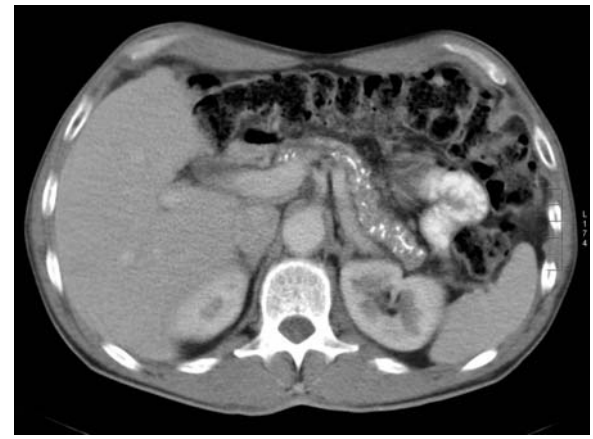

Fig. 4.20. Hereditary pancreatitis. CT image of shrunken pancreas with calcifications. The patient's father had a similar CT appearance

References

Arcement CM, Meza MP, Arumala S et al (2001) MRCP in the evaluation of pancreaticobiliary disease in children. Pediatr Radiol 31:92–97

Arrivé L, Tubiana JM (2003) Serial needle aspiration in polycystic liver disease. AJR Am J Roentgenol 181:1717

Baker LL, Hartman GE, Northway WH (1990) Sonographic detection of congenital pancreatic cysts in the newborn: report of a case and review of the literature. Pediatr Radiol 20:488–490

Behrman RE, Kliegman RM, Jenson HB (eds) (2004) Nelson textbook of pediatrics, 17th edn. Saunders

Brody AS, Seidel FG, Kuhn JP (1989) Metastatic Wilms' tumor to the liver with MR findings simulating cysts: case report emphasizing need for integrated imaging. Pediatr Radiol 19:337–338

Buetow PC, Buck JL, Pantongrag-Brown L et al (1997) Undifferentiated (embryonal) sarcoma of the liver: pathologic basis of imaging findings in 28 cases. Radiology 203:779–783

Carlson S.K, Johnson CD, Bender CE et al (2000) CT of focal nodular hyperplasia of the liver. AJR Am J Roentgenol 174:705–712

Cetin M, Demirpolat G, Elmas N et al (2002) Stromal predominant type mesenchymal hamartoma of liver: CT and MR features. Comput Med Imaging Graph 26:167–169

Chan JH, Tsui EYK, Luk SH et al (2001) Diffusion-weighted MR imaging of the liver: distinguishing hepatic abscess from cystic or necrotic tumor. Abdom Imaging 26:161–165

Chao HC, Lin SJ, Kong MS et al (2000) Sonographic evaluation of the pancreatic duct in normal children and children with pancreatitis. J Ultrasound Med 19:757–763

Chauveau D, Fakhouri F, Grunfeld JP (2000) Liver involvement in autosomal-dominant polycystic kidney disease: therapeutic dilemma. J Am Soc Nephrol 11:1767–1775

Chevallier P, Souci J, Buckley MJ et al (1999) Annular pancreas: MR imaging including MR cholangiopancreatography (MRCP). Pancreas 18:216–8

Cho JS, Shin KS, Kwonet ST et al (2000) Heterotopic pancreas in the stomach: CT findings. Radiology 217:139–144

Chowdhary SK, Trehan A, Das A et al (2004) Undifferentiated embryonal sarcoma in children: beware of the solitary liver cyst. J Pediatr Surg 39:E9–12

Choyke PL, Filling-Katz MR, Shawker TH et al (1990) Von Hippel-Lindau disease: radiologic screening for visceral manifestations. Radiology 174:815–820

Chung EM (2006) Pancreatic tumors in children. Radiologic-pathologic correlation. Radiographics 26:1211–1238

Czermak BV, Unsinn KM, Gotwald T et al (2001) Echinococcus granulosus revisited: radiologic patterns seen in pediatric and adult patients. AJR Am J Roentgenol 177:1051–1056

Dachman AH, Pakter RL, Ros PR et al (1987) Hepatoblastoma: radiologic-pathologic correlation in 50 cases. Radiology 164:15–19

Darbari A, Sabin KM, Shapiro CN et al (2003) Epidemiology of primary hepatic malignancies in US children. Hepatology 28:560–566

Elizondo G, Weissleder R, Stark DD et al (1987) Amebic liver abscess: diagnosis and treatment evaluation with MR imaging. Radiology 165:795–800

Feigelson J, Pecau Y, Poquet M et al (2000) Imaging changes in the pancreas in cystic fibrosis: a retrospective evaluation of 55 cases seen over a period of 9 years. J Pediatr Gastroenterol Nutr 30:145–151

Fulcher AS, Sterling RK (2002) Hepatic neoplasm: computed tomography and magnetic resonance features. J Clini Gastroenterol 34:463–471

Gazelle GS, Saini S, Mueller PR (1998) Hepatobiliary and pancreatic radiology imaging and intervention. Thieme, New York, p 4

Geier A, Lammert F, Gartung C et al (1990) Mediastinal pancreatic pseudocysts in children. J Pediatr Surg 25:843–845

Giovagnoni A, Gabrielli O, Coppa GV et al (1993) MRI appearances in amoebic granulomatous hepatitis: a case report. Pediatr Radiol 23:536–537

Gouya H, Vignaux O, Augui J et al (2003) CT, endoscopic sonography, and a combined protocol for preoperative evaluation of pancreatic insulinomas. AJR Am J Roentgenol 181:987–992

Gubernick JA, Rosenberg HK, Ilaslan H et al (2000) US approach to jaundice in infants and children. Radiographics 20:173–195

Gupta AK, Mitra DK, Berry M et al (2000) Sonography and CT of pancreatoblastoma in children. AJR Am J Roentgenol 174:1639–1641

Haliloglu, M, Hoffer FA, Gronemeyer SA et al (2000) 3D gadolinium-enhanced MRA: evaluation of hepatic vasculature in children with hepatoblastoma. J Magn Reson Imaging 11:65–68

Helmberger TK (1999) Pediatric liver neoplasms: a radiologic – pathologic correlation. Eur Radiol 9:1339–1347

Hinds R, Davenport M, Mieli-Vergani G et al (2004) Antenatal presentation of biliary atresia. J Pediatr 144:43-46

Hirohashi S, Hirohashi R, Uchida H et al (1997) Pancreatitis: evaluation with MR cholangiopancreatography in children. Radiology 203:411–415

Hough DM, Stephens DH, Johnson CD et al (1994) Pancreatic lesions in von Hippel-Lindau disease: prevalence, clinical significance, and CT findings. AJR Am J Roentgenol 162:1091–1094

Ichikawa T, Federle MP, Grazioli L et al (1999) Fibrolamellar hepatocellular carcinoma: imaging and pathologic findings in 31 recent cases. Radiology 213:352–361

Jaw TS, Kuo YT, Liu GC et al (1999) MR cholangiography in the evaluation of neonatal cholestasis. Radiology 212:249–256

Kanegawa K, Akasaka Y, Kitamura E et al (2003) Sonographic diagnosis of biliary atresia in pediatric patients using the "triangular cord" sign versus gall bladder length and contraction. AJR Am J Roentgenol 181:1387–1390

Katzenstein HM, Krailo MD, Malogolowkin MH et al (2003) Fibrolamellar hepatocellular carcinoma in children and adolescents. Cancer 97:2006–2012

Kelly DA (1999) Diseases of the liver and biliary system in children. Blackwell Science, Birmingham, p 375

Kim MJ, Han SJ, Yoon CS et al (2000) Biliary atresia in neonates and infants: triangular area of high signal intensity in the porta hepatis at T2-weighted MR cholangiography with US and histopathologic correlation. Radiology 215:395–401

King LR, Siegel MJ, Balfe DM (1995) Acute pancreatitis in children: CT findings of intra- and extrapancreatic fluid collections. Radiology 195:196–200

Kirks DR, Griscom NT (1998) Practical pediatric imaging: diagnostic radiology of infants and children, 3rd edn. Lippincott-Raven, Philadelphia, p 1226

Konez O, Goyal M, Vyas PK et al (2001) Mesenchymal hamartoma of the liver. Comput Med Imaging Graph 25:61–65

Krause D, Cercueil JP, Dranssart M et al (2002) MRI for evaluating congenital bile duct abnormalities. J Comput Assist Tomogr 26:541–552

Kuhn JP, Slovis TL, Haller JO, Caffey J (2004) Caffey's pediatric diagnostic imaging. Mosby/Elsevier Science, St Louis

Lack EE, Schloo BL, Azumi N et al (1991) Undifferentiated (embryonal) sarcoma of the liver. Clinical and pathologic study of 16 cases with emphasis on immunohistochemical features. Am J Surg Pathol 15:1–16

Lam WW, Lam TP, Saing H et al (1999) MR cholangiography and CT cholangiography of pediatric patients with choledochal cysts. AJR Am J Roentgenol 173:401–405

Manfredi R, Costamagna G, Brizi MG et al (2000) Pancreas divisum and „santorinicele": diagnosis with dynamic MR cholangiopancreatography with secretin stimulation. Radiology 217:403–408

Montemarano H, Lonergan GJ, Bulas DL et al (2000) Pancreatoblastoma: imaging findings in 10 patients and review of the literature. Radiology 214:476–482
Moon WK, Kim WS, Kim IO et al (1994) Undifferentiated embryonal sarcoma of the liver: US and CT findings. Pediatr Radiol 24:500–503
Mortele KM, Mergo PJ, Urrutia M et al (1998) Dynamic gadolinium-enhanced MR findings in infantile hepatic hemangioendothelioma. J Comput Assist Tomogr 22:714–717
Mortele KJ, Praet M, Van Vlierberghe H et al (2000) CT and MR imaging findings in focal nodular hyperplasia of the liver: radiologic-pathologic correlation. AJR Am J Roentgenol 175:687–692
Mortele KJ (2002) Solitary hepatic infantile hemangioendothelioma: dynamic gadolinium-enhanced MR imaging findings. Eur Radiol 12:862–865
Mortele KJ, Rocha TC, Streeter JL et al (2006) Multimodality imaging of pancreatic and biliary congenital anomalies. Radiographics 26:715–31
Mowat AP, Psacharopoulos HT, Williams R (1976) Extrahepatic biliary atresia versus neonatal hepatitis. Review of 137 prospectively investigated infants. Arch Dis Child 51:763–770
Nijs E (2005) Disorders of the pediatric pancreas: imaging features. Pediatr Radiol 35:358–373
Norton KI (2002) MR cholangiography in the evaluation of neonatal cholestasis: initial results. Radiology 222:687–691
O'Sullivan MJ, Swanson PE, Knoll J et al (2001) Undifferentiated embryonal sarcoma with unusual features arising within mesenchymal hamartoma of the liver: report of a case and review of the literature. Pediatr Dev Pathol 4:482–489
Oue T, Kubota A, Okuyama H et al (2003) Hepatoblastoma in children of extremely low birth weight: a report from a single perinatal center. J Pediatr Surg 38:134–137
Petersen C, Ure BM (2003) What's new in biliary atresia? Eur J Pediatr Surg 13:1–6
Pirson Y, Lannoy N, Peters D et al (1996) Isolated polycystic liver disease as a distinct genetic disease, unlinked to polycystic kidney disease 1 and polycystic kidney disease 2. Hepatology 23:249–252
Pobiel RS, Bisset GS 3rd (1995) Pictorial essay: imaging of liver tumors in the infant and child. Pediatr Radiol 25:495–506
Ramirez-Garredo F, De Dios LopezGonzalez-Garrido J, Ruiz-Lopez M-J et al (2003) Prenatal and postnatal imaging of an hepatic mesenchymal hamartoma. Eur J Pediatr 162:57–58
Richard S, Lindau J, Graff J et al (2004) Von Hippel-Lindau disease. Lancet 363:1231–1234
Roebuck DJ, Yang WT, Lam WWM et al (1998) Hepatobiliary rhabdomyosarcoma in children: diagnostic radiology. Pediatr Radiol 22:101–108
Roebuck DJ, Yuen MK, Wong YC et al (2001) Imaging features of pancreatoblastoma. Pediatr Radiol 31:501–506
Roebuck DJ (2006) Radiological staging in children with hepatoblastoma. Pediatr Radiol 36:176–182
Rosenthal P (1999) Biliary atresia and neonatal disorders of the bile ducts. In: Wyllie R, Hyams JS (eds) Pediatric gastrointestinal disease: pathophysiology, diagnosis and management, 2nd edn. WB Saunders Co, Philadelphia, pp 568-571
Sallah S, Semelka R, Kelekis N et al (1998) Diagnosis and monitoring response to treatment of hepatosplenic candidiasis in patients with acute leukemia using magnetic resonance imaging. Acta Haematol 100:77–81
Siegel MJ (2000) MR imaging of pediatric abdominal neoplasms. Magn Reson Imaging Clin N Am 8:837–851
Siegel MJ (2001a) Pediatric sonography. Lippincott Williams & Wilkins, Philadelphia, p 749
Siegel MJ (2001b) Pediatric liver imaging. Semin Liver Dis 21:251–269
Sokol RJ, Mack C,Narkewicz MR et al (2003) Pathogenesis and outcome of biliary atresia: current concepts. J Pediatr Gastroenterol Nutr 37:4–21
Somech R, Brazowski E, Kesller A et al (2001) Focal nodular hyperplasia in children. J Pediatr Gastroenterol Nutr 32:480–483
Soyupak SK, Narli N, Yapicioglu H et al (2002) Sonographic measurements of the liver, spleen and kidney dimensions in the healthy term and preterm newborns. Eur J Radiol 43:73–78
Sporcq C, Avni F, Sherer F et al (2007) Reappraisal of the sonographic chararacteristics of the fetal and newborn kidney: introducing the cortico-medullary ratio. European Society of Paediatric Radiology 44th Annual Meeting, June 5th-7th, 2007
Suchy FJ, Sokol RJ, Balistreri WF (eds) (2003) Liver disease in children. Sokol, Editor. Lippincott Williams & Wilkins, Philadelphia
Swischuk LE (2005) Imaging of the newborn, infant, and young child, 5th edn. Lippincott Williams & Wilkins, Philadelphia
Tattersall, DJ, Moore NR (2002) Von Hippel-Lindau disease: MRI of abdominal manifestations. Clin Radiol 57:85–92
Teele RL, Share JC (eds) (1991) Ultrasonography of infants and children. WB Saunders, Boston
Todani T, Watanabe Y, Toki A et al (2003) Classification of congenital biliary cystic disease: special reference to type Ic and IVA cysts with primary ductal stricture. J Hepatobiliary Pancreat Surg 10:340–344
Walker WA (1996) Pediatric gastrointestinal disease: pathophysiology, diagnosis, management. Mosby Year Book, St. Louis, p 2 v (xxiv, 2113)
Weinreb JC, Brateman L, Maravilla KR (1984) Magnetic resonance imaging of hepatic lymphoma. AJR Am J Roentgenol 143:1211–12114
Yen J-B, Kong MS, Lin JN (2003) Hepatic mesenchymal hamartoma. J Paediatr Child Health 39:632–634

The Small Bowel

5

Annick S. Devos, Morteza Meradji, and Johan G. Blickman

CONTENTS

A. S. Devos, MD
M. Meradji, MD
Erasmus MC, Sophia Children`s Hospital, 3000 DR Rotterdam, The Netherlands
J. G. Blickman, MD, PhD, FACR
Department of Radiology, UMC St Radboud, 6500 HB Nijmegen, The Netherlands

5.1 Introduction

The radiological approach to the pediatric upper and lower gastrointestinal (GI) tract varies according to the clinical condition of the child, the patient's age and the differential diagnostic considerations.

The imaging procedures should be performed in a problem-oriented fashion in order to minimize the risks and to maximize the diagnostic benefit.

All efforts must be made to reduce irradiation, the so-called ALARA principle. Especially in young children with chronic disease, repeated imaging evaluation should be as streamlined as possible.

Special attention should be paid to reduce any psychological trauma in these young children (e.g. catheterization of the urethra) and the environment of the radiology room should be adapted to calm and be user friendly for neonates and young children (e.g. the ambient experience) (Devos and Meradji 2003).

One can simplify the approach to analyzing the causes of disorders of the GI tract in children as congenital anomalies are not as prevalent in later life and the differential diagnosis is significantly affected by the age of the child. Thus, the entities

affecting the pediatric GI tract will be categorized into three groups: neonatal, infantile and childhood diseases, each subdivided into acute and non-acute conditions (Devos and Meradji 2003).

Some of the pathologies of the small intestine are discussed in Chapter 1. In the current chapter, therefore, little or no attention will be paid to (midgut volvulus) malrotation, the atresias, meconium ileus, meconium peritonitis, duplication cysts, necrotizing enterocolitis (NEC) and intussusception.

5.2 Imaging Techniques

5.2.1 The Abdominal Plain Film

An abdominal plain film is usually the first imaging procedure, especially in acute abdominal conditions. It can give worthwhile information and can positively influence the choice of subsequent imaging techniques.

In acute clinical conditions a child should have films in two directions (Fig. 5.1) instead of one, a supine and a cross-table horizontal beam radiograph.

On a supine film changes such as dilatation with or without obstruction, calcification and displacement of normal structures can all be identified and localized. Multiple (distended) loops are indicative of distal pathology (Fig. 5.2), whereas a few (distended) loops suggest proximal intestinal pathology (Fig. 5.3).

On a cross-table (or a left lateral decubitus) horizontal beam film the anatomic position of the small bowel and colonic loops is easily recognized (Fig. 5.1, arrows). Because of the dorsal (retroperitoneal) positioning of ascending and descending colon as well as rectum, these loops can be distinguished from the small bowel, which has an intraperitoneal ventral position. Fluid levels, as well as free intraperitoneal air collections due to intestinal perforation, are also better appreciated on a cross-table or left lateral decubitus film.

5.2.2 Contrast Examinations

In general the contrast medium used to evaluate the GI tract is a suspension of barium sulfate as it is cheap and easy to use. In patients at risk for aspiration, such as (pre-)term neonates, non-ionic contrast agent is preferred because of the lower risk of dehydration. Ionic water-soluble contrast media are used when a large amount of contrast medium is

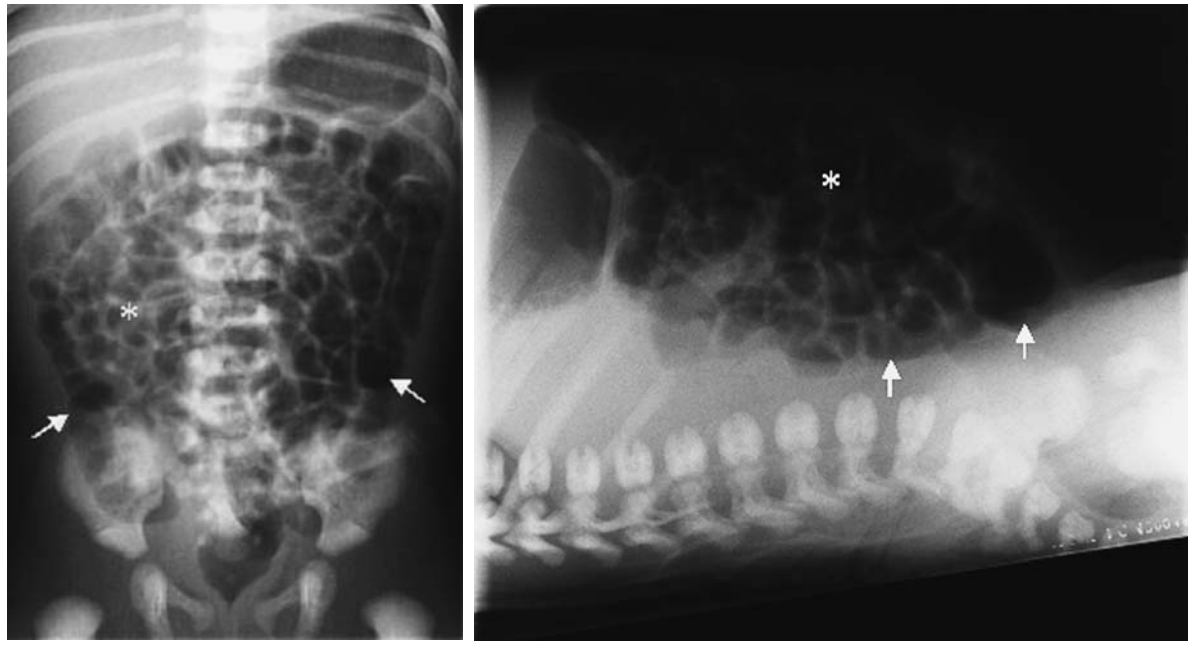

a b

Fig. 5.1a,b. Normal radiographs of abdomen in an infant with anatomic position and normal intestinal gas distribution. Peripheral (AP) low (lateral) location (*single arrow*) depicts colon; *asterisk* depicts small bowel

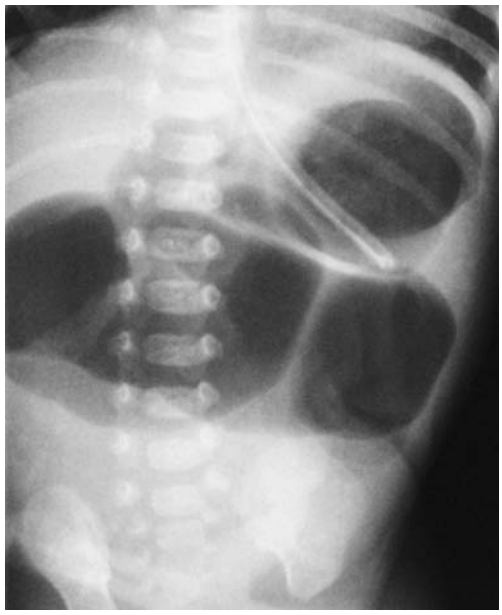

a

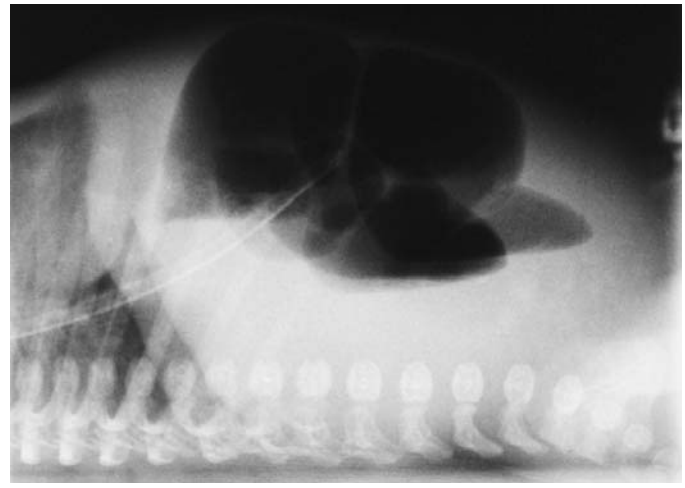

b

Fig. 5.2a,b. Jejunal atresia with multiple distended loops and fluid levels on lateral film

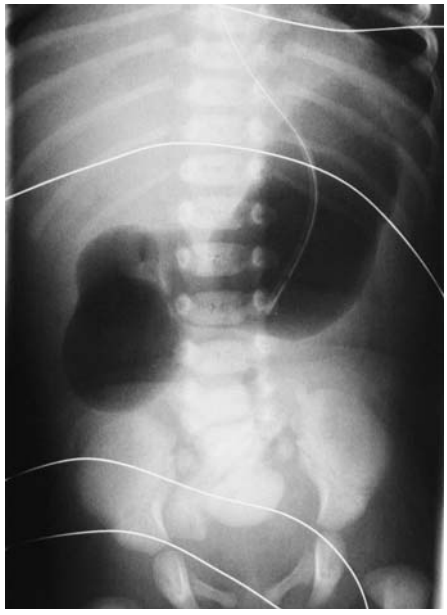

a

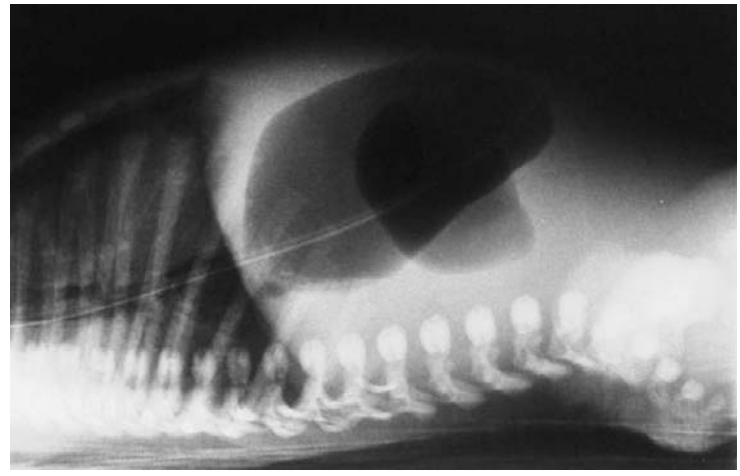

b

Fig. 5.3a,b. A neonate with a highly distended duodenum and stomach due to duodenal atresia. No passage of gas seen distally

needed, such as in enemas for hydrostatic reduction of an intussusception.

If bowel perforation or predisposition for pulmonary aspiration is suspected, barium is contraindicated because of the risk of granuloma formation in both lungs and the peritoneal cavity, in the abdomen adhesions or peritonitis. The reported side-effects of water-soluble contrast media such as hypothyroidism in neonates and allergic reaction in later life are rare.

In evaluating for abnormalities of the proximal digestive tract (proximal or few loops seen), contrast will be given orally or via a feeding tube placed in the stomach or selectively in another intestinal location. For suspected abnormalities of the ileum or below (distal or many loops seen), the contrast will be administered rectally.

Contrast examinations will elucidate the anatomy and the motility pattern of the GI tract.

5.2.3 Ultrasound (US)

As visualization with US is limited by intraluminal intestinal air, it can be useful to prepare the bowel with a mild laxative. Fasting should be a minimum of 3 h to optimally visualize the gallbladder and minimize gaseous distension. US is easy to perform, can be done at bedside, does not use ionizing radiation, is not cumbersome for the child and can be repeated as often as necessary.

US is the screening modality of choice in the child suspected of appendicitis, pyloric stenosis and intussusception, and has already proven its utility in diagnosing other diseases both as a screening and as a follow-up modality. Other indications will be discussed in the appropriate sections.

5.2.4 Computed Tomography (CT)

CT has a superior contrast resolution compared with that achieved on conventional radiographs. Optimal bowel filling and distension of the lumen with water or contrast media is essential to evaluate bowel loops and its surroundings. We must keep in mind that CT implies an increased radiation exposure. The information gained must justify the increased radiation burden. Indications for CT use include trauma, intestinal wall and liver/spleen parenchymal evaluation, abscesses and tumor staging (Devos and Meradji 2003; Nicolaou et al. 2005; Boudiaf et al. 2001).

5.2.5 Magnetic Resonance Imaging (MRI)

The superior tissue resolution and the multiplanar imaging capabilities without using any ionizing radiation are all advantages of MRI. However, the long examination times, the need for sedation or general anesthesia in young children and high costs are limiting factors for this technique. MRI plays an important role in staging primarily retroperitoneal, intraspinal mass lesions and postoperatively in anorectal/cloacal malformations. Recently it has been more frequently used in patients with inflammatory bowel disease (Devos and Meradji 2003; Frokjaer et al. 2005).

5.3 Congenital Diseases in the Newborn

5.3.1 Duodenal Obstruction

Duodenal obstruction is the most common cause of proximal (high) intestinal obstruction in newborns. It can be complete (atresia) or incomplete (stenosis). Atresia is caused by failure of recannulation. Approximately 30% of patients with duodenal atresia have Down syndrome. Duodenal stenosis can be the consequence of internal or external causes that impede re-canalization such as malrotation with or without volvulus, a duodenal web, pancreas annulare and duplication cysts (Carty et al. 2005; Parker 2003; Grier 1999; Devos and Meradji 2003; Berrocal et al. 1999). Prenatal diagnosis of a 'double bubble' with polyhydramnios in 40% of cases is more common today. Clinical manifestations are persistent (bilious) vomiting from the first hours of life, possibly complicated by dehydration. The abdomen is flat, scaphoid or minimally distended.

A conventional abdominal (plain) film in two directions (including a horizontal beam) may show a (markedly) dilated stomach and the proximal part of the duodenum.

Most important in these cases is to exclude conditions that are life-threatening for the patient. As intestinal malrotations may lead to bowel ischemia, which may subsequently lead to bowel necrosis, the patient's life is at risk when less than 3 in. of small bowel remain (Andrassy and Mahour 1981).

In the case of atresia, there will be no air in other parts of the intestinal tract, the so-called 'double bubble' sign (Fig. 5.3). No other imaging modality is then needed. However, the 'double bubble' sign may be absent if the patient has vomited, has a feeding tube or if there is intermittent passage of air.

In the case of duodenal obstruction with similar clinical signs as atresia, but with air distal to the duodenum, intestinal malrotation should be ruled out.

The sign of an intestinal malrotation is sometimes recognizable on an abdominal plain film in which the small bowel will be located in the right upper abdomen. When this is observed, color Doppler sonography shows in 85% of the cases an abnormal position and course of the superior mesenteric artery with dextroposition to the superior mesen-

teric vein and the small bowel will lie in the right instead of the left upper quadrant (Figs. 5.4 and 5.5) (Carty et al. 2005; Parker 2003; Grier 1999; Devos and Meradji 2003; Berrocal et al. 1999).

An upper GI tract examination (with low osmolar water soluble contrast medium) is the optimal study to verify whether normal bowel rotation has occurred, and the imaging hallmark for this is to identify the position of the duodenojejunal junction (ligament of Treitz) (Fig. 5.6a). Radiographically this implies, with an anteroposterior supine positioning of the patient, that the duodenojejunal junction is to the left of the vertebral column and at the same level or more superior than the duodenal

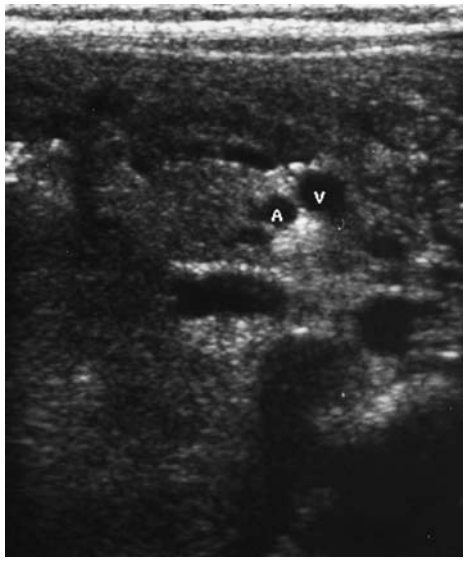

Fig. 5.4. An infant with intestinal malrotation on US. Abnormal position of the superior mesenteric arteria dextropositioned to the mesenteric vein

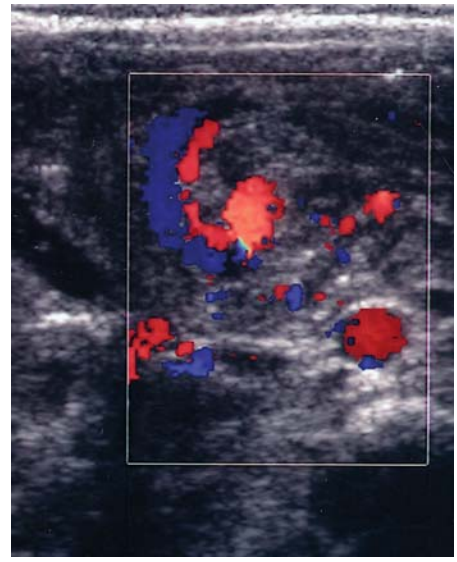

Fig. 5.5. An infant with intestinal malrotation. Note the abnormal position and course of the superior mesenteric artery and vein imaged by color Doppler sonogram (the "whirlpool sign")

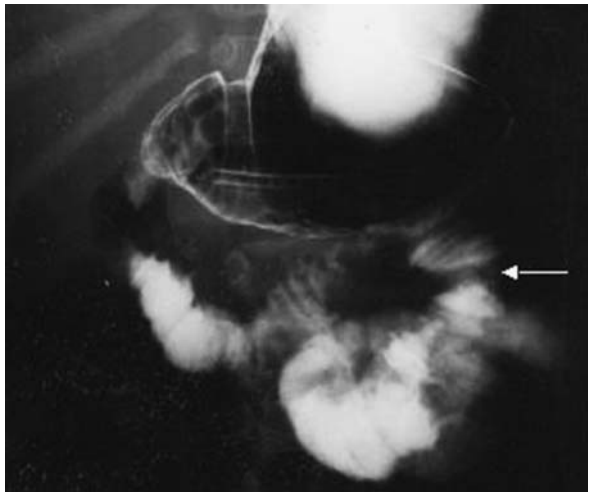

a

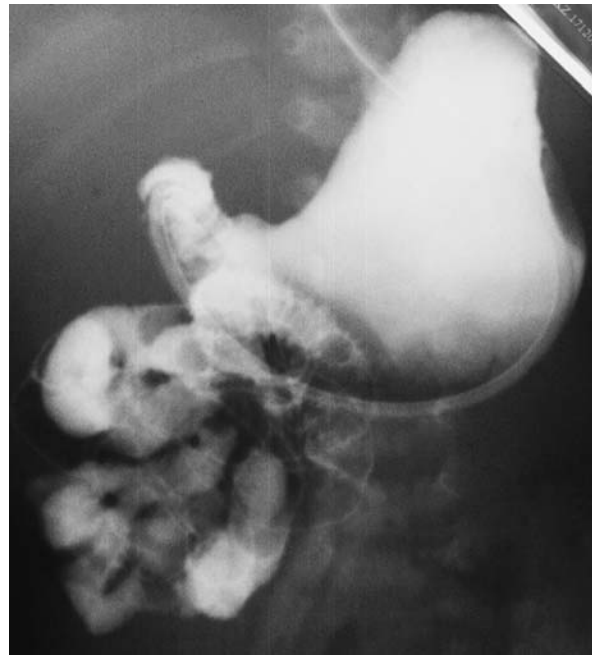

b

Fig. 5.6. a UGI: determines normal rotation by identifying the duodenojejunal junction (ligament of Treitz). **b** Intestinal malrotation demonstrated with a barium enema. Localization of jejunum in right upper quadrant. The duodenum does not cross the spine

bulb. In malrotation the duodenum courses into the right upper quadrant and does not cross the spine (Fig. 5.6b) (Carty et al. 2005; Parker 2003; Devos and Meradji 2003; Berrocal et al. 1999).

To avoid the risk of aspiration, the contrast medium is injected in very small proportions (Devos and Meradji 2003). A contrast enema cannot reliably exclude malrotation as in 15%–20% of normal neonates the caecum has not yet descended, which will occur in the subsequent 6–12 months (Berrocal et al. 1999).

A duodenal web or diaphragm is part of the spectrum from an atretic duodenum to a fully recanalized duodenum with a central opening. The radiological findings are identical to any other type of duodenal stenosis. The so-called 'windsock' appearance is easy to demonstrate as a curvilinear web that evacuates contrast medium through a tiny small central opening (Fig. 5.7a). The contrast medium is selectively administered through a feeding tube of which the tip is placed in the proximal duodenum (Devos and Meradji 2003).

Annular pancreas with complete or incomplete duodenal obstruction is another cause of duodenal obstruction. Its cause is persistence of the left lobe of the ventral pancreatic bud around the sixth week of gestation that then raps around the duodenum causing a ring-like eccentric narrowing (Fig. 5.7b). The clinical and radiological findings are the same as other types of duodenal obstruction (Carty et al. 2005; Parker 2003; Devos and Meradji 2003; Berrocal et al. 1999).

Duodenal duplication and diverticula are rare and incidentally cause a duodenal stenosis. A cystic non-communicating duplication is easy to detect sonographically while a communicating duplication and diverticulum can only be visualized by gastrointestinal contrast examinations.

5.3.2 Jejunal and Ileal Obstruction

Neonates with jejunal or ileal obstruction may also present with bilious vomiting depending on the level (most likely proximal) of obstruction. This clinical symptom is usually less severe than in duodenal obstruction.

A distended abdomen is virtually always present the more distal the level of intestinal obstruction. Failure to pass meconium may be an additional symptom. Atresia of the jejunum and ileum is twice as common as duodenal atresia, about equal in jejunum and ileum, with an incidence of 1 in 4–500 live births. Multiple atresias occur in 10%–20% of cases (Carty et al. 2005; Parker 2003; Grier 1999; Devos and Meradji 2003; Berrocal et al. 1999). Intestinal vascular accidents, such a thromboem-

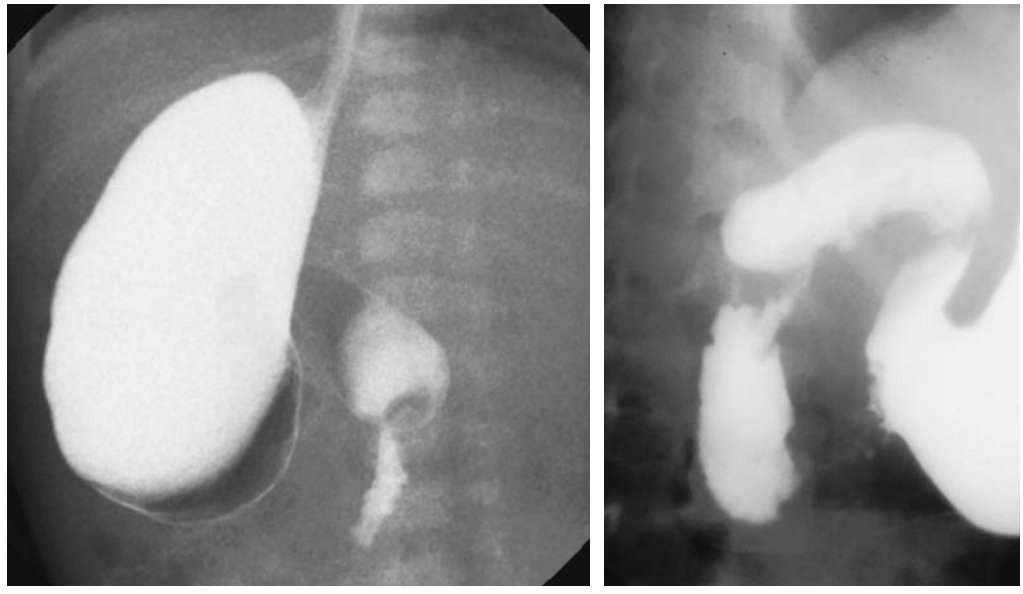

Fig. 5.7. a Duodenal stenosis caused by a duodenal web with a "windsock" appearance. **b** Eccentric narrowing of the descending duodenum at the level of the sphincter of Oddi: annular pancreas

bolic occlusion, hypoxia or volvulus, are thought to be the cause of an atretic jejunum or ileum. This ischemic event may also cause perforation leading to meconium peritonitis. The atretic or stenotic intestinal segment is mostly monoloculated and rarely multiloculated.

The radiological diagnosis of obstruction is usually visible on the conventional (plain) radiograph. In uncomplicated cases these radiographs of the abdomen are sufficient. The pre-atretic intestinal loops are dilated because of accumulation of large amounts of fluid and fluid levels are usually present on horizontal beam films. In case of jejunal atresia only a few loops of distended jejunum are present in the left upper abdomen, while in ileal atresia many dilated loops are identified. In complicated cases, especially with an abnormally distended and painful abdomen, a colon enema or US can be useful- particularly from the differential diagnostic point of view to exclude meconium ileus or meconium peritonitis. In case of atresia, a microcolon without the presence of meconium is usually found (Devos and Meradji 2003).

5.3.3 Meconium Peritonitis

An ante- or peri-natal perforation of the intestinal tract results in an aseptic chemical peritonitis as the sterile bowel contents (such as desquamated cells, lanugo hairs and vernix) escape into the peritoneal cavity causing an intense inflammatory reaction. This chemical peritonitis may lead to adhesions, granulomata, cystic changes and frequently to calcifications. The calcifications may extend into the scrotal cavity. Antenatal perforation due to meconium ileus in patients with cystic fibrosis is frequently the main cause of meconium peritonitis. A newborn with meconium peritonitis may have a distended, painful abdomen and may be lethargic. The child may have bilious vomiting and often produces no meconium.

Diagnosis is made by plain film and US. Plain film shows a swollen abdomen with a few or no air-containing bowel loops (Fig. 5.8). The bowel loops may be variably dilated. Often calcifications are visible. US shows not only the calcifications but also the extraluminal meconium and cystic fluid accumulations. The wall of the intestine is thickened (Fig. 5.9) (Parker 2003; Devos and Meradji 2003).

5.3.4 Meconium Ileus

For a more in depth discussion of meconium ileus please refer to Chapter 1.

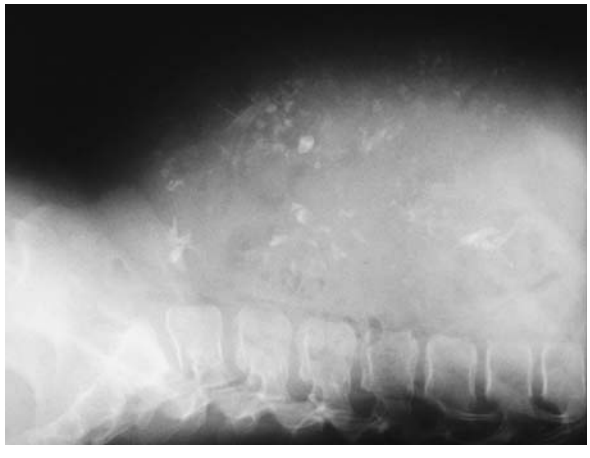

a

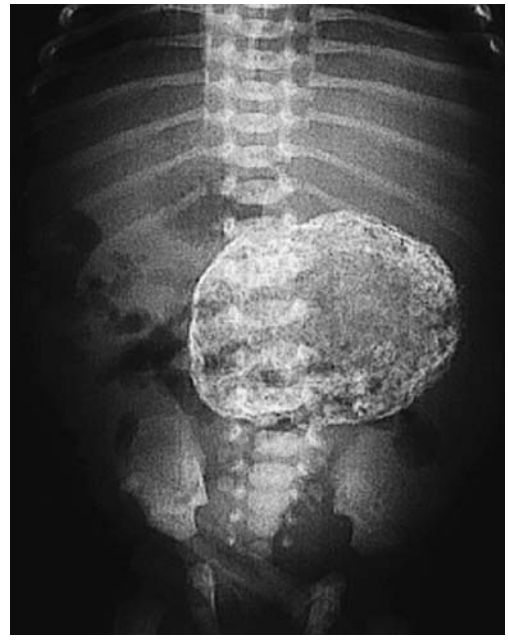

b

Fig. 5.8. a A neonate with a distended, practically gasless abdomen characteristic for meconium peritonitis. The streaky and flocculent calcifications in the peritoneal cavity are specific. **b** A neonate with meconium peritonitis and a rounded cystic calcification located intraperitoneally. Distended abdomen with reduced intestinal air

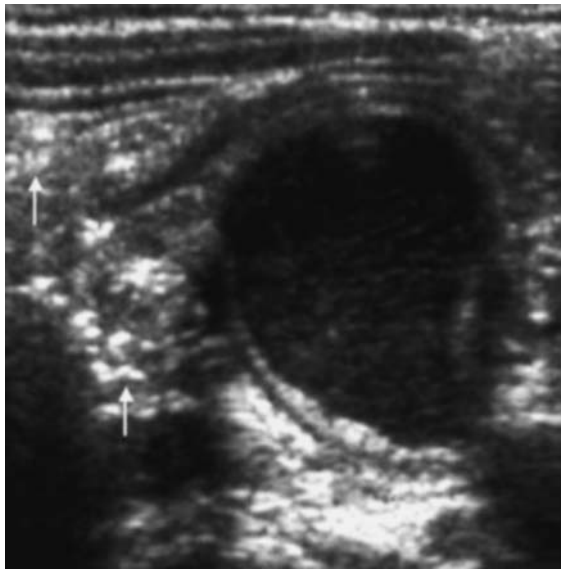

Fig. 5.9. Ileal duplication cyst in an infant with meconium peritonitis. Note the additional punctate calcifications and echogenic meconium intraperitoneally (*arrows*)

5.3.5 Megacystis-Microcolon-Malrotation-Intestinal-Hypoperistalsis Syndrome (MMMIHS)

The MMMIHS is a rare cause of intestinal obstruction and consists of a massively dilated bladder, malrotated microcolon and absent or ineffective peristaltic activity of the bowel. The disease is more common in females. Clinical symptoms are vomiting, failure to pass meconium, absent spontaneous micturition and a distended abdomen.

On abdominal plain film a highly distended abdomen caused by a distended urinary bladder may be identified.

A contrast examination of the upper GI tract may show dilated small bowel without peristaltic activity while on a colon enema a microcolon will be noticed (Fig. 5.10). US demonstrates a large urinary bladder with dilated ureters and pyelocaliceal systems.

5.4 Acquired Diseases in the Newborn

5.4.1 Perforation

Perforation of the GI tract is mostly iatrogenic. Both stomach and esophagus can incidentally be perforated by feeding tubes. The treatment with prostaglandins in case of patients with a patent ductus of Botalli can also be complicated with a perforation of the GI tract. Rectal use of a thermometer is inci-

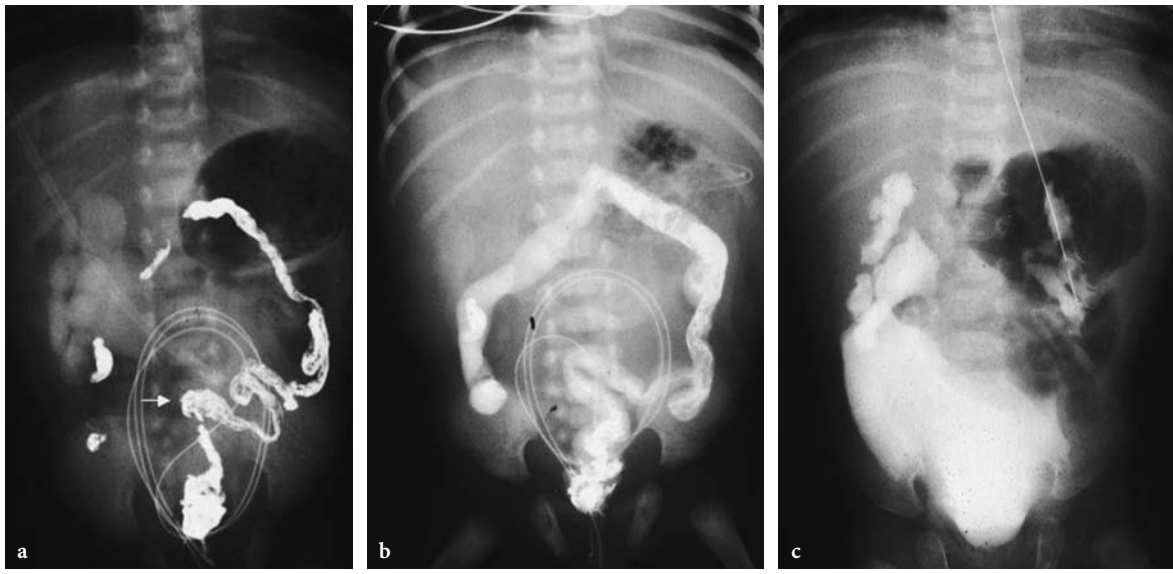

Fig. 5.10a–c. MMMIHS: highly distended stomach on contrast study with slow passage of contrast. Very little peristaltic activity. **a,b** Note the unusual microcolon and distended bladder (catheter). Secondary hydronephrosis because of dilated bladder. **c** Dilated system can be seen on EU, with the atonic, large bladder with dilatation of the pyelocaliceal system

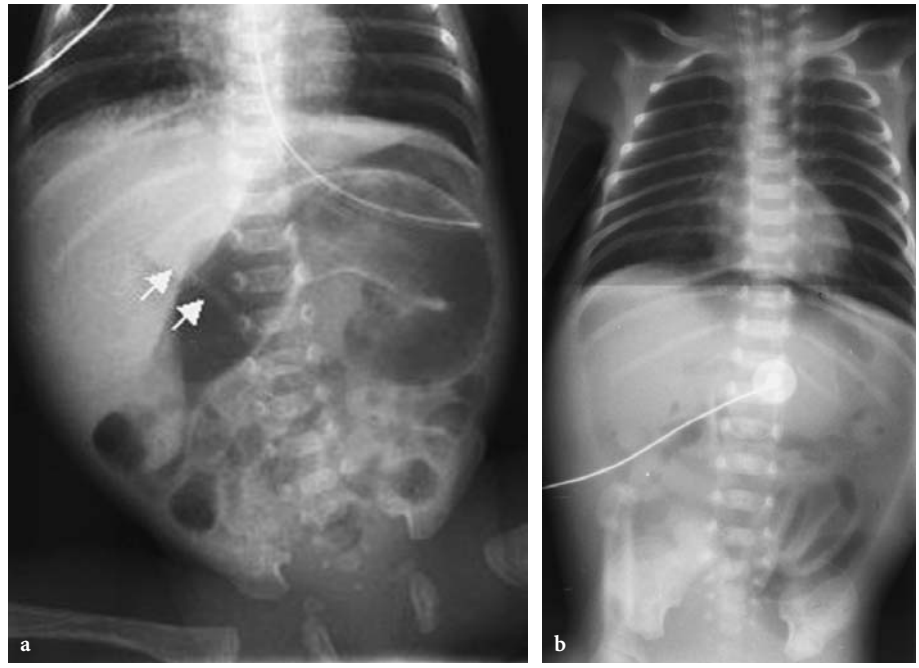

Fig. 5.11a,b. Pneumoperitoneum in an infant with ileal perforation. Free air outlining the GI tract. Note the visualized falciform ligament. **a** Supine film with "football sign"; **b** "cupula sign", free air under the cardiac silhouette

dentally followed by rectal perforation (Devos and Meradji 2003).

Sepsis, obstructions and vascular accidents, especially necrotizing enterocolitis, are all non-iatrogenic causes of enteral perforation.

A distended and painful abdomen with or without respiratory problems are clinical signs of perforation.

Perforation is most reliably demonstrated on abdominal plain films if taken in two directions. A supine film (Fig. 5.11) will demonstrate an abnormal lucency in the upper abdomen with gas outlining the right lobe of the liver, both sides of the wall of the stomach and bowel loops. The falciform ligament may be visible in the upper abdomen. In the newborn, a left-side down decubitus film will demonstrate free air between the liver and peritoneal wall, which is almost certainly impossible to confuse with intraluminal air. In case of an unstable neonate, a cross-table lateral view is preferred, but it can mask free air behind intraluminal air, unless the so-called 'triangle' sign (Fig. 5.12) is present.

5.4.2 Necrotizing Enterocolitis

For a more in depth discussion of necrotizing enterocolitis please refer to Chapter 1.

5.4.3 Functional Intestinal Obstruction of the Premature Newborn

Functional intestinal obstruction of the premature newborn is also called "meconium ileus-like syndrome" because, as in the case of meconium ileus, an obstruction exists at the distal ileum and caecum but meconium has passed. The obstruction is caused not by meconium but by stools.

As in meconium ileus, there is a motility disturbance of the bowel. However, it can also be related to absorption problems if inadequate feeding formula is used (so-called milk curd syndrome) (Devos and Meradji 2003). Clinical symptoms are similar to meconium plug syndrome or meconium ileus and are those of obstruction, such as progressive vomiting, progressive abdominal distension and failure to pass stools. Sometimes a mass can be felt in the (right) side of the abdomen.

Plain film shows most frequently a dilated small bowel with only a few or even no fluid levels and an absence of air in the rectum. Because of air-trapping in stools, a mottled appearance can be seen in the right side of the abdomen (Fig. 5.13a,b). US will show dilated small bowel loops (ileum) fully filled with huge hypoechogenic masses (Fig. 5.13c). A contrast enema with nonionic media shows fecal impaction in upper colonic segment or higher ileum. This pro-

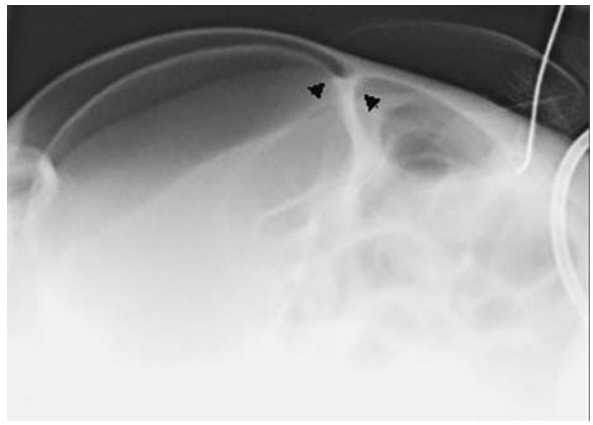

a

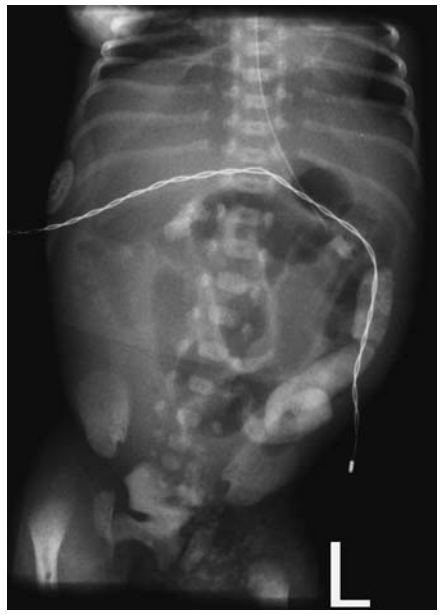

b

Fig. 5.12. a Pneumoperitoneum with a "triangle sign" on the cross-table lateral film. **b** Left lateral decubitus image (presented as if an AP view). Free air is located in the 'highest point': between abdominal wall and liver

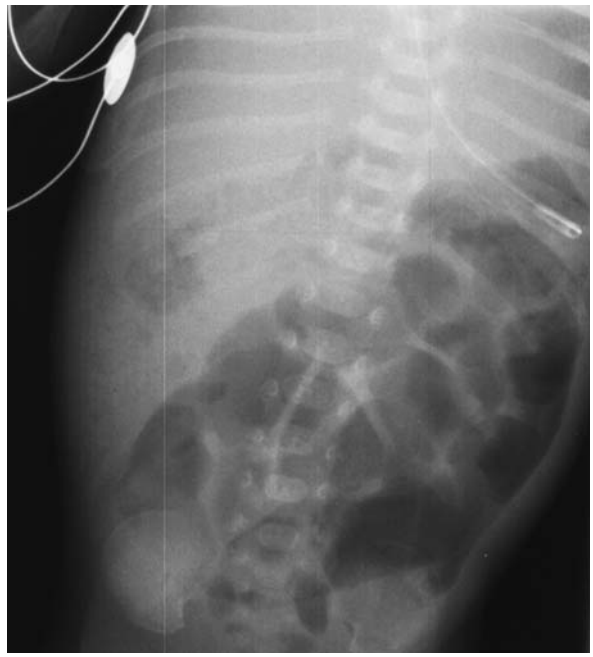

a

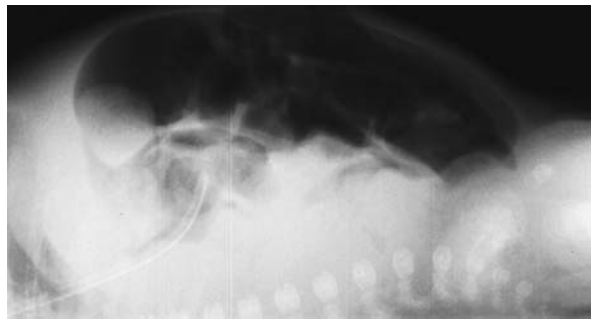

b

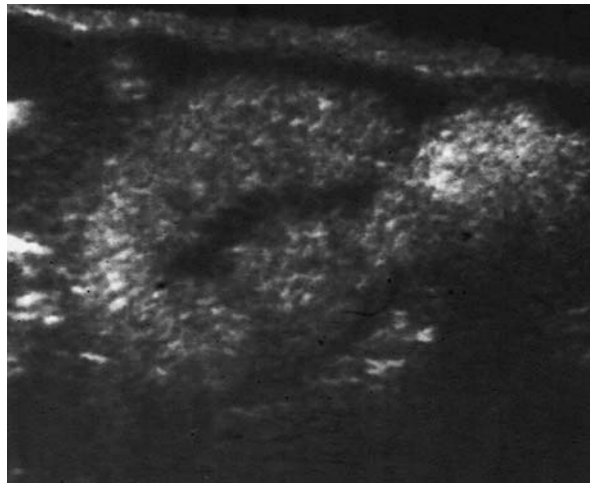

c

Fig. 5.13. a A premature infant with intestinal dysfunction, so-called meconium ileus-like syndrome. The supine abdominal film shows dilated intestinal loops because of fecal impaction in ileum. **b** Cross-table radiograph. Meconium-like ileus with dilated intestinal loops without fluid levels. The whole colonic tract and rectum are airless. **c** Ultrasound of the right lower quadrant of abdomen demonstrates the impacted and inspissated stool in the ileum

cedure may have a therapeutic effect (Carty et al. 2005; Parker 2003; Devos and Meradji 2003).

5.5 Congenital Diseases in the Infant

Congenital diseases are encountered less often in infants but can manifest after the neonatal period.

5.5.1 Volvulus

Clinical manifestations and diagnostic procedures remain the same as in newborns.

5.5.2 Meckel Diverticulum

A Meckel diverticulum results from an incomplete obliteration of the vitelline duct and is situated near the ileocaecal valve on the antimesenteric border of the ileum. It is usually about 2 cm long, located about 2 cm from the ileocecal valve. It is the most common form of congenital abnormality of the small intestine, occurring in about 2% of all infants, but mostly causes no clinical complaints. It contains all layers of the intestinal wall but the mucosa is (ectopic) gastric in origin in about 15%–20% of cases (Carty et al. 2005; Parker 2003; Berrocal et al. 1999).

In half of the patients with complaints clinical signs manifest in the first 2 years of life. Ulceration occurs only in those that contain ectopic gastric mucosa and thus is rare, but can cause occult fecal blood or frank blood in stool and anemia. Adhesions and formation of scar tissue can lead to obstructive ileus. The diverticulum can act as a lead point for ileocolic or ileoileal intussusception.

The visualization of a Meckel diverticulum is often unsuccessful. Plain films show only the complications caused by a Meckel diverticulum.

Plain film is indicated if obstruction or perforation is suspected. Meckel diverticulum is incidentally found by US (Fig. 5.14a), which may show cystic diverticula, and by enteroclysis. Small bowel or colon enemas can show the rather bigger diverticula. Scintigraphy may identify a Meckel diverticulum if it has gastric mucosa as a hot spot (Fig. 5.14b).

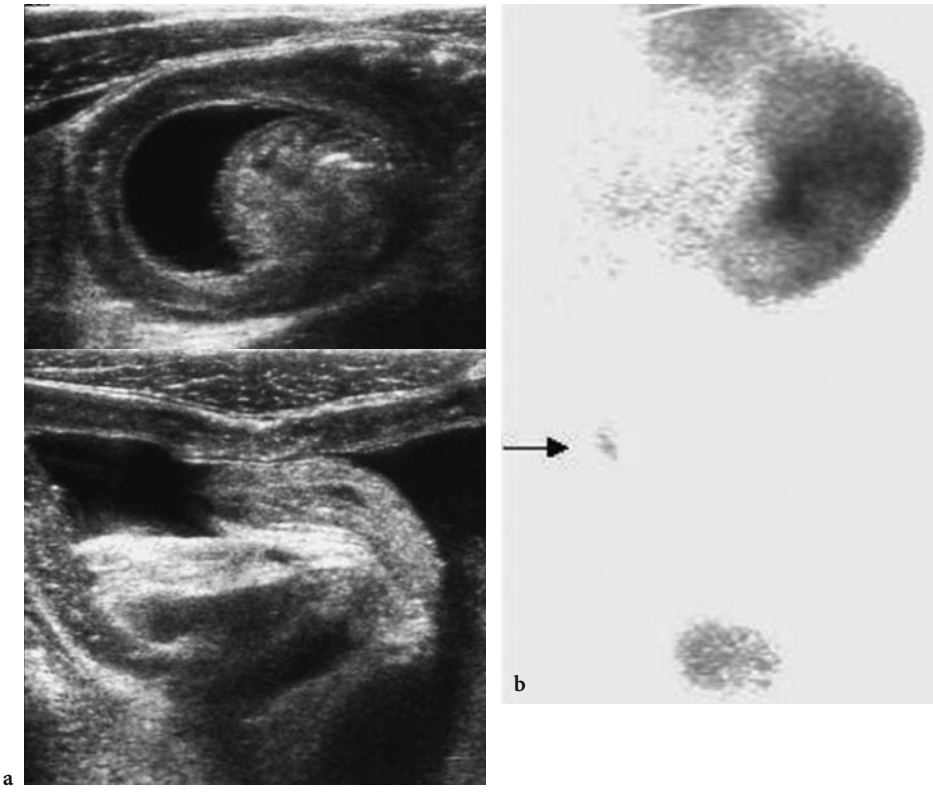

Fig. 5.14. a Meckel diverticulum as a lead point for an ileo-ileocolic intussusception. Note the surrounding of diverticulum by intraluminal intestinal fluid. **b** Radioisotope uptake in gastric mucosa in a Meckel diverticulum (*arrow*)

5.5.3 Duplication Cysts

A duplication cyst, the result of multiple twinning, persistent embryologic diverticula or aberrant luminal recanalisation, is a spherical or tubular structure that contains mucosa of the intestinal type and is surrounded by a layer of smooth muscle. They all have the same anatomic structure as normal bowel wall and are mostly (35%) located in the distal ileum on its mesenteric side, decreasing in frequency as one goes proximally. Sometimes there is a connection with adjoining bowel, but this exists in only a minority of cases. If they do communicate, its recognition as a tubular structure with intestinal content is more difficult. The non-communicating duplication cysts are cystic because of the mucosal secretions. The increasing number of prenatal and postnatal US examinations means that the non-communicating duplication cysts are recognized more often (Berrocal et al. 1999). The clinical manifestation and diagnostic procedures depend on the localization and type of duplication cyst. These cysts are asymptomatic; however, they can manifest later in life because of complications. A duplication cyst can contain ectopic gastric mucosa in which bleeding can occur. Clinical symptoms are bleeding (melena and hematemesis can cause serious anemia) and intermittent abdominal pain, vomiting and sometimes a palpable mass. Obstruction, volvulus and intussusception are well known complications.

Plain film, US, contrast examination, scintigraphy and even CT and MRI can be useful to diagnose a duplication cyst. Plain film may show obstruction. US may show the non-communicating anechoic cystic duplication cysts with the clearly visible,

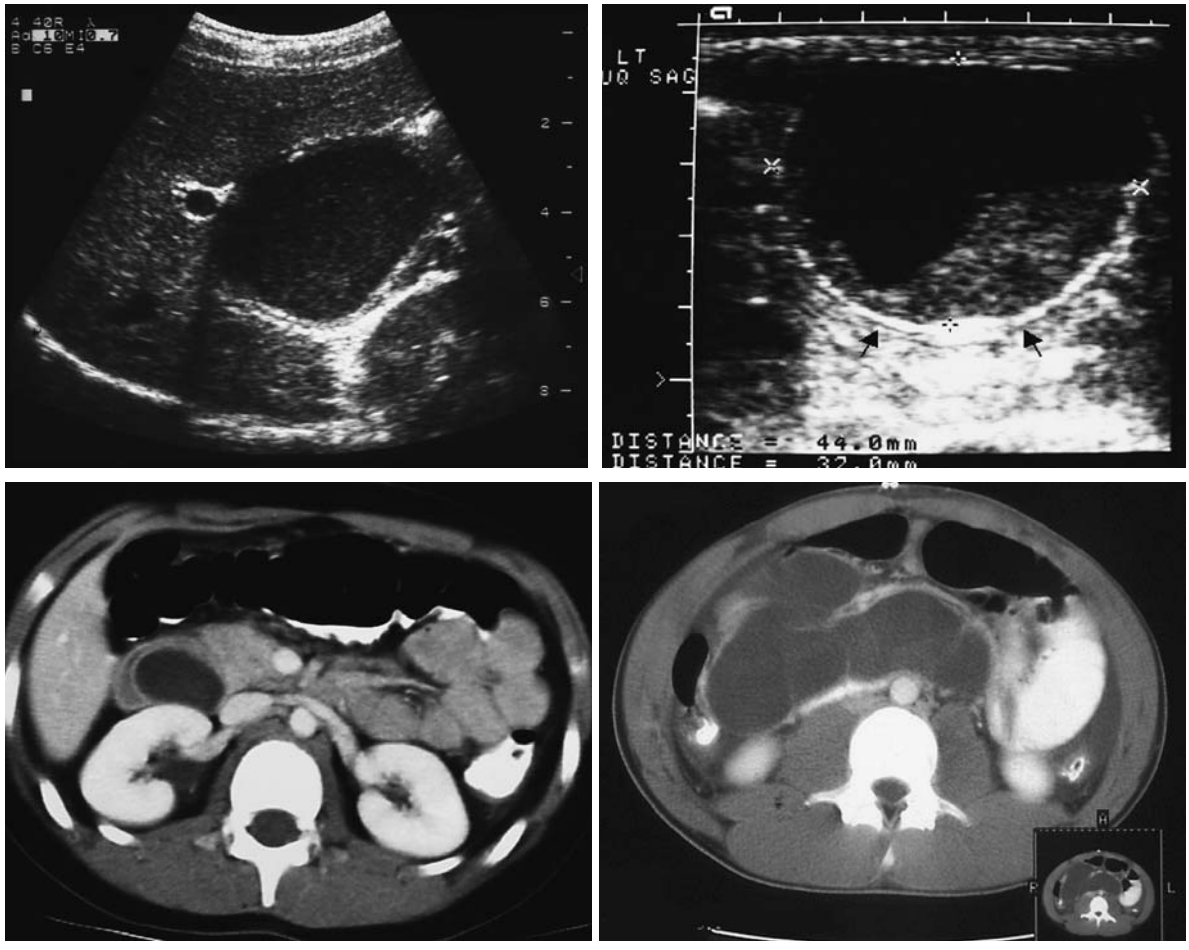

a b c (I) c (II)

Fig. 5.15. a A non-communicating duplication cyst of duodenum. Note the echogenic mucosal layer and hypoechoic muscular layer and the inhomogeneous content of the cyst. **b** Colonic duplication. US demonstrates mucosal echogenic "stripe"(*arrows*). **c** (I) & (II) CT of colon duplication

characteristic bowel wall in which the mucosa is echogenic and the muscularis hypoechogenic. The muscularis is typically shared with adjacent bowel wall but the mucosal layer is separated (Fig. 5.15a). They can be multi-locular and can contain echogenic debris because of bleeding or mucosal secretions. The contrast follow-through exam shows impression on the bowel wall and displacement of the bowel loops. In the case of communicating cysts the abnormal configuration of the bowel can be seen. CT and MRI show a cyst with an enhancing wall after contrast administration (Fig. 5.15b).

On plain film the cyst can be suspected by displacement of bowel loops and calcifications or by the signs of obstruction.

An upper GI tract examination may show displacement of bowel loops but is usually unremarkable.

On US these mostly multilocular cysts have fine septations and can be anechoic or, after bleeding or infection, filled with echogenic debris (Fig. 5.16)

CT and MRI are rarely indicated but show wall and septae enhancement after contrast injection.

5.5.4 Intraperitoneal Cysts

There are three types of lymphangiomas: the simple capillary, cavernous and cystic types. At least half have a haemangiomatous component. Most abdominal lymphangiomas are located in the mesentery and omentum, and are called mesenteric and omental cysts, respectively. They are caused by sequestration or obstruction of lymphatic vessels, are mono- or multilocular and can calcify in case of necrosis. The wall of mesenterial and omental cyst is unilayered, which is in contrast to the multilayered aspect of the wall of the duplication cyst. Most cysts are asymptomatic, but because of bleeding or infection they can cause fever and pain and can necrotize after torsion. Adherent cysts to the bowel can cause partial obstruction. Some cause a painless abdominal distension and palpable mass (Carty et al. 2005; Parker 2003; Devos and Meradji 2003).

5.6 Acquired Diseases in the Infant

5.6.1 Enteritis

Worldwide viruses, bacteria and parasites cause enteritis. Viral acute gastroenteritis and enterocolitis are most frequent in the first 2 years of life. Imaging is mostly not required but plain films are sometimes useful to differentiate enteritis from other more serious diseases such as obstruction, intussusception, perforated appendix with peritonitis, neuroblastoma and Hirschsprung disease.

Plain films in two directions may show moderate dilatation of small bowel and colon. Both may contain air-fluid levels, and particularly in the colon air-fluid levels suggest disturbed resorptive activity. Either there is too much intraluminal fluid (diar-

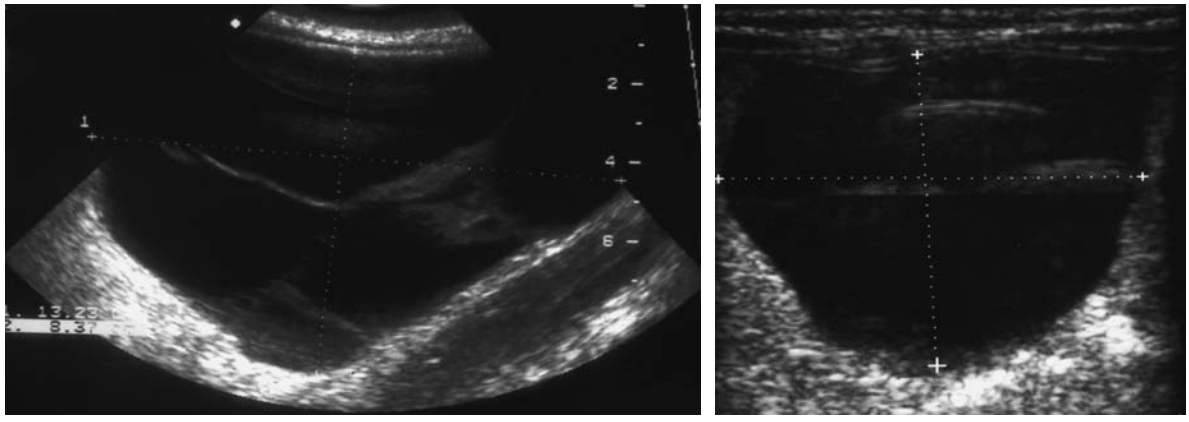

Fig. 5.16. a A huge mesenterial cyst located intraperitoneally and sharply encapsulated. **b** An omental cyst in the upper abdomen which is unlayered. Note wall: no mucosa pattern

rhea) or there is decreased peristaltic activity with resulting decreasing resorptive power. In case of persistent vomiting a relatively gasless abdomen can be seen. US, performed to exclude intussusception for example, may show fluid in the small intestine and even colon, hyperperistalsis, large mesenteric lymph nodes and sometimes bowel wall thickening (Parker 2003; Devos and Meradji 2003).

5.6.2 Intussusception

For a more in depth discussion of intussusception please refer to Chapter 1.

5.7 Diseases in Older Children

5.7.1 Small Bowel Intussusception

Intussusceptions are a pediatric GI emergency, most being ileocolic. Small bowel intussusceptions are less frequently diagnosed, but if searched for carefully, are relatively frequently encountered. Mostly these small bowel intussusceptions are also idiopathic and transient and of no clinical importance. Pathologic entities that might predispose a child to small bowel intussusception that can be clinically significant are infection, malabsorption syndromes, gastroenteritis with increased peristaltic activity of small bowel, lymphoma, cystic fibrosis, intramural hematomata (Henoch-Schönlein, posttraumatic), polyps, Meckel diverticulum, duplication, foreign body and adhesions.

Small bowel intussusceptions can be found incidentally when searching for other pathology, in which case patients will have no complaints.

Otherwise patients can present with transient cramping abdominal pain or with persistent abdominal pain, or even with symptoms of obstruction.

On sonography (Fig. 5.17) an intraluminal mass with a layered appearance may be seen. It can be seen to intussuscept and de-intussuscept, can have the 'pseudo-kidney' or 'donut' appearance and occasionally the lead point can be determined. CT (Fig.5.19c) findings correlate with the findings described for sonography. A layered or target appearance of the mass, fat within the mass, particularly if in continuity with mesenteric fat and mesenteric vessels entering the mass, are features suggestive of intussusception. Both on sonography and CT a crescent of gas or fluid may separate the mass (the intussusceptum) from the adjacent small bowel (the intussuscipiens).

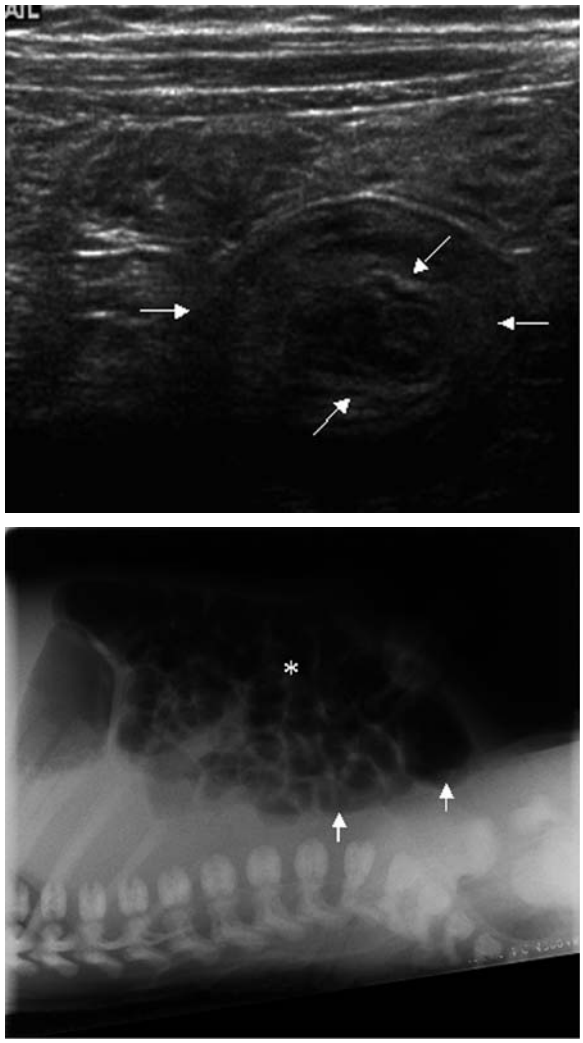

Fig. 5.17. a Transient small bowel intussusception. The intraluminal mass with layered appearance is the small bowel. **b** Small bowel (jejunal) intussusception caused by a bezoar

Idiopathic, transient small bowel intussusceptions need no treatment. The transient nature of the small bowel intussusception will be confirmed by reinvestigation of the small bowel, preferably by sonography, after a few minutes or hours. The intussusception will in most cases have then disappeared (Parker 2003; Strouse et al. 2003).

5.7.2 Ileus

Acquired ileus, encountered in older children or even infants, can be paralytic (adynamic) or obstructive (mechanical).

Paralytic ileus, due to intrinsic abnormalities of the bowel wall, can be caused for example by drugs, after laparotomy, sepsis or peritonitis. Obstructive ileus is most often due to extrinsic causes, for example adhesions (in 70% of cases), incarcerated hernia, small bowel wall hematoma posttraumatic, neoplasms, Crohn disease and intussusception (Parker 2003; Devos and Meradji 2003). Clinically the child has a distended and tender abdomen with failure to pass stools or no defecation and possibly (bilious) vomiting.

Imaging can indicate location, degree, and cause of obstruction and assess for the presence of ischemia.

Plain films remain the first line of imaging. CT is used increasingly because it provides essential diagnostic information not apparent on plain radiographs.

In paralytic ileus supine radiographs of the abdomen will show both dilated small bowel loops and colon, whereas in obstructive ileus usually only the loops proximal to the obstruction are dilated and those distal have a reduced caliber. The closer to the obstruction, the more the loops are dilated. Air-fluid levels on horizontal beam films can be seen in both types of ileus, but in case of obstructive ileus air-fluid levels are concentrated in the dilated loops (Figs. 5.18 and 5.19).

In the acute setting and with clinical symptoms such as (bilious) vomiting and the inability to drink contrast, studies such as a GI tract series and/or enteroclysis are usually not indicated.

Sonography may show dilated fluid-filled bowel loops. The obstructing cause can occasionally be visualized if it is a tumor or hernia. Absence of peristaltic movements, bowel wall thickening without perfusion on color Doppler imaging and dilated small bowel containing fluid can all indicate infarction in the appropriate clinical setting.

CT can be used to distinguish between paralytic (Fig. 5.19) and obstructive ileus or to localize the obstruction but should not be used routinely and care needs to be taken to minimize total radiation dose. Other advantages include the fact that no oral contrast material is needed as the retained intraluminal fluid serves as a natural (negative) contrast agent. It is a rapid, non-invasive, readily available technique with which also extraluminal pathology can be visualized. CT images of an obstructive ileus will identify dilated bowel loops proximally with normal caliber or collapsed loops distally. Sometimes the transition zone, which may resemble a beak, can be identified. This CT sign,

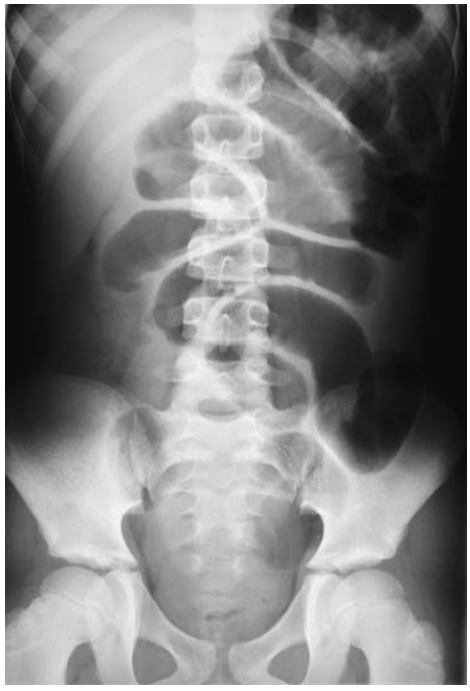

a

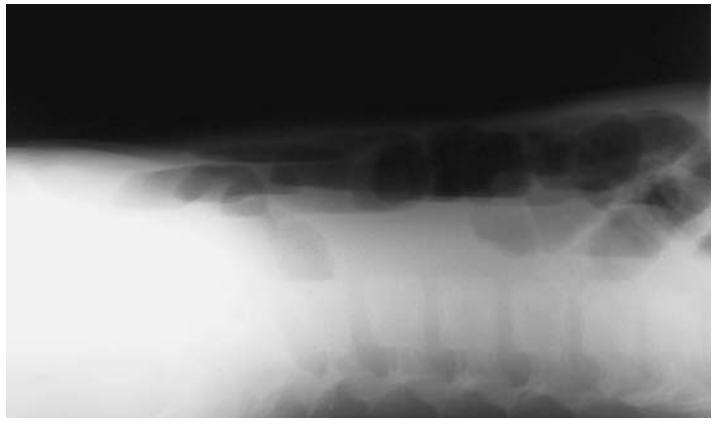

b

Fig. 5.18a,b. Mechanical intestinal obstruction after complicated and perforated appendectomy in a girl. Note the dilated intestinal loops (**a**) and multiple fluid levels on lateral film (**b**)

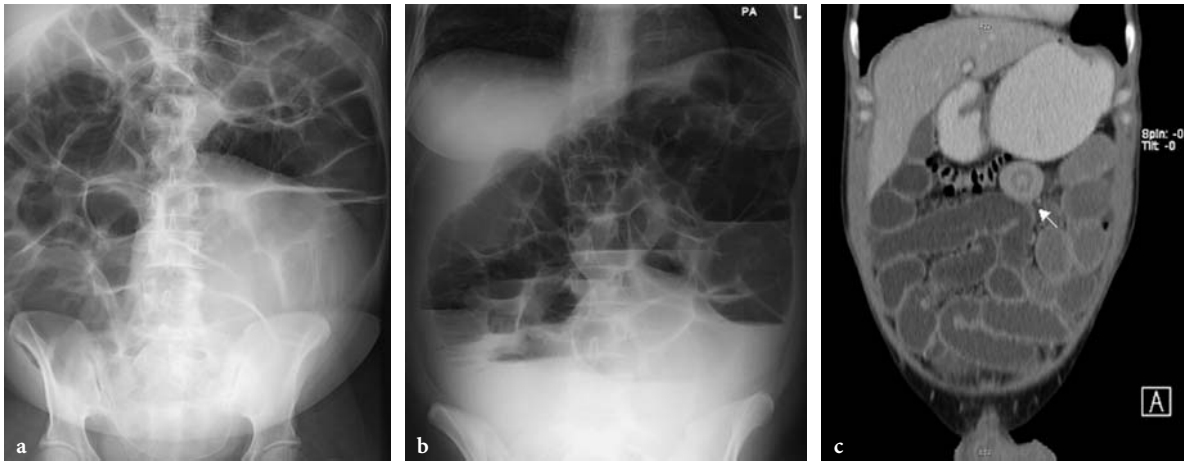

Fig. 5.19. a,b Paralytic ileus. Note the extremely dilated small bowel loops and also the colonic loops containing gas and fluid levels. **c** CT image shows multiple dilated loops of almost equal caliber: indicative of paralytic ileus. *Arrow* indicates small bowel intussusception

among others, is well described by Nicolaou et al. (2005). They also describe the so-called 'string-of-pearl' sign and small-bowel-faeces sign. The string-of-pearl sign is caused by slow resorption of intraluminal air leaving small bubbles trapped between the folds of the valvulae conniventes. The small-bowel-faeces sign results from stasis and mixing of small bowel content. Signs associated with ischemia include thickened bowel wall, ascites, the 'target' sign which refers to the trilaminar appearance of the bowel wall after IV contrast injection, poor or absent contrast enhancement of the bowel wall after IV injection, pneumatosis intestinalis and gas in mesenteric or portal veins, the 'whirl-pool' sign caused by twisting of the mesenteric vasculature around itself caused by a volvulus, tortuous engorged mesenteric vessels, mesenteric hemorrhage, and increased attenuation of bowel wall on non-contrast scans (Nicolaou et al. 2005; Boudiaf et al. 2001).

5.7.3 Tumors

Tumors of the small intestine are rare in children and with the exception of the pre-malignant polyposis syndromes, such as Gardner syndrome and Peutz-Jeghers syndrome, a malignant lesion of the small bowel in children is extremely rare.

Benign small bowel neoplasms are often associated with multi-organ syndromes such as Osler-Weber-Rendu (telangiectatic arteriovenous fistulae), Klippel-Trenaunay-Weber (solitary or multiple haemangiomas) or neurofibromas.

Benign mesenchymal lesions such as lipomas, fibromas and leiomyomas may also occur.

Any of these tend to present with symptoms of abdominal pain or obstruction, sometimes due to intussusception (Carty et al. 2005; Parker 2003).

Plain film is usually unremarkable. Diagnosis may be made with contrast studies. These may reveal polypoid filling defects or a classic intussusceptum.

US distinguishes solid from cystic lesions, and may reveal the polyps as intraluminal, floating lesions that are hyperechogenic, due to the mucosal secretions, and may be nodular or tubular structures. The so-called 'target' configuration on US is caused by the echogenic center that represents the polyp and the surrounding hypoechogenic region, which is the fluid collection in the dilated loops (Fig. 5.20).

CT and MRI can also reveal polyps, but the small bowel should then be filled with enough intraluminal contrast material that surrounds the polyps.

Malignant tumors of the small bowel in children, other than non-Hodgkin lymphoma, usually the B-cell Burkitt lymphoma, are exceedingly rare. Burkitt lymphoma can develop at any age, but is most common in children under the age of 8 years and then predominantly in males. It is a very fast growing non-Hodgkin lymphoma that originates from B-lymphocytes with a predilection for abdominal organs, particularly the distal ileum. Large numbers of lymphoma cells may accumulate in mesenterial lymph nodes. Over the age of 4 years it is the most

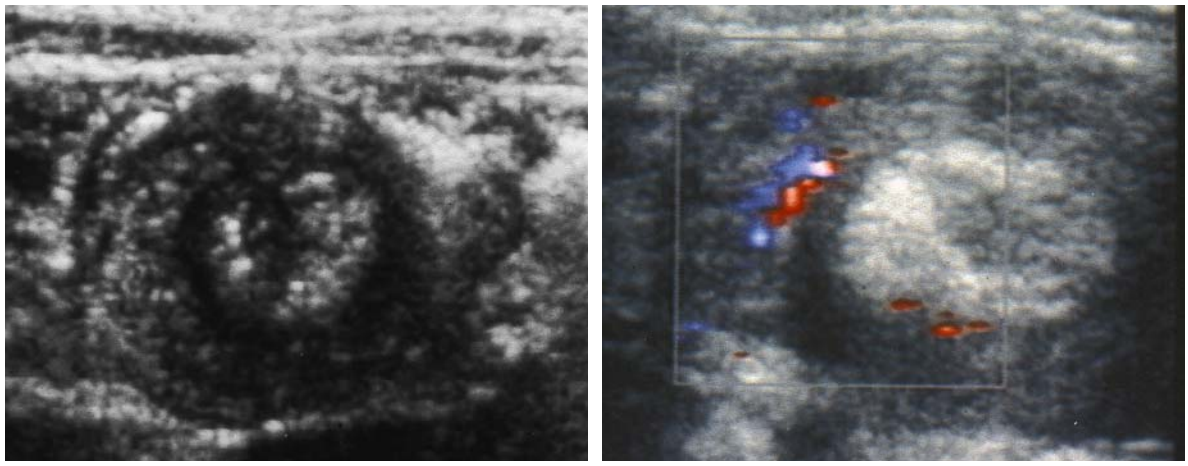

Fig. 5.20a,b. A child with intussusception. The echogenic mass, characteristic for a polyp, is visible as a lead point

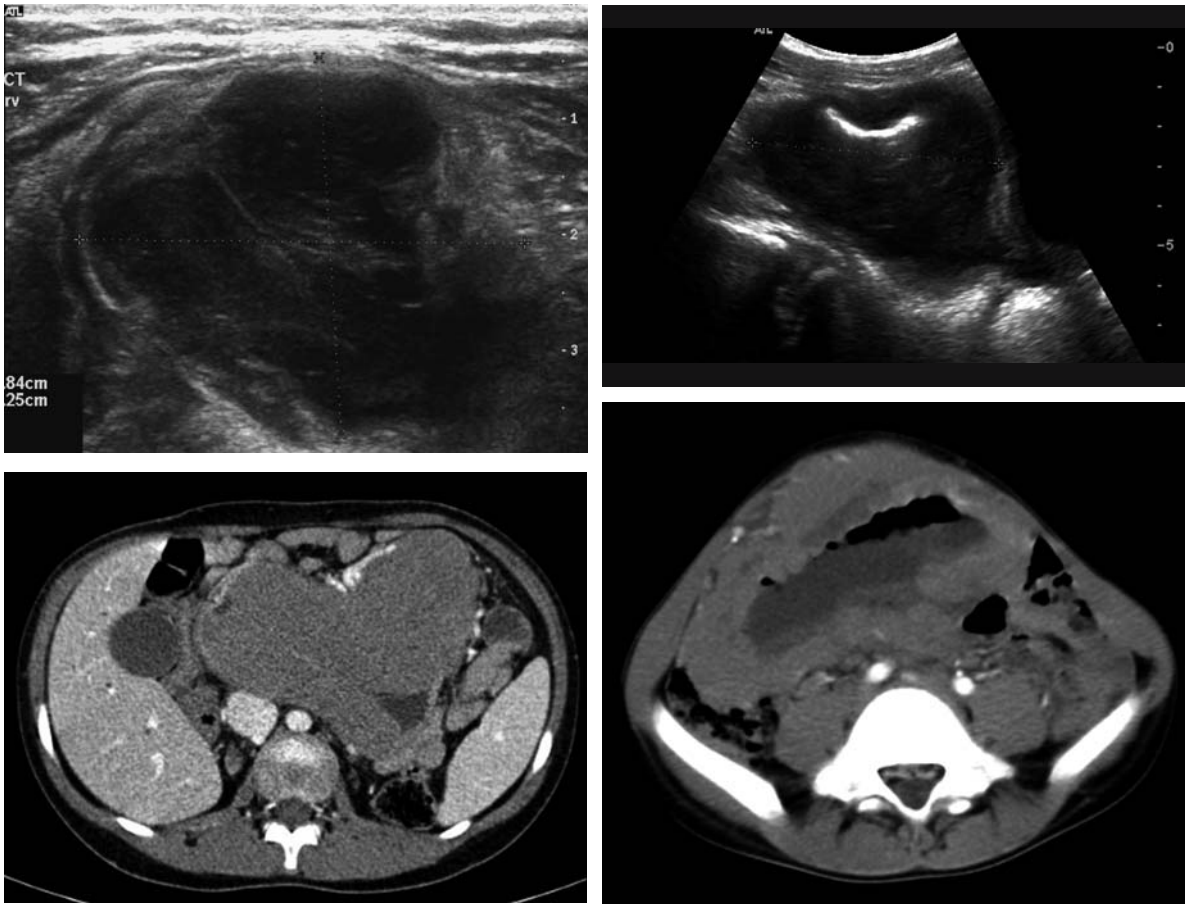

Fig. 5.21. a Burkitt lymphoma. Note the hypoechoic mass located in the ileum wall. **b** Burkitt lymphoma of the small bowel wall with visualization of air (hyperechogenic band) containing small bowel loop. **c,d** Burkitt lymphoma as a hypodense, contrast enhancing mass in the ileum. Dilated neighboring loops

common lead point in children with ileocolic intussusception. Burkitt lymphoma metastasizes often to bone marrow, blood and central nervous system (Parker 2003; Husband and Reznek 2004).

Patient complaints include loss of appetite, vomiting, abdominal pain, obstipation, GI bleeding or a palpable mass in the right lower quadrant.

Plain films may be normal or show signs of obstruction. This may include so-called aneurysmal dilatation, better appreciated on contrast studies as polypoid enlargement/thickening of the mucosal folds. Sometimes a mass in the right lower quadrant can be detected.

Ultrasound may show a hypoechoic or anechoic mass, localized eccentrically in the ileum of which the lumen is frequently dilated (Fig. 5.21a). Enlarged mesenterial lymph nodes and sometimes ascites may be seen.

CT and MRI may show infiltration of the bowel wall, dilatation of the lumen, sometimes ascites and enlarged mesenteric lymph nodes (Fig. 5.21b).

Unusual tumors in childhood also include the malignant counterparts of lipomas, fibromas, neurofibromas and leiomyomas (Parker 2003).

5.7.4 Protein-Losing Enteropathies

Many etiologies for protein-losing enteropathies (celiac disease, intestinal lymphangiectasis, allergic gastroenteritis, cow milk protein allergy, Crohn disease, cystic fibrosis, collagen vascular disease, short bowel, intestinal transplants and others) have been identified.

Celiac disease is the commonest cause of intestinal malabsorption in childhood. The etiology is an intolerance to the gliadin component of gluten. Most patients present early in childhood with failure to thrive, abdominal distension, diarrhea and stools that may be steatorrheic. Adolescents have delayed puberty, anorexia and clinical findings due to hypocalcemia and hypoproteinemia. It is distinctly unusual in people of Asian and African descent.

Diagnosis is made by clinical findings and jejunal biopsy that shows subtotal villous atrophy.

Imaging is done before diagnosis is made or to exclude other causes.

Plain film may be normal or show small bowel dilatation.

On US, hyperperistalsis, fluid-filled dilated small bowel loops, thickened bowel wall, enlarged mesenteric lymph nodes and ascites can be seen (Fig. 5.22).

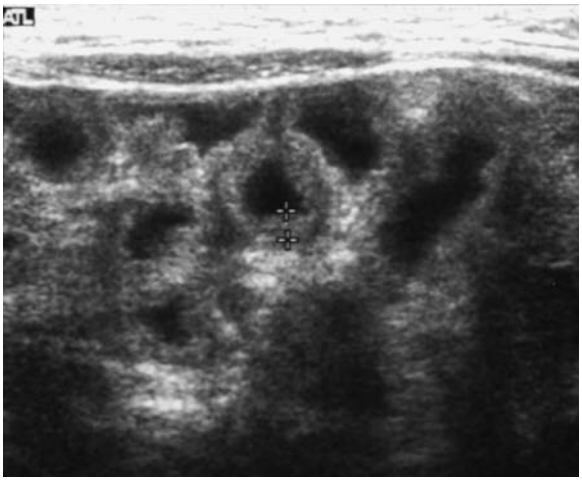

Fig. 5.22. Ultrasound in a patient with celiac disease. Fluid filled, dilated small bowel with a thickened wall is demonstrated

The upper GI tract examination may show dilated small bowel, thickened mucosal folds and rarely flocculation, as well as segmentation of the barium (Parker 2003).

Small intestinal lymphangiectasia is a primary or secondary protein-losing enteropathy. As a secondary disorder it is acquired as a result of surgical damage to the lymphatic vessels, chronic right-sided heart failure, ascites, constrictive pericarditis, retroperitoneal tumor, tuberculosis or inflammatory bowel disease. Primary intestinal lymphangiectasia is a rare congenital protein-losing enteropathy characterized by hypoplastic lymphatic vessels within the intestinal mucosa, submucosa and small bowel mesentery. Lymphatic flow is obstructed and small intestinal lymphatic channels will dilatate, causing the small bowel wall to appear thickened. Rupture of these dilated lymphatics into the small bowel lumen and occasionally into the peritoneal cavity results in hypoproteinemia, steatorrhea, lymphopenia, ascites and even pleural effusions.

Findings on plain film and contrast (barium) studies are similar to celiac disease.

On US, hyperperistalsis, fluid-filled dilated small bowel loops, thickened bowel wall, hyperechogenic, edematous mesentery and ascites can be seen.

Abdominal CT images may show diffuse small intestinal wall thickening and dilatation, mesenteric edema, ascites and possibly relatively low density confluent mesenteric soft tissue masses that represent lymphangiomas (Parker 2003).

5.7.5 Inflammatory Disease (M. Crohn)

In Crohn disease the underlying etiology is a segmental transmural granulomatous inflammation that can be seen to extend from mouth to anus. It is the most common chronic inflammatory condition of the small bowel in children. While a total of 25% of cases present during childhood, it is rare before the age of 5–8 years. Most affected are firstly the terminal ileum and secondly the colon. It is limited to the colon in 15% of cases. The inflammation can be localized in one or more segments. In the case of multiple segments, normal intestine lies interdispersed between inflamed intestine. Edema and fibrotic thickening of the affected wall and spasms cause a narrowing of the intestinal lumen and resulting pre-stenotic dilatation. In cases of inflammatory bowel disease patients present not only with diarrhea, abdominal pain, anorexia, a palpable abdominal mass and, if of long-standing, anorectal fistulas, but also with a failure to thrive, delayed puberty, fever, aphthous stomatitis, arthralgia, arthritis, sacroiliitis and erythema nodosum.

Plain film may be normal. Adynamic ileus, bowel wall thickening and occasionally focally abnormal dilated loops with thickened bowel wall can be seen in the case of acute exacerbation. Imaging the small bowel has always been difficult due to the long and winding shape of the lumen, overlapping segments and motility patterns. Small bowel lesions will be looked for with a barium contrast follow-through exam or enteroclysis. Granularity, reflecting mucosal edema, mucosal fold thickening and effacement of the mucosal pattern, cobblestone pattern because of linear and transverse ulceration, pseudopolyps, narrowed bowel loops and pre-stenotic dilatation, separation and retraction of bowel loops because of the inflamed, thickened and fibrotic mesentery, as well as enteroenteric and enterocolic fistulas can be seen (Fig. 5.23a,b) (Parker 2003).

US is useful as a screening tool and in the follow-up to evaluate the therapeutic result, as well as complications such as abscesses.

US is able to show thickened bowel walls, separation of bowel loops because of thickened and edematous, hyperechogenic mesentery and absence of peristaltic movements. Color Doppler is useful to detect a higher flow velocity in the superior mesenteric artery and to identify areas of active inflammation in which an increased Doppler signal will be found in and around the thickened bowel wall (Fig. 5.23c).

CT is only used to evaluate complications, when US is inconclusive or percutaneous drainage is required (Parker 2003; Devos and Merdji 2003).

Recent developments in MR techniques allow much faster and higher quality image acquisition. Frokjaer et al. (2005) showed that high quality MR images can reliably identify stenosis, cobblestone pattern, fissures, wall thickening, wall enhancement upon intravenous gadolinium and exoenteric changes such as mesenterial inflammation, fibrofatty proliferation, lymphadenopathy, hypervascularity, abscesses and fistulas. Luminal distension, achieved by oral or via the duodenal tube administration, is a necessity since collapsed bowel loops can conceal even large lesions, or the exact grade of obstruction can be underestimated. Certainly in cases where repeat evaluation during treatment is necessary, and when US is inconclusive, MR should gain acceptance.

5.7.6 Superior Mesenteric Artery Syndrome

Superior mesenteric artery (SMA) syndrome is an uncommon but well recognized clinical entity characterized by compression of the third, or transverse, portion of the duodenum against the aorta by the SMA, resulting in chronic, intermittent or acute complete or partial duodenal obstruction. Clinical symptoms are chronic upper abdominal symptoms such as epigastric pain, nausea, vomiting (bilious or partially digested food), postprandial discomfort and sometimes subacute small bowel obstruction. The stomach can be massively dilated and perforation has been described (Carty et al. 2005; Parker 2003).

An asthenic habitus is noted in about 80% of cases. Other possible etiologic factors are exaggerated lumbar lordosis, depletion of the mesenteric fat caused by rapid severe weight loss, anorexia nervosa, spinal disease or deformity, anatomic anomalies such as abnormally high and fixed position of the ligament of Treitz with an upward displacement of the duodenum and unusually low origin of the SMA and the familial SMA syndrome. An acute form of SMA syndrome is described following scoliosis treatment in which presumably the abrupt straightening of the spine changes the angle

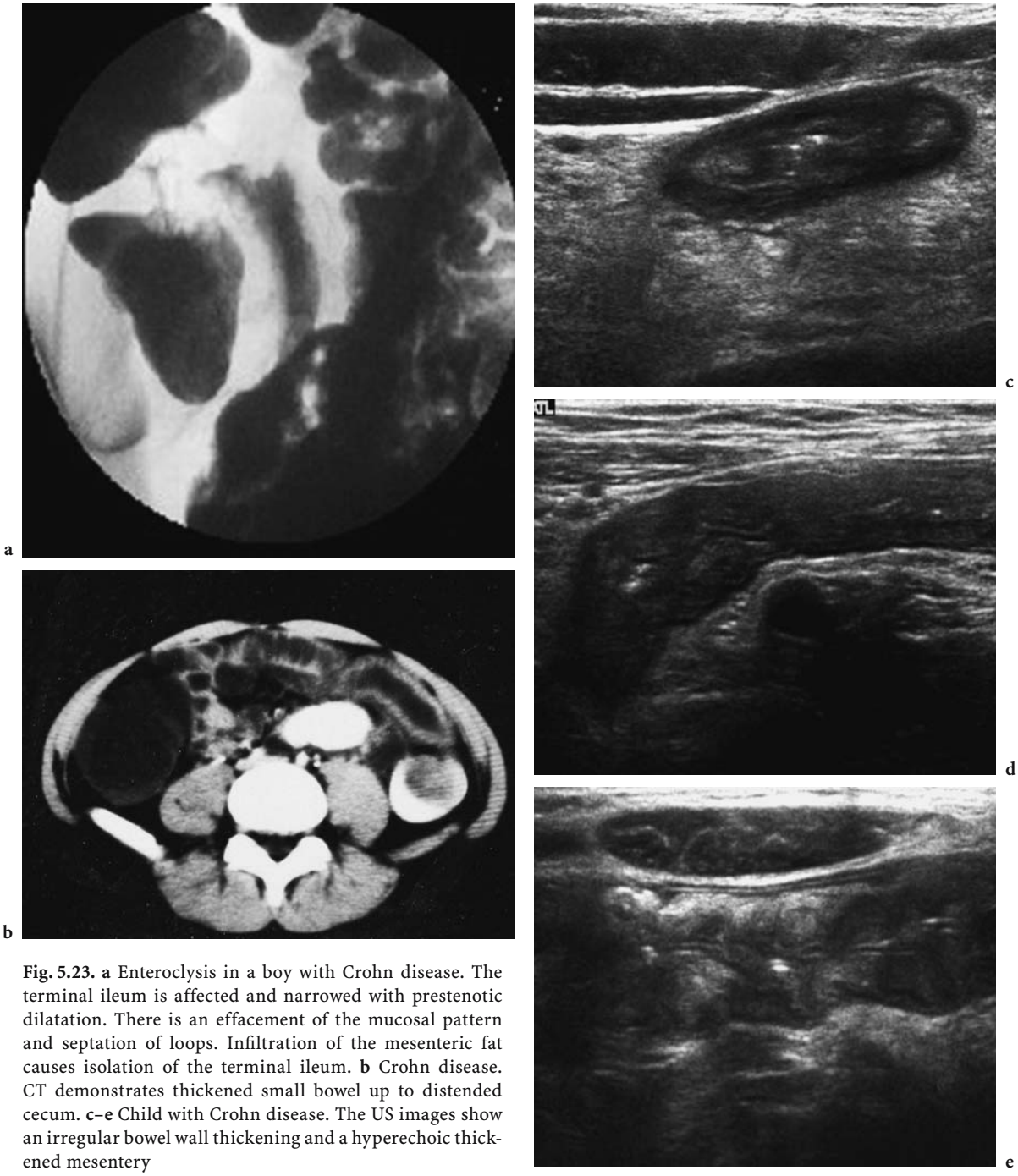

Fig. 5.23. a Enteroclysis in a boy with Crohn disease. The terminal ileum is affected and narrowed with prestenotic dilatation. There is an effacement of the mucosal pattern and septation of loops. Infiltration of the mesenteric fat causes isolation of the terminal ileum. **b** Crohn disease. CT demonstrates thickened small bowel up to distended cecum. **c–e** Child with Crohn disease. The US images show an irregular bowel wall thickening and a hyperechoic thickened mesentery

at which the SMA branches from the aorta causing duodenal compression.

Plain film may show gastric dilatation; however, the stomach may be decompressed by vomiting.

An upper GI tract exam with barium shows a high-grade partial obstruction of the third portion of the duodenum (Ortiz et al. 1990).

5.7.7 Cystic Fibrosis

Cystic fibrosis (CF) with an incidence of 1 in 2500 white live births, is the most common lethal, autosomal recessive disorder in white children (Chaudry et al. 2006; Lardenoye et al. 2004; Agrons et al.

1996) . This disorder is caused by mutations in the CF transmembrane regulator (CFTR) gene, which is located on the long arm of chromosome 7. Multiple different mutations of this gene exist.

The gastrointestinal manifestations are seen throughout childhood, from infancy to adolescence. They result from abnormally viscous luminal secretions within hollow viscera and the ducts of solid organs.

Bowel obstruction may be present at birth due to meconium ileus. Older children might present with distal intestinal obstruction syndrome (DIOS), colonic stricture(s) and, less commonly, intussusception, fecal impaction of the appendix, gastroesophageal reflux or recurrent rectal prolapse (Fig. 5.24).

5.7.7.1 Meconium Ileus

Between 10% and 15% of newborns with CF are affected by meconium ileus resulting from inspissated intraluminal meconium at the narrowest portion of the GI tract, the terminal ileum (Carty et al. 2005; Parker 2003; Grier 1999; Devos and Meradji 2003; Berrocal et al. 1999; Chaudry et al. 2006; Agrons et al. 1996).

Patients present with failure to pass meconium and a distended, painful abdomen.

Plain abdominal films will demonstrate a distended abdomen due to distal small bowel obstruction with many markedly dilated proximal small bowel loops and a bubbly appearance of the bowel in the right lower quadrant caused by mixing gas with viscous impacted meconium in the terminal ileum (Fig. 5.25).

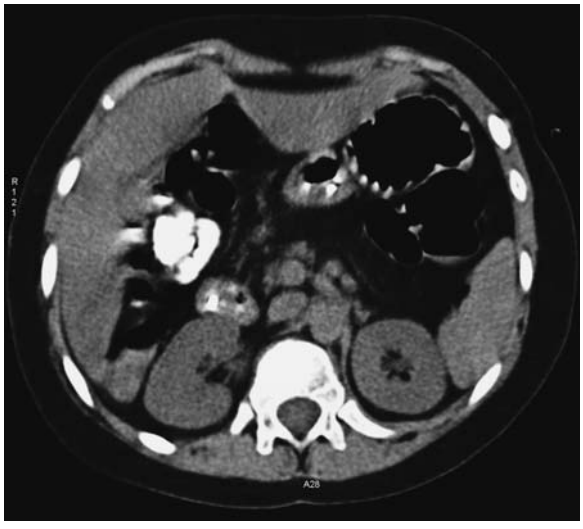

Fig. 5.24. CT image depicts the virtual disappearance of the pancreas in a patient with CF

On sonography this impacted meconium will be located in the ileum.

Contrast enema will demonstrate a microcolon with visualization of the meconium pellets in the terminal ileum. The microcolon results from the failure of the meconium to pass into the colon, which would thereby allow the colon to assume its normal caliber (Fig. 5.26). In about 50% of cases the enema will be curative.

Complications of meconium ileus are volvulus, perforation, small bowel atresia and meconium peritonitis with abdominal calcifications.

5.7.7.2 Distal Intestinal Obstruction Syndrome (DIOS)

DIOS will develop in approximately 15% of patients with CF (Carty et al. 2005; Parker 2003; Grier 1999; Devos and Meradji 2003; Berrocal et al. 1999; Chaudry et al. 2006; Agrons et al. 1996).

Clinical symptoms are related to those caused by a varying severity of bowel obstruction with recurrent abdominal pain and a palpable right lower quadrant mass.

Plain radiographs will show a proximal small bowel obstruction with faecal impaction in the terminal ileum and caecum (Fig. 5.27). The term 'meconium ileus equivalent' should be discarded.

A contrast enema with a water-soluble (diluted gastrographin) 1:3 contrast medium will show fecal impaction in the terminal ileum and proximal colon. This procedure may also have a therapeutic effect (Devos and Meradji 2003).

5.7.7.3 Intussusception

A tenacious intestinal residue, enlarged lymphoid follicles or a distended appendix may serve as a lead point for an intussusception. It is seen in only 1% of CF patients. The intussusception is usually ileocolic.

For clinical symptoms, radiographic imaging methods and (radiological) treatment, refer to Chapter 1.

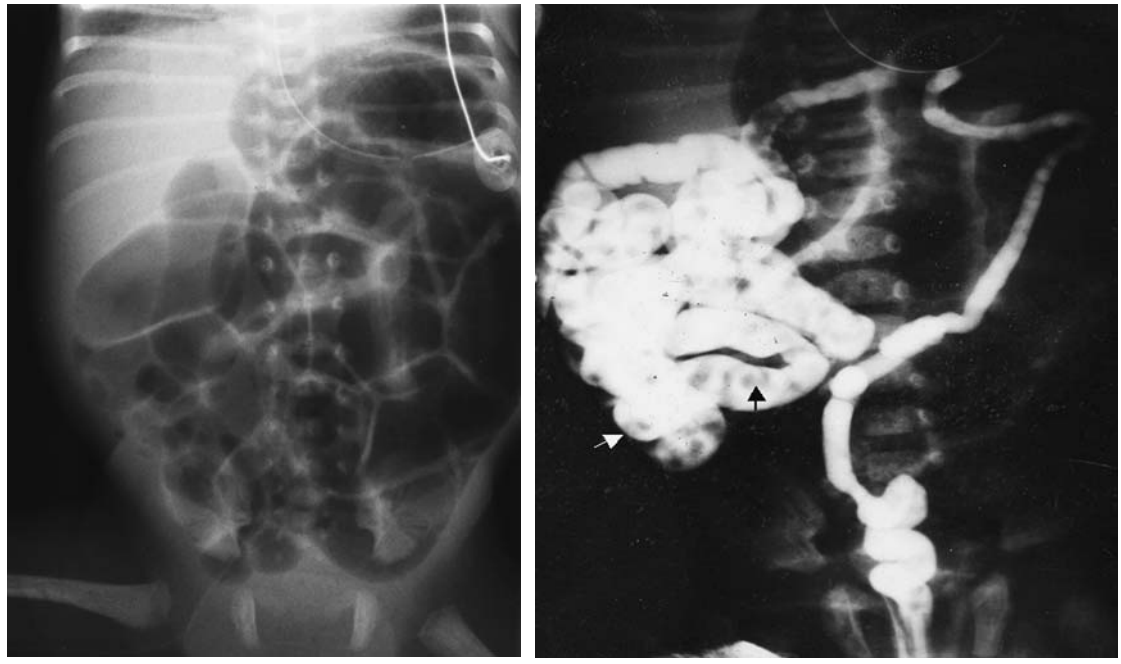

a

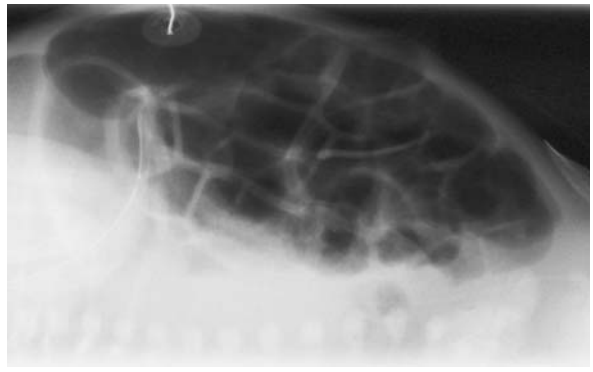

b

c

Fig. 5.25. a Meconium ileus in a 3-day-old neonate. The small bowel is dilated and has a bubbly irregularity in the right lower quadrant. **b** On the lateral film of the abdomen no colonic loops are visible. There are no gas-fluid levels. **c** Contrast enema shows "microcolon" as a result of meconium ileus. Meconium pellets demonstrated in the terminal ileum (*arrows*)

5.7.8 Abdominal Tuberculosis

Abdominal tuberculosis (TB) is rare in childhood and usually a diagnostic challenge, particularly in the absence of active pulmonary infection, and because clinical manifestations and results of laboratory studies are nonspecific. Intestinal TB can involve any segment of the gastrointestinal tract, but has a predilection for the ileocecal valve and the adjacent ileum and cecum (Parker 2003; Engin and Balk 2005).

Clinical features suggestive of TB are a history of fever, abdominal pain and weight loss.

Abdominal plain films may show no abnormalities or show a few or multiple air-fluid levels in the small bowel loops due to the enteritis component.

Upper GI examination reveals thickened folds, spasticity, irregular contours, and ulcers involving the cecum and terminal ileum. In the case of fibrosis, single or multiple short strictures that can be localized in a single segment or be present throughout the bowel will be found. Incidentally fistulae formation can be recognized radiographically.

Sonographic evaluation may show thickening of the wall of the cecum and terminal ileum, an inflammatory mass, dilated small bowel loops, an increase of mesenteric thickness and echogenicity (due to fat deposition), mesenteric lymphadenopathy and ascites. The lymph nodes are heterogeneous and can contain calcifications. Calcifications are virtually pathognomonic for TB (Jain et al. 1995).

Imaging with CT will show the same findings as with US, but is the preferred examination for obese

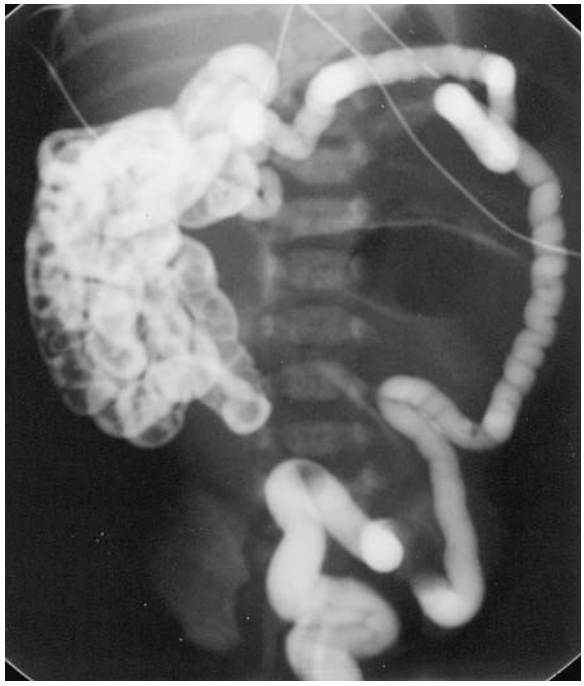

Fig. 5.26. Contrast enema with water-soluble medium which demonstrates a meconium ileus with impaction of meconium in the ileum and an unused colon

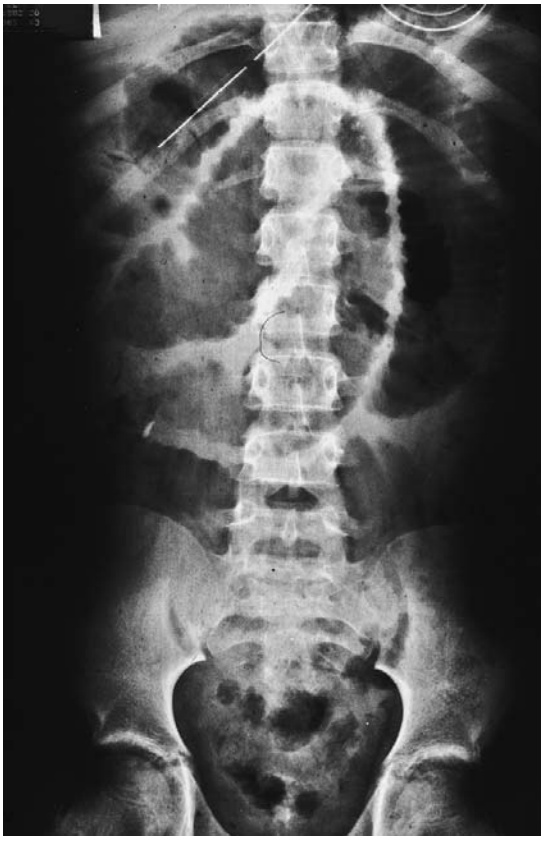

Fig. 5.27. A boy with cystic fibrosis complicated with distal intestinal obstruction syndrome. Note the dilated intestinal loops and huge fecal impaction in the terminal ileum and caecum

children, children in which US is difficult because of heavy pain when touching the abdomen, or if biopsy is needed (Fig. 5.28).

MRI of abdominal TB lymphadenopathy shows a variety of signal intensities and patterns of contrast enhancement and is described by De Backer et al. (2005). Mostly the signal intensities, in relation to abdominal wall muscle, are hyperintense on T2-WI with, in some cases, a hypointense peripheral rim and internal heterogeneity and hypo-/iso-intensity on T1-WI, also occasionally with a peripheral rim, but then hyperintense or internal heterogeneity. Contrast-enhanced fat-suppressed T1-WI demonstrate predominantly peripheral enhancement.

Crohn disease and peri-appendiceal abscesses should be considered as differential diagnoses, as well as, although less frequently in the case of children, carcinoma and lymphoma.

5.7.9 Henoch-Schönlein Purpura

Henoch-Schönlein is a type of hypersensitivity vasculitis and inflammatory response within the blood vessel. It is caused by an abnormal response of the immune system. The syndrome is usually seen in children and is more common in boys (Parker 2003).

Clinical symptoms are purple spots on the skin, joint pain, gastrointestinal symptoms and glomerulonephritis. Gastrointestinal symptoms include abdominal pain, nausea, vomiting, diarrhea and bloody stools. Bleeding into the bowel wall occurs in about half of patients and may act as a lead point for intussusception.

Routine abdominal radiographs (Fig. 5.29a) give no significant information and are not recommended, unless perforation is clinically suspected.

Ultrasound is the imaging modality of choice and will show thickened bowel wall, ascites, ileus of affected loops, bowel dilatation and possible entero-enteric intussusceptions (Fig. 5.29b) (Connolly and O'Halpin 1994).

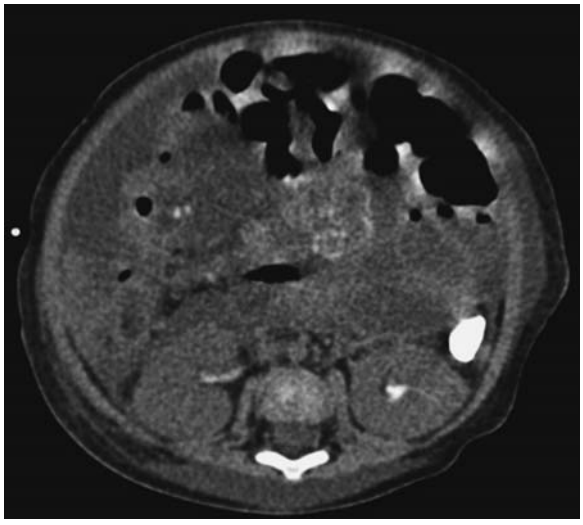

Fig. 5.28. Intestinal tuberculosis. CT scan shows the heterogenic, hypodense masses with peripheral ringlike calcifications following lymphadenitis and ascites

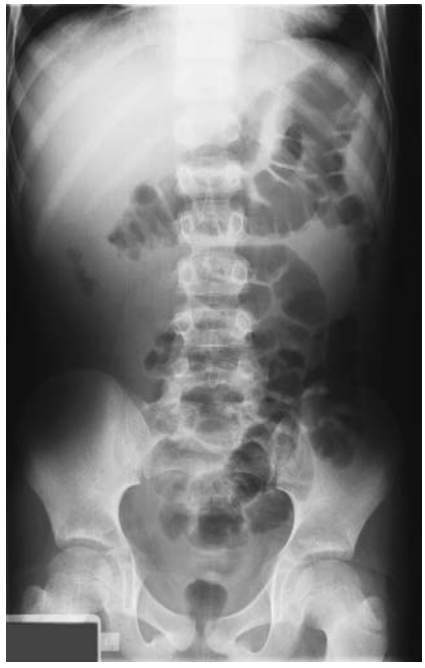

a

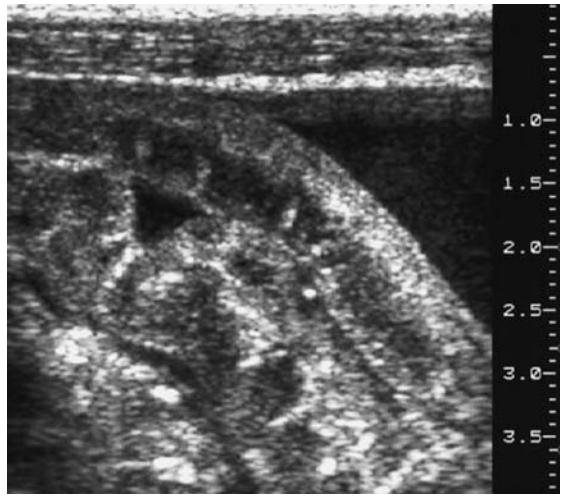

c

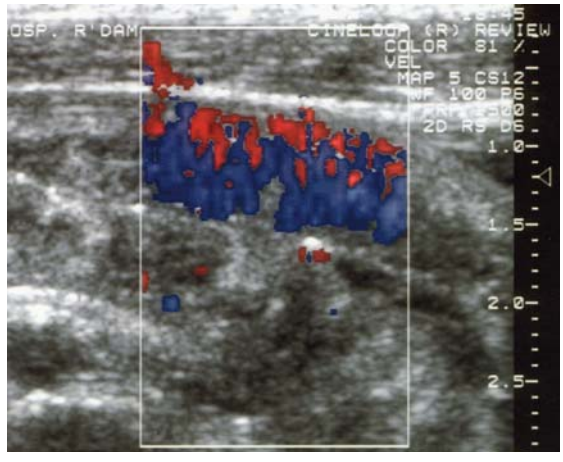

d

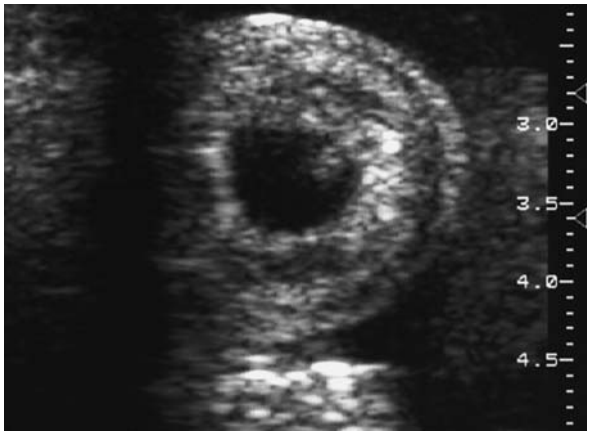

b

Fig. 5.29. a Supine abdominal film of a child with Henoch-Schönlein. Note the intestinal wall thickening on plain film. **b–d** A patient with Henoch-Schönlein disease. The thickened wall is demonstrated by ultrasound

References

Agrons GA, Corse WR, Markowitz RI et al. (1996) Gastrointestinal manifestations of cystic fibrosis: radiologic-pathologic correlation. Radiographics 16:871–893

Andrassy RJ, Mahour GH (1981) Malrotation of the midgut in infants and children: a 25-year review. Arch Surg 116:158–160

Berrocal T, Lamas M, Gutieerrez J et al. (1999) Congenital anomalies of the small intestine, colon, and rectum. Radiographics 19:1219–1236

Boudiaf M, Soyer P, Terem C et al. (2001) CT evaluation of small bowel obstruction. Radiographics 21:613–624 (review)

Carty H, Brunelle F, Stringer D, Kao S (2005) The gastrointestinal tract. In: Carty H, Brunelle F, Stringer D, Kao S (eds) Imaging children, 2nd edn, vol. 2. Elsevier Churchill Livingston, pp 1289–1545

Chaudry G, Navarro OM, Levine DS, Oudjhane K (2006) Abdominal manifestations of cystic fibrosis in children. Pediatr Radiol 36:233–240

Connolly B, O'Halpin D (1994) Sonographic evaluation of the abdomen in Henoch-Schönlein purpura. Clin radiol 49:320–323

De Backer AI, Mortele KJ, Deeren D et al. (2005) Abdominal tuberculosis lymphadenopathy: MRI features. Eur Radiol 15:2104–2109

Devos A, Meradji M (2003) Werkboek Kinderradiologie. Hoofdstuk VII: Maag-Darmkanaal. 2003 pp 72–99

Engin G, Balk E (2005) Imaging findings of intestinal tuberculosis. J Comput Assist Tomogr 29:37–41

Frokjaer JB, Larsen E, Steffensen E, Nielsen AH, Drewes AM (2005) Magnetic resonance imaging of the small bowel in Crohn's disease. Scand J Gastroenterol 40:832–842

Grier D (1999) Radiology of pediatric gastrointestinal emergencies. In: Carty H (ed) Emergency pediatric radiology. Springer, Berlin Heidelberg New York, pp 117–182

Husband JE, Reznek RH (2004) Imaging in oncology, 2nd edn, parts III and IV. Taylor and Francis, London, pp 817–874 and pp 921–998

Jain R, Sawhney S, Bhargava DK, Berry M (1995) Diagnosis of abdominal tuberculosis: sonographic findings in patients with early disease. AJR Am J Roentgenol 165:1391–1395

Lardenoye SW, Puylaert JB, Smit MJ, Holscher HC (2004) Appendix in children with cystic fibrosis: US features. Radiology 232:187–189

Nicolaou S, Kai B, Ho S et al (2005) Imaging of acute small bowel obstruction. AJR Am J Roentgenol 185:1036–1044 (review)

Ortiz C, Cleveland RH, Blickman JG, Jaramillo D, Kim SH (1990) Familial superior mesenteric artery syndrome. Pediatr Radiol 20:588–589

Parker BR (2003) Abdominal and gastrointestinal tract, small intestine. In: Kuhn J, Slovis T, Holler J (eds) Caffey`s pediatric diagnostic imaging, 10th edn. Mosby, Philadelphia . pp 1616–1648

Strouse PJ, DiPietro MA, Saez F (2003) Transient small-bowel intussusception in children on CT. Pediatr Radiol 33:316–320

The Colon

6

Melanie P. Hiorns and Christine M. Hall

CONTENTS

M. P. Hiorns, MBBS, MRCP, FRCR
Consultant Paediatric Radiologist and Honorary Senior Lecturer, Great Ormond Street Hospital, London, WC1N 3JH, UK
C. M. Hall, MBBS, DMRD, FRCR
Professor of Paediatric Radiology, Great Ormond Street Hospital, London, WC1N 3JH, UK

6.1 Appendicitis

6.1.1 Overview

Appendicitis most commonly occurs over the age of 5 years, is rare in those under 2 years, but may occur at any age and is the most common condition requiring emergency abdominal surgery in children (Janik and Firor 1979). Incidence in the paediatric age group shows wide geographical variation but overall incidence appears to be declining. Previ-

ous quoted incidence rates were approximately 1 in every 250 children but a recent study now suggests rates may be as low as 1 in 850 in children and young adults (Williams et al. 1998). The aetiology is that of appendiceal luminal obstruction, most commonly by lymphoid hyperplasia (60%) but also by hard concretions (faecoliths 33%), faecal impaction or appendiceal calculi (appendicolith). Rarer causes in children include tumour, stricture, parasites and Crohn's disease. Appendiceal obstruction is followed by luminal distention, ischaemia and bacterial invasion. Necrosis of the appendiceal wall then develops resulting in perforation and abscess formation.

Clinical criteria are most often used to make the diagnosis of appendicitis and the common clinical symptoms including cramping in the right iliac fossa and lower abdominal pain, vomiting, diarrhoea and sometimes dysuria. The signs are those of fever (56%), a leucocytosis (88%) of between 10,000 cells per milliliter and 20,000 cells per milliliter, guarding and tenderness in the right iliac fossa. However, the classic signs and symptoms are not present in up to 30% of patients and hence the clinical diagnosis is not always straightforward. Imaging plays an increasingly important role in the diagnostic pathway.

The main imaging technique in children with suspected appendicitis is compression graded ultrasound. Much has been written and described about the findings on the plain abdominal radiograph (AXR) but the AXR is typically normal in the early stages of appendicitis and can remain normal in more than 50% of cases. Plain films are insensitive and non-specific. Current practice is therefore either to make a clinical decision to go to appendicectomy, or to observe the child, or to proceed to ultrasound for diagnostic guidance. The sensitivity of ultrasound has ranged from 80%–94% and the specificity between 86% and 98% in various published series (Abu-Yousef et al. 1987; Jeffrey et al. 1988; Puylaert 1986; Sivit et al. 1992; Vignault et al. 1990). Ultrasound has several advantages as a diagnostic tool in the setting of appendicitis, and these include its lower cost than other techniques, lack of ionizing radiation and its ability to assess ovarian pathology that can often mimic acute appendicitis in young female patients. Furthermore, ultrasound is useful for excluding other differential diagnoses including intussusception. The disadvantages of ultrasound are a higher dependency on the skills of the operator, and its reduced sensitivity in obese patients or in patients whose degree of abdominal pain prevents a thorough examination.

In the last decade computed tomography (CT) has become widely utilized in the adult population in the diagnosis of the acute abdomen and this is now becoming more common practice in children. The main advantages of CT include less operator dependency than sonography and a subsequent higher diagnostic accuracy, and enhanced delineation of disease extent in perforated appendicitis. The disadvantages, particularly in children, are those of lack of intra-abdominal fat, a moderate to high radiation burden and, depending on the age of the child, the need for sedation or general anaesthesia.

The current suggested diagnostic approach is therefore to consider an AXR, not to make the diagnosis of appendicitis, but to exclude complications such as free intraperitoneal air, or to exclude other confounding diagnoses such as renal colic, small bowel obstruction or constipation. In the presence of a normal AXR or non-specific signs, ultrasound is then advised. If the clinical findings strongly suggest appendicitis ultrasound should be performed as the first investigation. Following the results of the ultrasound, clinical examination and laboratory tests, CT may then be considered depending on the degree of confidence in the diagnosis and the institution.

6.1.2 Graded Compression Sonography for Appendicitis

Graded compression sonography for appendicitis was first described by Puylaert (1986). Normal bowel is readily compressible when light pressure is applied with an ultrasound transducer. Processes affecting the bowel wall such as oedema, inflammation, neoplasm or haemorrhage alter the compliance of the bowel wall and render it relatively non-compressible. The basic principle underlying graded compression in diagnosing appendicitis is to compress away the normal lumen of the terminal ileum and the caecum and to allow better visualization of the non-compressible inflamed or obstructed appendix. A linear array transducer is used, typically a 6- to 8-MHz transducer depending on the patient's age and body habitus, although an 8- to 15-MHz transducer may be suitable in infants. The transducer must have sufficient penetration to image the iliac vessel and psoas muscles as visualization of these structures is necessary for an adequate examination, the appendix

lying anterior to these structures. It is often helpful with co-operative children to ask the patient to point to the site of maximal pain and tenderness. This can be particularly helpful if the appendix is in an atypical site. Initially the right flank is scanned with light pressure to identify the ascending colon, this being the largest luminal structure of the gastrointestinal tract (with little or no peristalsis), and is seen adjacent to the abdominal wall. The right colon is then followed inferiorly to termination at the caecum. To avoid inducing pain, pressure is gradually increased over the tip of the caecum. Bowel gas and fluid within the caecum and terminal ileum are gradually compressed away, allowing visualization of the appendix. The study is performed in both longitudinal and transverse planes.

Criteria to be sought according to the recent literature include: enlarged appendix, fluid in the appendiceal lumen, lack of compressibility of the appendix, colour in the appendiceal wall on colour Doppler ultrasound, inflammatory changes in the perienteric fat in the right lower quadrant, caecal wall thickening, right lower quadrant lymph nodes and peritoneal fluid (Kessler 2004).

The inability to visualise a normal appendix has previously been considered a major weakness of ultrasound in assessing patients with suspected appendicitis. However, with technological advances in equipment and increasing operator experience the normal appendix should be visualised in 64%–82% of healthy patients (Rioux 1992; Rettenbacher et al. 2001; Kessler et al. 2004).

6.1.2.1 Diagnostic Criteria

Sonographic criteria for acute appendicitis include a non-compressible appendix with an outer AP diameter of at least 6 mm (Kessler et al. 2004), mural thickness of 3 mm or greater, or the presence of an appendicolith in an appendix of any size (Figs. 6.1, 6.2). The two most useful ultrasound signs are those of an appendiceal diameter of ≥ 6 mm (sensitivity 98%, specificity 98%, positive predictive value (PPV) 98%, negative predictive values (NPV) 98%) and non-compressibility (sensitivity 96%, specificity 96%, PPV 96%, NPV 96% (Kessler et al. 2004)). If the appendix measures less than 6 mm in diameter, particularly if compressible, this should be considered normal. The use of colour Doppler may be helpful in showing hyperaemia associated with appendiceal wall inflammation.

Presence of a hypo-echoic fluid collection containing an appendicolith or a fluid collection adjacent to a gangrenous appendix is diagnostic for a peri-appendiceal abscess (Fig. 6.3).

Appendicitis may occur at the tip of the appendix and therefore the appendix must be visualized throughout its length to exclude a distal 'tip appendicitis'. The normal appendix may be difficult to visualize due to its small luminal diameter and easy compressibility. However, with operator experience it should be identified in the majority of cases. Features of a normal appendix include: (1) the typical normal sonographic appearance of bowel, with an

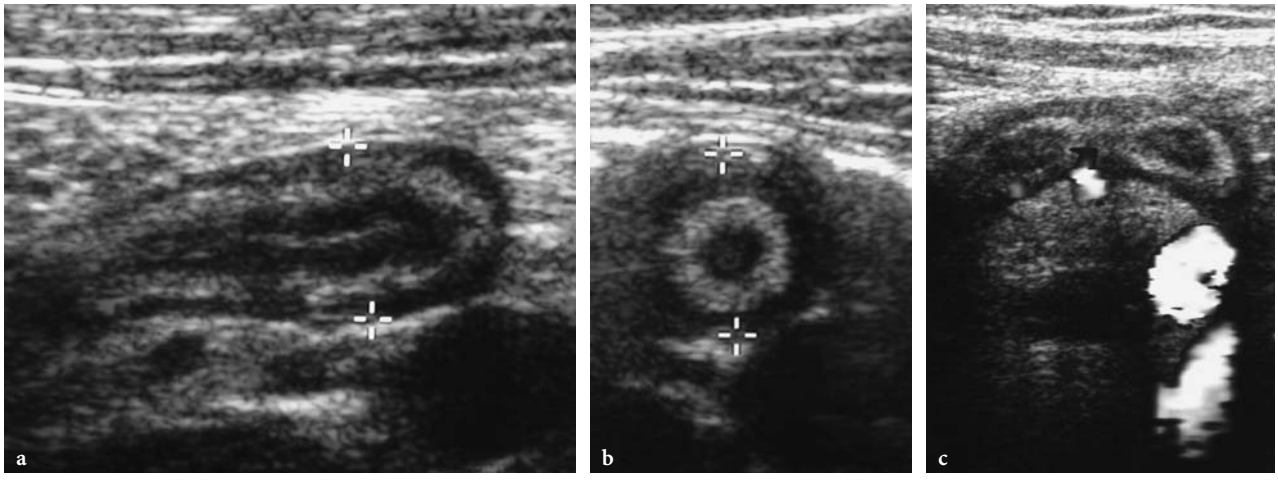

Fig. 6.1a–c. Acute appendicitis in a 12-year-old boy. **a** Longitudinal ultrasound image showing a swollen appendix (*markers*) which measured 7 mm. Note the increased echogenicity in the wall. **b** Transverse image (TS) showing the concentric layers of the inflamed appendix. **c** TS image showing two sections of the curved appendix and it's relationship to the iliac vessels

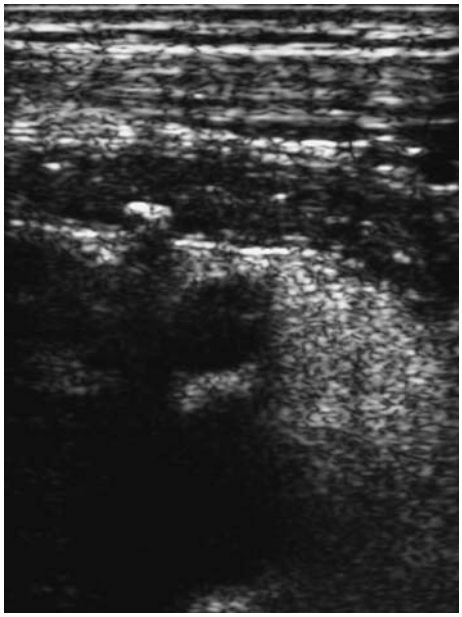

Fig. 6.2. Acute appendicitis in a 14-year-old boy showing the presence of an appendicolith with posterior acoustic shadowing on ultrasound

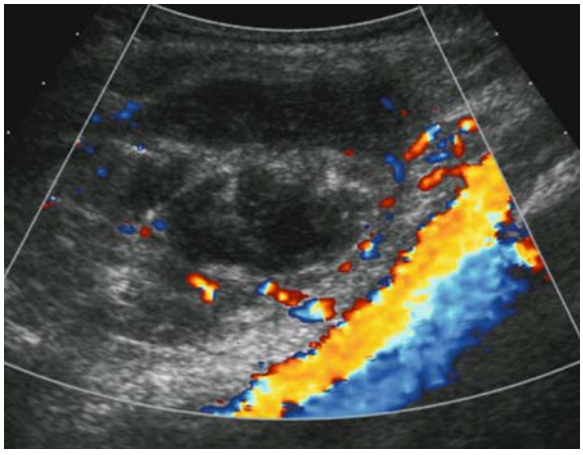

Fig. 6.3. Ultrasound of a heterogenous appendix mass in a 12-year-old girl

echogenic submucosal ring, (2) terminating with a blind tip (3), origin from the base of the caecum (4), and lack of peristalsis as it is part of the colon.

If the clinical signs and symptoms strongly suggest appendicitis, but it has not been possible to demonstrate the appendix, a retrocaecal appendix may be present. Various operator techniques can be employed to improve delineation of the retrocaecal appendix. These include manoeuvres to scan the patient in a left posterior oblique position. Ancillary techniques for demonstrating a 'hidden' appendix include the additional use of the posterior manual compression technique, upward graded compression technique (Lee et al. 2005), using a low frequency contrast transducer, or left/lateral decubitus change of body position.

It is reported that graded compression sonography with additional operator dependent techniques can yield a sensitivity of up to 99%, specificity of 99% and an accuracy of 99% for acute appendicitis (Lee et al. 2005).

The lack of visualization of the appendix with US has a negative predictive value of 90% in experienced hands (Kessler et al. 2004). The identification of an appendix measuring less than 6 mm in diameter is a very accurate indication to exclude appendicitis with a negative predictive value of between 98%–100% (Kessler et al. 2004; Rioux 1992; Rettenbacher et al. 2001).

Secondary signs may help the sonographer establish the diagnosis of appendicitis. These include prominent echogenic fat in the right lower quadrant suggestive of an inflammatory process, the presence of appendiceal mass, the presence of free fluid or of a collection, or the presence of free gas seen over the liver on ultrasound. However, the secondary signs are not specific for acute appendicitis because these may also be seen with other intra-abdominal pathology.

6.1.3 The Use of CT in Diagnosing Acute Appendicitis

CT is increasingly used to diagnose acute appendicitis in the adult population and to a lesser extent in the paediatric population. Ultrasound is still advised as the first line examination in children but CT may be considered in difficult cases. Numerous studies have looked at the use of intravenous, oral or rectal contrast media for CT scan for appendicitis. Some centers prefer un-enhanced scans and may do a focused CT scan of the lower abdomen, scanning from the lower pole of the right kidney inferiorly for approximately 15 cm. These scans are usually performed without intravenous contrast, but oral or rectal contrast is sometimes given. Other centers perform a standard CT of the abdomen following intravenous contrast. Suggested parameters for use in paediatric abdominal scans for this indication, on a typical 16-slice multidetector CT, would be those of 1.5-mm collimation, 100-kV, and approximately 30-mAs. A recent unenhanced CT study in

adult patients has shown no difference in sensitivity or specificity for appendicitis when using relatively low dose (30 effective mAs) against standard dose (100 effective mAs) (Keyzer et al. 2004). In children it may be possible to lower the dose even beyond the typical 30 mAs. A recent study looking at focused CT in children found no difference in the sensitivity, specificity of positive predicted value, or negative predicted value of interpretation of images whether they were focused below the right lower pole or whether they include the whole abdomen (Fefferman et al. 2001). Whilst practice varies it would seem a reasonable strategy when considering CT for appendicitis in children to only scan from the level of the lower pole of the right kidney, after intravenous contrast, and with an effective mAs of 30 or below.

Diagnostic signs on CT scan include the visualization of the oedematous appendix, the presence of an appendicolith, peri-appendiceal fat stranding, increased caecal wall thickness and abscess or phlegmon (Figs. 6.4, 6.5). Fat stranding may be difficult to visualise in children with little body fat. The diameter of the appendix would normally be measured and should be less than 6 mm.

Some authors have looked at the presence or absence of intraluminal air in the appendix as a discriminating sign for appendicitis. However, it has been shown that intraluminal air is frequently detected in both normal and abnormal appendices at CT and at ultrasound and is therefore a non-specific finding of little diagnostic value. (Rao et al. 1997).

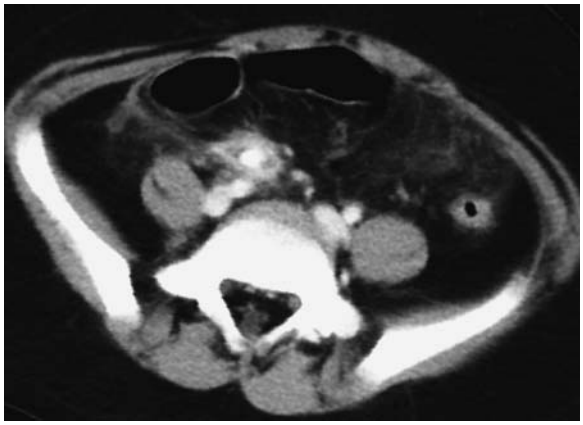

Fig. 6.4. CT of the lower abdomen showing a swollen appendix containing an appendicolith and with adjacent stranding of the intraperitoneal fat

6.2 Intussusception

Intussusception occurs when a length of bowel, the 'intussusceptum', prolapses and invaginates (or telescopes) into an adjacent segment, the 'intussuscipiens'. Four types of intussusception are described: ileocolic; ileo-ileocolic; colocolic; and ileoileal. Ileocolic is the most frequent and occurs in 90% of cases.

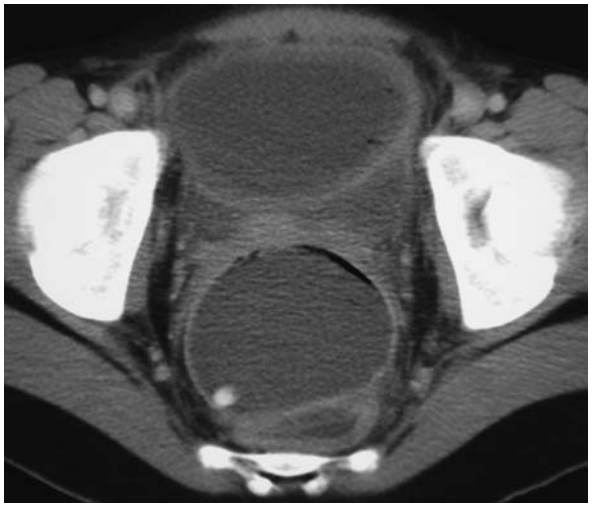

a

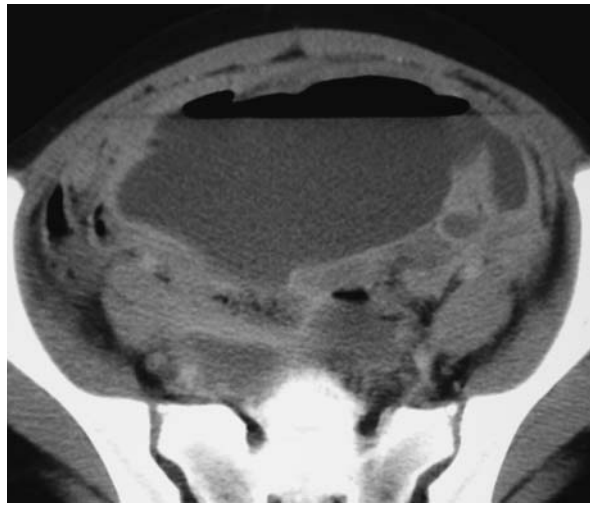

b

Fig. 6.5a,b. CT of the abdomen in a 12-year-old girl with a perforated appendicitis. **a** A large collection of fluid in the abdomen with an appendicolith seen low in the pelvis. **b** Fluid extending throughout the abdomen with an associated air-fluid level

The majority of symptomatic intussusceptions in children arise in the ileum due to mucosal oedema and lymphoid hyperplasia of Peyer's patches following viral gastroenteritis or upper respiratory tract infection. These so-called idiopathic intussusceptions occur predominantly at the ileocaecal valve (95%). A "lead point" (5%) may be the cause of the intussusception. Typical lead points include a Meckel's diverticulum, polyps, duplication cysts, suture granulomas, appendiceal inflammation, Henoch-Schönlein purpura, or occasionally inspissated meconium. Symptomatic ileocolic and ileo-ileocolic intussusceptions are generally idiopathic, rather than secondary to a lead point. There is a reported association between intussusception and malrotation / malfixation (Waugh's syndrome).

The peak incidence of idiopathic intussusception is between the ages of 3 and 9 months (40%) with a range between 3 months and 2 years (Carty 2002). Approximately 75% of cases are in children less than 2 years, and in children older than 2 years a cause for a secondary lead point should be sought. Idiopathic intussusceptions are more common in boys (male: female = 2:1). Incidence of idiopathic intussusception is often seasonal, being more common in the late spring and the autumn.

The clinical diagnosis of ileocolic and ileo-ileocolic intussusception is not always straightforward. The classical clinical triad of abdominal pain, red current jelly stool and a palpable abdominal mass is present in fewer than 50% of children with this condition. The child will typically draw up his legs to the abdomen during bouts of colic, which may be associated with facial pallor and the passage of red current jelly stools. Clinical examination of the abdomen may be difficult in a distressed child. The child may be shocked and peripherally shut down at the time of presentation. However, conversely, some children may be pain free at the time of presentation with only a history of bloody stools to suggest the diagnosis.

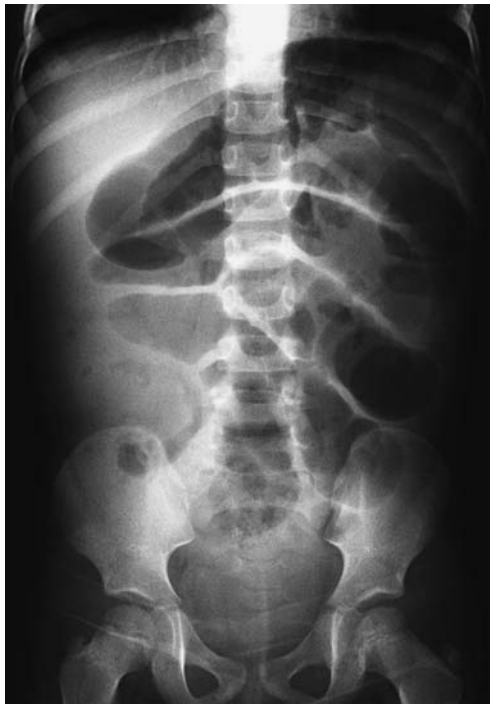

Fig. 6.6. AXR of a patient with intussusception. Note the soft tissue mass of the intussusception in the right iliac fossa and the dilated small bowel loops of obstruction

6.2.1 Imaging

Historically, the AXR has been the first investigation in children presenting with suspected intussusception. The most frequent plain film findings are those of reduced large bowel gas and the presence of a mass (Fig. 6.6) (Ratcliffe et al. 1993). Other signs include the meniscus sign and the target sign (Sargent et al. 1994; Lee et al. 1994). Exclusion of an ileocolic intussusception on AXR is based on the presence of gas and stool in the caecum (Sargent et al. 1994). However, in 45% of children aged less than 5 years the sigmoid colon is in the right lower quadrant of the abdomen and therefore sigmoid filled with air and stool can be misinterpreted for caecum. Also, sometimes loops of "pulled-up" small bowel will project over the right lower quadrant as a result of the bowel shortening secondary to intussusception. It has been shown that intussusception was correctly identified on AXR in only 45% of children with intussusception (Sargent et al. 1994). Hence, as the plain abdominal radiograph is unable to categorically confirm or refute the presence of intussusception in the majority of cases, although it may be helpful as part of the work-up for investigation of an acute abdomen, an alternative investigation will still be necessary to confirm intussusception. The investigation of choice is ultrasound, and it is suggested that in cases of suspected intussusception that the patient should proceed directly to ultrasound without an AXR.

6.2.2 Ultrasound in Intussusception

The use of sonography was first described in the late 1980s (Pracros et al. 1987) with a reported accuracy of 100% for intussusception. This accuracy rate has since been verified in many reports and the use of ultrasound for this indication has been validated. Ultrasound is now the first line of investigation in a child with suspected intussusception.

6.2.2.1 Ultrasound Technique

The ultrasound is performed with the child supine and at rest. It is recommended that initially a general survey of the abdomen is undertaken using a curvilinear probe of typically 6–8 MHz. If an intussusception is present this is most likely to be demonstrated in the right flank, but may also be demonstrated in the epigastrium, left flank or in the pelvis, depending on the extent of the intussusception. This general survey may also show the presence of other secondary signs such as small amounts of free fluid, the presence of lymphadenopathy both in the intussusception and elsewhere in the abdomen or, in the absence of an intussusception, may show an alternative underlying cause for the abdominal pain. It is then recommended that the operator switches to a higher frequency linear probe (typically an 8- to 15-MHz probe) for further evaluation of the intussusception. Doppler examination of the intussusceptum can also be performed.

Intussusception has a characteristic sonographic appearance (Pracros et al. 1987; del Pozo et al. 1996, 1999) making the diagnosis straightforward. The intussusceptum typically shows as a 3- to 5-cm diameter soft tissue concentric mass in transverse section, and a sausage-like mass in longitudinal section. The characteristic appearances are of the circular wall of the intussuscipiens, and the central echogenic mucosa of the intussusceptum, along with the appearance on transverse scans of the eccentric, semi-lunar, hyperechoic mesenteric fat that is pulled with vessels and lymph nodes into the intussusception by the intussusceptum, the so-called crescent and doughnut sign (Fig. 6.7) (del Pozo et al. 1996).

As with any ultrasound study the quality and diagnostic rate is determined by the operator. However, it has been shown that 100% accuracy rate can be achieved by 3rd and 4th year radiology residents who had completed a 3- to 5-month training period in adult sonography (Verschelden et al. 1992).

Whilst the sonographic appearances of an intussusception are straightforward, care must still be taken not to confuse these appearances with other causes of bowel wall thickening such as inflammation, oedema, haematoma or any area of volvulus. Nevertheless these other conditions will not show the characteristic "crescent and doughnut" sign.

Ultrasound is also extremely useful for demonstrating the presence or absence of pathological lead points, and these should be looked for in each examination. Ultrasound has been reported as demonstrating a lead point in up to 66% of patients when a lead point is present (Navarro et al. 2000) and allowing specific pathological diagnosis in up to one third of these patients.

With sonography now being the tool of choice for identifying intussusception, the use of a water-soluble contrast enema or barium enema to make the diagnosis is no longer justified.

6.2.2.2 Assessment for Reducibility

Ultrasound may also be used to make some assessment as to whether the intussusception is suitable for non-surgical reduction and the likelihood of success. Various sonographic signs have been evaluated, including a thick peripheral hypoechoic rim of the intussusception, free intraperitoneal fluid, trapped fluid within the intussusception and the absence of blood flow in the intussusception on Doppler interrogation. There appears to be no relation between the reduction rate and thickness of the external hypoechoic rim (Verschelden et al. 1992), and free intraperitoneal fluid is commonly associated due to transudation of fluid from the congested intussusception which is present in at least 50% of cases. Fluid trapped within the serosal layers of the entering and returning limbs of the intussusception has been shown to be associated with a lower reduction rate but at least 26% of these cases can still be reduced. Similarly the absence of flow on Doppler interrogation reduces the rate of successful reduction but does not preclude it, reduction still being successful in approximately 31% of cases (Kong et al. 1997). The absence of visualized blood flow on Doppler interrogation is therefore not a contra-indication for attempted air enema reduction. Similarly the identification of a pathological lead point does not necessarily mean that an intussusception will be irreducible (Navarro et al. 2000; Navarro and Daneman 2004).

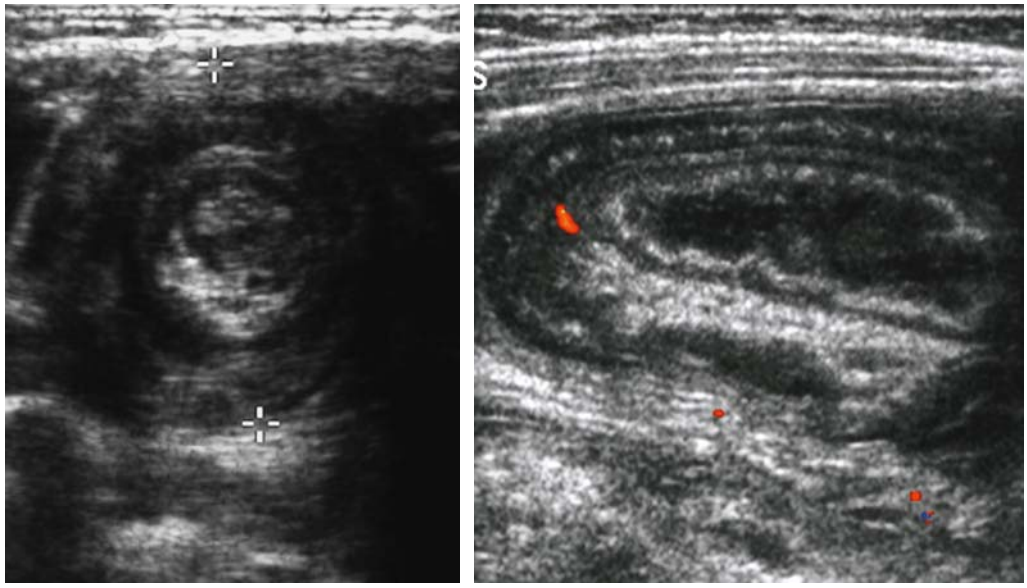

a b

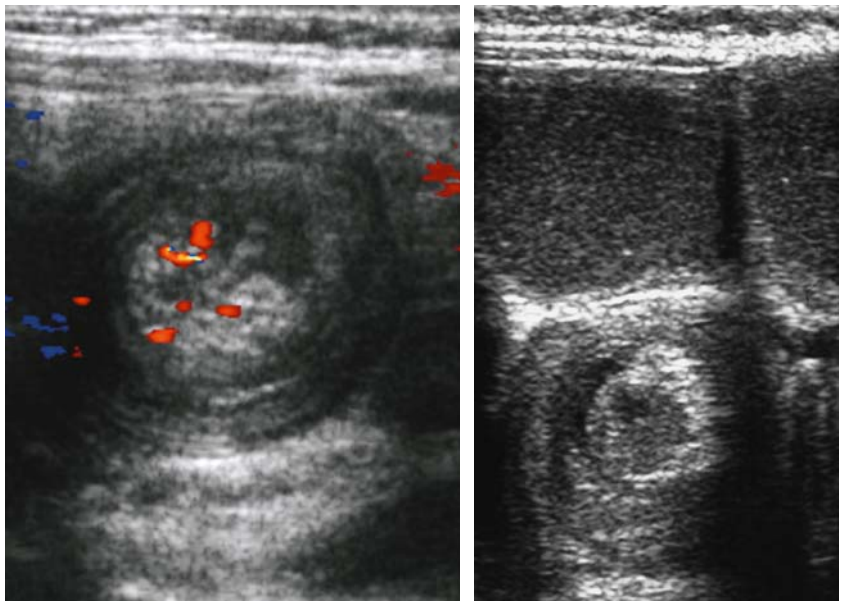

c d

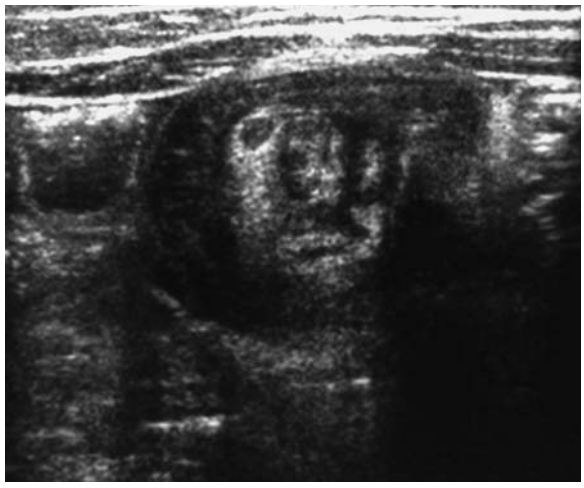

e

Fig. 6.7a–e. Ultrasound appearances of intussusception. **a** Transverse (TS) image showing the 'crescent and doughnut sign' as hyperechoic mesenteric fat is pulled into the intussusception. **b** Longitudinal image showing the 'sausage' appearance of the intussusception. **c** TS image with Doppler showing some blood flow present within the intussusception. **d** TS image showing dilated fluid-filled loops of small bowel which should not be mistaken for the intussusception which lies deep to them. Note the absence of the echogenic layers in the small bowel loops. **e** TS image showing lymph nodes pulled into the intussusception

6.2.3 Non-operative Reduction of Intussusception

Non-operative reduction is the treatment of choice. Historically barium or water-soluble contrast media have been used for the hydrostatic reduction of intussusception. These techniques have largely been replaced by the use of the air enema under fluoroscopic guidance, or ultrasound guided hydrostatic or air reduction. The fluoroscopic guided air enema is currently the most universal procedure but as experience grows, ultrasound guided reduction is also used in several centers. The basic principal is to raise the intraluminal pressure in the distal colon to push the intussusceptum retrogradely along the colon, thereby reducing the intussusception, until it is completely resolved, usually through the ileocaecal valve. Complete reduction is achieved when either air or contrast media flood back into multiple loops of terminal ileum. Whilst hydrostatic or pneumatic reduction can be successful in ileo-ileal intussusception, this is more commonly treated by surgery.

6.2.3.1 Technique for Fluoroscopic Air Enema

Once the presence of an intussusception has been confirmed by ultrasound, the child is taken to the fluoroscopy room. Some centers administer pain relief and/or sedation in anticipation of the procedure, but this is by no means universal and there is some evidence that the use of sedation (or the use of smooth muscle relaxants) may prevent the patient from performing the Valsalva manoeuvre which might otherwise enhance the chance of reduction and possibly reduce the chance of perforation. Children should be well resuscitated before attempted reduction, and should be monitored whilst the attempted reduction is in progress. This is particularly important in children who have received sedation as signs of clinical deterioration may not be so apparent.

A balloon catheter is placed per rectum (10 F–18 F). Many operators inflate the balloon on the Foley catheter but this is not universal practice and caution should be used when inflating a balloon catheter in the rectum because of the reported risk of mucosal ischaemia. The buttocks are subsequently taped or gripped firmly to complete a good seal at the anus. Air is then introduced into the distal colon, with a manometer or other monitoring device present on the system to ensure safe and constant pressures of air. The progress of the air (and the reduction of the intussusceptum) is closely observed under fluoroscopic guidance (Fig. 6.8a). It is usual practice to include the whole abdomen within the field of view so as not to miss a perfora-

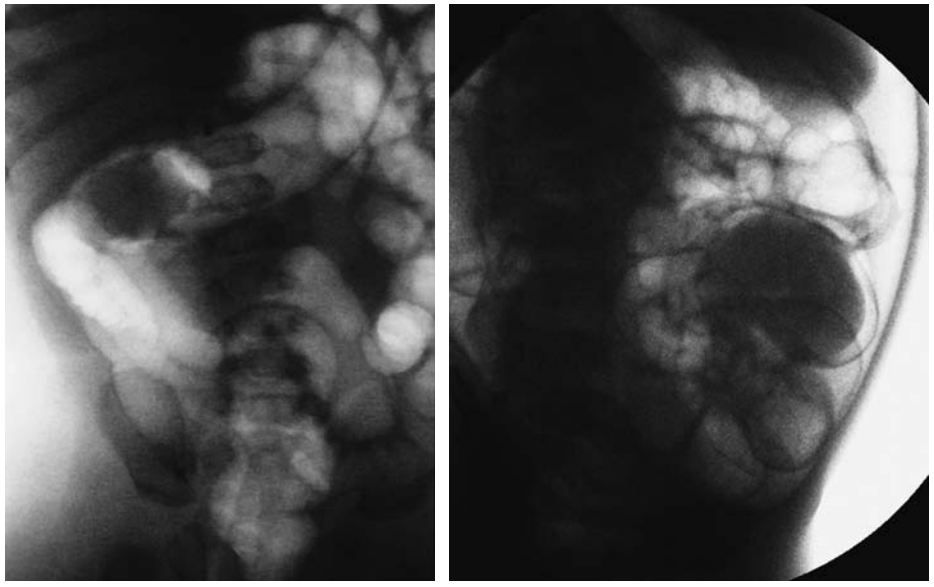

a b

Fig. 6.8a,b. Appearance of intussusception during reduction by air enema. **a** The soft tissue mass of the intussusception can be seen in the right flank and the remainder of the large bowel is distended by air. Air has not yet flooded back into the small bowel, which would indicate successful reduction. **b** Air enema in a different patient: the intussusception is shown as a soft tissue mass but perforation of the bowel has occurred

tion, which would necessitate the immediate termination of the procedure (Fig. 6.8b). In the case of a tension pneumoperitoneum an 18-G needle should immediately be positioned in the midline to relieve the abdominal distension, thereby preventing respiratory collapse. Typically the pressure is raised to 80 mm of mercury equivalent and sustained at this level for approximately 3 min. This may then be repeated either at the same pressure, or at 100 mm of mercury or 120 mm of mercury until reduction is complete. Typically three attempts of 3 min each are made at each pressure. The whole procedure may be performed with the infant supine or prone at the operator's discretion and preference. Advantages for the supine position include being able to observe the child more closely and for a normally orientated radiographic view. Advantages for the prone position include it being easier to obtain a complete seal on the child's buttocks if these are uppermost.

6.2.3.2 Ultrasound Guided Hydrostatic or Air Reduction

Once the diagnosis of intussusception has been made by ultrasound a 10- to 18-F balloon catheter is placed per rectum as above. In the case of hydrostatic reduction this is normally performed with the child supine. The child may be placed on a plastic enema ring approximately 50 cm in diameter, which allows a suction device to continuously remove fluid which has escaped per rectum during the procedure. Fluid is then introduced per rectum, which may be water, saline, or isotonic Hartmann's solution and a constant pressure of injection is maintained, typically 100 mm of mercury. During the reduction the intussusceptum is observed under continuous ultrasound guidance as it proceeds to the caecum and reduces across the ileocaecal valve (Khong et al. 2000). One advantage of ultrasound guided hydrostatic reduction is that it may allow identification of an ileo-ileocolic intussusception. This has a characteristic complex fronded appearance, compared with the otherwise smooth appearance of an ileocolic intussusception.

6.2.3.3 Ultrasound Guided Pneumatic Reduction

Whilst this is still a relatively new technique it is reported to have similar success rates to the fluoroscopic air enema technique (Yoon et al. 2001). Yoon et al. describe their technique as follows: A balloon catheter (10–18 F) is inserted per rectum, and 20–25 ml of air injected to inflate the balloon. The Foley catheter is gently pulled as low as possible. Tape is applied to secure the catheter to the buttocks. By means of a pressure monitoring device linked to a T connector and with ultrasound guidance, air is injected manually to the initial intra-colonic pressure of approximately 60 mm of mercury and held for 30 s and then released. Ultrasound criteria for successful reduction after deflation of the air includes the disappearance of the intussusceptum with the presence of a single concentric echogenic ring representing the swollen terminal ileum instead of the multiple concentric rings of the intussusception, and the abrupt transition of bowel wall thickness between the swollen terminal ileum and the proximal normal ileum when scanned along the axis of the ileum. If the intussusception is still visible air is reintroduced by gradually increasing pressures up to a limit of 120 mm of mercury. Air is typically insufflated and deflated three times at each increment. If there is an abrupt decrease in pressure during air insufflation, sudden abdominal distention or clinical improvement, the air is then deflated to allow further ultrasound assessment. To detect free intraperitoneal air caused by bowel perforation, intermittent ultrasound of the epigastrium is performed to look for a 'ring-down' (or 'comet-tail') reverberation artefact in the subphrenic area obscuring the inferior hepatic margin.

Overall, using one of these techniques, an expected reduction rate of at least 70% would be expected, with a perforation rate of approximately 1% or less. Guidelines to the performance of intussusception reduction are published by various bodies (American College of Radiology 1997; see also BSPR Standards for intussusception reduction, www.bspr.org.uk/intuss.doc) and the clinician should be aware of these pertaining to his region of practice.

6.2.4 Delayed Repeat Enema

If the attempted intussusception reduction has been partly successful, there is value in a delayed repeat enema if the child is clinically stable. It has been shown that a delayed repeated enema can be successful in reducing the intussusception in a further 50% of those patients in whom it is used, and thus has a place in the management of the

infant who remains clinically stable with no evidence of peritonitis, where there has been a partial reduction of the intussusception at the first attempt (Navarro and Daneman 2004; Navarro et al. 2003). The best time interval between the two enemas remains uncertain and the number of times a delayed enema can be reasonably repeated is also unproven. In published series (Navarro et al. 2003) the delay has varied between 15 min and 12 h (Gorenstein et al. 1998; Navarro et al. 2003). Some centers allow a planned delay of between 45 and 60 min between three consecutive air enema attempts (Gorenstein et al. 1998), but other centers wait between 4 and 6 h, to allow resolution of oedema. In any event, repeated delayed reduction attempts increase the overall success rate and should be advocated in a stable patient. Finally, the use of multiple delayed reduction attempts is not contra-indicated in the presence of a pathological lead point as successful reduction may facilitate subsequent surgery for resection of the lead point. Multiple recurrences of intussusception in this context are not a contra-indication to repeated reduction. A careful search for a pathological lead point is mandatory. Surgery should be reserved for irreducible recurrences or for a demonstrated pathological lead point (Daneman et al. 1998; Navarro and Daneman 2004).

6.2.5 Summary

A diagnosis of intussusception is preferentially made by ultrasound. The plain abdominal radiograph has been shown to be of only limited value, and may be omitted safely in the vast majority of children suspected of having an intussusception, provided sonography is available.

The preferred reduction technique is either that of the air enema under fluoroscopic guidance or of air or hydrostatic enema under ultrasound guidance. The only absolute contra-indication to attempted enema reduction is full thickness bowel necrosis (which will present with features of shock and peritonitis) or if there is imaging evidence of perforation with free air.

6.3 Constipation

Constipation is a common problem in infants and children and accounts for approximately 3% of visits to paediatric outpatients (Loening-Baucke 1993); it is also likely that constipation is the most common digestive complaint outnumbering all other chronic gastrointestinal conditions (Mezwa et al. 1993).

Constipation is defined clinically as an alteration in the frequency, size, consistency or ease of passage of stools (Seth and Heyman 1994). A common working definition for constipation in children is a stool frequency of less than three per week, but painful bowel movements and/or stool retention can be regarded as constipation even if the stool frequency is three or more per week (Loening-Baucke 1993; Seth and Heyman 1994). Encopresis is the voluntary or involuntary passage of a normal bowel movement into the underwear after the age of 4 years, and faecal soiling is defined as the involuntary seepage of faeces which is often associated with faecal impaction and is reflected in the staining of the underwear (Benning et al. 1994; Partin et al. 1992).

Causes of constipation in infants and children include functional constipation, neurogenic constipation [aganglionosis, hypoganglionosis, neuronal intestinal dysplasia (NID)], chronic intestinal pseudo-obstruction, disorders of the spinal cord, cerebral palsy, constipation secondary to anal fissures and strictures, neonatal hypothyroidism and drug induced constipation (Fotter 1998).

6.3.1 Functional Constipation

Approximately 90%–95% of cases of childhood constipation are likely to represent functional constipation. Rectal distention is present in nearly all cases and failure of the external anal sphincter and/or puborectalis muscle to relax during defaecation attempts has been found in the majority of these children. Whilst delayed colonic transit time may be part of the problem, pelvic floor dysfunction seems to be the dominating factor (Loening-Baucke 1993).

6.3.2 Neurogenic Constipation

6.3.2.1 Hirschsprung's Disease

Hirschsprung's disease is the most common cause of neonatal obstruction of the colon and accounts for 33% of all neonatal obstructions. It is characterized by congenital absence or deficiency of the ganglion cells in the myenteric and submucosal plexuses of the rectum and the distal, non-dilated part of the colon, together with a hyperplasia of cholinergic nerve fibres in the circular muscle layer, muscularis mucosae and mucosa with a high activity of acetylcholinesterase (Fotter 1998). This results from failure of neural crest cells to migrate into the wall of the colon during the fifth to seventh week of embryological life and subsequent failure of development of the parasympathetic ganglion cells. The absence of the intramural ganglion cells interferes with normal relaxation and peristalsis of the bowel wall and the internal anal sphincter. The abnormally innervated segment of colon becomes hypertonic and behaves as a functional stenosis leading to partial or complete colonic obstruction. Immediately proximal to the aganglionic segment the intestine becomes markedly dilated with faeces and gas. In most cases aganglionosis is limited to the rectum or the rectum and a short distal segment of the sigmoid colon. This so-called short segment disease occurs in approximately 80% of cases, with long segment disease occurring in 15% and total colonic aganglionosis (Zuelzer-Wilson syndrome) accounting for approximately 2%–13%. Ultra-short segment Hirschsprung's disease accounts for up to 10% in some series. In ultra-short segment Hirschsprung's disease the aganglionic segment is usually confined to the internal anal sphincter or up to 3–4 cm above the pectinate line (Meir-Ruge and Scharli 1986).

Overall there is an incidence of approximately 1 in 5000 to 1 in 8000 live births. Occurrence is usually sporadic but is reported to be familial in 4%. There is an increased incidence in children with Down syndrome. Presentation is most common in the full term infant during the first 6 weeks of life (70%–80%) and is extremely rare in premature infants. In classic Hirschsprung's disease and in ultra-short segment disease there is a male-to-female ratio of 3:1 and in total colonic aganglionosis the ratio is 1.8:1.

Complications of Hirschsprung's disease include an enterocolitis with or without intraluminal air, intermittent dilatation after surgical treatment which may give a picture of pseudo-obstruction. Following a Duhamel procedure ('pull through' procedure) there may be persistent narrowing at the anastomosis site.

Hirschsprung's disease has now been shown to be one of several disorders in intestinal innervation due to an abnormal number of neurones. These disorders are known as dysganglionoses and include congenital intestinal aganglionosis (Hirschsprung's disease), hypoganglionosis and hyperganglionosis (Kapur 2000). Hypoganglionosis is described histologically as a variable length of gut with abnormal numbers of ganglion cells. It is believed to be the primary cause of intestinal pseudo-obstruction (see Sect. 6.3.3) and may represent a *forme fruste* of Hirschsprung's disease. The patient may present with multiple loops of dilated bowel with an obstructive picture but with no cause of mechanical obstruction found.

Hyperganglionosis is described as having two distinct patterns: ganglioneuromas (nodular proliferations of ganglion cells often associated with multiple endocrine neoplasia type 2B and not seen in children) and intestinal neuronal dysplasia (NID). NID is a controversial entity but a consistently described feature is of increased density of the submucosal ganglia. Patients may present with intestinal dysmotility clinically indistinguishable from Hirschsprung's disease.

In view of these overlapping presentations these disorders should be considered in the differential diagnosis of Hirschsprung's disease until histological confirmation has been made.

6.3.2.2 Chronic Intestinal Pseudo-obstruction

Chronic intestinal pseudo-obstruction is a rare clinical condition also known as chronic adynamic ileus, pseudo-Hirschsprung's disease, and adynamic bowel syndrome. Megacystis-microcolon-intestinal hypoperistalsis syndrome is the most severe form of chronic intestinal pseudo-obstruction.

Onset of chronic intestinal pseudo-obstruction can be at any age but tends to be more severe with the earlier presentation. In the neonatal period symptoms include failure to pass meconium, abdominal distention or bilious vomiting. Constipation may subsequently develop. In older children presenta-

tion may be abrupt or slowly progressive. Urinary tract involvement occurs in up to 50% of patients. Histologically abnormalities are either seen in the myenteric plexus with an associated visceral myopathy, or show argyophobic cells or argyrophilic cells on silver stains. The overall result is a lack of coordinated intestinal motility. Inheritance may be autosomal dominant but the majority of cases are sporadic. There is an association with malrotation. Overall there is a high morbidity and high mortality (Heneyke et al. 1999).

6.3.3 Imaging in Constipation

In the newborn period the patient may present with a delay or failure to pass meconium, distension of the abdomen, bilious vomiting or signs of neonatal intestinal obstruction. An AXR will show evidence of low obstruction but will be non-specific; however, it may allow assessment of the lower spine and in Hirschsprung's disease a lack of air in the distal colon or rectum may be a sign of congenital aganglionosis (Fig. 6.9a).

In suspected neurogenic causes of constipation (Hirschsprung's disease, NID and hypoganglionosis) a contrast enema is often performed. It is not advisable to prepare the bowel before this procedure because the narrow segment may be dilated up and therefore missed.

In the neonatal period water soluble contrast is instilled preferentially as this may wash out the colonic contents and relieve obstruction in cases of neonatal small left colon syndrome or in meconium plug syndrome. In infants or older children either water soluble contrast medium or barium can be used. It is not usually appropriate to inflate a balloon catheter as this may obscure visualization of a narrow segment in congenital aganglionosis. The infant or child is usually placed in a lateral position at the beginning of the study to allow observation of the anorectal junction during filling, and in cases of aganglionosis, bowel filling should be limited to as far as the transitional zone. The transitional zone should be sought and is identified by change in calibre from relatively small or normal calibre/collapsed lower bowel to distended stool filled proximal bowel (an 'inverted cone' appearance). In the case of Hirschsprung's disease the most common site for the transitional zone is in the recto-sigmoid (Fig. 6.9b,c). It should be noted that the aganglionic segment appears normal in size. The recto-sigmoid ratio may be used to assess the relative size of the rectum to the sigmoid. This should normally be 1:1 and if greater than this suggests a diagnosis of Hirschsprung's disease (i.e. in normality the rectum may be larger than the sigmoid but the sigmoid should not be larger than the rectum).

Filling with contrast should continue slowly, leaving enough time for the bowel to adapt to the instilled volume. The aganglionic segment may need some time to contract to its former diameter. One suggested technique in infants and older children is to use barium, with secondary insufflation with air. As air does not expand a narrow segment as much as barium the transition zone can be demonstrated more easily and more accurately. A 24-h delayed film can show a complete lack of evacuation of contrast medium especially in cases of total colonic aganglionosis (O'Donovan et al. 1996).

6.3.3.1 Imaging Findings in Hirschsprung's Disease

The cardinal sign in Hirschsprung's disease, shown on a contrast or barium enema, is the transitional zone between the narrow and dilated bowel segment, most often seen at the recto-sigmoid junction (Fig. 6.9b,c). It may be represented by an abrupt change of calibre, or may have a more conical appearance (Fig. 6.9d). The absence of a demonstrated transitional zone does not exclude the diagnosis of Hirschsprung's disease. A classic aganglionic segment may not be visible before days 10–14 of life. A narrow segment refers to a segment of rectum where the relationship of the diameter of the rectum to the sigmoid colon is 1:1 or less. A transitional zone with a mega colon may be seen only after 4–6 weeks. The wall of the colon often has a 'saw-tooth' appearance as a result of non-peristaltic contractions. There may be marked retention of barium on delayed films after 24 h, and mixing of barium and stools after 24 h is a common finding.

The differential diagnosis in the neonatal period is that of small left colon syndrome. In this condition the left colon is a reduced calibre, typically, from the level of the splenic flexure distally, with an abrupt transitional zone between the dilated transverse colon and the narrow calibre descending colon. These findings are visible right from the first few days of life in small left colon syndrome, but would not typically be present in Hirschsprung's disease for some delayed period.

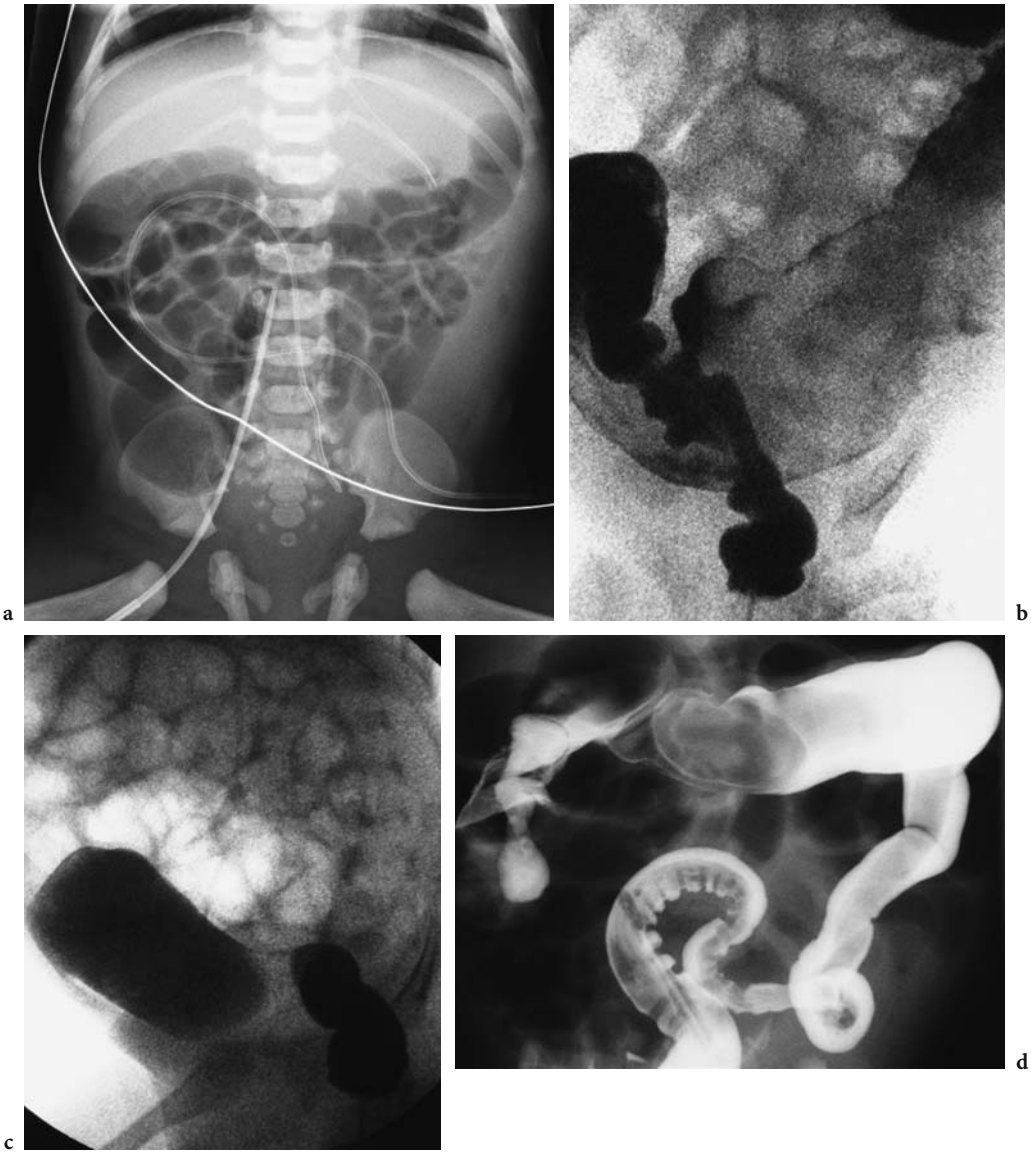

Fig. 6.9a–d. Imaging of Hirschsprung's disease. **a** AXR in total colonic Hirschsprung's disease showing the absence of gas in the large bowel but otherwise non-specific appearances. **b** Contrast enema showing an irregular and non-dilated rectum with a transition to a markedly dilated and stool-filled sigmoid colon. **c** Contrast enema showing a transition zone at the recto-sigmoid junction. The recto-sigmoid ratio is greater than 1. **d** Contrast enema in a neonate with Hirschsprung's disease with a conical transition zone at the splenic flexure. There is also a long meconium plug in the distal colon and the differential diagnosis would be functional immaturity of the colon. The final diagnosis was made by biopsy

6.3.3.2 Imaging Findings in NID, Hypoganglionosis, Chronic Intestinal Pseudo-obstruction, Ultra Short Segment Hirschsprung's Disease and Total Colonic Aganglionosis

The appearances at contrast or barium enema in these remaining conditions are often non-specific. In ultra-short segment Hirschsprung's disease the barium enema may show a large mega-rectum but no other specific findings. In NID, chronic intestinal pseudo-obstruction and total colonic aganglionosis the barium enema is often non-contributory. However, total colonic aganglionosis may sometimes have the appearance of a microcolon and therefore needs to be differentiated form ileal atresia and meconium ileus.

In all these conditions the final diagnosis is usually made by histology, most commonly following suction biopsy via the rectum. This technique is fast and simple and can be carried out in neonates without a general anaesthetic. In some cases full thickness biopsy will be required to obtain all layers of the intestinal wall, in which case a general anaesthetic is required. Complex enzyme histochemistry and immune histochemistry is frequently necessary. If contrast enema is required it should be performed pre-biopsy or at least 24 h post biopsy.

6.3.3.3 Imaging in Functional Constipation

The plain abdominal radiograph is no longer indicated in cases of chronic functional constipation. Barium enema may still be performed to assess the degree of bowel dilatation and the degree of colonic loading. However, a conclusive diagnosis is rarely reached by this method alone. Biopsies are routinely performed to exclude a previously missed diagnosis of Hirschsprung's disease. Pellet studies may be performed for transit times: the patient is given a pellet containing tiny radio-opaque markers on each of the 3 days preceding an AXR. The markers in the pellets are different on each day allowing for estimation of transit time. Defecography is performed in some children with chronic constipation and defaecation disorders after the third to fourth year of life. Defecography allows assessment of the degree or relaxation of the internal anal sphincter during retrograde filling and during defaecation. The anorectal angle can be assessed as can the degree of relaxation of the external anal sphincter during defaectation. The combined function of the puborectalis muscle and the external sphincter can be demonstrated. A detailed description of the procedure of defecography and the range of findings is beyond the scope of this chapter.

6.4 Functional Immaturity of the Colon (Small Left Colon and Meconium Plug Syndrome)

Historically 'meconium plug syndrome' and small left colon syndrome have been considered as separate, if possibly overlapping, entities. The main finding in both entities is that of a narrow rectosigmoid and descending colon with a transition to normal size or dilated colon typically at the level of the splenic flexure. The term 'meconium plug syndrome' was used initially, reflecting the belief that the obstruction was probably due to 'an alteration in the character of the most distal portion of the meconium mass' (Clatworthy et al. 1956). Subsequent authors observed that a small left colon with proximal obstruction could be seen in the absence of the meconium plug, and termed the syndrome 'small left colon syndrome', in the belief that the abnormality was due to the smallness of the colon rather than the abnormality of the meconium. Finally the term 'functional immaturity of the colon' has come into widespread use and reflects the overlapping or synonymous entities of 'small left colon syndrome' and 'meconium plug syndrome' (Berdon et al. 1977).

The underlying aetiology remains unknown but is likely due to impaired intestinal motility, leading to local inspissation of meconium and secondary low colonic obstruction. Presentation is in new born infants, normally within the first 24 h of life. Approximately 50% of infants have diabetic mothers. The signs are those of abdominal distention, vomiting and failure to pass meconium. The AXR will show evidence of a low obstruction with multiple dilated loops of bowel. Occasionally there is a bubbly appearance in the colon which raises concern about the differential diagnosis of submucosal air including necrotising enterocolitis. Investigation is by water soluble contrast enema. A catheter is passed per rectum and contrast introduced under fluoroscopic guidance. If a meconium plug is present there may be a ribbon-like filling defect in the small left colon with a larger filling defect in an otherwise normal appearing transverse colon (Fig. 6.10). The hyper-osmolality of the contrast medium often causes the meconium plug to shell away from the bowel wall and meconium is usually evacuated during or soon after the enema examination, resulting in relief of obstruction. If a meconium plug is not present, a small left colon will be seen usually with an abrupt change of calibre at the splenic flexure. The images confirm the diagnosis and usually no further treatment is necessary with the infant normally passing meconium from the ascending and transverse colon soon after the study. Though infants with functional immaturity of the colon usually do well, a benign course is not invariable and perforation may occur.

A differential diagnosis in infants with these findings includes that of Hirschsprung's disease. However, it is unusual for a case of Hirschsprung's

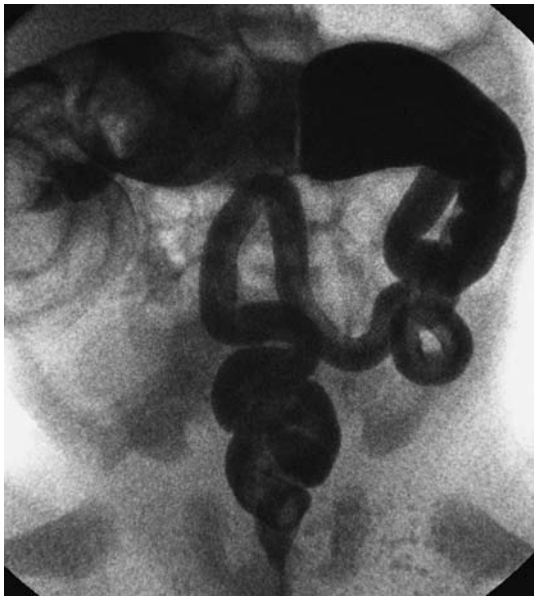

Fig. 6.10. Contrast enema appearances in functional immaturity of the colon: a small left-sided colon filled with meconium

disease to have a transition zone at the splenic flexure, the transition zone in functional immaturity is often quite abrupt whereas the transition zone in Hirschsprung's disease may be cone shaped and gradual, and finally in Hirschsprung's disease aganglionic colon is usually of near normal calibre whereas in functional immaturity the left colon is usually small. In newborns with functional immaturity the rectum is usually quite distensible unlike in Hirschsprung's disease when the aganglionic colon usually remains of uniform calibre to the anus. If any doubt about the diagnosis remains after treatment by contrast enema, a rectal biopsy should be obtained.

6.5 Colon Agenesis, Colonic Atresia and Stenosis

Complete absence of the colon and rectum is extremely rare. However, segmental atresias or stenosis of the colon are seen more often and are believed to be secondary to an intrauterine vascular insult. Nevertheless they are still quite unusual and are seen much less commonly than atresias in the small bowel. The colon typically accounts for only 5%–15% of total intestinal atresias (Powell and Raffensperger 1982). The atresia may be represented simply by a membrane across the lumen of the colon, by a fibrous band connecting the two ends of the large bowel, by a complete atresia with no fibrous connection, or by multiple series of atresias.

In complete colonic agenesis or atresia the child will present with failure to pass meconium in the first 24 h and with clinical features of obstruction. In colonic stenosis the degree of obstruction will be variable. The AXR will show features of a low intestinal obstruction. At contrast enema the distal colon is likely to be a micro-colon, never having been used, and it will not be possible to pass contrast beyond the level of the atresia (Fig. 6.11a,b). In cases of stenosis, rather than complete atresia, the stenotic portion may be demonstrated with contrast material and the colon proximal to the stenosis is likely to be very dilated and filled with meconium or stool. The colon proximal to the obstruction can become over distended and ischaemic secondary to compression by the massive intraluminal contents. Some authors have described an association between colonic atresia and Hirschsprung's disease. However, it now seems likely that this anecdotal link is due to the vascular insult rendering the colon atretic and also rendering the involved segment aganglionic.

Acquired stenosis can also occur following necrotising enterocolitis and this is described later in this chapter.

6.6 Duplication Cysts

A gastrointestinal tract duplication cyst represents a congenital anomaly found anywhere along the alimentary tract, with the colon being an uncommon site and representing only 13%–30% of cases. It shares a common muscle wall and blood supply but has a separate mucosal lining. The aetiology is unclear but the duplication is thought to occur early in embryological development, usually as a failure of recanalisation. These cysts are located in or adjacent to the wall of part of the gastrointestinal tract, have smooth muscle in their walls, and are lined by mucosa similar to that of some other portion of the alimentary tract. However, there may be ectopic squamous mucosa, transitional ciliated mucosa, lymphoid aggregates or ganglion cells. Gastric mucosa and pancreatic tissue

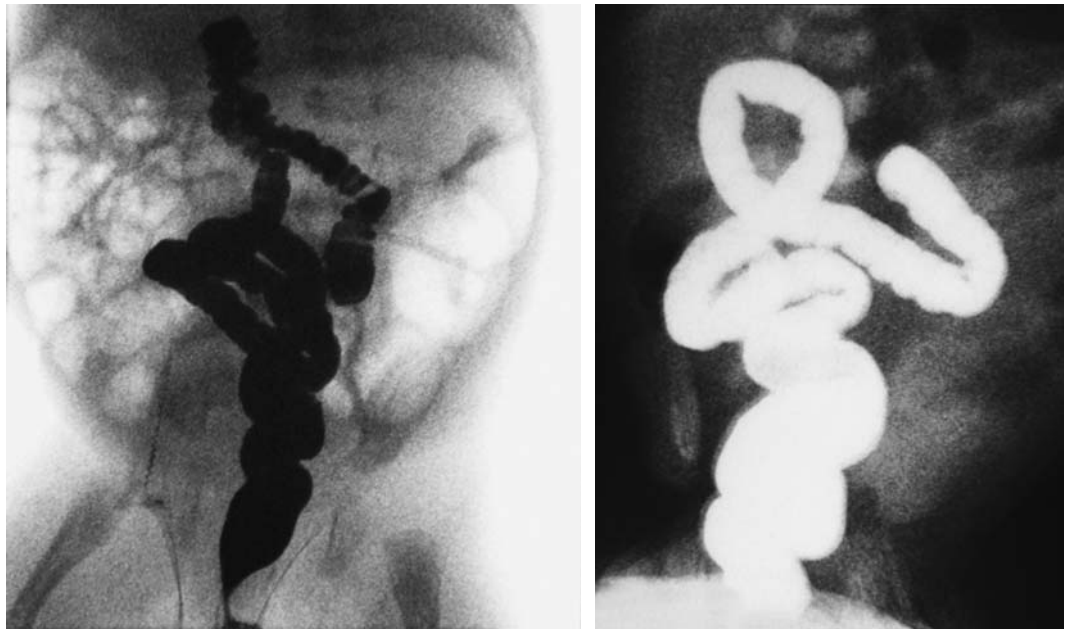

a b

Fig. 6.11a,b. Colonic atresia and stenosis. **a** Colonic atresia in a neonate with a small distal colon and a blind upper end. **b** Colonic atresia showing a lower bowel well distended with contrast but with no connection to the more proximal bowel

are the only ectopic tissues of clinical importance. Technetium isotope studies may help demonstrate ectopic gastric mucosa Duplications are most commonly spherical cysts but may be tubular structures that parallel the normal gut, most commonly being on the mesenteric aspect of the alimentary canal. They may or may not communicate with the enteric lumen. The colon is the least frequently involved site and there is a gradient of decreasing frequency from the caecum to the rectum. Of the large bowel duplication cysts approximately 40% are within the caecum. Their variation includes the colorectal tubular duplication cyst (duplication of the hind gut). This is a double-barreled duplication involving part or all of the large bowel with a "twin" segment on the mesenteric or ante-mesenteric side.

Patients normally present in the neonatal period or in infancy and there is a male-to-female ratio of 1:2. The patient may present with constipation, with obstruction if the cyst is of large size, or may present with bleeding if the cyst communicates with the normal gut lumen, and if there is ulceration of gastric mucosa within the duplication cyst. Duplication cysts may be associated with recto-genital or recto-urinary fistula, duplication of the internal or external genitalia, vertebral anomalies and multi-system congenital anomaly complexes. Female patients may present with the passage of faeces through the vagina. Approximately 20% of rectal duplications communicate with the rectal lumen or may connect with the perineum as a chronic peri-anal fistula.

At contrast enema there may be simultaneous opacification of the true and the twin lumen. The cystic duplication may or may not contain air depending on whether it communicates with the lumen of the colon.

The most effective imaging is cross sectional, with ultrasound being the modality of choice although cysts may also be seen on fluoroscopy as filling defects (Fig. 6.12a). Ultrasound may show a sonolucent mass with through transmission if the cyst contains clear fluid contents, or may show an echogenic mass if the cyst contains haemorrhage or debris (Fig. 6.12b,c). Typically the inner echogenic mucosal, and outer hypo-echoic muscle layers are seen confirming the diagnosis. CT or MRI can be used for greater clarification. MRI would be the investigation of preference given the absence of ionizing radiation and the additional information which can be obtained about the cyst contents on different sequences. The intra-cystic fluid will be of mid-signal intensity on T1-weighted MR images and may be heterogeneous; it will return a homogeneous high signal intensity on T2-weighted images.

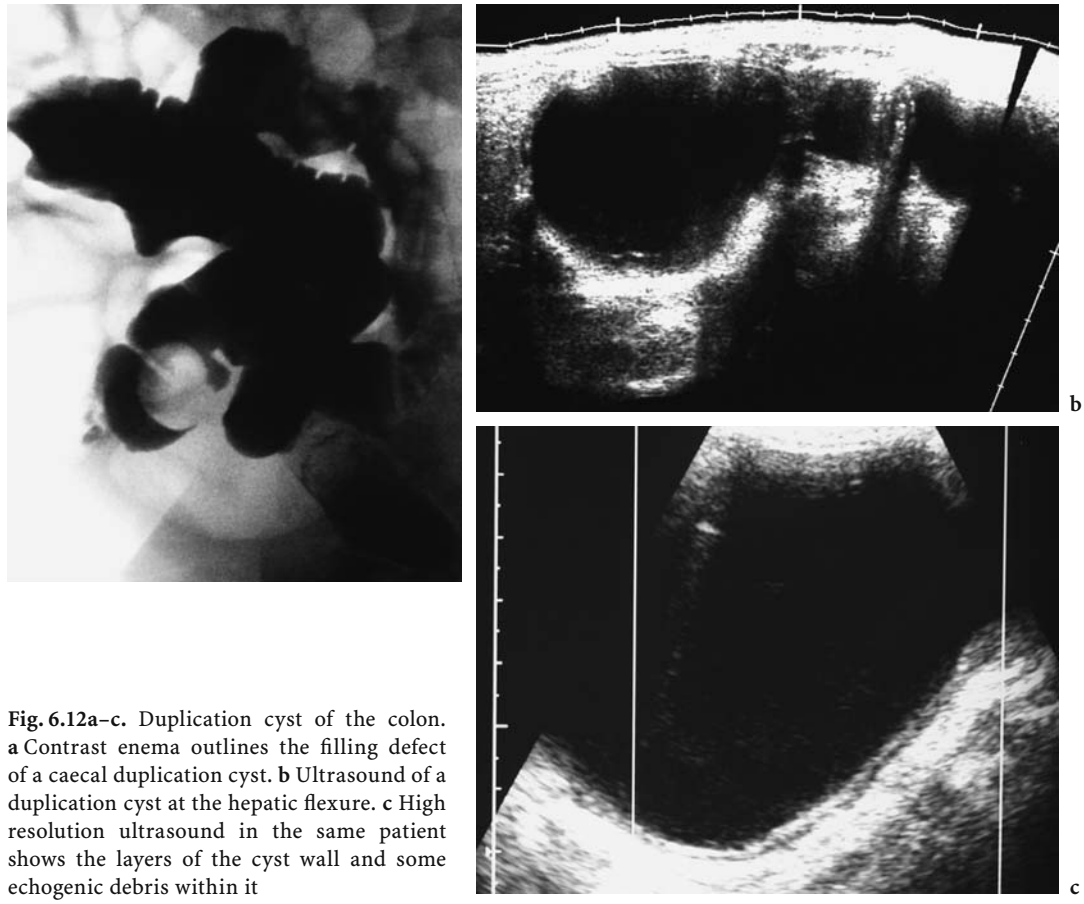

Fig. 6.12a–c. Duplication cyst of the colon. **a** Contrast enema outlines the filling defect of a caecal duplication cyst. **b** Ultrasound of a duplication cyst at the hepatic flexure. **c** High resolution ultrasound in the same patient shows the layers of the cyst wall and some echogenic debris within it

6.7 Anorectal Anomalies

Anorectal anomalies occur in approximately 1 per 5000 live births and are more common in males.

The embryological development of the anorectal segment is complex and as a result many anomalies are possible. Many classification schemes have been proposed, and whilst one of the simplest and earliest outlines (Gans 1970) is still in use it has been superseded by the "Wingspread" classification (see below). This is itself now likely to be superseded by a new classifcation (Krickenberg 2005), but publication of this is still awaited.

The Wingspread classification divides anorectal malformations into high, intermediate or low form (Stephens and Smith 1988). The classification is based on the level of the rectal pouch relative to the levator ani muscle, i.e. above the levator ani is designated a supralevator or high, at the level of the levator ani is termed intermediate, and below levator ani is termed translevator or low. The majority of anorectal malformations are of the communicating type, in which the enteric component joins into the urinary or genital tract, or to the perineum. This abnormally located opening to the exterior is usually termed 'fistula', however, recent work suggests that embryologically this is not a fistula but an ectopic anal orifice (Nievelstein et al. 1994, 1998a).

Depending on the exact level of the distal end of the colon, it may have passed through the puborectal sling. In cases of a high ending colon, the colon ends at or above the puborectal sling which may be hypoplastic or absent. If the colon ends low, it will have passed through the puborectal sling, which will usually be well developed and functional. The level of the distal end of a colon will affect the imaging required, and the subsequent surgical approach.

Anorectal malformations are frequently associated with other congenital anomalies, especially of

the vertebra, kidney, esophagus or trachea. Anorectal anomalies may present as part of the VACTERL pattern of anomalies (i.e. vertebral, anal, cardiac, tracheal, esophageal, renal and limb anomalies). The overall incidence of associated anomalies is approximately 50%. Associated genitourinary tract abnormalities occur in 28%–72% of cases. The anomalies are twice as common with high, as opposed to low anorectal malformations, although up to 30% of patients with low imperforate anus have associated urologic anomalies which may still cause significant morbidity (Misra et al. 1996). Many of the associated anomalies are significant, and the long-term outcome for children with anorectal malformations is often dependent on the extent of the associated anomalies more than on the anorectal malformation itself.

When anorectal malformations are associated with several other congenital abnormalities, involving the spinal cord, spine, and urogenital system it is often called the caudal regression syndrome, which has an association with maternal diabetes. A further associated syndrome, Currarino's triad is the rare autosomal dominant genetic disorder characterised by the complex of a congenital sacral bony abnormality with a 'sickle-shape', anorectal malformation and a pre-sacral mass (anterior meningocele, teratoma, dermoid cyst or enteric duplication cyst) (Currarino et al. 1980).

A separate, more complex group of anomalies is formed by the cloacal malformations, in which the urinary, genital and intestinal tracts converge to form a common channel with a single perineal orifice, i.e. the cloaca. These malformations are found exclusively in phenotypic females.

6.7.1 Imaging for Anorectal Anomalies

An anorectal anomaly is usually identified clinically. There may be an anal dimple present on the perineum or there may be an apparently patent external orifice but with a digitally palpable membrane on examination. Meconium may be passed per urethra in boys or per vagina in girls.

It is still common that plain radiography is performed and this will show a low obstruction early in the neonatal period (Fig. 13a). A prone lateral shoot through radiograph may be helpful in determining the level of the atresia, and allow assessment of the sacrum (Figs. 13b,c)

Ultrasound has been used to delineate the distance from the distal gas-filled colon to the perineum although its use is not widespread (Donaldson et al. 1989); less than 10 mm indicates a low lesion, and 15 mm or greater indicates a high lesion that will require diversion with colostomy.

Given the high incidence of associated anomalies all patients should have a renal tract ultrasound early in the newborn period. If this shows hydronephrosis, hydroureter or other renal abnormality (Fig. 6.13d) a full urological workup should be performed before a colostomy is fashioned or immediately after (Pena 1993). It would be appropriate to perform spinal ultrasound at the same examination to assess the integrity of the spinal cord and any associated dysraphic abnormalities (Fig. 6.13e). If this is normal only plain radiographs of the lumbar spine will be required, but if any further anomalies are demonstrated MRI of the lumbosacral spine should be obtained later when clinically appropriate (Fig. 6.13f). Possible associated intraspinal pathology includes caudal regression syndrome, cord tethering, hydromyelia or lipoma of the filum terminale. Newborn females with a cloaca may need drainage of a hydrocolpos.

Many centres make a clinical decision whether to proceed to definitive primary repair by perineal anoplasty (for low malformations) or to perform a colostomy only, deferring further imaging until definitive repair can be performed at a later date (in high malformations). Most centers routinely use a combination of a micturating cystogram (MCU) and a loopogram through the loop colostomy (high pressure distal colostogram) to outline any associated connection or 'fistula' between the distal bowel and the urinary tract (Fig. 6.13g,h). The MCU will also demonstrate the degree of any associated vesicoureteric reflux. An increasing number of centers are additionally using MR imaging, as it can help determine the presence of the puborectalis muscle and external sphincter as well as the rectal pouch prior to surgery. The definitive surgical approach for high malformations is dependent on the type of fistula demonstrated. The posterior sagittal anorectoplasty (PSARP) is most often used in this group but in cases with an additional rectovesical fistula a laparotomy is also required in addition to the posterior sagittal approach.

A PSARP is performed prone. A midline posterior sagittal incision is made extending from the mid level of the sacrum to the anterior edge of the external sphincter.

The sphincter mechanism is divided in the midline hence preserving the nerve fibers. The gluteal

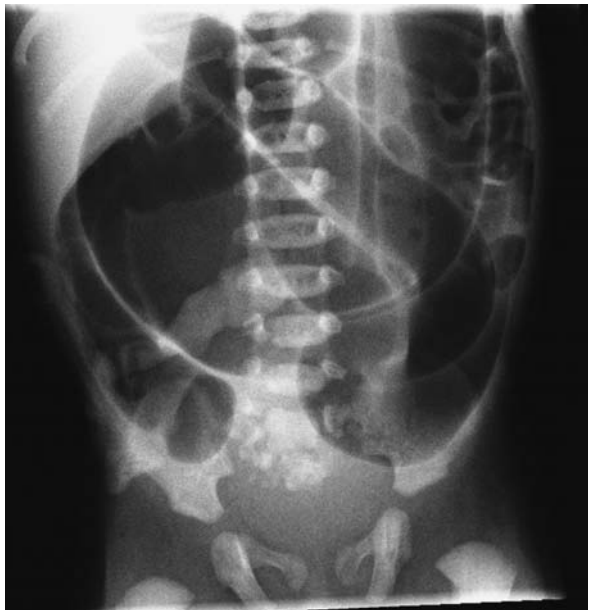
a

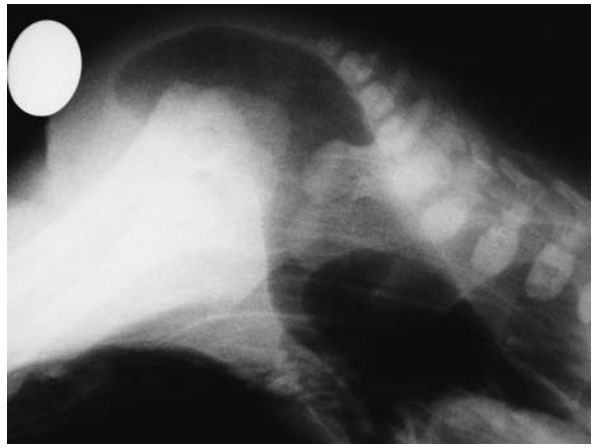
b

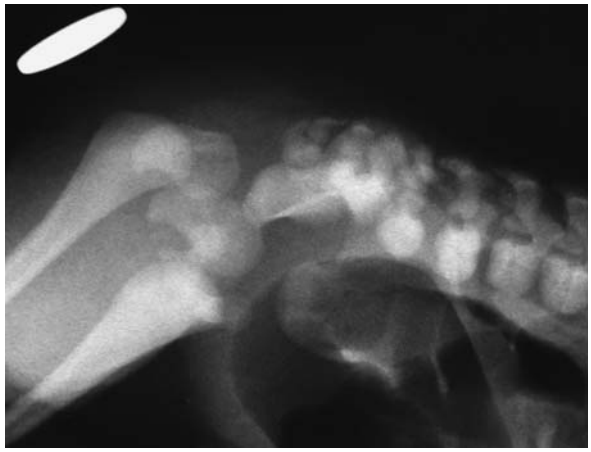
c

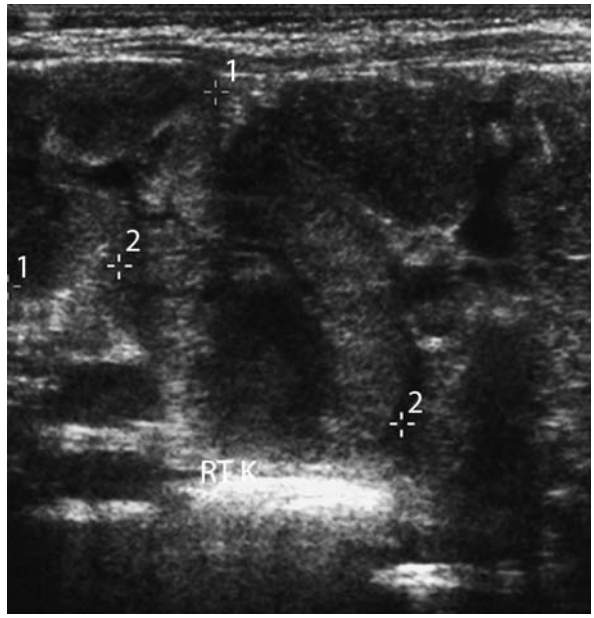

d

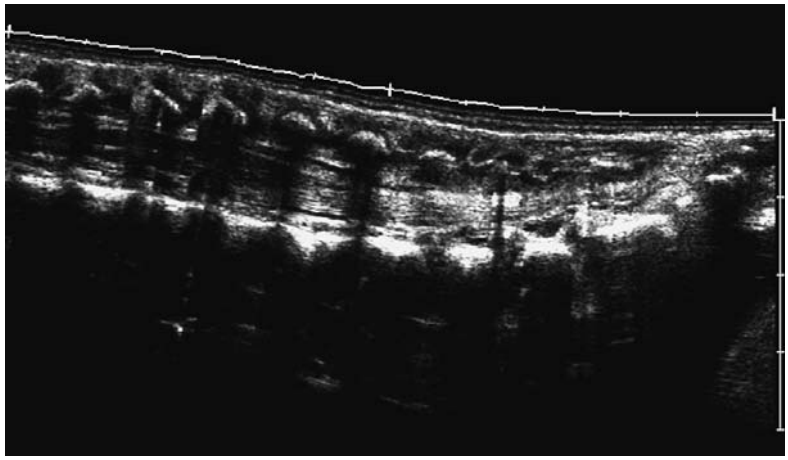
e

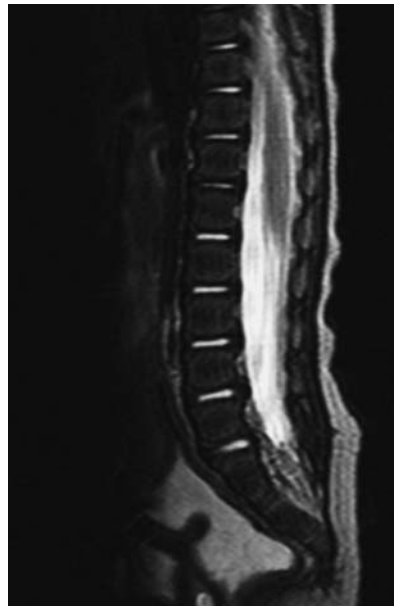
f

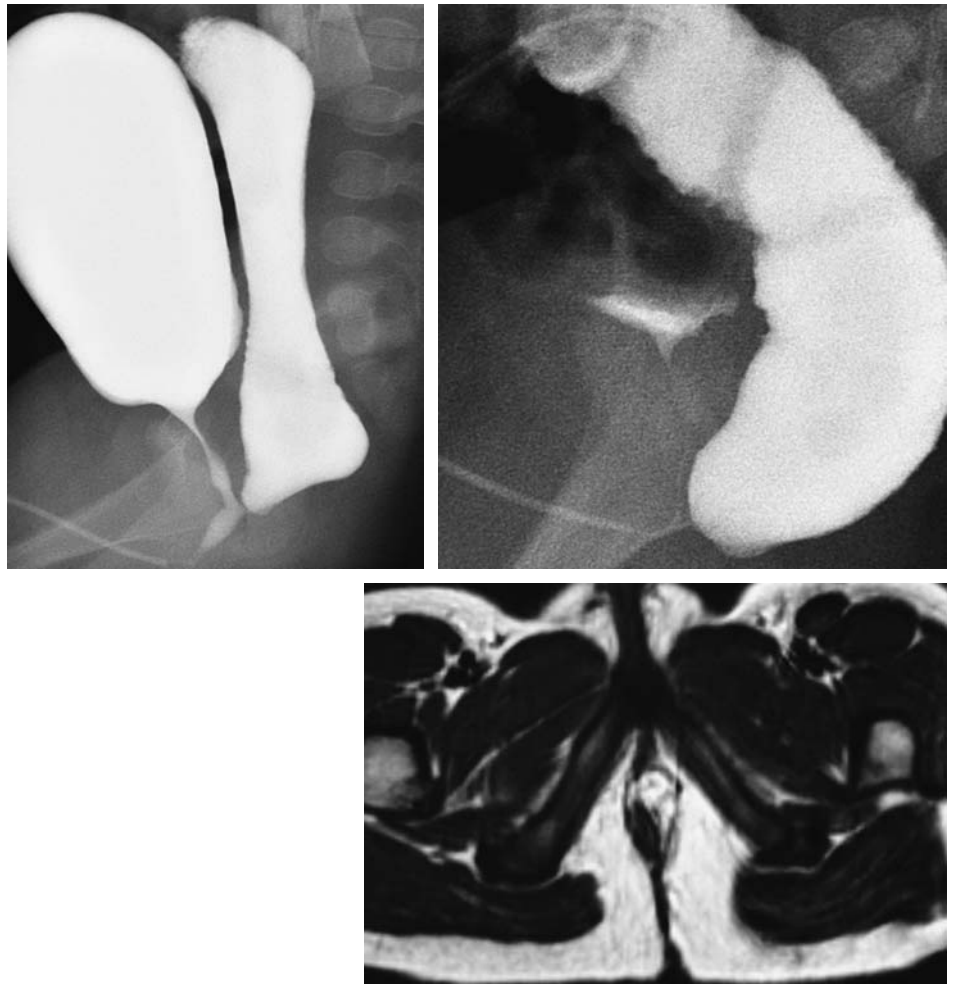

g h i

a–f

Fig. 6.13. a Abdominal radiograph on day 1 of life. The bowel is distended with air but this comes to an abrupt end low in the pelvis. Note the associated deficient sacrum. **b** A prone lateral shoot through radiograph showing the lowest gas filled bowel which is near the radio-opaque marker place in the natal cleft. This is a 'low' anomaly. **c** A prone lateral shoot through radiograph showing the lowest gas filled bowel which is near the radio-opaque marker place in the natal cleft. This is a higher anomaly. **d** Renal US showing crossed fused ectopia in an infant with an anorectal malformation. The fused right and left kidneys are shown by the markers. **e** Spine ultrasound in the patient shown in (**a**) showing the deficient sacrum, the cord was normal. **f** T2-weighted sagittal sequence of the spine showing the partly absent sacrum. **g** A 'fistula' inserting into the posterior urethra of a male infant. **h** Loopogram study demonstrating distension of the distal colon with retrograde filling of the bladder via the very narrow fistula. **i** MR of the pelvic floor following surgery showing mesenteric fat that has inadvertently been brought down into the rectal complex

muscles are opened like a book, and all internal structures including the 'fistula' are exposed. The rectum is then separated from the genitourinary tract, dissected, and freed enough to reach its normal orifice without tension. The fistula site is then closed.

With the use of an electrical muscle stimulator, the limits of the sphincter mechanism are determined and the rectum is placed in its optimal location to achieve the best functional results. Adequate placement of the neo-rectum in both the puborectalis muscle and the external anal sphincter is essential in achieving an acceptable functional outcome (Fig. 6.13i) (Nievelstein et al. 1998b).

6.7.1.1 MCU and Loopogram Technique

The combined MCU and loopogram is usually performed when the child is a few months old. An MCU is performed first using a urethral catheter, and good

distention of the bladder must be achieved. The 'fistula', if present, is often demonstrated at MCU when the child voids with retrograde filling of the fistula connecting to the distal bowel loop. The loopogram is then performed using water-soluble contrast, with a good seal being obtained at the stomal orifice by careful inflation of the catheter balloon. With maximal filling of the distal pouch the fistula may again be delineated, and the inferior limit of the distal pouch can be demonstrated. It is essential to get good pressure in the distal segment to be certain that any possible ectopic insertion of the bowel has been demonstrated.

6.7.1.2 MRI Imaging Technique in the Neonatal or Infantile Period

Suggested sequences are given in Table 6.1 (Nievelstein et al. 1998b). The level of the anorectal malformation can be adequately demonstrated on T1-weighted images but T2-weighted images are particularly helpful in the evaluation of intermediate and low malformation because the highest signal intensity of the anorectal mucosa allows better delineation of the anorectum with respect to this sphincter muscle complex and perineum (Nievelstein et al. 1998b). The sagittal and coronal sequences allow accurate determination of the level of the malformation. The use of FSE T2-weighted sagittal and axial images allows detection of a fistula, although the exact level of connection to the urogenital system may still be difficult to ascertain. If MRI is performed in the neonatal period the hyperintense meconium inside the rectal pouch on T1-weighted images may serve as an excellent MRI contrast agent. For further details of specialized MRI anatomy and techniques the interested reader is referred to the cited literature (Pena 1993; Nievelstein et al. 1998b; Pringle et al. 1987; Sato et al. 1988; Vade et al. 1989; Taconne et al. 1992; Fukuya et al. 1993).

Table 6.1. Suggested guidelines (Nievelstein et al. 1998b) for MR protocol for neonates and infants with anorectal malformations (based on a 1-T or 1.5-T magnet using a head coil for neonates and a phased array body coil for older children). Axial and coronal planes should be angled to be parallel and perpendicular to the pelvic floor. Imaging of the spinal cord and kidneys is only necessary if associated anomalies are suspected

Sequence	Plane	Anatomic region
SE T1	Sagittal	Pelvis, spine from T10, kidneys
SE T1	Axial, coronal	Pelvis
FSE T2	Sagittal, axial, coronal	Pelvis
SE T1	Axial, coronal	Spinal cord and/or kidneys
GRE T2	Sagittal	Spinal cord and spine
GRE T2	Axial	Spinal cord and cauda equina

6.8 Typhlitis

Typhlitis, also known as ileocaecal syndrome or neutropenic colitis, is an acute inflammation of the caecum, appendix and occasionally terminal ileum. It is primarily described in children with leukemia and a severe neutropenia. Histologically the changes are of oedema and ulceration of the entire bowel wall, with transmural necrosis and perforation possible. It is thought to be due to a leukemia or lymphomatous infiltrate, ischaemia, focal pseudo membranous colitis and/or infection. The most common organisms found include cytomegalovirus virus, *Pseudomonas*, *Candida*, *Klebsiella*, *E Coli*, *B Fragilis* and *Enterobacter*. Whilst being most common in childhood leukemia, it is also seen in aplastic anaemia, lymphoma and during immunosuppressive therapy. Children present with abdominal pain (which may be localized to the right iliac fossa), watery diarrhoea, a palpable mass in the right iliac fossa, fever in neutropenia or with bloody stools.

The caecum and ascending colon are the most common sites of involvement, the appendix and the terminal ileum may be secondarily involved. The plain abdominal radiograph may show distention of nearby small bowel loops, possibly a fluid-filled mass-like density in the right iliac fossa, representing the caecum, thumb printing of the ascending colon and thickening of the caecal wall to greater than 4 mm. Typhlitis may be associated with pneumatosis coli which is a common finding in markedly immunosuppressed children. Ultrasound examination can be either by a curvilinear or a linear probe. The circumferential thickening of the caecal wall, and possibly the terminal ileum, will be seen. There may be adjacent oedema. Some centers advocate the use of CT where the main findings will again be of

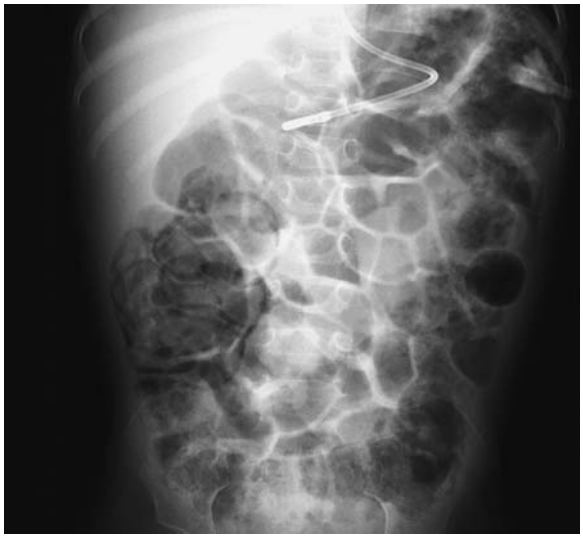

Fig. 6.14. Abdominal radiograph showing thickening of the cecal wall and intramural gas consistent with typhlitis in this immunocompromised patient

wall thickening of the caecum, decreased bowel wall attenuation due to oedema, streaking and stranding of the adjacent fat and thickening of the fascial planes, as well as fluid around the colon associated with intramural pneumatosis.

Contrast studies should not be attempted due to the risk of perforation. In the absence of perforation surgery is not indicated.

The differential diagnosis includes appendicitis with an appendicular abscess, inflammatory bowel disease or leukaemic deposit (in which case the wall thickening is likely to be eccentric) (Alexander et al. 1988) (Fig. 6.14).

6.9 Volvulus

Volvulus of the colon is rare in children and infants but when seen it most commonly involves the sigmoid colon, although caecal volvulus can also occur. The sigmoid colon in infants and children is often redundant and therefore the extra length is believed to be prone to twisting. In a recent review of the literature (Salas et al. 2000) the median age at presentation was 7 years, ranging from 4 h to 18 years. Boys were more commonly affected than girls (ratio: 3.5 to 1) and presentation could be either acute or recurrent. In acute cases, the mean duration of symptoms, including severe pain that may escalate to shock and circulatory collapse, was 1.5 days. In recurrent cases, the chronic and intermittent episodes of pain had been present, on average, for 1 year. The most common symptoms are abdominal pain that is relieved by passage of stool or flatus, abdominal distention and vomiting.

A plain abdominal radiograph shows colonic dilatation. A sigmoid volvulus tends to point to the right upper quadrant and will be shown by enclosed loop of dilated bowel. As in adults, a caecal volvulus will tend to lie in the left upper quadrant. The diagnosis is usually made from the plain abdominal film; however, if a contrast enema is performed this may demonstrate a typical beak deformity showing the point of obstruction as a result of twisting by the volvulus. The volvulus may resolve spontaneously, but if persistent will need to be reduced surgically, although in some patients a contrast examination may reduce the volvulus (Mellor and Drake 1994).

6.10 Lymphoid Hyperplasia

Lymphoid hyperplasia affecting the colon in infants and children is well recognised and best seen on a double contrast barium enema. The classical finding is a mucosa studded with innumerable 1- to 3-mm small uniform nodules. Some of these lesions may show an umbilicated center but this is not always seen. Whilst it is normal to find some lymphoid follicles in the pediatric gut they are usually sparser and more diffuse.

Lymphoid hyperplasia is most commonly seen in children less than 2 years old but is also seen in older children and adults. The histology is that of hyperplastic lymph follicles in the lamina propria (Peyer's patches) and these follicles probably represent a compensatory attempt for immunoglobulin deficiency. In adults lymphoid hyperplasia is associated with late onset immunoglobulin deficiency (IgA, IgM). Occasionally lymphoid hyperplasia can take the form of large polypoid growths in the ileocaecal region. Clinical presentation may be indistinguishable from acute appendicitis. In this variant of lymphoid hyperplasia there is increased risk of bleeding and intussusception, with secondary obstruction. The condition may require surgical intervention.

6.11 Necrotising Enterocolitis

Necrotising enterocolitis (NEC) in modern paediatric practice refers to the idiopathic, often severe enterocolitis that occurs in premature infants in neonatal intensive care units. The only definite risk factor for NEC is prematurity and the majority of cases occur in infants who weigh less than 2000 g, with both the incidence and mortality increasing with decreasing birth weight and gestational age (Holman et al. 1997). NEC may also occur in full-term infants with a predisposition, such as those who have had surgery for congenital heart disease or who have had abdominal surgery. An acute enteritis may be seen in Hirschsprung's disease. Vascular lines and generalized sepsis have been loosely associated with NEC.

Inflammation begins in the mucosa of the bowel wall and then extends through the whole bowel wall. The terminal ileum and the proximal colon are the most commonly affected areas.

Details of the acute radiological findings are described elsewhere in the text as they are not specific to the colon. However, the complications of NEC often do involve the colon with approximately 10%–20% of survivors developing strictures of the bowel which may be single or multiple. Despite NEC most commonly affecting the distal ileum and the ascending colon the majority of strictures affect the descending colon (Fig. 6.15). Infants who have developed strictures may be asymptomatic but most present clinically within weeks to months of the initial diagnosis of NEC, usually with a distended abdomen, intolerance of feeds or with obstruction. In those infants who have had surgery to raise an ileostomy or colostomy it is essential to assess the distal bowel using a loopogram or contrast enema before reversal of the stoma.

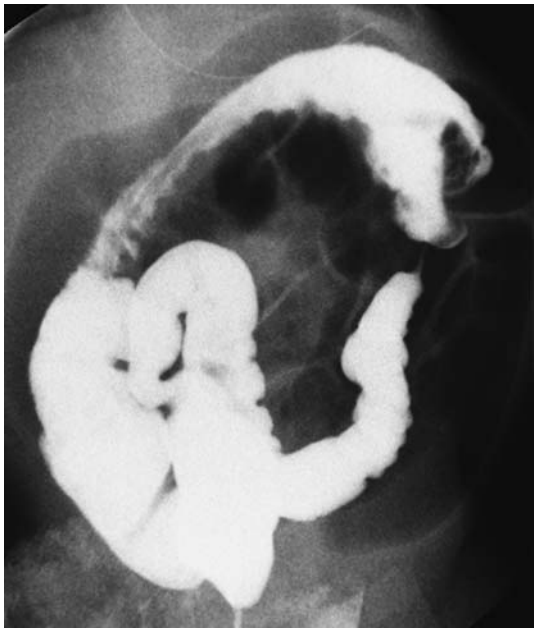

Fig. 6.15. Contrast enema showing a stricture of the descending colon following necrotising enterocolitis

6.12 Inflammatory Bowel Disease Affecting the Colon

In infants and young children the majority of the colitides are thought to be infectious in origin, although ulcerative colitis (UC) and Crohn's disease (CD) are also seen. In the neonatal period, inflammatory processes of the colon are often related to necrotising enterocolitis, but the enterocolitis of Hirschsprung's disease and colitis associated with milk allergy are also seen. UC and CD are the main inflammatory diseases of the colon that come to the attention of the paediatric radiologist and hence are discussed below.

6.12.1 Chronic Inflammatory Bowel Disease

UC and CD are both considered 'idiopathic' types of inflammatory bowel disease (IBD). They are distinguished by their morphological, histological, clinical and epidemiological features and by their distribution in the gut. In some cases it is not possible to differentiate the two conditions by the standard criteria and in such patients the colitis is considered 'indeterminate'. Patients may present with abdominal symptoms such as pain, cramping, diarrhoea, bloody stools and weight loss, but also with associated symptoms including anorexia, arthritis, failure to thrive and other extra-intestinal symptoms. The aetiology is unclear but childhood infection, early diarrhoea, immunological hypersensitivity and vasculitis have all been linked to both CD and UC. Affected relatives/family history are reported in up

to 20% of patients suggesting a genetic contribution in at least some cases.

6.12.2 Imaging in Inflammatory Bowel Disease of the Colon

Colonoscopy and biopsy is the mainstay in the investigation of suspected IBD affecting the colon or terminal ileum. However, imaging can add important information during disease exacerbations and complications. Plain abdominal radiographs may demonstrate an acute colitis, bowel perforation or obstruction. The features of acute colitis include increased thickness of the colonic wall, irregularity of the mucosal surface, bowel dilatation, and an abnormal stool distribution (stool being non-adherent to inflamed mucosa). Absence of any stool suggests significant and widespread inflammation, and associated spasm may result in the absence of any bowel contents (stool or air). Nuclear medicine examinations provide an adjunct to endoscopy and radiological techniques with technetium-leukocyte scans (white cell scans) useful for assessing the presence and location of active disease in children (Fig. 6.16a). Whilst this technique cannot give anatomical detail regarding strictures and fistulae, it is able to confirm active disease using a lower radiation dose than the barium follow through or barium enema.

Whilst the barium follow through is the main contrast examination for assessing the small bowel in IBD (Fig. 6.16b) it may still provide information on the colon if delayed views are obtained; however, the barium enema is mainly used in the colon. A double-contrast technique is necessary for mucosal delineation although for patients with advanced disease a single contrast study may be adequate. Some centers have a preference for performing small bowel enteroclysis.

More recently there has been increasing use of MRI in the imaging of Crohn's disease in children. Various protocols are in use (Wiarda et al. 2005; Horsthuis et al. 2005; Gourtsoyiannis et al. 2004; Kim and Ha 2003). Typically this may be performed using 1 l of 2.5% mannitol solution as an oral preparation, taken over the hour leading up to the imaging, and following a 6-h fast. Hyoscine butylbromide and gadolinium are given intravenously at the start of the scan and sequences typically including heavily T2-weighted (HASTE), true FISPs and VIBEs (3D volume acquisition) are obtained in a coronal plane.

6.12.2.1 Imaging Finding in Ulcerative Colitis

Ulcerative colitis is well recognised in children, but tends to occur in older children, with a similar pattern to that seen in adults. The inflammatory process is confined to the mucosa and superficial mucosa of the colon and the inflammation typically extends for a varying distance retrogradely from the rectum. Colonoscopy is the investigation of choice and barium enemas are rarely performed. If a double contrast enema is obtained the findings are those of superficial ulceration of the mucosa, often appearing as a fine mucosal granularity and loss of haustration. The presacral space may be widened with active disease in the rectum. As the disease progresses the ulceration will become more prominent with spicules and serrated bowel margins. Deeper ulcers are described as being "collar button" and there may be "double tracking" representing longitudinal submucosal ulceration. "Thumb printing" demonstrates symmetric thickening of the colonic folds. As the disease progresses inflammatory polyps may be seen, the mucosa becomes coarsened, and eventually the colon becomes shortened, distensible and without haustral markings or a mucosal pattern.

6.12.2.2 Imaging Findings in Crohn's Disease

In contrast, Crohn's disease shows transmural inflammation and characteristically affects some areas of bowel and not others. Compared to ulcerative colitis, the colon is less affected in Crohn's disease but overall, Crohn's disease is more common than ulcerative colitis in children and therefore inflammatory bowel disease affecting the colon in children is most commonly Crohn's disease. Crohn's disease particularly affects the right side of the colon with sparing of the rectum and sigmoid colon. In the early stages barium enema will show nodular enlargement of lymphoid follicles and aphthous ulcers. As the disease progresses the findings are similar to those in adults, i.e. a cobblestone appearance to the bowel wall caused by longitudinal and transverse ulcers separated by areas of oedema, straightening and rigidity of the affected part of the colon, strictures and fistulae. Barium studies remain the mainstay of investigations, however, white cell studies (nuclear medicine) are useful for confirming acute exacerbation when anatomical detail is not required. Ultrasound is useful for showing

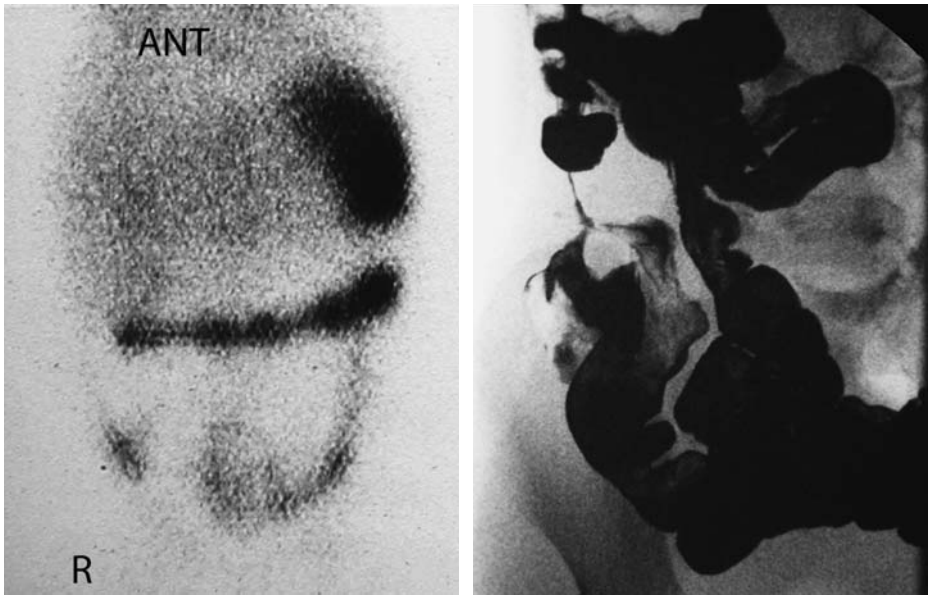

a b

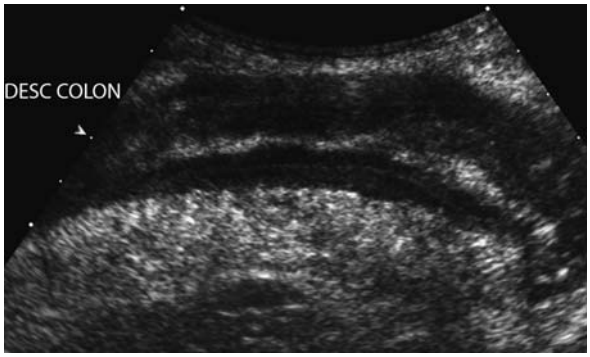

c

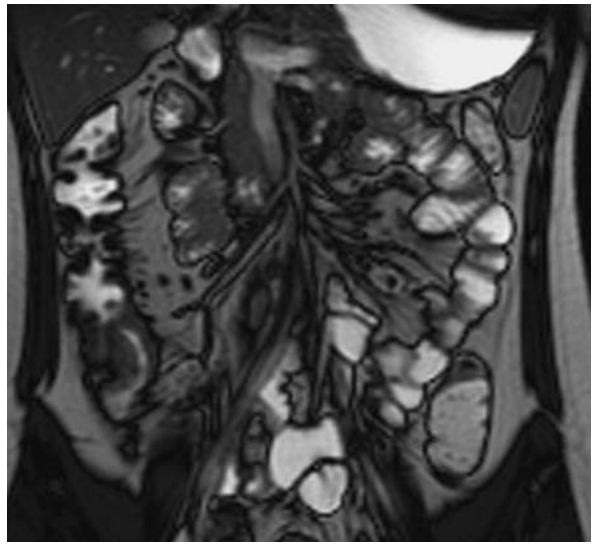

d

Fig. 6.16a–d. Crohn's disease of the colon. **a** Indium labelled white cell scan in active disease with widespread involvement of the caecum, transverse and descending colon. **b** Barium follow through demonstrating stricture formation of the ascending colon with displaced adjacent bowel consistent with an inflammatory mass. **c** Ultrasound of the descending colon in a patient with active disease. Note the thickened bowel wall and the obliterated bowel lumen. **d** Coronal MRI showing marked wall thickening of the caecal pole with a narrowed lumen

thickening of the bowel wall, typically to 8 mm or more (Fig. 6.16c), and can also show the presence of abscesses and distended loops. MRI is increasingly used to examine the bowel wall (Fig. 6.16d) and also to show the presence and configuration of fistulae, especially in the peri-anal region.

As both Crohn's disease and ulcerative colitis are similar in adults and children the reader is referred to the adult literature for further reading.

References

Abu-Yousef MM, Bleicher JJ, Maher JW et al (1987) High-resolution sonography of acute appendicitis. AJR Am J Roentgenol 149:53–58

Alexander JE, Williamson SL, Seibert JJ et al (1988) The ultrasonographic diagnosis of Typhlitis (neutropenic colitis). Pediatr Radiol 18:200–204

American College of Radiology (1997) Standard for the performance of pediatric contrast enema examinations. Revised 2001 (Res 28)

Benning MA, Buller HA, Heymans HAS et al (1994) Is encopresis always the result of constipation? Arch Dis Child 59:649–652
Berdon WE, Slovis TL, Campbell JB et al (1977) Neonatal small left colon syndrome: its relationship to aganglionosis and meconium plug syndrome. Radiology 125:457–462
Carty HML (2002) Paediatric emergencies: non-traumatic abdominal emergencies. Eur Radiol 12:2835–2848
Clatworthy H, Howard W, Lloyd J (1956) The meconium plug syndrome. Surgery 39:132–141
Currarino G, Coln D, Votteler T (1980) Triad of anorectal, sacral and presacral anomalies. AJR Am J Roentgenol 137:395–398
Daneman A, Alton DJ, Lobo E et al (1998) Patterns of recurrence of intussusception in children: a 17-year review. Pediatr Radiol 28:913–191
del Pozo G, Albillos JC, Tejedor D et al (1996) Intussusception: US findings with pathologic correlation – the crescent-in-doughnut sign. Radiology 199:688–692
del Pozo G, Albillos JC, Tejedor D et al (1999) Intussusception in children: current concepts in diagnosis and enema reduction. Radiographics 19:299–319
Donaldson JS, Black T, Reynolds M et al (1989) Ultrasound of the distal pouch in infants with imperforate anus. J Pediatr Surg 24:465–468
Fefferman NR, Roche KJ, Pinkney LP (2001) Suspected appendicitis in children: focuses CT technique for evaluation. Radiology 220:691–695
Fotter R (1998) Imaging of constipation in infants and children. Eur Radiol 8:248–258
Fukuya T, Honda H, Kubota M et al (1993) Post operative MRI evaluation of anorectal malformations with clinical correlation. Pediatr Radiol 23:583–586
Gans SL (1970) Classification of anorectal anomalies: a critical analysis. J Pediatr Surg 5:511–513
Gorenstein A, Raucher A, Serour F et al (1998) Intussusception in children: reduction with repeated, delayed air enema. Radiology 206:721–724
Gourtsoyiannis N, Papanikolaou N, Grammatikakis J et al (2004) Assessment of Crohn's disease activity in the small bowel with MR and conventional enteroclysis: preliminary results. Eur Radiol 14:1017–24. Epub 2004 Apr 1
Heneyke S, Smith VV, Spitz L et al (1999) Chronic intestinal pseudo-obstruction: treatment and long term follow up of 44 patients. Arch Dis Child 81:21–27
Holman RC, Stoll BS, Clarke MJ (1997) The epidemiology of necrotising enterocolitis: Infant mortality in the United States. Am J Public Health 87:2026–2031
Horsthuis K, Lavini Mphil C, Stoker J (2005) MRI in Crohn's disease. J Magn Reson Imaging 22:1–12
Janik JS, Firor HV (1979) Pediatric appendicitis. A 20-year study of 1,640 children at Cook County (Illinois) Hospital. Arch Surg 114:717–719
Jeffrey RB, Laing FC, Townsend RR (1988) Acute appendicitis: sonographic criteria based on 250 cases. Radiology 167:327–329
Kapur RP (2000) Developmental disorders of the enteric nervous system. Gut [Suppl IV]47:iv81–iv83
Kessler N, Cyteval C, Gallix B et al (2004) Appendicitis: evaluation of sensitivity, specificity, and predictive values of US, Doppler US, and laboratory findings. Radiology 230:472–478
Keyzer C, Tack D, de Maertelaer V et al (2004) Acute appendicitis: comparison of low-dose and standard-dose unenhanced multi-detector row CT. Radiology 232:164–172
Khong PL, Peh WC, Lam CH et al (2000) Ultrasound-guided hydrostatic reduction of childhood intussusception: technique and demonstration. Radiographics 20:E1 (Erratum in: Radiographics 2000 20:1818)
Kim KW, Ha HK (2003) MRI for small bowel diseases. Semin Ultrasound CT MR 24:387–402
Kong MS, Wong HF, Lin SL et al (1997) Factors related to detection of blood flow by color Doppler ultrasonography in intussusception. J Ultrasound Med 16:141–144
Lee JH, Jeong YK, Park KB et al (2005) Operator-dependent techniques for graded compression sonography to detect the appendix and diagnose acute appendicitis. AJR Am J Roentgenol 184:91–97
Lee JM, Kim H, Byun JY et al (1994) Intussusception: characteristic radiolucencies in the abdominal radiograph. Pediatr Radiol 24:293–295
Loening-Baucke V (1993) Chronic constipation in children. Gastroenterology 105:1557–1564
Meir-Ruge W, Scharli AF (1986) The epidemiology and enzyme histotopochemical characterisation of ultrashort-segment Hirschsprung's disease. Pediatr Surg Int 1:37–42
Mellor MFA, Drake DG (1994) Colonic volvulus in children: value of barium enema for diagnosis and treatment in 14 children. AJR Am J Roentgenol 162:1157–1159
Mezwa DG, Feczko PJ, Bosanko C (1993) Radiologic evaluation of constipation and anorectal disorders. Radiol Clin North Am 31:1375–1393
Misra D, Mushtaq I, Drake DP et al (1996) Associated urologic anomalies in low imperforate anus are capable of causing significant morbidity; a 15-year experience. Urology 48:281–283
Navarro O, Daneman A (2004) Intussusception. Part 3: diagnosis and management of those with an identifiable or predisposing cause and those that reduce spontaneously. Pediatr Radiol 34:305–312
Navarro O, Dugougeat F, Kornecki A et al (2000) The impact of imaging in the management of intussusception owing to pathologic lead points in children. A review of 43 cases. Pediatr Radiol 30:594–603
Navarro OM, Daneman A, Chae A (2003) Intussusception: the use of delayed, repeated reduction attempts and the management of intussusceptions due to pathologic lead points in pediatric patients. AJR Am J Roentgenol 182:1169–1176
Nievelstein RAJ, Valk J, Smit LME et al (1994) MR of the caudal regression syndrome: embryologic implications. AJNR 15:1021–1029
Nievelstein RA, van der Werff JF, Verbeek FJ et al (1998a) Normal and abnormal embryonic development of the anorectum in human embryos. Teratology 57:70–78
Nievelstein RAJ, Vos A, Valk J (1998b) MR imaging of anorectal malformations and associated anomalies. Eur Radiol 8:573–581
O'Donovan AN, Habra G, Sommers S et al (1996) Diagnosis of Hirschsprung's disease. AJR Am J Roentgenol 167:517–520
Pracros JP, Tran-Minh VA, Morin DE et al (1987) Acute intestinal intussusception in children: contribution of ultrasonography (145 cases). Ann Radiol 30:525–530

Partin JC, Hamill SK, Fischel JE et al (1992) Painful defecation and faecal soiling in children. Pediatrics 89:1007–1009
Pena A (1993) Management of anorectal malformations in the new-born period. World J Surg 17:385–392
Powell RW, Raffensperger JG (1982) Congenital colonic atresia. J Pediatr Surg 17:166
Pringle KC, Sato Y, Soper RT (1987) Magnetic resonance imaging as an adjunct to planning an anorectal pull-through. J Pediatr Surg 22:571–574
Puylaert JB (1986) Acute appendicitis: US evaluation using graded compression. Radiology 158:355–360
Rao PM , Rhea JT, Novelline RA (1997) Appendiceal and peri-appendiceal air at CT: prevalence, appearance and clinical significance. Clin Rad 52:750–754
Ratcliffe JF, Fong S, Cheong I et al (1993) The plain abdominal film in intussusception: the accuracy and incidence of radiographic signs. Paed Radiol 22:110–111
Rettenbacher T, Hollerweger A, Macheiner P et al (2001) Outer diameter of the vermiform appendix as a sign of acute appendicitis: evaluation at US. Radiology 218:757–762
Rioux M (1992) Sonographic detection of the normal and abnormal appendix. AJR Am J Roentgenol 158:773–778
Salas S, Angel CA, Salas N et al (2000) Sigmoid volvulus in children and adolescents. J Am Coll Surg 190:717–723
Sargent MA, Babyn P, Alton DJ (1994) Plain abdominal radiography in suspected intussusception: a reassessment. Pediatr Radiol 24:17–20
Sato Y, Pringle KC, Bergman RA et al (1988) Congenital anorectal anomalies: MR imaging. Radiology 168:157–162
Seth R, Heyman MB (1994) Management of constipation and encopresis in infants and children. Gastroenterol Clin North Am 23:1375–1393
Sivit CJ, Newman KD, Boenning DA et al (1992) Appendicitis: usefulness of US in diagnosis in a paediatric population. Radiology 185:549–552
Stephens FD, Smith ED (eds) (1988) Anorectal malformations in children: update 1988. Birth defects original article Series 24 (4) Liss, New York
Taccone A, Martucciello G, Dodero P et al (1992) New concepts in preoperative imaging of anorectal malformations. Pediatr Radiol 22:196–199
Vade A, Reyes H, Wilbur A et al (1989) The anorectal sphincter after rectal pull-through surgery for anorectal anomalies: MRI evaluation. Pediatr Radiol 19:179–183
Verschelden P, Filiatrault D, Garel L et al (1992) Intussusception in children: reliability of US in diagnosis – a prospective study. Radiology 184:741–744
Vignault F, Filiatrault D, Brandt ML et al (1990) Acute appendicitis in children: evaluation with US. Radiology 176:501–504
Wiarda BM, Kuipers EJ, Houdijk LP et al (2005) MR enteroclysis: imaging technique of choice in diagnosis of small bowel diseases. Dig Dis Sci 50:1036–1040
Williams NM, Jackson D, Everson NW et al (1998) Is the incidence of acute appendicitis really falling? Ann R Coll Surg 80:122–124
Yoon CH, Kim HJ, Goo HY (2001) Intussusception in children: US-guided pneumatic reduction – initial experience. Radiology 218:85–88

Radiological Gastrointestinal Interventions in Childhood: A Review

7

Rick R. van Rijn and Johan S. Laméris

CONTENTS

7.1 Introduction

In recent decades, image-guided interventions have become daily routine in radiology departments worldwide. Radiologists and clinicians alike clearly see the advantages of image-guided interventions, as it is minimally invasive, well tolerated by patients and has shown to have a low level of complications.

R. R. van Rijn; J. S. Laméris
Department of Radiology, Academic Medical Centre/Emma Children's Hospital Amsterdam, the Netherlands

In paediatrics this level of acceptance has yet to be reached, and currently interventional radiology in this particular group of patients is mostly performed in specialized paediatric hospitals. As we all know and should appreciate, children are not miniature adults, a fact reflected by age specific pathology and psychological development. This means that when a paediatric interventional program is initiated one should keep in mind specific problems when dealing with children. Generally speaking, one should plan ample time and be prepared to do fewer interventions in a given time frame than in an adult setting. If one is prepared to do the proverbial extra mile, one will be rewarded by satisfied patients and parents alike.

In this chapter we will discuss sedation and interventional procedures related to the gastrointestinal tract.

7.2 Sedation

One of the hallmarks of paediatric radiological interventions is the need for sedation in combination with analgesia. Where in the adult population local anaesthesia will mostly suffice, this will almost never be the case in children. This aspect of the interventional procedure may be one of the reasons for the lower level of acceptance of interventional radiology in children.

Although the situation will differ from country to country and most likely even from hospital to hospital, we would like to present a number of guidelines for running a sedation program in a radiology department.

Our first advice is to cooperate with your anaesthesiologists in order to develop a set of guidelines

along which the decision can be made whether to perform the procedure under sedation or under total anaesthesia.

Secondly, talk with the parents and where possible with the child. Explain the procedure and try to assess whether it will be possible to perform the procedure under sedation or whether general anaesthesia should be used.

Finally, when in doubt do not use sedation but consult the appropriate experts, since, after all, we are first and foremost radiologists.

For a more in-depth discussion of what sedation is, we refer to the American Society of Anaesthesia (ASA) (1996) and the American College of Radiology (ACR) (2004). Sedation can be classified into three different levels. Level I is light sedation or anxiolysis. This category is defined as 'the administration of oral medications for the reduction of anxiety' and 'a drug induced state during which the patient responds normally to verbal commands'. The ASA further states that 'although cognitive function and coordination may be impaired, ventilatory and cardiovascular functions are unaffected. Level II is moderate or conscious sedation, which is defined as 'a minimally depressed level of consciousness induced by the administration of pharmacological agents in which the patient retains conscious and independent ability to maintain protective reflexes and a patent airway and to be aroused by physical or verbal stimulation'. Level II sedation is actually quite difficult to achieve and maintain as it may easily lead to the next level (level III), i.e. deep sedation which is 'a controlled state of depressed consciousness or unconsciousness from which the patient is not easily aroused' (ASA 1996). Sedation level IV is general anaesthesia, which is beyond the scope of this article.

Sedation should always be performed by or under the supervision of a physician. This is especially so in the case of a radiological intervention as both sedation and analgesia are necessary. The latter combination makes it all the more difficult to adequately monitor the patient in question, thus it is essential that all persons responsible for the administration of medication and/or monitoring of the patient should be fully knowledgeable of the equipment and medication in use. Furthermore, they should possess basic life support skills in order to intervene in case of complications.

The current situation in Europe is that in many centres anaesthesia resources are relatively limited, which has led to the situation where more and more non-anaesthesiologists are administering sedatives. A possible solution to this problem in paediatric interventional radiology could be the use of a nurse-led sedation program. Several publications show excellent results of these programs for MRI units (Sury et al. 1999; Beebe et al. 2000). Sury et al. (1999) report on a total of 1155 sedations for MRI with a failure rate of only 5%, without cases of adverse reactions.

Finally, which patients are eligible for sedation? According to the ASA only class I and II patients (healthy patient and patient with mild systemic disease, respectively) are eligible (see Table 7.1). ASA Class III and higher require general anaesthesia (ASA 1996).

When an interventional procedure is performed under sedation the radiologist is also responsible for the pre-procedural management. In neonates the last feeding should be withheld, while in older children the policy is nil-by-mouth for at least 4 hours prior to sedation. Several drugs can be used for sedation (Table 7.2). However, the choice of drugs will depend on the experience of the radiologist, availability of the drugs and hospital policy. In an excellent review article by Towbin et al. (1988) they describe a strategy that, in their hands, has a 98% success rate. In children less than 2 years of age, oral chloral hydrate, at a dose of 50 mg/kg, is their drug of first choice. If more sedation is needed, for instance in case of a painful procedure, intravenous Fentanyl can be given, albeit in small doses of 1 mcg/kg. In children aged 2 years and above, oral chloral hydrate will generally not suffice. Intravenous Nembutal (Pentobarbital sodium), 2 mg/kg, is then preferred. Nembutal is a quick acting drug with relatively few side effects. When using Nembutal in interventional radiology, Fentanyl should be added,

Table 7.1. American Society of Anaesthesia physical status classification

Class I	A normal, healthy patient
Class II	A patient with mild systemic disease
Class III	A patient with severe systemic disease
Class IV	A patient with severe systemic disease that is a constant threat to life
Class V	A moribund patient who is not expected to survive without the operation
Class VI	A brain-dead patient whose organs are being removed for donor purposes

Table 7.2. Drugs used in sedation (Towbin and Ball 1988; Kaye et al. 2000a)

Drug	Dose	Range	Administration
Chloral hydrate	50 mg/kg	50–75 mg/kg	Oral
Nembutal	2 mg/kg	2–8 mg/kg	Intravenous
Fentanyl	1 µg/kg	1–5 µg/kg	Intravenous
Midazolam		0.1–0.3 mg/kg	Intranasally

as Nembutal tends to make children hypersensitive to stimulation. Nembutal should be given in 2- to 3-mg/kg boluses, titrated to the preferred level of sedation. Rubin et al. (2004) presented their experience with oral or intravenous caffeine for the treatment of post-sedation paradoxical hyperactivity. Of the children treated, 63% showed a positive effect and returned to baseline behavioural status significantly sooner than untreated children.

The use of midazolam intranasally as premedication has been described in several publications (Weber et al. 2003; Kogan et al. 2002; Ljungman et al. 2000). Its use reduces anxiety, induces amnesia in a significant number of patients and also has a sedative effect. The latter, however, is hardly ever satisfactory to allow an interventional procedure to be performed, but it will facilitate insertion of a venous access (Kaye et al. 2000a). The most common adverse reaction is nasal discomfort, reported to be as high as 45% of the cases; one case of an allergic reaction has also been published (Ljungman et al. 2000; McIlwain et al. 2004).

In a publication by Reeves et al. (2004) reported that conscious sedation using propofol actually amounted to deep sedation. The use of this medicine should therefore be restricted to personnel trained in anaesthesia and airway management.

Following an interventional procedure, the children should be observed and, depending on the intervention, feeding can be started, but only if the child has regained full consciousness.

7.3 Balloon Dilatation of Oesophageal Stricture

Oesophageal strictures in childhood can be the result of oesophageal surgery performed in the case of congenital oesophageal atresia (with strictures occurring in up to 70% of patients), or as a complication of ingestion of caustic agents, severe gastroesophageal reflux or oesophagitis and in rare cases epidermolysis bullosa (Huang et al. 2004; Fasulakis and Andronikou 2003; Sato et al. 1988; Naehrlich et al. 2000; Said et al. 2003; Erdogan et al. 2003; Jayakrishnan and Wilkinson 2001). Prior to the London et al. publication in 1981 on the use of a balloon catheter in order to treat oesophageal strictures, these strictures were treated with serial bougienage, with an increasing diameter, under general anaesthesia. Balloon dilatation has now become the initial choice of treatment in cases of oesophageal stricture.

In this fluoroscopy-guided procedure, a balloon catheter is passed over a guidewire after which dilation is performed (Fig. 7.1) (Fasulakis and Andronikou 2003). Prior to the procedure the patient is kept nil-by-mouth and an oesophagram is performed for precise location of the stricture. Thereafter a small feeding tube is placed just cranial of the stricture, through which a guidewire is passed and negotiated beyond the stricture, and finally placed within the stomach for the duration of the procedure. The feeding tube is exchanged for a balloon catheter, of which the markers on the balloon are placed across the stricture. The size of the balloon can be measured on a calibrated oesophagram; however, the 'rule of thumb' is as effective (Hamza et al. 2003). According to this latter rule, the calibre of the balloon is equal to the diameter of the patient's thumb. The balloon is inflated using a water-soluble contrast medium, enabling visual inspection during the procedure. Some recommend the use of serial dilatations in one session whereas others claim that a prolonged inflation of the balloon is as effective. After the procedure has been completed, a repeat oesophagram, using water-soluble contrast medium, is performed to rule out perforation.

The success rate of balloon dilatation is reported to range from 62.5% to 79%. In cases of post-surgical stenosis and gastroesophageal reflux-induced ste-

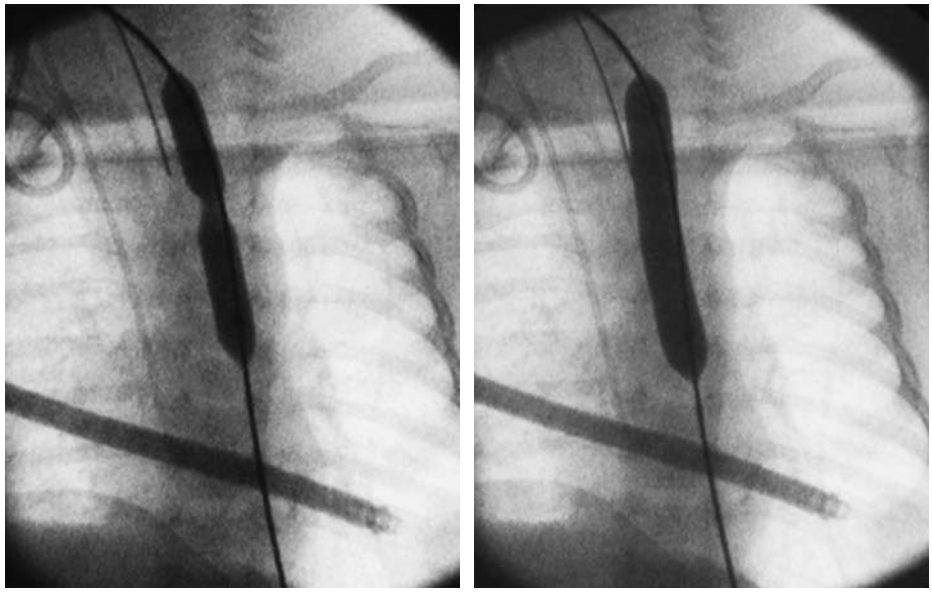

Fig. 7.1. a A 2-month-old boy with a history of esophageal atresia. Post-operatively a stricture developed at the level of the anastomosis. Dilatation with a 7-mm balloon shows a clear waist in the balloon at the level of the stenosis. **b** The balloon is fully inflated and the stenosis is no longer visible

nosis, the procedure has shown to be most effective (Lisy et al. 1998; Sandgren and Malmfors 1998). Lang et al. (2001) compared balloon dilatation with bougienage in a paediatric population and found that in the balloon group 1–7 procedures (median 2) were required while in the bougienage group it required 1–60 (median 9, $p = 0.002$) procedures.

Balloon dilation is a multi-session procedure. Serial dilation has the advantage that it minimizes the risk of tears and perforation. The advantage of balloon dilation over bougienage is that, when the balloon is inflated, it exerts a radial force on the stricture opposed to the shearing forces induced by bougienage (McLean and Le Veen 1989; Yeming et al. 2002; Kim et al. 1993). This leads to a decreased risk in perforation, which in balloon dilation has been reported to be as low as 0%–1.8% compared to a 5.8% risk in bougienage (Fasulakis and Andronikou 2003; Sato et al. 1988; Said et al. 2003; Jayakrishnan and Wilkinson 2001; Sandgren and Malmfors 1998; McLean and Le Veen 1989; Kim et al. 1993).

Although a safe procedure, contraindications for balloon dilation do exist, and these are considered to be multiple (> 3) strictures, long strictures (> 5 cm), tortuous strictures, or patients with tracheoesophageal fistulas (Hamza et al. 2003).

7.4 Percutaneous Gastrostomy

The use of percutaneous feeding techniques is well appreciated by clinicians and patients alike, and in most instances will be the preferred technique for nutritional supplementation. Percutaneous techniques surpass surgical procedures as in most cases they can be performed under IV sedation in combination with local anaesthesia. Chait et al. (1996) reported on 505 children in which 77.5% of all procedures were done successfully under IV sedation in combination with local anaesthesia. Additionally, the percutaneous procedure is less time consuming, has a lower complication rate and is less expensive (Kaye et al. 2000a; Kaye and Towbin 2002; Cory et al. 1988). Compared to endoscopic techniques it has the advantage of visualizing the liver prior to puncture of the abdominal wall, thus reducing the risk of passing the tube through the left liver lobe (Stellato and Gauderer 1987). Due to the relative ease of the procedure the number of indications has increased over the years. One can state that each child that needs nutritional support for a period of more than 6–8 weeks is a candidate for this procedure.

Currently there are two different approaches to percutaneous gastrostomy placement: the retrograde or 'push' technique, and the antegrade or 'pull' technique (Towbin and Ball 1988; Kaye et al. 2000a; Kaye and Towbin 2002). Both techniques have a high reported success rate (84%–100%) and a low rate of complications (major 0.5%–5% and minor 12%–16%). In the largest retrospective study to date by Dewald et al. (1999), of 701 adult cases only three (0.4%) experienced major complications (two cases of peritonitis and one case of external leakage requiring removal of the catheter) occurred. Friedman et al. (2004) presented data on 253 tubes (208 gastrostomy tubes, 41 gastrojejunostomy tubes and four gastrostomy and gastrojejunostomy tubes) in 208 children. In their study they found a major complication rate of 5% (including one death after peritonitis). Chait et al. (1996) reported on retrograde gastrostomies and gastrojejunostomies in 505 children. They found that in 1.2% access to the stomach could not be achieved, while in only two patients of their series did the gastrostomy tube require modification by surgical intervention. No procedure-related deaths were reported.

Occasionally the transverse colon or the splenic flexure can be interposed between the stomach and abdominal wall; usually inflation of the stomach will displace the colon caudally. However, if this does not occur safe access cannot be obtained. Wiebe et al. (2004) recently described a safe technique in which a 27- or 25-gauge needle can be used to deflate the colonic loop so as to obtain a safe entrance into the stomach.

Preprocedural preparation is relatively simple and consists of withholding the last feeding in children younger than 4 months and nil-by-mouth for older children. Antibiotics are not routinely administered; however, in children with a depressed immunological system or with a ventriculoperitoneal drain there is an indication for prophylactic antibiotics. In case of perforation during the procedure or free air after the procedure, antibiotics should always be administered.

As both procedures are safe to perform, the number of contraindications is relatively low. However, in children with a severe non-correctable coagulopathy, severe respiratory or cardiac problems a surgical approach would be more advisable. In some children their inherent anatomy, i.e. the absence of a good percutaneous route, or previous gastric surgery, will preclude a percutaneous approach. Dewald et al. (1999) reported this to occur in 4.4% of their patients. For the 'pull' technique the oesophagus should be sufficiently in diameter(> 12 mm) to pass the tube. If this is not the case, a push approach should be chosen.

7.4.1 Retrograde Gastrostomy 'Push'

The retrograde or 'push' technique is the most widely used technique for both the adult and paediatric populations. One should start by performing an upper abdominal ultrasound scan to assess and mark the position of the liver and transverse colon. The colon can be opacified using contrast medium to better delineate its position and thereby decreasing the risk of inadvertently puncturing it during the procedure.

A nasogastric tube is inserted and the stomach inflated. Thereafter it is punctured under fluoroscopic guidance and a T-fastener is inserted (Fig. 7.2). Some radiologists will place up to three T-fasteners in order to secure the gastric wall to the anterior abdominal wall. The advantage of using only one T-fastener is that the procedure can be done with a single puncture of the stomach.

Under fluoroscopic guidance the stomach is punctured and a guidewire is inserted. Using dilators the needle tract is dilated and a gastrostomy tube is placed within the stomach. The retention balloon is inflated and the gastrostomy tube is fixed to the abdominal wall using the supplied external stabilizer.

At the end of the procedure a cross table radiograph should be taken to rule out free intraperitoneal air. Post procedure the patient is kept nil-by-mouth and the tube is not used for at least 6 hours after the procedure. In practice this will mean that the first feeding over the gastrostomy tube will occur the morning after the procedure. Medication and fluid should be given intravenously during this period. Both the patient and his/hers parents should be carefully instructed on the use of the gastrostomy tube.

7.4.2 Antegrade Gastrostomy 'Pull'

The intervention starts with an ultrasound exam of the upper abdomen to assess and mark the position of the liver and transverse colon. Thereafter a naso-

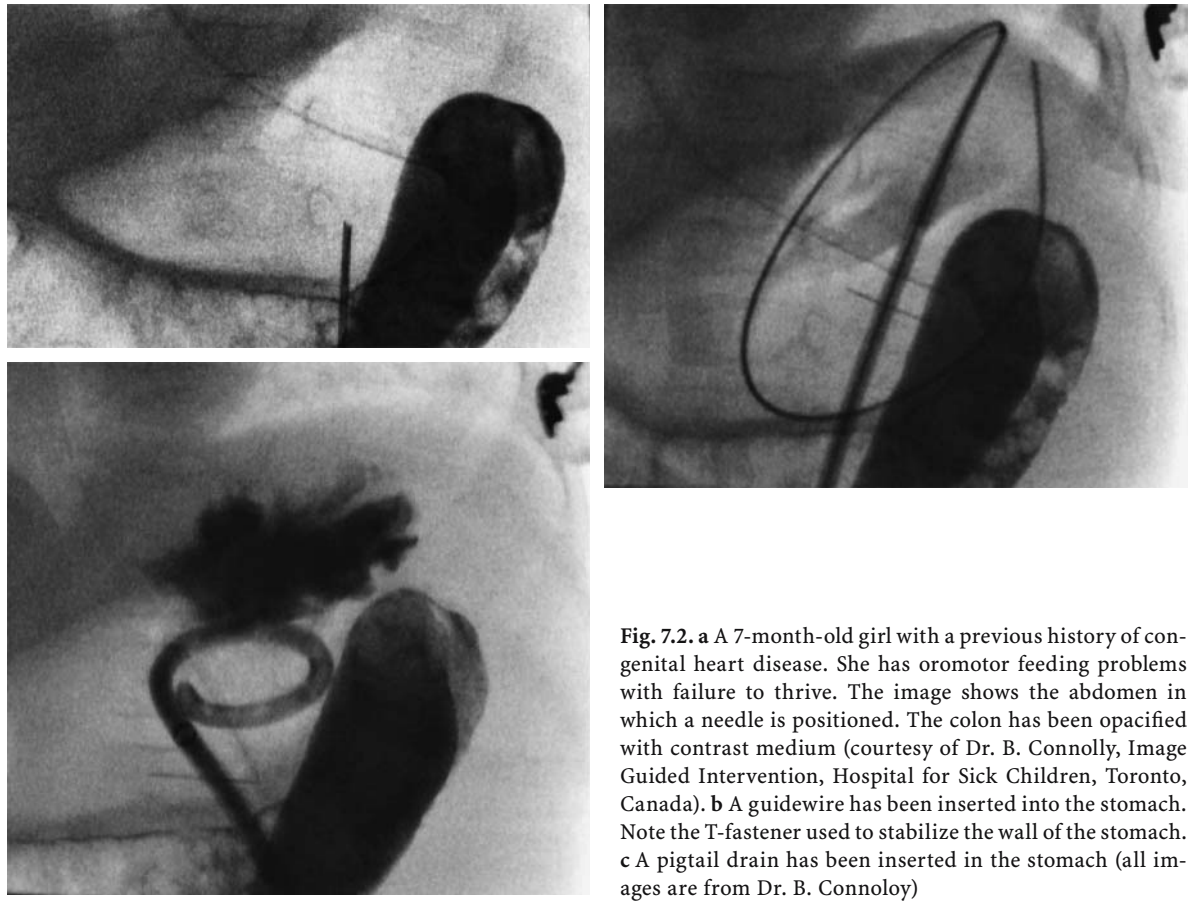

Fig. 7.2. a A 7-month-old girl with a previous history of congenital heart disease. She has oromotor feeding problems with failure to thrive. The image shows the abdomen in which a needle is positioned. The colon has been opacified with contrast medium (courtesy of Dr. B. Connolly, Image Guided Intervention, Hospital for Sick Children, Toronto, Canada). **b** A guidewire has been inserted into the stomach. Note the T-fastener used to stabilize the wall of the stomach. **c** A pigtail drain has been inserted in the stomach (all images are from Dr. B. Connoloy)

gastric and an orogastric feeding tube are inserted into the stomach. A snare is passed through the orogastric tube and positioned in the stomach. With the snare in place, the stomach is inflated, displacing the transverse colon inferiorly, and punctured with a needle. Through the needle a long guidewire (260 cm) is inserted into the stomach and, under fluoroscopic guidance, grasped by the snare (Fig. 7.3a,b) to be subsequently pulled up the oesophagus and out of the mouth. This now means that the guidewire runs through the mouth into the stomach and out via the puncture site. Over this guidewire a gastrostomy tube with a fixed terminal retention disk is fitted and fed until the tip of the dilator is visible at the puncture site (Fig. 7.3c). It is important to keep in mind that the collapsed retention disk has a diameter of approximately 12 mm. The calibre of the oesophagus should be large enough to capacitate its passage. The tip of the gastrostomy tube dilator is grasped and pulled through the anterior abdominal wall. Care should be taken not to cause damage to teeth at the time when the retention disk enters the mouth. The gastrostomy tube is fixed using the external stabilizer, which comes with the set. One should not place too much pressure on the abdominal wall when fixing the stabilizer, because pressure necrosis of gastric mucosa can occur. The post-procedural approach is identical to the 'push' technique.

The advantage of the 'pull' technique is the use of fixed retention disks allowing for a lower number of cases of gastrostomy tube dislodgement. Most authors state that when the time has arrived to remove the gastrostomy tube it suffices to cut the gastrostomy tube and push the retention disk into the stomach. This way it will leave the patient's body via the natural route. However, Kaye et al. (2000a) describe two complications of this approach and advocate the retrieval of the retention disk. The procedure entails passing a snare through the gastrostomy tube and a guidewire down the oesophagus, the guidewire is grasped under fluoroscopy and pulled out of the stomach via the gastrostomy tube. A dilatation (PTA) balloon, with a sufficient balloon diameter, is passed antegrade and inflated when it

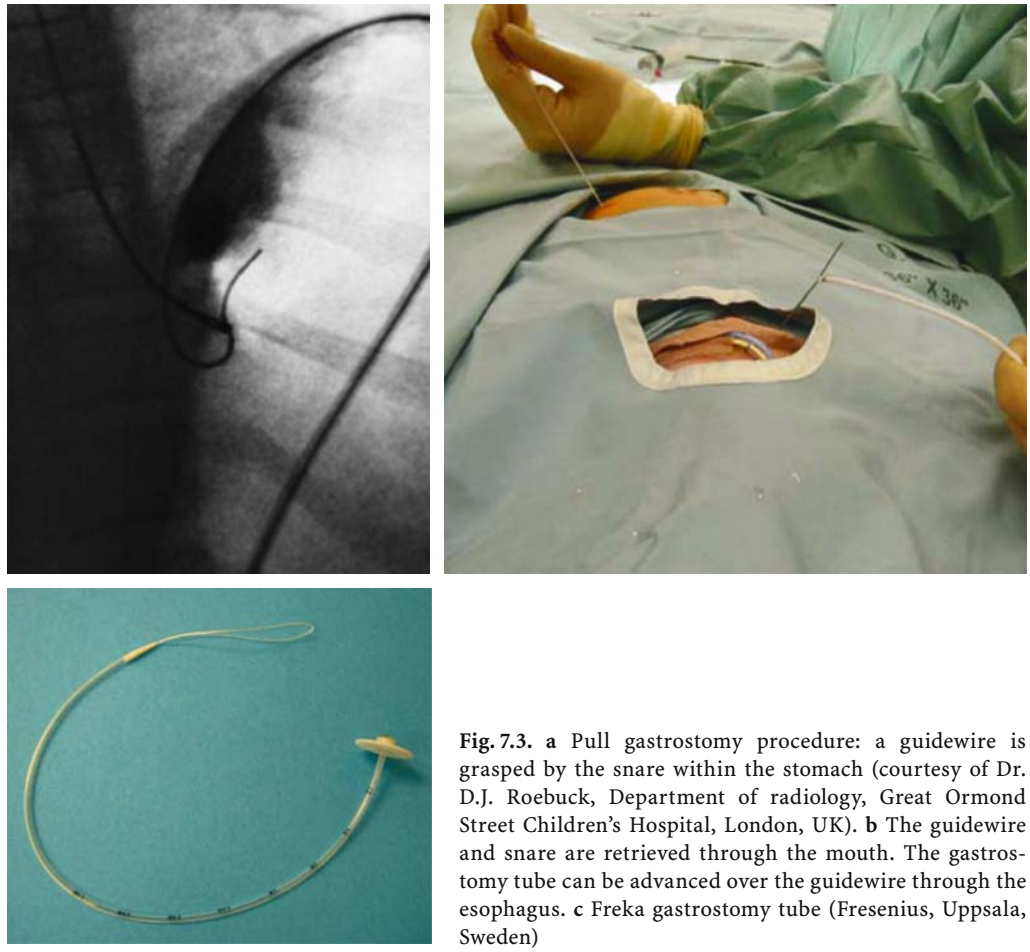

Fig. 7.3. **a** Pull gastrostomy procedure: a guidewire is grasped by the snare within the stomach (courtesy of Dr. D.J. Roebuck, Department of radiology, Great Ormond Street Children's Hospital, London, UK). **b** The guidewire and snare are retrieved through the mouth. The gastrostomy tube can be advanced over the guidewire through the esophagus. **c** Freka gastrostomy tube (Fresenius, Uppsala, Sweden)

has passed the gastrostomy tube. The PTA balloon and gastrostomy tube are pulled into the stomach, where the PTA balloon is inflated *further*, and both the PTA balloon and gastrostomy tube are retrieved via the mouth.

7.5 Gastrojejunostomy

The indications for placement of a gastrojejunostomy tube in children include severe gastro-oesophageal reflux or gastric emptying abnormalities. A gastrojejunostomy tube is placed coaxially via a gastrostomy tube. This can be done either in the same session as the gastrostomy placement or at a later moment in time. The procedure itself is relatively simple. A catheter is placed into the stomach and directed towards the pylorus. Using a guidewire the catheter is advanced beyond the ligament of Treitz after which the catheter is exchanged for a gastrojejunostomy tube (Kaye et al. 2000a; Norman 2001).

The gastrojejunostomy procedure knows virtually no serious complications, besides those related to the placement of the gastrostomy tube. Minor complications consist of leakage of feeding from the puncture site and dislodgement of the gastrojejunostomy tube. A rare complication has been described by Connolly et al. (1998) in five patients in whom small bowel intussusception was seen around the gastrojejunostomy tube. We experienced the same rare complication in the case of a surgically placed jejunostomy tube (Fig. 7.4). Reduction of these intussusceptions can be achieved by bolus injection of air or water-soluble contrast medium through the gastrojejunostomy tube or by exchanging the jejunostomy tube over a guidewire.

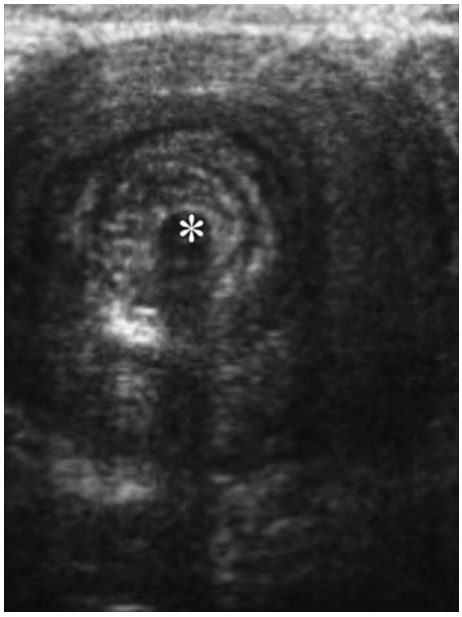

Fig. 7.4. A 7-year-old girl with HSAN type II. A jejunostomy was placed because of feeding problems. Despite her condition she complained of cramping abdominal pain. The ultrasound image shows an ileo-ileal intussusception around the jejunostomy tube (*asterisk*). The abdominal pain was relieved after changing the jejunostomy catheter

7.6 Cecostomy

In children faecal incontinence encompasses both encopresis and soiling (Di Lorenzo and Benninga 2004). Encopresis is defined as the repeated expulsion of a normal bowel movement, whether involuntary or intentional in inappropriate places by a child aged 4 years or over. Soiling is defined as the involuntary leakage of small amounts of stool resulting in staining of underwear. Faecal incontinence is a serious problem in the paediatric population. In the USA it is estimated that at least 3 million children are affected (Kaye and Towbin 2002). Children with faecal incontinence can be classified into four main groups: children with functional faecal retention and overflow soiling; children with functional non-retentive faecal soiling; children with anorectal malformations; and children with spinal deformities. The cecostomy technique described below is primarily aimed at the last two categories.

To date the most effective therapeutic method is the use of high volume enema, as this ensures complete evacuation of the colonic tract. This approach minimizes the risk of unwanted bowel evacuation, which is not only cumbersome but also humiliating for both patient as well as carers. The major disadvantage is the level of acceptance in patients, especially during puberty. In patients with paresis or paralysis of limbs it is impossible to perform the procedure without aid, lowering the level of compliance in this population.

In order to overcome the above mentioned problems, Malone et al. (1990) introduced an operation to perform an antegrade colonic enema (ACE). The advantage of ACE over retrograde colonic enemas is that the procedure is cleaner to perform and patients are more independent as they can more easily perform the procedure themselves (Malone et al. 1990). In this operation Malone et al. (1990) used the appendix as a conduit to irrigate the colon (see also Graf et al. 1998; Griffiths and Malone 1995; Squire et al. 1993). Although the procedure is effective, well tolerated and the level of acceptance in patients is high, complications have been described in a significant number of patients (Griffiths and Malone 1995; Squire et al. 1993; Ekmark and Adams 2000; Searles et al. 2000; Cascio et al. 2004). These complications consist of stoma prolapse, stenosis of the fistula, accidental perforation of the conduit and faecal soiling at the stoma site. In a retrospective literature study Graf et al. (1998) report a prevalence of 27% of necrosis/stenosis of the stoma, 6.6% catheter leak, 3.7% difficulty in catheterization, 3% pain with enema administration and 2.9% wound infection. Besides the surgical approach, endoscopic approaches to the ACE procedure have also been described (Rivera et al. 2001). Rivera et al. (2001) described their experience with percutaneous endoscopic cecostomy (PEC) in 13 patients. In one patient the PEC could not be placed after multiple attempts. In the 12 patients in whom the PEC could be placed one child died of underlying disease 9 months after the procedure. The remaining 11 patients have all improved after PEC placement.

In 1996, Shandling and Chait were the first to describe a percutaneous approach to cecostomy placement in 15 patients. In more recent publications, Kaye et al. (2000a), Kaye and Towbin (2002) and Chait et al. (2003) describe the percutaneous ACE procedure in detail. The patient is placed on a two-day pre-admission fluid diet and Fleet (CB Fleet CO. Inc., Lynchburg, Va., Canada) phospho-soda bowel regimen (45 ml on the night before admission

and a repeat dose on the day of the procedure). The bowel should be clear of stools. Within 30 minutes prior to the procedure a single dose of Cefotaxime 20 mg/kg is administered.

Ultrasound is used to identify the liver, right kidney and bladder, and possibly other masses. The procedure is quite similar to the 'push' gastrostomy technique. The colon is inflated and after confirmation of its location, the cecum is punctured and transfixed using T-fasteners (Fig. 7.5). A stiff guidewire is inserted into the ascending colon through the puncture needle. The puncture site can be dilated over the guidewire in order to capacitate the placement of an 8-F pigtail catheter. The position of the catheter is confirmed and secured in place.

After approximately 8 days antegrade enemas can commence. To prevent clogging of the pigtail, a daily flush with 10–15 ml of saline is performed.

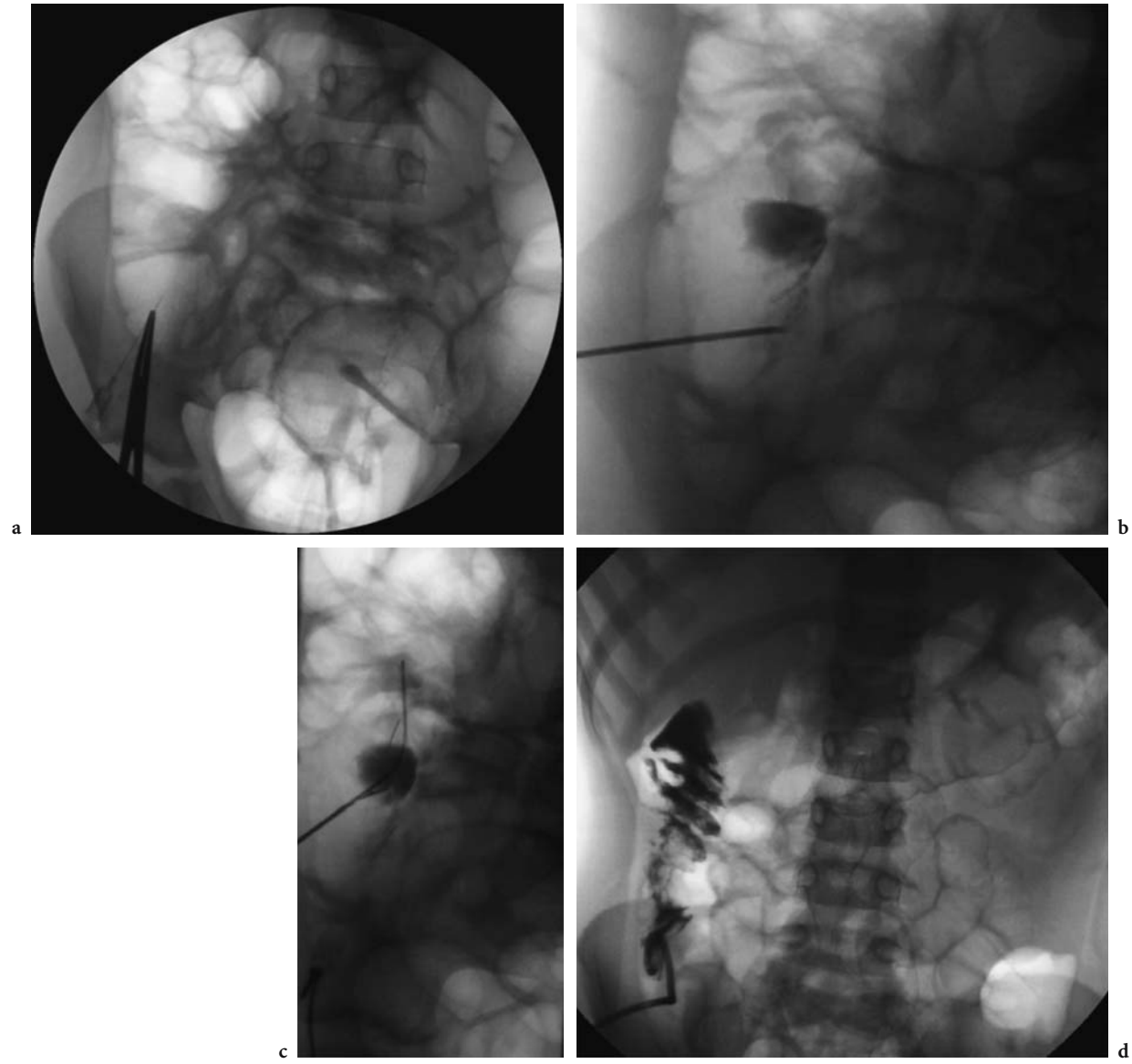

Fig. 7.5. a A 5-and-a-half-year-old boy with bifid spine and faecal incontinence. The image shows an overview of the abdomen with the cecum outlined in the right lower abdomen (courtesy of Dr. P.G. Chait, Image Guided Intervention, Hospital for Sick Children, Toronto, Canada). **b** The caecum has been punctured and the intraluminal position of the needle is confirmed using contrast medium. **c** A guidewire is inserted into the caecum along with two T-fasteners. **d** An 8.5-F pigtail catheter is placed within the lumen of the caecum. All images are from Dr. P.G. Chait

After 6–12 weeks the pigtail can be exchanged for a cecostomy button.

In 1997 Chait et al. (1997a) presented an improved cecostomy button that protrudes no more than 1 cm from the abdominal wall, which constitutes an enormous cosmetic improvement as the button or trapdoor can easily be hidden under garments (Fig. 7.6).

As in all procedures complications have been described. In one of the largest studies thus far, Chait et al. (1997b) report one case of local cellulites and one case of transient ileus. Minor complications consist of nausea, constipation, granulation of the puncture site, soiling and accidental dislodgement of the cecostomy tube. Chait et al. (2003) reported results of their 7-year experience with this technique, achieving a 100% success rate for the procedure. The majority of patients (79%) reported that the number of soiling accidents had decreased and, additionally, their independence had increased by being able to perform the antegrade enema themselves. In four cases the cecostomy tube had to be removed twice due to problems with tube maintenance and twice because of aesthetic reasons. The most impressive result in their study was that 97% of respondents stated that they would recommend the procedure to others in the same position (Chait et al. 2003). Another study, on surgical ACE procedures, also reported a high patient satisfaction, with 84% completely continent or soiling less than once a month (Dey et al. 2003).

The advantage of the percutaneous ACE procedure over the surgical approach is the fact that it can be performed without general anaesthesia (Kaye and Towbin 2002; Chait et al. 1997, 2003). An additional advantage is that in case of a surgical ACE procedure the appendix is used, thus precluding its use in urinary incontinence, which these patients also frequently face. A surgical approach using a cecal flap, thus sparing the appendix, is currently also in use (Squire et al. 1993; Ahn et al. 2004).

Fig. 7.6. The low-profile Chait Trapdoor (Chait, Cook, Bloomington, IN) catheter has a pigtail configuration for internal retention (courtesy of Dr. P. Chait, Hospital for Sick Children, Toronto, Canada)

7.7 Drainage

7.7.1 Abscesses

Percutaneous abscess drainage is a relatively straight forward technique with a wide field of indications, the most common being peri-appendiceal abscesses and Crohn's abscesses (Norman 2001; Hubbard and Fellows 1993; Safrit et al. 1987). The aim of the procedure is either to gain time in order to reduce surgery related morbidity and to be able to perform a one-stage operation or to obtain complete cure. The latter has been described in patients with Crohn's disease, making surgery at the time unnecessary (Safrit et al. 1987). The only contraindications for percutaneous drainage are uncorrectable coagulopathy and the inability to approach the collection without transgressing major vessels, bowel loops, solid organs or the pleural cavity (Lang et al. 1986). Studies performed in adult patients show a high success rate of up to 90% and low mortality rates (Lang et al. 1986).

Depending on the location of the abscess the intervention can be performed using ultrasound, sometimes in combination with fluoroscopy or CT guidance. Ultrasound will be used for larger and superficial abscesses whereas CT will be used for smaller and more deeply located collections (Maher et al. 2004). In case of multiple abscesses or loculated abscesses, more than one drain should be placed ensuring complete drainage of all locations. In case of deep pelvic abscesses or a perirectal abscess, a transrectal approach can be chosen (Fig. 7.9), performing abdominal ultrasonography to visualize the abscess. Under ultrasound guidance a finger is placed within the rectum up to the level of the abscess. A trocar is guided upwards along this finger and the abscess is punctured. With the trocar in place, a guidewire and subsequently a pigtail can

be inserted into the abscess. In children this procedure has been reported to be as effective as a percutaneous or a surgical approach and better tolerated (Pereira et al. 1996).

Although some radiologists will use the trocar technique, which encompasses placing a catheter mounted on a sharp trocar into the abscess, a safer and more elegant way is the use of the Seldinger technique (Norman 2001). The Seldinger technique entails puncturing the skin with a thin (22- to 20-G) or thick (18- to 19-G) needle and placing the tip of the needle within the collection. When a thin needle is used one will need to upgrade to a system capable of accepting a 0.038-in. guidewire. Commercial kits are available for this purpose, one of which is the Neff-set (Cook, Bloomington, IN) (Fig. 7.7). Once the needle is in place, a stiff guidewire is placed within the collection and a catheter is advanced into the collection. Smaller calibre catheters (7–8.5 F)will only be used in liquefied collections, whereas thicker, more viscous collections will require a 12- to 14-F catheter. In general, self-retaining pigtail catheters (Cook, Bloomington, IN) will be used, as they have a lower risk of inadvertent dislocation (Fig. 7.8). We also always secure the drain to the skin, either by using a suture or by the supplied retention device. Decompression of the abscess is generally attained using a syringe attached to the catheter. Some radiologists advocate flushing the abscess cavity with saline. However, care should be taken to use less fluid than was drained, as an increased pressure within the cavity can result in bacteraemia and sepsis (Gervais et al. 2004). Towbin et al. (1991) report the use of contrast medium to identify catheter position and possible connections between the abscess and surrounding structures.

The drain is attached to a bag and left to drain by gravity. Ward nurses are supplied with written instructions from the radiologist responsible for the intervention on how to care for the catheter. The drain is removed once the patient's symptoms have resolved and no drain production is noted. In the case of a complex abscess a control study, CT (or in

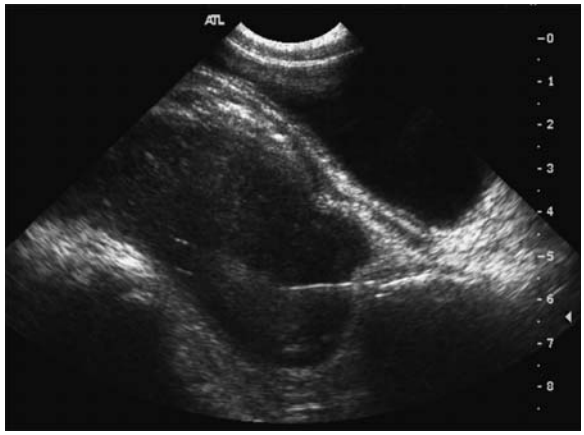

Fig. 7.9. An 8-year-old boy with a perirectal appendiceal abscess. The image shows the needle positioned, using ultrasound guidance, through the posterior rectal wall within the abscess (courtesy of Dr. L. Fontalva, Hospital for Sick Children, Toronto, Canada)

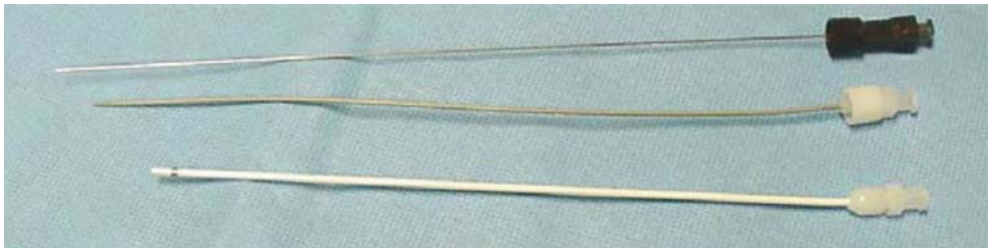

Fig. 7.7. Neff set (Cook, Bloomington, IN)

Fig. 7.8. Pigtail catheters (Cook, Bloomington, IN)

superficial collections, ultrasound) should be performed prior to removal of the drain. In a study by Lang et al. (1986) in 12 out of 136 patients (8.8%), premature withdrawal of the catheter resulted in failure of the intervention.

7.7.2 Biliary System

The need for biliary drainage in children is less frequent than in adults; however, there are a number of indications for performing a percutaneous transhepatic cholangiogram (PTC) (Diament et al. 1985). The most common indications for PTC is obstructive jaundice resulting from either a malignancy, most commonly rhabdomyosarcoma of the bile ducts or pancreas and neuroblastoma, or post liver transplantation. Cholithiasis is less frequently a causative agent (Lorenz et al. 2001; Roebuck and Stanley 2000; Rose et al. 2001). Cholangitis, which is a relatively common indication for PTC in adults, is rarely seen in children.

As in all percutaneous procedures, an uncorrectable coagulopathy is a definite contraindication for PTC. In children the procedure should be performed under general anaesthesia. Access to the biliary tree is gained by needle puncture; this can be done using fluoroscopy guidance, ultrasonography or a combination of both. We routinely use ultrasonography to access the biliary tree after which a small amount of contrast is injected to confirm appropriate placement of a 22-gauge needle. This stage of the procedure is usually performed using a Neff set (Cook, Bloomington, IN), thus reducing the risk of bile spill into the abdominal cavity. Using a guidewire the sheath is exchanged for a 6- or 8-F catheter. At this stage in the procedure one can either choose external biliary drainage or internal-external biliary drainage (Fig. 7.10) (Roebuck and Stanley 2000). In the latter a modified pigtail catheter is used: the modification consists of the presence of additional holes in the catheter along the intrahepatic tract of the catheter. The decision to perform external biliary drainage or internal-external biliary drainage is dependent on the findings of the cholangiogram. If passage into the duodenum is deemed possible, one should choose internal-external biliary drainage. If it is not possible in the first procedure it may be possible to convert external biliary drainage into internal-external biliary drainage at a later stage.

The advantage of internal-external biliary drainage over external biliary drainage is first of all that it re-establishes the flow of bile into the duodenum,

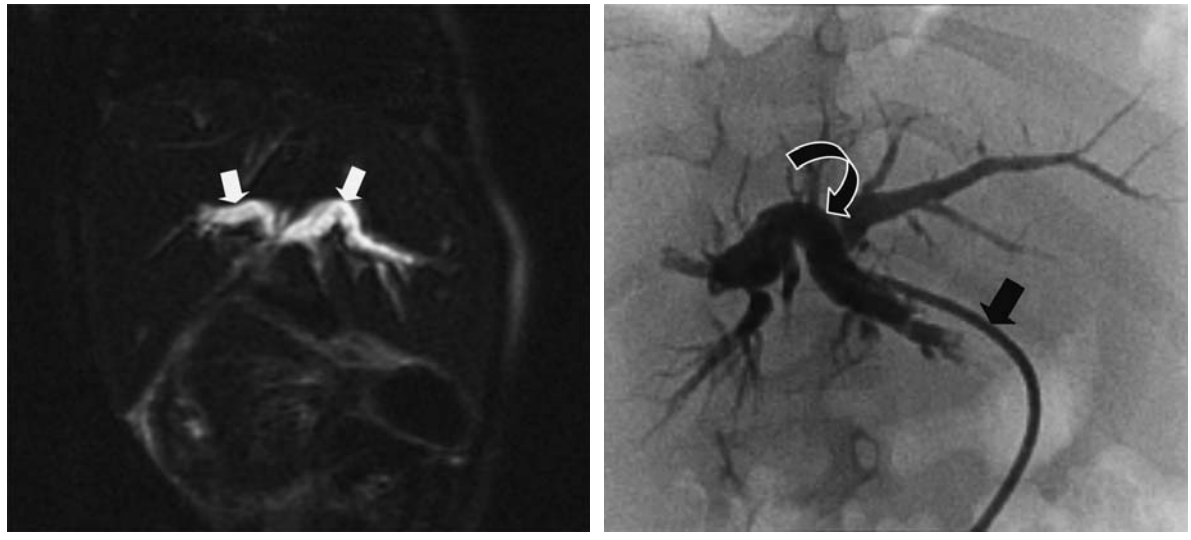

a b

Fig. 7.10. a A 4-year-old boy with jaundice. The medical history of the boy revealed a neuroblastoma for which ^{131}I-MIBG therapy was given. Magnetic resonance cholangiopancreatography (MRCP) coronal thin slice (TR 1837 ms, TE 249.2 ms, slice thickness 3 mm, flip angle 90°) shows clear dilatation of the intrahepatic bile ducts (*arrows*) and no visualization of the common bile duct. **b** Percutaneous transhepatic cholangiography in the same patient. Access route was via the left liver lobe, with dilatation of the left intrahepatic bile ducts (*curved arrow*). There is no passage of contrast to the right side of the gall tree or the duodenum. An 8.5-F pigtail drain (*arrow*) was placed and satisfactory extra biliary drainage was obtained. A second stage elective hepatico-jejunostomy was successfully performed several weeks later

thus enhancing the absorption of dietary fats. An additional advantage is that positioning of the catheter into the duodenum increases catheter stability, which of course is advantageous in smaller children.

PTC is not only used for catheter drainage but it also allows for dilatation of strictures of the biliary tree, which in children is mostly in cases of biliary-enteric anastomoses (Sze and Esquivel 2002). The advantage of balloon dilatation of strictures is the relatively minimal invasive approach and that, if dilatation fails, surgical options remain viable. Lorenz et al. (2005) reported their experience in 19 children over a 7-year period. In their study, 58% of patients showed a patent biliary-enteric anastomosis after 1 year (continued patency ranged from 1.4 to 5.4 years, mean patency 3.6 years).

Complications of PTC can be mild, such as haemobilia, pancreatitis, and bacteraemia, or severe, such as haemoperitoneum and sepsis (Lorenz et al. 2001). However, there is insufficient data to calculate the risk of the procedure in children.

If it is difficult to identify the bile duct, as can be the case in very young children, an alternative approach is to drain the biliary system via the gallbladder. This can of course only be done in cases of a distal obstruction (Fig. 7.11).

Another approach to the treatment of biliary obstructive jaundice is the use of endoscopic antegrade cholangiography (ERC). The main advantage of PTC over ERC is that it is a percutaneous technique that allows for easier access to the catheter in case of obstruction or infection. Secondly, PTC will be successful in cases of complete obstruction of the common bile duct because then external biliary drainage can be performed. Finally, ERC has a higher number of complications, such as pancreatitis and perforation, especially when the operator does not do the procedure on a regular basis. This is even more the case in children where special scopes are needed to perform a successful ERC. This procedure will therefore only be performed in specialized centres. The advantage of ERC over PTC lies mainly

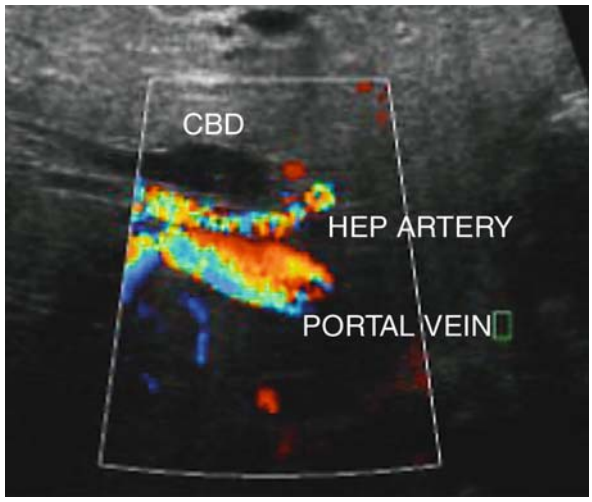

a

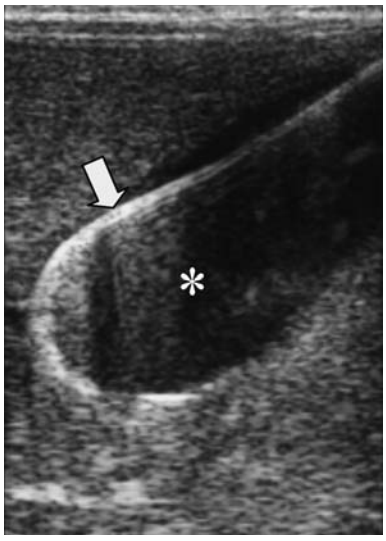

b

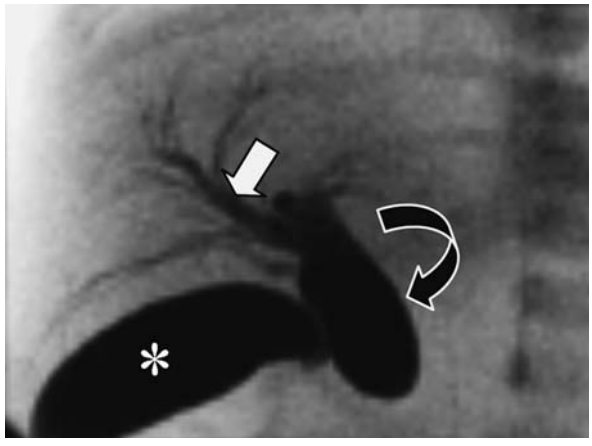

c

Fig. 7.11. a A 3-week-old boy with a history of urethral valves and obstructive ureters (diagnosed on prenatal ultrasound). Post-urological intervention (placement of bilateral sober stomata) the baby developed progressive jaundice. The ultrasound exam reveals dilation of the intrahepatic bile ducts and the common bile duct (CBD), which could be visualized into the pancreatic head. The gallbladder was also dilated. **b** Biliary drainage via the dilated bile duct. The oblique-coronal image shows an Amplatz guidewire (*arrow*) placed within the gallbladder (*asterisk*). **c** Post-intervention fluoroscopy image shows the dilated intrahepatic bile ducts (*arrow*), gallbladder (*asterisk*) and the dilated common bile duct (*curved arrow*). The latter is blind ended at the level of the pancreatic head. At surgery a choledochal cyst was found

in treating cholelithiasis induced jaundice, as stone removal using a dormia basket and sphincterotomy can be performed (Guelrud et al. 1992).

7.8 Transjugular Intrahepatic Portosystemic Shunt (TIPS)

Portal hypertension is a relatively rare disorder in childhood compared to adults, where the majority of cases are caused by alcohol abuse (in western parts of the world), and viral hepatitis and cirrhosis (in Africa and Asia). In children the cause of portal hypertension lies in extra-hepatic biliary atresia, portal vein thrombosis, hepatitis and toxic liver injury (Cwikiel 2002; Cwikiel et al. 2003; Huppert et al. 1998). Clinical manifestations of portal hypertension consist of ascites production and the development of oesophageal varices. Oesophageal varices have a tendency to bleed and this can cause a life-threatening situation. The first line of treatment is repeated paracentesis for the reduction of ascites and endoscopic sclerotherapy or rubber banding for oesophageal variceal haemorrhage. In case of repeated haemorrhage from oesophageal varices, shunting of blood away from the portal system thereby reducing the pressure in the collateral vessels, is necessary. Initially portosystemic shunts consisted of surgical spleno-renal, porto-caval or meso-caval shunts. These surgical procedures however, carry a high morbidity and mortality rate. As far back as 1969, Rösch et al. suggested creating an intrahepatic shunt. However, it was not until the development of endovascular stents that this gained momentum (Rösch et al. 1969). In 1994, The United States National Digestive Diseases Advisory Board established the following clinical indications for Tips: first, acute variceal bleeding that cannot be successfully controlled with medical treatment, including sclerotherapy. Second, recurrent and refractory variceal bleeding or recurrent variceal bleeding in patients who cannot tolerate conventional medical treatment, including sclerotherapy and pharmacologic therapy (Shiffman et al. 1995). There are also some indications for which there is no scientific proof of the effectiveness of TIPS. These consist of medically refractory ascites, refractory hepatic hydrothorax, Budd-Chiari syndrome, veno-occlusive disease, hepatorenal syndrome and hypersplenism (Heyman et al. 1997). To date there is no indication that TIPS is useful in preventing variceal haemorrhage in patients who are awaiting liver transplantation. Its use for initial prevention of variceal haemorrhage is also discouraged.

There are several contraindications for TIPS: absolute contraindications consist of right-sided heart failure with elevated central venous pressure, polycystic liver disease, and severe hepatic failure (Shiffman et al. 1995). The latter contraindication is based on the fact that the TIPS shunts blood away from the liver, thus further compromising liver function. Relative contraindications consist of active or systemic infection, as TIPS makes use of a foreign device that could act as a colonization site for bacteria, severe hepatic encephalopathy poorly controlled by medical therapy and portal vein thrombosis.

Due to the nature of the procedure TIPS will always be performed under general anaesthesia. The right jugular vein is punctured and a sheath is inserted. A catheter and a guidewire are advanced into the inferior caval vein and from there into preferably the middle or else the left hepatic vein. A special TIPS stainless steel angled catheter is exchanged over the guidewire and positioned in the middle or left hepatic vein. Under ultrasonic guidance or a wedged venogram an intrahepatic portal vein is punctured transhepatically using a special needle. Performing TIPS requires a thorough knowledge of the venous hepatic anatomy and its variations. After confirmation of intrahepatic portal venous position by use of contrast medium, a needle catheter is passed into the portal vein. When intrahepatic portal vein location is proven, the parenchymal tract is dilated and lined with a stent (Fig. 7.12). A TIPS is considered to be successful if the pressure gradient is less than 15 mm Hg. Care should be taken in placing the stent. It should not protrude into the inferior caval vein, since most children will at some point in time require a liver transplant. A stent placed into the inferior caval vein can complicate transplantation surgery.

TIPS has been shown to be a safe and effective treatment for portal hypertension and compared to endoscopic sclerotherapy it has proven to be a more effective and safer technique (Garcia-Villarreal et al. 1999). In primary cases endoscopic band ligation has shown to be as effective as TIPS in a randomized control study (Pomier-Layrargues et al. 2001). In a long term follow up study in adult TIPS patients, rates of rebleed from oesophageal vari-

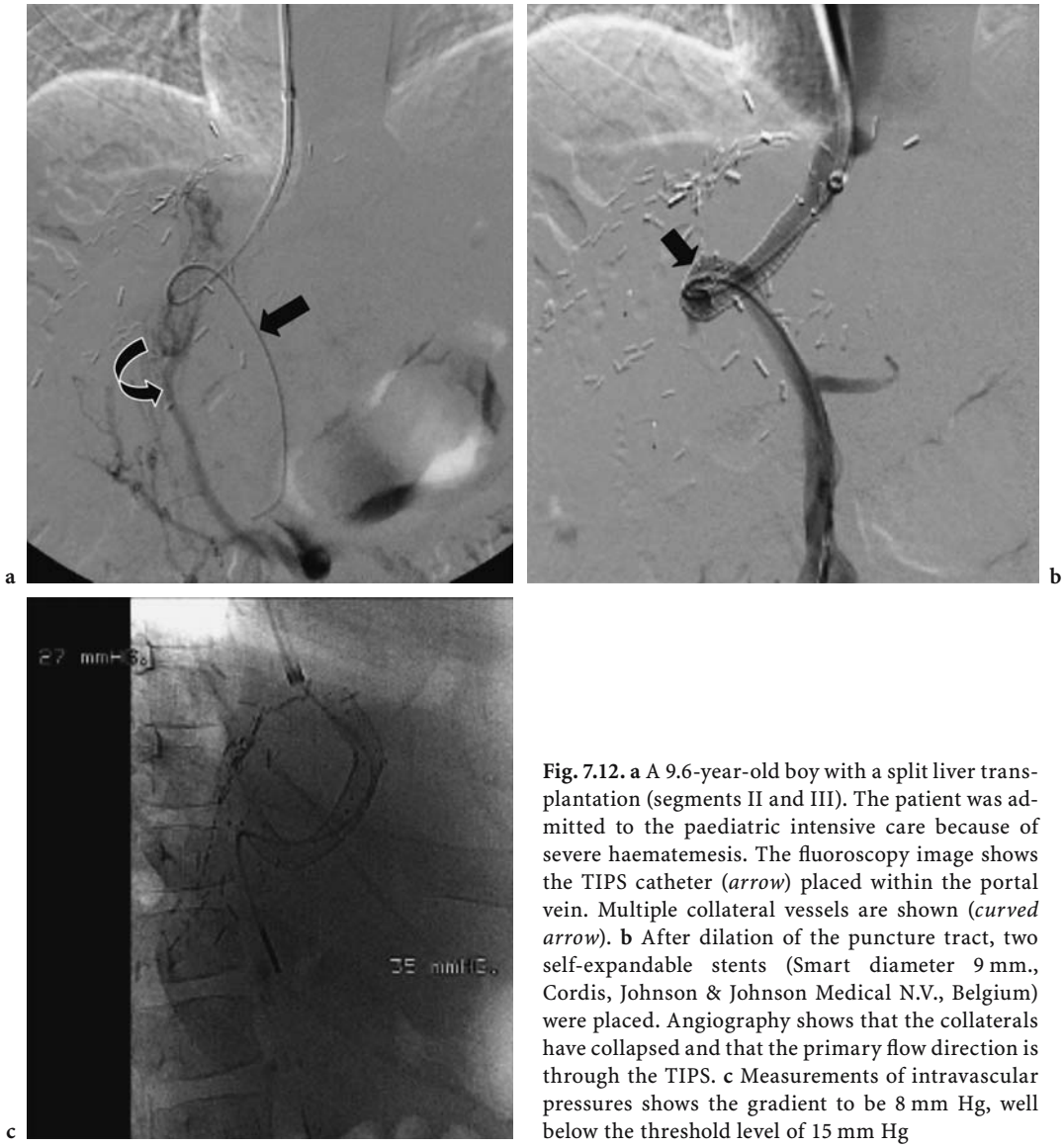

Fig. 7.12. a A 9.6-year-old boy with a split liver transplantation (segments II and III). The patient was admitted to the paediatric intensive care because of severe haematemesis. The fluoroscopy image shows the TIPS catheter (*arrow*) placed within the portal vein. Multiple collateral vessels are shown (*curved arrow*). **b** After dilation of the puncture tract, two self-expandable stents (Smart diameter 9 mm., Cordis, Johnson & Johnson Medical N.V., Belgium) were placed. Angiography shows that the collaterals have collapsed and that the primary flow direction is through the TIPS. **c** Measurements of intravascular pressures shows the gradient to be 8 mm Hg, well below the threshold level of 15 mm Hg

ces after 1, 2 and 5 years were 21%, 21% and 27%, respectively (ter Borg et al. 2004).

A major concern of TIPS has been the development of encephalopathy. In a study by Pomier-Layrargues et al. (2001), 47% of the TIPS patients developed encephalopathy versus 44% in the endoscopic band ligation population; however, this difference was not significant. Of note is that encephalopathy does occur less frequent in children than in adults, although there is no clear reason for this observed difference in risk (Heyman and LaBerge 1999).

As with all interventional procedures, TIPS has its complications. The main complication is procedure-related mortality, which has been reported to be 2% (Freedman et al. 1993). The 30-day mortality of emergency surgical shunts ranges from 40%–100% compared to 7%–45% for TIPS (Heyman et al. 1997). In TIPS the majority of cases of mortality and morbidity are related to severity of disease, with death occurring in those with the worst Child-Pugh classification. Complications related to the TIPS itself are shunt occlusion and stenosis. Intimal hyperplasia is the most common cause of stenosis and subsequent occlusion, although the use of covered stents should largely overcome this problem. In case of stenosis, restenting or balloon dilatation will, for the majority, successfully solve the problem (Heyman et al. 1997).

In adults the initial technical success rate of TIPS is reported to be over 95%. A Dutch study on long term outcome of TIPS in adult patients showed that the risk of definitive loss of shunt function was 17% at 5 years follow up (ter Borg et al. 2004). Heyman et al. (1999) presented literature data on 40 paediatric TIPS procedures. In this overview, six (6.6%) complications were found, and although patency was not assessed, the longest follow-up was over 800 days.

7.9 Biopsy

The use and effectiveness of image guided percutaneous biopsy, either by fine needle aspiration (FNA) or core needle biopsy (CNB), has been well documented in adult radiology. In children there seems to be some reluctance amongst clinicians and pathologists to use this technique and therefore surgical excision biopsies are frequently obtained. The obvious advantage of percutaneous over surgical excision biopsies is that it can be done under local anaesthesia and mild sedation, although in some cases deep sedation will still be necessary. In the adult population percutaneous biopsies of soft tissue masses have almost completely replaced surgical excision biopsies. Indications for performing a biopsy are obtaining pathologic information on a mass which can modify patient treatment, confirmation of metastases or in case of diagnosis of hepatic disease (Norman 2001; Hoffer 1997).

The advantage of CNB over FNA is the fact that a larger specimen is obtained which makes it possible to perform histological studies, showing not only the absence or presence of malignant cells but also the architectural composition of the mass (Cheung et al. 2000). Therefore, whenever possible, CNB should be the biopsy method of choice (Fig. 7.13). The relative drawback of CNB over FNA is that it is somewhat more invasive. An advantage of FNA is that the procedure is relatively easy to perform and that the material can be screened on-site. In our clinic we always have a pathologist in the room for immediate assessment of the quality of the aspirated material. The choice for FNA depends largely on the availability of an experienced cytologist and the type of lesion to be biopsied. In particular, more deeply located lesions, such as pancreatic lesions, will be more approachable for FNA than CNB, for example using a transgastric approach.

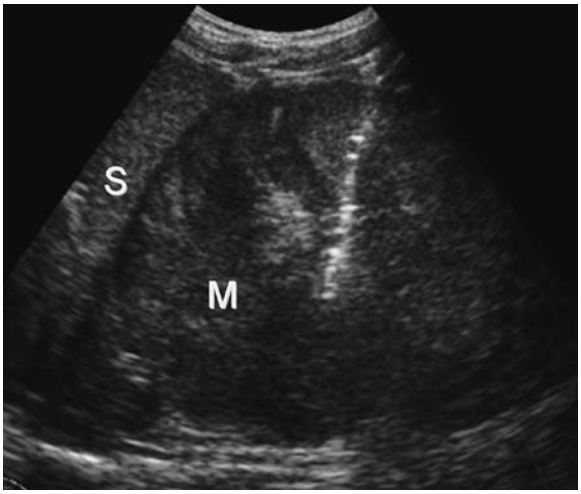

Fig. 7.13. A 1-year-old boy with a solid tumour arising from the adrenal gland. Biopsy was performed to confirm the diagnosis of neuroblastoma and to obtain specimen for genetic marker studies. The biopsy was done using freehand technique, the arrow delineates the biopsy needle. *S*, spleen; *M*, mass

For CNB one can choose for either a cutting-edge or so called 'tru-cut' needle with or without an automated biopsy device. Numerous variants of both devices are on the market, with personal experience usually guiding the choice for a specific device. The same applies for the use of a biopsy adaptor attached to the head of the ultrasound probe, which guides the needle, or the use of freehand technique. When the biopsy adaptor is used the needle follows the path that is overlain over the ultrasound image by special biopsy software, thus allowing for a highly accurate biopsy. A much-used technique is working coaxially. A needle is advanced into or near to the lesion, the biopsy needle is inserted and biopsies are taken. Using this technique multiple passes are easily possible with a low risk of spill and thus avoiding potential complications of the procedure. A second advantage is that due to the coaxial needle configuration haemostatic material can be deposited into the needle tract. This has been reported to be a very effective technique for reducing the risk of CNB-induced haemorrhage, especially in liver lesions (Kaye and Towbin 2002; Hoffer 2000).

Several studies into the effectiveness of FNA and CNB in children have been published (Cheung et al. 2000; Hoffer 2000; Guo et al. 2002; Lieberman et al. 2003; Muraca et al. 2001; Nobili et al. 2003; Saarinen et al. 1991; Scheimann et al. 2000;

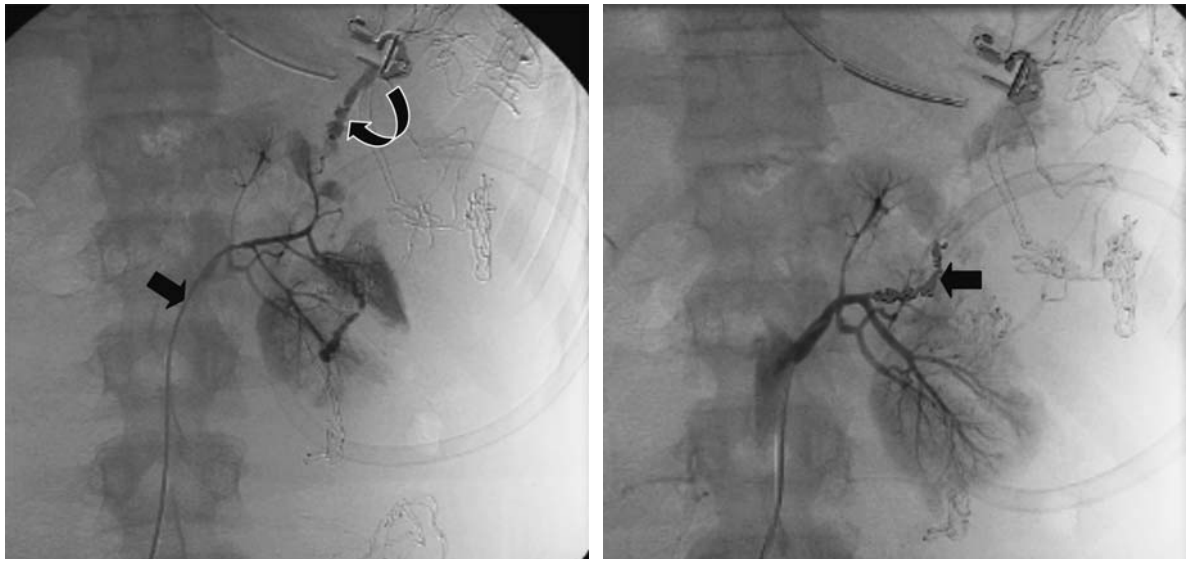

Fig. 7.14. a A 17-year-old boy who was involved in a motor vehicle accident. At presentation at the emergency department, ultrasound imaging showed free fluid surrounding the left kidney. Computed tomography revealed a left renal laceration. The ensuing selective renal angiography (*arrow* denotes the angiography catheter) clearly demonstrates contrast extravasation (*curved arrow*). **b** After embolization with multiple coils no contrast extravasation was seen thus preserving renal function

Sklair-Levy et al. 2001; Yu et al. 2001; Roebuck 2004). The diagnostic yield ranged from 83% to 100%. The rate of complications depends largely on the biopsy site, with the highest number of complications found in hepatic biopsies (up to 14% post-procedural haemorrhage).

Although one would expect a significant difference in complication rates of blind versus image guided biopsies, relatively few studies have been performed to demonstrate this. Nobili et al. (2003) reported a retrospective analysis on 140 biopsies (64 blind versus 76 ultrasound guided), in which 95% of the blind biopsies and 100% of the ultrasound guided biopsies were of diagnostic quality. Moreover, in the blind biopsy population three patients developed significant haemorrhage versus none in the ultrasound guided population.

A special approach to biopsies is that for liver biopsy in children with a coagulopathy or a significant amount of ascites. If in this category of patients a liver biopsy is needed, a transjugular approach should be used. The right jugular vein is punctured under ultrasound guidance. Using guidewires and catheters the middle or right hepatic vein is catheterised. Subsequently a stainless steel trocar is placed over the guidewire. Up to this stage the procedure is in effect identical to TIPS. Using a spring-loaded transjugular biopsy needle biopsies of hepatic tissue can be obtained. Drawbacks of the transjugular approach are the use of a more invasive technique, higher costs and smaller (18 gauge) histological samples (Kaye and Towbin 2002; Kaye et al. 2000b). In a large retrospective study in adults by Smith et al. (2003) tissue diagnosis was possible in 98% of cases using a 18 gauge biopsy needle (Quick-Core, Cook, Bloomington, IN) (Smith et al. 2003). There was an overall 2.4% complication rate; one patient died as a result of haemorrhage; however, in this case the family's request to withhold invasive treatment was honoured.

7.10 Abdominal Trauma

Interventional radiology has evolved into a 24/7 service and as such it has acquired a role in the field of emergency medicine. Classically, angiography in the trauma setting was used to identify the site of haemorrhage in order to direct subsequent surgical approach. However, due to rapidly progressing technical innovations transcatheter therapeutic options have become available (Kushimoto et al. 2003; Towbin 1989).

Patients involved in motor vehicle accidents, for example, are likely to have severe intra-abdominal pathology with consequent haemorrhage. These patients can become caught up in the cycle of coagulopathy, acidosis and hypothermia (Kushimoto et al. 2003). The first priority in these patients is to control haemorrhage, for which transcatheter arterial embolization (TAE) has been shown to be rapid and highly effective (Christensen 2001; Kushimoto et al. 2003). In abdominal trauma four sites, the pelvis, liver, spleen and kidneys, are of main importance in controlling haemorrhage.

Pelvic injuries accompanied by haemorrhage are associated with high mortality rates. Unfortunately, surgical exploration is hindered by the often-associated haematoma and the surgical procedure itself can release the tamponade effect of the haematoma leading to a subsequent increase in haemorrhage. TAE results in control in 90% of cases of pelvic haemorrhage in trauma patients.

Due to the dual blood supply to the liver, patients with blunt hepatic injuries (BHI) are ideal candidates for TAE, with success percentages of TAE reported to be as high as 98%. Complication rates of hepatic TAE are low, although one must keep in mind that necrosis can occur if portal venous supply is also disrupted due to trauma. In a retrospective study of 21 paediatric trauma patients with BHI, 18 patients could be managed conservatively, two of whom successfully underwent TAE in order to stop haemorrhage (Ohtsuka et al. 2003).

In splenic trauma, with a life-long increased risk of sepsis after splenectomy, non-operative treatment is the management of choice. In several studies the efficacy of TAE has been shown to be over 90% (Hagiwara et al. 1996). Embolization of the splenic artery, distal to the pancreatic artery, leads to splenic preservation resulting from collaterization by pancreatic and gastric branches.

The majority of renal injuries are a result of blunt abdominal trauma. In severe blunt renal injury controversy exists on treatment, with some advocating surgical exploration, accompanied with a significant increase in nephrectomy rates, whereas others advocate conservative treatment. Selective TAE has a high success rate without significant complications; post-procedural hypertension can occur but is generally temporary in nature.

TAE is achieved by using co-axial micro-catheters in order to be able to achieve selective embolization. Most radiologists will use either coils (permanent) or gelfoam (temporary) to embolize vessels. The advantage of coils is their relative ease of use and the capacity to be placed accurately. Gelfoam has only a temporary effect, lasting up to 3 weeks, and can be used in cases where haemostasis will normalize within this time frame. Other embolization materials, such as poly-vinyl-alcohol particles and bovine collagen are not normally used for this specific indication.

7.11 Conclusion

The aim of this review was to highlight the increasing importance of image guided interventions in children. The ever increasing capabilities of interventional radiology combined with the increasing awareness amongst paediatricians and paediatric surgeons will lead to an increase in the number and level of image guided interventions in the future. In addition, we strove to convey clearly that only close cooperation between attending paediatrician, paediatric surgeon, paediatric radiologist, interventional radiologist and, whenever necessary, paediatric anaesthesiologist is mandatory for a successful image guided intervention program.

References

Ahn SM, Han SW, Choi SH (2004) The results of antegrade continence enema using a retubularized sigmoidostomy. Ped Surg Int 20:488–491

American College of Radiology (2004) ACR guideline for pediatric sedation/analgesia. http://www acr org/, January 1; accessed on 11-5-2007

American Society of Anesthesiologists Task Force on sedation and analgesia by non-anesthesiologists (1996) Practice guidelines for sedation and analgesia by non-anesthesiologists. Anesthesiology 89:459–471

Beebe DS, Tran P, Bragg M, Stillman A, Truwitt C, Belani KG (2000) Trained nurses can provide safe and effective sedation for MRI in pediatric patients. Can J Anaesth 47:205–210

Cascio S, Flett ME, De la Hunt M, Barrett AM, Jaffray B (2004) MACE or caecostomy button for idiopathic constipation in children: a comparison of complications and outcomes. Ped Surg Int 20:484–487

Chait PG, Weinberg J, Connolly B, Pencharez P, Richards H, Clift JE et al (1996) Retrograde percutaneous gastrostomy and gastrojejunostomy in 505 children: a four-and-a-half year experience. Radiology 201:691–695

Chait PG, Shandling B, Richards HF (1997a) The cecostomy button. J Pediatr Surg 32:849–851
Chait PG, Shandling B, Richards HM, Connolly BL (1997b) Fecal incontinence in children: treatment with percutaneous cecostomy tube placement – a prospective study. Radiology 203:621–624
Chait PG, Shlomovitz E, Connolly BL, Temple MJ, Restrepo R, Amaral JG et al (2003) Percutaneous cecostomy: updates in technique and patient care. Radiology 227:246–250
Cheung YC, Wan YL, Lui KW, Lee KF (2000) Sonographically guided core-needle biopsy in the diagnosis of superficial lymphadenopathy. J Clin Ultrasound 28:283–289
Christensen R (2001) Invasive radiology for pediatric trauma. Sem Ped Surg 10:7–11
Connolly BL, Chait PG, Siva-Nandan R, Duncan D, Peer M (1998) Recognition of intussusception around gastrojejunostomy tubes in children. AJR Am J Roentgenol 170:467–470
Cory DA, Fitzgerald JF, Cohen MD (1988) Percutaneous nonendoscopic gastrostomy in children. AJR Am J Roentgenol 151:995–997
Cwikiel W (2002) Transjugular intrahepatic portosystemic shunt. Acta Paediatr 91:374–375
Cwikiel W, Keussen I, Larsson L, Solvig J, Kullendorff CM (2003) Interventional treatment of children with portal hypertension secondary to portal vein occlusion. Eur J Pediatr Surg 13:312–218
Dewald CL, Hiette PO, Sewall LE, Fredenberg PG, Palestrant AM (1999) Percutaneous gastrostomy and gastrojejunostomy with gastropexy: experience in 701 procedures. Radiology 211:651–656
Dey R, Ferguson C, Kenny SE, Shankar KR, Coldicutt P, Baillie CT et al (2003) After the honeymoon – medium-term outcome of antegrade continence enema procedure. J Pediatr Surg 38:65–68
Diament MJ, Boechat MI, Kangarloo H (1985) Interventional radiology in infants and children: clinical and technical aspects. Radiology 154:359–361
Di Lorenzo C, Benninga MA (2004) Pathophysiology of pediatric fecal incontinence. Gastroenterology 126[1 Suppl 1]: S33–S40
Ekmark E, Adams RC (2000) The antegrade continence enema (ACE) surgical procedures: patient selection, outcomes, long-term patient management. Eur J Pediatr Surg 10[Suppl 1]:49–51
Erdogan E, Eroglu E, Tekant G, Yeker Y, Emir H, Sarimurat N et al (2003) Management of esophagogastric corrosive injuries in children. Eur J Pediatr Surg 13:289–293
Fasulakis S, Andronikou S (2003) Balloon dilatation in children for oesophageal strictures other than those due to primary repair of oesophageal atresia, interposition or restrictive fundoplication. Pediatr Radiol 33:682–687
Freedman AM, Sanyal AJ, Tisnado J, et al (1993) Complications of transjugular intrahepatic portosystemic shunt: a comprehensive review. Radiographics 13:1185–1210
Friedman JN, Ahmed S, Connolly B, Chait PG, Mahant S (2004) Complications associated with image-guided gastrostomy and gastrojejunostomy tubes in children. Pediatrics 114:458–461
Garcia-Villarreal L, Martinez-Lagares F, Sierra A, Guevara C, Marrero JM, Jimenez E et al (1999) Transjugular intrahepatic portosystemic shunt versus endoscopic sclerotherapy for the prevention of variceal rebleeding after recent variceal hemorrhage. Hepatology 29:27–32
Gervais DA, Brown SD, Connolly SA, Brec SL, Harisinghani MG, Mueller PR (2004) Percutaneous imaging-guided abdominal and pelvic abscess drainage in children. Radiographics 24:737–754
Graf JL, Strear C, Bratton B, Housley HT, Jennings RW, Harrison MR et al (1998) The antegrade continence enema procedure: a review of the literature. J Pediatr Surg 33:1294–1296
Griffiths DM, Malone PS (1995) The Malone antegrade continence enema. J Pediatr Surg 30:68–71
Guelrud M, Mendoza S, Jaen D, Plaz J, Machuca J, Torres P (1992) ERCP and endoscopic sphincterotomy in infants and children with jaundice due to common bile duct stones. Gastrointest Endosc 38:450–453
Guo Z, Kurtycz DF, Salem R, Las Casas LE, Caya JG, Hoerl HD (2002) Radiologically guided percutaneous fine-needle aspiration biopsy of the liver: retrospective study of 119 cases evaluating diagnostic effectiveness and clinical complications. Diagn Cytopathol 26:283–289
Hagiwara A, Yukioka T, Ohta S, Nitatori T, Matsuda H, Shimazaki S (1996) Nonsurgical management of patients with blunt splenic injury: efficacy of transcatheter arterial embolization. AJR Am J Roentgenol 167:159–66
Hamza AF, Abdelhay S, Hasan T, Soliman H, Kabesh A, Bassiouny I et al (2003) Caustic esophageal strictures in children; 30 years' experience. J Pediatr Surg 38:828–833
Heyman MB, LaBerge JM (1999) Role of transjugular intrahepatic portosystemic shunt in the treatment of portal hypertension in pediatric patients. J Pediatr Gastroenterol Nutr 29:240–249
Heyman MB, LaBerge JM, Somberg KA, Rosenthal P, Mudge C, Ring EJ et al (1997) Transjugular intrahepatic portosystemic shunts (TIPS) in children. J Pediatr 131:914–919
Hoffer FA (1997) Interventional radiology in the acute pediatric abdomen. Radiol Clin North Am 35:977–987
Hoffer FA (2000) Liver biopsy methods for pediatric oncology patients. Pediatr Radiol 30:481–488
Huang Y, Ni Y, Lai H, Chang M (2004) Corrosive esophagitis in children. Ped Surg Int 20:207–211
Hubbard AM, Fellows KE (1993) Pediatric interventional radiology: current practice and innovations. Cardiovasc Intervent Radiol 16:267–274
Huppert PE, Astfalk W, Brambs HJ, Schweizer P, Schott U, Pereira P et al (1998) [Transjugular intrahepatic portosystemic shunt in children. Initial clinical experiences and literature review]. Rofo Fortschr Geb Rontgenstr Neuen Bildgeb Verfahr 168:595–603
Jayakrishnan VK, Wilkinson AG (2001) Treatment of oesophageal strictures in children: a comparison of fluoroscopically guided balloon dilatation with surgical bouginage. Pediatr Radiol 31:98–101
Kang SG, Song HY, Lim MK, Yoon HK, Goo DE, Sung KB (1998) Esophageal rupture during balloon dilation of strictures of benign or malignant causes: prevalence and clinical importance. Radiology 209:741–746
Kaye RD, Towbin RB (2002) Imaging and intervention in the gastrointestinal tract in children. Gastroenterol Clin North Am 31:897–923
Kaye R, Sane SS, Towbin RB (2000a) Pediatric intervention: an update-part II. J Vasc Interv Radiol 11:807–822

Kaye RD, Sane SS, Towbin RB (2000b) Pediatric intervention: an update-part I. J Vasc Interv Radiol 11:683–697

Kim IO, Yeon KM, Kim WS, Park KW, Kim JH, Han MC (1993) Perforation complicating balloon dilation of esophageal strictures in infants and children. Radiology 189:741–744

Kogan A, Katz J, Efrat R, Eidelman LA (2002) Premedication with midazolam in young children: a comparison of four routes of administration. Paediatr Anaesth 12:685–689

Kushimoto S, Arai M, Aiboshi J, Harada N, Tosaka N, Koido Y et al (2003) The role of interventional radiology in patients requiring damage control laparotomy. J Trauma 54:171–176

Lang EK, Springer RM, Glorioso LW3, Cammarata CA (1986) Abdominal abscess drainage under radiologic guidance: causes of failure. Radiology 159:329–336

Lang T, Hummer HP, Behrens R (2001) Balloon dilation is preferable to bougienage in children with esophageal atresia. Endoscopy 33:329–335

Lieberman S, Libson E, Maly B, Lebensart P, Ben Yehuda D, Bloom AI (2003) Imaging-guided percutaneous splenic biopsy using a 20- or 22-gauge cutting-edge core biopsy needle for the diagnosis of malignant lymphoma. AJR Am J Roentgenol 181:1025–1027

Lisy J, Hetkova M, Snajdauf J, Vyhnanek M, Tuma S (1998) Long-term outcomes of balloon dilation of esophageal strictures in children. Acad Radiol 5:832–835

Ljungman G, Kreuger A, Andreasson S, Gordh T, Sorensen S (2000) Midazolam nasal spray reduces procedural anxiety in children. Pediatrics 105(1 Pt 1):73–78

London RL, Trotman RW, DiMarino AJJr, Oleaga JA, Freiman DB, Ring EJ et al (1981) Dilatation severe oesophageal strictures by an inflatable balloon catheter. Gastroenterology 80:173–175

Lorenz JM, Leef JA, Chou CH, Funaki B, Straus CM, Rosenblum JD (2001) Sonographic needle guidance in cholangiography in children. J Vasc Interv Radiol 12:342–346

Lorenz JM, Denison G, Funaki B, Leef JA, van Ha T, Rosenblum JD (2005) Balloon dilatation of biliary-enteric strictures in children. AJR Am J Roentgenol 184:151–155

Maher MM, Gervais DA, Kalra MK, Lucey B, Sahani DV, Arellano R et al (2004) The inaccessible or undrainable abscess: how to drain it. Radiographics 24:717–735

Malone PS, Ransley PG, Kiely EM (1990) Preliminary report: the antegrade continence enema. Lancet 336:1217–1218

McIlwain M, Primosch R, Bimstein E (2004) Allergic reaction to intranasal midazolam HCl: a case report. Pediatr Dent 26:359–361

McLean GK, Le Veen RF (1989) Shear stress in the performance of esophageal dilation: comparison of balloon dilatation with bougienage. Radiology 172:983–986

Muraca S, Chait PG, Connolly BL, Baskin KM, Temple MJ (2001) US-guided core biopsy of the spleen in children. Radiology 218:200–206

Naehrlich L, Lang T, Schamberger U, Behrens R (2000) Balloon dilation of an esophageal stenosis in a patient with recessive dystrophic epidermolysis bullosa. Pediatr Dermatol 17:477–479

Nobili V, Comparcola D, Sartorelli MR, Natali G, Monti L, Falappa P et al (2003) Blind and ultrasound-guided percutaneous liver biopsy in children. Pediatr Radiol 33:772–775

Norman J (2001) Practical pediatric interventional radiology. Curr Probl Diagn Radiol 30:61–86

Ohtsuka Y, Iwasaki K, Okazumi S, Yoshida H, Matsunaga T, Kouchi K et al (2003) Management of blunt hepatic injury in children: usefulness of emergency transcatheter arterial embolization. Pediatr Surg Int 19(1–2):29–34

Pereira JK, Chait PG, Miller SF (1996) Deep pelvic abscesses in children: transrectal drainage under radiologic guidance. Radiology 198:393–396

Pomier-Layrargues G, Villeneuve JP, Deschenes M, Bui B, Perreault P, Fenyves D et al (2001) Transjugular intrahepatic portosystemic shunt (TIPS) versus endoscopic variceal ligation in the prevention of variceal rebleeding in patients with cirrhosis: a randomised trial. Gut 48:390–396

Reeves ST, Havidich JE, Tobin DP (2004) Conscious sedation of children with propofol is anything but conscious. Pediatrics 114:e74–e76

Rivera MT, Kugathasan S, Berger W, Werlin SL (2001) Percutaneous colonoscopic cecostomy for management of chronic constipation in children. Gastrointest Endosc 53:225–228

Roebuck DJ (2004) Ultrasound-guided core needle biopsy of primary liver tumours in young children. Pediatr Radiol 34:S127

Roebuck DJ, Stanley P (2000) External and internal-external biliary drainage in children with malignant obstructive jaundice. Pediatr Radiol 30(10):659–664

Rösch J, Hanafee WN, Snow H (1969) Transjugular portal venography and radiologic portacaval shunt: an experimental study. Radiology 92:1112–1114

Rose SC, Andre MP, Roberts AC, Kinney TB, Valji K, Ronaghi AH et al (2001) Integral role of interventional radiology in the development of a pediatric liver transplantation program. Pediatr Transplant 5:331–338

Rubin JT, Towbin RB, Bartko M, Baskin KM, Cahill AM, Kaye RD (2004) Oral and intravenous caffeine for treatment of children with post-sedation paradoxical hyperactivity. Ped Radiol 34:980–984

Saarinen UM, Wikstrom S, Koskimies O, Sariola H (1991) Percutaneous needle biopsy preceding preoperative chemotherapy in the management of massive renal tumors in children. J Clin Oncol 1991 9:406–415

Safrit HD, Mauro MA, Jaques PF (1987) Percutaneous abscess drainage in Crohn's disease. AJR Am J Roentgenol 148:859–862

Said M, Mekki M, Golli M, Memmi F, Hafsa C, Braham R et al (2003) Balloon dilatation of anastomotic strictures secondary to surgical repair of oesophageal atresia. Br J Radiol 76:26–31

Sandgren K, Malmfors G. Balloon dilatation of oesophageal strictures in children. Eur J Pediatr Surg 8:9–11

Sato Y, Frey EE, Smith WL, Pringle KC, Soper RT, Franken EA, Jr. (1988) Balloon dilatation of esophageal stenosis in children. AJR Am J Roentgenol 150:639–642

Scheimann AO, Barrios JM, Al Tawil YS, Gray KM, Gilger MA (2000) Percutaneous liver biopsy in children: impact of ultrasonography and spring-loaded biopsy needles. J Pediatr Gastroenterol Nutr 31:536–539

Searles JM, Roberts JP, MacKinnon AE (2000) The ACE procedure-problems behind the success. Eur J Pediatr Surg 10[Suppl 1]:51–52

Shandling B, Chait PG, Richards HF (1996) Percutaneous cecostomy: a new technique in the management of fecal incontinence. J Pediatr Surg 31:534–537

Shiffman ML, Jeffers L, Hoofnagle JH, Tralka TS (1995) The role of transjugular intrahepatic portosystemic shunt for treatment of portal hypertension and its complications: a conference sponsored by the National Digestive Diseases Advisory Board. Hepatology 22:1591–1597

Sklair-Levy M, Lebensart PD, Applbaum YH, Ramu N, Freeman A, Gozal D et al (2001) Percutaneous image-guided needle biopsy in children – summary of our experience with 57 children. Pediatr Radiol 31:732–736

Smith TP, Presson TL, Heneghan MA, Ryan JM (2003) Transjugular biopsy of the liver in pediatric and adult patients using an 18-gauge automated core biopsy needle: a retrospective review of 410 consecutive procedures. AJR Am J Roentgenol 180167–172

Squire R, Kiely EM, Carr B, Ransley PG, Duffy PG (1993) The clinical application of the Malone antegrade colonic enema. J Pediatr Surg 28:1012–1015

Stellato TA, Gauderer MWL (1987) Percutaneous endoscopic gastrostomy for gastrointestinal decompression. Ann Surg 205:119–122

Sury MR, Hatch DJ, Deeley T, Dicks-Mireaux C, Chong WK (1999) Development of a nurse-led sedation service for paediatric magnetic resonance imaging. Lancet 353:1667–1671

Sze DY, Esquivel CO (2002) The role of interventional radiology in a pediatric liver transplant program. Pediatr Transplant 6:1–4

ter Borg PC, Hollemans M, Van Buuren HR, Vleggaar FP, Groeneweg M, Hop WC et al (2004) Transjugular intrahepatic portosystemic shunts: long-term patency and clinical results in a patient cohort observed for 3–9 years. Radiology 231:537–545

Towbin RB (1989) Current advances in pediatric interventional radiology. Curr Opin Radiol 1:572–576

Towbin RB (1991) Pediatric interventional radiology. Curr Opin Radiol 3:931–935

Towbin RB, Ball WS, Jr. (1988) Pediatric interventional radiology. Radiol Clin North Am 26:419–440

Weber F, Wulf H, el Saeidi G (2003) Premedication with nasal s-ketamine and midazolam provides good conditions for induction of anesthesia in preschool children. Can J Anaesth 50:470–475

Wiebe S, Cohen J, Connolly B, Chait PG (2004) Percutaneous decompression of the bowel with a small-caliber needle: a method to facilitate percutaneous abdominal access. AJR Am J Roentgenol 184:227–229

Yeming W, Chenren S, Huiming J, Ming Z, Liu DC (2002) Balloon catheter dilatation in children with congenital and acquired esophageal anomalies. J Pediatr Surg 37:398–402

Yu SC, Liew CT, Lau WY, Leung TW, Metreweli C (2001) US-guided percutaneous biopsy of small (< or = 1-cm) hepatic lesions. Radiology 218:195–199

Subject Index

C

D

E

F

G

H

I

J

K

L

M

N

O

P

R

S

T

U

V

W

Y

Z

List of Contributors

Teresa Berrocal, MD, PhD
Pediatric Radiologist, Department of Radiology
Division of Pediatric Radiology
University Hospital La Paz
Madrid
Spain

Susan A. Connolly, MD
Department/Division Radiology
Area of Clinical Expertise, Musculoskeletal Radiology
Children's Hospital Boston, Department of Radiology
300 Longwood Avenue, Main 2
Boston, MA 02115
USA

Gloria del Pozo, MD, PhD
Associate Professor of Radiology, Pediatric Radiologist
Department of Radiology
Pediatric Radiology Section
University Hospital 12 de Octubre
Madrid
Spain

Ronald B. J. Glass, MD
Department of Radiology
Children's Memorial Hospital
2300 Children's Plaza
Chicago, IL 60614
USA
and
Associate Professor of Radiology
Feinberg School of Medicine
Northwestern University
Chicago, IL
USA

Christine M. Hall, MBBS, DMRD, FRCR
Professor of Paediatric Radiology
Great Ormond Street Hospital
London WC1N 3JH
UK

Melanie P. Hiorns, MBBS, MRCP, FRCR
Consultant Paediatric Radiologist
and Honorary Senior Lecturer
Department of Radiology
Great Ormond Street Hospital
London WC1N 3JH
London
UK

Yvonne. L. Hoogeveen, PhD
Department of Radiology
UMCN St Radboud
P.O. Box 9101, route 667
6500 HB Nijmegen
The Netherlands

Rafael M. Jiménez, MD
Department/Division Radiology
Area of Clinical Expertise
Musculoskeletal Radiology
Children's Hospital Boston
Department of Radiology
300 Longwood Avenue, Main 2
Boston, MA 02115
USA

Johan S. Laméris, MD, PhD
Department of Radiology
Academic Medical Centre/
Emma Children's Hospital Amsterdam
Meibergdreef 9
1105 AZ Amsterdam Zuid-Oost
The Netherlands

Morteza Meradji, MD, PhD
Erasmus MC
Sophia Children's Hospital
Dr. Molewaterplein 40
P.O. Box 1738
3000 DR Rotterdam
The Netherlands

Els Nijs, MD
Department of Radiology
University Hospitals Gasthuisberg
Katholieke Universiteit Leuven
Herestraat 49
3000 Leuven
Belgium

Rick R. van Rijn, MD, PhD
Paediatric Radiologist
Department of Radiology
Academic Medical Centre Amsterdam
Emma Children's Hospital
Meibergdreef 9
1105 AZ Amsterdam Zuid-Oost
The Netherlands

Medical Radiology Diagnostic Imaging and Radiation Oncology

Titles in the series already published

Diagnostic Imaging

Innovations in Diagnostic Imaging
Edited by J. H. Anderson

Radiology of the Upper Urinary Tract
Edited by E. K. Lang

The Thymus - Diagnostic Imaging, Functions, and Pathologic Anatomy
Edited by E. Walter, E. Willich, and W. R. Webb

Interventional Neuroradiology
Edited by A. Valavanis

Radiology of the Pancreas
Edited by A. L. Baert, co-edited by G. Delorme

Radiology of the Lower Urinary Tract
Edited by E. K. Lang

Magnetic Resonance Angiography
Edited by I. P. Arlart, G. M. Bongartz, and G. Marchal

Contrast-Enhanced MRI of the Breast
S. Heywang-Köbrunner and R. Beck

Spiral CT of the Chest
Edited by M. Rémy-Jardin and J. Rémy

Radiological Diagnosis of Breast Diseases
Edited by M. Friedrich and E.A. Sickles

Radiology of the Trauma
Edited by M. Heller and A. Fink

Biliary Tract Radiology
Edited by P. Rossi, co-edited by M. Brezi

Radiological Imaging of Sports Injuries
Edited by C. Masciocchi

Modern Imaging of the Alimentary Tube
Edited by A. R. Margulis

Diagnosis and Therapy of Spinal Tumors
Edited by P. R. Algra, J. Valk, and J. J. Heimans

Interventional Magnetic Resonance Imaging
Edited by J. F. Debatin and G. Adam

Abdominal and Pelvic MRI
Edited by A. Heuck and M. Reiser

Orthopedic Imaging
Techniques and Applications
Edited by A. M. Davies and H. Pettersson

Radiology of the Female Pelvic Organs
Edited by E. K.Lang

Magnetic Resonance of the Heart and Great Vessels
Clinical Applications
Edited by J. Bogaert, A.J. Duerinckx, and F. E. Rademakers

Modern Head and Neck Imaging
Edited by S. K. Mukherji and J. A. Castelijns

Radiological Imaging of Endocrine Diseases
Edited by J. N. Bruneton in collaboration with B. Padovani and M.-Y. Mourou

Trends in Contrast Media
Edited by H. S. Thomsen, R. N. Muller, and R. F. Mattrey

Functional MRI
Edited by C. T. W. Moonen and P. A. Bandettini

Radiology of the Pancreas
2nd Revised Edition
Edited by A. L. Baert. Co-edited by G. Delorme and L. Van Hoe

Emergency Pediatric Radiology
Edited by H. Carty

Spiral CT of the Abdomen
Edited by F. Terrier, M. Grossholz, and C. D. Becker

Liver Malignancies
Diagnostic and Interventional Radiology
Edited by C. Bartolozzi and R. Lencioni

Medical Imaging of the Spleen
Edited by A. M. De Schepper and F. Vanhoenacker

Radiology of Peripheral Vascular Diseases
Edited by E. Zeitler

Diagnostic Nuclear Medicine
Edited by C. Schiepers

Radiology of Blunt Trauma of the Chest
P. Schnyder and M. Wintermark

Portal Hypertension
Diagnostic Imaging-Guided Therapy
Edited by P. Rossi
Co-edited by P. Ricci and L. Broglia

Recent Advances in Diagnostic Neuroradiology
Edited by Ph. Demaerel

Virtual Endoscopy and Related 3D Techniques
Edited by P. Rogalla, J. Terwisscha Van Scheltinga, and B. Hamm

Multislice CT
Edited by M. F. Reiser, M. Takahashi, M. Modic, and R. Bruening

Pediatric Uroradiology
Edited by R. Fotter

Transfontanellar Doppler Imaging in Neonates
A. Couture and C. Veyrac

Radiology of AIDS
A Practical Approach
Edited by J.W.A.J. Reeders and P.C. Goodman

CT of the Peritoneum
Armando Rossi and Giorgio Rossi

Magnetic Resonance Angiography
2nd Revised Edition
Edited by I. P. Arlart, G. M. Bongratz, and G. Marchal

Pediatric Chest Imaging
Edited by Javier Lucaya and Janet L. Strife

Applications of Sonography in Head and Neck Pathology
Edited by J. N. Bruneton in collaboration with C. Raffaelli and O. Dassonville

Imaging of the Larynx
Edited by R. Hermans

3D Image Processing
Techniques and Clinical Applications
Edited by D. Caramella and C. Bartolozzi

Imaging of Orbital and Visual Pathway Pathology
Edited by W. S. Müller-Forell

Pediatric ENT Radiology
Edited by S. J. King and A. E. Boothroyd

Radiological Imaging of the Small Intestine
Edited by N. C. Gourtsoyiannis

Imaging of the Knee
Techniques and Applications
Edited by A. M. Davies and V. N. Cassar-Pullicino

Perinatal Imaging
From Ultrasound to MR Imaging
Edited by Fred E. Avni

Radiological Imaging of the Neonatal Chest
Edited by V. Donoghue

Diagnostic and Interventional Radiology in Liver Transplantation
Edited by E. Bücheler, V. Nicolas, C. E. Broelsch, X. Rogiers, and G. Krupski

Radiology of Osteoporosis
Edited by S. Grampp

Imaging Pelvic Floor Disorders
Edited by C. I. Bartram and J. O. L. DeLancey
Associate Editors: S. Halligan, F. M. Kelvin, and J. Stoker

Imaging of the Pancreas
Cystic and Rare Tumors
Edited by C. Procacci and A. J. Megibow

High Resolution Sonography of the Peripheral Nervous System
Edited by S. Peer and G. Bodner

Imaging of the Foot and Ankle
Techniques and Applications
Edited by A. M. Davies, R. W. Whitehouse, and J. P. R. Jenkins

Radiology Imaging of the Ureter
Edited by F. Joffre, Ph. Otal, and M. Soulie

Imaging of the Shoulder
Techniques and Applications
Edited by A. M. Davies and J. Hodler

Radiology of the Petrous Bone
Edited by M. Lemmerling and S. S. Kollias

Interventional Radiology in Cancer
Edited by A. Adam, R. F. Dondelinger, and P. R. Mueller

Duplex and Color Doppler Imaging of the Venous System
Edited by G. H. Mostbeck

Multidetector-Row CT of the Thorax
Edited by U. J. Schoepf

Functional Imaging of the Chest
Edited by H.-U. Kauczor

Radiology of the Pharynx and the Esophagus
Edited by O. Ekberg

Radiological Imaging in Hematological Malignancies
Edited by A. Guermazi

Imaging and Intervention in Abdominal Trauma
Edited by R. F. Dondelinger

Multislice CT
2nd Revised Edition
Edited by M. F. Reiser, M. Takahashi, M. Modic, and C. R. Becker

Intracranial Vascular Malformations and Aneurysms
From Diagnostic Work-Up to Endovascular Therapy
Edited by M. Forsting

Radiology and Imaging of the Colon
Edited by A. H. Chapman

Coronary Radiology
Edited by M. Oudkerk

Dynamic Contrast-Enhanced Magnetic Resonance Imaging in Oncology
Edited by A. Jackson, D. L. Buckley, and G. J. M. Parker

Imaging in Treatment Planning for Sinonasal Diseases
Edited by R. Maroldi and P. Nicolai

Clinical Cardiac MRI
With Interactive CD-ROM
Edited by J. Bogaert, S. Dymarkowski, and A. M. Taylor

Focal Liver Lesions
Detection, Characterization, Ablation
Edited by R. Lencioni, D. Cioni, and C. Bartolozzi

Multidetector-Row CT Angiography
Edited by C. Catalano and R. Passariello

Paediatric Musculoskeletal Diseases
With an Emphasis on Ultrasound
Edited by D. Wilson

Contrast Media in Ultrasonography
Basic Principles and Clinical Applications
Edited by Emilio Quaia

MR Imaging in White Matter Diseases of the Brain and Spinal Cord
Edited by M. Filippi, N. De Stefano, V. Dousset, and J. C. McGowan

Diagnostic Nuclear Medicine
2nd Revised Edition
Edited by C. Schiepers

Imaging of the Kidney Cancer
Edited by A. Guermazi

Magnetic Resonance Imaging in Ischemic Stroke
Edited by R. von Kummer and T. Back

Imaging of the Hip & Bony Pelvis
Techniques and Applications
Edited by A. M. Davies, K. J. Johnson, and R. W. Whitehouse

Imaging of Occupational and Environmental Disorders of the Chest
Edited by P. A. Gevenois and P. De Vuyst

Contrast Media
Safety Issues and ESUR Guidelines
Edited by H. S. Thomsen

Virtual Colonoscopy
A Practical Guide
Edited by P. Lefere and S. Gryspeerdt

Vascular Embolotherapy
A Comprehensive Approach
Volume 1: *General Principles, Chest, Abdomen, and Great Vessels*
Edited by J. Golzarian. Co-edited by S. Sun and M. J. Sharafuddin

Vascular Embolotherapy
A Comprehensive Approach
Volume 2: *Oncology, Trauma, Gene Therapy, Vascular Malformations, and Neck*
Edited by J. Golzarian. Co-edited by S. Sun and M. J. Sharafuddin

Head and Neck Cancer Imaging
Edited by R. Hermans

Vascular Interventional Radiology
Current Evidence in Endovascular Surgery
Edited by M. G. Cowling

Ultrasound of the Gastrointestinal Tract
Edited by G. Maconi and G. Bianchi Porro

Imaging of Orthopedic Sports Injuries
Edited by F. M. Vanhoenacker, M. Maas, J. L. M. A. Gielen

Parallel Imaging in Clinical MR Applications
Edited by S. O. Schoenberg, O. Dietrich, and F. M. Reiser

MR and CT of the Female Pelvis
Edited by B. Hamm and R. Forstner

Ultrasound of the Musculoskeletal System
S. Bianchi and C. Martinoli

Spinal Imaging
Diagnostic Imaging of the Spine and Spinal Cord
Edited by J. W. M. Van Goethem, L. Van den Hauwe, and P. M. Parizel

Radiation Dose from Adult and Pediatric Multidetector Computed Tomography
Edited by D. Tack and P. A. Gevenois

Computed Tomography of the Lung
A Pattern Approach
J. A. Verschakelen and W. De Wever

Clinical Functional MRI
Presurgical Functional Neuroimaging
Edited bei C. Stippich

Imaging in Transplantation
Edited by A. A. Bankier

Radiological Imaging of the Digestive System in Infants and Children
Edited by A. S. Devos and J. G. Blickman

Pediatric Chest Imaging
Chest Imaging in Infants and Children
2nd Revised Edition
Edited by J. Lucaya and J. L. Strife

Radiological Imaging of the Neonatal Chest
2nd Revised Edition
Edited by V. Donoghue

Radiology of the Stomach and Duodenum
Edited by A. H. Freeman and E. Sala

Imaging in Pediatric Skeletal Trauma
Techniques and Applications
Edited by K. J. Johnson and E. Bache

Percutaneous Tumor Ablation in Medical Radiology
Edited by T. J. Vogl, T. K. Helmberger, M. G. Mack, and M. F. Reiser

Screening and Preventive Diagnosis with Radiological Imaging
Edited by M. F. Reiser, G. van Kaick, C. Fink, and S. O. Schoenberg

Color Doppler US of the Penis
Edited by M. Bertolotto

Image Processing in Radiology
Current Applications
Edited by E. Neri, D. Caramella, and C. Bartolozzi

Springer

Medical Radiology Diagnostic Imaging and Radiation Oncology

Titles in the series already published

Radiation Oncology

Lung Cancer
Edited by C.W. Scarantino

Innovations in Radiation Oncology
Edited by H. R. Withers
and L. J. Peters

Radiation Therapy
of Head and Neck Cancer
Edited by G. E. Laramore

Gastrointestinal Cancer –
Radiation Therapy
Edited by R.R. Dobelbower, Jr.

Radiation Exposure
and Occupational Risks
Edited by E. Scherer, C. Streffer,
and K.-R. Trott

Radiation Therapy of Benign Diseases
A Clinical Guide
S. E. Order and S. S. Donaldson

Interventional Radiation
Therapy Techniques – Brachytherapy
Edited by R. Sauer

Radiopathology of Organs and Tissues
Edited by E. Scherer, C. Streffer,
and K.-R. Trott

Concomitant Continuous Infusion
Chemotherapy and Radiation
Edited by M. Rotman
and C. J. Rosenthal

Intraoperative Radiotherapy –
Clinical Experiences and Results
Edited by F. A. Calvo, M. Santos,
and L.W. Brady

Radiotherapy of Intraocular
and Orbital Tumors
Edited by W. E. Alberti and
R. H. Sagerman

Interstitial and Intracavitary
Thermoradiotherapy
Edited by M. H. Seegenschmiedt
and R. Sauer

Non-Disseminated Breast Cancer
Controversial Issues in Management
Edited by G. H. Fletcher and S.H. Levitt

Current Topics in
Clinical Radiobiology of Tumors
Edited by H.-P. Beck-Bornholdt

Practical Approaches to
Cancer Invasion and Metastases
A Compendium of Radiation
Oncologists' Responses to 40 Histories
Edited by A. R. Kagan with the
Assistance of R. J. Steckel

Radiation Therapy in Pediatric Oncology
Edited by J. R. Cassady

Radiation Therapy Physics
Edited by A. R. Smith

Late Sequelae in Oncology
Edited by J. Dunst and R. Sauer

Mediastinal Tumors. Update 1995
Edited by D. E. Wood and
C. R. Thomas, Jr.

Thermoradiotherapy
and Thermochemotherapy
Volume 1:
Biology, Physiology, and Physics
Volume 2:
Clinical Applications
Edited by M.H. Seegenschmiedt,
P. Fessenden, and C.C. Vernon

Carcinoma of the Prostate
Innovations in Management
Edited by Z. Petrovich, L. Baert,
and L.W. Brady

Radiation Oncology
of Gynecological Cancers
Edited by H.W. Vahrson

Carcinoma of the Bladder
Innovations in Management
Edited by Z. Petrovich, L. Baert,
and L.W. Brady

Blood Perfusion and
Microenvironment of Human Tumors
Implications for
Clinical Radiooncology
Edited by M. Molls and P. Vaupel

Radiation Therapy of Benign Diseases
A Clinical Guide
2nd Revised Edition
S. E. Order and S. S. Donaldson

Carcinoma of the Kidney and Testis,
and Rare Urologic Malignancies
Innovations in Management
Edited by Z. Petrovich, L. Baert,
and L.W. Brady

Progress and Perspectives in the
Treatment of Lung Cancer
Edited by P. Van Houtte,
J. Klastersky, and P. Rocmans

Combined Modality Therapy of
Central Nervous System Tumors
Edited by Z. Petrovich, L. W. Brady,
M. L. Apuzzo, and M. Bamberg

Age-Related Macular Degeneration
Current Treatment Concepts
Edited by W. A. Alberti, G. Richard,
and R. H. Sagerman

Radiotherapy of Intraocular
and Orbital Tumors
2nd Revised Edition
Edited by R. H. Sagerman,
and W. E. Alberti

Modification of Radiation Response
Cytokines, Growth Factors,
and Other Biolgical Targets
Edited by C. Nieder, L. Milas,
and K. K. Ang

Radiation Oncology for Cure and Palliation
R. G. Parker, N. A. Janjan,
and M. T. Selch

Clinical Target Volumes in Conformal and
Intensity Modulated Radiation Therapy
A Clinical Guide to Cancer Treatment
Edited by V. Grégoire, P. Scalliet,
and K. K. Ang

Advances in Radiation Oncology
in Lung Cancer
Edited by Branislav Jeremić

New Technologies in Radiation Oncology
Edited by W. Schlegel, T. Bortfeld,
and A.-L. Grosu

Technical Basis of Radiation Therapy
4th Revised Edition
Edited by S. H. Levitt, J. A. Purdy,
C. A. Perez, and S. Vijayakumar

CURED I • LENT – Late Effects of Cancer
Treatment
on Normal Tissues
Edited by P. Rubin, L. S. Constine,
L. B. Marks, and P. Okunieff

Clinical Practice of Radiation Therapy for
Benign Diseases
Contemporary Concepts and Clinical
Results
Edited by M. H. Seegenschmiedt,
H.-B. Makoski, K.-R. Trott, and
L. W. Brady

Springer